THE UNIVERSITY OF HULL

Solubilisation and emulsification of silicone oils in aqueous surfactant systems

being a Thesis submitted for the Degree of Doctor of Philosophy in the University of Hull

by

Jinfeng Dong, BSc, MSc

March 1999

Acknowledgements

The author would like to express her gratitude to her supervisor, Dr. Bernard Paul Binks, for his high standard of supervision and guidance. He has always been enthusiastic, available, supportive and encouraging.

The author thanks S.C. Johnson and Son, Inc. (Racine, USA) and the University of Hull for the provision of a studentship, and Dr. Ian C. Callaghan, formerly of S.C. Johnson Wax, Egham for regular meetings and useful discussions.

The author is grateful for the support and encouragement she received from Prof. Paul Fletcher, Dr. John Clint and Prof. Robert Aveyard during her stay in Hull. The past and present members of the Surfactant Science Group are thanked for their friendship and good times.

The author gratefully acknowledges Miss Natasa Rebolj from the University of Ljubljana, Slovenia for carrying out some of the experiments detailed in chapters 7 and 8.

Parts of this thesis have been presented at the following conferences:

- 10th European Colloid and Interface Society (ECIS) Conference, September 1996, Turku.
- Emulsion Conference (CISG), March 1997, Hull.
- 4th UK Surface and Colloid Science Student Meeting, July 1997, Greenwich.
- Polymers and Surfactants Conference (CISG/CSCG), September 1997, Wrexham.
- 12th Surfactant in Solution (SIS) Conference, June 1998, Stockholm.
- 12th European Colloid and Interface Society (ECIS) Conference, September 1998, Dubrovnik-Cavtat.

This thesis has led to the following publications:

- B.P. Binks, J. Dong and N. Rebolj "Equilibrium Phase Behaviour and Emulsion Stability in Silicone Oil+Water+AOT Mixtures", *Phys. Chem. Chem. Phys.*, in press.
- B.P. Binks and J. Dong, *Patent* to S.C. Johnson Wax, filed.
- B.P. Binks and J. Dong, "Mixing of Silicone Oils with Monolayers of Nonionic Surfactant at the Air-water Surface", *J. Chem. Soc. Faraday Trans.*, **94,** 401 (1998).
- B.P. Binks and J. Dong, "Emulsions and Equilibrium Phase Behaviour in Silicone Oil+Water+Nonionic Surfactant Mixtures", *Colloids and Surfaces A*, **132**, 289 (1998).

Nothing in the world is too difficult to achieve for one

who sets one's heart on it.

Chinese Proverb

ABSTRACT

ABSTRACT

Solubilisation and emulsification of polydimethylsiloxane (PDMS) oils into aqueous surfactant solutions have been investigated with a series of nonionic surfactants and an anionic surfactant (AOT).

For nonionic surfactants at oil-water interfaces, the effect of temperature, surfactant structure, electrolyte concentration and PDMS molecular weight on the emulsion phase inversion of water/PDMS/surfactant systems has been studied in detail. For certain nonionic surfactants the equilibrium phase behaviour of equal volumes of water and oil has been studied in Winsor systems. At air-water surfaces, the spreading behaviour of PDMS on aqueous nonionic surfactant solutions has been investigated for a range of surfactant structures. Above the critical micelle concentration (cmc) and with 50 cS PDMS, the initial and equilibrium spreading coefficients have been determined. For $C_{12}E_5$, the dependence of the spreading coefficients on oil molecular weight also was investigated. The complete adsorption isotherms of the volatile PDMS oils on $C_{12}E_5$ solutions have been measured, which yields the composition of the mixed layer of surfactant and oil. The competition for the surface between PDMS and surfactant has been studied by opening up the monolayer of $C_{12}E_5$ and L-77 by dilution below the cmc. The preliminary neutron reflectivity study showed that PDMS forms a thin layer on top of the surfactant chain region.

For the anionic surfactant AOT, the transition of Winsor systems at equilibrium for hexamethyldisiloxane (0.65 cS)+AOT+aqueous NaCl from I-III-II is effected by increasing the electrolyte concentration. In single phase microemulsions, the uptake of oil into aqueous surfactant solutions and the solubilisation of water into surfactant solutions in oil are determined both as a function of salt concentration and temperature. The partitioning of salt between dispersed and excess water phases is considered. The stability of macroemulsions prepared from the coexisting phases in Winsor systems is investigated. Correlation between the emulsion phase inversion, Winsor phase transition and oil-water interfacial tension is discussed. The mixing behaviour of 0.65 cS PDMS oil and AOT at air-water surfaces has been studied as a function of oil activity, surfactant and electrolyte concentrations.

CONTENTS

Chapter 1 Introduction 1

1.1 Introduction and industrial relevance 1

1.2 Nature of silicone oil 2

1.2.1 Introduction to silicone oil 2

1.2.2 Physical properties 3

1.2.3 Industrial applications 6

1.3 Surfactant phase behaviour 6

1.3.1 General structure of surfactants 6

1.3.2 Adsorption at surfaces and aggregation in bulk 8

1.3.3 Microemulsion phase behaviour 13

1.3.4 Emulsion type and stability 19

1.4 Mixing of oil and surfactant at air-water interfaces 25

1.4.1 Spreading behaviour and spreading coefficients 26

1.4.2 Adsorption isotherm studies 28

1.4.3 Neutron reflection studies 30

1.5 Relevant literature review 32

1.6 Presentation of thesis 36

Chapter 2 Experimental 38

2.1 Materials 38

2.1.1 Water 38

2.1.2 Silicone oil 38

2.1.3 Surfactants 39

2.1.4 Other chemicals 40

2.2 Preparation of glassware 40

2.3 Experimental methods 41

2.3.1 Equilibrium phase behaviour of oil+water+surfactant mixtures 41

2.3.2 Turbidity titration 41

2.3.3 Emulsion preparation and stability 42

2.3.4 Spreading behaviour of oils on surfactant solutions 43

2.4 Measurement of surface and interfacial tensions 43

2.4.1 du Noüy ring method 44

2.4.2 Drop-volume technique 47

2.4.3 Spinning drop method 48

2.4.4 Vapour adsorption apparatus 52

2.5 Analytical determinations 54

2.5.1 Determination of ionic surfactant 54

2.5.2 Karl Fischer titration of water 56

2.6 Additional experimental techniques 57

2.6.1 Conductivity 57

2.6.2 Density 57

2.6.3 Refractive index 57

2.6.4 Viscosity measurements 58

2.6.5 Image analysis of emulsions 58

2.7 Laser diffraction for sizing emulsions 59

2.8 Neutron reflectivity 60

Chapter 3 Emulsion Phase Inversion in Nonionic Surfactant Systems **62**

3.1 Introduction 62

3.2 C_nE_m surfactant systems 64

3.2.1 Conductivity of PDMS oils and aqueous salt 64

3.2.2 Effect of surfactant concentration on the PIT 64

3.2.3 Variation of the PIT with surfactant structure 65

3.2.4 Effect of electrolyte concentration on emulsion phase inversion 68

3.2.5 Effect of oil molecular weight on emulsion phase inversion 69

3.3 Emulsion phase inversion in other surfactant systems 70

3.3.1 Extended surfactant 70

3.3.2 Silicone surfactant (Silwet L-77) 71

3.4 Conclusions 72

Chapter 4 Equilibrium Phase Behaviour in Nonionic Surfactants/PDMS/Water Systems **74**

4.1 Introduction 74

4.2 Systems containing $C_{12}E_3$ 75

4.2.1 Temperature dependence of the Winsor phase transition 75

4.2.2 Effect of surfactant concentration 77

4.2.3 Effect of electrolyte concentration 78

4.3 Systems containing other surfactants 82

4.3.1 $C_{16}P_8E_1$ systems 82

4.3.2 L-77 systems 83

4.3.3 Sugar surfactant systems 85

4.4 Oil-in-water single phase microemulsion formation with PDMS 85

4.4.1 Dependence of cloud point of $C_{12}E_5$ on PDMS uptake 86

4.4.2 Dependence of cloud point of L-77 on oil uptake 87

4.4.3 Microemulsion formation in modified PDMS oil systems 90

4.5 Conclusions 91

Chapter 5 Mixing of Silicone Oil and Nonionic Surfactants at Air-Water Interfaces **93**

5.1 Introduction 93

5.2 Observation of the spreading behaviour 97

5.3 Spreading coefficients of PDMS on C_nE_m monolayers 98

5.3.1 Air-oil tensions 99

5.3.2 Air-water tensions of surfactant solutions with and without PDMS oil 99

5.3.3 Equilibrium oil-water tensions 103

5.3.4 Spreading coefficients of 50 cS PDMS oil for C_nE_m surfactants 104

5.3.5 Effect of PDMS oil molecular weight for $C_{12}E_5$ above the cmc 105

5.4 PDMS oil adsorption isotherm on aqueous solutions above the cmc 106

5.5 Adsorption of PDMS into surfactant monolayers below the cmc 108
5.5.1 $C_{12}E_5$ systems 109
5.5.2 L-77 systems 110
5.6 Spreading behaviour of PDMS oil studied by neutron reflection 112
5.6.1 Introduction 112
5.6.2 Basic terms used in neutron reflection 114
5.6.3 Neutron reflection experimental procedure and data analysis models 115
5.6.4 Results and discussion 117
5.7 Conclusions 118

Chapter 6 Equilibrium Phase Behaviour in Ionic Surfactant Systems 120
6.1 Introduction 120
6.2 Equilibrium multiphase systems 122
6.2.1 Effect of electrolyte in 0.65 cS PDMS oil systems 122
6.2.2 Nature of Winsor III and Winsor II phases 126
6.2.3 Effect of temperature on the Winsor phase behaviour in 0.65 cS oil 129
6.2.4 Effect of oil molecular weight on multiphase behaviour 130
6.2.5 Correlation between phase behaviour and oil-water tensions 132
6.3 Water-in-oil microemulsion single phase systems 134

6.3.1 Theory 134

6.3.2 Effect of electrolyte concentration in the dispersed aqueous phase 135

6.3.3 Effect of temperature 137

6.4 Oil-in-water microemulsion single phase systems 138

6.4.1 Effect of electrolyte concentration 138

6.4.2 Effect of temperature 140

6.5 Conclusions 141

Chapter 7 Stability of Emulsions Prepared from Equilibrium Winsor Systems **144**

7.1 Introduction 144

7.2 Correlation between Winsor phase behaviour, emulsion type and o-w interfacial tensions 146

7.3 Effects of salt concentration of the stability of emulsions 147

7.3.1 Stability of o/w emulsions in Winsor I systems 148

7.3.2 Stability of w/o emulsions in Winsor II systems 152

7.3.3 Stability of emulsions in Winsor III systems 153

7.4 Emulsion inversion and stability for different PDMS oil 155

7.4.1 Phase inversion 155

7.4.2 Drop size and stability 156

7.5 Conclusions 157

Chapter 8 Mixing of 0.65 cS PDMS Oil with AOT at Air-Water Surface **159**

8.1 Introduction 159

8.2 Observation of the spreading behaviour of silicone oils on AOT aqueous surfaces 160

8.3 Effect of electrolyte concentration on the spreading coefficients 161

8.4 Effect of electrolyte concentration on 0.65 cS oil adsorption 162

8.4.1 Oil adsorption isotherms 162

8.4.2 Correlation between tension lowering and oil-water tension 164

8.5 Correlation between the minimum in the tension lowering and surfactant aggregate structure in bulk 168

8.5.1 Aggregation of AOT in electrolyte solutions 168

8.5.2 Effect of surfactant concentration on $\Delta\gamma$ 171

8.5.3 Effect of equilibrium on the minimum in $\Delta\gamma$ 172

8.6 Conclusions 173

Chapter 9 Overall Conclusions and Summary **174**

References **179**

Appendices **188**

CHAPTER ONE

CHAPTER 1

Introduction

1.1 Introduction and industrial relevance

This thesis is concerned with the interaction of polydimethylsiloxane (PDMS) oils with surfactants with respect to emulsion behaviour, equilibrium phase studies and the mixing of oil with surfactant at air-water interfaces. This is of fundamental importance in attempting to gain a detailed understanding of adsorption, aggregation and phase behaviour in ternary mixtures of surfactant, PDMS oils and water. Systems involving PDMS oils, water and surfactant have widespread application in products including antifoam agents, paints, cosmetics and drug delivery formulations. In comparison to hydrocarbon oils such as alkanes, there currently exist few publications related to the interactions between silicone oil and surfactant at the molecular level.

The work described in this thesis was initiated by the fact that there is a good understanding of the behaviour of alkane/water/surfactant systems, but no systematic study of the behaviour of PDMS oils and surfactant. Hence, a number of the experiments and methodologies described in this thesis are limited to allow comparison with simple hydrocarbon oils.

In this first chapter, a brief review of the current understanding about PDMS oils and some relevant aspects of surfactant behaviour at interfaces and in solution are presented together with a literature review related to the present study of silicone oils.

1.2 Nature of silicone oil

1.2.1 Introduction to silicone oils

The silicone oils used throughout are based on the polymer polydimethylsiloxane (PDMS) which has the following general structure (MD_nM):

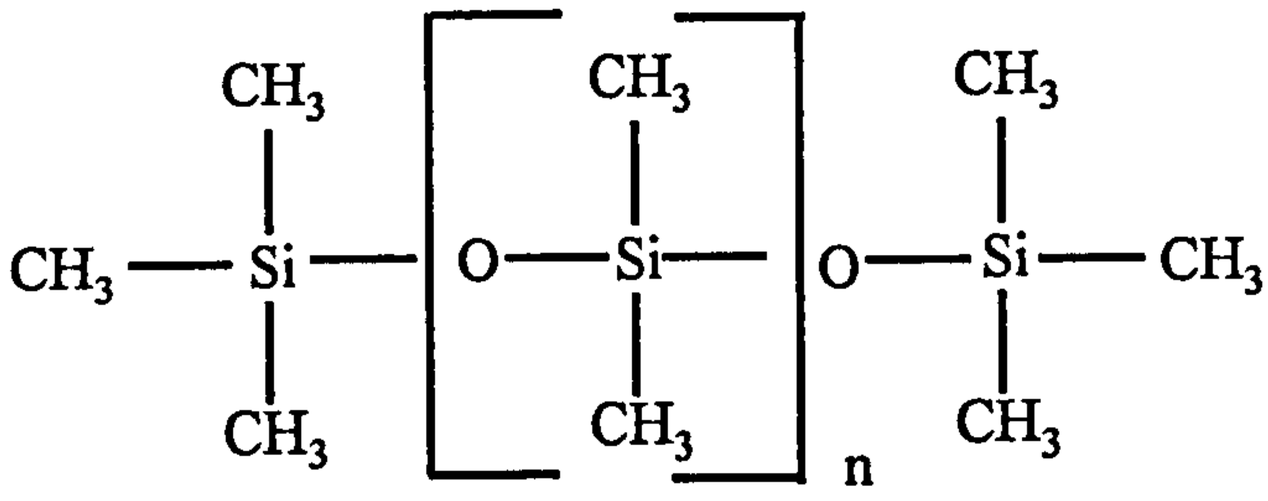

where, M = $(CH_3)_3Si$, D = $(CH_3)_2SiO$, and n varies between 0 and at least 2000. The viscosity of PDMS varies with the molecular weight, from 0.65 to 100,000 centistokes (cS) at 25°C.[1] The structure shows that PDMS oil has low surface energy pendant groups, the methyl groups, which are arranged along the siloxane chain. This siloxane chain is the most flexible backbone due to several characteristics.[2] Firstly, the Si-O skeletal bond has a length (1.64 Å) which is significantly longer than that of the C-C bond (1.53 Å) central to all of organic chemistry. As a result, steric interference or intramolecular congestion is diminished.[3] Secondly, the oxygen skeletal atoms are not only unencumbered by side groups, they are as small as an atom can be and still have the multivalency needed to continue a chain structure. Finally, the Si-O-Si bond angle of ~ 143° is much more open than the usual tetrahedral bond angle of ~ 110°. These three structural features have the effect of increasing the flexibility of the chain, which is the ability of

a chain to be compact when in the form of a random coil. They also account for the many physical properties and applications of PDMS oils.

1.2.2 Physical Properties

PDMS oils have some interesting physicochemical properties resulting from their unique flexible structure. Table 1.1 lists several common physical constants[1] of PDMS oils as a function of average molecular weight $\overline{M}_w$ determined by viscosity measurements.

Table 1.1 Some physical constants of PDMS at 25°C. n is the average number of dimethylsiloxane groups in PDMS, ρ is the density, $n_{25}{}^{\circ}_{C}$ is the refractive index, ε is the dielectric constant, and γ is the surface tension.

n	Viscosity (cS)	$\overline{M}_w$ (g mol^{-1})	ρ (g cm^{-3})	$n_{25}{}^{\circ}_{C}$	ε	γ (mN m^{-1})
0	0.65	162	0.761	1.3750	2.20	15.9
1	1	237	0.818	1.3825	2.30	17.4
8	5	770	0.918	1.3970	2.60	19.7
15	10	1,250	0.935	1.3990	2.68	20.1
25	20	2,000	0.950	1.4000	2.72	20.6
36	50	3,780	0.960	1.4015	2.75	20.8
76	100	5,970	0.966	1.4025	2.75	20.9
241	500	17,250	0.971	1.4033	2.75	21.1
339	1000	28,000	0.971	1.4034	2.75	21.2

It is worth pointing out that the solubility of PDMS oils in water is less than 0.2%. They have the general solubility behaviour of nonpolar liquids, but to

a certain extent the solubility varies with viscosity grade. Those with a viscosity at 25°C of 10 cS or less are often completely soluble in solvents (e.g. toluene) with which the higher members of the series are only partially miscible. The presence of water in the organic solvent greatly reduces the solubility of PDMS oils.[1]

From the physical constants in Table 1.1, it can be seen that the densities of the PDMS oils range from 0.76 to 0.97 g cm^{-3}, whereas the refractive index changes from 1.375 to 1.403 at 25°C. Both increase sharply with molecular weight in the lower molecular weight ranges, but vary only slightly with increasing molecular weight in polymers above twenty units due to the smaller influence of the trimethylsiloxy end groups. Viscosity relationships, on the other hand, show an effect of nearly the opposite nature where small increases in molecular weight cause progressively greater increases.[1] Figure 1.1 demonstrates the dependence of viscosity on temperature of the 50 cS PDMS oil. In comparison, petroleum hydraulic oil is also shown. It can be seen that the dependence of viscosity on temperature for PDMS oil is not as pronounced as that of petroleum hydraulic oil. Since viscosity is a manifestation of the physical interaction between molecules, the unique shallow slope of the viscosity-temperature curve is due in part to the low intermolecular forces existing between PDMS molecules.

Table 1.1 also shows the surface tensions of PDMS oils, ranging from 16 to 21 mN m^{-1} at room temperature, depending on molecular weight. These values are lower than the surface tensions of most other polymer

systems, which is probable the most familiar surface characteristic of PDMS oils. Only aliphatic fluorocarbon species have lower surface tension.[4,5] This is more evidence for the low intermolecular forces between the methyl groups in PDMS oils.

However, the most astonishing feature of PDMS oils is its maintenance of liquid nature to unusually high molecular weights.[1] The glass transition temperature (below which the polymer becomes glassy) of PDMS oils is about –125°C, the lowest recorded for any polymer.[2] This again reflects the low intermolecular forces and high chain flexibility within this polymer.

The boiling point is a very important physical constant for materials. However, it is not shown in Table 1.1 due to the unavailability of the literature data for PDMS oils. Hunter *et al.*[6] compared the boiling points of low molecular weight PDMS oils, cyclic siloxane polymers with those of normal alkanes, branched alkanes and the corresponding tetraalkylsilanes. The results are redrawn in Figure 1.2. They found that in both alkanes and PDMS oils the boiling points depend proportionally on the molecular weight not the geometric structure, either linear or cyclic, of the molecules. The boiling point/molecular weight curves have similar slopes in both the normal and branched alkane series. Likewise, the introduction of a silicone atom into a branched alkane alters the boiling point dependence only slightly. The siloxane systems which contain silicon-oxygen structures, however, have a very different dependence of the boiling point on molecular weight. It

Figure 1.1

Comparison of the viscosity of a PDMS oil with a hydrocarbon redrawn from ref.1

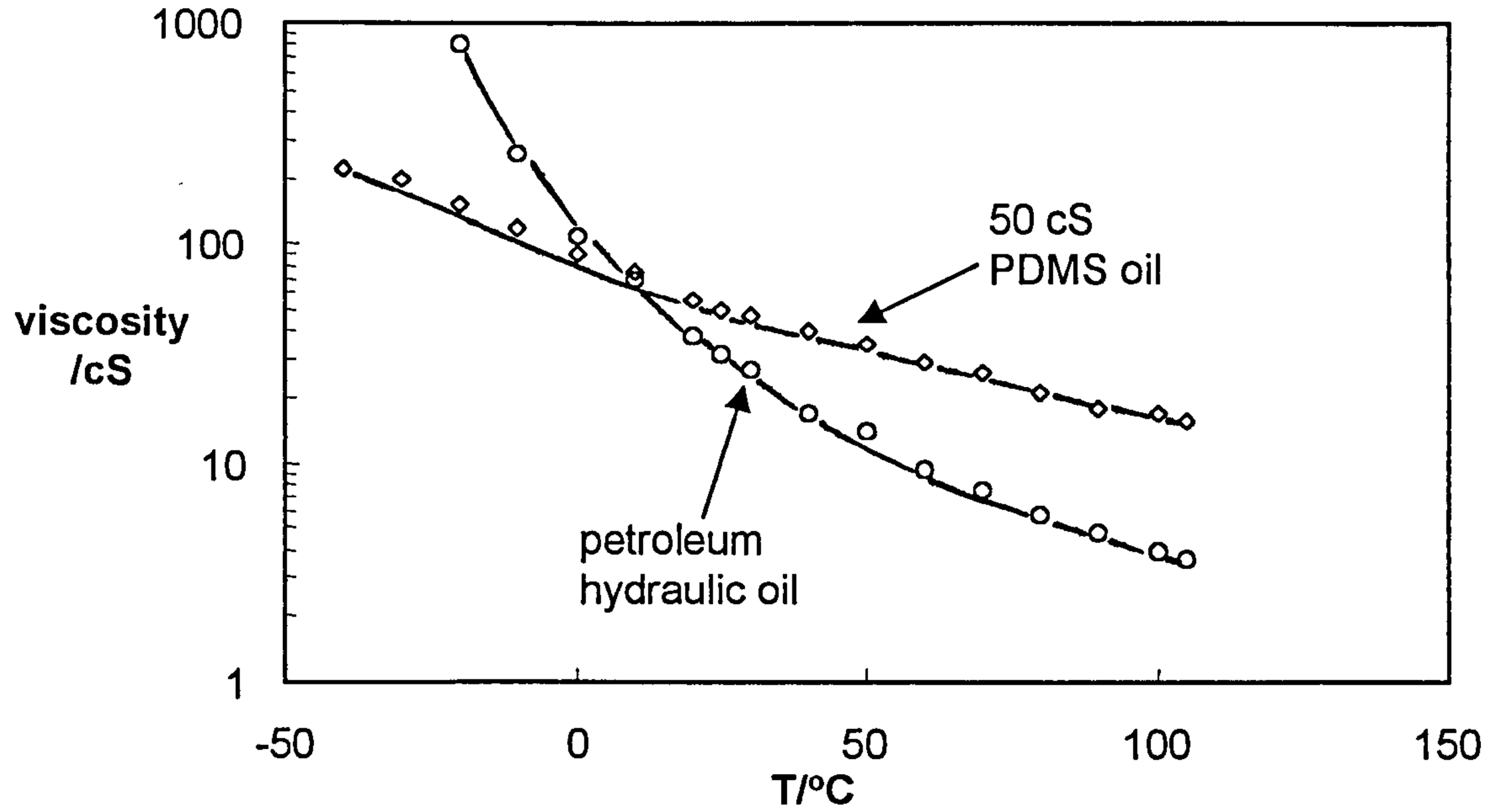

Figure 1.2

Comparison of the boiling points (bp)of PDMS oils with hydrocarbons having comparable molecular weights, redrawn from ref.6

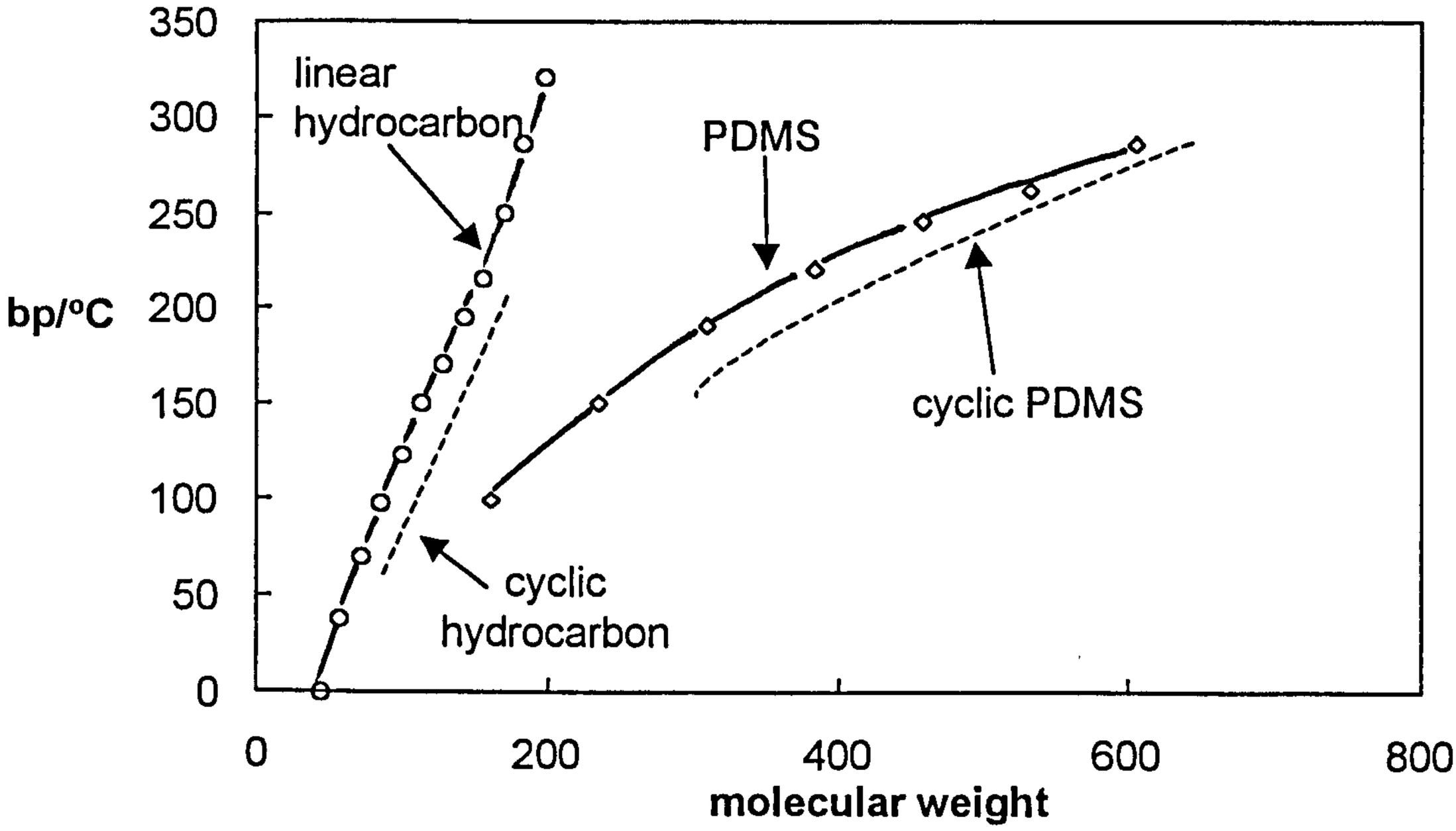

is claimed that the presence of the siloxane structure is responsible for these remarkable differences.

1.2.3 Industrial applications

The main consequence of the low surface tension of PDMS oils resulting from London dispersion force interaction of methyl groups is that this polymer spreads not only over any high surface energy substrate as shown by Zisman and co-workers[7] for materials such as metals, silica and water, but also on some organic liquids e.g. hexadecane. This is exploited in numerous applications, notably in release materials, foam control agents, lubricants and mechanical fluids in a number of products like cosmetics and polishes. In the electrical/electronics industry, PDMS oils are important because they possess the stability and good electric properties associated with glass, quartz and the mineral silicates to which they are chemically related.

1.3 Surfactant phase behaviour

1.3.1 General structure of surfactants

The word surfactant comes from the phrase SURFace ACTive AgeNT. Not only does this show the origin of the word itself, it also sheds some light on the properties of surfactants i.e. they tend to accumulate at surfaces. Surfactants are amphiphilic molecules, which means they consist of two distinct and diverse regions. The molecule can be divided into polar and non-polar parts. The non-polar region, which is hydrophobic, is typically

a straight or branched hydrocarbon or fluorocarbon chain. The headgroup is polar and hydrophilic in nature and can be anionic, cationic, nonionic or zwitterionic.[8] The classification of surfactants is due to the nature of the headgroup.

(a) Ionic surfactants – Depending on the charge of the headgroup, ionic surfactants can be classified as anionic, cationic or zwitterionic. Anionic surfactants have negatively charged headgroups and include sulphates, sulphonates and the traditional soaps containing $-CO_2^-$. They are mainly used in cleaning formulations. Cationic surfactants have positively charged headgroups, *e.g.* quaternary ammonium and alkyl pyridinium compounds. These surfactants are generally used in fabric and hair conditioners given that the positive charge on the headgroup has an attraction for negatively charged fibres such as hair and cotton. The zwitterionic surfactants, having both a positively and negatively charged group present, include betaines and sulphobetaines ($-N^+(CH_3)_2CH_2SO_3^-$). These surfactants are used in the formulation of baby shampoos and toiletries because they generally have a milder effect on the skin relative to the anionic surfactants.

(b) Nonionic surfactants – The headgroups mostly contain a polyoxyethylene group of general structure ($-(OCH_2CH_2)_mOH$) or a sugar ring. These surfactants are used in detergency and as emulsifiers especially at low temperatures. The straight alkyl chain polyoxyethylene surfactants, of general structure $C_nH_{2n+1}(OCH_2CH_2)_mOH$ (abbreviated to C_nE_m), have the

advantage that the balance of hydrophobic/hydrophilic properties can be easily optimised for a particular application through variation of n and m.

For most solutes in water, increasing the temperature usually produces a gradual increase in solubility. For surfactants, however, there is a temperature at which the solubility suddenly increases very dramatically. This is known as the Krafft temperature or Krafft point T_k.[8] For a given nonionic aqueous surfactant solution, an increase in temperature will cause the solution to become cloudy at a well-defined temperature. This is often referred to as the 'cloud point'. This value will depend on the concentration of surfactant amongst other things.

1.3.2 Adsorption at surfaces and aggregation in bulk

As mentioned above, surfactant molecules are amphiphiles which consist of a hydrophobic group and a hydrophilic group. The insolubility of the hydrophobic group in water causes the molecule to concentrate at the air-water interface, with its hydrocarbon chain oriented toward the vapour phase. Since the surface tension (γ) of water is higher than that of hydrocarbons, adding surfactant results in a decrease in surface tension.

As the surfactant concentration in the bulk is increased, the amount of surfactant adsorbed at the interface increases and the surface tension decreases. The surface tension becomes virtually constant when no more surfactant can be accommodated at the surface. This occurs at a concentration of surfactant known as the critical micelle concentration (cmc) at which the surfactant forms normal micelles in water. Figure 1.3 is a

schematic illustration of a typical surface tension versus ln(surfactant concentration) plot.

The relationship between the amount of surfactant adsorbed and the surface tension lowering is given by the Gibbs adsorption equation, a thermodynamic expression which relates the surface concentration (or excess) of a species to both the tension and the bulk activity of the adsorbate. The general form of this equation (for constant temperature and pressure) can be written as[9]

$$-d\gamma = \sum_i \Gamma_i d\mu_i \qquad (1.1)$$

where Γ_i is the total or excess surface concentration of species i, μ_i is the chemical potential of species i and $\sum_i$ denotes the summation over all the species i. μ_i is related to the molar concentration c_i in the bulk phases by:

$$\mu_i = \mu_i^\circ + RTlnf_ic_i \qquad (1.2)$$

where f_i is the activity coefficient of species i in the same phase and μ_i° is the standard chemical potential of i in that phase (pure liquid status). When the surfactant concentration is below the cmc, the solution can be treated as ideal and f_i equals 1. Hence, for an ionic surfactant like SDS (sodium dodecyl sulphate), the surfactant chemical potential is

$$\mu_2 = \mu_2^\circ + RT \ln c_{DS^-} + RT \ln c_{Na^+} \qquad (1.3)$$

In the absence of electrolyte, the electroneutrality requires that $c_{DS^-} = c_{Na^+}$ and equation 1.1 becomes:

$$\Gamma_{surf} = -\frac{1}{2RT}\frac{d\gamma}{d\ln c} \qquad (1.4)$$

where the factor 2 indicates adsorption of both surfactant ion and counterion. For ionic surfactants in the presence of swamping electrolyte (i.e. sufficient salt to make electrostatic effects unimportant), and for nonionic surfactants, we have

$$\Gamma_{surf} = -\frac{1}{RT}\frac{d\gamma}{d\ln c} \qquad (1.5)$$

Therefore, below the cmc the slope in Figure 1.3 may be used to calculate the surface excess concentration of surfactant Γ_{surf} using equations 1.4 or 1.5.

As more and more surfactant is added to water, the surface tension becomes almost constant above the cmc, which means that the surface eventually becomes saturated with surfactant. What happens upon further addition of surfactant is a compromise between the extremes of complete phase separation and a molecularly disperse solution. The surfactant molecules self-assemble to create a microphase in which the hydrocarbon chains sequester themselves inside the aggregate and the polar groups orient themselves toward the aqueous phase. In the micellar aggregates, the surfactant again arranges itself in such a way that the contact of surfactant tails with water is minimised.[10]

The occurrence of a cmc is the result of two competing factors. Transfer of the hydrocarbon chain out of water and into the oil-like interior of the micelle drives micellization. Repulsion between headgroups as they come close together opposes it. Under these conditions the growth process has specific limits, and aggregates cease to grow when they have reached a certain size. Above the cmc, adding more surfactant simply produces more

micelles over a considerable concentration range rather than further growth of existing micelles.[11]

When air is replaced by an oil phase in Figure 1.3, the surfactant molecules can adsorb at the interface and reduce the interfacial tension between oil and water. The Gibbs equation is still valid. The difference arises when the concentration of surfactant is above the break point. This means that the surfactant can also form aggregates in the oil phase. The aggregates are known as *reverse micelles* where the surfactant tails point towards oil and the headgroups aggregate as a hydrophilic core. Because of the static electric repulsion between the headgroups, the reverse micelles are normally much smaller than the normal micelles. The overall surfactant concentration at this point is sometimes referred to as the *critical aggregation concentration (cac)* to distinguish aggregate formation in both water and oil phases from that only in water (cmc).

The structure of the aggregates is dependent on the geometry of the surfactant molecules. The surfactant packing parameter (P) defined as[12]

$$P = \frac{v}{lA_h} \tag{1.6}$$

where l is the molecular length of the hydrocarbon chain, A_h is the optimal surface area of the surfactant headgroup, and v is the hydrocarbon chain volume. According to Tanford,[11] for a saturated linear hydrocarbon chain with n carbon atoms,

$$l\ (nm) = (0.15 + 0.127n) \tag{1.7}$$

and

$$v\ (nm^3) = (27.4 + 26.9n) \times 10^{-3} \qquad (1.8)$$

The 0.15 nm in equation (1.7) comes from the van der Waals radius of the terminal methyl group (0.21 nm) minus half the bond length of the first atom not contained in the hydrocarbon core (0.06 nm). The factor 0.127 is the carbon-carbon bond length (0.154 nm) projected onto the direction of the chain in the all-trans configuration.

The surfactant packing parameter relates the properties of the molecule to the preferred curvature properties of the aggregates. Small values of P imply highly curved aggregates, but when P is close to unity, planar bilayers usually form. For spheres, cylinders and bilayers, a simple relation exists between volume, area, and radius (thickness), and a comparison of the P values shows that optimal stability of the different aggregates occurs as follows:

spherical micelles	$P < 1/3$
infinite cylinders	$1/3 < P < 1/2$
vesicles or bilayers	$1/2 < P < 1$
inverted micelles, cylinders and vesicles	$P > 1$

Obviously, the surfactant packing parameter can represent only an approximate model of the nature of surfactant self-assembly. In spite of this, the theory provides valuable insight into the way that changes in solution conditions and molecular structure affect aggregate size and shape.

1.3.3 Microemulsion phase behaviour

The surfactant aggregates in both oil and water phases have the ability to dissolve substances which are general insoluble in these phases, and become swollen. This phenomenon is called solubilisation. For example, oil can be solubilised into the aqueous surfactant aggregates. When sufficient oil or water solubilisation occurs such that the dispersed material forms separate liquid cores within the aggregates, the resultant dispersions are known as *microemulsions*. Microemulsions may be defined as thermodynamically stable dispersions of oil-in-water (o/w) or water-in-oil (w/o) stabilised by surfactant. They contain aggregates in the size range 5-100 nm, are isotropic and general scatter light only weakly. Figure 1.4 represents the typical spherical droplet structures in microemulsions.

For spherical, monodisperse microemulsion droplets, geometrical considerations give the following relationship between the droplet radius of the core (r_c) and the composition,

$$r_c = \frac{3V_{dc}}{A_s}\left\{\frac{[\text{dispersed component}]}{[\text{surfactant}]-\text{cmc}}\right\} \qquad (1.9)$$

where A_s is the area per surfactant at the surface of the droplet and V_{dc} is the molecular volume of the dispersed component. This simple model predicts that the droplet radius is proportional to the ratio of the molar concentration of the dispersed oil or water to that of the surfactant (term in curly brackets), i.e. to the extent of solubilisation of the dispersed component by the surfactant.

Figure 1.3

Schematic illustration of the surface tension of aqueous surfactant solution versus surfactant concentration

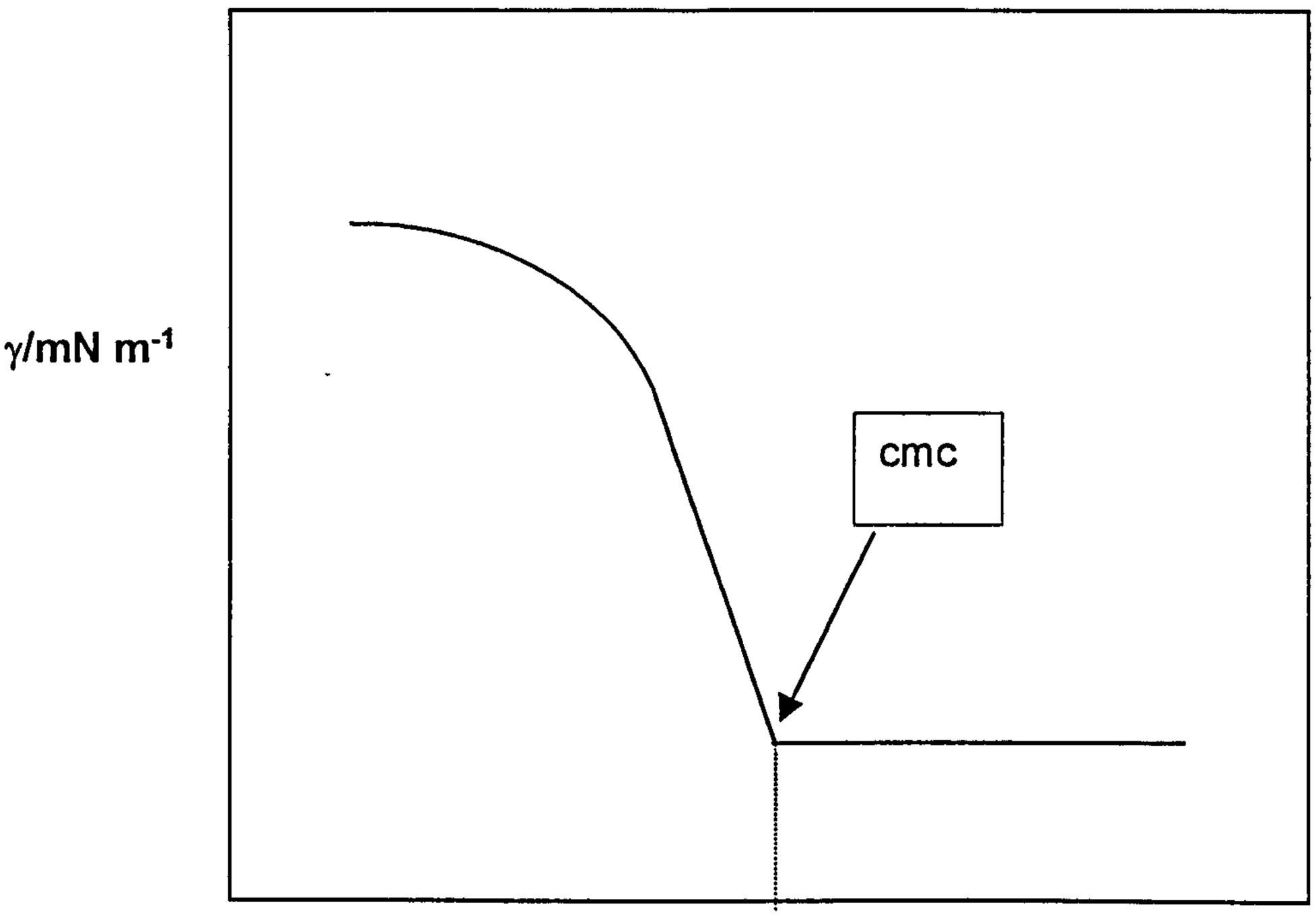

Figure 1.4

Schematic representation of microemulsion droplets

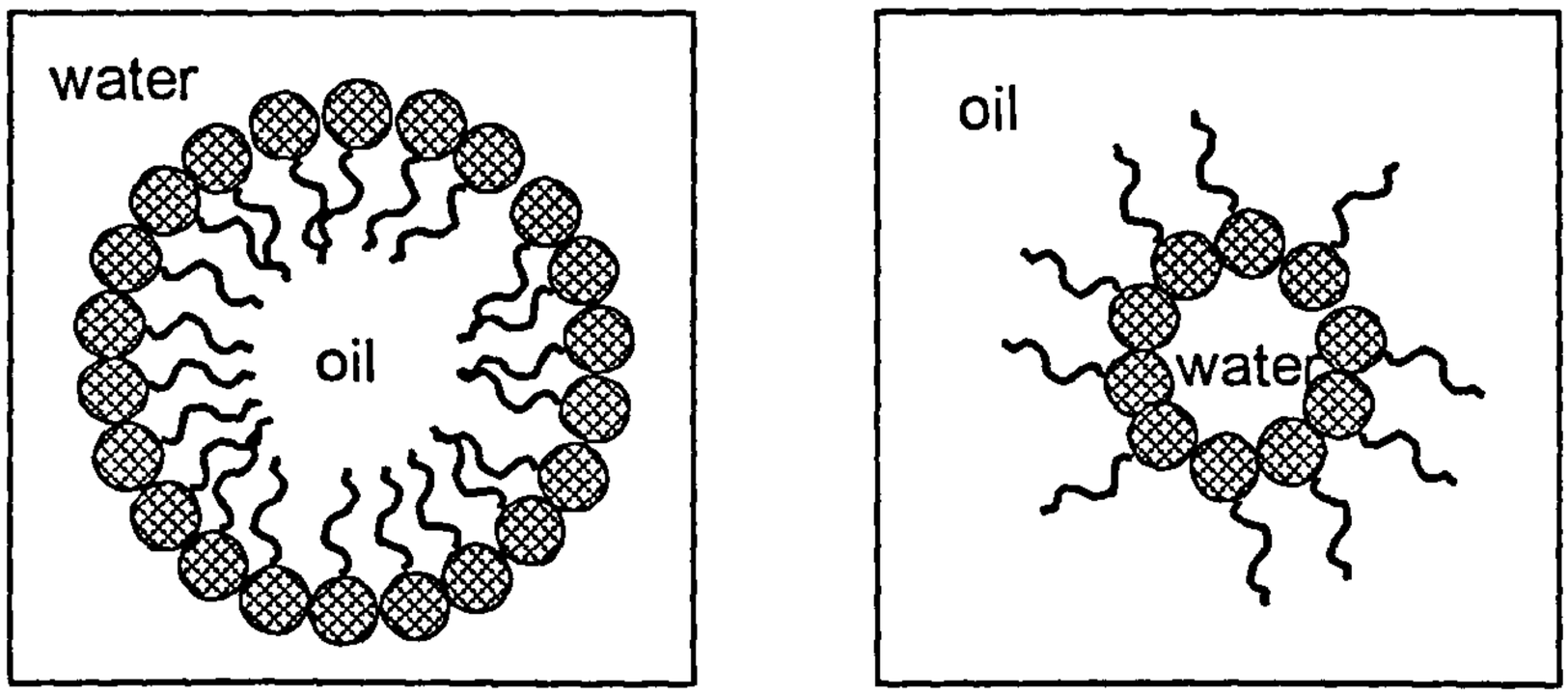

o/w **w/o**

The free energy of formation ΔG of a liquid-in-liquid dispersion can be expressed as

$$\Delta G = \gamma_{ow} \Delta A - T\Delta S \qquad (1.10)$$

where γ_{ow} is the oil-water tension, ΔA is the increase in oil-water surface area and ΔS is the entropy change arising from dispersion of the droplets.

Thermodynamically stable microemulsions form when the oil-water tension is ultralow (less than approximately 0.1 mN m^{-1}) such that the favourable entropy term outweighs the unfavourable tension term. For highly curved oil-water monolayers with ultralow tensions such as those coating microemulsion droplets, the effect of monolayer curvature on the tension becomes significant. Microemulsion stability is thus dominated by the tendency of oil-water surfactant monolayers to curve. Qualitatively, a low tendency to curve together with an ultralow tension favours large microemulsion droplets and hence large solubilisation of the dispersed component.

The tendency of a surfactant monolayer to curve is related to the surfactant packing parameter P. If the surfactant chain area A_t = v/l, equation 1.6 can be written as

$$P = \frac{A_t}{A_h} \qquad (1.11)$$

Thus, when $P<1$, $A_h>A_t$ and the preferred curvature is such that the headgroups form the exterior surface of the aggregate and o/w microemulsion droplets are favoured. When $P>1$, w/o microemulsions are favoured. Solubilisation is maximised when A_h is approximately equal to A_t.

The areas A_h and A_t are not only determined by the molecular structure of the surfactant, but also are modified by factors such as penetration of the surfactant layer by water or oil, temperature and the addition of electrolyte which alter the interactions between adjacent surfactant head and tail groups in the monolayer. These variables are sometimes called HLB (hydrophile-lipophile balance) variables which induce a wealth of phase behaviour. For example, consider an ionic surfactant with oil and water which forms an o/w microemulsion phase in equilibrium with excess oil. Addition of electrolyte to the aqueous phase screens the electrostatic repulsion between adjacent headgroups in the monolayer causing A_h to decrease. If A_h decreases such that it is smaller than A_t, the system undergoes phase inversion of the microemulsion to give a w/o microemulsion phase in equilibrium with excess water. In this way, the preferred monolayer curvature can be 'tuned' to optimise solubilisation for a particular application.

In systems that contain equal volumes of oil and aqueous phases, the general phase behaviour of a microemulsion tuned by one HLB variable is shown schematically in Figure 1.5. The most commonly used classification for phase diagrams in oil/water/surfactant mixtures is that due to Winsor[13] who first described three types of system. Firstly, the system in which excess oil and o/w microemulsion coexist is called Winsor I; no surfactant aggregates exist in the oil phase in this region. For ionic surfactants, no surfactant monomers exist in the oil phase either. For nonionic surfactants, however, the monomer concentration of surfactant in

Figure 1.5

Sequence of phases produced by inversion from an o/w microemulsion to a w/o microemulsion and the corresponding oil-water interfacial tension as a function of the system HLB variable. Shaded areas indicate the location of surfactant aggregates.

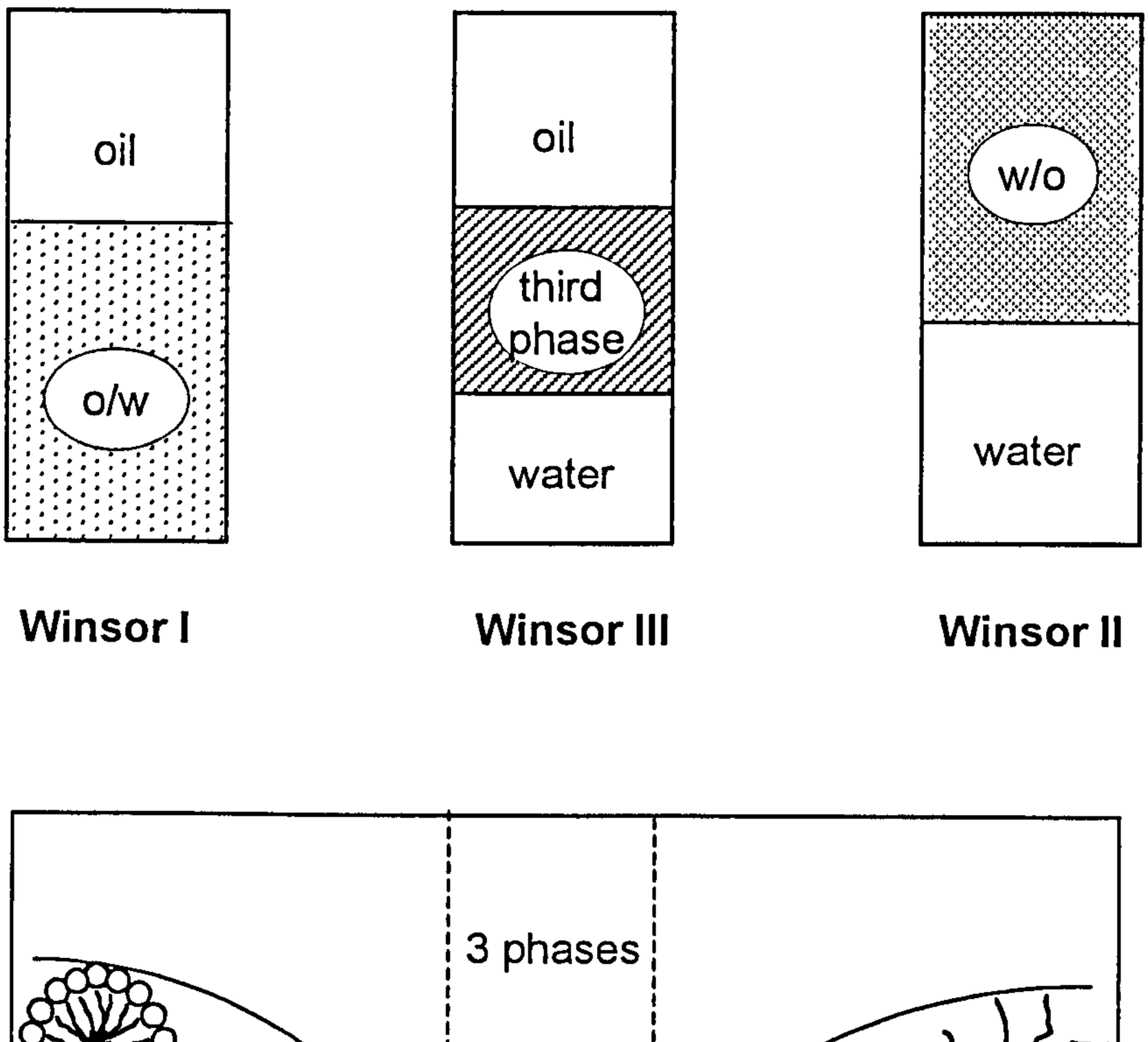

oil can be high. Secondly, excess water and w/o microemulsion coexist in Winsor II systems. No surfactant aggregates are present in the aqueous phase, merely a small concentration of monomer (at the cmc) with which the microemulsion is in equilibrium. In progressing from Winsor I to Winsor II, there exists a three phase region, consisting of oil, water and a third phase. The third phase can contain oil, water and the majority of the surfactant, which is referred to as a third-phase bicontinuous microemulsion. No surfactant aggregates now exist in either the aqueous or the oil phase. This three phase region is classified as Winsor III. It is worth pointing out that if the HLB variable in the system is electrolyte such as sodium chloride concentration, the Winsor phase transition progress is the same for both nonionic and ionic surfactants. (i.e. Winsor I to Winsor II via Winsor III as the increase in electrolyte concentration). However, if the HLB variable is temperature, the Winsor phase progress in ionic surfactant systems is opposite to that of nonionic surfactant systems, which means for ionic surfactants, the phase inverts from Winsor II to Winsor I via Winsor III with the increase in temperature.

The Winsor systems described above contain a monolayer of surfactant at the planar interface separating the bulk phases which is in equilibrium with the curved monolayer coating the microemulsion aggregates.[14,15] In these cases the oil/water ratio and consequently the nature of the microemulsion phase depend on the spontaneous curvature c_o and the elastic properties of the monolayer. Helfrich[16] obtained an expression for the bending energy per unit area of an interface as

$$E_{bend} = \frac{K}{2}\left(\frac{1}{r_1}+\frac{1}{r_2}-\frac{2}{c_o}\right)^2 + \frac{\overline{K}}{r_1 r_2} \qquad (1.12)$$

where r_1 and r_2 are the principal radii of curvature, K is the monolayer bending rigidity constant, which is twice the energy required to bend unit area of interface by a unit amount of curvature away from the spontaneous curvature.[17] $\overline{K}$ is the Gaussian curvature elastic modulus. c_o is controlled by steric interactions and electrostatic repulsion for ionic surfactants.[18] Roughly, one can say that c_o changes progressively from positive in the Winsor I system to negative in the Winsor II case. When the mean spontaneous curvature c_o vanishes Winsor III systems appear. Different types of aggregate structure in Winsor III systems occur which depend on the bending elasticity of the surfactant monolayer:[17] lamellar phases, bicontinuous microemulsions and the so-called L_3 phases. Lamellar phases are water and oil layers separated by surfactant monolayers.[19] Bicontinuous microemulsions are isotropic phases containing roughly equal amounts of oil and water. The structure is a random 'sponge–like' structure of interconnected oil and water domains.[20,21] L_3 phases are mainly composed of surfactant and water (or oil) and made up of multiconnected surfactant bilayers, eventually swollen by thin films of oil (or water), separating two equivalent domains of water (or oil).[22]

The oil-water interfacial tension γ_{ow} passes through a minimum with respect to the HLB variable. Assuming that the contribution arising from the droplet dispersion entropy can be neglected, the relationship between the

interfacial tension of the planar monolayer and the microemulsion droplet radius, r_c, is approximated by[23]

$$\gamma_{ow} = \frac{(2K + \bar{K})}{r_c^2} \tag{1.13}$$

Hence, it can be seen that the interfacial tension is inversely proportional to the square of the droplet radius. As Winsor III approaches from either side (Winsor I or Winsor II), the maximum solubilisation and hence maximum microemulsion droplet size are achieved under the conditions corresponding to zero spontaneous curvature and the interfacial tension reaches its minimum value. The minimum corresponds to the phase inversion condition within the Winsor III systems, also shown in Figure 1.5.

In comparison with multiphase Winsor systems, single phase microemulsions formed directly by the swelling of micelles are sometimes referred to as Winsor IV systems. In micellar dispersions, the aggregates are made of surfactant only. In microemulsions, the aggregates are much larger. They have large liquid cores surrounded by a surfactant monolayer that stabilises the dispersion. The limiting extent of solubilisation of the micelles is related to c_o and the bending energy. When starting with spherical micelles in water, c_o being large, one finds that the micelles cannot accommodate more than that a few molecules of oil. This frequently produces a rod-to-sphere transition upon swelling,[24] as expected from simple packing considerations. For alkanes, the extent of swelling depends on the hydrocarbon chain length; swelling is larger for shorter alkanes. This can be understood in terms of oil penetration in the surfactant layer; short

chain alkanes penetrate the layer increasing the surfactant chain area and decreasing the value of the packing parameter. Further addition of oil leads to an excess phase. This two phase equilibria corresponds to the Winsor I system as described earlier. The process leading to Winsor II systems is entirely analogous.[25]

1.3.4 Emulsion type and stability

An emulsion may be defined as a heterogeneous system of two immiscible liquid phases ('oil' and 'water') where one of the phases is dispersed in the other as drops of microscopic or colloidal size (typically around 1 μm).[26] There are two kinds of simple emulsions; oil-in-water (o/w) and water-in-oil (w/o), depending on which phase comprises the drops. Emulsions made by agitation of the pure immiscible liquids are very unstable and break rapidly to the bulk phases. Such emulsions may be stabilised by the addition of surfactant which protects the newly formed drops from re-coalescence. Emulsions are thermodynamically unstable. The final fate of an emulsion is clear- it will separate into two or more equilibrium phases. The processes causing emulsion instability include phase inversion, creaming, flocculation, coalescence and Ostwald ripening.

Whether an emulsion is o/w or w/o depends on a number of variables like oil:water ratio, electrolyte concentration, temperature *etc.* For most of this century, emulsion chemists have known that surfactants more 'soluble' in water tend to make o/w emulsions and surfactants more 'soluble' in oil tend to make w/o emulsions. This is the essence of Bancroft's rule which

states that the continuous phase of an emulsion tends to be the phase in which the emulsifier is preferentially soluble.[27] However, in a minority of emulsion systems, Bancroft's rule fails due to two reasons. Firstly, a surfactant may be more soluble in e.g. oil than in water in a binary system, but in the ternary system of oil-water-surfactant it may partition more into water, and hence give an o/w emulsion. Secondly, no distinction is made between the solubility of monomeric or aggregated surfactant in oil or water. This was discussed in detail recently by Binks.[28]

Griffin[29] introduced the concept of the hydrophile-lipophile balance (HLB) as a way of predicting emulsion type from surfactant molecular composition. Later Davis[30] suggested a simple group contribution method to evaluate the HLB of different surfactants from their molecular structure. A major problem of the HLB concept is that the HLB numbers assigned to the neat surfactant take no account of the effective HLB of a surfactant *in situ* adsorbed at an oil-water interface. The prevailing conditions such as temperature, electrolyte concentration, oil type and chain length, and co-surfactant concentration can all modify the geometry of the surfactant at an interface[31] and thus change the curvature of the surfactant monolayer, which in some way affects the preferred emulsion type.[32,33]

Shinoda and Friberg[34] defined a phase inversion temperature (PIT) for emulsions stabilised by nonionic surfactants. Below the PIT the micellar phase is water continuous and above the PIT the reverse micellar phase is oil continuous. For ionic surfactant-stabilised emulsions, the location of surfactant micelles (or reversed micelles) is opposite that above. The PIT

represents the temperature for emulsion phase inversion from an o/w emulsion to a w/o emulsion. The PIT rule works even in circumstances when Bancroft's rule and Griffin's HLB scale have failed. It is now generally acceptable that the phase containing the surfactant aggregates becomes the continuous phase of an emulsion. Bancroft's rule and the system HLB apply to surfactant aggregates rather than to total surfactant present in the system.[28]

It is frequently observed that the type of emulsion (o/w, w/o, or intermediate type) formed by homogenisation of the Winsor system is the same as that of the equilibrium microemulsion[35,36]as shown in Figure 1.6. For example, emulsification of a Winsor I system (o/w microemulsion plus excess oil) generally gives an o/w emulsion, the continuous phase of which is itself an o/w microemulsion. It is hard to believe that the correlation between the microemulsion phase behaviour and emulsion type is purely coincidental. Kabalnov and Wennerström[37] proposed a model to argue that the properties which control the equilibrium phase behaviour and emulsion stability are the surfactant monolayer bending parameters, the spontaneous curvature and bending saddle splay moduli. In particular, the value and sign of the monolayer spontaneous curvature controls the type (o/w or w/o) and stability of the emulsion formed. There have been developments in understanding how the type of emulsion is related to the type of microemulsion at equilibrium in a variety of particular systems.[38,39] It is likely that the spontaneous curvature of the surfactant monolayer plays a major role in this emulsion and microemulsion correlation.

Figure 1.6

Schematic illustration of the correspondence between the microemulsion and emulsion types (o/w or w/o)

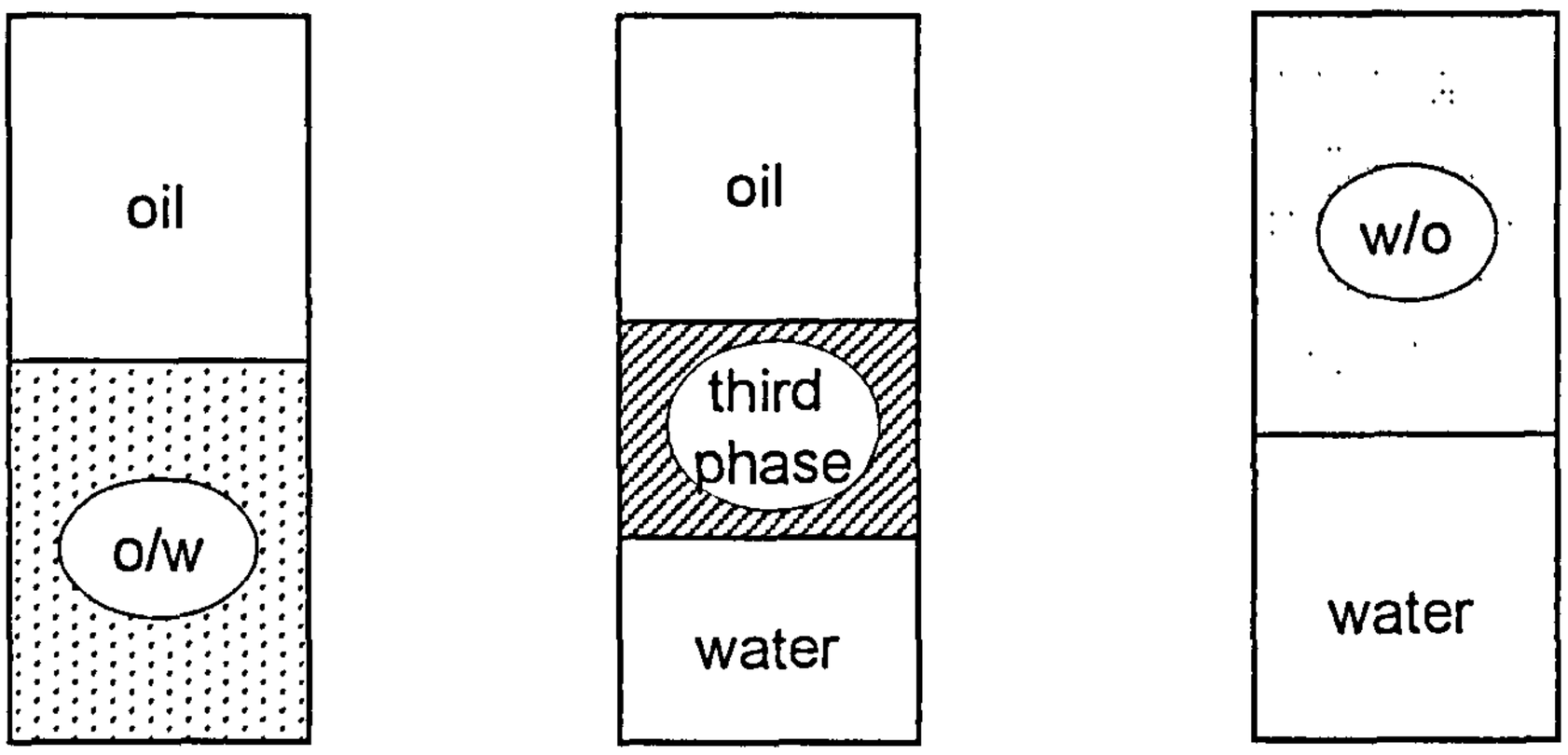

Phase inversion in emulsions can be one of two types.[34] Transitional inversion is induced by changing factors which affect the HLB of the system such as temperature and electrolyte concentration. Catastrophic inversion is induced by increasing the fraction of the dispersed phase and has the characteristics of a catastrophe, meaning a sudden change in behaviour of the system as a result of gradually changing conditions. The work carried out in this thesis has been limited to a fixed volume of continuous and dispersed phases. Therefore, only transitional inversion is considered.

Similar to the concept of PIT, if the HLB variable in transitional inversion is electrolyte concentration, the inversion concentration is often referred to the phase inversion salt concentration (PIS). Phase inversion in emulsions is accompanied by sharp changes in their physical properties. This can be used to detect the PIT and PIS by different methods such as measurements of electrical conductivity, viscosity and dielectric constant.[40]

Emulsion stability is a kinetic concept. The instability may involve a number of processes which take place simultaneously or consecutively depending on conditions. The four main ways in which an emulsion may become unstable are creaming (or sedimentation), flocculation, coalescence and Ostwald ripening.[26] Figure 1.7 is a schematic illustration of the instability processes in emulsions.

Creaming- In an o/w emulsion, creaming is the movement of oil drops under gravity or in a centrifuge to form a concentrated layer at the top of the sample, but with no accompanying change in the drop-size distribution. Initially, a concentration gradient of drops develops in the vertical direction,

Figure 1.7

Schematic illustration of different types of emulsion instability, shown for an o/w emulsion

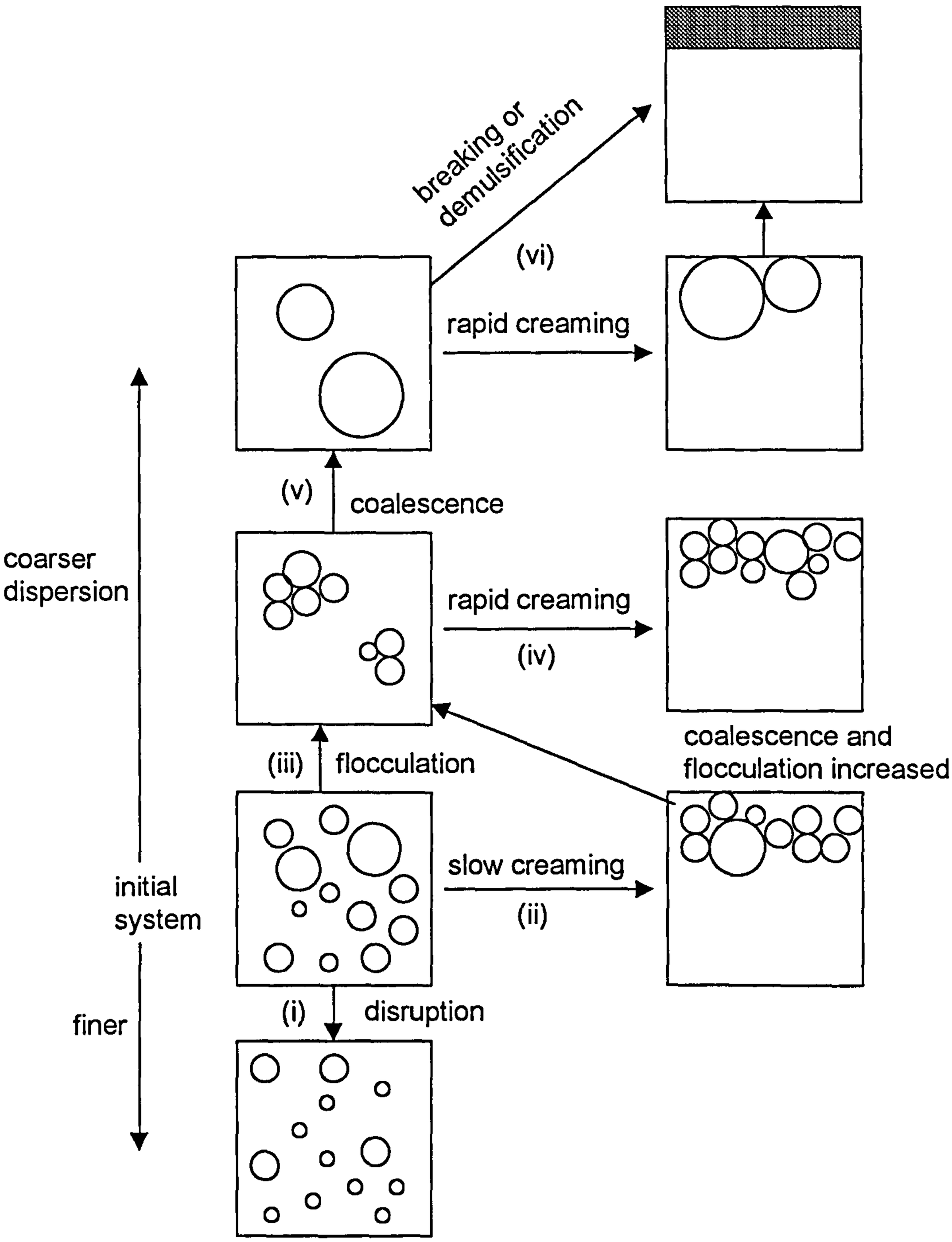

often followed by the appearance of a distinct boundary between an upper cream layer and a lower depleted emulsion layer. In a w/o emulsion, the equivalent phenomenon is called sedimentation. Creaming arises from the action of gravity on drops of lower density than that of the continuous phase and is reversible in that gentle agitation can re-establish the original uniform distribution of drops.

Flocculation- Flocculation is the process in which emulsion drops aggregate, without rupture of the stabilising layer at the interface, if the pair-interaction free energy becomes appreciably negative at a certain separation. It may be weak (reversible) or strong (not easily reversible) depending on the strength of the inter-drop forces. Flocculation usually leads to enhanced creaming because flocs rise faster than individual drops due to their larger effective radius.

Coalescence- Coalescence is the process in which two or more emulsion drops fuse together to form a single larger drop, and is irreversible. For coalescence to occur, the forces between the drop surfaces must be such that the film of continuous phase separating them can become sufficiently thin that film rupture becomes probable.

Ostwald ripening- Ostwald ripening is the growth of large droplets at the expense of smaller ones and occurs when the dispersed phase has a finite solubility in the continuous phase. The driving force is the higher internal pressure (and hence higher chemical potential) in the smaller drops due to the higher Laplace pressure.

A number of microscopic events contribute to the destabilisation of an emulsion. The basis for stability is the existence of a repulsive regime for the force between drops. The general *DLVO theory* (after Derjaguin, Landau, Verwey and Overbeek) can be used to describe the qualitative features of the droplet-droplet interaction.[41] The DLVO theory assumes that more long-ranged drop interactions mainly control colloidal stability. Two types of forces are considered; long range van der Waals attractive (V_A) forces operate irrespective of the chemical nature of the drops or the medium. Furthermore, for most emulsion drops a charge exists either from surface charge groups or by specific ion adsorption from the solution. For similar drops this charge leads to a repulsive double-layer force (V_R). The total interaction potential V is written as

$$V = V_A + V_R \qquad (1.14)$$

V_A and V_R are functions of the distance (h) between the drops. Depending on the relative strength of the attractive and repulsive terms, we can generate the interaction potential versus distance curves as shown schematically in Figure 1.8. The attractive term V_A may dominate the repulsive term V_R when h is very large or very small. At intermediate separations the double-layer force gives rise to a potential energy barrier to drop coagulation if the surface is sufficiently charged and if the electrolyte ions do not screen the charge completely. Generally the primary minimum is so deep that once drops have passed over it, aggregation becomes irreversible.

In an emulsion, if the mean distance between the drops is larger than the distance corresponding to *secondary minimum*, the system gains energy by bringing drops together and *flocculation* occurs. Once drops have been brought into proximity by flocculation and/or creaming, they can coagulate into the *primary minimum* while still keeping their identity as separate droplets. If the surfactant film surrounding the drops breaks, *coalescence* occurs. This is the final stage in the life of an emulsion drop.

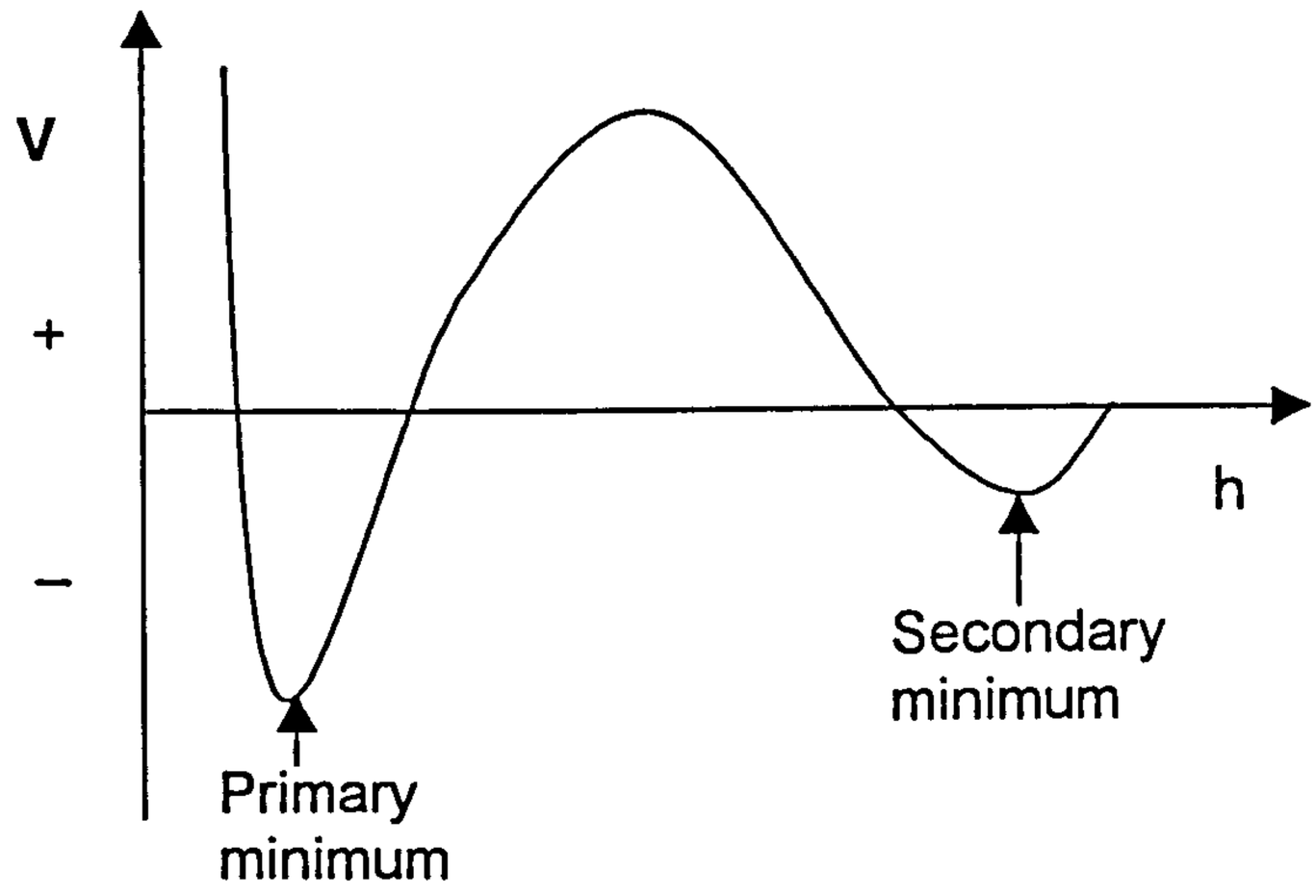

Figure 1.8 Schematic representation of the interaction potential energy versus distance curve between two drops

1.4 Mixing of oil and surfactant at air-water interfaces

In section 1.3 we mentioned that the solubilisation (penetration) of oil at the oil-water interface has a number of important consequences. Particularly interesting are the ways in which oil penetration can affect the spontaneous curvature of surfactant monolayers and hence microemulsion phase behaviour in Winsor systems. However, it is difficult to quantify

directly the solubilisation of oil in the surfactant chain region at oil-water interfaces. An alternative way to study the oil-surfactant mixing behaviour is to look at the solubilisation of oil into flat monolayers at the air-water surface, since the quantitative determination of the extent of oil mixing with surfactant molecules is possible. Presumably the solubilisation of oil into planar and curved monolayers is linked,[42,43] and this may provide some insight into the mixing of oil and surfactant at the oil-water interface. Furthermore, one of the major applications of PDMS oils in industry is as antifoam agents, related to the interactions of PDMS oils and surfactant at air-water surfaces directly. Here we describe the behaviour when small amounts of oil are added to the aqueous surfactant surface.

1.4.1 Spreading behaviour and spreading coefficients

Several situations may occur on addition of a drop to the surface of an aqueous surfactant solution. Figure 1.9 is a schematic illustration of the possible spreading behaviour of oil on aqueous surfactant solutions:

(a) The oil spreads as a macroscopic (on the molecular scale) film over the surface of the solution. These films give characteristic interference colours making them easily recognisable. For spreading oils, the measured surface tension of the solution falls from the value of the aqueous solution to the sum of the oil-water and oil-air tensions. A recent study of the adsorption of n-pentane on the surface of pure water at a temperature where the van der Waals forces across the film switch from attractive to repulsive has shown to be this case.[44]

Figure 1.9

Three possible situations following the addition of a drop of oil onto a surfactant solution at the air-water surface

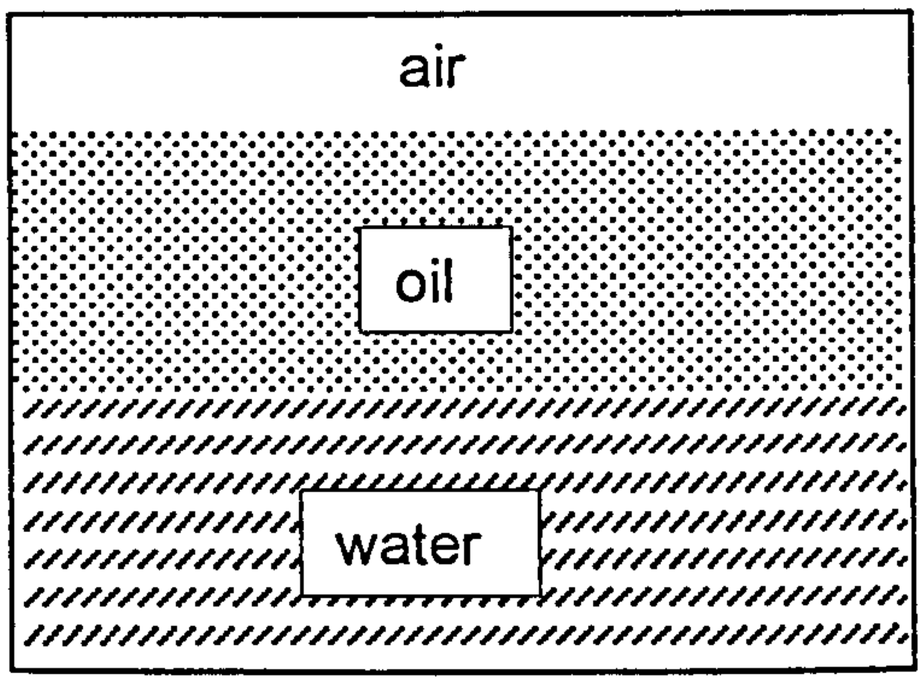

(a)

macroscopic spreading, thick oil layer on water surface

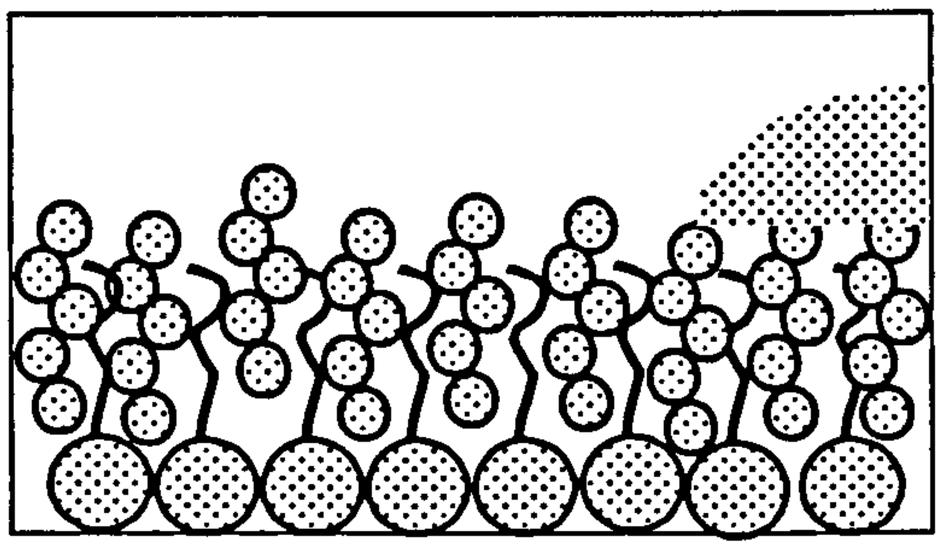

(b)

mixed monolayer formation and nonspreading oil lens

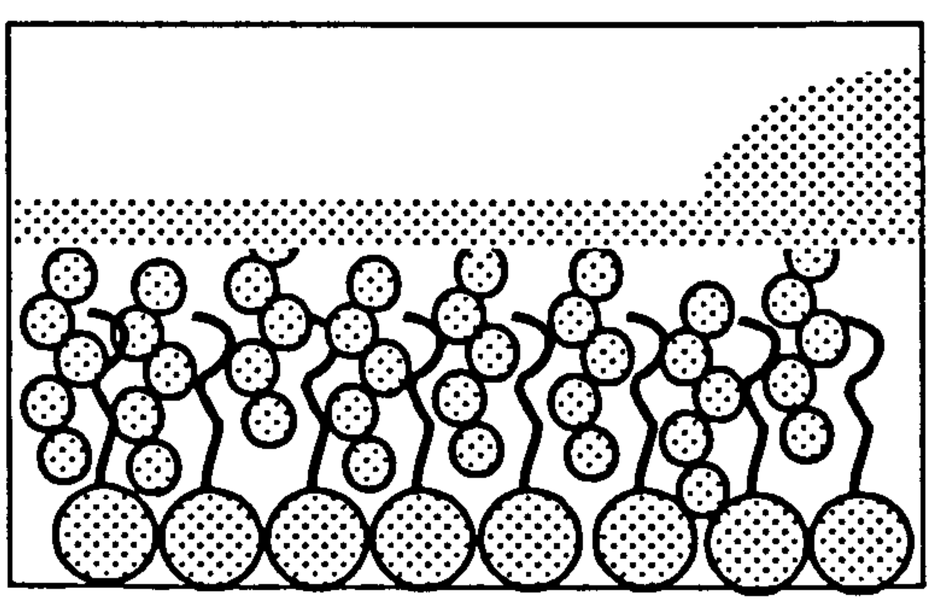

(c)

Pseudo-partial wetting, thin oil film on top of the mixed monolayer and oil lens

oil molecule

surfactant molecule

(b) The oil forms stable lenses on the surface, with or without molecular spreading at the surface. In the molecular spreading process, oil molecules are solubilised by surfactant chains in the monolayer. In this case, the tension again falls after oil addition because the tension of the mixed surfactant/oil film is lower than the tension of the pure surfactant monolayer. The spreading behaviour of dodecane on CTAB (cetyl trimethyl ammonium bromide) solutions described by Aveyard *et al.*[42] belongs to this group.

(c) The oil drop coexists with a thin oil film on the top of the mixed monolayer of surfactant and oil molecules. This situation is commonly known as pseudo-partial wetting. Such a situation may result from a competition between an attractive van der Waals potential and a short range repulsive potential. The total interaction potential between the interfaces shows a minimum at a small but non-zero separation, favouring the case of a surface coated by a thin film coexisting with a residual drop. It has been reported for short alkanes on AOT solutions.[45]

The spreading behaviour of oil can be explained by the spreading coefficients, related to the three tensions which are present in the system. The initial spreading coefficient is defined as

$$S_i = \gamma^i_{AW} - \gamma^i_{AO} - \gamma_{OW} \qquad (1.15)$$

where γ^i_{AW}, γ^i_{AO} and γ_{OW} are the initial air-aqueous, air-oil and oil-aqueous solution tensions respectively. S_i is positive if spreading is spontaneous. However, when oil and water are in contact, they will become mutually saturated, so that γ^i_{AW} and γ^i_{AO} will change to the equilibrium tension. The

corresponding spreading coefficient is then known as the equilibrium spreading coefficient,

$$S_e = \gamma^e_{AW} - \gamma^e_{AO} - \gamma_{OW} \qquad (1.16)$$

Assuming that γ^e_{AW} is the largest of the three tensions, there is a limit to the possible values of S_e, since[46]

$$\gamma^e_{AW} \leq \gamma_{AO} + \gamma_{OW} \qquad (1.17)$$

from which $S_e \leq 0$. If $S_e = 0$ spreading will occur, whereas if $S_e < 0$ the drop remains as a lens on the surface. Values of $S_e > 0$ indicate either experimental error in the tensions or lack of equilibrium.

1.4.2 Adsorption isotherm studies

To understand the spreading behaviour of oil on a surfactant layer fully, it is necessary to study the adsorption isotherm of the oil. The Gibbs adsorption equation (at constant temperature and total pressure) leads to the following expression for the surface concentration of oil, Γ_o, in the mixed monolayer

$$\Gamma_o = \frac{a_o}{RT}\frac{d\Delta\gamma}{da_o} \qquad (1.18)$$

where a_o is the mole fraction activity of oil, $\Delta\gamma$ is the reduction in surface tension caused by the adsorption of oil, R is the gas constant and T is the absolute temperature.

There are two methods of varying the oil activity, a_o. One way was developed recently by Aveyard *et al.*[47] Here the liquid mixture of pure alkane and a diluent oil (e.g. squalane) was used in order to vary the oil mole

fraction. The activity of the adsorbing alkane in the oil mixture is equal to the product of the activity coefficient and the mole fraction. In what follows, the activity scale used is that for which the activity of the pure liquid is unity i.e. the standard state is the pure liquid. For this choice, the activity coefficient of alkane tends to unity as its mole fraction tends to unity. When $\Delta\gamma$ increases linearly with a_o and the surface concentration of diluent oil is zero, the quantity $(d\Delta\gamma/d\ln a_o)$ in the limit that a_o tends to 1 is equal to the *maximum* tension lowering $\Delta\gamma(max)$ obtained following the addition of a drop of pure adsorbing oil to the surfactant solution. The *maximum* surface concentration of adsorbing alkane $\Gamma_o(max)$ is then

$$\Gamma_o(max) = \frac{\Delta\gamma(max)}{RT} \qquad (1.19)$$

In this case, the maximum surface concentration of adsorbed oil can be obtained from a single measurement of the tension lowering following the addition of a drop of pure oil to the surface.

Alternatively, a_o can be determined by varying the partial pressure of the adsorbing oil (P/P_o) as has been done previously for the surface of pure water,[48] adopted on surfactant solutions recently in this group.[49] PDMS oils used in this thesis are commercial products which contain mixtures of different chain lengths. Moreover, a diluent oil for the adsorption isotherm study is not available. Hence, we adopt the vapour partial pressure method to investigate the adsorption isotherm of the volatile PDMS oils (0.65 and 1 cS oils) on surfactant solutions.

1.4.3 Neutron reflection studies

The effect adsorbing oils have on the surface tension of surfactant monolayers no doubt provides information on the spreading behaviour. However, to understand the detailed structure such as the molecular orientation and position of the oil and surfactant molecules in mixed oil-surfactant films, we need to use the neutron reflection technique.[50] This method involves determining the intensity of a specularly reflected beam of neutrons as a function of either the angle of incidence or neutron wavelength. Neutron reflection from a deuterated species is of much higher intensity than from the protonated species. Therefore, by deuterating different components within a system containing a surfactant solution and an oil film, important information concerning the molecular make-up of the interface can be ascertained.

There have been studies using ionic surfactants, investigating the change in area per molecule of the surfactant before and after the addition of oil and also analysing where the oil lies in the interface in relation to the surfactant monolayer.[51] This study showed that a mixed monolayer of TTAB (tetradecyltrimethylammonium bromide) and dodecane exists at the aqueous-air surface rather than a multilayer oil film coexisting with a lens. This distinction would probably not be possible with tension measurements alone. For the same system, it was concluded that the area per surfactant at the interface in the mixed film derived from neutron reflection agrees, within experimental error, with that derived from surface tension measurements. The main conclusion found for this system was that the oil

adsorption occurs via "chain filling" with straightening of the surfactant chains. Only a slight change in the surfactant headgroup area was found. The oil was found to penetrate toward the water level giving a mixed monolayer such that the oil chains protrude above those of the surfactant chains.

More recently, the adsorption of dodecane on nonionic surfactant ($C_{12}E_5$) monolayers has been studied in detail with variation of the oil activity using neutron reflection.[49] Here comparison of the isotherm of dodecane on the surfactant monolayer with that obtained directly using neutron reflectivity indicates that changes in the surfactant chemical potential following oil addition are negligible within the timescale of the tension measurements. It is also shown that the surface concentration of surfactant, scattering length density of the surfactant film and surfactant layer thickness are all independent of the activity of the oil, consistent with the idea that oil adsorption occurs primarily by filling of the voids present between the surfactant chains. However, the surface concentration of oil, scattering length density of oil and oil layer thickness change with oil activity. The changes are dependent on the bulk concentration of surfactant.

It can be seen from this that neutron reflection is a useful technique to complement surface tension studies, giving an insight into the actual position and spacing of the molecules at the surface.

1.5 Relevant literature review

This thesis concerns the mixing behaviour of PDMS oils and surfactant both at oil-water and air-water interfaces. The structure and dynamic features of these oils differ from hydrocarbon oils in a number of fundamental respects, giving rise to important physical properties as described in section 1.2. In this section we mainly focus on the interaction between PDMS oils and surfactant carried out previously.

PDMS oils are amphiphilic and can spread on the surface of water,[52,53] and of organic solvents,[54,55] which was established half a century ago. More recently, Langevin and co-workers[56-60] have studied the structure of PDMS layers on water and on a variety of surfactant solutions ($C_{10}E_5$, AOT, C_9-C_{16}TAB) using surface pressure, capillary wave spectroscopy, ellipsometry, Brewster angle microscopy and neutron reflectivity techniques. They found that PDMS oils spread more easily on a dense surfactant layer than on pure water. In the latter case, the polymer chains must accommodate themselves near the polar water surface and this chain configuration favours multilayer formation. On surfactant solutions, the resultant mixed film is a superposition of two layers; one surfactant-rich and the other surfactant-lean. The degree of mixing of the layers depends on the surfactant type. Significant penetration of the polymer into a monolayer of the nonoinic surfactant $C_{10}E_5$ occurs, whereas no interpenetration of the two layers occurs for the double-chain anionic surfactant Aerosol OT. For the homologous series of cationic alkyltrimethylammonium bromide surfactants, a critical chain length of 14 is found, above which PDMS oils displays

'complete' wetting (homogeneous layer), and below which 'pseudopartial' wetting (heterogeneous PDMS surface coverages) occurs.

Kanellopoulos and Owen[61] have measured the air-water surface tensions and the silicone oil-water interfacial tensions as a function of surfactant concentration for a series of PDMS polyether block copolymers as surfactant. High siloxane-content copolymers were preferentially adsorbed at the air-water surface, whereas low siloxane-content copolymers adsorbed preferentially at the oil-water interface. Rouviere *et al.*[62,63] found no swelling of the lamellar or hexagonal phase formed in water-octylphenol ethoxylated surfactant systems following the addition of silicone oil, unlike the increase in bilayer separation caused by incorporation of decane. This indicates that the silicone oil is dispersed into drops which form the dispersing medium. In lamellar phases formed from C_9E_5 however, swelling is observed on addition of PDMS oils with molecular weight < 500, while longer chain oils leave the phase unaltered. The solubilisation of several PDMS oils into solutions of TTAB in the presence of sodium salicylate has been studied by light scattering.[64] These solutions initially contain large entangled rod-like micelles, which become shorter and transform to spheres with increasing concentration of the additive. The PDMS oils were either cyclic (D_n) or linear siloxanes of low molecular weight (M_2, MDM, MD_2M, MD_3M, D_3-D_5). The maximum solubilisation ratio of [PDMS]:[surfactant] is only 0.6, decreasing with an increase in the molar volume of the oil. Katayama *et al.*[65] shows that microemulsions (of various types) can be formed in aqueous salt+aminofunctionalised PDMS+N,N-

dimethylethanolamine myristate+alcohol quinary systems. Microemulsions were not formed in non-functionalised oil systems pointing to the important role of the NH_2 group in promoting microemulsion formation. Mayer has described the preparation of silicone oil-in-water microemulsions from concentrates.[66,67] Here, anhydrous concentrates containing almost 100% silicone oil are simply poured into an aqueous medium giving rise to translucent solutions containing droplets in the 10-80 nm size range. No details of the oil type or of the surfactant type are given, although it appears that at least two surfactants are necessary and that both may be siloxane-containing themselves.

Steytler *et al.*[68] reported the formation of single phase w/o microemulsions stabilised by Aerosol-OT in two low molecular weight silicone oils, hexamethyldisiloxane (HMDS) and diphenyltetramethyldisiloxane (DPTMDS). The maximum amount of water solubilised in w/o microemulsions with silicone oils can also be altered by electrolyte concentration, temperature and the addition of cosurfactant. The characteristics of the microemulsions were studied by photon correlation spectroscopy and small angle neutron scattering. They found that the attractive interactions between w/o microemulsions droplets in HMDS are stronger than those in hydrocarbon oils of comparable molecular weight. Gee[69] claimed the formation of an aminosilicone polymer oil-in-water microemulsion with a nonionic surfactant, which is time and procedure dependent. This procedure involves forming an associated complex of oil, water and surfactant, possibly inverse micellar, where an ultralow oil-water

interfacial tension (0.0001 mN m^{-1}) was found, then instantaneous dilution with water to produce a silicone oil-in-water microemulsion. If the dilution with water is gradual, making o/w microemulsions is impossible, instead an opaque mixture with two or more phases appeared. By contrast, John *et al.*[70] investigated the phase behaviour of the water/$C_{12}E_6$/isopropyl myristate+PDMS oil (30 cS) system. They found that the presence of PDMS oils in the isopropyl myristate enhanced the lipophilic nature of the oil phase and thereby decreased the solubility of oil in surfactant aggregates.

Various patents exist claiming the formation of silicone oil microemulsions or emulsions with small particle size. Dumoulin[71] reported that a complex mix of anionic surfactant+nonionic surfactant+fatty acid+amine compounds is required for this purpose. Harashima *et al.*[72] used emulsion polymerisation with cyclic silicone oils, whilst Osaki and Ona[73] microemulsified PDMS oils which contained cyclohexylamino groups. Likewise, Gee[74] prepared emulsions of size < 0.14 μm with oils that posses one polar radical.

Regarding (macro)-emulsions, Obey *et al.*[75,76] descried the preparation of surfactant-stabilised silicone oil-in-water emulsions of low polydispersity involving the base-catalysed hydrolysis and polymerisation of dimethyldiethoxysilane. In systems with copolymers of PDMS with PPO/PEO (PPO refers to polypropylene oxide and PEO to polyethylene oxide) chains as surfactant, very small (~25 nm) droplet sizes were formed, possibly in the form of microemulsions.

It can be appreciated from the literature survey given above that the conditions required to solubilise silicone oils into aqueous surfactant systems are very specific and that little systematic work has been carried out with these oils. This thesis attempts to gain a detailed understanding of the fundamental interactions between PDMS and surfactant systems in relation to emulsions, microemulsions and monolayer mixing at air-water interfaces.

1.6 Presentation of thesis

The overall aim of this study is to increase the understanding of the interactions of PDMS oils with surfactants. A series of nonionic surfactants (C_nE_m) and a double-chained anionic surfactant (AOT) have been studied and the major subjects of interest are:

1. In chapter 3, we start by using the 50 cS oil (which is the most popular one employed in industry) to describe PDMS oil and water emulsions stabilised by nonionic surfactants in order to determine the phase inversion temperatures. Factors that affect emulsion PIT's are also investigated.
2. In chapter 4, following the finding in the previous chapter, we choose several systems to study the equilibrium phase behaviour of 50 cS PDMS oil with nonionic surfactants. The possibility of making single phase microemulsions with low molecular weight PDMS oils has been explored in $C_{12}E_5$ and a silicone surfactant (L-77) systems.

3. In chapter 5, the mixing behaviour of PDMS oils and nonionic surfactants at air-water surfaces is described. Above the cmc, the spreading coefficients of PDMS oils on C_nE_m surfactant solutions are determined. The oil adsorption isotherms with volatile low molecular weight PDMS oils (0.65 and 1 cS) on $C_{12}E_5$ solution are measured. The surfactant adsorption isotherms with $C_{12}E_5$ and L-77 are also studied in the presence of a liquid drop of 50 cS PDMS oil. We also report the preliminary neutron reflection results of a deuterated PDMS oil on C_nE_m solutions.
4. In chapter 6, we start to consider the behaviour of PDMS oils with an anionic surfactant (AOT). We mainly focus on the Winsor phase behaviour of the low molecular weight PDMS oil (0.65 cS) and the formation of both o/w and w/o microemulsions.
5. In chapter 7, the stability of emulsions formed from all Winsor systems described in chapter 6 has been investigated.
6. In chapter 8, we discuss the spreading behaviour of 0.65 cS PDMS oil on AOT aqueous solutions. The oil adsorption isotherm on the surfactant solution is investigated as a function of electrolyte concentration in the bulk. We also propose a possible correlation between the tension lowering of surfactant solutions caused by the adsorption of oil and the presence of surfactant aggregates in bulk.

CHAPTER TWO

CHAPTER 2

Experimental

2.1 Materials

2.1.1 Water

Water was passed through a reverse osmosis unit and then a Milli-Q reagent water system. The surface tension of the water treated in this way was 71.9 ± 0.1 mN m^{-1} at 25°C in good agreement with the best literature values,[77] indicating the absence of surface active impurities and conducting ions. The resistivity was always above 18 mΩ cm.

2.1.2 Silicone oils

Except for the 2 cS and 3 cS PDMS samples which were purchased from Gelest (Germany), all the PDMS oils used were PDMS Dow Corning® 200 fluids of various viscosity. These oils are commercial products containing a mixture of oils of different molecular weight oils and their purity is unknown. They were used without further treatment. Details of the oil viscosity and sample reference number are in Table 2.1. The aminofunctionalised PDMS oil had a viscosity of 1500 cS. The average molecular weights for each oil were calculated according to the information in the Dow Corning data sheet.[1]

Table 2.1 Viscosity (at 25°C) and the viscosity-averaged molecular weight of PDMS oils used

Oil viscosity / cS	Average molecular weight	Lot. ref.
0.65	162	AA077034
1	237	AA057367
2	410	175373547
3	550	461447056-8E20-0
5	770	AA085775
10	1,250	WC015329
20	2,000	WC045334
50	3,780	WC094332
100	5,970	WC114316
500	17,250	WC094326
1000	28,000	WC114341

2.1.3 Surfactants

(a) Nonionic

The nonionic surfactants, all of the alkyl polyoxyethylene glycol ether type (C_nE_m), were obtained from Nikkol (Japan) or Fluka (UK). The purity was >99%. They have the following general structure:

$$C_nH_{2n+1}(OCH_2CH_2)_mOH$$

where n = 8, 10, 12, 14, 16 and m = 2, 3, 4, 5, 6. A space filled molecular model of $C_{12}E_3$ is shown in Figure 2.1.

Commercial samples of $C_{16}P_8E_1$ (PBC-41, ref. 5167) and $C_{16}P_4E_1$ (PBC-31, ref. 5065) where P refers to a propyleneoxide group were from Nikkol. The silicone surfactant Silwet L-77 ($[(CH_3)_3SiO]_2Si(CH_3)(CH_2)_4(OCH_2CH_2)_{7.5}OCH_3$) was a gift from the Union

Carbide Corporation (ref. 8610QUO62391). Figure 2.1 also shows a space filled molecular model of L-77.

(b) Ionic

The ionic surfactant used in this study is the anionic surfactant AOT (sodium bis-2-ethylhexylsulphosuccinate) which was purchased from Sigma with purity >99%. A space filled molecular model of AOT is shown in Figure 2.2.

2.1.4 Other chemicals

Table 2.2 lists the sources and purity of the electrolytes and other chemicals used in this study. They were all used as received.

Table 2.2 Purity and sources of other chemicals

Material	Source	Purity
sodium chloride (NaCl)	Prolabo Analar	>99.9%
tetrabutylammonium bromide (TBAB)	Fluka 'puriss'	>99.5%
disulfan blue	Fluka 'standard'	unknown
dimidium bromide	Fluka	95%
Karl Fischer reagent	BDH 'improved'	unknown
chloroform	Fisher	99%
Hyamine 1622	BDH	99%

2.2 Preparation of glassware

All glassware was washed thoroughly in alcoholic KOH, rinsed several times with hot water and then at least three times with ultra-pure Milli-Q water. The glassware was dried in a clean oven at 100-105°C.

Figure 2.1

Space filled molecular model of $C_{12}E_3$ and L-77

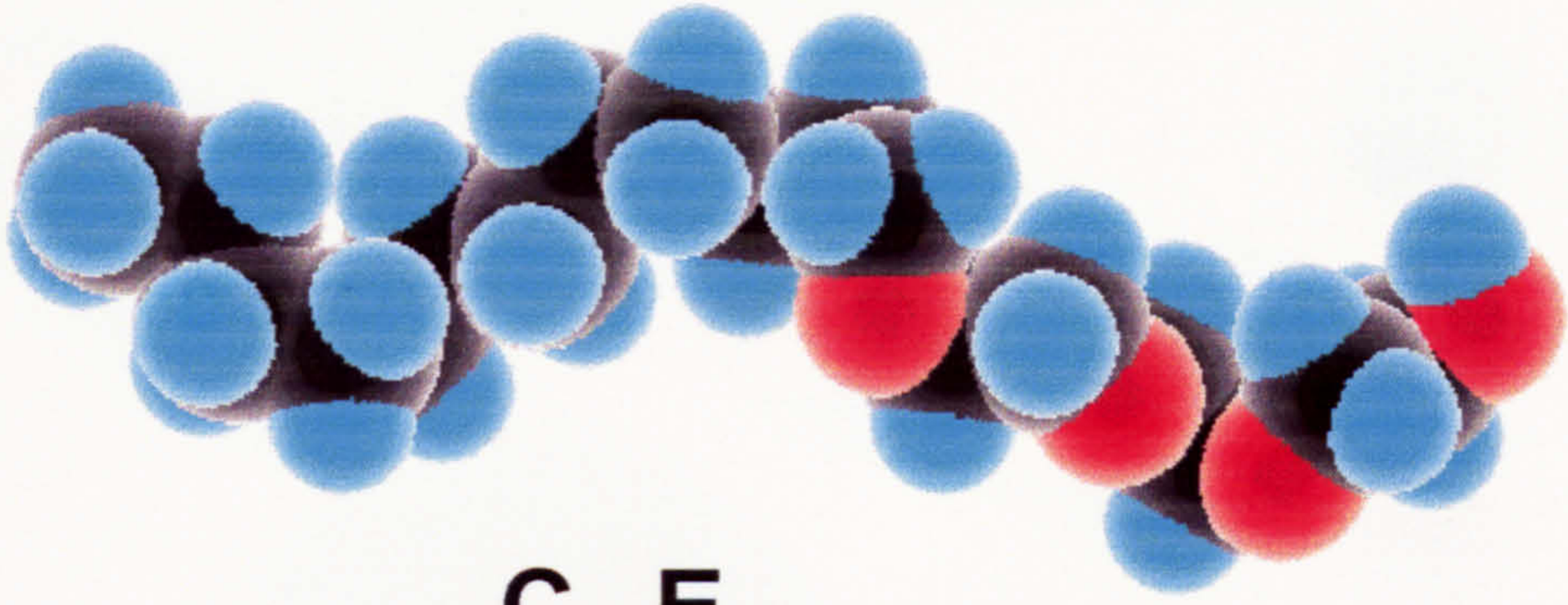

$C_{12}E_3$

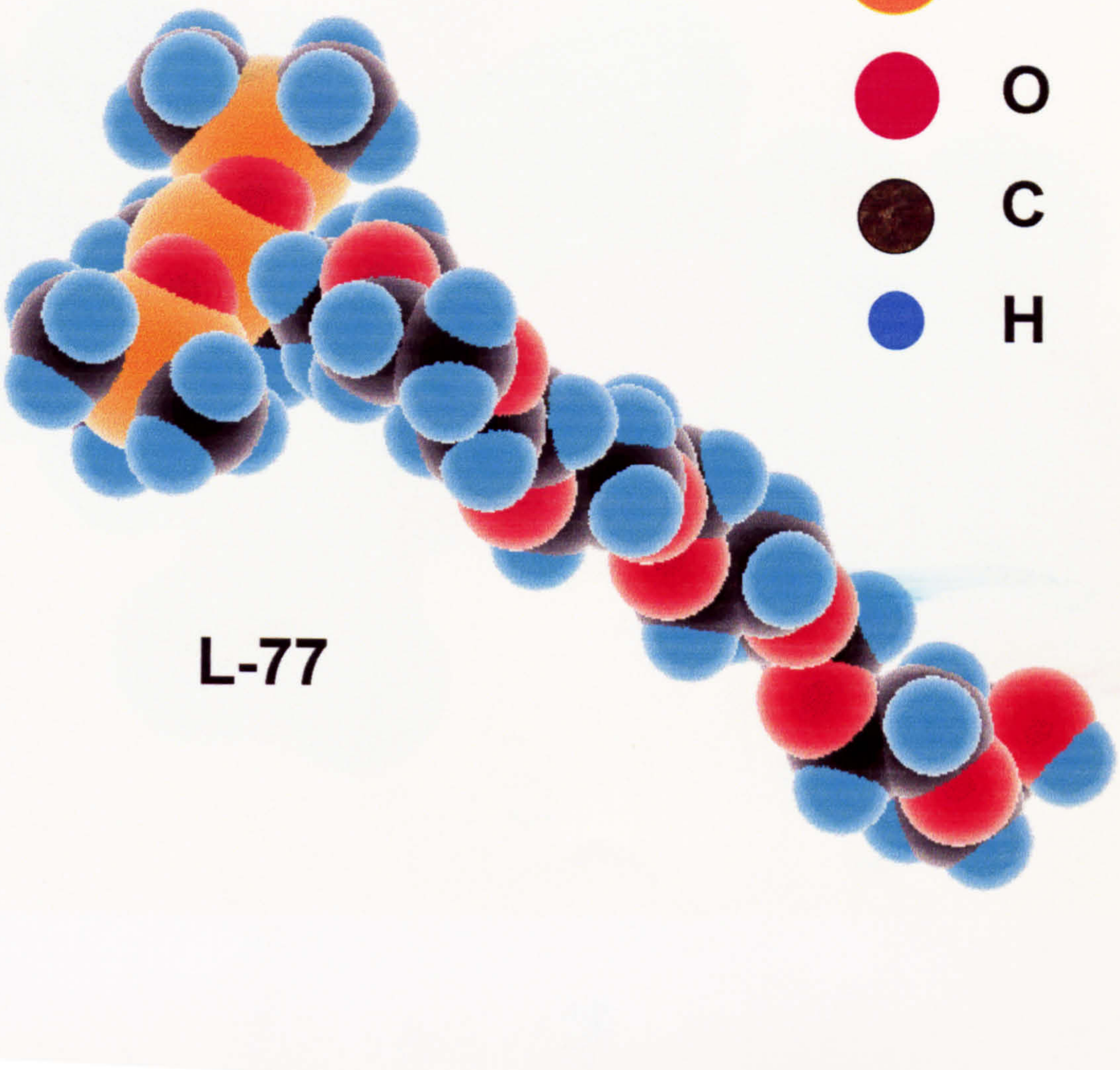

L-77

Figure 2.2

Space filled molecular model of Aerosol - OT (AOT)

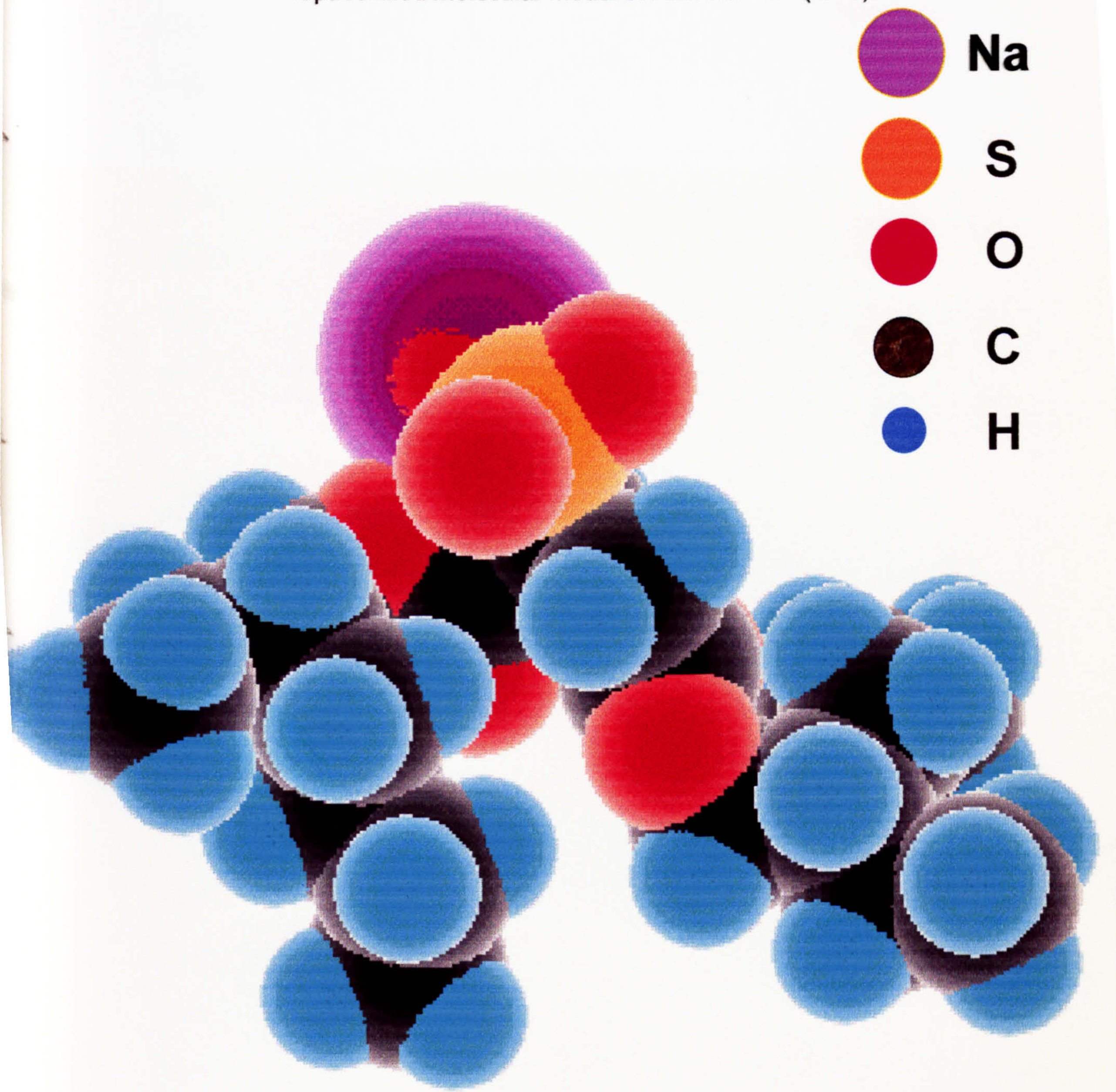

2.3 Experimental methods

2.3.1 Equilibrium phase behaviour of oil+water+surfactant mixtures

The equilibrium phase behaviour was determined by preparing mixtures of aqueous electrolyte and PDMS oil (equal volumes, 5 cm^3) and adding appropriate amounts of surfactant. The glass phase tubes were 13 mm internal diameter and of length 100 mm and were graduated. For efficient mixing without macroemulsion formation, the mixtures were shaken gently by inverting the tubes a number of times and thermostatted at the appropriate temperature. Gentle inversion was performed occasionally during the equilibration period until the final equilibrium state was reached, in which there was no change in the volume of each phase.

2.3.2 Turbidity titration

A turbidity titration method was employed to determine the solubilisation boundaries of surfactant solutions in conditions pertaining to oil-in-water or water-in-oil droplets. A tightly stopped tube with a side arm was thermostatted in a water jacket (Figure 2.3). 10 ml of surfactant solution (oil or water) was pipetted into the tube. The contents were stirred rapidly using a magnetic stirrer and thermostatted to the required temperature. This initially transparent mixture was titrated with oil (or water) until a second phase was visually observed. The composition of the mixture at this point was taken as being the phase boundary at which separation of an excess phase occurs. The phase change from clear to turbid or vice versa was sharp.

Figure 2.3

Schematic representation of the turbidity titration apparatus

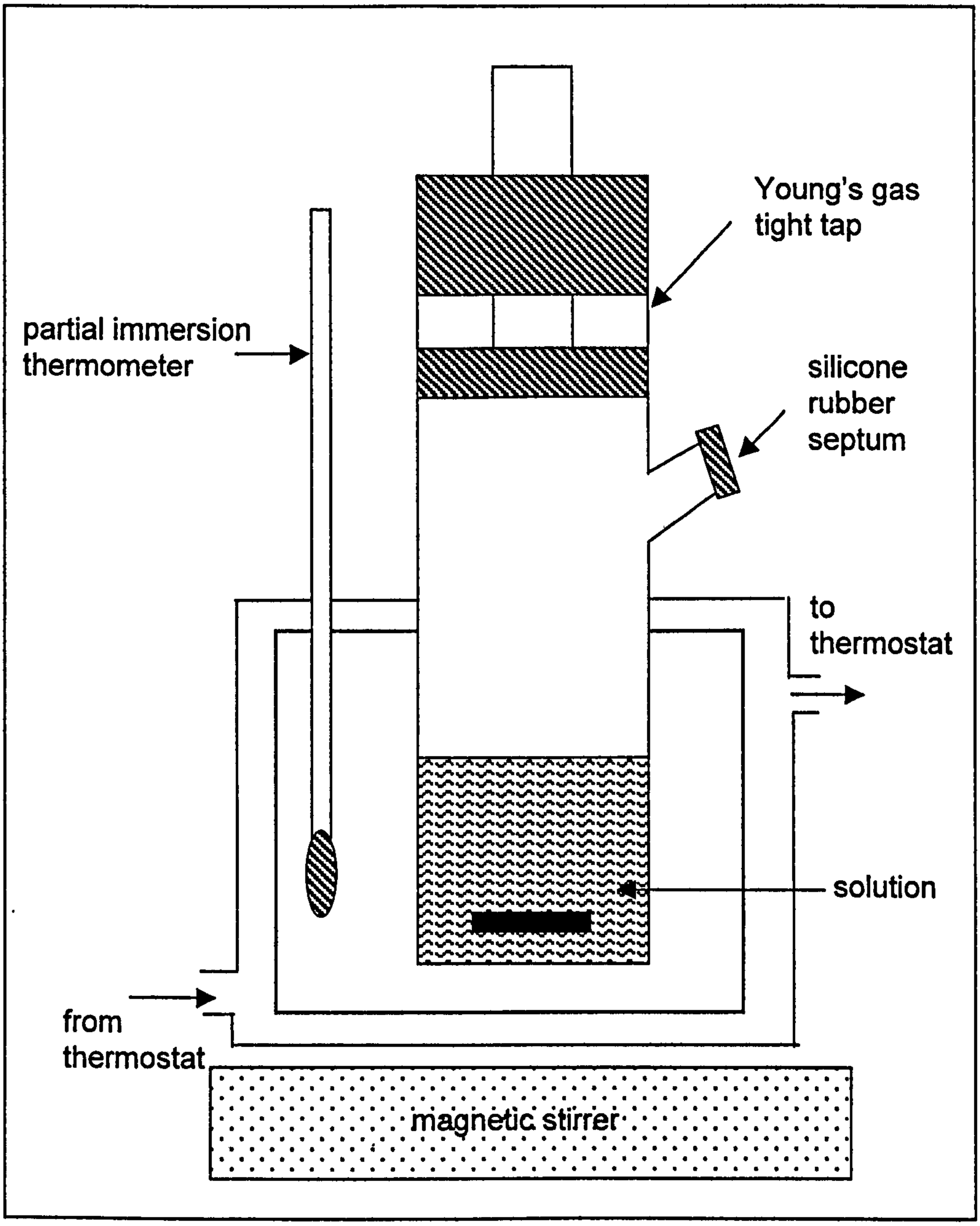

2.3.3 *Emulsion preparation and stability*

All the emulsions were made from non-pre-equilibrated phases using a Janke and Kunkel Ultra-turrax T25 homogeniser (rotor-stator mechanism) with shaft 8G at 8000 rpm for 2 minutes. Equal volumes (8 cm^3) of an aqueous electrolyte solution were mixed with PDMS oil, surfactant added to this in varying amounts. The conductivity of the emulsions was measured using a Peak Scientific PTI-58 digital conductivity meter with a Pt/Pt black dip cell. The sample tube was thermostatted using a Grant LTD 6 or a Haake F3 thermostat. To determine the PIT of emulsions stabilised by nonionic surfactants, emulsions were prepared at ambient temperature and heated in 2°C intervals with occasional re-homogenisation. For ionic surfactant, emulsions with different salt concentration were prepared individually and the conductivity of the emulsions was measured immediately after homogenisation.

Emulsion stability, that is the volume of water or/and oil resolved, were determined visually as a function of time from the height of clear aqueous or/and oil phase in the stopped, graduated glass tubes at specific temperature. For example, in o/w emulsions where creaming occurs a distinct boundary between an upper cream layer and a lower depleted emulsion layer appears, the position of the boundary was measured. When coalescence happens, a clear oil layer forms on the top of the upper cream layer, a second distinct boundary appears which was also followed with time.

2.3.4 Spreading behaviour of oils on surfactant solutions

The spreading behaviour of oils on surfactant solutions was observed by using a teflon dish contained within a thermostatted glass vessel with a thermostatted lid and a teflon stopper, through which the oil was introduced with a syringe (Figure 2.4). All the apparatus was cleaned, prior to use, by using alcoholic KOH and Milli-Q water in the usual way.

The procedure used to investigate the spreading behaviour was to fill the teflon dish with the surfactant solution. The glass vessel was then covered with the lid. The apparatus was allowed to thermostat for about 20 minutes to make sure that the surfactant solution reached the required temperature. The oil (~20 μl) was then added to the surface of the surfactant solution by using a 50 μl syringe inserted through the small hole in the teflon stopper. The apparatus was illuminated, from behind, by a lamp. There were three types of observations: (a) On initial contact, oil spread fast and interference colours were seen near the side of the dish; (b) Oil spread initially, then retracted to form patches of film showing interference colour; (c) Oil formed a circular lens initially, the lens then spread slowly and became flatter gradually. For volatile oils, the vapour within the apparatus was saturated by placing filter papers soaked in oil around the teflon dish.

2.4 Measurement of surface and interfacial tensions

Measurements of surface and interfacial tension were carried out by using either the du Noüy ring method, the drop volume method or the spinning drop method depending on experimental requirements.

Figure 2.4

Apparatus used to visually observe the spreading behaviour of oils on surfactant solutions

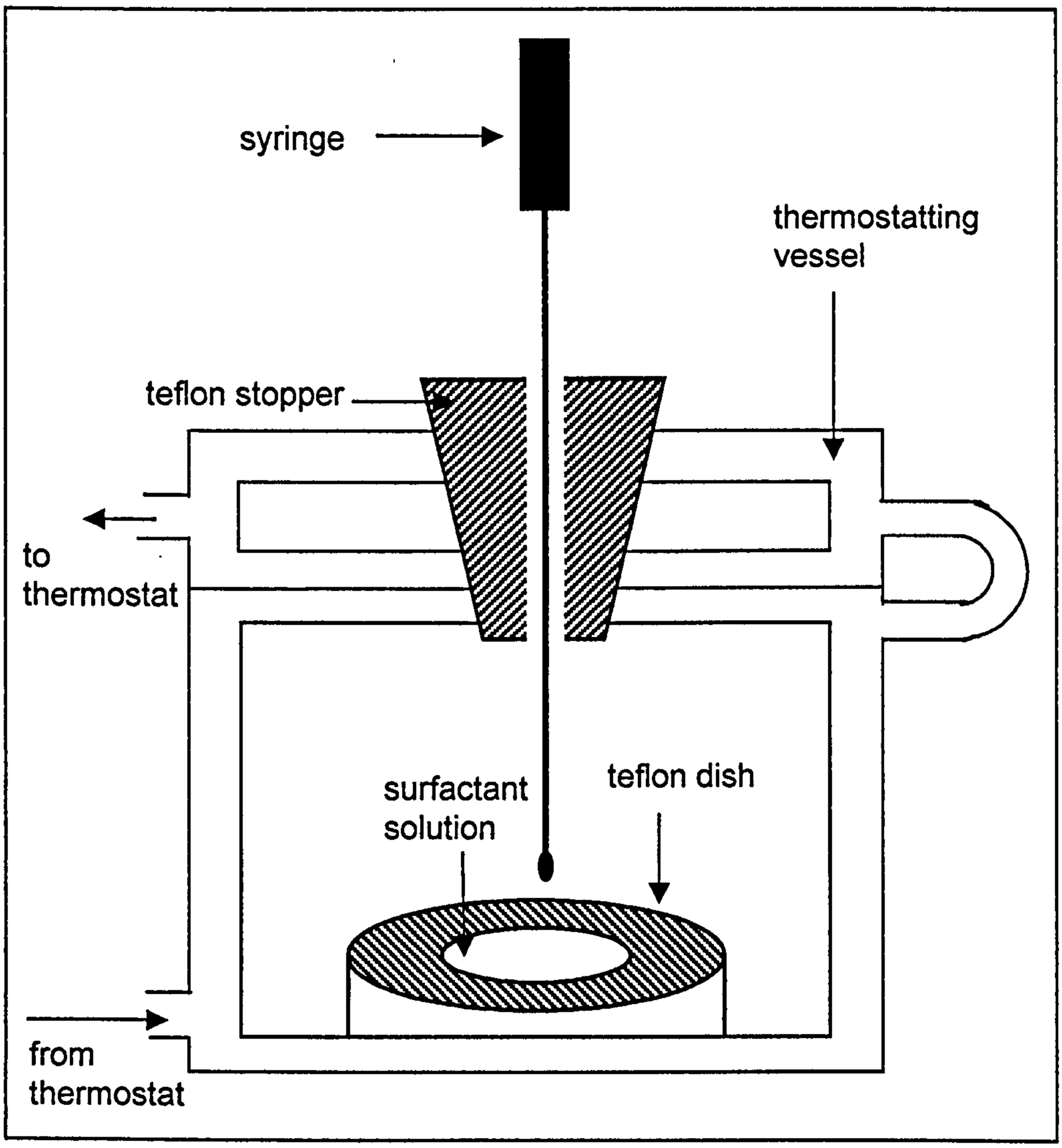

2.4.1 du Noüy ring method

(a) Surface tension of aqueous surfactant solution in the absence of oil

The air-water surface tensions of surfactant solutions were measured using the du Noüy ring method. A modern du Noüy ring tensiometer consists of a ring made from a chemically inert alloy material, usually platinum/iridium (Pt/Ir) which is suspended from a torsion balance horizontally in the surface of the liquid (or interface between two liquids). Historically, the du Noüy ring involved the detachment of the ring from the interface and was used without the application of any correction factors. The force required to pull the ring from the surface was thought to equal the surface/interfacial tension according to $mg = 4\pi R\gamma$, where mg is the maximum force applied to a ring of inner radius R. Harkins and Jordan[78] showed that this simple equation could be in error by as much as 25%. Therefore, a correction factor F is necessary to attain the correct tension. The physical significance of the correction factor is best understood by reference to Figure 2.5a which shows three successive stages of pulling a ring from the surface of a liquid. Provided that the wire is completely wetted, the meniscus begins to form as a force is applied. When lifting the ring, the tension is acting along its wetted line. The resultant, due to the forces acting on the ring, reaches a maximum as soon as the tangent at the point of wetting is vertical to the surface. Further raising of the ring results in the interruption of the lamella. Besides the resultant of the tension, the hydrostatic weight of the liquid volume underneath the ring is also measured. This additional force is eliminated by the correction factor.

Harkins and Jordan determined empirically values for the correction factor F, which in a separate paper by Freud and Freud[79] was given a solid

theoretical foundation. Hence, the force required to achieve maximum pull of the ring in the surface is given by

$$\gamma = \frac{mgF}{4\pi R} = \frac{\Delta\rho VgF}{4\pi R} \qquad (2.1)$$

The correction factor F is a function of R^3/V and R/r, where V is the volume of liquid raised above the plane surface by the maximum pull of the ring, and r is the radius of the wire from which the ring is made. The correction factors are applied by measuring the radii of the ring (R), and wire (r), and the density difference between the fluids $\Delta\rho$. A value of R^3/V is calculated for each determination and the correction factor F is obtained from the tables according to the value of R/r. The accuracy of these tables has been shown to be within 0.25% of those obtained from theoretical variations in meniscus shapes by Freud and Freud. The data of Harkins and Jordan has been extended by Zuidema and Waters[80] to include the measurement of the interfacial tensions below 25 mN m^{-1}.

The tensiometer used for determination of surface and relatively high interfacial tensions was supplied by Krüss (model K10). This modern tensiometer has the advantage of enabling tensions to be measured without the necessity for detachment of the ring. Detachment is unnecessary because the maximum force acting on the ring is achieved before detachment from the meniscus occurs. The tensiometer consists of a water thermostatted vessel which can be raised by motors and a torsion balance. Th ring is made from Pt/Ir and has the following dimensions: R = 9.545 mm and r = 0.185 mm (Figure 2.5b). The ring was cleaned by a procedure of immersing in alcoholic KOH, rinsing with high purity water and flaming by

Figure 2.5

(a) Cross-sectional view of the dü Nöuy ring showing the different stages of measurement

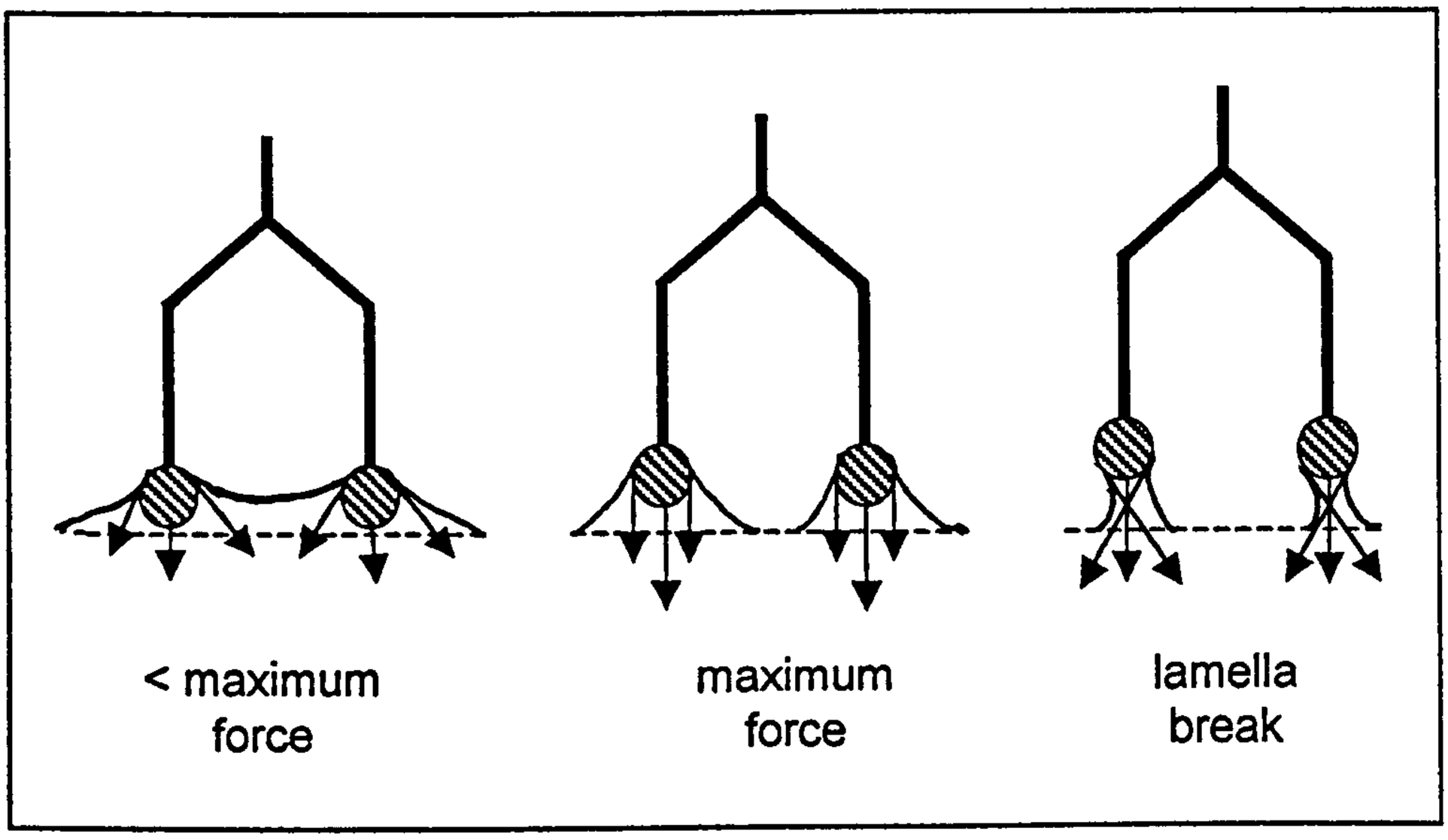

(b) Schematic diagram of the ring

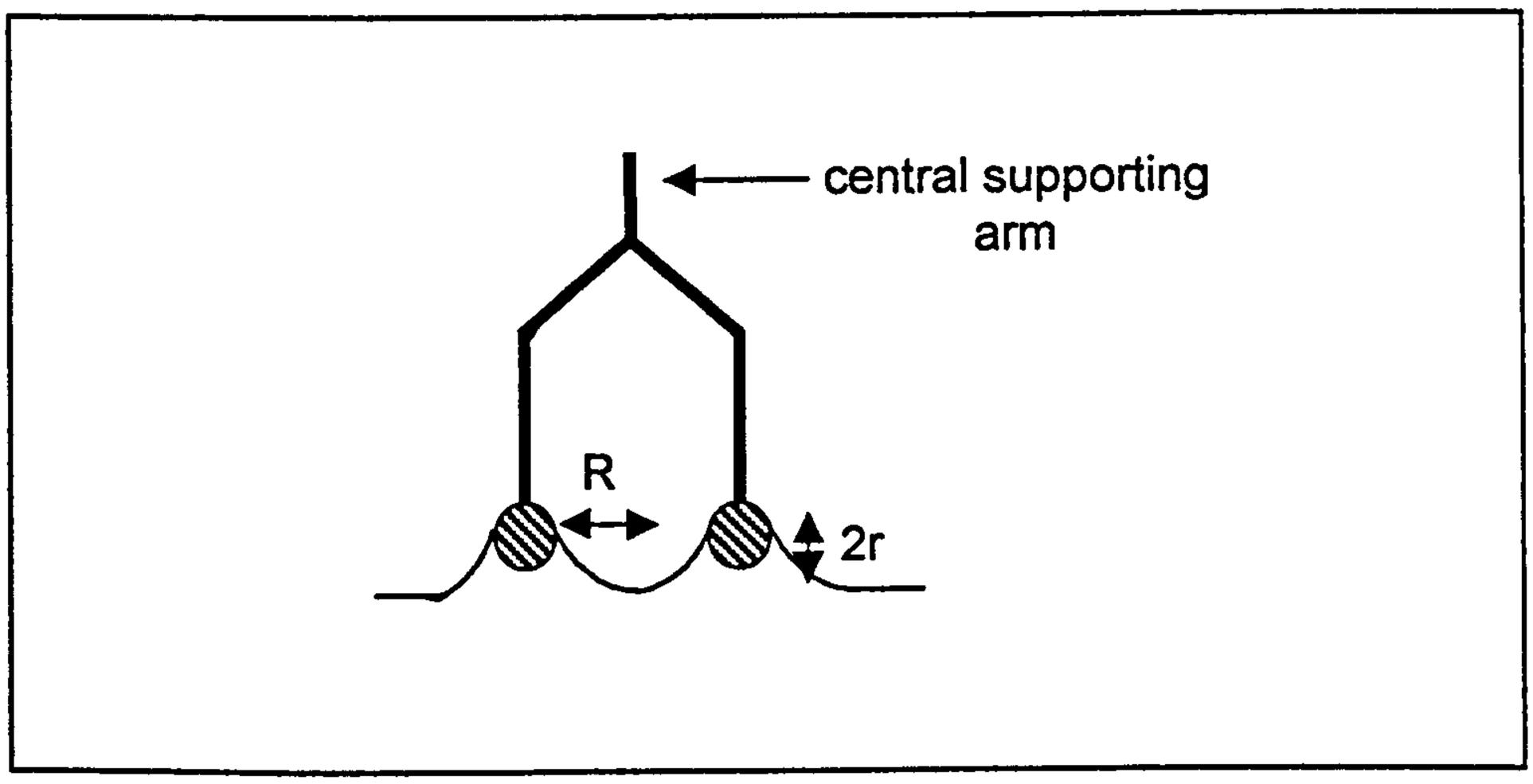

holding above a Bunsen burner. The glass vessels for holding the liquid were cleaned by the standard procedure used for all glassware and dried in a clean oven. The vessels were filled with an appropriate amount of liquid (or liquids), and allowed 20 minutes to attain the correct temperature before measurements were made. Frequent checks of the orientation of the ring in the plane of the surface, and its curvature were made to ensure maximum accuracy in the measurements. It has been shown that deviations of 1° from the horizontal introduces an error of 0.5%, and 2° an error of 1.5%.

For the determination of the surface tensions of liquids, the balance is first zeroed with the ring suspended in air close to the surface of the liquid. The vessel is then raised until the ring is immersed in the liquid. The servo motors start and lower the vessel until a maximum force is measured. For oil-water interfacial tensions, the balance is zeroed in the upper oil phase. This procedure compensates for the buoyancy and surface tension that acts upon the vertical supports. The tensiometer is calibrated, using internal potentiometers such that the corrected value for the surface tension of water at 25°C reads 71.9 mN m^{-1}. Tensions are reproducible to ± 0.1 mN m^{-1}.

(b) Surface tension of aqueous surfactant solution in the presence of oil

Surface tensions in the presence of small volumes of PDMS oil (10 µl) were determined with the same instrument, but the vapour space above the solution was also thermostatted using a double-walled glass lid. In addition, filter papers soaked in oil were contained in small glass dishes around the solution vessel to ensure that the vapour remains saturated throughout the measurement for volatile oils. The tension of the aqueous solution in the

absence of oil was determined as above. The liquid surface was then raised slightly with the meniscus still attached to the ring and 10 µl of oil was added to the surface. The new (lower) tension of aqueous solution was then measured at least 3 times and the reproducibility was within ± 0.1 mN m^{-1}.

(c) Surface tension of aqueous surfactant solutions pre-equilibrated with oil

In order to measure the true equilibrium surface tension of aqueous solutions in the presence of oil, the oil and aqueous phases were first equilibrated for 2 days at the required temperature using gentle hand shaking. The upper phase oil was removed quickly by using a pipette. The tension of the equilibrated aqueous phase was measured. Similar precautions were taken as described in (b) to ensure saturation of the vapour space for volatile oils.

2.4.2 Drop-volume technique

Drop volume tensiometry (DVT) is a well established technique, which was used to measure surface and interfacial tensions. Two advantages of using this technique over others are that only small (0.6 ml) amounts of solutions are required, and thermostatting is also relatively straightforward.

A drop was suspended from a cylindrical tip of known radius (see Figure 2.6) mounted onto a syringe containing the solution of interest. The tip was made of stainless steel and was accurately ground and of circular cross-section, diameter 1.999 mm. The contact between the stainless steel and the glass syringe end was improved by using carborundum occasionally. Using a micrometer to drive the plunger of the syringe into the barrel, the

Figure 2.6

Schematic diagram of the drop volume apparatus

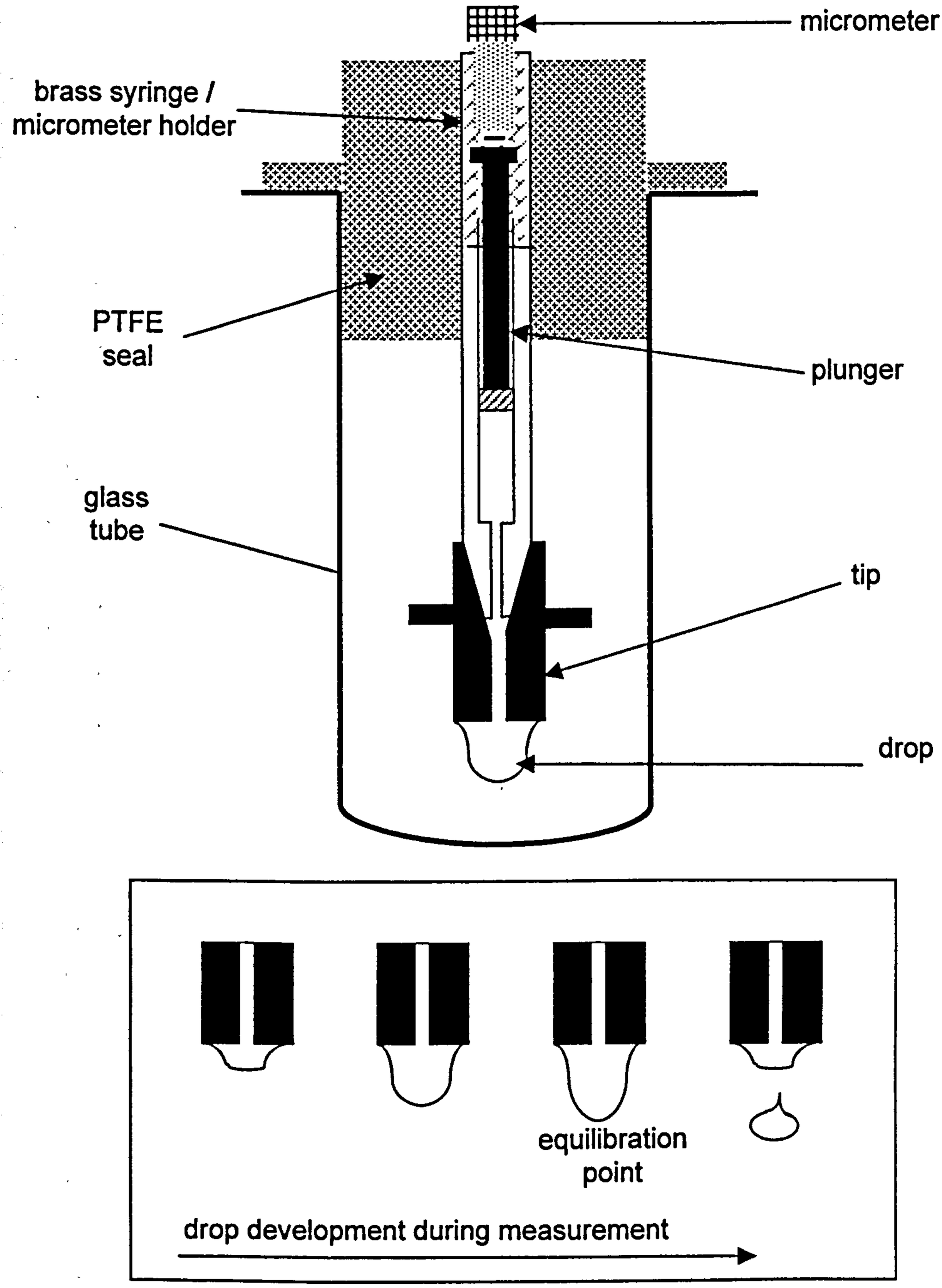

drop was enlarged until the maximum size that would remain on the tip was approached. The drop was allowed some time for the surface to equilibrate, and then enlarged slowly until it finally detached. This procedure was then repeated, and the difference between successive micrometer reading at the point of detachment was used to calculate the drop volume. Equation 2.2 was used to calculate the tension, γ,

$$\gamma = \frac{\Delta\rho\Delta h A g}{2\pi f} \tag{2.2}$$

where $\Delta\rho$ is the density difference between the two phases, Δh is the mean of at least 10 micrometer increments, A is the cross sectional area of the syringe, g is the acceleration due to gravity, and f is a correction factor which allows for the shape of the drop.

The FORTRAN program in Appendix 1 was used to calculate the tension. The correction factor was calculated using polynomial fits to data for the correction factor obtained by Wilkinson.[81] This method was used to attain the interfacial tensions of higher molecular weight PDMS oils (5 cS and above) and aqueous phase due to the relatively low $\Delta\rho$ that is undesirable in the spinning drop method. Typically, before the contact of the aqueous phase with the oil phase, the tip was wetted by the aqueous phase in the barrel to avoid the formation of air bubbles, then a drop of the aqueous phase was formed in the PDMS oil phase.

2.4.3 Spinning drop method

The spinning drop technique was developed during the 1940's by Vonnegut[82] and is particularly suitable for measuring low interfacial tensions

(10^{-4} – 5 mN m^{-1}). The spinning-drop tensiometer used was supplied by Krüss (model Site 04). Figure 2.7 depicts the layout of the apparatus. As seen, the tensiometer consists of a high speed rotating capillary tube (internal diameter ~ 2.5 mm) open at both ends. The tube in its housing is pivoted and sealed so that the open ends rotate inside the chambers filled with the denser aqueous phase, and its middle section is observable through the cylinder windows. This arrangements allows the injection of a drop of the less dense oil phase into the filled and rotating system, so that the drop may be stabilised in the axis of rotation. Illumination of the capillary is with a stroboscope 'in-phase' with the rotation of the capillary. The control box of the instrument displays the speed of rotation of the capillary, n, up to 10,000 r.p.m., which can be controlled to ± 5 r.p.m. There is also a digital read-out of the temperature. Thermostatting of the capillary is achieved by circulating a thin lubricating oil around it from a Colora thermostat. Temperature can be controlled to ±0.2°C.

The tension is obtained by the measurement of the shape of the drop. When a closed vessel containing a liquid and a drop of a lighter immiscible liquid (oil) is rotated about the horizontal axis, the drop will take up an equilibrium position on the axis of rotation because of the pressure caused by the centrifugal force. As a result, the drop will come to an equilibrium length balanced by rotation forces and opposing interfacial tension forces.

A mathematical solution for the shape of the drop is complex, but if the effects of gravity are neglected and the drop shape can be approximated by a cylinder with hemispherical caps, the treatment is simplified. The expression relating the tension of the drop surface to the angular velocity,

Figure 2.7

Schematic diagram of the spinning drop tensiometer

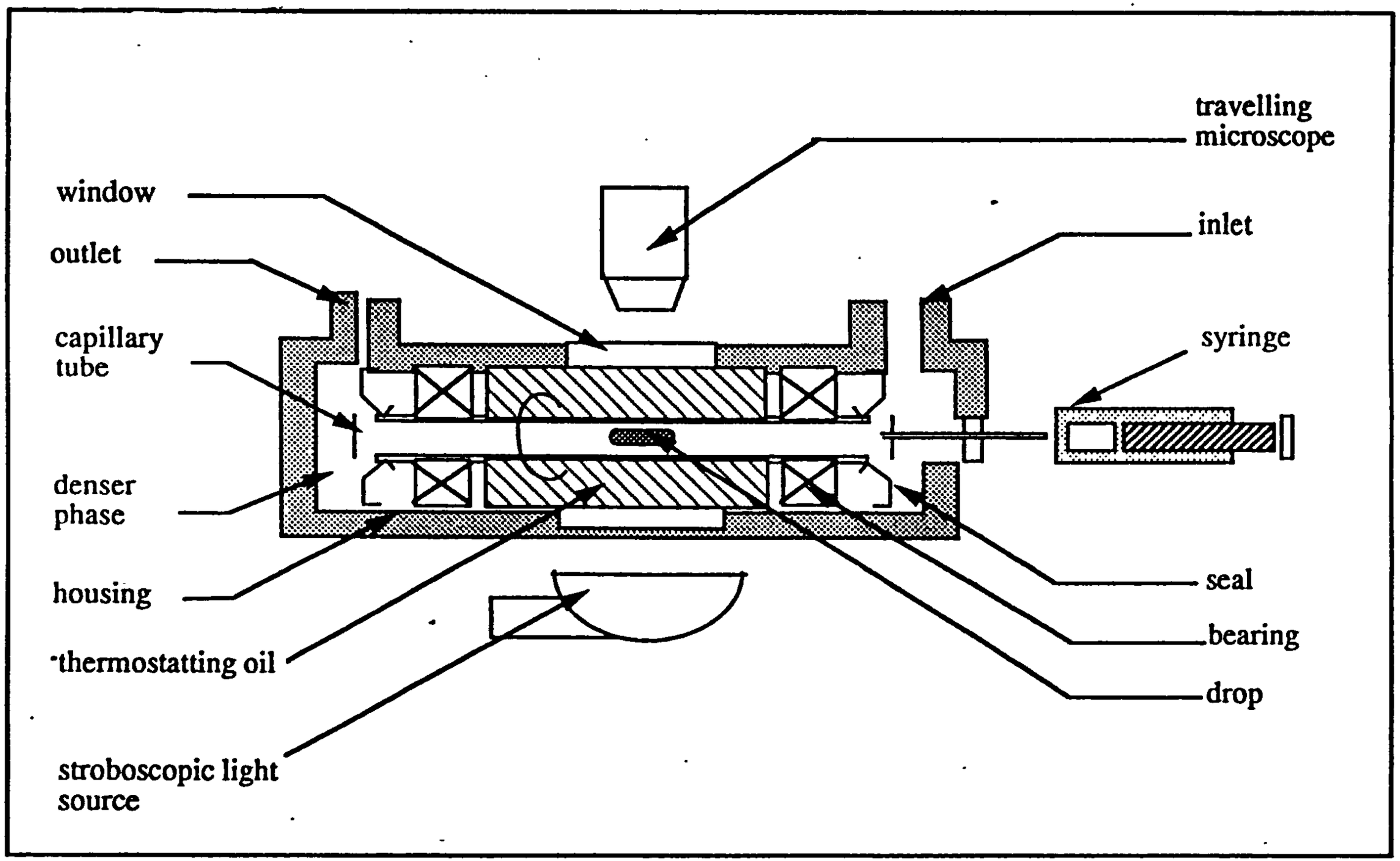

the dimensions of the drop and the densities of the two phases can be derived in several ways. Probably the simplest method is that developed by Vonnegut, who sets up an expression for the energy of the drop and solves it for the equilibrium shape in which the total energy is a minimum. Couper *et al.*[83] have presented a simpler derivation of Vonnegut's equation by calculating the kinetic energy of rotation of the system from a consideration of its moment of inertia. The most thorough treatment of the problem is provided by Princen *et al.*[84] They compute drop shape factors for various extents of deformation, from slightly deformed spheres to long cylindrical droplets. They find that if the drop length exceeds about four times its width, it has a central section which is a near-perfect circular cylinder. Slattery and Chen[85] have also presented a procedure by which the interfacial tension may be calculated for all drop shapes. In this case the determination requires the measurement of both the maximum radius and maximum length of the drop, and the tension is given by

$$\gamma = 0.5\left(\frac{r_{max}}{r^*_{max}}\right)^3 \Delta\rho\omega^2 \qquad (2.3)$$

where r^*_{max} is a function of the maximum radius r_{max} and the maximum length l_{max} of the drop and ω is the angular velocity.

Determination of l_{max} is in practice difficult and introduces a source of error in the calculation of γ. However, it can be shown that if the condition $l_{max} \geq 8\ r_{max}$ is satisfied, equation 2.3 reduces to

$$\gamma = 0.25 r^3 \Delta\rho\omega^2 \qquad (2.4)$$

where r is the radius of the cylindrical part of the drop.

Equation 2.4 shows that the accuracy of this method is strongly dependent on the accuracy by which the droplet diameter (2r) can be measured. Any error in r will result in a threefold percentage error in γ. In the Krüss Site 04 instrument a precision-measuring microscope with two eyepieces of 2.5 and 3.5 times magnification is used to determine the drop diameter. After focussing on the drop, the ocular on the microscope is adjusted until the horizontal crosshair line is parallel to the upper edge of the drop. The zero on the scale is then brought to coincide with the upper edge of the drop whilst the crosshair line is made to coincide with the lower edge. The whole number of the scale reading can be seen in the ocular, the tenth and hundredth on the micrometer. Thus, optical reading of drop diameter can be made to an accuracy of three decimal places (on a vernier scale).

The measuring process is very straightforward. The capillary system is filled, through valves, with the heavy phase e.g. aqueous surfactant solution. With the tube in motion (~ 2,000 r.p.m.), a small volume of the lighter oil phase is injected from a microsyringe. The oil drop formed is brought into the field of view by inclination of the apparatus, and the rotation speed is adjusted to produce a cylindrical drop. The diameter is measured as a function of time in order that equilibrium be attained. In general, the tension quoted is from drops whose diameters remained constant for at least 1 hour. The drop volume varies depending on the tension. Typically, for ultralow tensions (< 0.1 mN m^{-1}) 5 mm^3 are injected at low speeds (~2,000 r.p.m.), but volumes as high as 50 mm^3 and speeds > 5,000 r.p.m. are needed to measure tensions of the order of 20 mN m^{-1}.

For tensions measured at temperatures above 40°C, it was necessary to degas the aqueous samples first, since air bubbles developed in the capillary. Degassing was achieved by attaching a water pump and causing the solution to foam.

2.4.4 Vapour adsorption apparatus

The surface tension of an aqueous solution can be lowered by the adsorption of oil. By measuring the variation of the tension lowering with the oil activity, the oil adsorption isotherm can be determined.

The adsorption isotherms for the volatile PDMS oils (0.65 and 1 cS) were measured by determination of the solution-vapour tension as a function of oil vapour pressure. The apparatus employed was built in-house[49] and is shown schematically in Figure 2.8. A stream of nitrogen gas is filtered using a column of activated charcoal (Puritube, Phase Separation Ltd.) and saturated with oil vapour by passage through several oil bubblers at temperature T_3 set to be a few degrees centigrade above the temperature of the adsorption isotherm (25°C). The vapour saturated nitrogen is passed through two long glass spirals fitted with receivers to trap condensed liquid thermostatted at a lower temperature T_2. Since T_2 is the lowest temperature in the gas flow train, condensation occurs in the spirals until the silicone oil vapour reaches its saturation value at T_2. Silicone oil vapour condensation occurred only in the first spiral indicating that equilibration of the vapour pressure is complete within the first spiral. The vapour stream is then fed through an additional spiral and water bubbler at the adsorption temperature T_1 in order to achieve temperature equilibrium

Figure 2.8

Schematic diagram of the vapour adsorption train

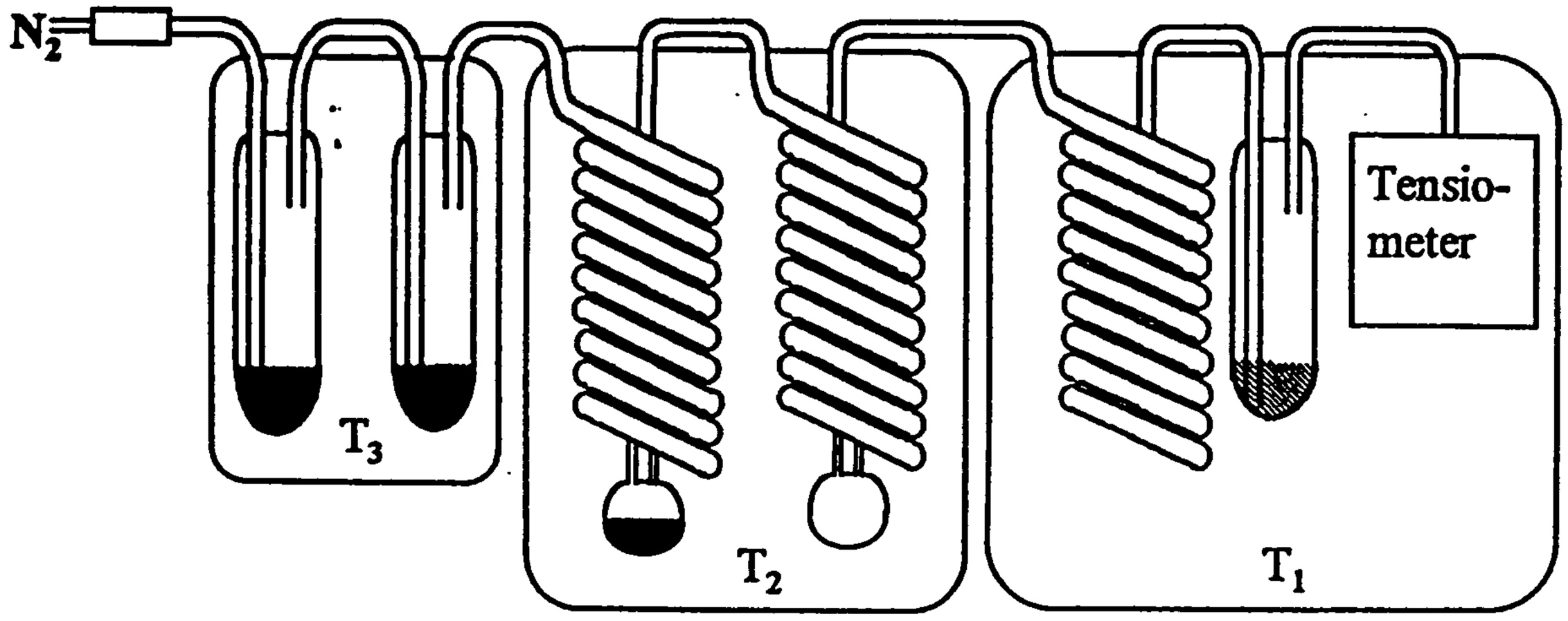

and saturation of the vapour stream with water. Finally, the gas stream enters the tensiometer chamber where it fills the vapour space above the surfactant solution. Assuming ideal gas behaviour, the silicone oil activity is equal to the relative pressure P/P_o, where P is the vapour pressure of the silicone oil in the gas stream (determined by T_2) and P_o is the saturation vapour pressure at T_1, calculated using the Clausius-Clapeyron equation:[86]

$$\frac{d\ln p}{dT} \approx \frac{\Delta_{vap}H}{RT^2} \tag{2.5}$$

where R is the gas constant, $\Delta_{vap}H$ (J mol^{-1}) is the enthalpy of vaporisation for silicone oil at temperature T. Integrating equation 2.5 gives,

$$\ln P = \frac{-\Delta_{vap}H}{RT} + \text{constant} \tag{2.6}$$

which can be related to the vapour pressure of the adsorbing oil at T_1 and T_2. Assuming that $\Delta_{vap}H$ is independent of temperature, equation 2.6 becomes,

$$\ln\frac{P}{P_o} = -\frac{\Delta_{vap}H}{R}\left(\frac{1}{T_2} - \frac{1}{T_1}\right) \tag{2.7}$$

where P_o is the saturation vapour pressure of the oil vapour at the adsorption temperature T_1. Thus the activity of the adsorbing oil can be determined from the enthalpy of vaporisation using equation 2.7. The value of $\Delta_{vap}H$ used to determine the PDMS oil activity was derived from the pressure versus temperature data given in the Dow Corning data sheet.[1]

The surface tension was determined using the static, maximum pull exerted on a du Noüy ring in the aqueous surface. The pull was adjusted to the maximum value manually using a precision laboratory jack (Ealing) and

the maximum pull was measured using a Precisa 125A balance from which the ring was suspended. The tension is calculated using equation 2.1 as described earlier. It was ascertained that blowing pure nitrogen over the solution (in the absence of silicone oil) did not affect the measured tension. In the presence of silicone oil vapour, tensions were independent of gas flow rate over the range 500 to 1500 cm^3 min^{-1}, and a flow rate of 1000 cm^3 min^{-1} was used for the measurements. In order to ensure that the gas flow train had no 'cold spots', the entire apparatus was contained within a tent which was air thermostatted to a temperature a few degrees above T_1. Repeated cycles of passing silicone oil vapour over the solution followed by exposure to a stream of pure nitrogen caused the tension to switch reversibly between the values with and without silicone oil. A constant tension was reached within about a minute of exposure to oil vapour and remained constant thereafter for up to several hours.

2.5 Analytical determinations

2.5.1 Determination of ionic surfactant

To determine quantitatively for AOT, the two-phase Epton titration[87] was employed. The principle of the method is that an anionic surfactant reacts with a cationic material to form a salt which usually loses surfactant properties and dissolves in an organic phase. The end point is determined by a mixed indicator. The mixed indicator is a mixture of an anionic dye Disulfan Blue and a cationic dye Dimidium Bromide dissolved in an acidic aqueous solvent. The cationic surfactant used is a tetra-substituted ammonium salt, Hyamine 1622. The endpoint is very distinctive. The

mechanism of the colour changes which take place in a two-phase titration by using the mixed dyes is as follows:

$$CD/AS + AD + CT \rightarrow AD/CT + CD + CT/AS$$

where, CT, AS, AD and CD are the Cationic Titrant, Anionic Sample, Anionic Dye and Cationic Dye respectively.

The colour change with Dimidium Bromide/Disulfan Blue mixed indicator is observed in the chloroform layer, which is coloured pink in the presence of excess of anionic sample and blue with excess cationic titrant. The endpoint is a grey-blue colour which probably coincides with the complete transfer of Dimidium Bromide to the water layer and the transfer of a very small quantity of the Disulfan Blue cationic salt to the chloroform layer. The clarity of the mixed indicator is superior to that on any indicator for two-phase titrations which have been examined.

The data concerned with the stoichiometry of the reaction indicates that one mole of anionic-active material reacts with 0.96-0.97 moles of Hymine. It appears desirable to employ a pure anionic-active material as reference standard, therefore, in order that this deviation from true stoichiometry does not affect the accuracy of the analysis. Analytical tests indicated that the specially purified grade of sodium dodecyl sulphate (SDS) obtained from B.D.H. was of adequate purity for use as a reference standard.

The method described above may be applied to the analysis of alkyl sulphates, alkylbenzene sulphonates and dialkylsulphosuccinates amongst others. The accuracy of the method is of the order of ± 2% of the determined value. A weighed amount of SDS from B.D.H. was dried in a clean oven at

105-110°C for 4 hours. After cooling, an exact amount of SDS was weighed to make a 0.004 mol dm^{-3} solution in water. The Hyamine was then standardised by taking 20.0 cm^3 of this solution, adding 10 cm^3 of water, 15 cm^3 of AnalaR chloroform and 10 cm^3 of the acid indicator solution, This was titrated with 0.004 mol dm^{-3} Hyamine solution, with vigorous shaking between each addition.

A similar titration procedure was employed to determine unknown concentration of surfactant in equilibrium aqueous, oil or third phases. At least two determinations were made per sample.

2.5.2 Karl Fischer titration of water

The analysis for water in oil phases was performed via the Karl Fischer technique using a Baird and Tatlock AF3 automatic titrator. The method, as formulated by Fischer and modified by Smith *et al.*[88], relies on the chemical reaction between iodine, sulphur dioxide and water in the presence of anhydrous methanol and pyridine. It may be represented as:

$$SO_2 + I_2 + H_2O + 3C_5H_5N \rightarrow 2C_5H_5N.HI + C_5H_5N$$

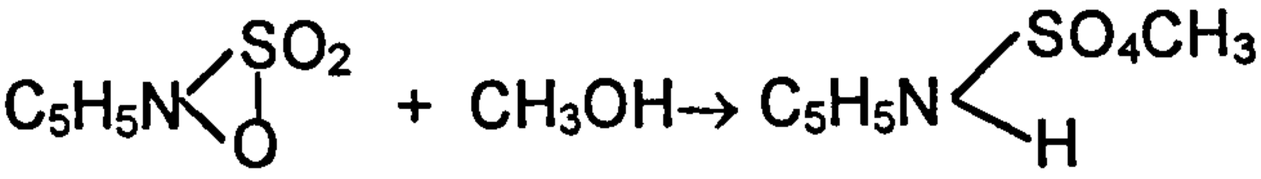

Since each mole of iodine is equivalent to one mole of water, the principle is that the sample is dissolved in a moisture free solvent e.g. methanol, and titrated with standardised Karl Fischer reagent to an endpoint detected in this case electrometrically.

Prior to any measurements, the initial calibration using pure water was necessary in order to determine the water equivalent of the Karl Fischer reagent (BDH) due to the instability of the reagent. Care was taken to ensure

that the conditions of the determination conformed as closely as possible to those of standardisation. Weighed amounts of oil phase were then admitted to the titration vessel as quickly as possible and a digital readout of mg H_2O was taken. At least two separate determinations were made for each solution. The accuracy was better than 1 mg cm^{-3} and concentrations were always greater than 5 mg cm^{-3}.

2.6 Additional experimental techniques

2.6.1 Conductivity

The conductivity of emulsions was measured using a Peak Scientific PTI-58 digital conductivity meter with a Pt/Pt black dip cell. The sample tube was thermostatted using a Grant LTD 6 or a Haake F3 thermostat.

2.6.2 Density

The densities of the oil and aqueous phases required for the calculation of γ were measured using a Paar DMA 55 densimeter. Thermostatting was by means of a Hetofrig water thermostat.

2.6.3 Refractive index

An Abbé refractometer (Hilger) and sodium lamp were employed to measure the refractive indices of samples. Thermostatting was by means of a Hetofrig water thermostat.

2.6.4 Viscosity measurements

When an aqueous surfactant micellar solution incorporates oil, the micelle shape may change, which is reflected by the viscosity of the solution. For example, if the micelle shape changes from a sphere to a cylinder, the viscosity rises. The measurement of the viscosity was done by using an Ubbelohde capillary viscometer, thermostatted by immersion in a water bath controlled to ± 0.1°C. The time t required for a given volume of solution to flow through the capillary was measured. The flow time of the solutions are related to the kinematic viscosity. It is sufficient for our purposes to determine the relative viscosity for the system. The viscosity of the solution (η) relative to that of the solvent (η_o) can be calculated by

$$\frac{\eta}{\eta_o} = \frac{t}{t_o}\frac{\rho}{\rho_o} \approx \frac{t}{t_o} \qquad (2.8)$$

where t and t_o are the flow times of the solution and the solvent respectively with densities ρ and ρ_o.

2.6.5 Image analysis of emulsions

Microscope images of emulsions allows one to view the distribution of emulsion droplets and sometimes to measure the contact angle of two or more flocculated drops. In the image analysis system, the optical equipment consists of a Nikon Labophot microscope, using an LWD Achromat condenser (numerical aperture N.A. = 0.65) and an LWD Achromat 40x Nikon objective (N.A. = 0.65). The images were recorded with a Hitachi CCTV camera (model HV-720K) which was connected to a DIC-U Imaging

Software for Windows system via a frame grabber. Frames were stored digitally as 512 x 512 pixels with 0-255 grey levels.

After homogenisation of the emulsions (5 vol% dispersed phase), samples were diluted with aqueous electrolyte solutions containing surfactant at the cmc. Small samples (< 0.2 cm^3) were then taken from the middle of the diluted emulsion and spotted onto a clean microscope slide. A coverslip was positioned over the sample, and was bridged at either end by coverslip spacers (approximately 0.2 mm clearance). This prevented the droplets being compressed which could give rise to a possible erroneous size distribution. The emulsion was viewed and the image of the emulsion was printed out.

2.7 Laser diffraction for sizing emulsions

A Malvern 2600c laser diffractometer (resolution limit 1 μm) was used to measure the drop size distributions in emulsions.[89]

Figure 2.9 shows the basic configuration of the instrument. A low power helium-neon laser provides a collimated and monochromatic beam of light which is incident on the emulsion sample. The light is diffracted by the emulsion droplets, circulating with liquid in the small volume sample presentation unit: larger drops scatter at small angles and small drops at large angles. The scattered light is incident on the receiver lens. This operates as a Fourier transform lens forming the far field diffraction pattern of the scattered light at its focal plane. The special configuration of the receiver lens means that regardless of the position or movement of the drops its diffraction pattern is stationary and focuses onto the multi-element photo-

Figure 2.9

Schematic diagram of the 2600c laser diffractometer

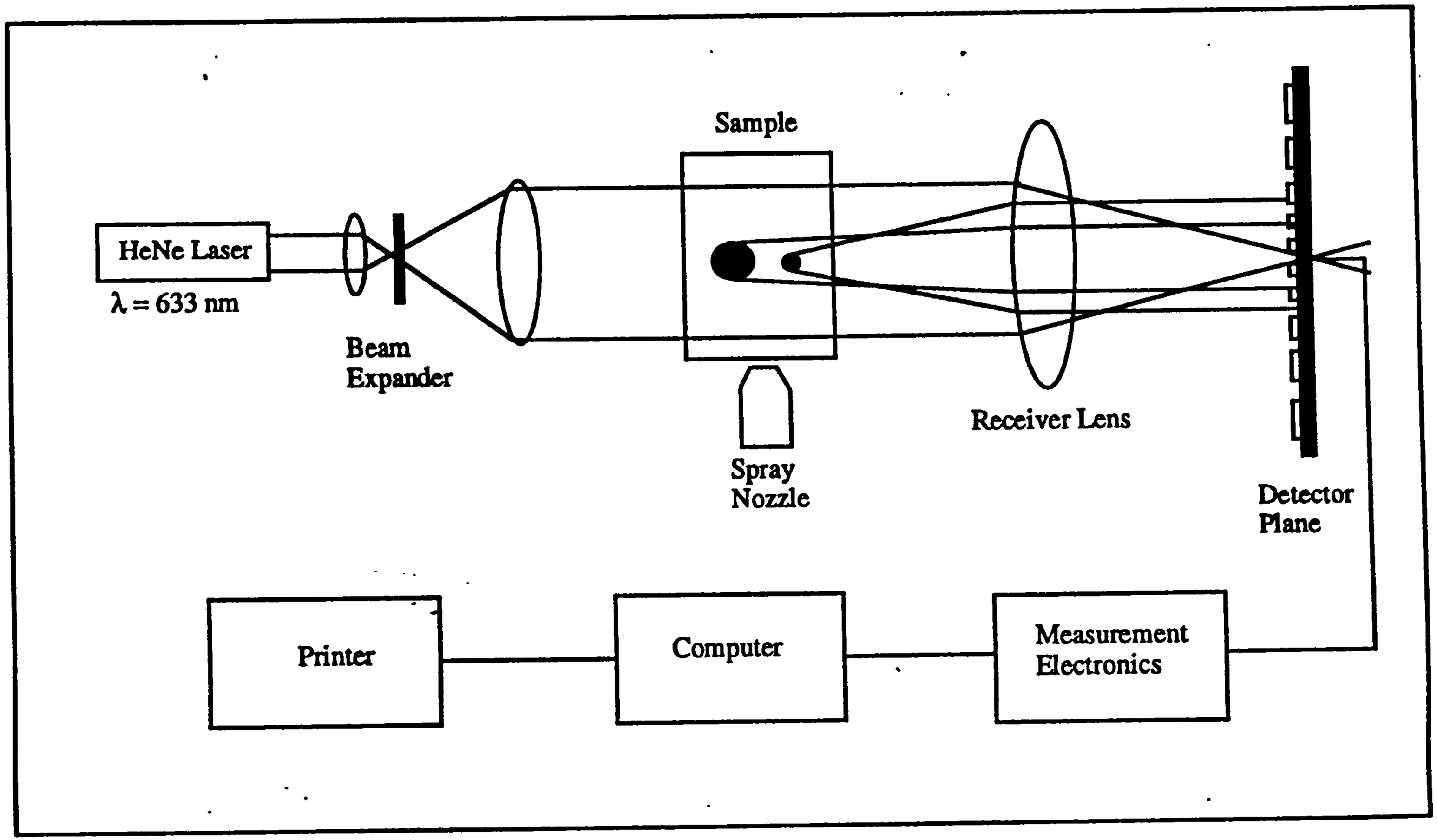

electric detector. Each element produces an electronic output signal proportional to the light intensity falling on it. The computer reads this signal and performs time averaging from successive detector readings over the designated measurement time which means a representative bulk sample of the drops contributes to the final diffraction pattern. The computer deduces the volume size distribution by constrained least squares fitting of theoretical scattering to the observed data. Results are presented as a histogram of volume frequency and the cumulative volume undersize on a log scale. The volume diameter d (v, 0.5) is defined as the diameter such that 50% of the volume of drops are ≤ this value. Typically, two or three drops (0.1 - 0.2 cm^3) of emulsion immediately after homogenisation were diluted into ~200 cm^3 of aqueous electrolyte solutions containing surfactant at the cmc corresponding to the particular salt concentration. Emulsion preparation and sizing were all performed at ambient temperature (23°C).

2.8 Neutron reflectivity

Neutron reflection gives information on the neutron refractive index profile normal to an interface and is a powerful investigative tool in studying mixed films of oil+surfactant at surfaces. The neutron reflectivity measurements of PDMS oils on various nonionic surfactant solutions were performed in collaboration with Prof. T. Cosgrove and Dr. R.M. Richardson at the University of Bristol. The experiments were carried out on the NG7 reflectometer at the cold source reactor in NIST, Gaithersburg, Maryland, USA. The surfactant solution was contained in a PTFE trough. The trough was enclosed in a sealed double-walled temperature controlled

compartment, as described elsewhere.[90] A known amount of PDMS was added by syringe to the surface through a small re-sealable inlet. The deuterated PDMS-protonated surfactant-D_2O contrast was utilised.

CHAPTER THREE

CHAPTER 3

Emulsion Phase Inversion in Nonionic Surfactant Systems

3.1 Introduction

In this chapter, the emulsion type and phase inversion temperatures (PIT) in emulsions made from equal volumes of PDMS oil and aqueous nonionic surfactant solutions were investigated. Aggregates of nonionic surfactant usually dissolve in the water phase at low temperature, and dissolve in the oil phase at high temperature. The preferentially adsorbed nonionic surfactant at the oil-water interface forms an adsorbed monolayer. The convex or concave curvature of the adsorbed monolayer against water (oil) is closely related to the dissolution state of the nonionic surfactant. The hydration forces between the hydrophilic groups of surfactant and water are stronger at lower temperatures, and the adsorbed monolayer may have a convex curvature toward water. The resulting emulsion is an o/w type. As the temperature increases, the hydration force between the head groups and water gradually decreases. The convex curvature of the adsorbed monolayer towards water will gradually change to a concave curvature, and a w/o emulsion results.[91] Accordingly, at the intermediate temperature the emulsion undergoes phase inversion. This temperature refers to *phase inversion temperature* (PIT). The PIT is naturally related to the type, inversion and stability of emulsions. It is also closely related to the optimum

temperature for the solubilisation of oil in aqueous surfactant solutions and of water in nonaqueous surfactant solutions. Hence, the PIT is an experimental value which reflects all variables, such as the concentration of surfactant, the type of oil and the effect of additives.

In many surfactant systems, it has been shown that the type of emulsion formed from an equilibrium microemulsion plus its excess phase is the same as that of the microemulsion.[28, 92] Thus, homogenisation of the two phases in a Winsor I system produces an oil-in-water (o/w) emulsion. In addition, macroemulsions invert from oil-in-water to water-in-oil (w/o) or vice-versa at or around the same conditions as the corresponding microemulsion. This fact is useful in rapidly locating the experimental window of interest for microemulsions, since emulsion type can readily be determined by simple conductivity measurements. For o/w emulsions, the continuous phase is water and therefore has high conductivity. For w/o emulsions, the continuous phase is oil and hence the conductivity is low.

For the systems containing nonionic surfactants, a low level of electrolyte (0.01 M) was added to the aqueous phase in order to examine the type of the continuous phase, and o/w emulsions which conduct form at low temperatures inverting to non-conducting w/o emulsions at higher temperatures. The PIT's of the emulsions were determined as a function of the system HLB variables such as surfactant concentration, surfactant chain length, surfactant headgroup size, electrolyte concentration and PDMS oil molecular weight (viscosity). The surfactants employed were conventional C_nE_m, extended nonionics $C_{16}P_8E_1$ and $C_{16}P_4E_1$ and a silicone surfactant Silwet L-77.

3.2 C_nE_m surfactant systems

3.2.1 Conductivity of PDMS oils and aqueous salt

The PDMS oils contain Si^+-O^- weak dipole moments (2.8 D)[4] in their molecules. It was necessary to establish whether the conductivity of neat PDMS oils is affected by temperature. Therefore, the conductivity of all the PDMS oils was measured as a function of temperature and found to be less than 0.1 $\mu S\ cm^{-1}$ from 5 to 70°C. This is similar to the conductivity of most of the hydrocarbon oils. In comparison, the conductivity of 0.01 M NaCl aqueous solution was also measured which amounts to 233 $\mu S\ cm^{-1}$.

3.2.2 Effect of surfactant concentration on the PIT

The nonionic surfactant $C_{12}E_5$ has been extensively used in the research fields of emulsions and microemulsions. Part of the reason is its moderate cloud point (31°C) which is easy to modify to lower or higher values. This was our standpoint for choosing it as the surfactant in this systematic study. Figure 3.1 shows how the emulsion conductivity varies with temperature for 50 cS PDMS+0.01 M aq. NaCl (1:1)+$C_{12}E_5$ mixtures for different concentrations of surfactant. It can be seen that emulsions are conducting at low temperatures (< 50°C) but become less conducting above ~ 52°C. Although the conductivity at high temperature does not fall to the conductivity of neat PDMS oil (< 0.1 $\mu S\ cm^{-1}$), the temperature at which it changes markedly may be indicative of phase inversion to w/o emulsions. It is observed that below this temperature, the emulsions are white, foaming and stable. Above it the emulsions become less stable and non-foaming. The instability of the emulsion at high temperature can be explained by the

Figure 3.1

Variation of emulsion conductivity with temperature for the systems:
0.01 M NaCl + 50 cS PDMS oil (1:1 volume), plus x% (in water)
$C_{12}E_5$

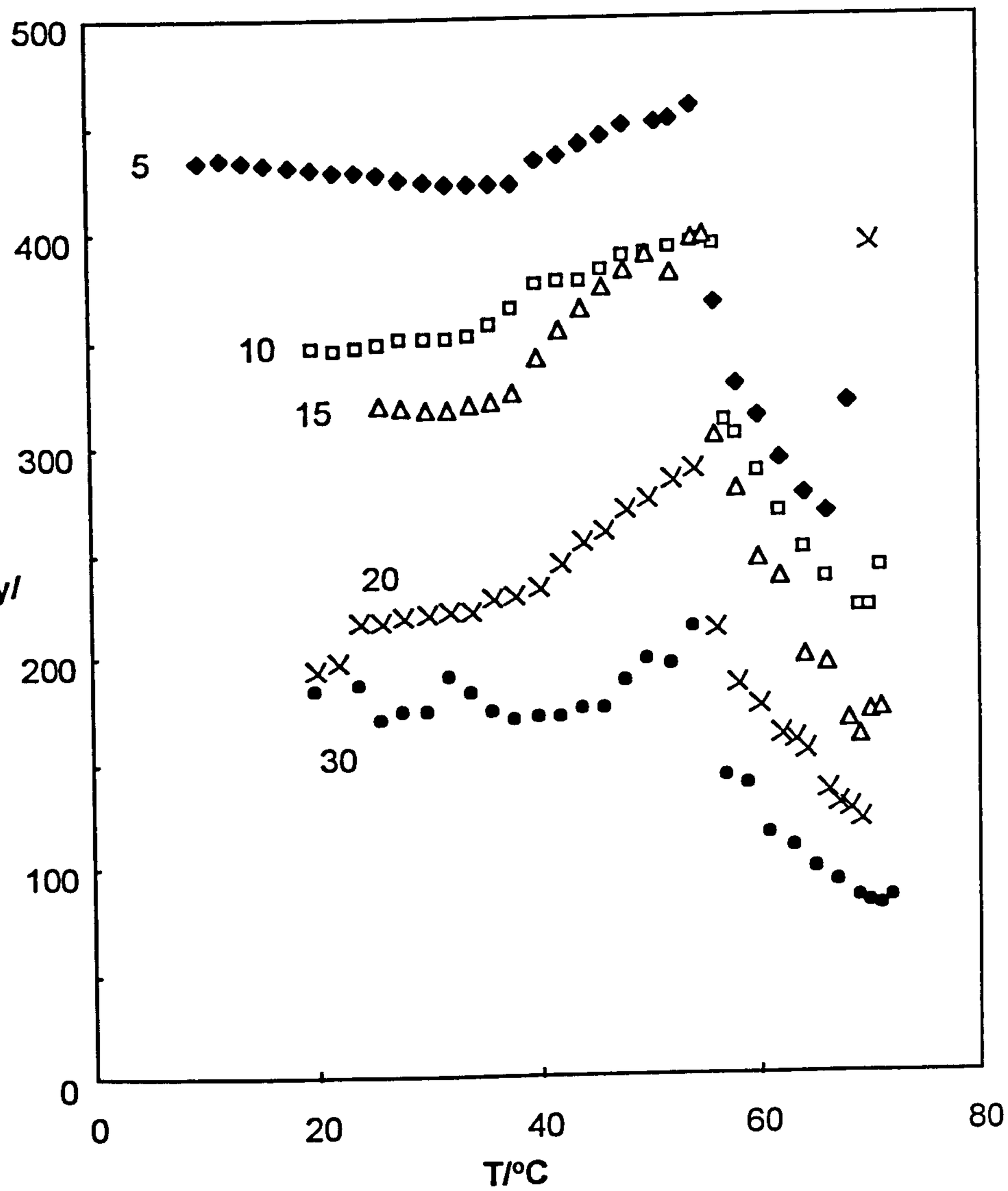

thermal motion of the molecules and the low viscosity of the continuous phase.[93] This temperature is virtually independent of surfactant concentration, a result known for alkane oil systems with pure surfactants when the overall surfactant concentration is above the cmc,[34] indicating there is enough surfactant in the system to cover the emulsion droplets and the surfactant is pure $C_{12}E_5$ not a mixture of its homologues. The decrease in the magnitude of the conductivity with increasing surfactant concentration may arise due to a number of effects. Firstly, the average emulsion drop size will decrease but the volume fraction of drops (approximately equal to the volume fraction of dispersed phase + surfactant) will increase causing a fall in conductivity due to obstruction. Alternatively, the salt concentration in water itself decreases as surfactant dilutes the aqueous phase. A third possibility is that sodium ions may bind to the ethyleneoxide moieties of the surfactant via ion-dipole forces and thus reduce the mobility of such ions. The apparent phase inversion temperature or PIT for this surfactant is similar to the PIT of the emulsion where octadecane is the oil.[94]

3.2.3 Variation of the PIT with surfactant structure

It is expected that in an emulsion system where the aqueous composition and oil are fixed, the longer the hydrophilic headgroup in the nonionic surfactant, the higher the PIT. The reason is obvious since the PIT correlates with the cloud point in the binary surfactant-water system. The longer the hydrophilic headgroup, the stronger the hydration force between the surfactant and water, the higher the cloud point will be. For alkane as oil, the change in PIT is found to be approximately 14°C per oxyethylene

group.[95] This also holds in PDMS oil systems as well. Figure 3.2 shows the effect of the number of E groups in the headgroup, and hence the surfactant hydrophile-lipophile balance (HLB), on the emulsion behaviour for a fixed chain length (12 carbons) at 10% surfactant. Emulsions are non-conducting and probably w/o for $C_{12}E_2$ at all temperatures investigated, whereas they are conducting and probably always o/w for $C_{12}E_6$. For $C_{12}E_3$, the conductivity of o/w emulsions decrease to low values at ~ 30°C followed by a sharp increase again to 40°C. Emulsions are then extremely unstable, separating into separate phases typical of three phase emulsions in under two minutes, between 40 and 65°C so that no conductivity can be determined. They re-stabilise as w/o emulsions above 65°C. This system may be phase inverting through three phase emulsions known to be unstable. For $C_{12}E_4$, the conductivity of o/w emulsions initially increases with temperature and decreases around 20°C. Overall, the temperature at the onset of the change in conductivity (and hence apparent phase inversion) decreases with a decrease in the number of ethyleneoxy groups, but it is difficult to specify this increment.

Conductivity of emulsions containing 10% surfactant in which the head group is fixed at E_5 are given in Figure 3.3 where the alkyl chain length is varied from 10 to 16. $C_{10}E_5$ emulsions remain o/w with increasing temperature, whereas the other chain length surfactants show sharp changes in conductivity at particular temperatures. This temperature decreases with an increase in the chain length, from about 54°C for C_{12} to 29°C for C_{16}. In alkane emulsion systems the PIT decreases 10°C as the nonionic surfactant chain length increases one CH_2 unit. Kahlweit[96] has

Figure 3.2

Variation of emulsion conductivity with temperature for 0.01 M NaCl + 50 cS PDMS oil (1:1), plus 10% (in water) $C_{12}E_m$

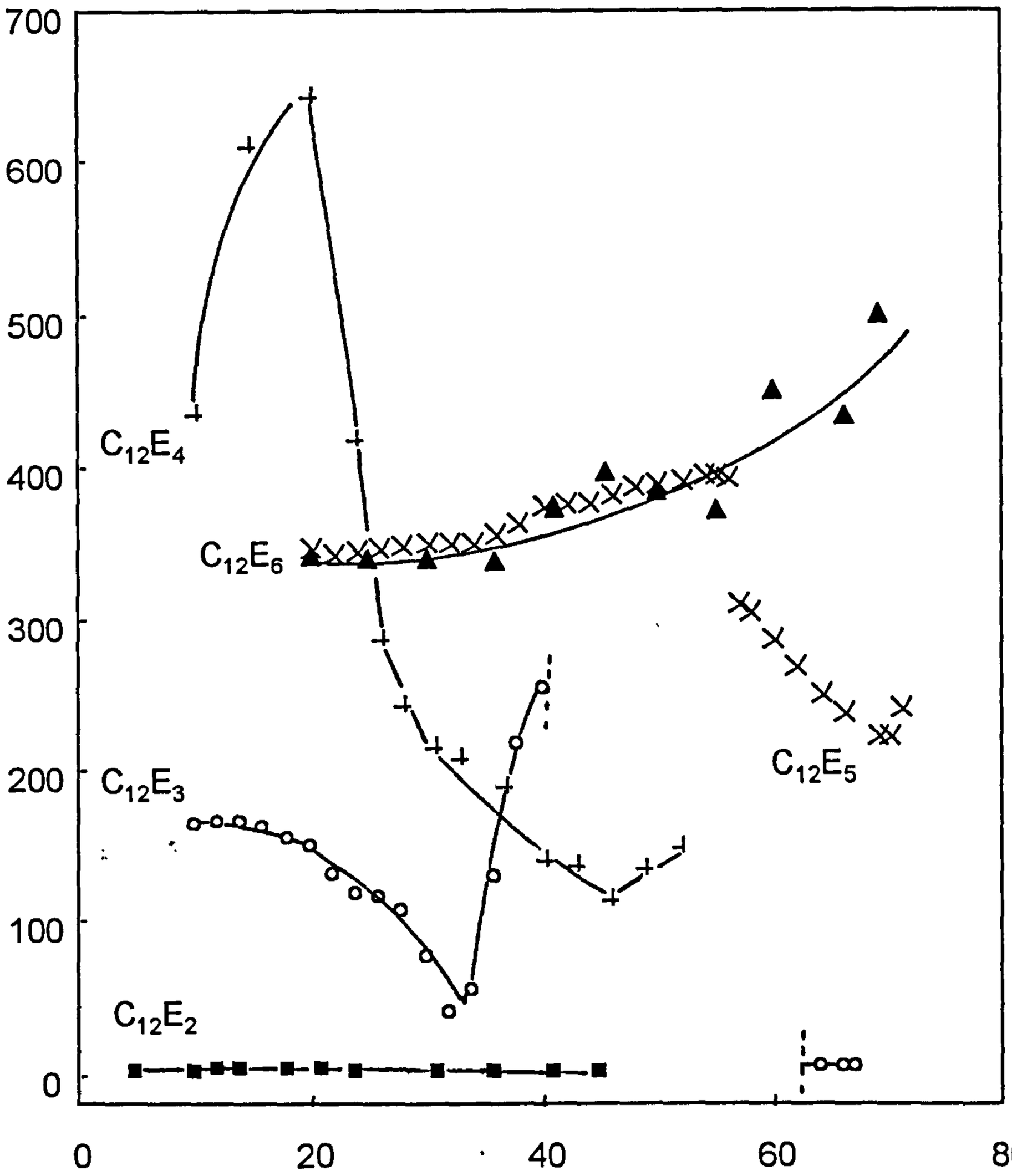

Figure 3.3

Variation of emulsion conductivity with temperature for 0.01 M NaCl + 50 cS PDMS oil (1:1), plus 10% (in water) C_nE_5

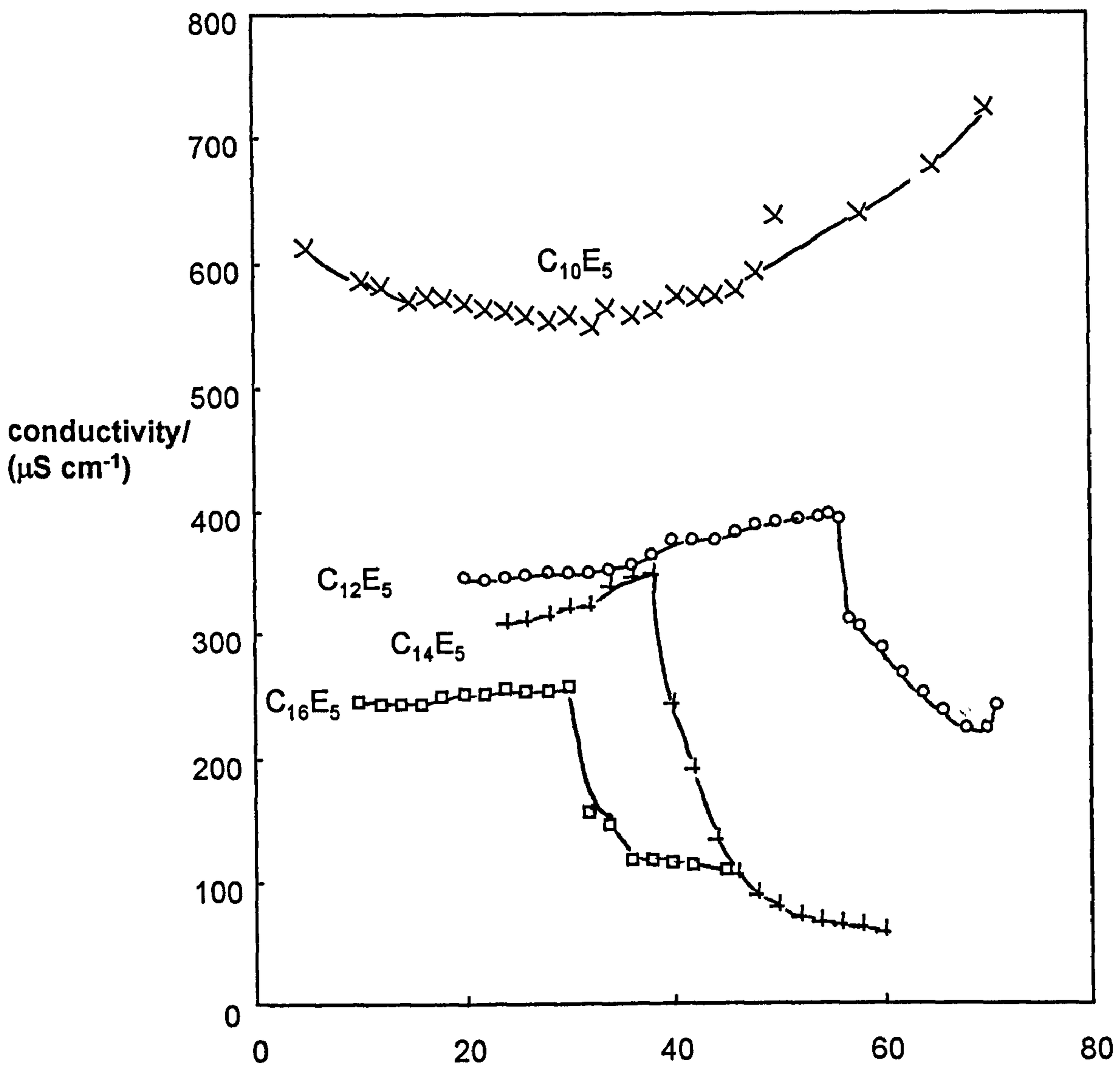

correlated the shape of the emulsion conductivity/temperature curves with the amphiphilic strength of the surfactant in water-alkane emulsions. The curves are very shallow for surfactants like C_4E_1 which form weakly structured mixtures but become sharper and more pronounced as one moves to longer chain surfactants like $C_{12}E_5$ which form structured microemulsions. A similar change in the type of curve with PDMS as oil can be observed here.

Table 3.1 lists the PIT's of PDMS oil (50 cS) emulsions as a function of surfactant structure. For those systems where no phase inversion occurred in the experimental temperature range, the emulsion type is given (o/w or w/o). Also given are the cloud points of these surfactants taken from the literature.[95] Clearly, the higher the cloud point, the higher the PIT. This correlation holds for silicone oil systems as well.

Table 3.1 Relation between the PIT of PDMS emulsions and cloud point for C_nE_m nonionic surfactants

surfactant	m or n	PIT / °C or emulsion type	cloud point / °C refers to column 5	%surf.
$C_{12}E_m$	2	w/o from 5-70°C	< 0	/
	3	16	< 0	/
	4	24	7.0	0.8
	5	54	31.5	1
	6	o/w from 5-70°C	53.0	1.5
C_nE_5	10	o/w from 5-70°C	45.5	2.1
	12	54	31.5	1
	14	40	20	/
	16	29	/	/

3.2.4 Effect of electrolyte concentration on emulsion phase inversion

In anticipation of work on the phase behaviour at constant temperature, we have also investigated the effect of electrolyte concentration on the possible inversion of emulsions. It is known that electrolyte has a significant effect[34] on an emulsion phase inversion. Systems can be phase inverted from o/w to w/o with salt alone, this is related to the effect of electrolyte on aqueous surfactant properties such as the cloud point and the cmc[34]. The effect of added salts on the PIT, cloud point, cmc and/or surface activity of nonionic surfactant exhibits the same trend.[97,98] It is generally accepted that the added electrolytes affect the solvent property of water, hence the activity of nonionic surfactant.[99] We have chosen two types of electrolyte. One is sodium chloride (NaCl), a lyotropic salt which decreases the mutual solubility between water and surfactant and reduces the PIT in nonionic systems. The other is tetrabutylammonium bromide (TBAB), a hydrotropic salt which increases the mutual solubility between water and surfactant and which increases the PIT.[100]

Figure 3.4 shows how the emulsion conductivity falls at a specific NaCl concentration with temperature, although non-conducting emulsions never form. The temperature at the onset of the change decreases with added salt being only 12°C in 4 M NaCl. This is due to the fact that NaCl salts out the surfactant into the oil phase by dehydration.[101] With TBAB (Figure 3.5), emulsions became very unstable in 0.01 M salt above 45°C as with NaCl, probably approaching three phase emulsions. However, further increase in temperature did not produce w/o emulsions, indicating a wide three phase region. In 0.1 and 1 M TBAB, the emulsions become more

Figure 3.4

Emulsion conductivity vs temperature for x M NaCl
+ 50 cS PDMS oil (1:1), plus 10% (in water) $C_{12}E_5$

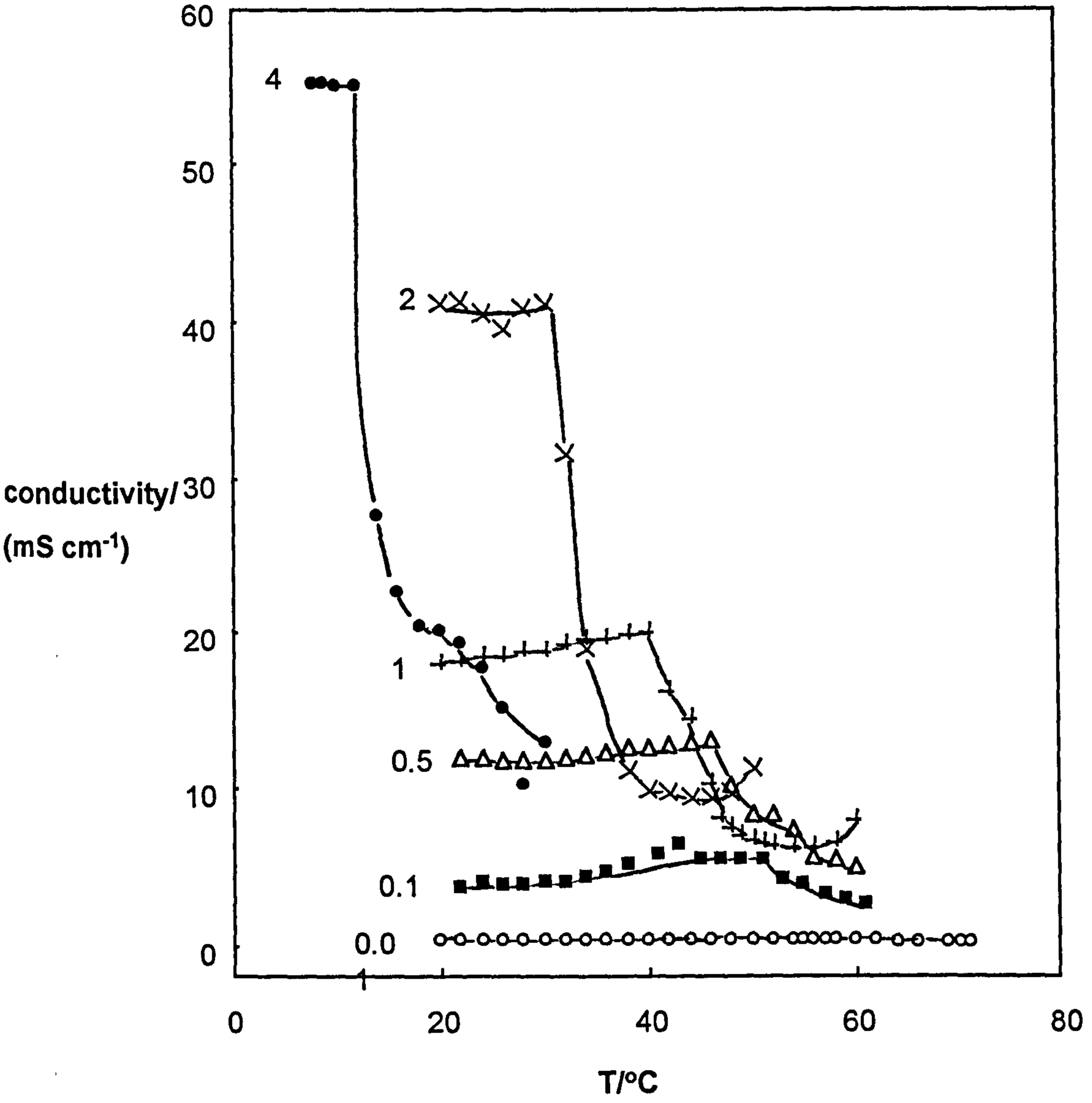

Figure 3.5

Emulsion conductivity vs temperature for x M TBAB + 50 cS PDMS oil (1:1), plus 10% (in water) $C_{12}E_3$

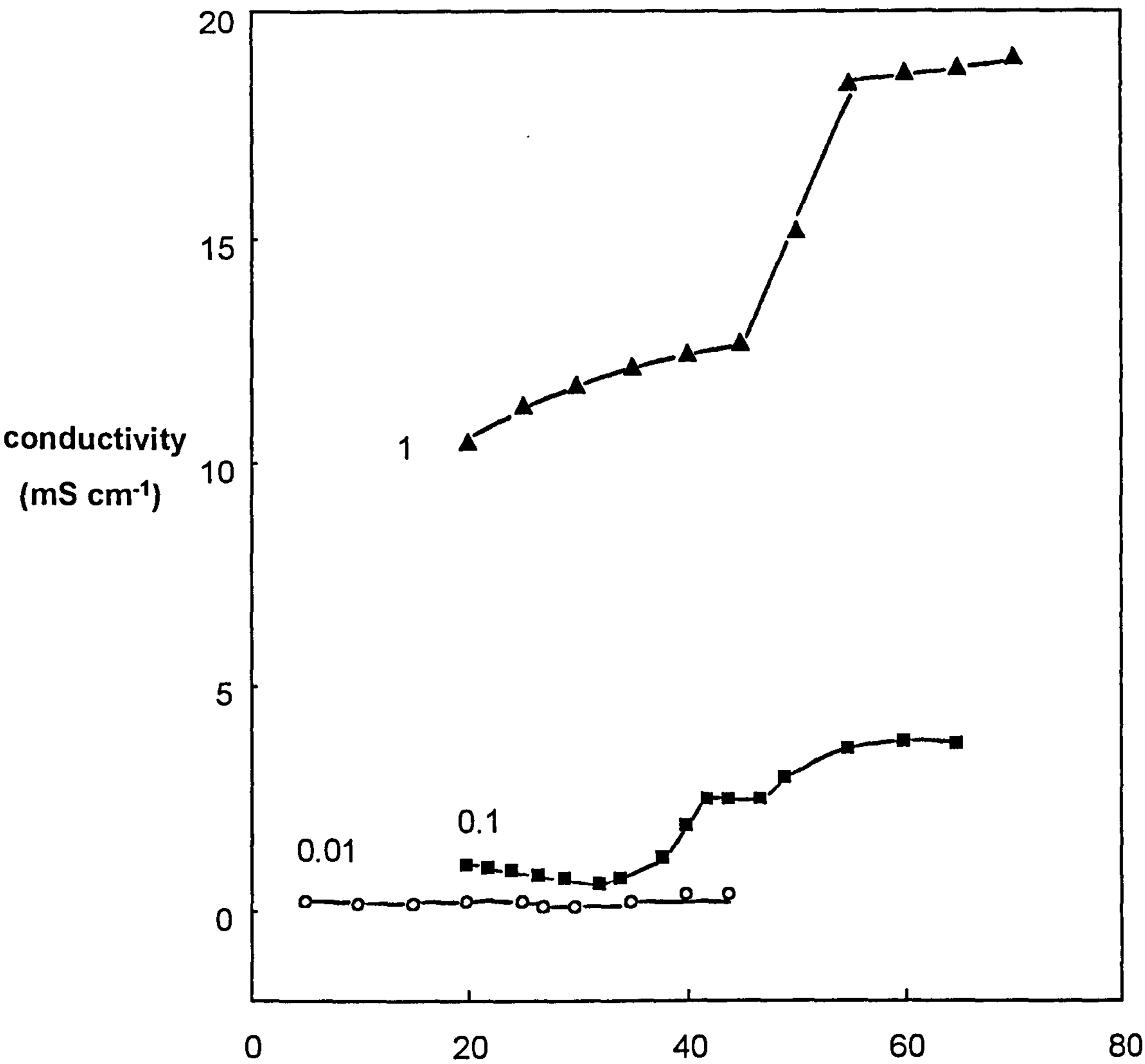

stable and the conductivity only increases with temperature, indicating that the PIT has probably been raised (salting-in) to over 70°C, the limit of these experiments. Tetraalkylammonium salts are known to have hydrophobic effects on nonionic surfactants due to hydrotropy.[101] This means that TBAB can break the structure of water and reduce the extent of hydrogen bonding among the water molecules, thereby increasing the hydration of the oxyethylene groups by hydrogen bonding, which elevates the cloud point of $C_{12}E_3$ in water and hence, increases the PIT of the emulsions. The conductivity of the emulsions is plotted as a function of [TBAB] at 18°C in Figure 3.6; no phase inversion occurs at this temperature.

3.2.5 Effect of oil molecular weight on emulsion phase inversion

The PIT in an emulsion differs widely for different oils.[102] This is related to the solubility of the emulsifier in the various oils. The more soluble the oil for a given hydrated nonionic surfactant, the lower the PIT. The higher the cloud point in aqueous surfactant solution saturated with various oils, the higher the PIT.[103] For PDMS oils, the PIT for different molecular weights (viscosity) was determined with $C_{12}E_2$ as surfactant. Figure 3.7 shows the effect of PDMS oil molecular weight on the PIT for 10% surfactant. We recall in Figure 3.2 that with 50 cS PDMS oil, the emulsions are w/o throughout the whole temperature range. On increasing the PDMS oil viscosity to 100 cS, the emulsion becomes conducting until the temperature reaches 28°C, at which the conductivity decreases to a very low value within a narrow temperature range (2°C), indicating complete phase inversion. The PIT increases with an increase in molecular weight from 50 cS to 100 cS as

Figure 3.6

Emulsion conductivity vs [TBAB] for 10% (in water) $C_{12}E_3$ + 50 cS PDMS oil (1:1) at 18° C

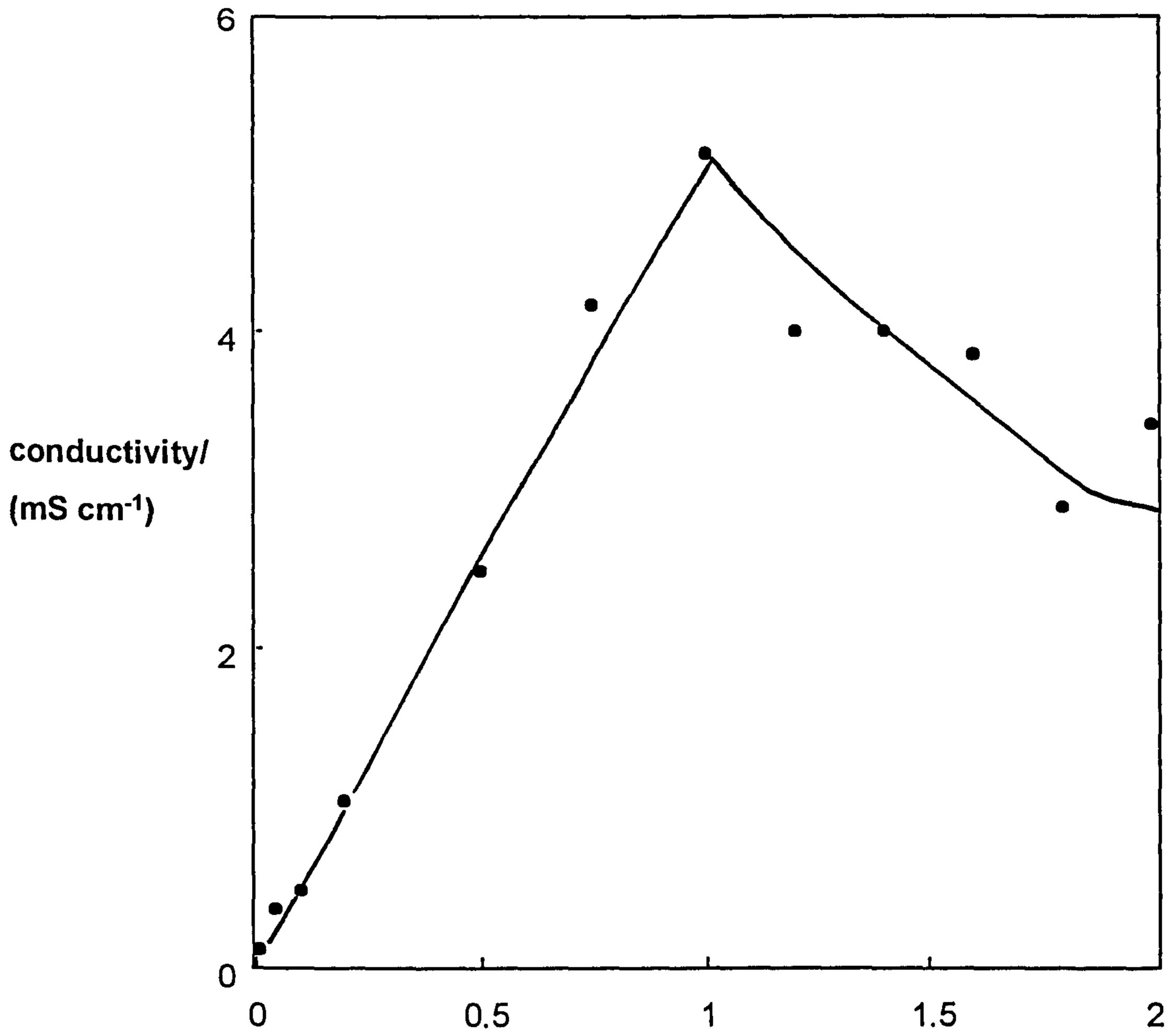

Figure 3.7

Variation of conductivity vs temperature of the system:
10% $C_{12}E_2$ + x cS PDMS oils + 0.01 M NaCl

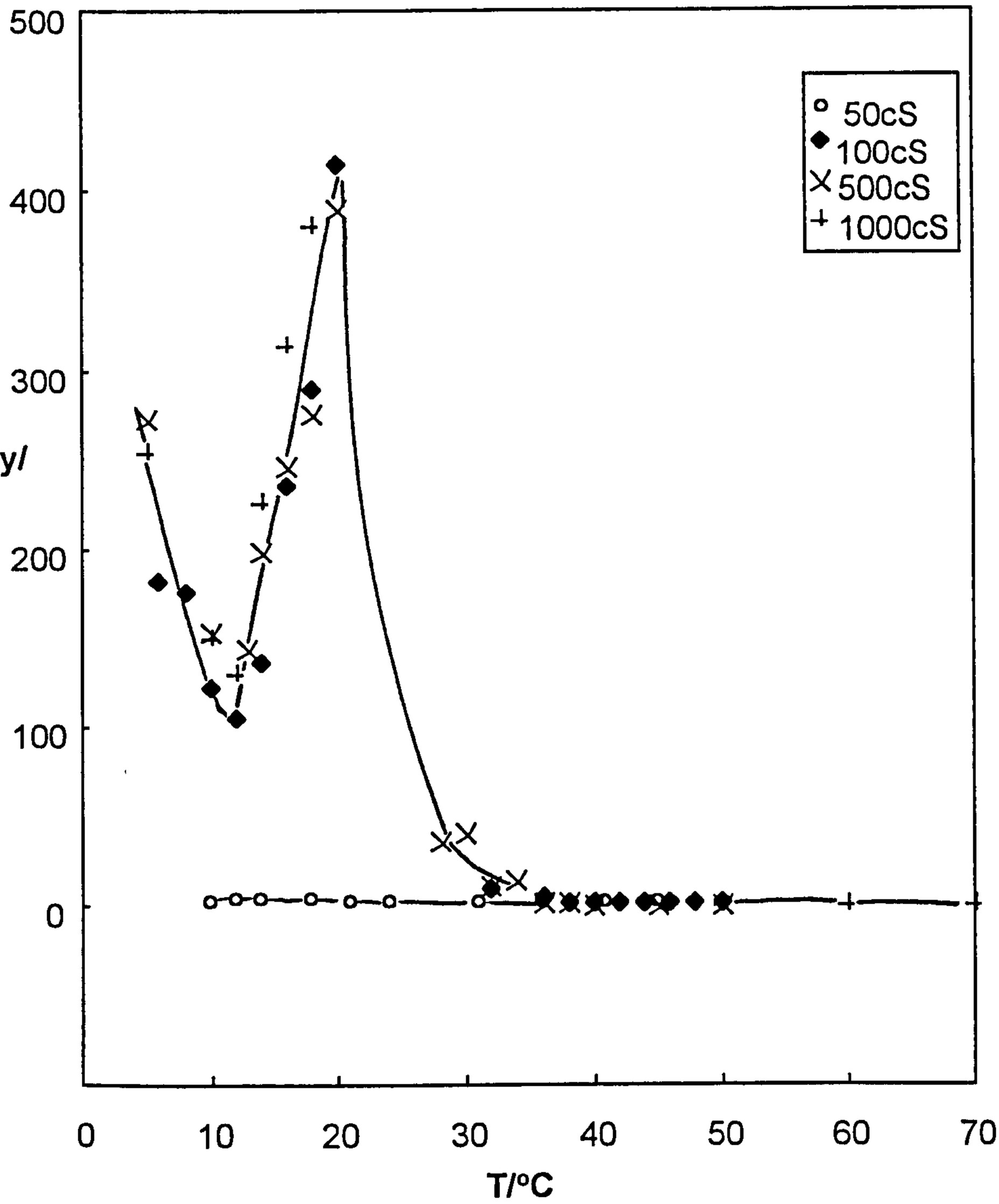

expected. However, by increasing the oil viscosity further beyond 100 cS there is no significant change in this behaviour. The reason may be that the PDMS oils are commercial products which are blends of different chain lengths. Low molecular weight components may be preferentially solubilised into the surfactant chain region which is responsible for the change in the cloud point and the PIT. However, in the absence of knowledge concerning the ratio of the individual component in PDMS oils, it is hard to interpret the data here. The PIT's of emulsions in which the oil phase consists of alkane mixtures are expressed as follows:[104]

$$\text{PIT (mixture)} = \text{PIT (A)}\ \phi_A + \text{PIT (B)}\ \phi_B \qquad (3.1)$$

where ϕ_A and ϕ_B are the volume fractions of oils A and B, and PIT (mixture), PIT (A) and PIT (B) are the phase inversion temperatures of emulsions in which the oil phase consists of an oil mixture, oil A and oil B, respectively. Thus, the PITs of emulsions of oil mixtures are given exactly by the volume (or weight) average of the individual PITS. In the case of PDMS oils, the lack of change in the PITs when the PDMS viscosity varied from 100 cS to 1000 cS indicates that this equation is invalid for higher viscosity PDMS oil mixtures.

3.3 Emulsion phase inversion in other surfactant systems

3.3.1 Extended surfactant

Minana-Perez *et al.*[105] have synthesised so-called *extended* surfactants in which propyleneoxide (P) groups are inserted between the usual hydrocarbon chain and an ethyleneoxy sulphate head group. These surfactants are capable of allowing significant solubilisation of triglyceride

oils (which are notoriously difficult to solubilise with ordinary surfactants) into aqueous solutions. It is unclear however whether this effect is due to the increase in the effective chain length or whether the chemical nature of the P groups in some way facilitates the oil to mix with the surfactant chains. We have obtained similar materials from Nikkol which are nonionic ended in an attempt to see if solubilisation of silicone oil becomes possible. The emulsion data is shown in Figure 3.8 for two such compounds. The $C_{16}P_8E_1$ surfactant shows *normal* phase inversion from o/w to w/o emulsions at 28°C, the first surfactant exhibiting a sharp decrease in conductivity to very low values over a narrow temperature range. The $C_{16}P_4E_1$ surfactant by contrast displays an unusual rise in the conductivity around 25°C superimposed on a typical phase inversion curve. The rise is possibly associated with emulsion instability around inversion.

In Figure 3.9, the effect of PDMS oil molecular weight on the PIT for $C_{16}P_8E_1$ is shown. Interestingly, the increase in PDMS oil molecular weight has virtually no effect on the PIT, which resembles the behaviour for $C_{12}E_2$ described earlier.

3.3.2 *Silicone surfactant (Silwet L-77)*

It is argued that chain compatibility between the oil and surfactant plays a major role in emulsions and solubilisation.[16,17,36] We chose a silicone surfactant Silwet L-77 to emulsify PDMS oils. As described earlier, L-77 has the trisiloxane hydrophobic group. The emulsion type and phase inversion with respect to temperature are shown in Figure 3.10. An apparent phase inversion occurs around 46°C, the shape of the curve resembling that of

Figure 3.8

Emulsion conductivity vs temperature for 0.01 M NaCl + 50 cS PDMS oil (1:1), plus 10% (in water) surfactant

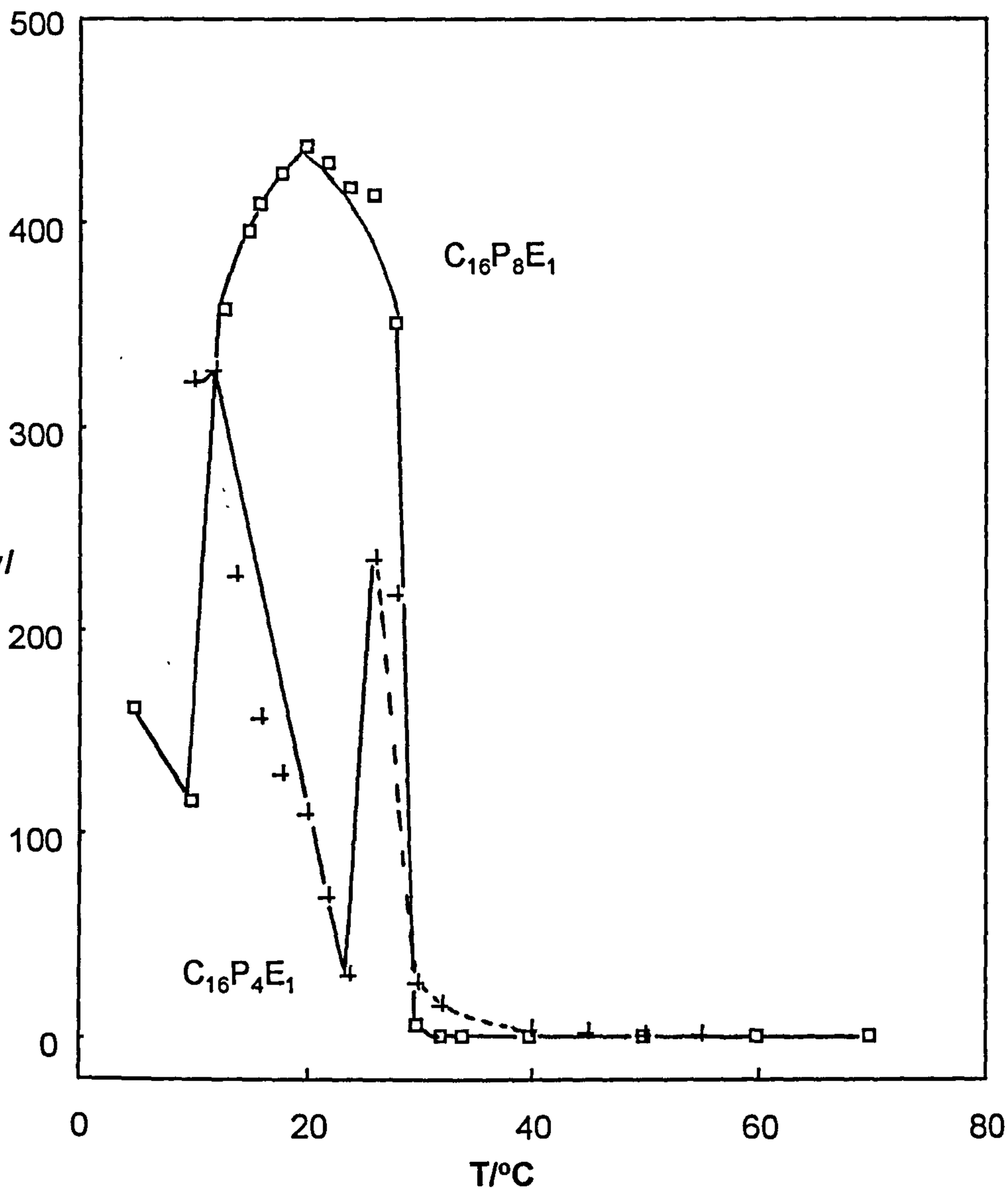

Figure 3.9

Variation of conductivity vs temperature of the system:
10% $C_{16}P_8E_1$ + x cS PDMS oils + 0.01 M NaCl

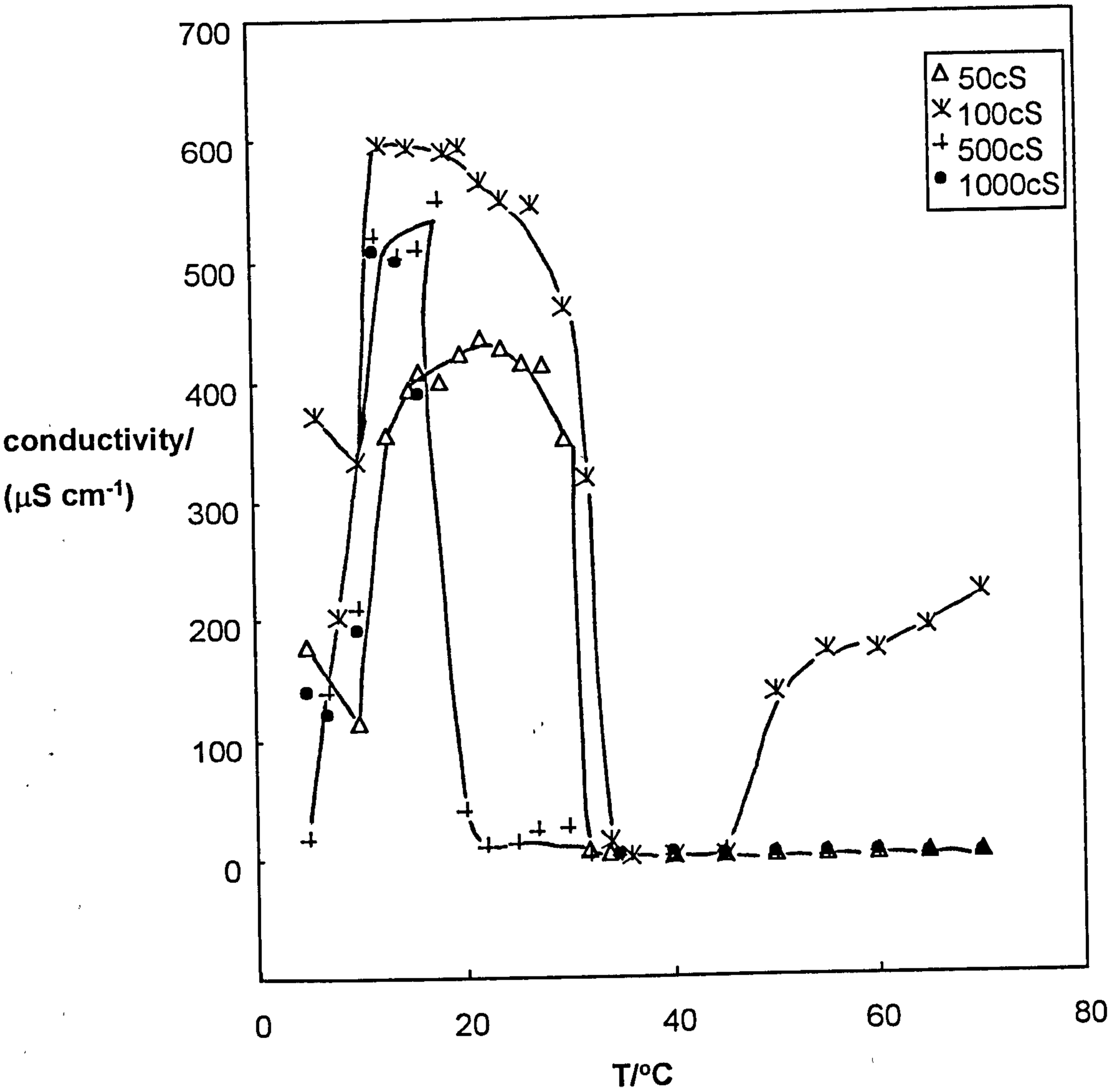

Figure 3.10

Emulsion conductivity vs temperature for 0.01 M NaCl + 50 cS PDMS oil (1:1),plus x% L-77 (in water)

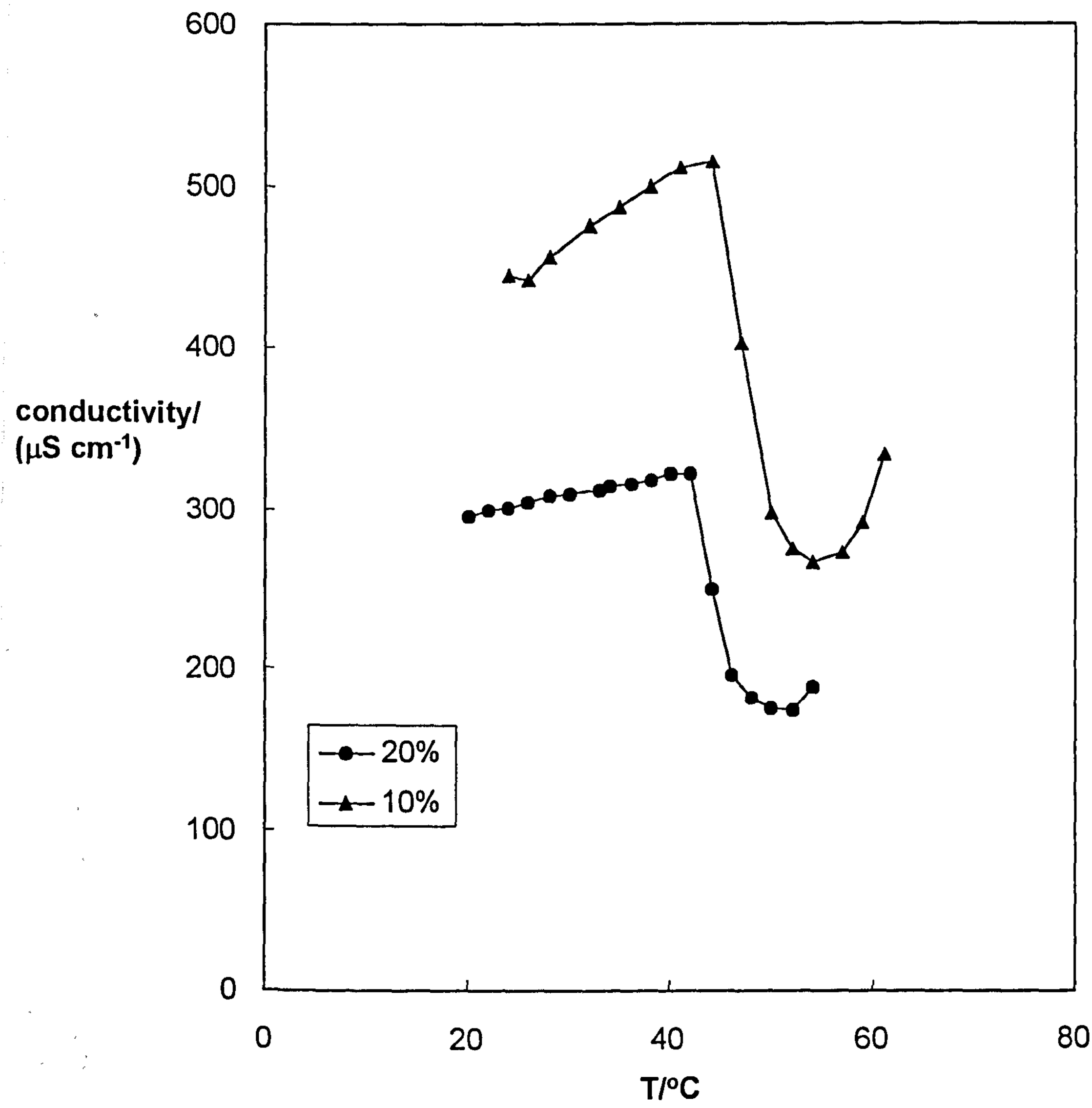

$C_{12}E_5$ as surfactant. Increasing the concentration of L-77 does not affect the PIT, even though the magnitude of the conductivity is reduced. Gradzielski *et al.*[106] showed that the hydrophobicity of the trisiloxane hydrophobe is comparable to that of the linear dodecyl hydrophobe. Molecular packing calculations of the type illustrated by Mitchell *et al.*[107] indicate that L-77 should favour lamellar packing similar to that of $C_{12}E_5$. Hill *et al.*[108] compared the water-surfactant binary phase behaviour of L-77 with that of $C_{12}E_5$ and found there are significant similarities. The similarity of the emulsion phase inversion observed here might be related to the binary phase behaviour.

3.4 Conclusions

The following conclusions can be drawn from the emulsion type and phase inversion results, which lay the foundation for the further study of the equilibrium phase behaviour of PDMS oils with surfactants and water.

(i). For C_nE_m surfactants, emulsions may be inverted from o/w to w/o with increasing temperature. The temperature at which the conductivity changes markedly increases with increasing E number (m), and decreases with increasing chain length (n).

(ii). With $C_{12}E_3$, emulsions were very unstable to coalescence around the conditions of phase inversion.

(iii). Addition of NaCl to emulsions of $C_{12}E_5$ reduces the phase inversion temperature, whereas addition of TBAB to $C_{12}E_3$ emulsions raises it.

(iv). For the extended surfactant $C_{16}P_8E_1$ complete phase inversion occurs.

(v). For the silicone surfactant Sil-wet L-77 the emulsion phase inversion resembles that for $C_{12}E_5$.

(vi). Changes in oil viscosity from 50 cS to 100 cS raises the PIT. However, further increase in viscosity from 100 cS to 1000 cS does not significantly affect the PIT.

CHAPTER FOUR

CHAPTER 4

Equilibrium Phase Behaviour in Nonionic Surfactants/PDMS/Water Systems

4.1 Introduction

The understanding of the oil-water-surfactant ternary phase behaviour is the basis for the discussion of the system properties. The properties of this system have attracted intense attention for the last two decades for both practical and theoretical reasons. The practical reasons result from the fact that with an appropriate surfactant one can prepare so-called "microemulsions". Closely related herewith is the separation of the system into three phases with ultra-low interfacial tensions between them, a property which appears to be of interest for tertiary oil recovery.[109] The theoretical reasons result from the growing interest in critical phenomena in such systems, in particular, in the properties of multicritical points.[110,111] There has been good understanding toward the system properties with hydrocarbon as oil.[112,113] There is no systematic study concerning the phase behaviour with silicone oils in the literature.

Based on the findings in chapter 3, we have selected several systems and determined the phase behaviour in 1:1 (by volume) oil:water mixtures in an attempt to understand the inversion of aggregated surfactant from water

to oil either as micelles or as microemulsion droplets. Phase changes as a function of surfactant concentration, temperature and electrolyte concentration are discussed. In addition, $C_{12}E_5$ and L-77 are chosen to explore the possibility of the formation of single phase o/w microemulsions.

4.2 Systems containing $C_{12}E_3$

In chapter 3 we found that the emulsions of 50 cS PDMS oil and water with $C_{12}E_3$ as surfactant were very unstable in the temperature range around the inversion, which is probably due to the formation of a wide three phase region. This is an interesting system to address a series of questions in the study of the equilibrium phase behaviour, e.g. how does the third phase form? What is its composition?

4.2.1 Temperature dependence of the Winsor phase transition

Figure 4.1 shows the appearance of the phase equilibria for $C_{12}E_3$ as a function of temperature in 0.01 M NaCl systems. We recall from Figure 3.2 that emulsions were impossible to stabilise in this system between 40 and 65°C, possibly owing to the formation of three phase emulsions involving low tensions, where the coalescence probability is high.[26] We observe a two phase-three phase-two phase transition with increasing temperature, with three phases forming over at least 30°C. It can be noticed that the solubilisation of oil into the third phase is low (oil volume fraction in excess phase is close to 0.5) and that, with increasing temperature, the third phase (containing mostly surfactant+water) loses water and becomes more concentrated. Eventually, above 62°C a two-phase system is formed with the

Figure 4.1

Appearance of phases at equilibrium for the system: 0.01M NaCl + 50 cS PDMS oil (1:1), plus 10% $C_{12}E_3$ at different temperatures

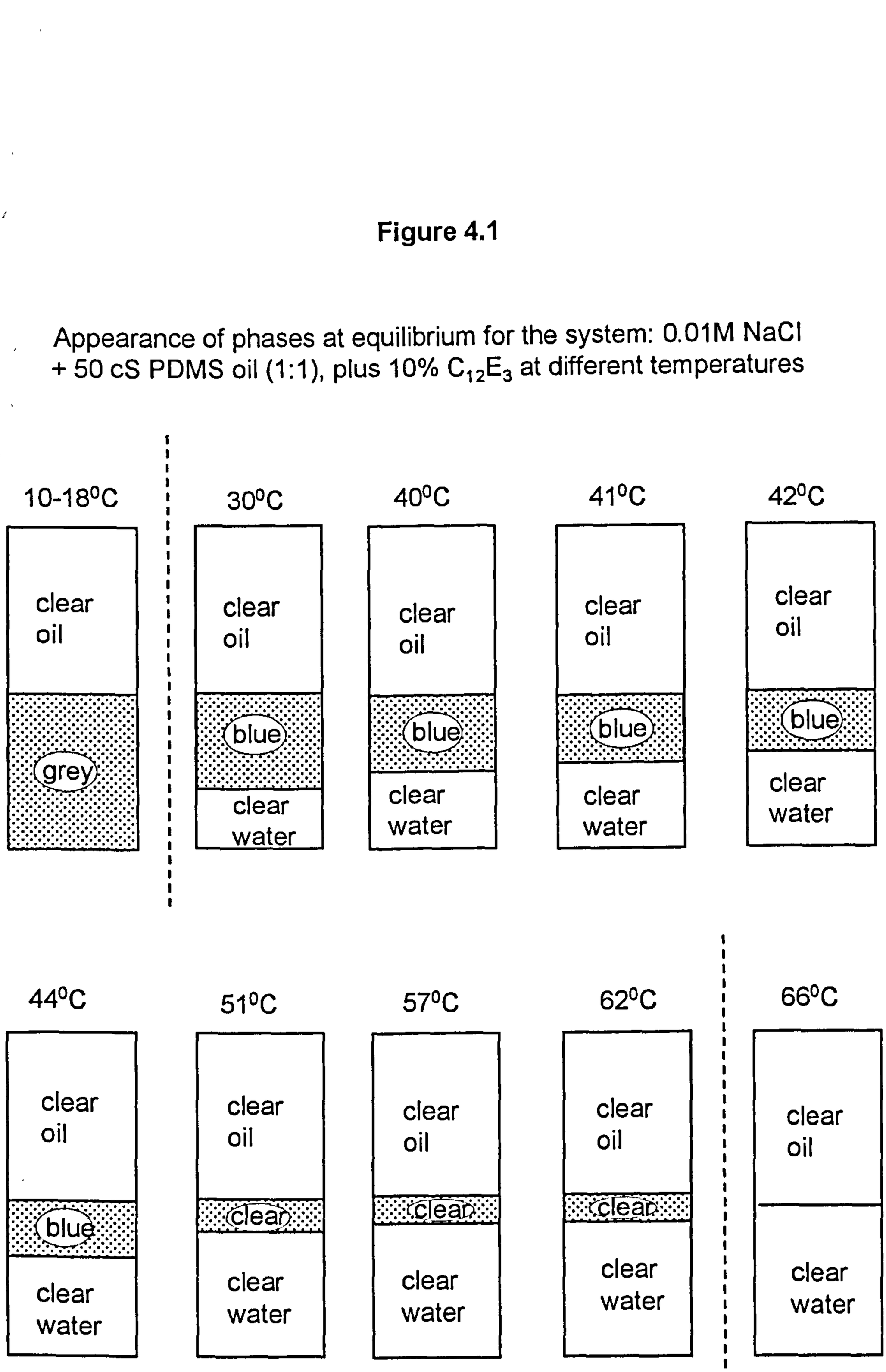

aggregated surfactant probably located in the oil phase. The behaviour seen here with temperature as the HLB variable is reminiscent of what has been observed for phase changes as a function of salt concentration in systems stabilised by the ionic surfactant Aerosol OT with long chain alkanes.[114] Here, the third phase contained little solubilised oil and its structure, determined by small angle neutron scattering, corresponded to that of the L_3 phase in which fluctuating bilayers of surfactant, swollen very slightly by oil, separate domains of aqueous solvent. The preference for this phase over that of the more common bicontinuous microemulsion (in which fluctuating surfactant monolayers separate domains of near equal volume fraction of oil and water formed with short chain alkanes) is thought to be related to the reduced extent of oil penetration into the surfactant chain region for the higher molecular weight oils. The temperature range in which a third phase is formed in the PDMS oil system resembles that where an L_3 phase appears in the binary $C_{12}E_3$-H_2O systems.[115] However, at 10% $C_{12}E_3$ in water, the L_3 phase forms at 39°C and disappears at 58.1°C, and so it appears that the presence of small amounts of silicone oil in this phase changes these temperature boundaries by several degrees. The result may be due to a change in the spontaneous curvature of the monolayer as a result of the (limited) solubilisation of silicone oil.

The solubilisation capacity of oil into aqueous surfactant micelles or the third phase is related to the oil-water interfacial tension. The post-cmc PDMS oil-water interfacial tension (γ_{OW}) is given in Figure 4.2 as a function of temperature over the three phase range, where it is virtually constant and high (2 mN m^{-1}). Also shown is that of the system with pentadecane as oil

redrawn from reference 130. For typical Winsor behaviour in alkane systems[130] the interfacial tension passes through an ultra-low value (less than 0.01 mN m^{-1}) at a certain temperature (T*, corresponding to the PIT), and a large amount of both oil and water can be solubilised into the third phase. Generally, as the alkane chain length increases, the temperature T* for minimum tension increases and the tension versus temperature curve becomes broader and more shallow. For $C_{12}E_3$, T* falls to less than 12°C for a various alkane chain length (from 7 to 15). Here, with 50 cS PDMS oil we do not observe the existence of T*, instead a wide Winsor III temperature region occurs. This indicates the low degree of PDMS oil solubilisation into the third phase as shown by the relative phase volume of each phase at equilibrium.

4.2.2 Effect of surfactant concentration

One way of increasing the solubilisation of oil into surfactant-rich third phases is to increase the overall surfactant concentration in the system at temperatures where three phases form. Figure 4.3 for 30°C is representative of the behaviour seen. At 1% surfactant, only two phases appear because this concentration is below the critical aggregation concentration in the system. The latter can be viewed as the sum of the critical micelle concentration (cmc) in water (typically low for these surfactants, ~ 10^{-5} M) and the critical micelle concentration in oil (can be as high as 10^{-2} M).[116] By 2% surfactant, three phases form, the volume fraction of the third phase increasing with further surfactant addition at the expense of the excess water phase. Figure 4.4, in which the phase volume fractions are plotted against

Figure 4.2

Post cmc PDMS-water interfacial tension as a function of temperature in pre-equilibrated $C_{12}E_3$ aqueous+50 cS PDMS systems (circles), triangles are those for pentadecane systems redrawn from ref. 130

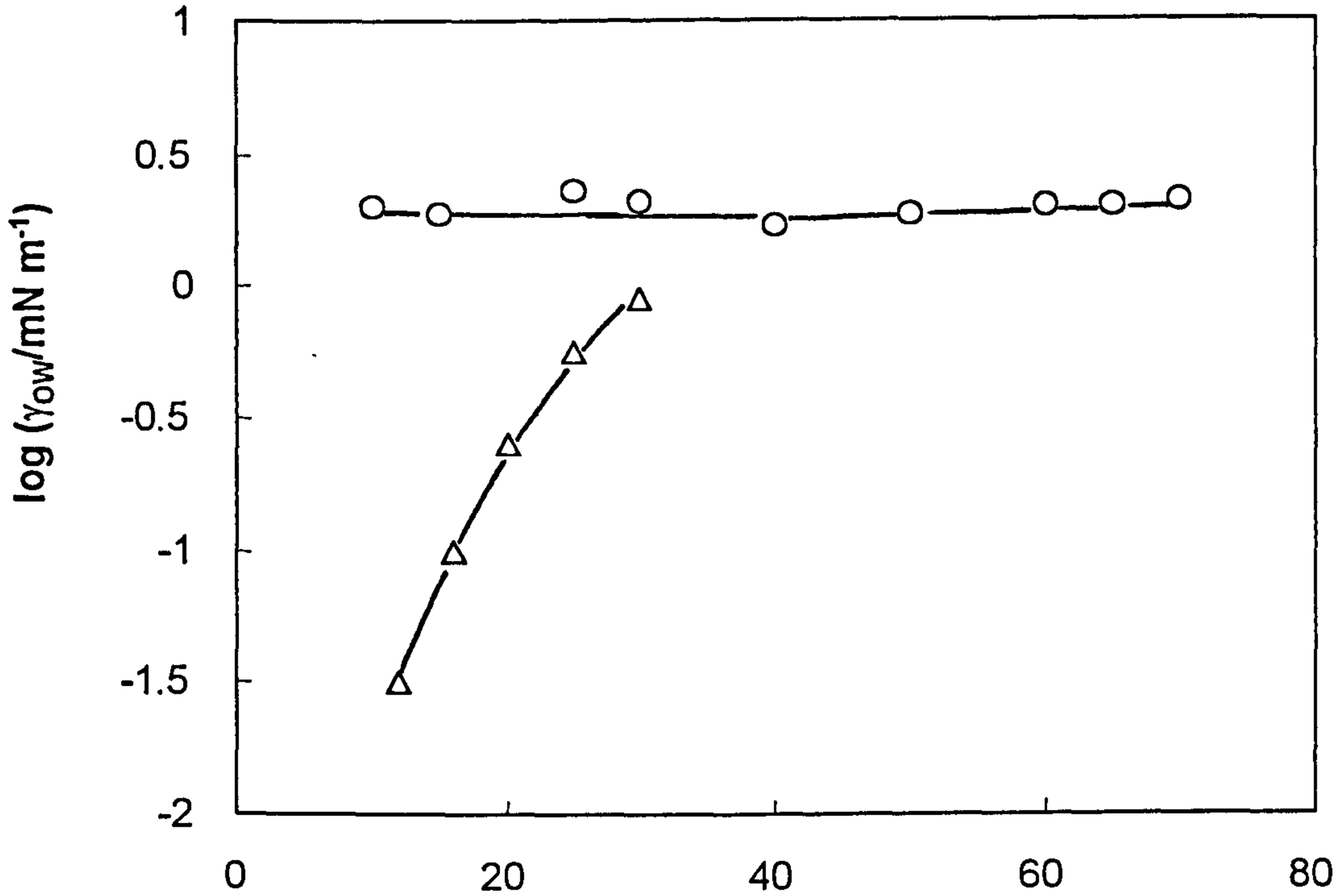

Figure 4.3

Appearance of phases at equilibrium for the system: 0.01 M NaCl+50 cS PDMS oil (1:1), plus x% $C_{12}E_3$ in aqueous phase at 30°C

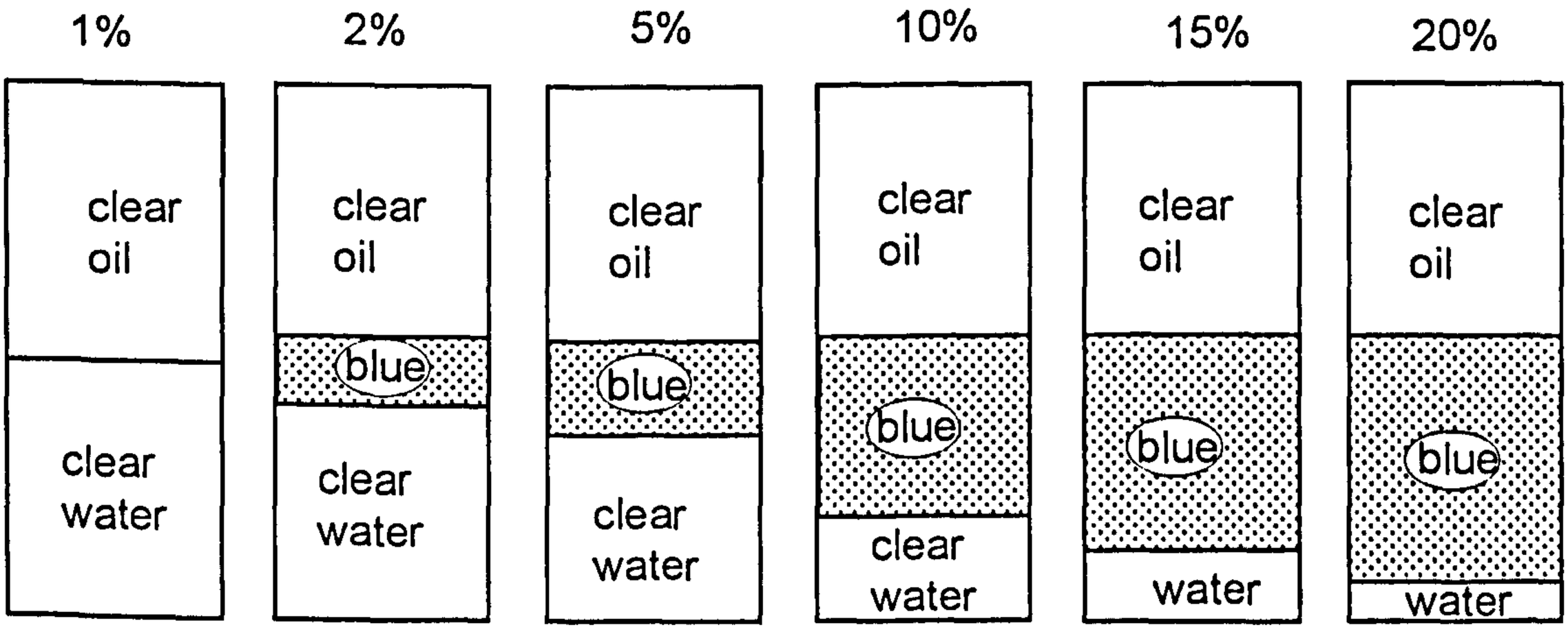

Figure 4.4

Effect of [surfactant] on the volume fraction of each phase for 0.01 M NaCl + 50 cS PDMS oil (1:1), plus $C_{12}E_3$ at different temperatures

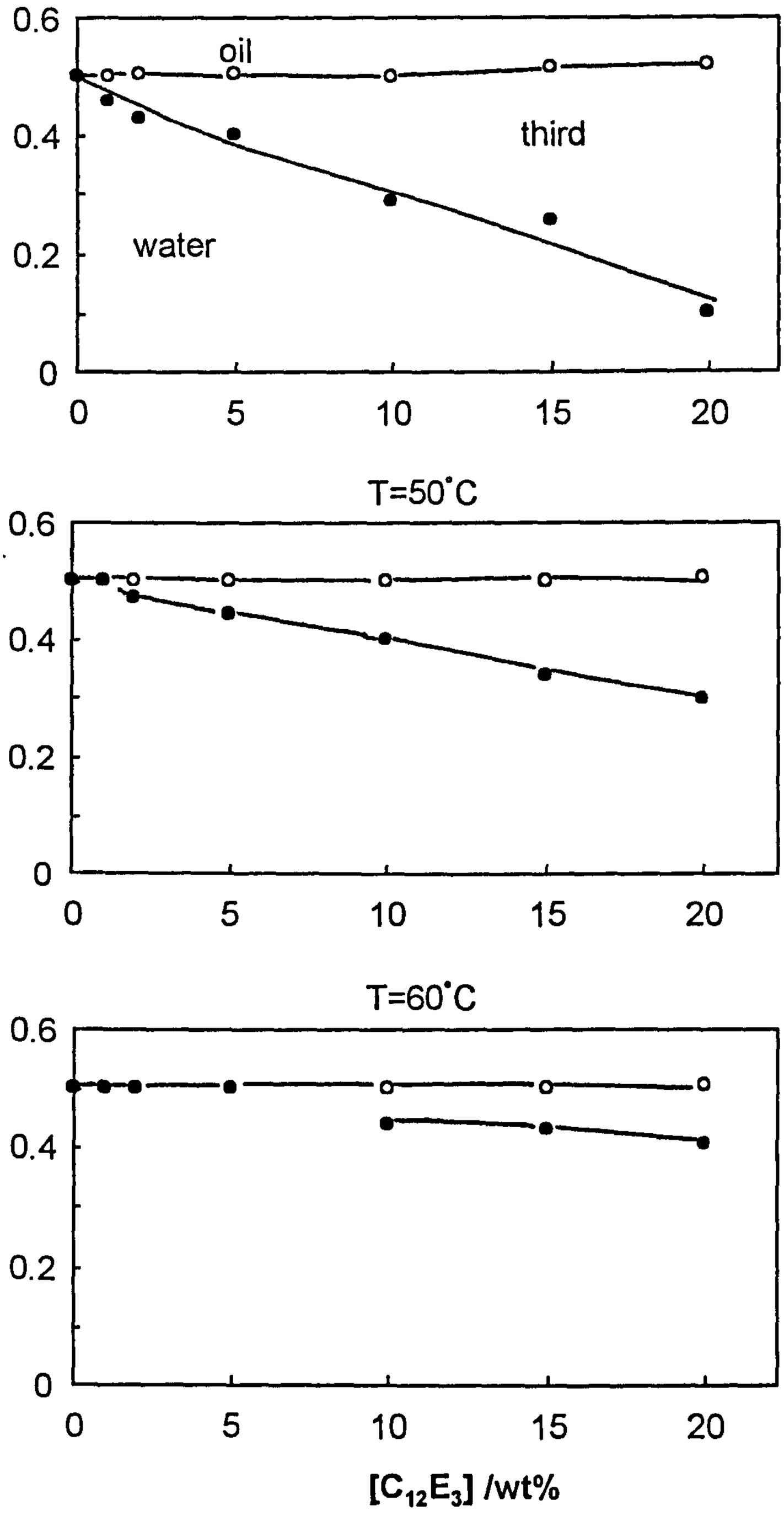

surfactant concentration for 30, 50 and 60°C, shows how the appearance of the third phase in the system increases from between 0-1% at low temperatures to above 5% at high temperatures. These values are close to those for $C_{12}E_5$ in heptane+water systems,[116] suggesting that the monomeric solubility of nonionic surfactant in silicone oil is not too high.

From this temperature dependence, it can be concluded that the enthalpy of transfer of monomeric surfactant from solution in oil to the preferred curvature monolayer of the third phase is negative. This transfer changes the environment of the surfactant headgroup from that of oil to that of water whereas the chain group environment remains essentially 'oily'. The enthalpy change is mainly associated with changes in hydration of the polyoxyethylene headgroup. As the temperature increases, the EO groups of the surfactant molecules become dehydrated.

4.2.3 Effect of electrolyte concentration

The effect of added electrolyte on the mutual solubility between water and organic compounds was studied systematically first by Hofmeister[117] about a century ago. He found the electrolyte effect to be mainly determined by the nature of the anion. As a rule, the mutual solubility is decreased (salting-out effect) by inorganic electrolytes and in the order $SO_4^{2-} > CrO_4^{2-} > CO_3^{2-} > Cl^- > NO_3^-$, whereas ClO_4^- and SCN^- and tetraalkylammonium bromide increase the mutual solubility (salting-in effect). The reasons for the effect of the inorganic anions have been extensively studied since then. Generally, there are two opinions that have been proposed to describe the Hofmeister series. One[118] is that salts affect the "solvent property" of water,

i.e. the salts which have a salting-out effect are believed to be "structure makers" while those salting-in nonionic surfactants are "structure breakers". The other opinion[119] interprets the salting-in and salting-out phenomena from an interfacial origin. Salts are thought to adsorb or desorb at the water-organic solute (surfactant) interface, producing an increment in the solute free energy and, therefore, modifying the phase behaviour. More recently, Kabalnov *et al.*[120] proposed a model which is based on the interfacial origin, describing the effect of depletion on the bending properties of a nonionic surfactant monolayer. They argued that the salting-in and salting-out effects are in fact driven by a weak adsorption/depletion at the monolayer. For instance, in the case of depletion, a depleted salt exerts osmotic pressure on the surfactant "palisade layer"; this alters the monolayer spontaneous curvature and, as a consequence, the microemulsion phase equilibrium.

The salt effects on the equilibrium phase behaviour of nonionic microemulsions have been extensively studied in alkane systems.[96, 100] In understanding the interaction between PDMS oils and nonionic surfactants, it is necessary to investigate the salt effects. Two types of electrolyte were employed, one is known to have a salting-out effect (NaCl) whereas the other has a salting-in effect (tetrabutylammonium bromide, TBAB).

The effect of sodium chloride concentration on phase inversion in $C_{12}E_3$ systems is shown in Figure 4.5 for two temperatures. At 10°C, two-phase systems form up to 2.5 M NaCl where the aggregated surfactant is most likely in the water phase. Between 2.7 M and 5 M NaCl, three phases exist, the third phase being blue and birefringent (as viewed between crossed polarisers). From the way in which its volume fraction decreases

Figure 4.5

Appearance of phases at equilibrium for the system: x M NaCl + 50 cS PDMS oil (1:1), plus 5% $C_{12}E_3$ at two temperatures

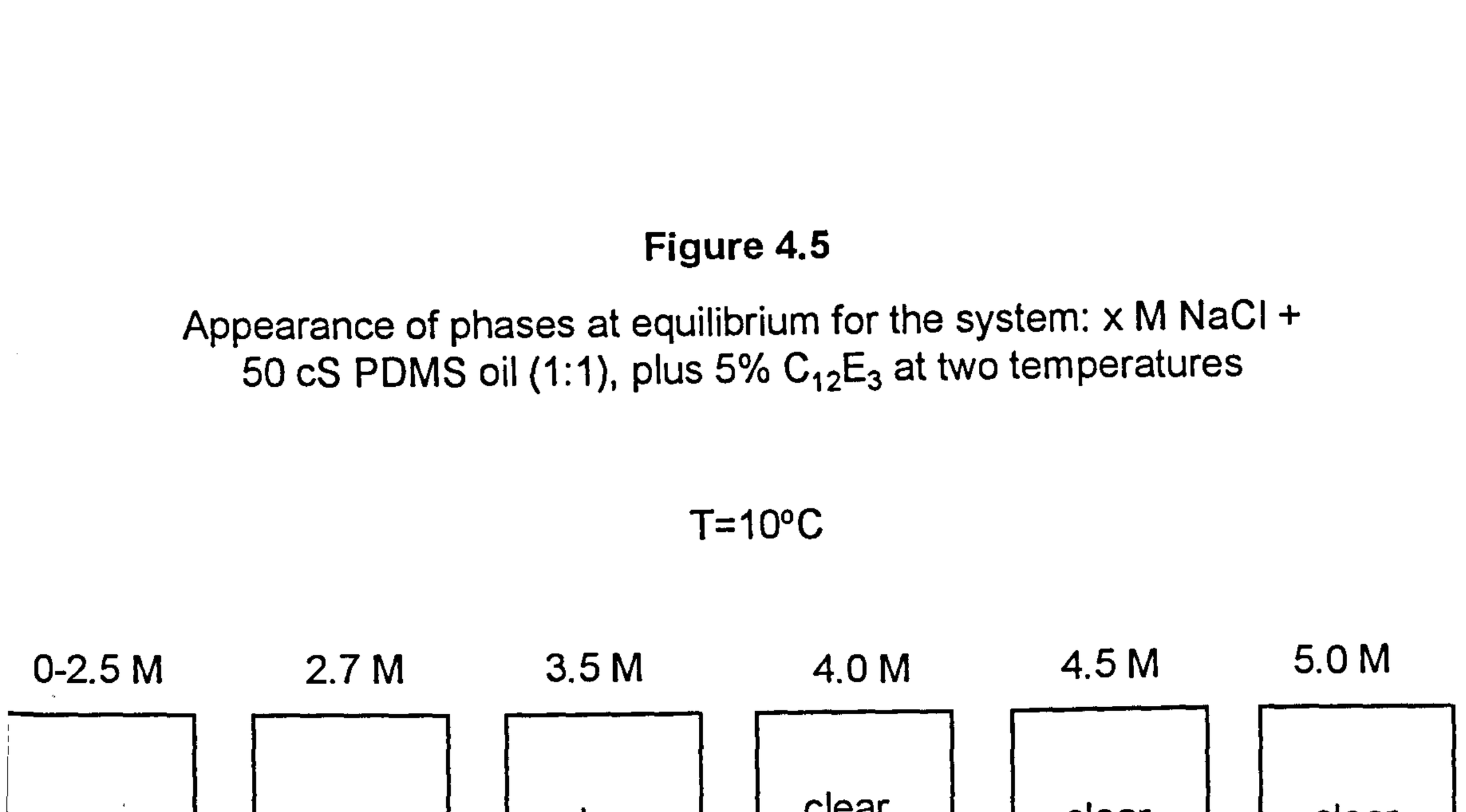

with added salt, we can predict that two phases, in which aggregated surfactant will reside in oil, will form (hypothetically) above 5 M. At 30°C, three phases are present below 1 M and transform to two phases above 4 M NaCl. In both cases however, the solubilisation of oil into the third phase is not as high as that of water. The volume fraction plots versus [NaCl] concentration at 6 temperatures are given in Figure 4.6, where it can be seen that the concentration of salt required to produce three-phase systems decreases upon increasing the temperature. The range of existence of three-phase mixtures with respect to temperature is given in Figure 4.7 as a function of salt concentration. Below the curve of the filled points, two-phases exist (Winsor I), and above the curve of the open points two phases exist (Winsor II). The bars at some of the salt concentrations indicate that the exact temperature of the transition has not been determined. As with hydrocarbon oils, the three phase region falls in temperature on addition of NaCl.

Similar experiments have been carried out with TBAB as salt, and Figure 4.8 and 4.9 show how the phase separation at 50°C varies with added TBAB. The third phase, already present in 0.01 M salt, increases in volume at the expense of the excess water phase up to around 0.42 M salt. It then decreases losing the bluish tinge until eventually above 0.75 M salt a clear two phase system results. By dispersing the upper phase into both neat oil and pure water, we have checked that in all mixtures it is the oil phase. A similar uncharacteristic 3-2-3-2 phase transition occurs at 41°C, but the effect is over by 60°C (Figure 4.10). The salt concentration at which the first 3-2 transition occurs increases with temperature (from around 0.2 M to

Figure 4.6

Effect of [NaCl] on the volume fraction of each phase for aqueous NaCl + 50 cS PDMS oil (1:1), plus 5% $C_{12}E_3$ at different temperatures

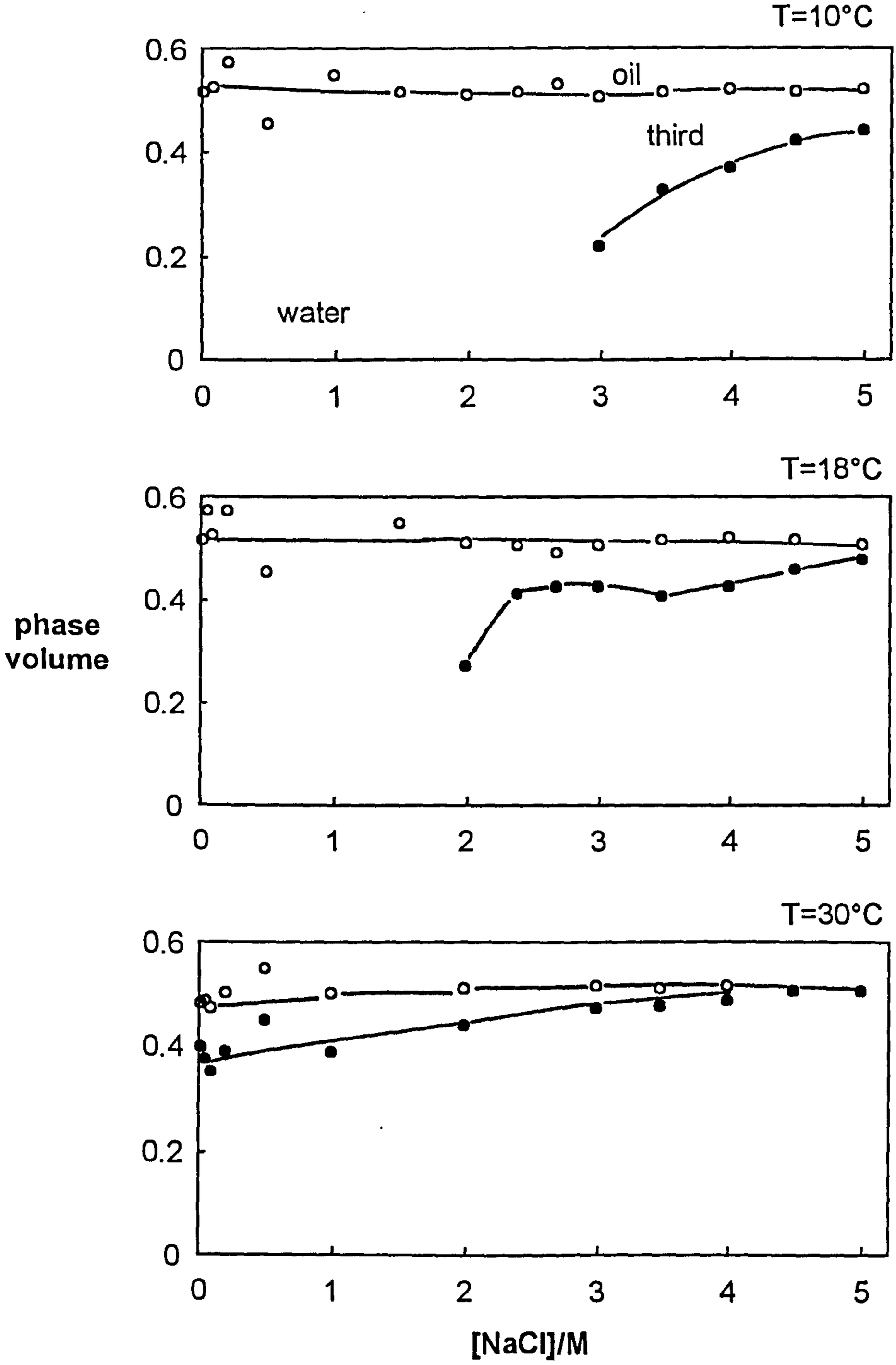

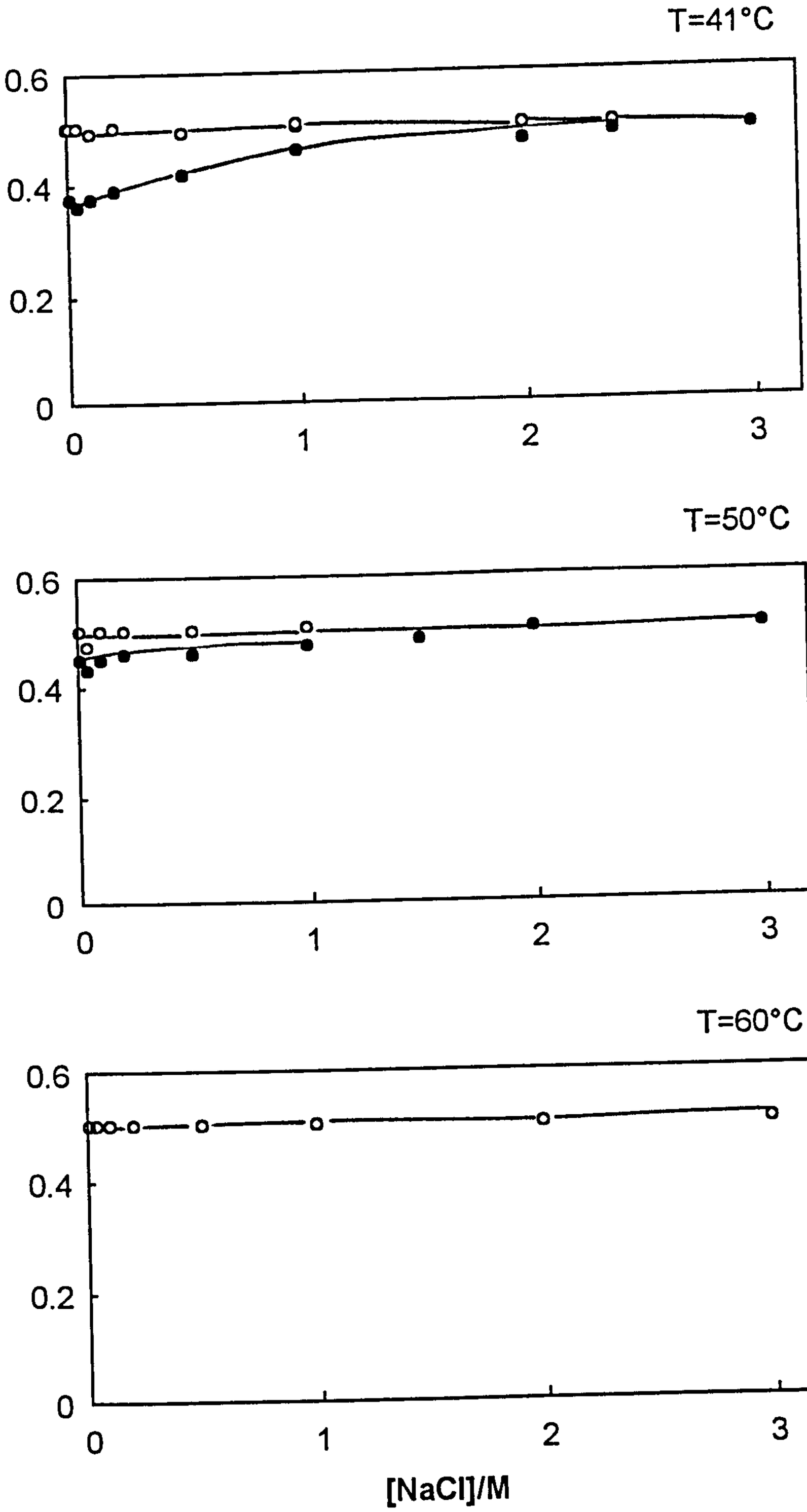
T=41°C
0.6
0.4
0.2
0
0
1
2
3
T=50°C
0.6
0.4
0.2
0
0
1
2
3
T=60°C
0.6
0.4
0.2
0
0
1
2
3
phase volume
[NaCl]/M

Figure 4.7

Temperature dependence of the three phase region as a function of salt concentration for the system H_2O-50 cS PDMS oil-$C_{12}E_3$-NaCl

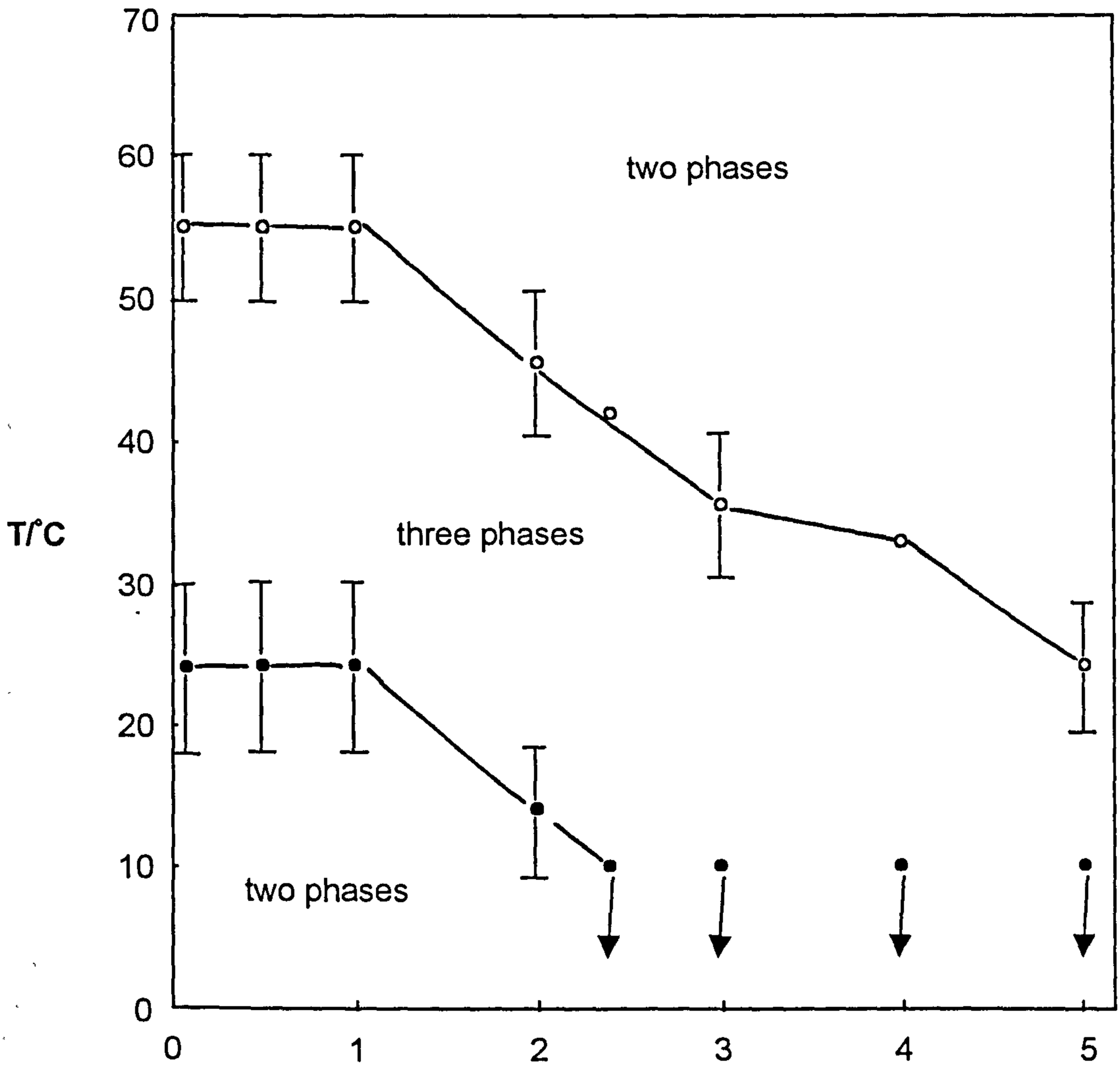

Figure 4.8

Appearance of phases at equilibrium for the system: x M TBAB + 50 cS PDMS oil (1:1), plus 10 % $C_{12}E_3$ (in water) at 50°C

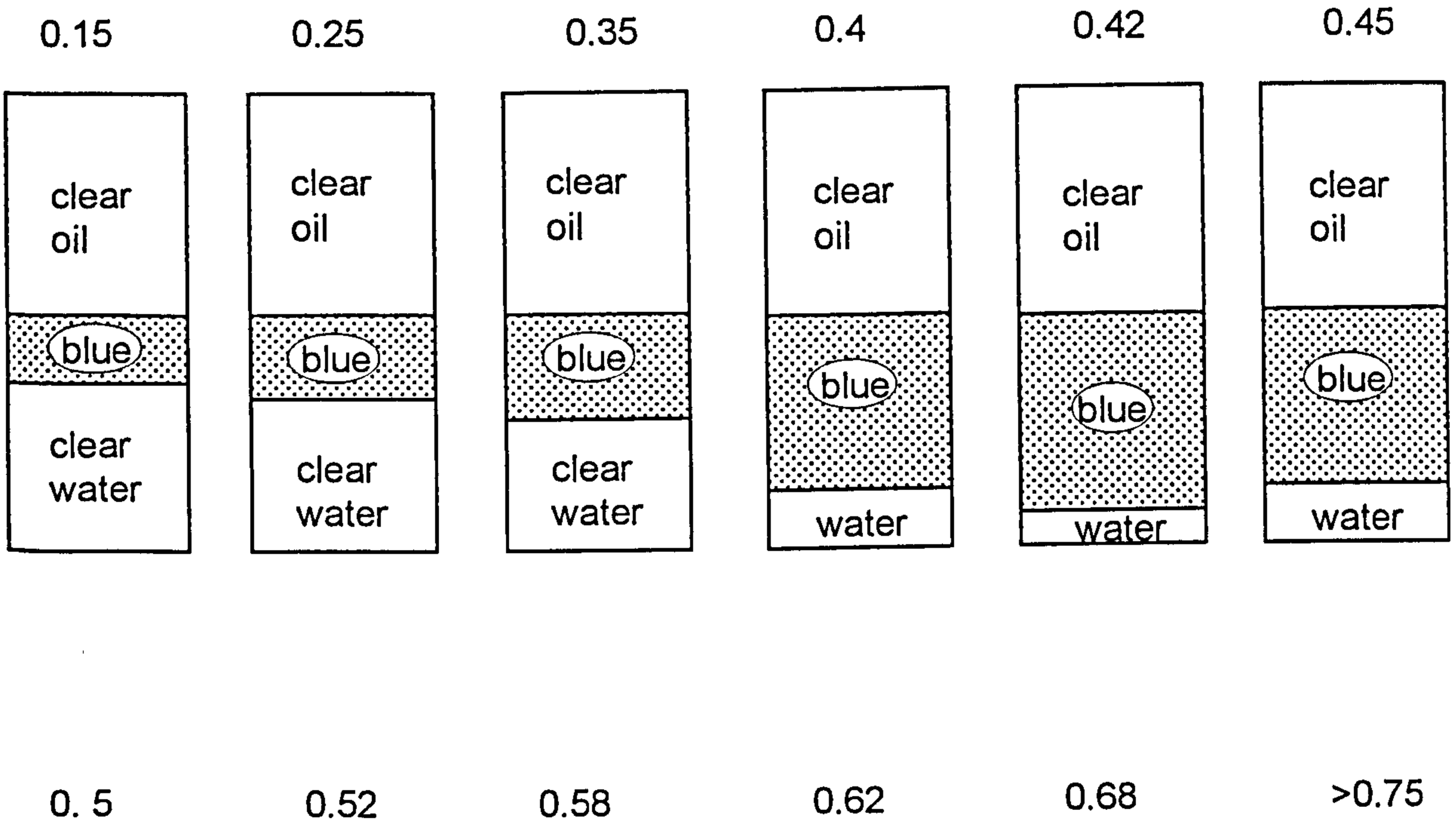

Figure 4.9

Effect of [TBAB] on the volume fraction of each phase for $C_{12}E_3$ in aqueous TBAB+ 50 cS PDMS oil systems at 50°C

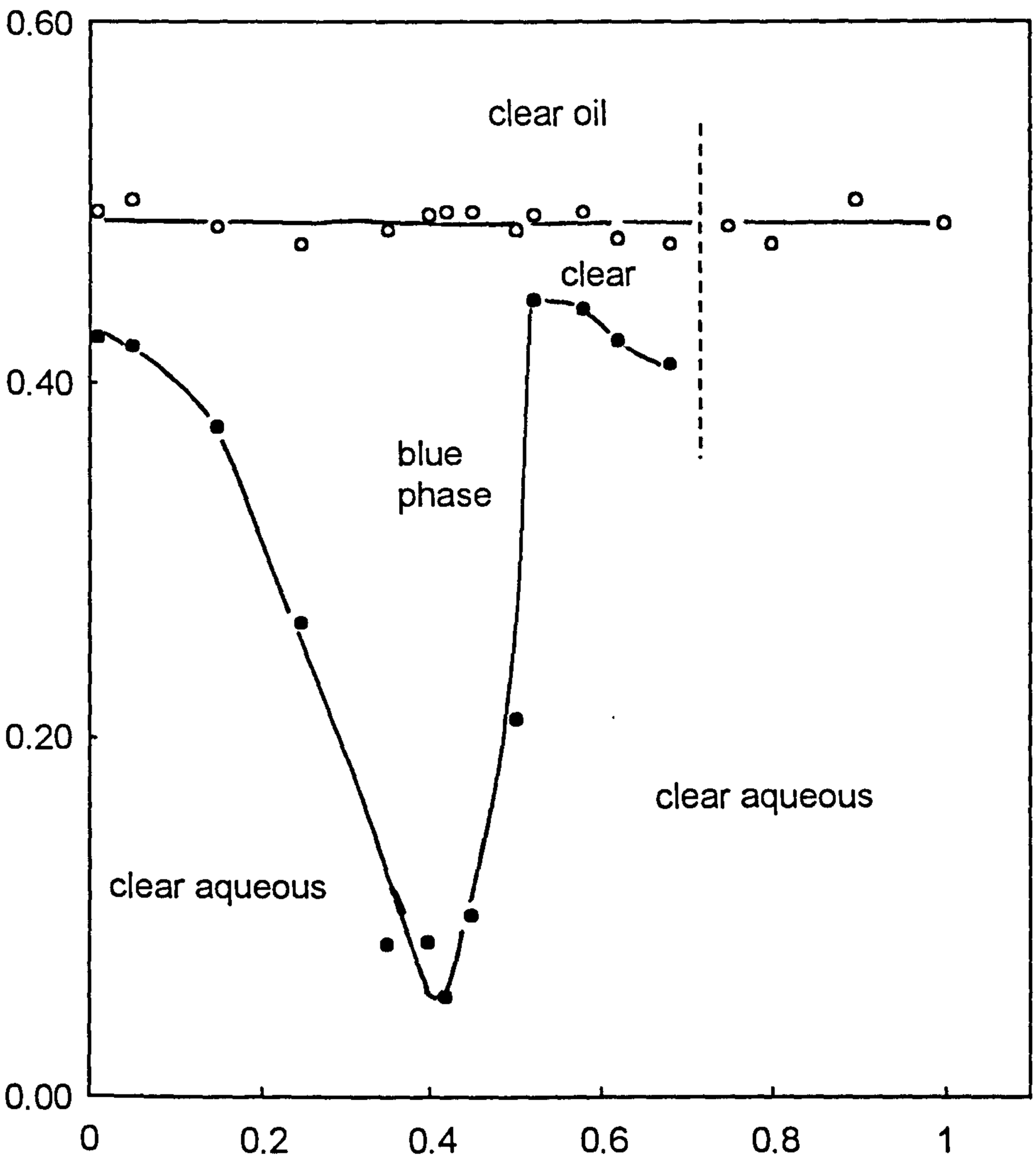

Figure 4.10

Effect of [TBAB] on the volume fraction of each phase for $C_{12}E_3$ in aqueous TBAB+ 50 cS PDMS oil systems at 41 and 60°C

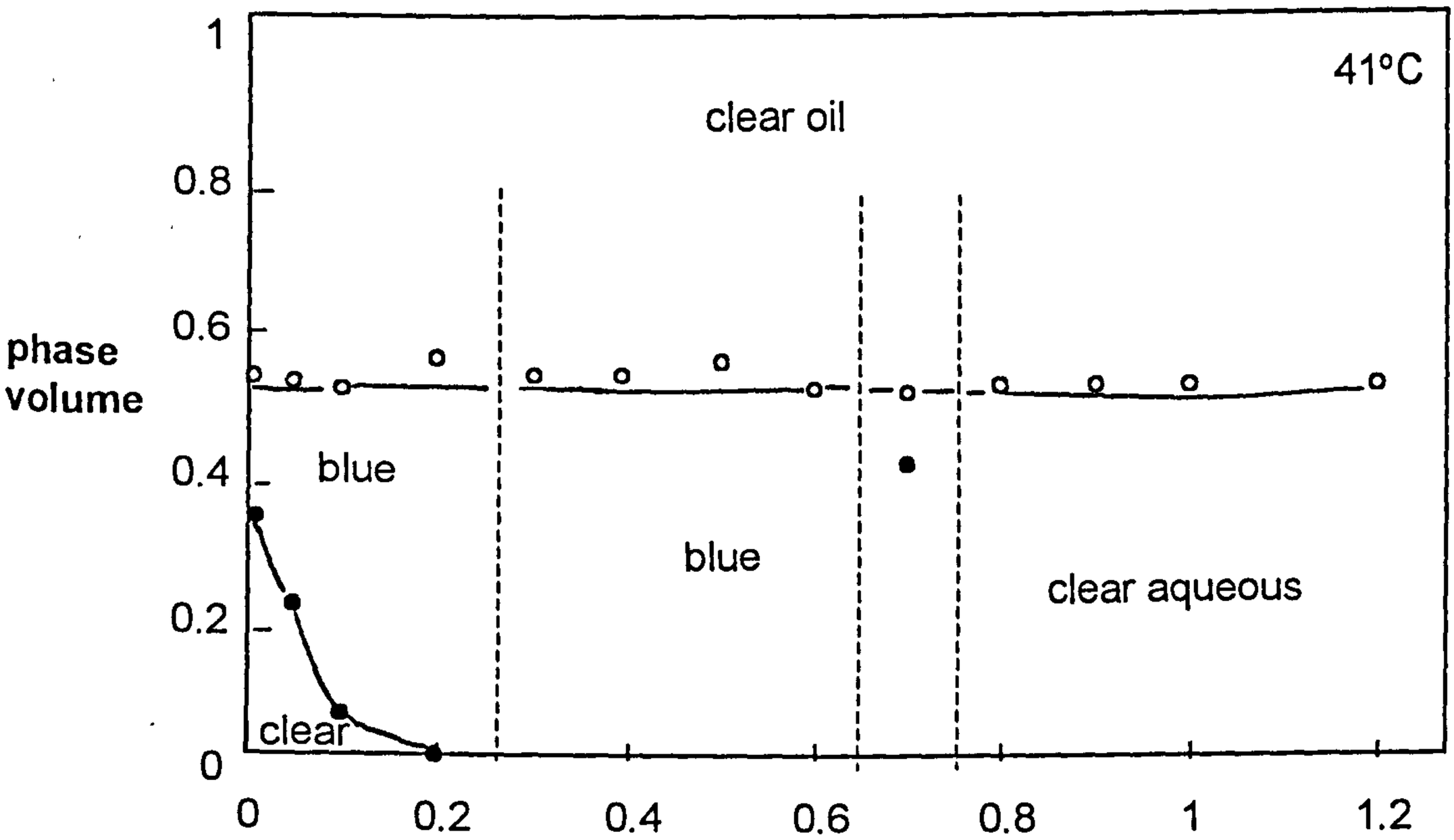

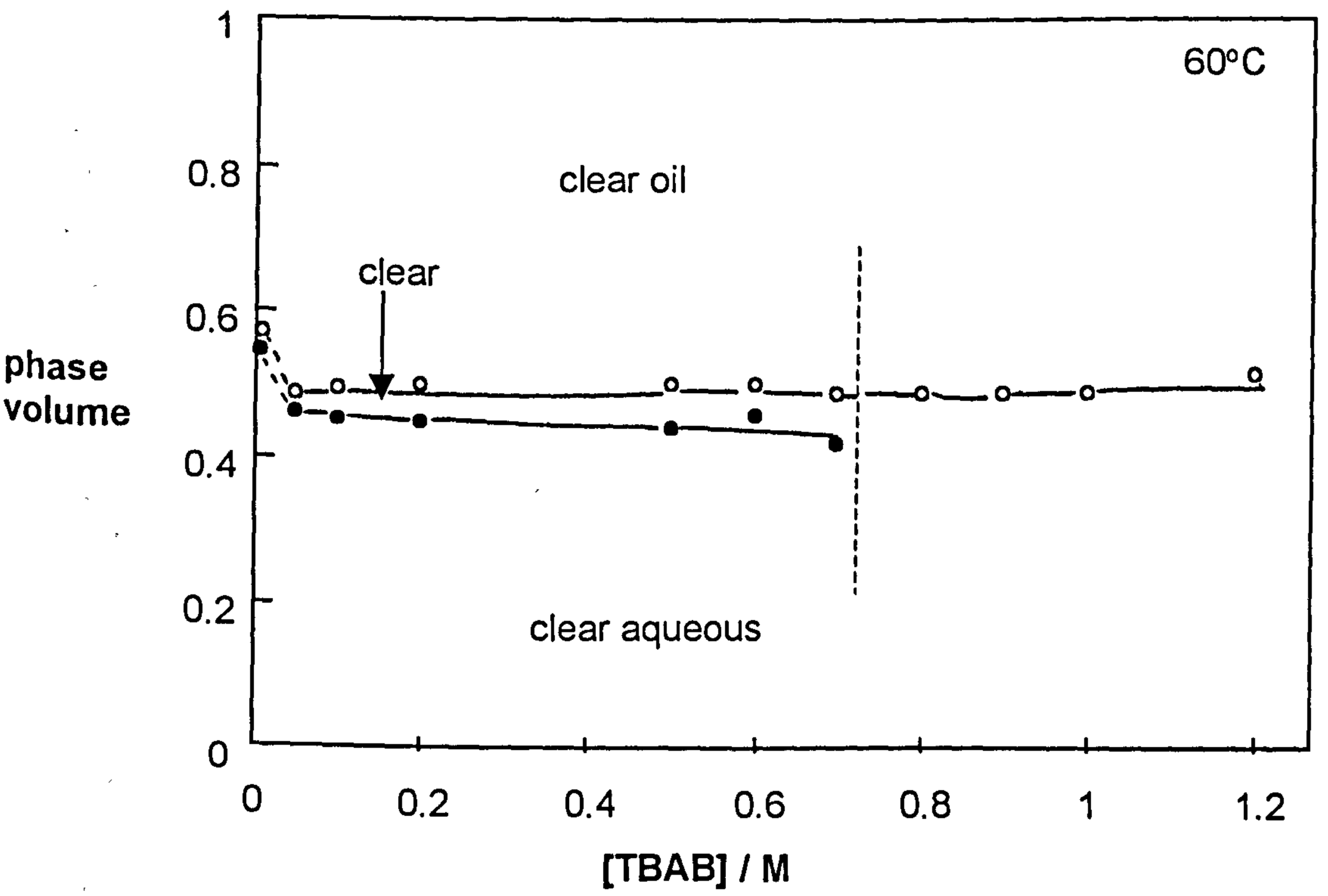

>0.4 M). The volume fraction of the bluish third phase increases with an increase in [TBAB] demonstrating the opposite trend as observed in the lyotropic salt (NaCl) case. In all cases the volume fraction of the PDMS oil phase remains at around 0.5 indicating little solubilisation of PDMS oil into the third or aqueous phases. This result may be explained as follows. The addition of a lyotropic salt is equivalent to a decrease in the effective hydrophilicity of the nonionic surfactant, whereas the addition of a hydrotropic salt is equivalent to an increase in it. Thus, initially the system transforms from Winsor III at lower [TBAB] towards Winsor I when the TBAB concentration increases. As [TBAB] increases further, the volume fraction of the second third phase is very small. It appears that surfactant suddenly becomes dehydrated and depletes most of the aqueous phase. The reason for this hydrotropic to lyotropic transition of the TBAB is not clear. This behaviour may be due to the properties of the electrolyte itself, changing from a hydrotropic salt at low levels to a lyotropic salt at higher concentrations. A similar effect has been observed with short chain nonionic surfactants and $NaClO_4$ systems by Kahlweit *et al.*[100] The phase sequence may thus be Winsor III-I-III-II. Furthermore, the phase transition at 60°C is only Winsor III-II, the volume fraction and appearance of the third phase at this temperature is similar to that of the second third phase at 41°C and 50°C. It seems that TBAB has lost its hydrotropic effect (salting-in) at 60°C. The resultant phase behaviour of $C_{12}E_3$-PDMS-TBAB systems reflects that there exists a competition between the increase in temperature and hydrotropic salt concentration. The increase in temperature dehydrates

nonionic surfactants whereas the increase in TBAB concentration salt-in them.

4.3 Systems containing other surfactants

4.3.1 $C_{16}P_8E_1$ systems

It was mentioned earlier that Minana-Perez *et al.*[105] have synthesised so-called "extended" surfactants in which propyleneoxide (P) groups are inserted between the usual hydrocarbon chain and an ethyleneoxy sulphate head group. These surfactants are capable of promoting significant solubilisation of triglyceride oils into aqueous solutions. Their idea is that the interaction of the hydrocarbon chain with the oil phase is enhanced through the intermediate polarity of the P groups. It is unclear, however, whether this result is due to the large increase in the overall surfactant chain length, which is known to increase the extent of solubilisation. We have employed $C_{16}P_8E_1$ in an attempt to see if solubilisation of silicone oils become possible. The emulsion conductivity/temperature data for $C_{16}P_8E_1$ was shown in Figure 3.8, where it can be seen that typical phase inversion from o/w to w/o emulsions occurs around 28 °C, the curve exhibiting a sharp decrease in conductivity to very low values over a narrow temperature range. Since emulsion conductivity measurements alone do not indicate how many phases are present at each temperature, we have determined the phase sequence as a function of surfactant concentration at one temperature below 28°C and at one temperature above it. Results from both gentle mixing of the components and from homogenising them at 8000 rpm for 1 min using an Ultra-turrax were identical. At 18°C Figure 4.11 shows that three phase

Figure 4.11

Phase separation at equilibrium for 0.01 M NaCl+50 cS PDMS oil (1:1 vol.), plus x wt % (rel. water) $C_{16}P_8E_1$) at two temperatures.

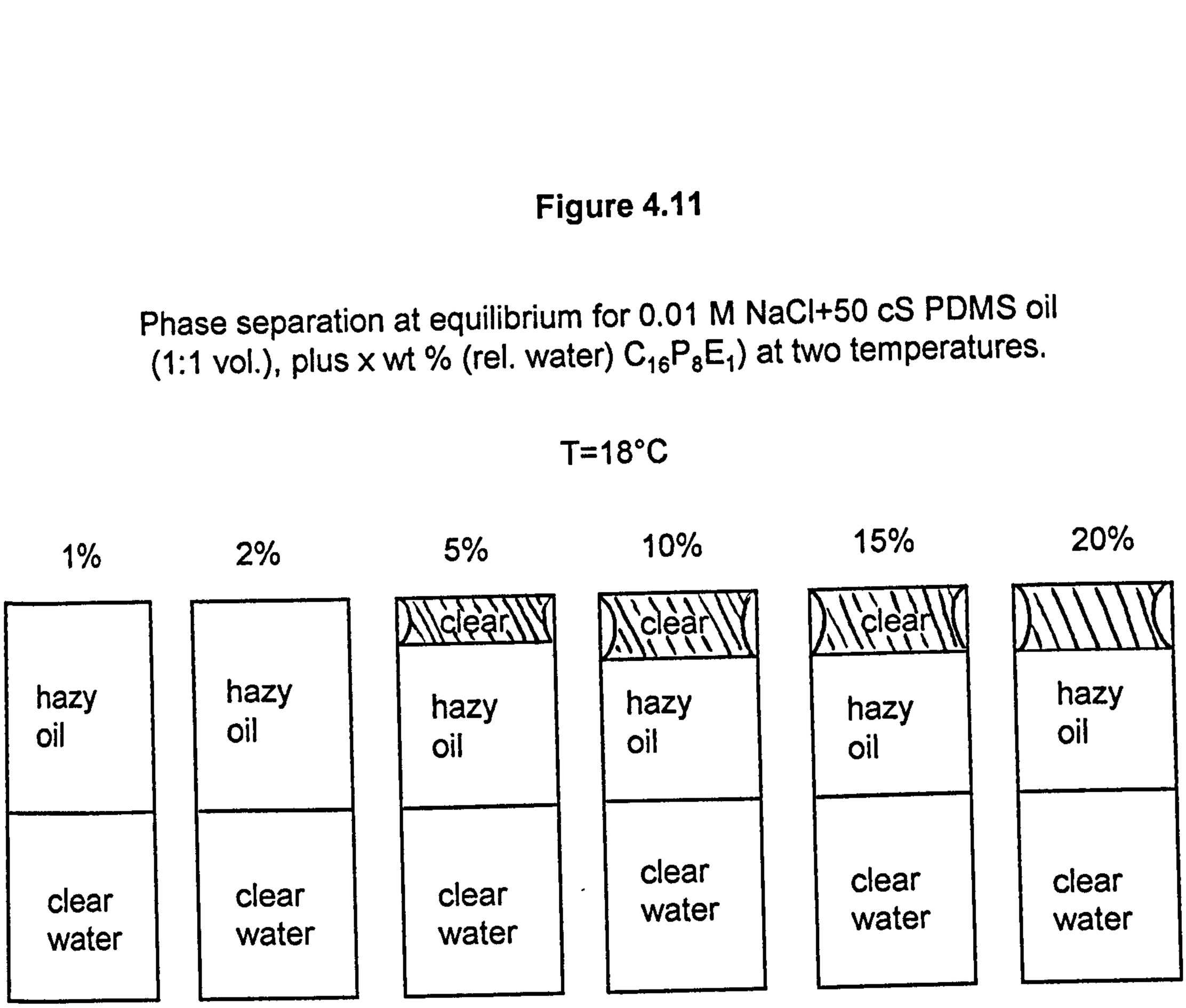

systems begin to form between 2 and 5 wt.% surfactant, with the surfactant-rich phase being the upper phase. This phase does not wet the sides of the glass tubes completely and so the meniscus with the walls is curved. Its volume fraction increases slightly by incorporating more oil. It most likely contains silicone oil and surfactant, the volume fraction of the excess water phase remaining close to 0.5. The findings are similar at 30°C, except that three phases form above 5 wt.%, a consequence of the increasing oil phase cmc with temperature. At both temperatures, addition of very low concentrations of NaCl (<0.05 M) results in two phase systems, in which the oil phase is slightly hazy indicating the presence of water along with aggregated surfactant. Thus, unlike the conventional nonionic surfactant $C_{12}E_3$ whose third phase contains mainly surfactant plus water, this extended surfactant forms a third phase with little water. Therefore, it is of interest to investigate the phase behaviour further by using mixed surfactants, which may provide a way to solubilise silicone oil into aqueous surfactant solutions.

4.3.2 L-77 systems

L-77 is a nonionic trisiloxane surfactant. The difference between L-77 and C_nE_m surfactants is their hydrophobic moiety, which is a siloxane chain in the former and a hydrocarbon chain in the latter. The area[121] per L-77 molecule obtained from the surface tension measurements at the surfactant-air interface is about 70 $Å^2$, which is considerably larger than that of the $C_{12}E_3$ molecule (40 $Å^2$).[122] $C_{12}E_3$ consists of a long narrow hydrophobic chain whereas L-77 consists of a much fatter and shorter T-shaped or umbrella-

like hydrophobic group. This difference in the proportions of the hydrophobe compared with those of the headgroup is an important feature of L-77.[123] L-77 is known to exhibit "superwetting" or "superspreading", an unusually rapid spreading of a dilute (about 0.1 wt.%) aqueous dispersion of the surfactant over a hydrophobic surface (such as a paraffin film or a waxy leaf surface).

In order to establish if the presence of a silicone chain in the surfactant is necessary for the solubilisation of PDMS oil into aqueous aggregates, we looked at previously the nonionic silicone surfactant L-77 with the 50 cS PDMS oil. Without added salt, the apparent PIT was just above 40°C. We have therefore chosen a temperature close to this and have investigated the equilibrium phase sequence as a function of [NaCl] and [surfactant], to see if phase inversion can be effected by salt, and if the third phase is oil-containing. At 10 wt.% surfactant and 35°C, two phase systems (with aggregation in the aqueous phase) occur up to at least 1 M NaCl. Three phases then form from 2 M up to 5 M salt, but the surfactant-rich middle phase contains very little oil (Figure 4.12). Figure 4.13 shows the phase sequence as a function of surfactant concentration in 2 M NaCl systems at 35°C. The third phase begins to appear between 5 and 10 wt. % L-77, but increasing the [L-77] further simply concentrates up the third phase by expelling excess water i.e. no more solubilisation of PDMS is seen at high [surfactant]. Clearly, from this comparison it can be concluded that having a silicone chain in the surfactant does not lead to any significant differences in the phase behaviour in PDMS oil systems compared with those containing hydrogenated nonionic surfactants.

Figure 4.12

(a) Appearance of phases at equilibium in the system:10% L-77 in x M aqueous NaCl + 50 cS PDMS oil at 35°C

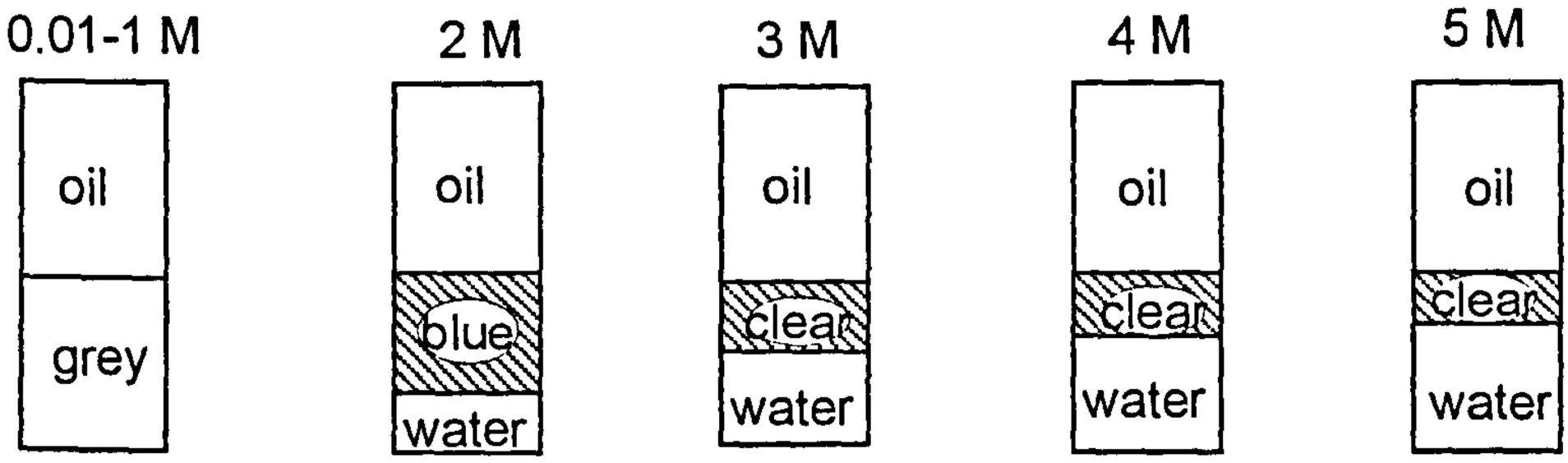

(b) Effect of [NaCl] on the volume fraction of each phase in the above system

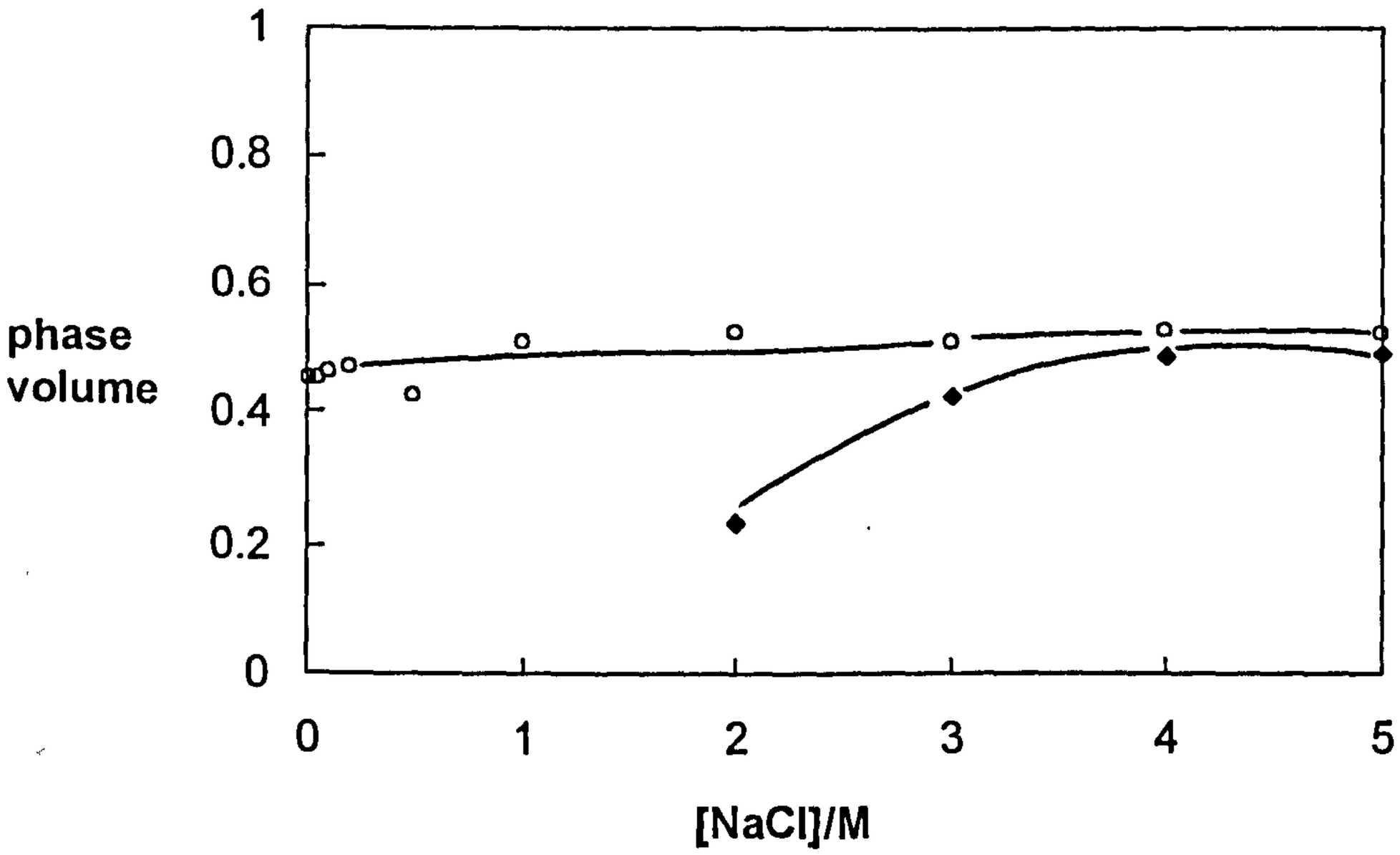

Figure 4.13

(a) Appearance of phases of the system: x% L-77 based on water and equal volume of 2 M NaCl aqueous and PDMS oil (50 cS) at 35°C

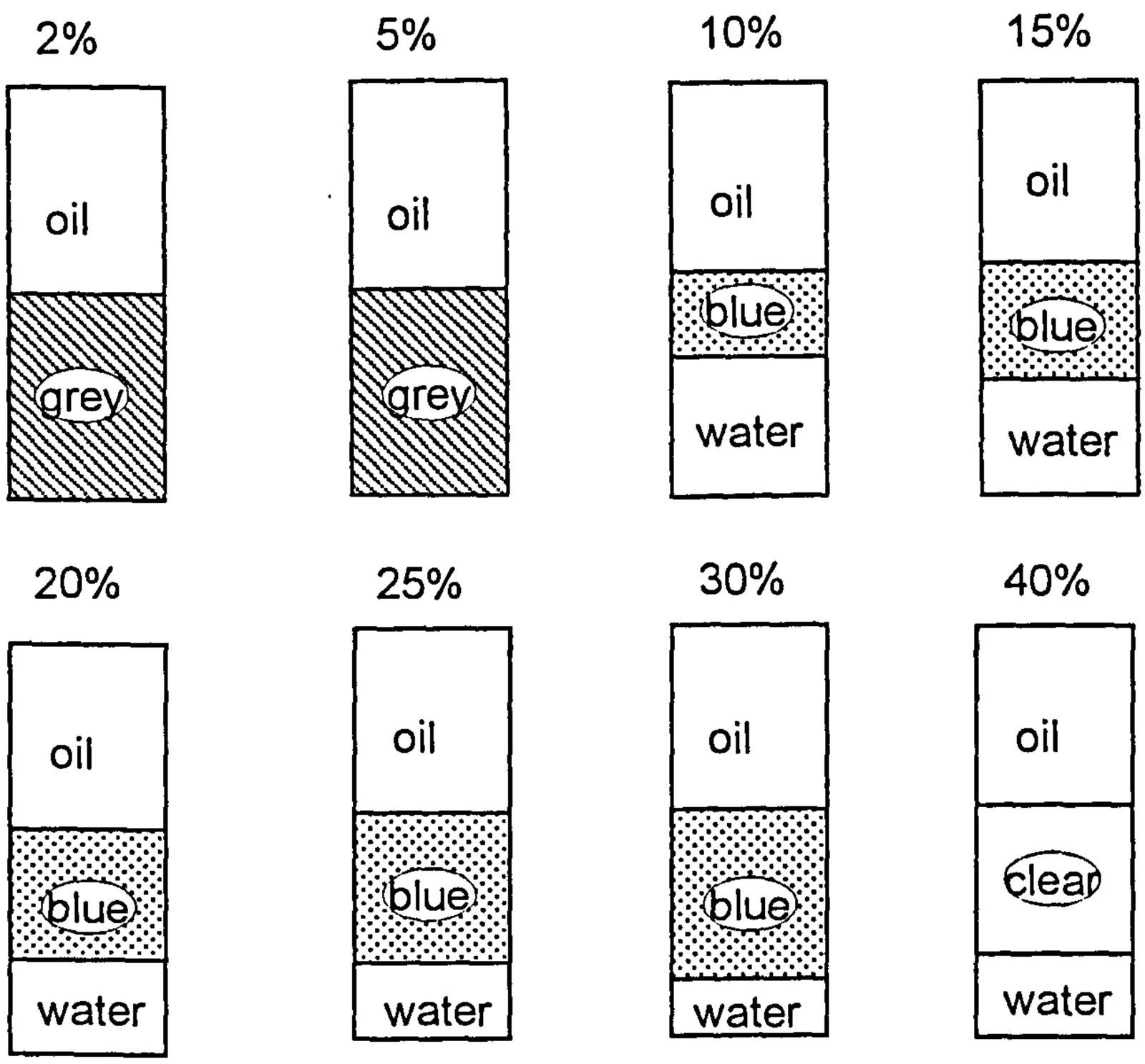

(b) Effect of [L-77] on the volume fraction of each phase in the above system

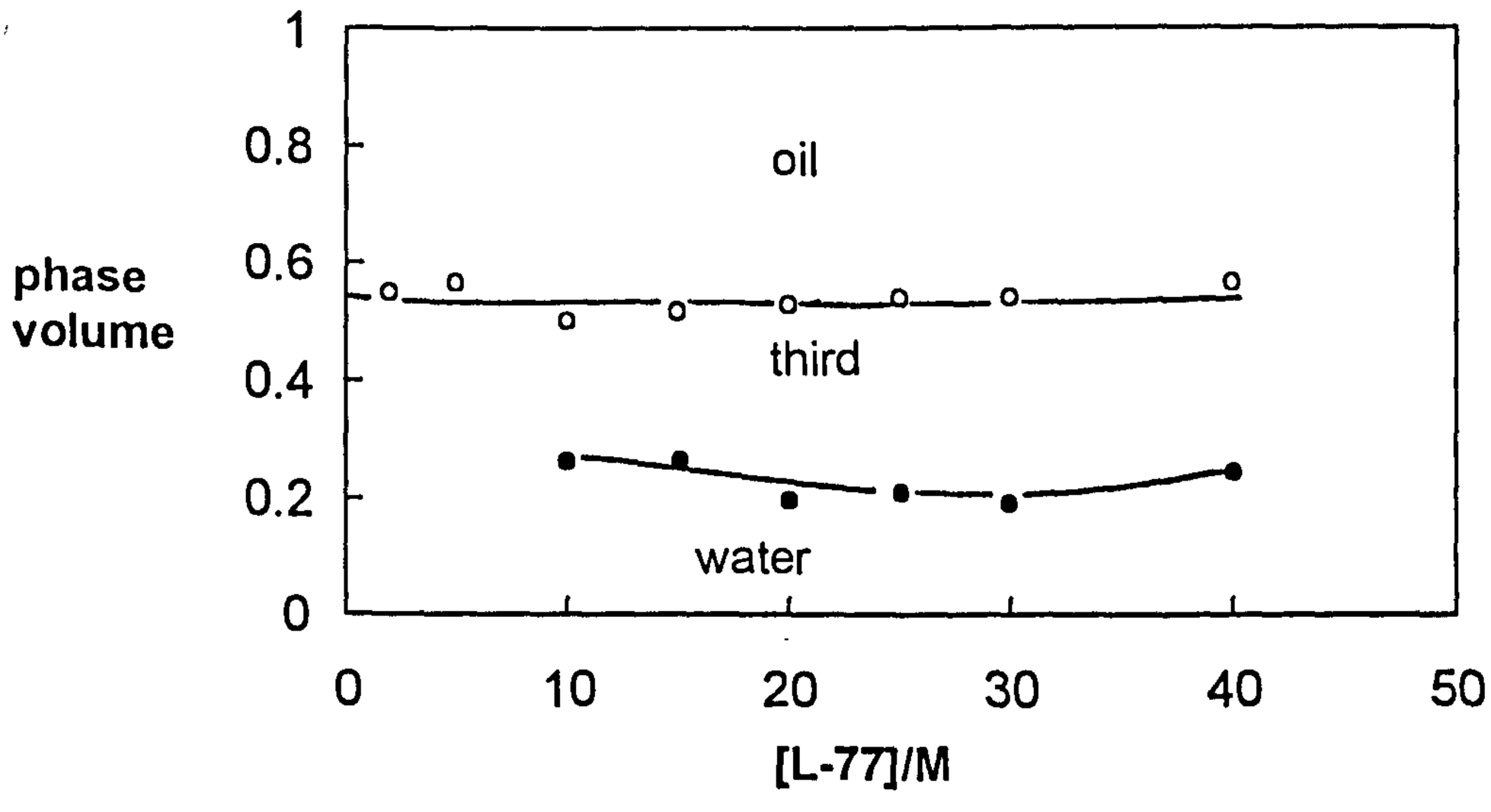

4.3.3 Sugar surfactant systems

Certain sugar surfactants have glucose rings and their micellar solutions may solubilise silicone oil. We have used 15 mM C_{12} ß-D-maltoside (its cmc in water is 0.15 mM at 25°C[124]) in 50 cS PDMS oil systems in order to investigate whether the PDMS oil can be solubilised. Figure 4.14 shows the structure of the surfactant and the volume fraction of each phase on varying the salt concentration. All the tubes were shaken vigorously at 25°C and the phase separation was rapid (within 12 hours). The upper phase is clear oil and the bottom phase is clear water. The temperature was increased to 50°C and all the tubes were re-shaken, the separation being the same. This may be because the sugar surfactant used contains seven hydroxyl groups and is therefore very hydrophilic and hence has extremely high HLB. In addition, the high molecular weight of PDMS oil also made the system more difficult to invert.

4.4 Oil-in-water single phase microemulsions formation with PDMS

Oil can be solubilised in aqueous surfactant micellar solutions to form single phase o/w microemulsions. If sufficient oil is added, an excess oil phase will eventually separate which corresponds to the Winsor I system as discussed earlier. The solubilisation of oil into aqueous micelles can change the surfactant solution properties such as the cloud point and viscosity of nonionic surfactant solutions. The changes in these properties provide a means of following the solubilisation of oils.

Figure 4.14

Structure of decyl β-maltoside, R represent decyl group

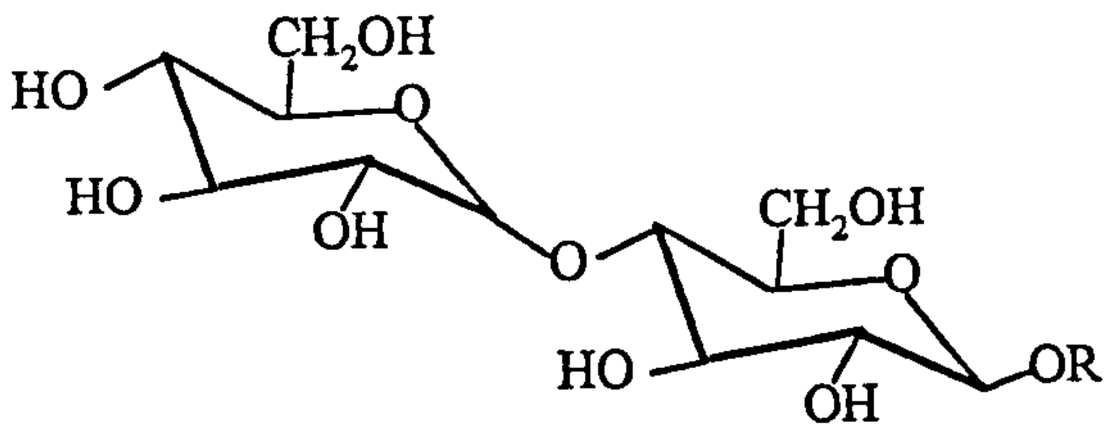

Effect of [NaCl] on the volume fraction of each phase for 15 mM C_{12}β-D-maltoside in x M NaCl aqueous + 50 cS PDMS oil at 25°C

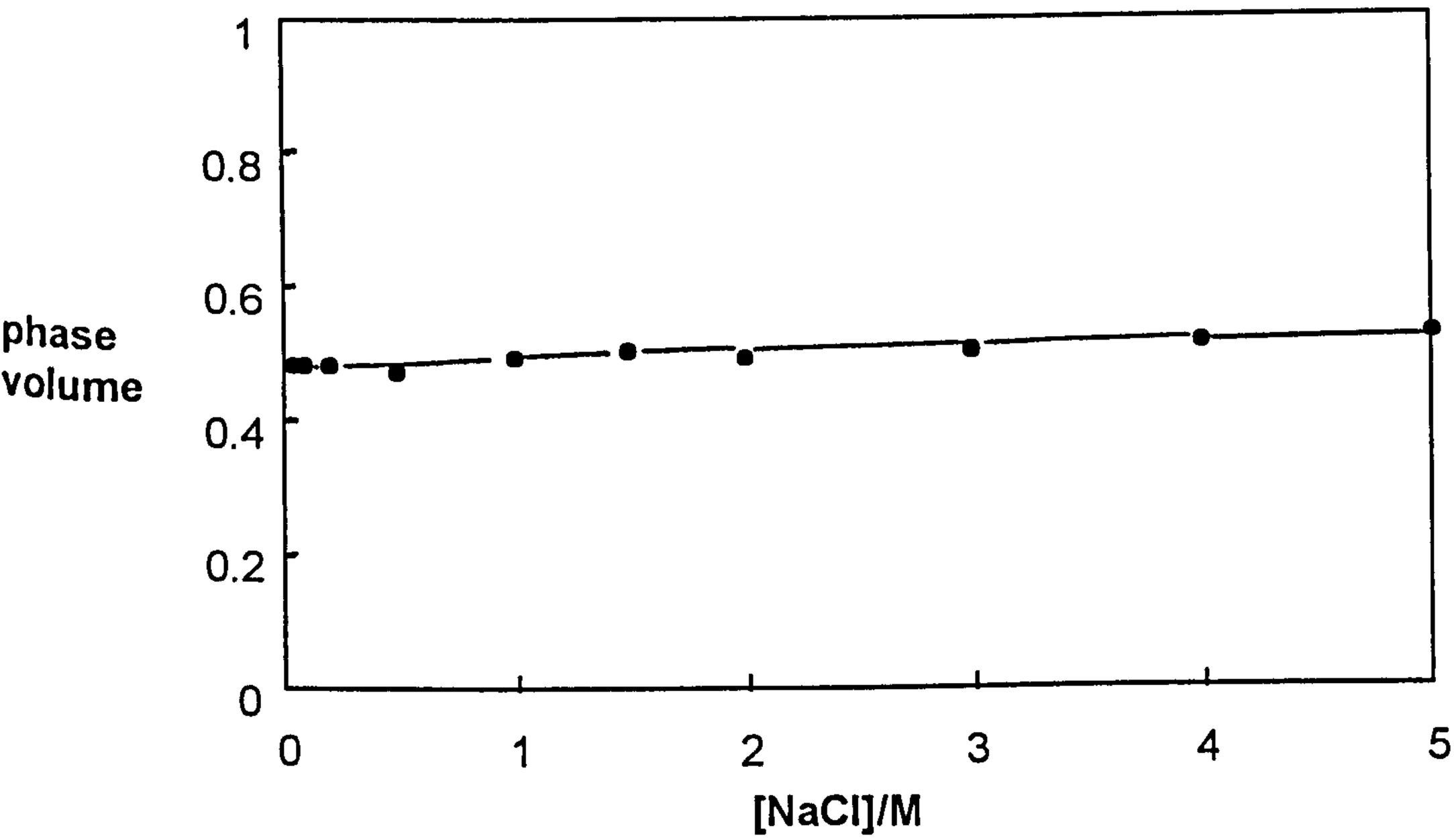

4.4.1 Dependence of cloud point of $C_{12}E_5$ on the uptake of PDMS

It is well known that aqueous solutions of nonionic surfactants when heated undergo a phase separation and become turbid at the so-called cloud point.[34] The cloud point (temperature) is markedly affected by relatively small amounts of various additives such as inorganic and organic salts, polar organic materials and hydrocarbons. The mechanisms by which the various classes of materials bring about changes in cloud points are presumably different, but the changes may often ultimately depend on changes in hydration and/or shape of the micelles. It is generally believed that hydration of the EO groups on the surface of the micelles stabilises the micelles against aggregation. Increasing the temperature is thought to dehydrate the micelles to some extent causing the intermicellar interactions to become increasingly attractive[107] and hence leading to phase separation. However, micellar shape changes are also expected to accompany dehydration for the following reasons. Suppose the hydrated EO group has a cross-sectional area a_h, and the corresponding chain area is a_c. Then, in simple terms, because of geometrical constraints, the micelle shape is governed by the packing parameter P as described earlier. Increasing the temperature, which leads to dehydration, would be expected to decrease a_h and thus increase P. This is expected to lead to the formation of aggregates of decreased curvature (i.e. rod or disc shaped micelles as compared with spherical micelles). The formation of these more elongated structures necessarily involves an increase in aggregation number as is observed by the time-resolved-fluorescence technique.[125] The mutual attraction between micelles is expected to depend on the extent of hydration of the micelle and also on

the area of mutual contact between touching micelles, This area will be larger for disc or rod shaped micelles as compared with spherical micelles. Hence, temperature variation is likely to induce inter-related changes in the micelle size, shape and intermicellar interactions; all these factors combine to determine the cloud point of the system. If the effects of additives on cloud points are associated with greater (or smaller) micelle asymmetry as suggested, this should be reflected in the viscosity of the solution. It is argued by Aveyard *et al.*[126] that the viscosity and cloud point changes are inversely related.

The effect of alkanes on the cloud point and viscosity depends very much on the oil chain length.[126] Short alkanes such as octane that can be solubilised in high amounts reduce the cloud point initially which then steadily rises with the addition of further amounts. In the case of long alkanes, which are solubilised much less, the cloud point rises markedly however. It has been argued earlier that short alkanes initially penetrate in the surfactant chain region promoting the formation of more asymmetric structures like rods. This would cause the cloud point to fall since this temperature is a measure of the attractive interactions between micelles, which is greater for rods than spheres. Once the chain region is saturated with oil, further oil goes into it to form a core, transforming the asymmetric structures to larger spherical ones, raising the cloud point. Since we know that penetration of oils into surfactant monolayers decreases with an increase in the oil chain length, then long oils form a core immediately with little chain solubilisation. From viscosity of the solution considerations, it

reflects the shape of the particles and hence changes in the opposite sense to the cloud point.

Figure 4.15 gives the variation of the cloud point of $C_{12}E_5$ solutions with oil concentration, for pure heptane (which is solubilised), pure 50 cS PDMS oil and some of their mixtures. No change in cloud point is found in pure PDMS oil systems, but decreases are seen on addition of heptane. The changes for the mixtures roughly correlate with the ratio of heptane in the oil suggesting that it is taken up in preference to the silicone oil.

Since the uptake of the 50 cS PDMS oil into aqueous micelles has found to be extremely low, the low viscosity PDMS oils were employed to investigate the interaction between surfactant micelles and oils. Figure 4.16 shows the effect of oil viscosity on the cloud point changes in aqueous 0.5 wt.% $C_{12}E_5$ solutions. Here, all the oils cause the cloud point to rise, indicating that the oil probably forms a core inside the micelle. The mole ratio of oil:surfactant at saturation varies from 6 (0.65 cS) to 2 (1 cS) to 0.2 (5 cS). This finding is consistent with the lamellar phase swelling results,[63] where short chain PDMS ($\overline{M}_w$ < 500) found to make a lamellar system swell, while polymer-like long chains PDMS does not swell the lamellar phase, but disperses it into smaller liquid crystals with the initial structure.

4.4.2 Dependence of cloud point of L-77 on oil uptake

In comparison with $C_{12}E_5$, Figure 4.17 shows the cloud point of aqueous 0.5 wt.% L-77 as a function of added PDMS oils. Without oil, the surfactant has a cloud point of 11.7°C at this concentration. The solution remains turbid until 48°C, at which point it clears again, going turbid a

Figure 4.15

Cloud point of 0.5% aqueous $C_{12}E_5$ solution with added oil. The oil contains x wt % 50 cS PDMS in heptane

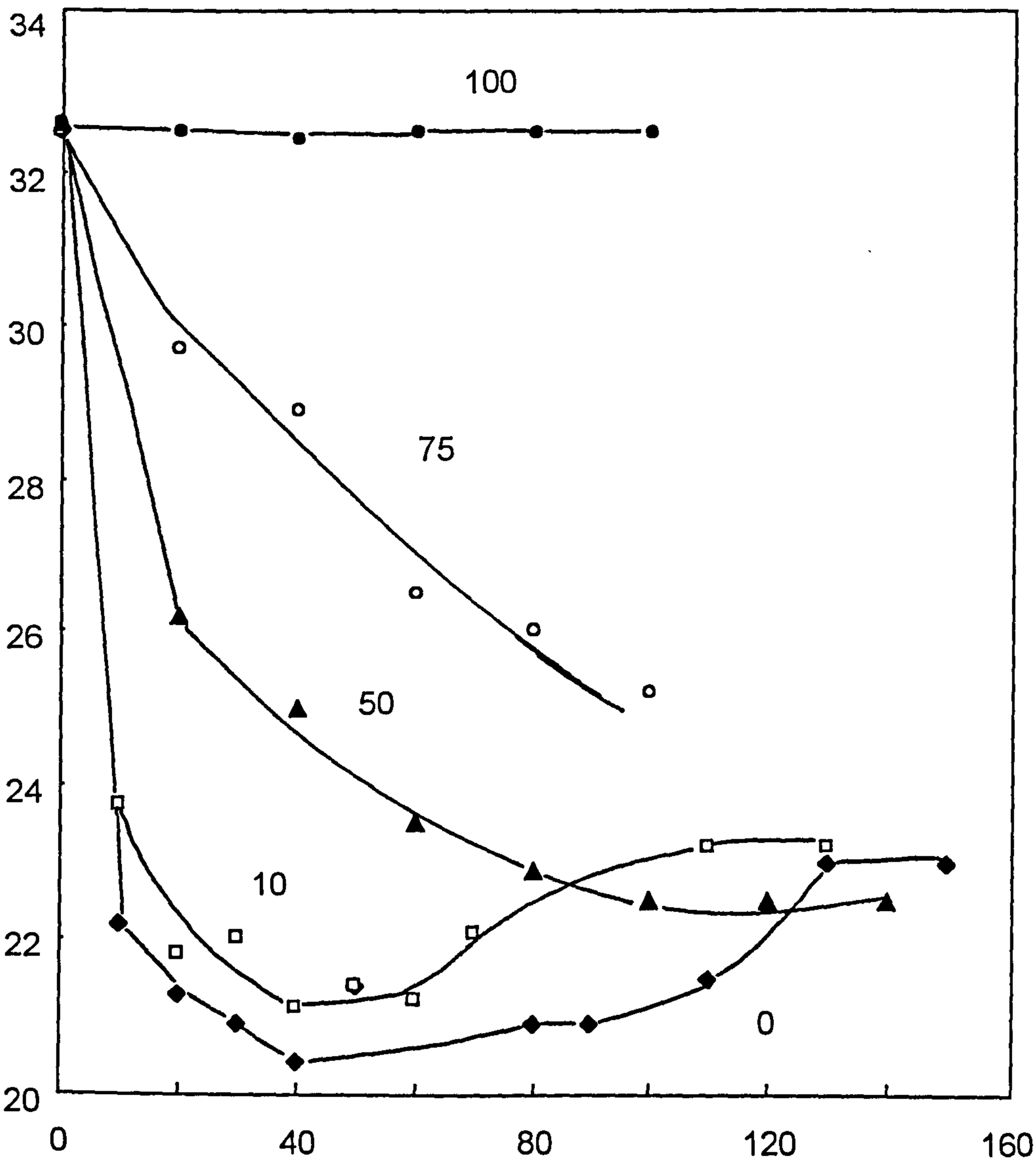

Figure 4.16

Cloud point of 0.5% aqueous $C_{12}E_5$ solution on addition of PDMS oils of viscosity given

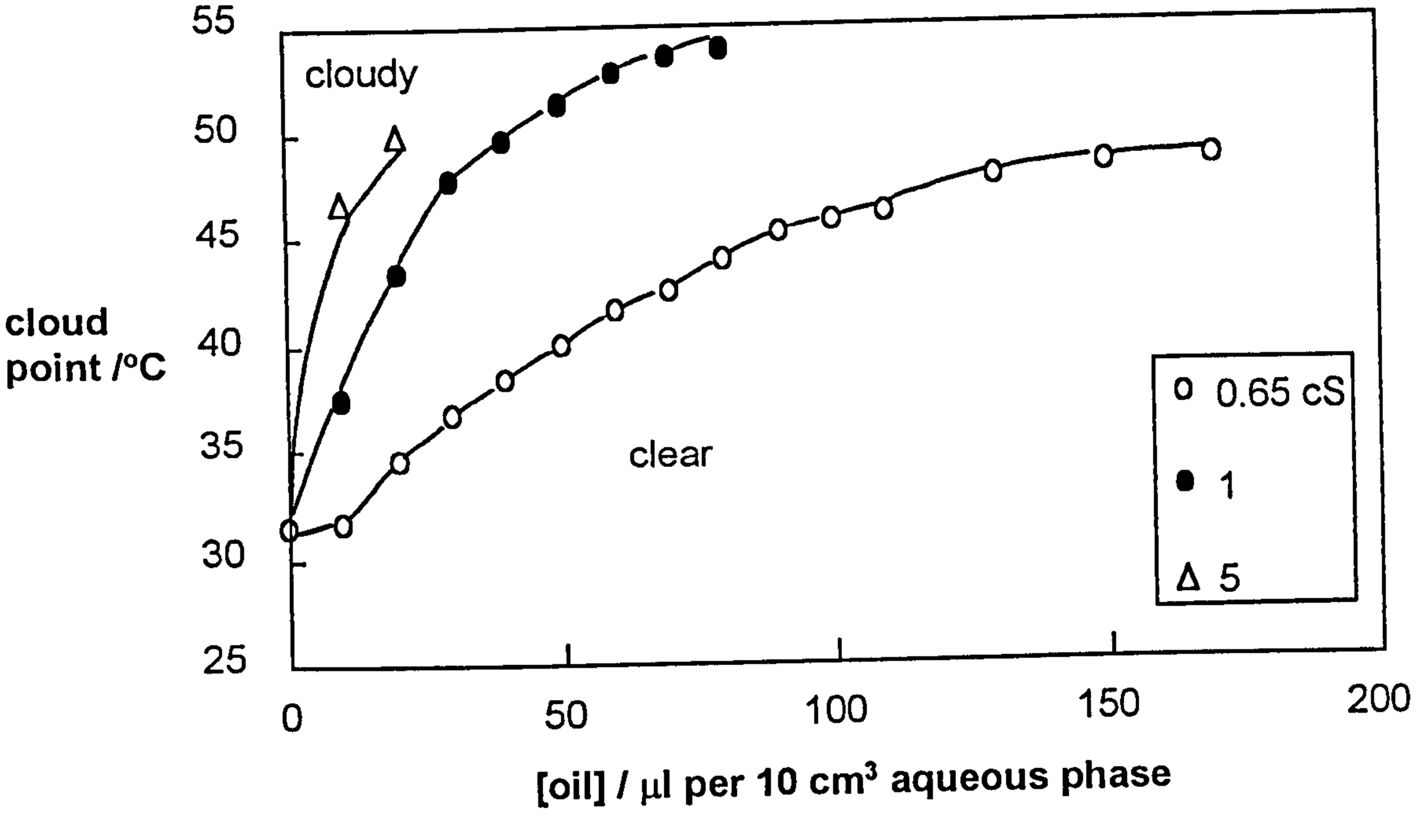

Figure 4.17

Cloud point of 0.5% aqueous L-77 solution on addition of PDMS oils of viscosity given

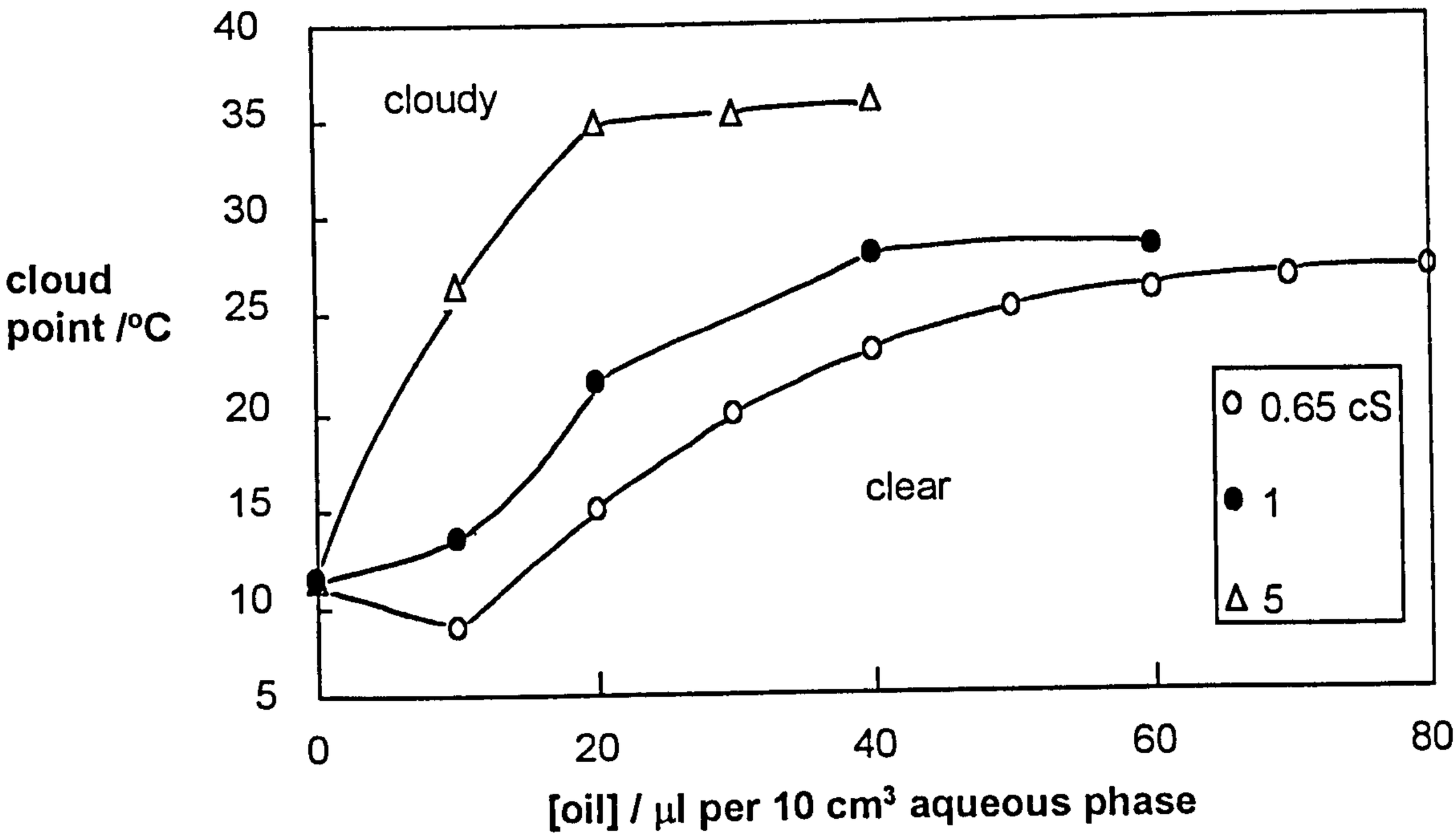

second time above 50°C. This sequence of phases is in agreement with the findings of Hill *et al.*[108] at higher surfactant concentration. The second clear phase is an L_3 phase of bilayer structure. On the addition of small volumes of 0.65 cS PDMS oil, the cloud point initially falls 3 degrees and then further solubilised oil raises it progressively to around 26°C at saturation. Beyond the saturation point, solutions were turbid at all temperatures i.e. the oil phase separates from solution. An increase in the viscosity of the oil leads to a larger increase in the cloud point and a decrease in the saturation volume of oil that can be solubilised. The changes are in line with predictions from behaviour with alkanes. Single phase water-in-oil microemulsions stabilised by L-77 in cyclohexane have been studied by Steytler *et al.*[127] In this work it was concluded that the extent of solubilisation of water in the L_2 phase did not exceed the maximum hydration requirement of the hydrophilic EO groups, which means that hydrated reversed micelles rather than w/o microemulsion droplets are formed in the system. Their results are in agreement with those for C_nE_m surfactants.[128,129]

It can be appreciated that the PDMS oil solubilisation capacity of L-77 is less than that of $C_{12}E_5$. Since the cmc's of the two surfactants are comparable, this is not an effect of micelle concentration, but an inherent effect due to the different chemical constituents. In certain systems, the cloud point at saturation with oil is close to the phase inversion temperature made in mixtures with excess oil.[130] Comparison of the PIT and the cloud point at saturation for L-77 shows that this is not the case here. Intermediate phases (like $L\alpha$) can intervene between the oil content at saturation and the

amount of oil used in emulsion experiments (typically ϕ=0.5) which obscure this relation.

4.4.3 Microemulsion formation in modified PDMS oil systems

It is known that stable aqueous phases containing significant amounts of PDMS oils can be prepared if the PDMS oil has been modified in some way.[65] We chose the aminofunctionalised PDMS oil Q2-8166 (viscosity 1500 cS, density 0.97 g cm^{-3}) to study microemulsion formation with L-77. The cloud points and viscosity changes of L-77 micellar solutions were measured on addition of oil.

The apparent solubilisation of oil in aqueous solutions of L-77 above the cmc at 10°C has been studied. Transitions of turbid - clear - blue - turbid were observed with increasing oil content. Figure 4.18 shows the uptake of oil as a function of [L-77]. The first turbid phase could appear because the cloud points of the solutions are still below 10°C. The structures in clear and blue solution regions may be microemulsions. Since the molecular weight of the oil is unknown, it is impossible to calculate the molar ratio R_o=*[oil]/[L-77]*. We define a mass ratio R_m=*m(oil)/m(L-77)* and calculate it from the slope of the boundary where the blue solutions become turbid again in the figure. R_m =1.52, i.e. 1.52 g oil per gram of surfactant. The value R_o would be much lower because the molecular weight of the oil is much higher than that of the surfactant. Figure 4.19 shows how the cloud point and the viscosity of L-77 solutions are affected by the solubilisation of aminofunctionalised PDMS oil. The increase in the cloud point is accompanied by the decrease in the outflow time required for the same volume of solutions with and without the

Figure 4.18

Oil uptake dependence of the phase boundaries as a function of [L-77] for the system H_2O-aminofunctionalised PDMS oil-L-77 (in 10 cm^3 water) at 10°C

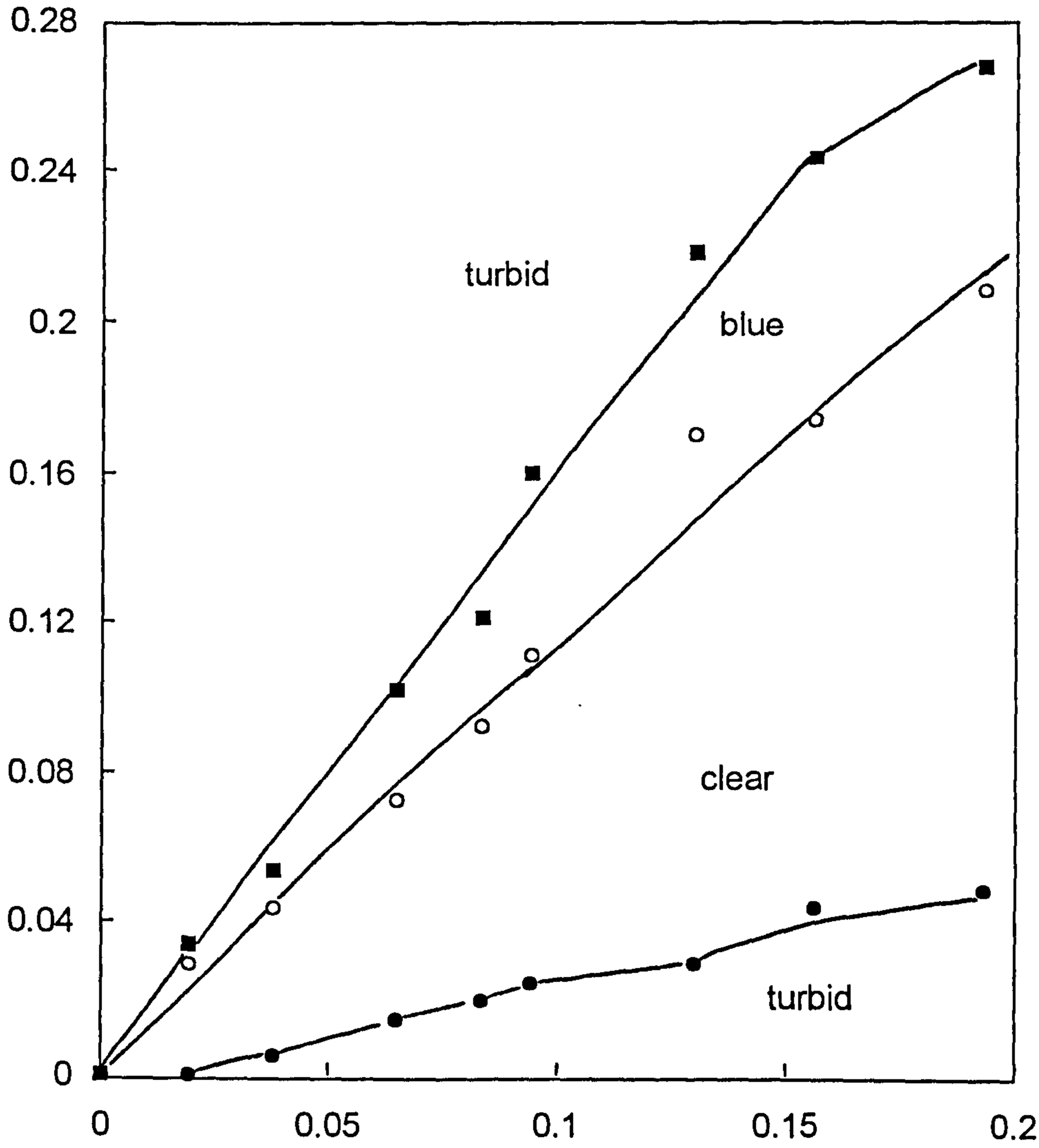

Figure 4.19

Variation of cloud point (o) with added aminofunctionalised PDMS oil for 0.5 wt% aqueous solution of L-77. Also shown is the ratio of the outflow time for solutions containing oil to that of the solution without oil (●)

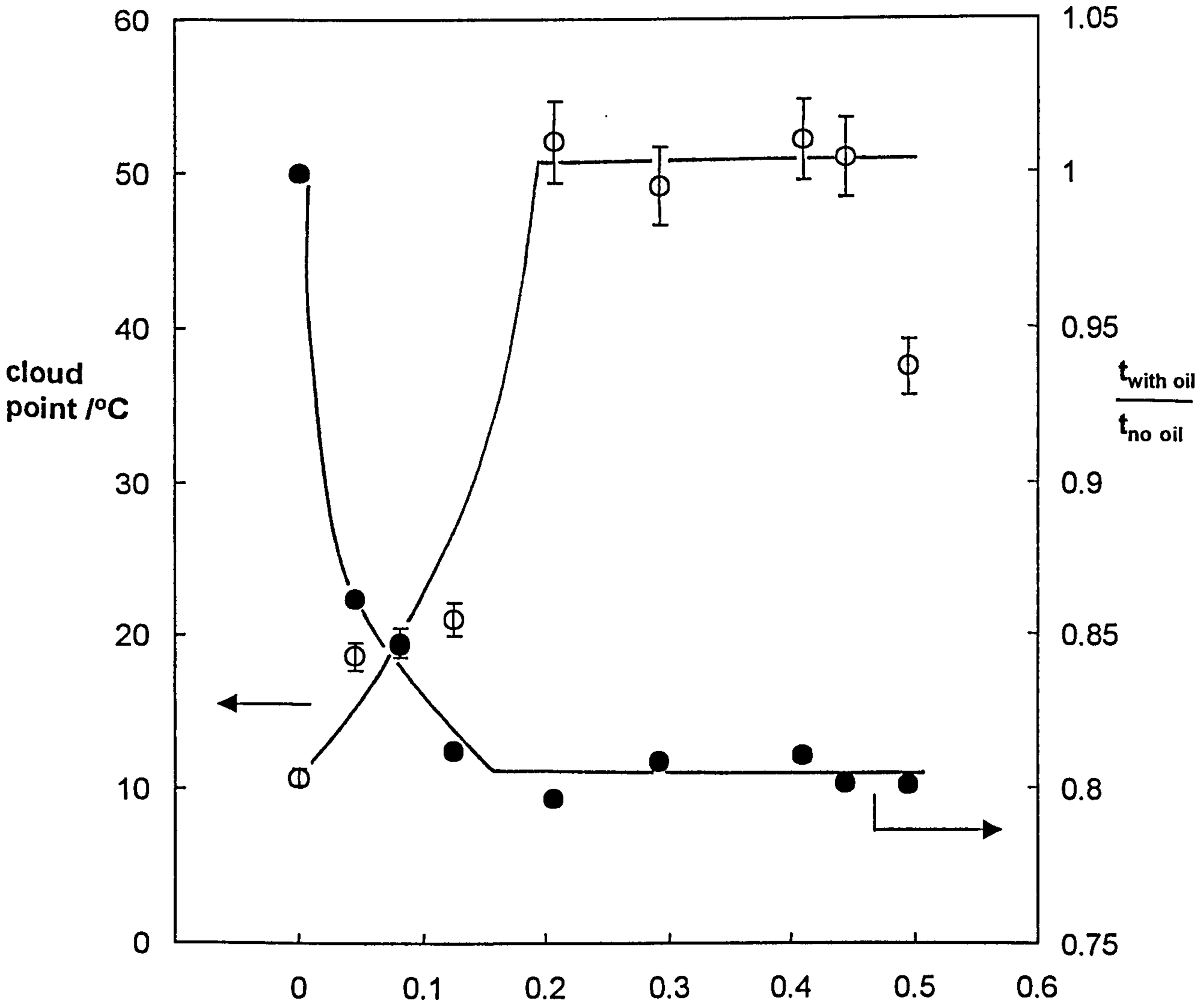

addition of the oil. The outflow time is closely related to the relative viscosity of the solutions, which may indicate that dry micelles which are non-spherical become spherical microemulsion droplets upon incorporation of the oil as expected.

4.5 Conclusions

The equilibrium phase behaviour of PDMS oil + water + nonionic surfactants + electrolyte systems studied in this chapter gave the following conclusions.

For the 50 cS oil

(i) For $C_{12}E_3$ in 0.01 M NaCl, a Winsor I-III-II transition occurs with increasing temperature in equilibrium systems. The third phase contains mainly surfactant and water. At 10, 18, 30, 41 and 50°C, inversion from Winsor I-III or III-II equilibria occurs on increasing the [NaCl].

(ii) For $C_{12}E_3$, increasing the concentration of TBAB results in two types of third phase, one rich in water and the other rich in surfactant.

(iii) For $C_{16}P_8E_1$, three phase systems occur at 18 and 30°C which become two phase systems on addition of NaCl. The third phase is the upper phase and contains mainly oil and surfactant.

(iv) For L-77 at 35 and 40°C, a Winsor I-III transition occurs upon increasing the [NaCl].

For other oils

(v) The solubilisation of low molecular weight PDMS oils into aqueous aggregates of nonionic surfactant raises the cloud point of $C_{12}E_5$ and L-77. $C_{12}E_5$ is capable of solubilising more oil per surfactant than L-77.

(vi) The aminofunctionalised PDMS can be solubilised into L-77 aqueous solutions, raising the cloud point and decreasing the viscosity of the solution.

CHAPTER FIVE

CHAPTER 5

Mixing of Silicone Oil and Nonionic Surfactants at Air-Water Interfaces

5.1 Introduction

The interaction of oils with the chain region of surfactant monolayers at the air-water interface has important consequences on a number of phenomena in surfactant systems. Thus, for example, short chain alkanes when added to air-water surfaces in foams destabilise them relative to the no oil situation, whereas long chain alkanes have a stabilising effect.[131] PDMS oil has been used widely in anti-foaming agents. It is believed that the reason is related to the spreading characteristics of PDMS oil, since it can spread on both water and organic liquid surfaces. Apparently, spreading oil entrains subsurface fluid that then drains the individual foam films, causing film rupture and eventual destruction of the foam. The spreading coefficients proposed by Harkins[132] based on the Dupré theorem reflect the possibility of the spreading of one phase on the surface of another.

From the previous chapters about the aspects of emulsion and equilibrium phase behaviour in silicone oil + water + nonionic surfactant systems, it was found that the solubilisation of silicone oils into surfactant aqueous or surfactant-rich third phases depends on temperature, electrolyte concentration and oil molecular weight. For the 50 cS PDMS oil, using different structures of nonionic surfactant ($C_{12}E_3$, L-77, $C_{16}P_8E_1$) revealed that little solubilisation occurred in all cases. Since the direct determination of

the amount of oil associated with the surfactant monolayer at the oil-water interface is not advanced yet experimentally, the measurement of the extent of oil and surfactant mixing at the air-water interface is possible by surface tension measurements, which may shed light on the behaviour at the oil-water interface.

In this chapter, the spreading behaviour of silicone oils on aqueous solutions of nonionic surfactant is discussed.

Firstly, we discuss the spreading behaviour of silicone oils on the air-water surface in the absence of surfactant. For many years it has been known[5,53,133] that when linear PDMS oils are spread at the air-water surface, a surface pressure develops that is analogous to the osmotic pressure characteristic of a three-dimensional solution. Figure 5.1 shows a typical example of the surface pressure-molecular area curve obtained. There are three regions of interest. In the dilute region of surface coverage, molecules interact little and the surface pressure in this region is very low. The PDMS oils form a dense layer with their chains elongated at the water surface. The Si-O-Si bonds are oriented towards water whilst the methyl groups are predominantly on the side of the chain away from the water. Recently, this layer was demonstrated directly with neutron reflectivity.[57] At higher surface coverages a transition region follows. Here the surface pressure rises much more rapidly than proportional to the surface concentration and is independent of molecular weight. It was thought that as the molecules of PDMS oils on the water surface are compressed in this region, weakly associated water molecules in the film are displaced until at about 20 $Å^2$ per monomer the extended siloxane chains begin fitting into a close-packed

array. As the polymers are compressed below 20 $Å^2$ per monomer, the film pressure increases rapidly and the siloxane chains orient with the methyl groups outmost and in closest packing. Since further compression is impossible while maintaining all Si-O-Si groups in contact with water, subsequent decreases in area lead to one siloxane after another lifting off the surface and coiling into a series of spirals, averaging 6 siloxane units per spiral, and the force-area curve reaches a plateau region. It is generally agreed that the plateau reflects collapse of the monolayer to a three-dimensional state. Two general scenarios are observed; a direct transition from the monolayer to a bulk phase or a progressive transition through a series of multilayers and have been investigated recently by Brewster angle microscopy and scanning force microscopy.[134] Topographic images show that the growth of the second layer begins with the nucleation of three-dimensional islands, which then appear to spread in the form of ribbons 0.5 μm wide and 7.5 Å high. The number of ribbons increases as the extent of the second layer increases, but the width of the ribbons remains constant. Multilayer formation is also confirmed using neutron reflectivity.[57,59]

PDMS oils were also studied as insoluble monolayers on a variety of organic liquids like ethylene glycol, oleic acid and hexadecane[55,135,136] In many instances the PDMS oil films are extremely stable and can give film pressures as high or higher than normally found at the same area/monomer on water. In most cases, the minimum surface tensions of the monolayer-covered organic liquids were not much above that of the pure liquid PDMS oil, but no well-defined collapse pressures were observed. The low surface tensions indicate complete coverage of the surfaces by the PDMS oil films.

Surfactants can form insoluble monolayers on the water surface and modify the surface properties. The polarity of the surface depends on the surfactant structure such as the headgroup size and hydrophobic chain length. As mentioned in chapter 1, the spreading behaviour of PDMS oils on surfactant aqueous solutions of surfactant was investigated a cationic (CTAB), a nonionic ($C_{10}E_5$) and an anionic (AOT) surfactant.[56-60] Here, the differences in the spreading behaviour of PDMS oils are mainly associated to the surfactant structure. However, the difference in the surfactant structures is too diverse. In order to gain a systematic understanding of the effect of surfactant structure on PDMS oil spreading behaviour, this chapter will focus on the following:

(i) We first describe the visual observations following the addition of various PDMS oils to aqueous nonionic surfactant solutions.

(ii) The behaviour of the 50 cS PDMS oil with monolayers of alkylpolyoxyethyleneglycol either, C_nE_m, surfactants above the cmc is given next. These data, combined with oil/water interfacial tensions, allow the determination of the spreading coefficients as a function of n and m.

(iii) Thirdly, we investigate the effect of the viscosity of the oil on the mixing for $C_{12}E_5$ above its cmc.

(iv) We then show what happens when the surfactant solution is diluted below the cmc, and compare results for a hydrocarbon surfactant and a silicone surfactant.

(v) For a volatile silicone oil, the oil adsorption isotherm on $C_{12}E_5$ is measured to assess the surface concentration of oil.

(vi) Finally, we report preliminary results of the spreading behaviour of

PDMS oils determined by neutron reflectivity.

5.2 Observation of the spreading behaviour

Two systems have been investigated visually. In the first, drops of the 50 cS PDMS oil have been added to surfactant solutions at 1.5xcmc in the series $C_{12}E_m$ (m=2-6) and C_nE_5 (n=8, 10, 12, 14, 16). In the second, $C_{12}E_5$ in the presence of PDMS oils of various viscosities have been studied. Table 5.1 summarises the visual observations. In order to investigate the effect of adding surfactant to the oil on the spreading behaviour, two methods have been compared where the 50 cS oil is either neat or contains 1 wt. % surfactant. Without surfactant in oil, the drops do not spread initially on any surfactant solution but form lenses with appreciable contact angles. With time, the lenses flatten and for both short alkyl chains and small head group size, they disappear completely. In other systems, the changes continue to occur for at least 72 hours. By contrast, surfactant-containing oil drops spread rapidly on all solutions and characteristic interference colours were seen around the edges of the film near the vessel sides. These spread films appear to be the equilibrium situation except for $C_{12}E_2$ and $C_{16}E_5$ where a very flat lens appears within 10 minutes. The effect of oil viscosity on the PDMS spreading on $C_{12}E_5$ solution was carried out by adding 1 wt. % $C_{12}E_5$ in the oil phase. The lower viscosity oils up to 50 cS all spread on $C_{12}E_5$, but the more viscous homologues spread partially and an oil lens remains on the surface.

Table 5.1 Observations following addition of PDMS oils to surfaces of aqueous solutions of nonionic surfactants at 1.5xcmc at 25°C

(a) Addition of 50 cS PDMS oil

system	no surfactant in oil		1 wt.% surfactant in oil	
	initial (<5 s)	after 72 hrs	initial (<5 s)	after 10 mins.
H_2O	spreads with colours	colours seen	On all surfactant solutions, the oil spread rapidly giving interference colours at the edge of the vessel	
$C_{12}E_2$	lens	no lens		flat lens
$C_{12}E_3$	lens	flatter lens		no colours
$C_{12}E_4$	lens	flatter lens		no colours
$C_{12}E_5$	lens	flatter lens		colours seen
$C_{12}E_6$	lens	flatter lens		colours seen
C_8E_5	flat lens	no lens, colours seen		colours seen
$C_{10}E_5$	flat lens			colours seen
$C_{14}E_5$	lens	flatter lens		colours seen
$C_{16}E_5$	flat lens	no lens		flat lens

(b) Addition of various PDMS oils containing 1 wt.% $C_{12}E_5$ to $C_{12}E_5$ solutions

PDMS oils viscosity / cS	0.65	1	5	10	20	50	100	500	1000
initially (<5s)	Oil spreads rapidly and colours visible at edge of vessel						Partially spreads, lens remains		
after 10 mins	Oil remains spread. Colours still visible at edge of vessel						no lens	lens	

5.3 Spreading coefficients of PDMS on C_nE_m monolayers

The spreading behaviour of oil on water can be described quantitatively by the spreading coefficients S_i and S_e which have been determined for the 50 cS PDMS oil on monolayers of C_nE_m above the cmc.

In addition, $C_{12}E_5$ was chosen to investigate the effect of PDMS oil molecular weight on the spreading coefficients. As described in chapter 1, three tensions are needed to calculate the spreading coefficients.

5.3.1 Air-oil tensions

The surface tensions of the PDMS oils at 25°C were measured by using the du Noüy ring method. In order to check if water itself changes the tension of the oil, equal volumes of water and PDMS oil were equilibrated and the tension of the (wet) oil phase was measured. Figure 5.2 shows the results. Clearly, the difference is negligible demonstrating the immiscibility of water and PDMS oils.

5.3.2 Air-water tensions of surfactant solutions with and without PDMS oil

(a) C_nE_5 series

For measurements with aqueous surfactant solutions at air-water surfaces, it is necessary to ensure that sufficient surfactant is present at the surface in the presence of oil. Since nonionic surfactants can partition as monomer into oil phases,[113] and the extent of this partitioning is unknown in the case of PDMS oils, precautions have been taken to ensure that even with this possible loss, the aqueous phase remains at or above the cmc. Figure 5.3 shows the time dependence of γ_{AW} following the addition of 10 μl of neat PDMS oils to surfactant solutions at 1.5xcmc. For C_8E_5 and $C_{10}E_5$, the tension change becomes constant within 5 minutes as a flat lens forms very quickly. This time increases to over 40 minutes for $C_{12}E_5$ and $C_{14}E_5$ as the oil drop slowly disappears, and in the case of $C_{16}E_5$ the tension initially

Figure 5.1

Surface pressure of 50 cS PDMS oil on pure H_2O, redrawn from ref. 55

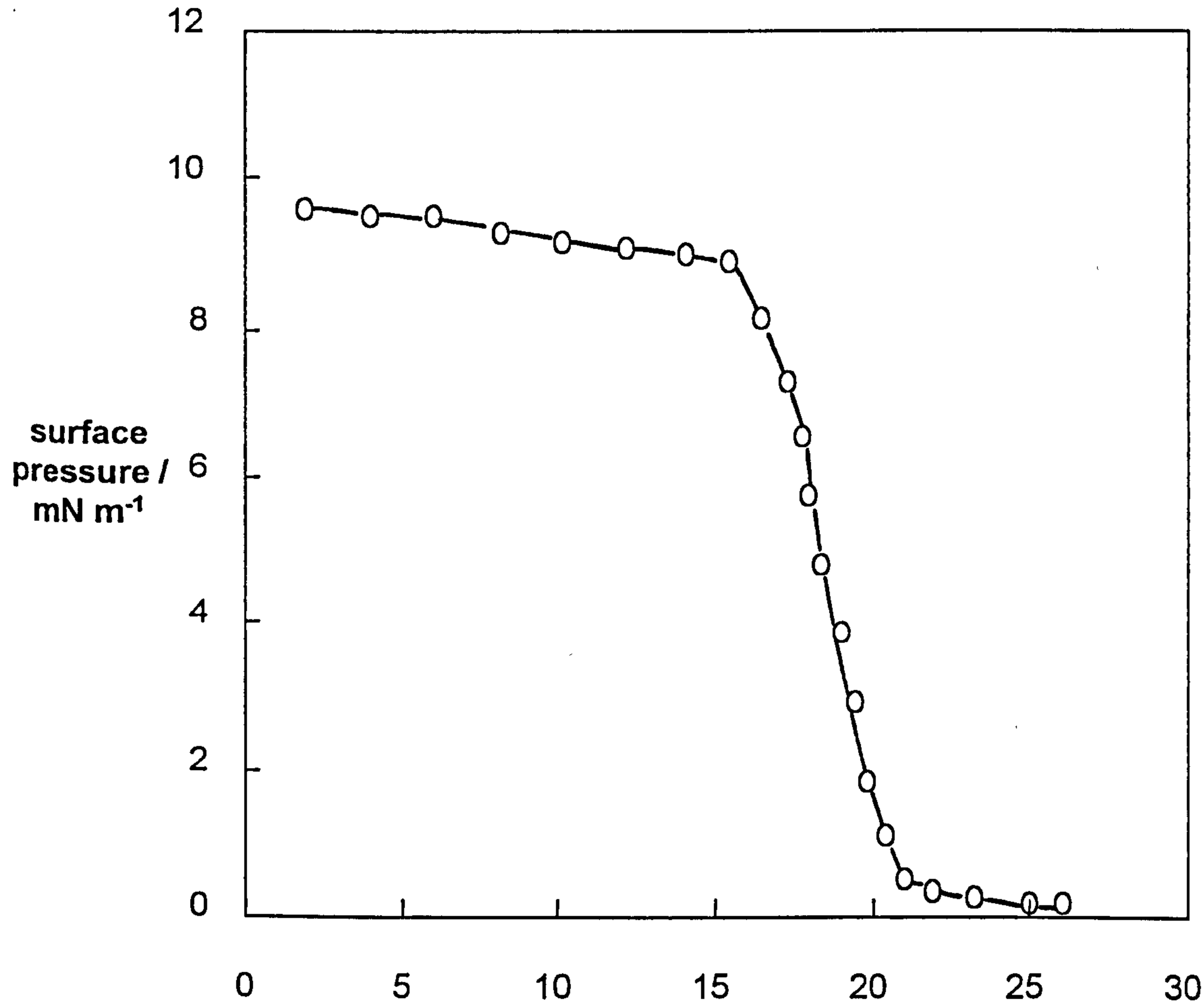

Figure 5.2

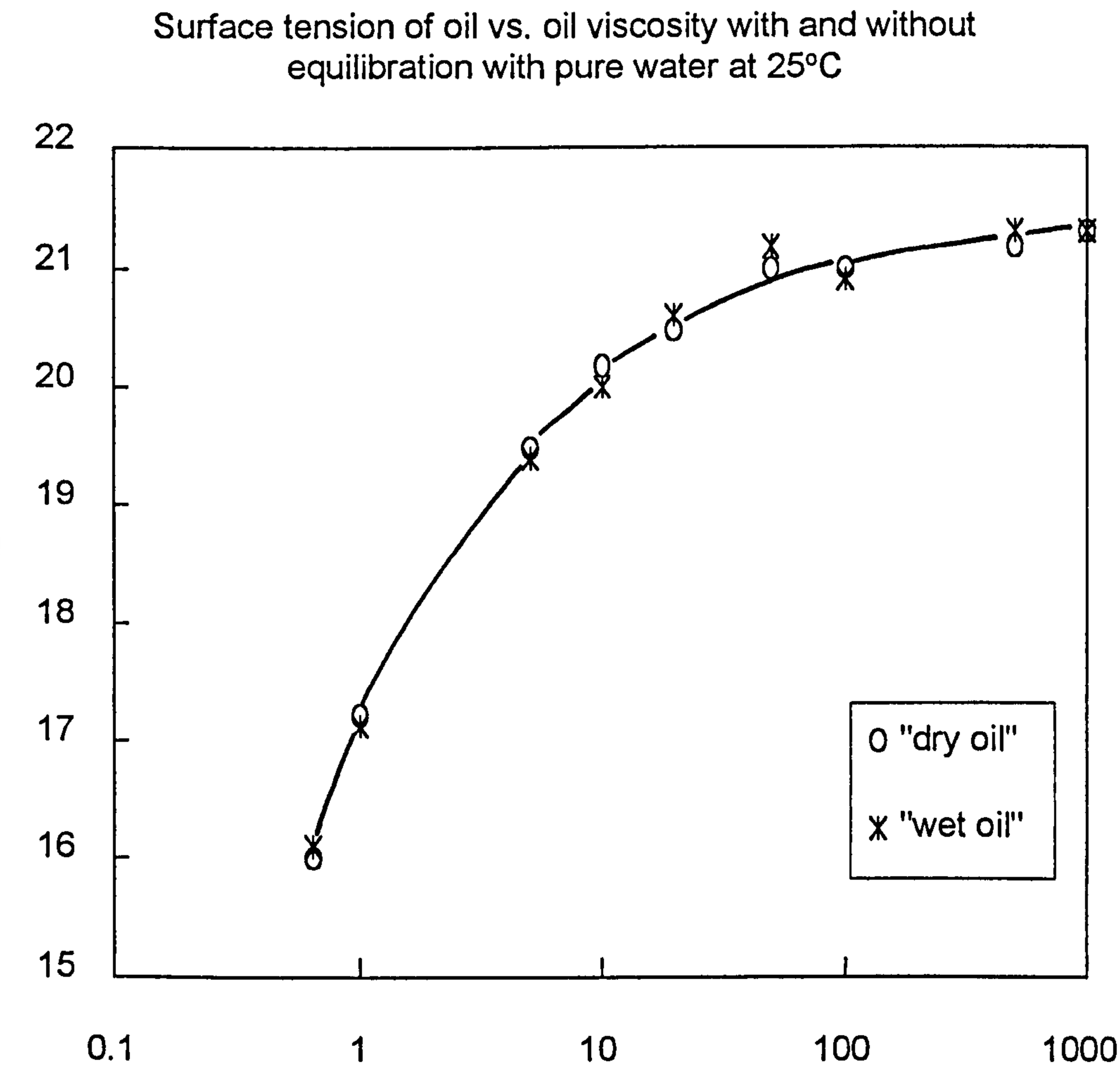
Surface tension of oil vs. oil viscosity with and without equilibration with pure water at 25°C
22
21
20
19
18
17
16
15
/ mN m-1
0 "dry oil"
x "wet oil"
0.1
1
10
100
1000
PDMS viscosity/cS

Figure 5.3

Variation of air-water surface tension with time following addition of 10 μl of 50 cS PDMS oil to aqueous solutions of 1.5 x cmc C_nE_5 surfactants at 25°C

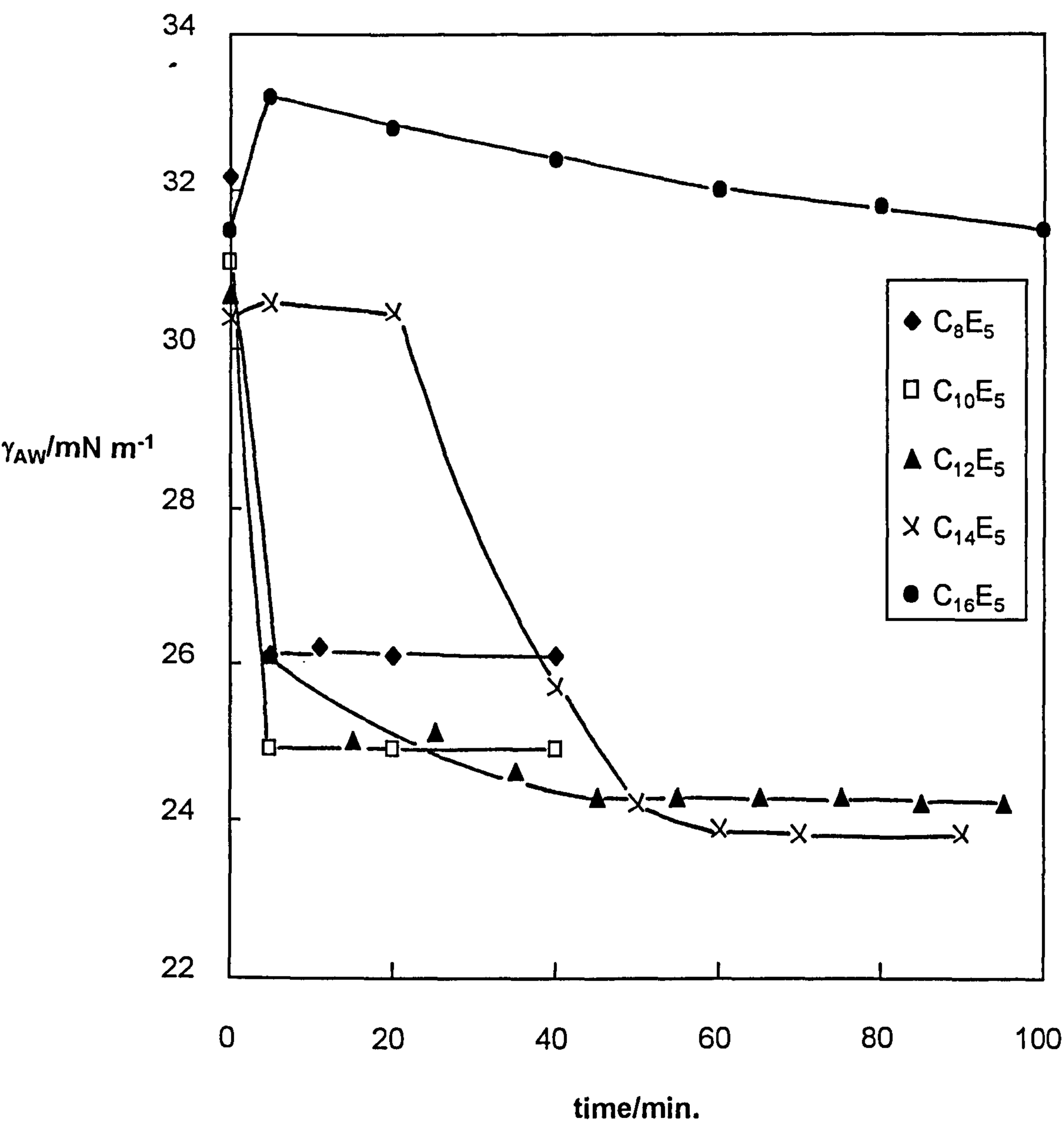

increases and continues to change even after 2 hours. Clearly, as the surfactant chain length increases it may be that transfer of surfactant from water to oil occurs making it more difficult for PDMS oils to spread. Figure 5.4a shows the results of a series of experiments in which drops of PDMS oils containing different concentrations of surfactant were placed on aqueous phases at 1.5xcmc. Here, the oil drop spreads immediately on all surfactant solutions and the systems reach equilibrium within 5 minutes. For $C_{16}E_5$, at least 0.2 wt.% surfactant is required in the oil phase for a true $\Delta\gamma$, the difference in surface tension after the addition of the oil drops on the same surfactant solution, to be attained. By comparison, using neat oil but increasing the surfactant concentration in water to 50xcmc, restores the time dependence of the tension changes with the result that the data for $C_{16}E_5$ are unreliable (Figure 5.4b). The findings from all 3 sets of experiments are consistent and we also verified that the tensions remain at their new values for up to at least 30 hours.

In Figure 5.5, the variation of $\Delta\gamma$ for the C_nE_5 series of surfactants is shown. Within the errors ($\pm$0.2 mN m^{-1}), $\Delta\gamma$ increases slightly with the increase in chain length from 8 to 14, but the change is much less than for the addition of dodecane and tetradecane to C_nE_7 surfactants.[47] As described in chapter 1, $\Delta\gamma$ is equivalent to the surface pressure of oil on the surfaces. If the simple space filling mechanism holds, $\Delta\gamma$ should depend on at least two factors. One is the space available on the surfactant solution surface which depends on the area per surfactant molecule (A_s). For a nonionic surfactant, A_s is mainly determined by the size of the headgroup.

Figure 5.4a

Effect of surfactant concentration in 50 cS PDMS oil drop on the equilibrium surface tension in the presence of oil. Aqueous phase surfactant concentration is 1.5 x cmc

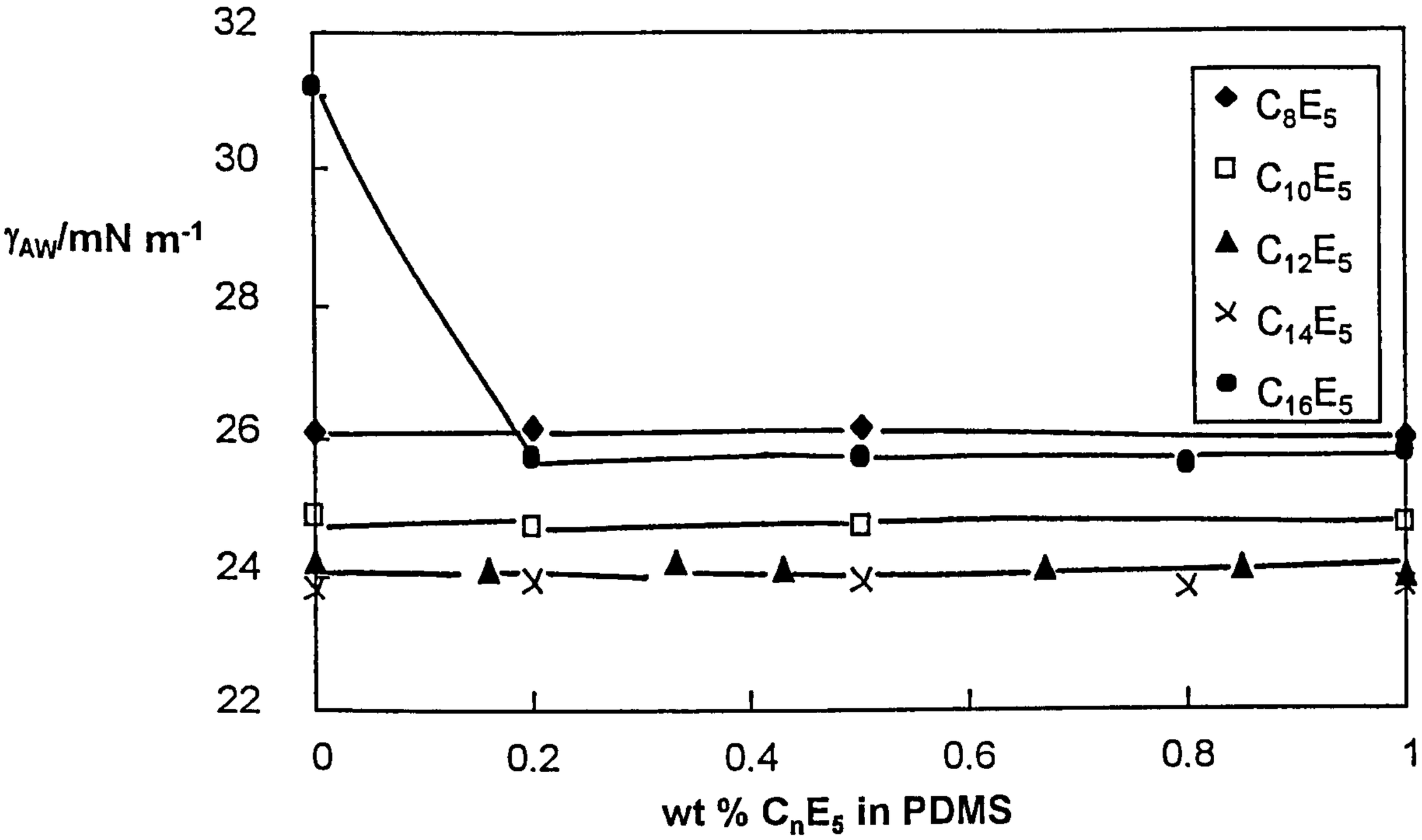

Figure 5.4b

Time dependence of surface tension after addition of 10 μl of 50 cS PDMS oil to 50 x cmc aqueous C_nE_5 solutions

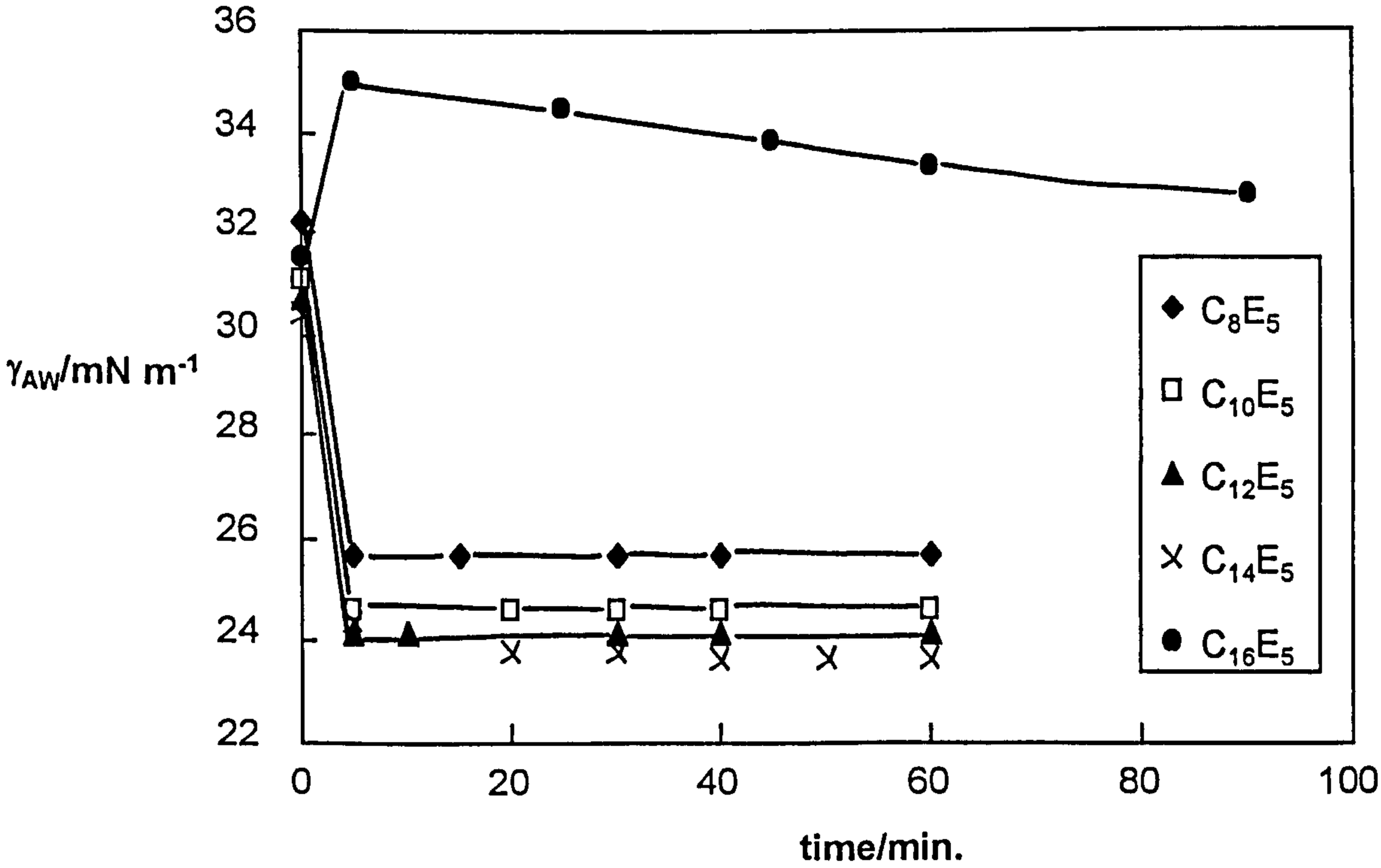

Figure 5.5

Tension lowering by 50 cS PDMS oil for aqueous solutions of C_nE_5 surfactants above the cmc (filled circles). Also shown is the tension lowering of C_nE_7 by dodecane (open circles) and tetradecane (triangles) redrawn from ref. 47

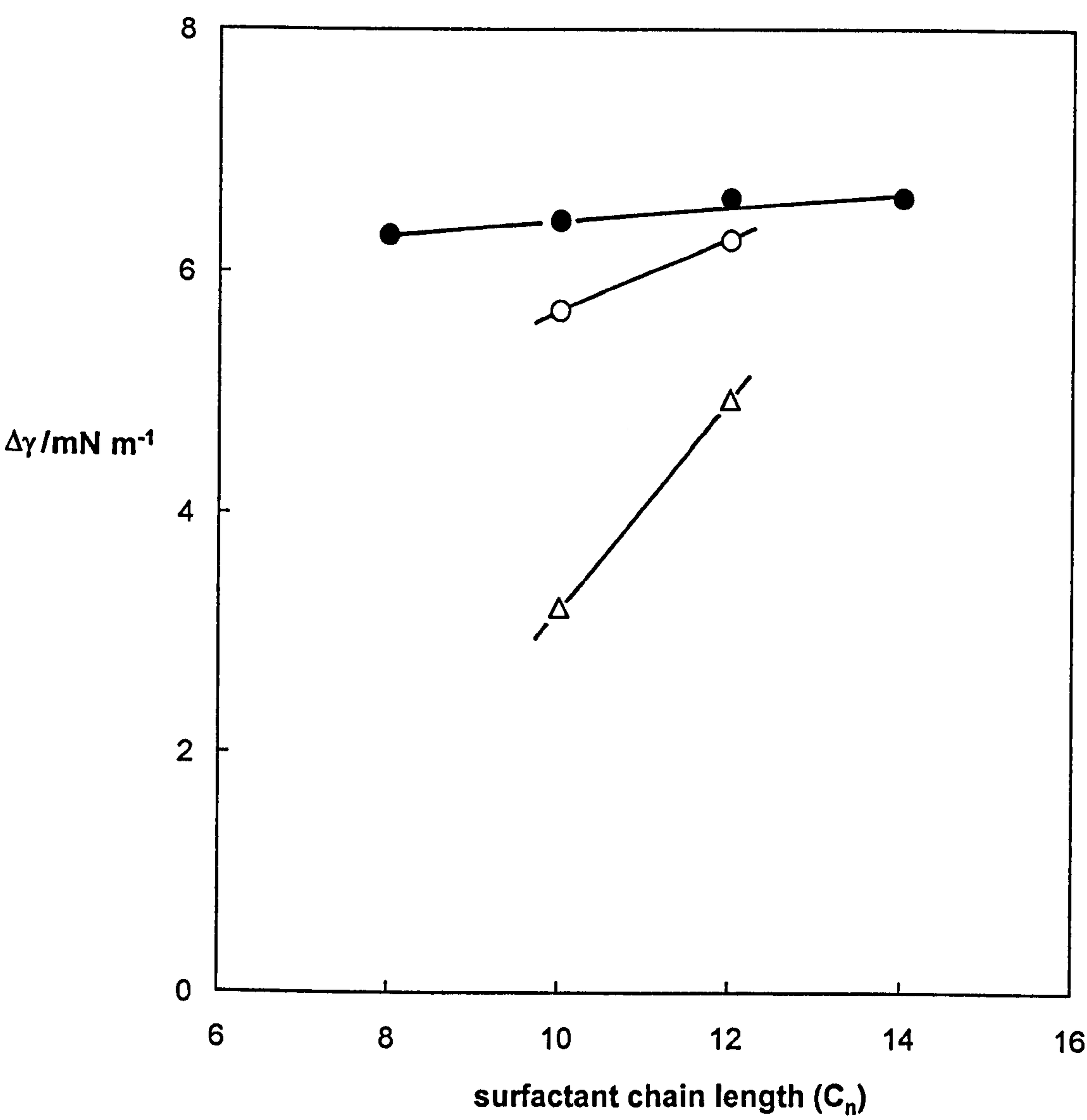

The other is the molecular volume of the oil itself. Clearly, the large molecular volume of PDMS oil compared with dodecane makes the oil penetration into the surfactant chain region very difficult. Hence, the dependence of $\Delta\gamma$ on surfactant chain length is less pronounced.

(b) $C_{12}E_m$ series

The effect of the number of ethyleneoxy groups on the spreading behaviour of PDMS oil was also investigated for a fixed chain length of C_{12}. For aqueous phase surfactant concentrations at 50xcmc, neat PDMS oil drops added spread rapidly on $C_{12}E_4$, $C_{12}E_5$ and $C_{12}E_6$ surfaces, whereas they sit as lenses initially on $C_{12}E_2$ and $C_{12}E_3$ solutions. It can be seen in Figure 5.6a that the tension lowering is time-dependent for $C_{12}E_3$ as the drop finally spreads. In experiments where surfactant was initially in both oil and aqueous phases, the $\Delta\gamma$ values after 1 hour remains the same over 10 hours (Figure 5.6b). The magnitude of $\Delta\gamma$ increases markedly with the size of the surfactant head group from 2.9 mN m^{-1} for $C_{12}E_2$ to 7.4 mN m^{-1} for $C_{12}E_6$ (Figure 5.7), which can be explained by the space filling mechanism.

It can be appreciated from this and other work that the amount by which the surface tension is lowered following the addition of PDMS oils is very dependent on the surfactant type. On pure water containing no surfactant, fast spreading takes place and a $\Delta\gamma$ of 10±1 mN m^{-1} was measured, close to the maximum surface pressure monitored using a Langmuir trough of around 9.5 mN m^{-1}.[137] It is argued that the Si-O groups interact favourably with interfacial water. As the surface becomes covered by

Figure 5.6a

Lowering of air-water tension with time after addition of 10 μl 50 cS PDMS oil to 50 x cmc $C_{12}E_m$ aqueous solutions at 25°C

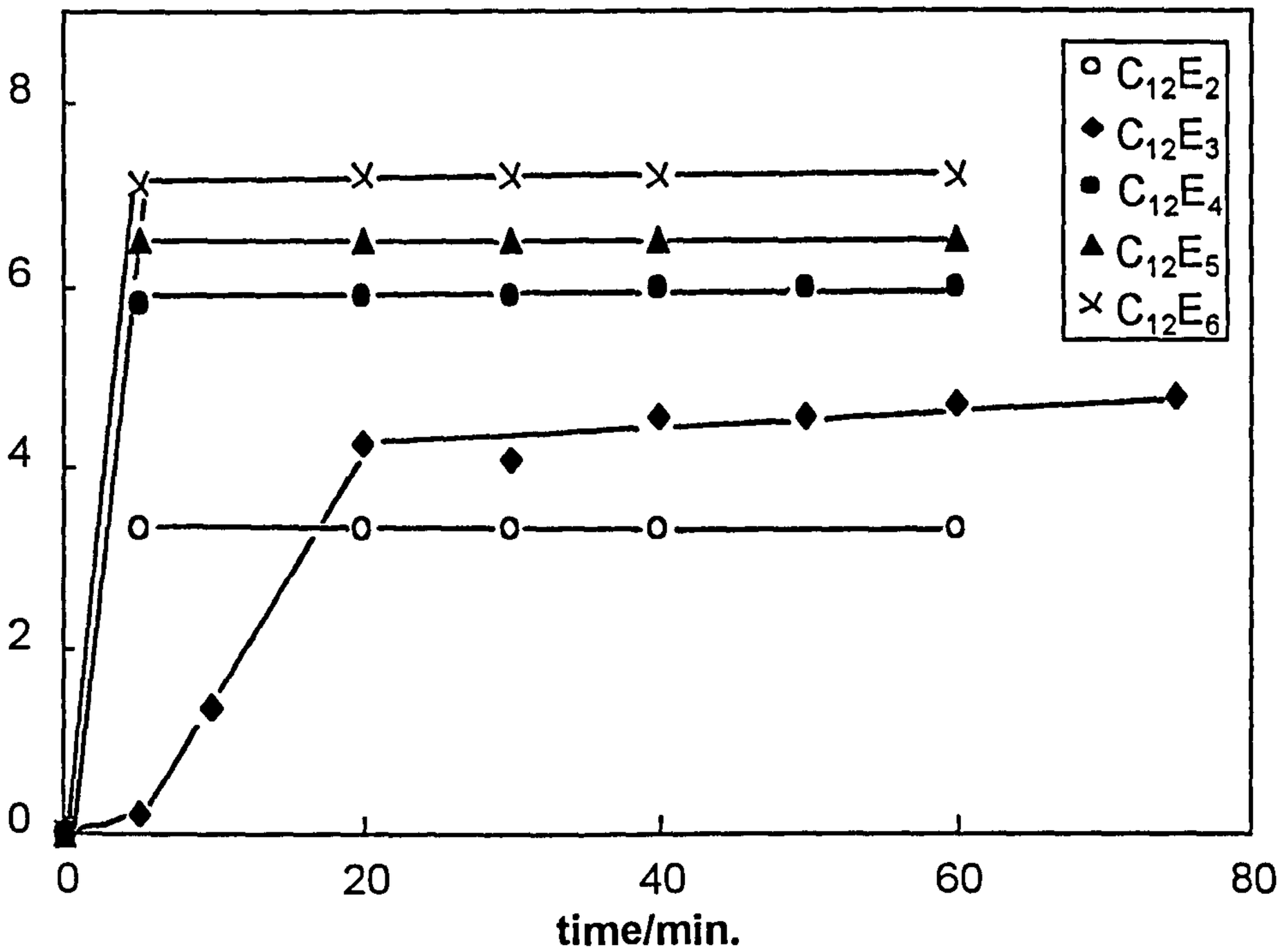

Figure 5.6b

Time dependence of surface tension after adding 50 cS PDMS oil containing 1 wt.% surfactant to 1.5 x cmc $C_{12}E_m$ aqueous solutions

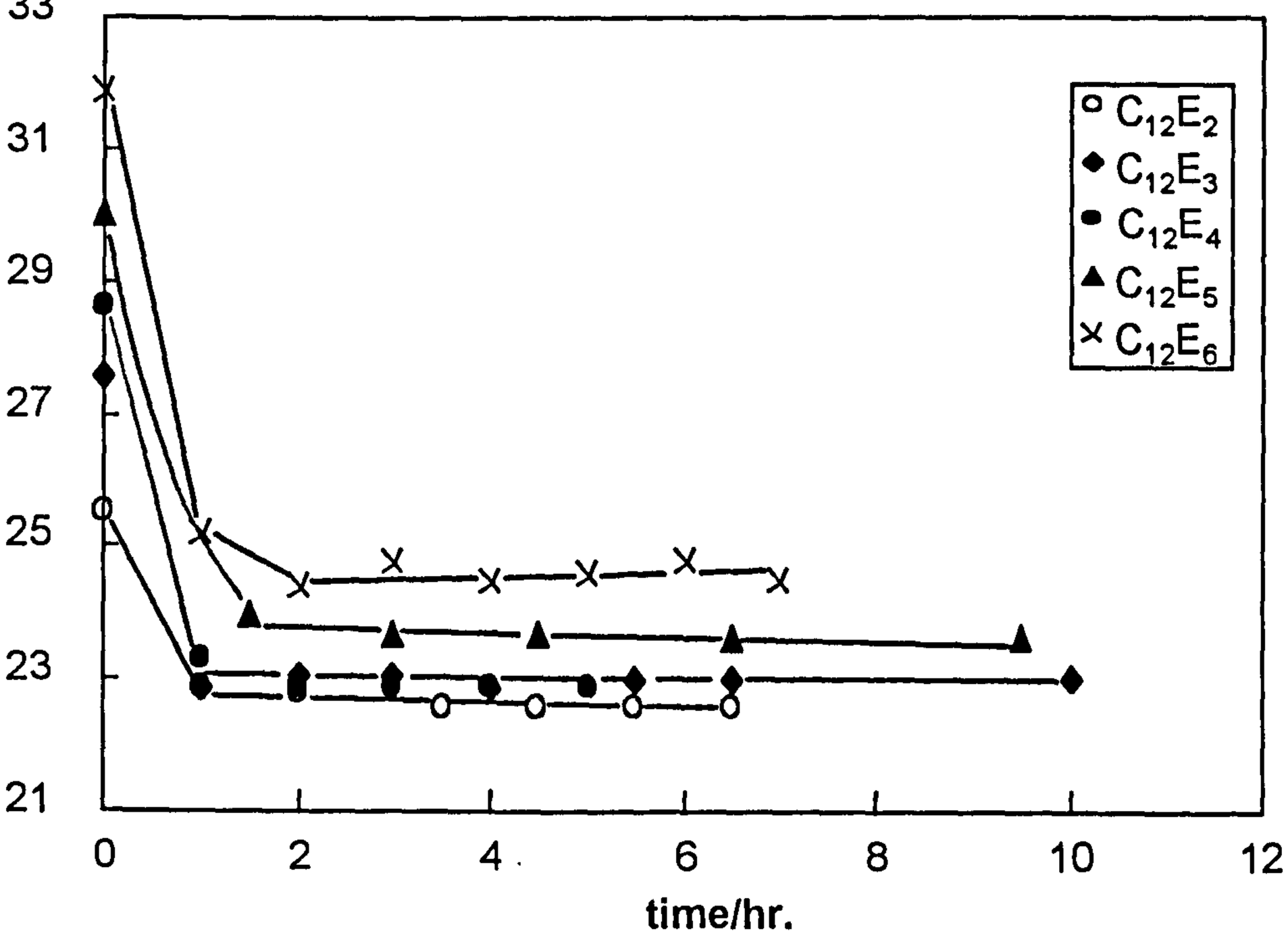

Figure 5.7

Comparison of the tension lowering by 50 cS PDMS oil and the area per surfactant molecule in the absence of oil for aqueous solutions of $C_{12}E_m$ surfactants above the cmc. Areas taken from neutron reflectivity data given in ref.139

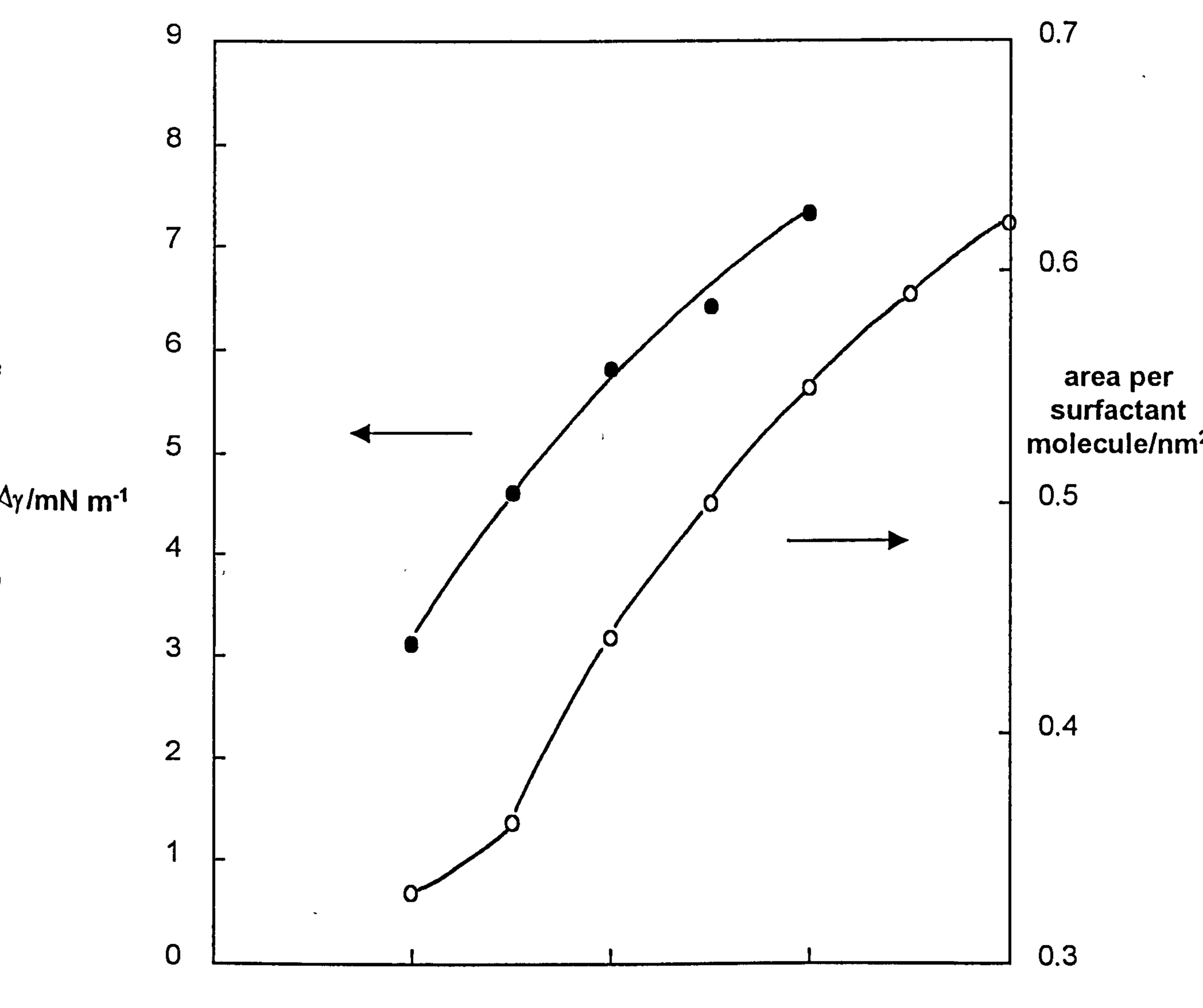

surfactant, the driving force for oil spreading is reduced. If the packing of surfactant at the surface is important, and the area occupied per surfactant molecule (A_s) is unchanged on adding oil, then there should be a correlation between $\Delta\gamma$ and A_s. In this work, $\Delta\gamma$ is found to be weakly dependent on surfactant alkyl chain length for the E_5 series. Although reliable values of A_s are not available for these nonionics, this finding is in line with results for PDMS oil of M_w=10,000 added to C_nTAB solutions, where the ($\Delta\gamma$, A_s) pairs are (7.5, 0.46), (6.6, 0.46) and (7.1, 0.43) for n equal to 12, 14 and 16 respectively.[60,138] In contrast, $\Delta\gamma$ increases progressively with the head group size, and A_s values at the cmc taken form neutron reflectivity results,[139] show that this effect goes alongside the increase in the area per molecule as the surfactant chains are spaced. If in the spreading cases observed here, PDMS oil is initially solubilised in the chain region and the excess forms a thin layer above the mixed monolayer, then there will be a contribution to the measured $\Delta\gamma$ value from this monolayer mixing. On a volume-filling mechanism, monolayer solubilisation might be considered hypothetically to occur in two stages. First, the surfactant chains become more extended and secondly, oil fills the space so generated. Calculations of the density of the surfactant chain region (in the absence of oil) from measured values of A_s[138] and the chain thickness reveal that the chain density is around 80% of liquid dodecane for $C_{12}E_2$ falling to around 50% for $C_{12}E_8$. Thus, part of the increase in $\Delta\gamma$ seems to arise from an increase in the volume of oil needed to saturate the monolayer chain region.

5.3.3 Equilibrium oil-water tensions

For the PDMS oil-water interfacial tension, since the density difference is only 0.04 g cm^{-3}, use of the smallest tip in drop-volume method resulted in too large a water drop formed in oil to detach from one syringe barrel. D_2O ($\Delta\rho$=0.105 g cm^{-3}) was used instead of H_2O for which 3 drops per barrel could be detached. The average tension for 10 drops formed was 38.0±0.2 mN m^{-1}. For oil-water tensions with surfactants, the aqueous phase initially contained a surfactant concentration of 1.5xcmc and the oil phase initially contained 1 wt.% surfactant were pre-equilibrated for 24 hours by shaking the mixture before re-combining the two phases in the drop-volume set-up. Figure 5.8 shows the variation of γ_{ow} with the surfactant structure. As the surfactant chain length increases, there is a decrease in γ_{ow} and a shallow minimum in γ_{ow} as surfactant headgroup size increases. However, in both cases, no ultra-low (less than 0.1 mN m^{-1}) interfacial tension was found. The oil-water tension depends on the monolayer curvature of the surfactant at the oil-water interface. This curvature is not only related to the surfactant structure, but also to the oil penetration into the surfactant monolayer. From the high tensions in this experiment, it is clear that by varying the surfactant structure this does not significantly change the 50 cS PDMS oil penetration into the surfactant monolayer. In other words, the solubilisation of 50 cS PDMS oil into the surfactant monolayer at the oil-water interface is very small which is consistent with the equilibrium Winsor phase behaviour discussed in chapter 4.

Figure 5.8

Variation of the 50 cS PDMS oil-water interfacial tension above the cmc with surfactant structure in C_nE_m at 25°C

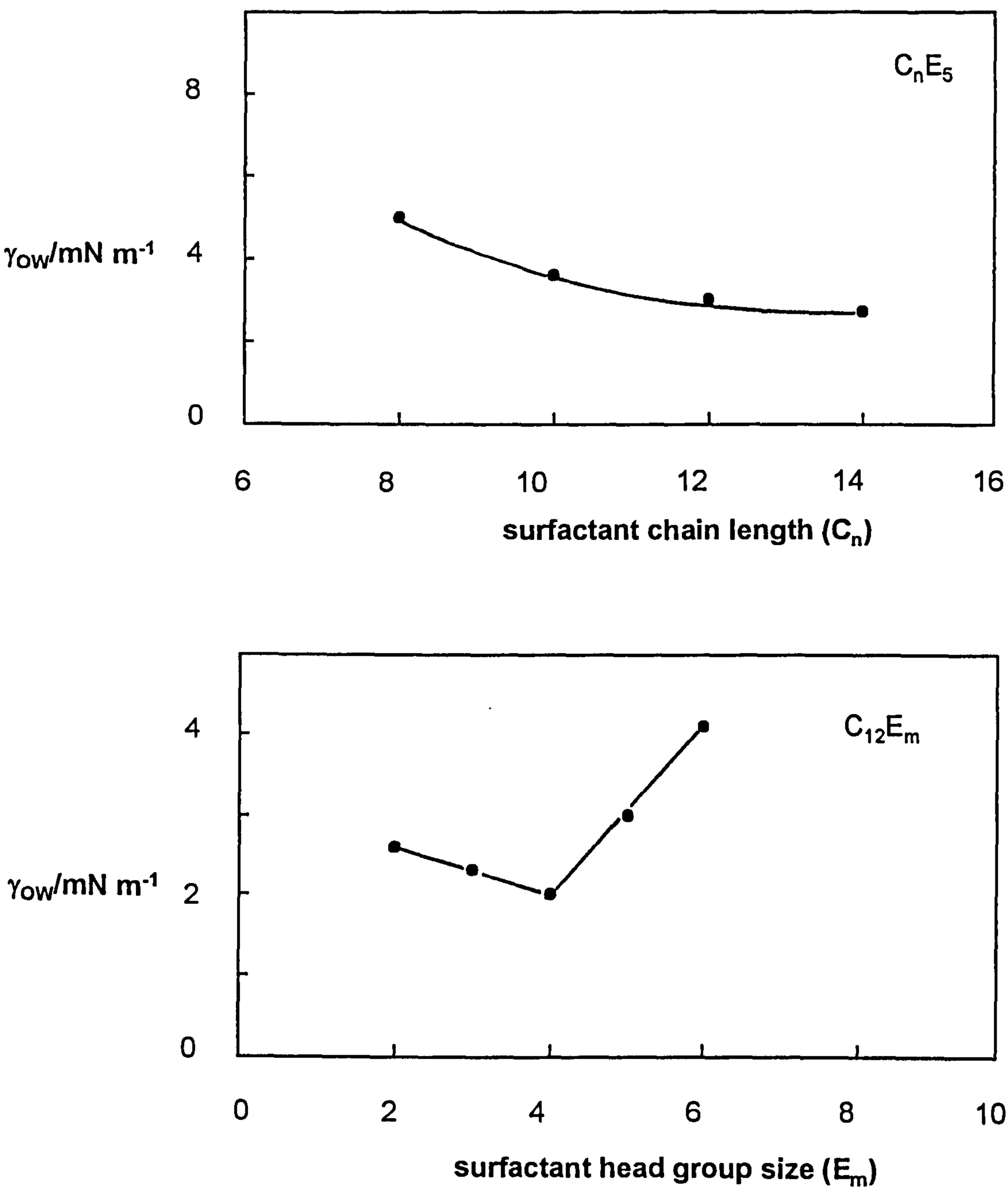

5.3.4 Spreading coefficients of 50 cS PDMS oil for C_nE_m surfactants

By combining the three tensions- air-oil, oil-water and air-water, both the initial and equilibrium spreading coefficients of 50 cS PDMS oil on surfactant solutions can be calculated using equations 1.15 and 1.16. The initial spreading coefficients in the C_nE_5 series are given in Figure 5.9. Interestingly, S_i remains nearly constant, which is a result of the fact that the initial air-water tension decreases with chain length by about the same amount as the oil-water tension does. S_e is close to zero for all chain lengths, consistent with the visual observation that rapid spreading occurs with no oil lens visible at long time. Figure 5.10 shows the initial and equilibrium spreading coefficients in the $C_{12}E_m$ series. S_i values are all positive and S_e values are again close to zero, meaning that oil addition reduces the surface tension to a value equal to the sum of the oil-air and oil-water tensions. The relevant data are given in Table 5.2.

Table 5.2 Air-water surface tensions γ_{AW} (before and after adding oil), oil-water interfacial tensions γ_{OW} and spreading coefficients S in the systems post-cmc aqueous C_nE_m+50 cS PDMS oil at 25°C

Surf.	γ_{AW}/ mN m^{-1}	γ_{AW}^{+oil}/ mN m^{-1}	$\Delta\gamma$/ mN m^{-1}	γ_{OW}/ mN m^{-1}	S_i/ mN m^{-1}	S_e/ mN m^{-1}
Water$^+$	71.9	61.4	10.5	38.0	12.9	2.4
C_8E_5	32.2	25.9	6.3	5.0	6.2	-0.1
$C_{10}E_5$	31.1	24.7	6.4	3.6	6.5	+0.1
$C_{12}E_5$	30.7	24.1	6.6	3.0	6.7	+0.1
$C_{14}E_5$	30.4	23.8	6.6	2.7	6.7	+0.1
$C_{12}E_2$	25.9	22.8	3.1	2.6	2.4	-0.8
$C_{12}E_3$	27.7	23.2	4.6	2.3	4.4	-0.2
$C_{12}E_4$	28.8	23.0	5.8	2.0	5.8	0.0
$C_{12}E_5$	30.4	24.0	6.4	3.0	6.4	-0.1
$C_{12}E_6$	32.2	24.9	7.3	4.1	7.1	-0.2

Figure 5.9

Initial and equilibrium spreading coefficients of 50 cS PDMS oil on aqueous solutions of C_nE_5 surfactants above the cmc.

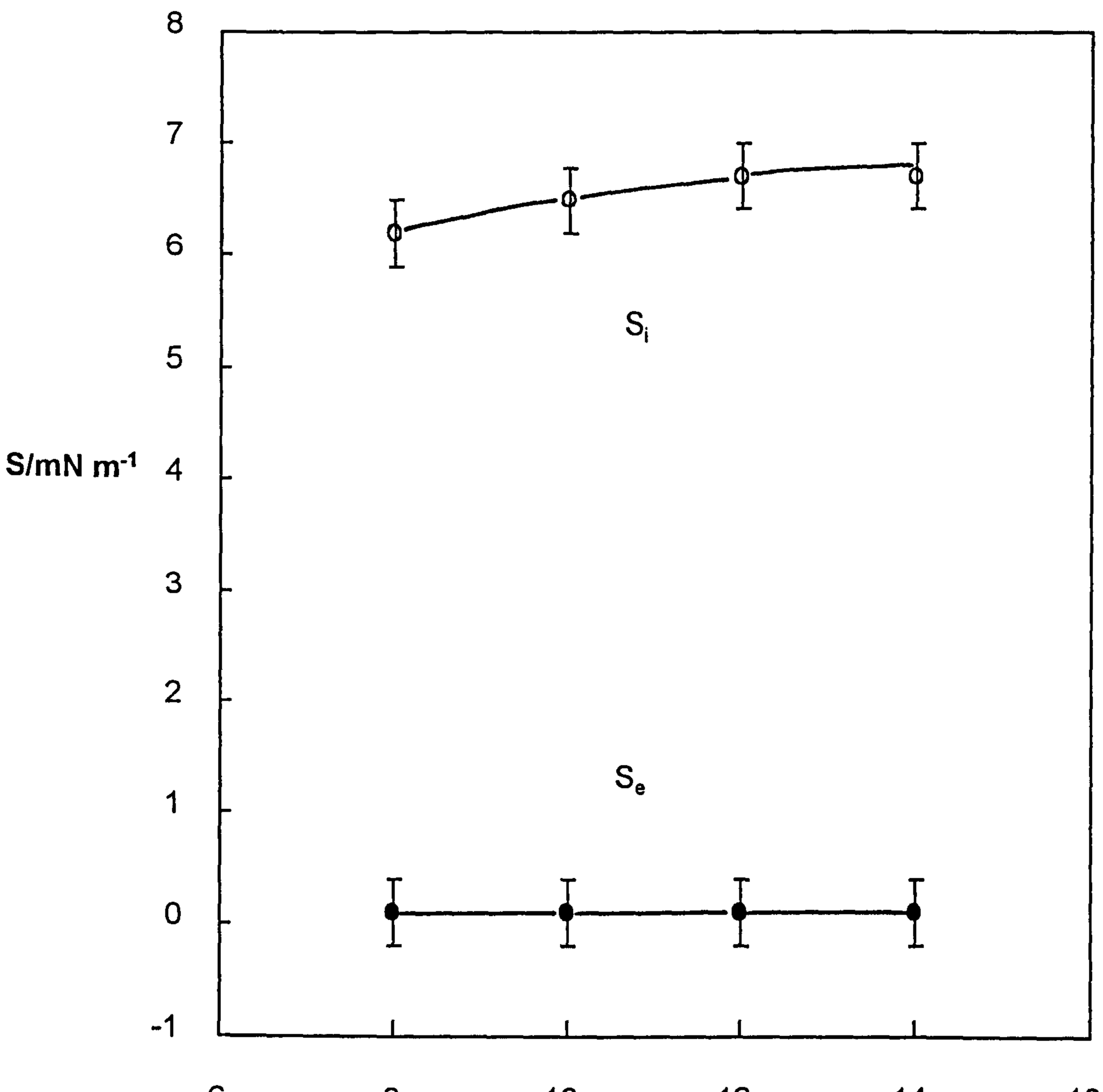

Figure 5.10

Initial and equilibrium spreading coefficients of 50 cS PDMS oil on aqueous solutions of $C_{12}E_m$ surfactants above the cmc.

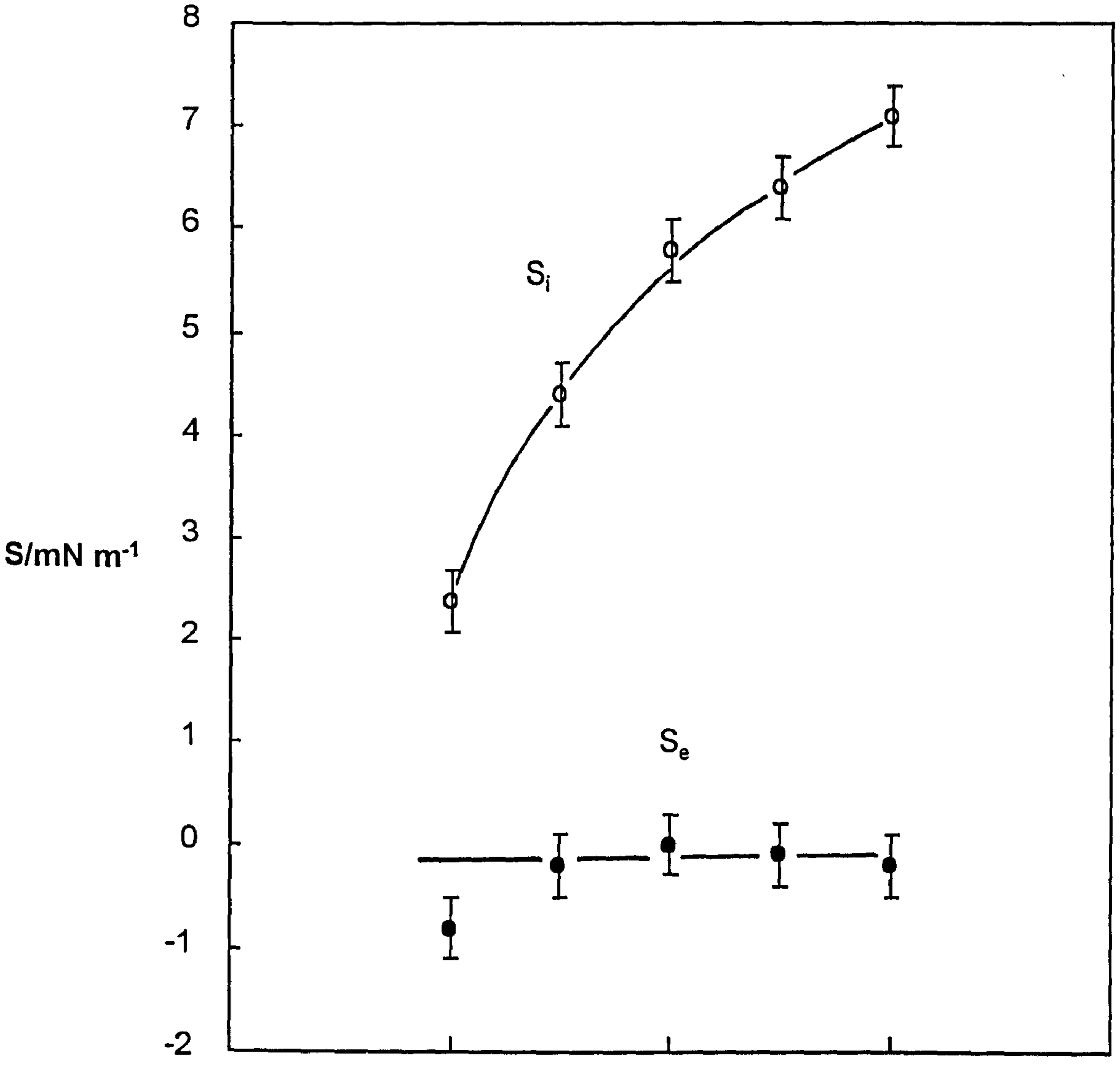

+Average of 5 determinations, error ±1 mN m^{-1}

γ_{OA} is 21.0 mN m^{-1} in all cases

5.3.5 *Effect of PDMS oil molecular weight for $C_{12}E_5$ above the cmc*

For both planar air-water surfactant monolayers and curved monolayers coating microemulsion droplets, adsorption of alkanes is known to increase with decreasing alkane chain length.[42, 47] We have likewise investigated the mixing of a range of PDMS oils of varying molecular weight (hence viscosity) with monolayers of $C_{12}E_5$. For oils of viscosity 5 cS and higher, their vapour pressures are sufficiently low that no noticeable evaporation of oil occurs from the monolayers. The oils of viscosity 0.65 to 100 cS inclusive spread rapidly with no lens being visible at long time. The 500 and 1,000 cS oils do not spread completely but remain as visible lenses. From Figure 5.11a it is seen that the surface tension becomes constant within 10 minutes for the non-volatile oils added as a 1 wt.% solution of $C_{12}E_5$ in oil to aqueous phases at 1.5xcmc. Exactly the same results were obtained for the addition of 10 μl of neat oil to aqueous phases at 50xcmc. For the more volatile oils, the K10 tensiometer was used where the vapour space is thermostatted and small vessels containing oil and filter paper strips soaked in oil were placed around the dish holding the surfactant solution. On placing a drop of oil on the aqueous surface, the tension is lowered immediately. The tension was then monitored for at least one hour to be certain of an equilibrium value, after which the cover was removed. As oil evaporated the tension reassuringly returns to its original value in the absence of oil (Figure 5.11b). Quite remarkably, the surface tension is

Figure 5.11

(a) Surface tension lowering with time after addition of 10 μl PDMS oil (viscosity given) containing 1 wt. % surfactant to 1.5xcmc aqueous $C_{12}E_5$ solutions at 25°C

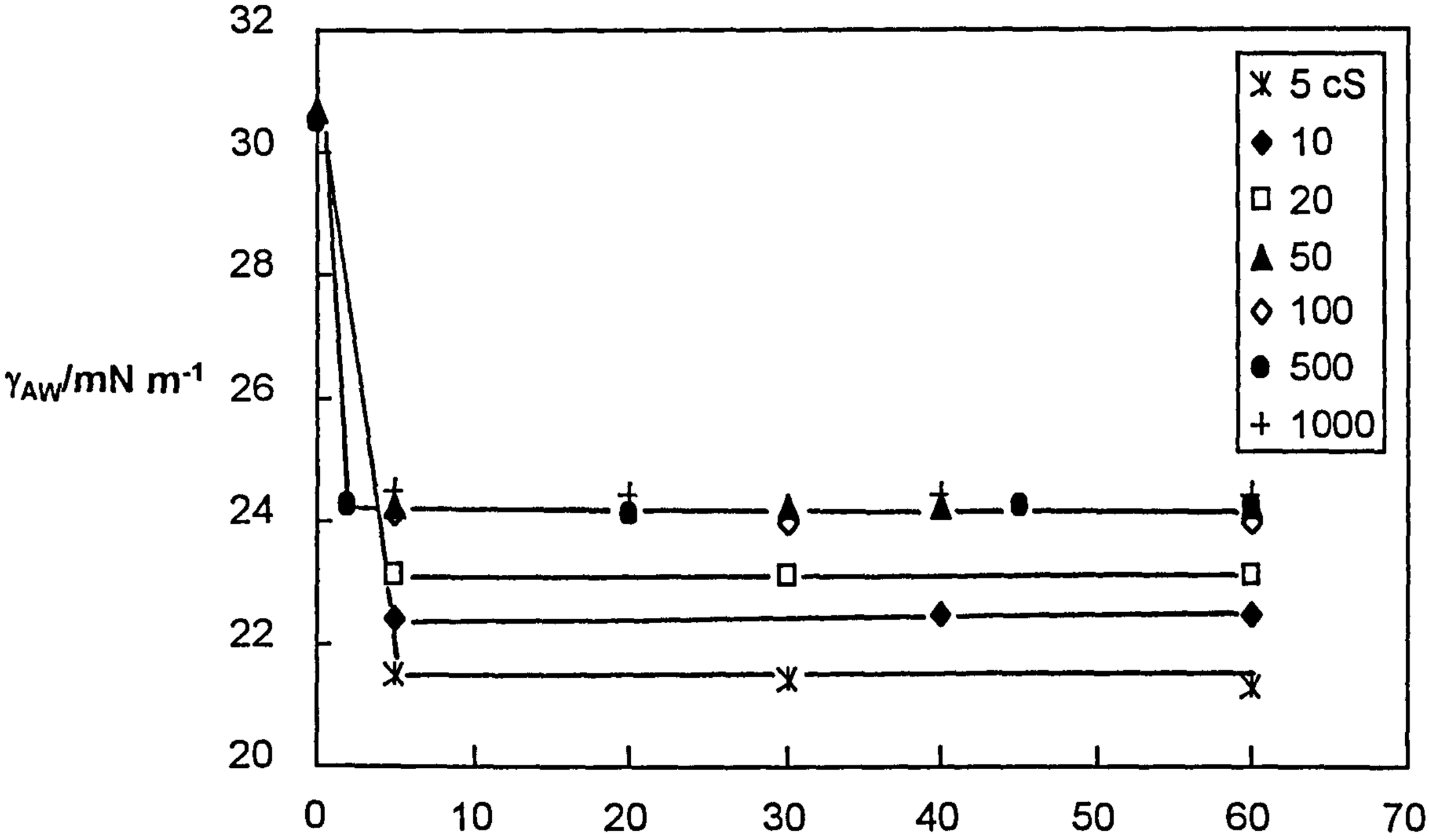

(b) For volatile oils-the dotted lines indicate the time when the glass slides over the solution dish and the thermostatted dome above the solution were removed

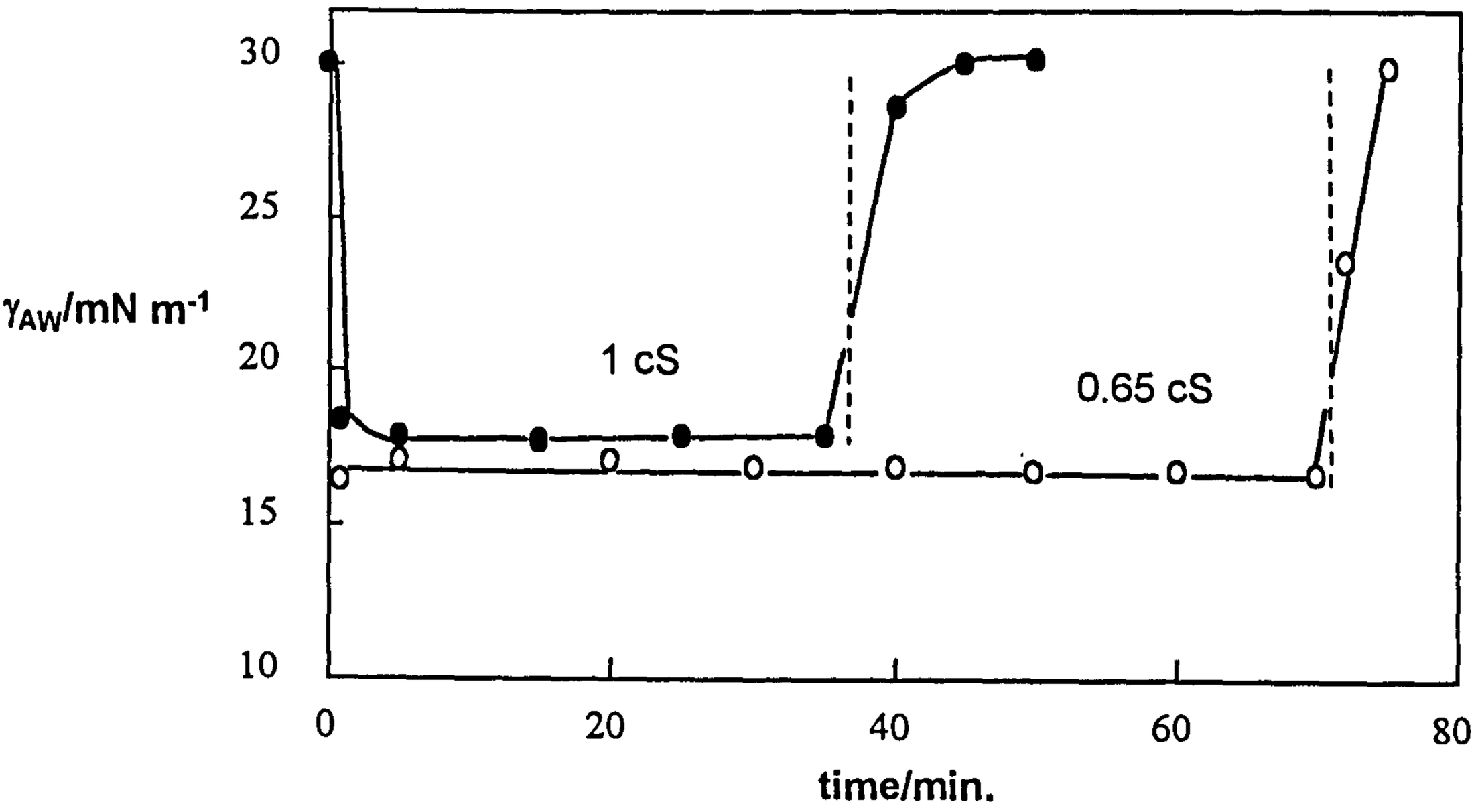

lowered to 16.8 mN m^{-1} for the 0.65 cS PDMS oil which is close to its own surface tension of 16 mN m^{-1}. The calculated spreading coefficients are given in Figure 5.12 as a function of oil viscosity. Values of S_i fall smoothly up to around 50 cS and then appear to level off. The equilibrium values lie around zero, even for the 2 highest viscosity oils. Here, although the bulk drop remains, oil molecules diffuse from it as a spreading front and lower the tension. All the tension data is given in Table 5.3.

Table 5.3 Air-water surface tensions (before and after adding oil), oil-water interfacial tensions and spreading coefficients in the systems post-cmc aqueous $C_{12}E_5$+x cS PDMS oils at 25°C

PDMS visc./cS	γ_{AW}/ mN m^{-1}	γ_{AW}^{+oil}/ mN m^{-1}	$\Delta\gamma$/ mN m^{-1}	γ_{OW}/ mN m^{-1}	γ_{OA}/ mN m^{-1}	S_i/ mN m^{-1}	S_e/ mN m^{-1}
0.65	30.1	16.8	13.3	0.9	16.0	13.2	-0.1
1	30.1	17.8	12.3	1.3	17.2	11.6	-0.7
5	30.5	21.4	9.1	2.2	19.5	8.8	-0.3
10	30.5	22.4	8.1	2.3	20.2	8.0	-0.1
20	30.5	23.1	7.4	2.6	20.5	7.4	0.0
50	30.4	24.0	6.4	3.0	21.0	6.4	0.0
100	30.5	24.0	6.5	3.2	21.0	6.3	-0.2
500	30.5	24.2	6.3	3.0	21.2	6.3	0.0
1000	30.4	24.4	6.0	3.0	21.3	6.1	+0.1

5.4 PDMS oil adsorption isotherms on aqueous solutions above the cmc

As mentioned earlier, for the more volatile oils the activity of oil a_{oil} may be obtained by varying the vapour pressure P above the surfactant solution. The oil adsorption isotherm can be determined by measuring the

Figure 5.12

Initial and equilibrium spreading coefficients of PDMS oils of different viscosity on aqueous solutions of $C_{12}E_5$ above the cmc.

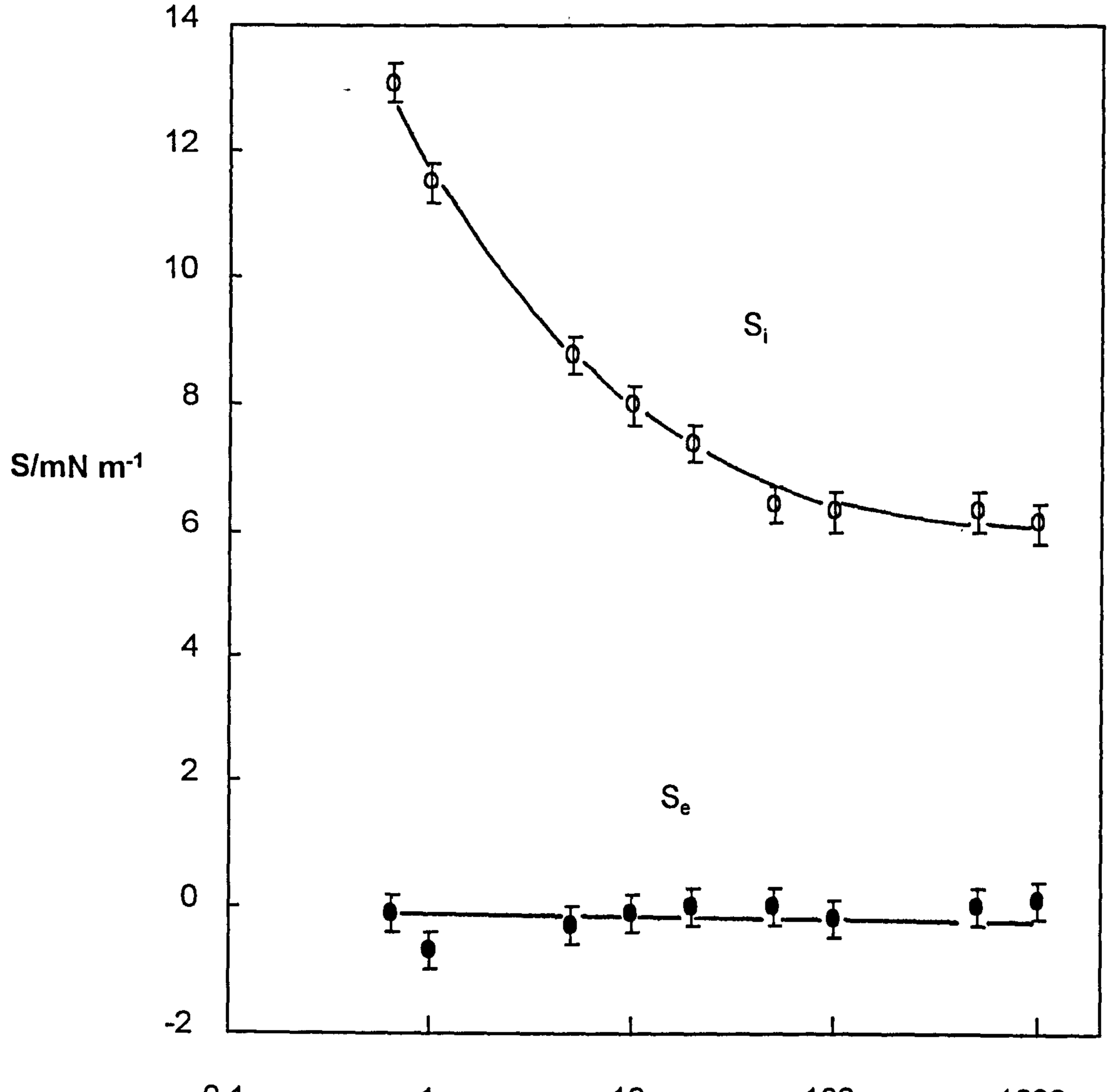

surface tension lowering as a function of the vapour pressure of an adsorbing oil.

The tension lowering for 0.65 cS and 1 cS PDMS oils adsorption onto 6.4 mM aqueous solutions of $C_{12}E_5$ (100xcmc) have been determined. Figure 5.13a shows the variation of $\Delta\gamma$ with a_{oil}. For the 0.65 cS oil that is >99% pure, there is excellent agreement between the $\Delta\gamma$ value at unit activity measured via the vapour phase and from the liquid drop. For the 1 cS oil, which is prepared as a blend, the tension lowering is higher when adsorbed from the vapour, and the data before saturation for the two oils virtually overlap. This is understandable since it is likely that the more volatile low molecular weight fraction is preferentially adsorbed from the vapour. Assuming that micelle solubilisation does not occur in the experimental timescale, the surface concentration of oil Γ_o can be obtained by differentiation of the polynomial fitting of $\Delta\gamma$ vs. P/P_o curves and is given in Figure 5.13b. At unit activity of the 0.65 cS hexamethyldisiloxane oil there are approximately 2.25 molecules of oil adsorbed into the monolayer per nm^2 of surface. Since the surface concentration of surfactant at this concentration is 2.2 molecules nm^{-2} (section 5.5), there is a 1:1 ratio of oil to surfactant molecules in the mixed monolayer. Using numbers given by Tanford,[11] the volume of a C_{12} chain is 0.351 nm^3 and so the volume occupied by dodecyl chains per nm^2 of surface is 0.351/0.45 = 0.78 nm^3. Since the length of a vertical *all-trans* C_{12} chain is 1.67 nm, 1 nm^2 of surface has a volume equal to 1.67 nm^3. Therefore, the volume available for oil is 0.89 nm^3/nm^2 surface. This compares well with the volume of oil determined experimentally of 0.8 nm^3, calculated from (Γ_o^{max} x molar volume/Avagadro's

Figure 5.13a

Lowering of surface tension as a function of oil activity for PDMS oils on aqueous solutions of $C_{12}E_5$ at 6.4 mM and 25°C. Open points are 0.65 cS, filled are 1 cS. The triangles at unit activity are from the liquid drop

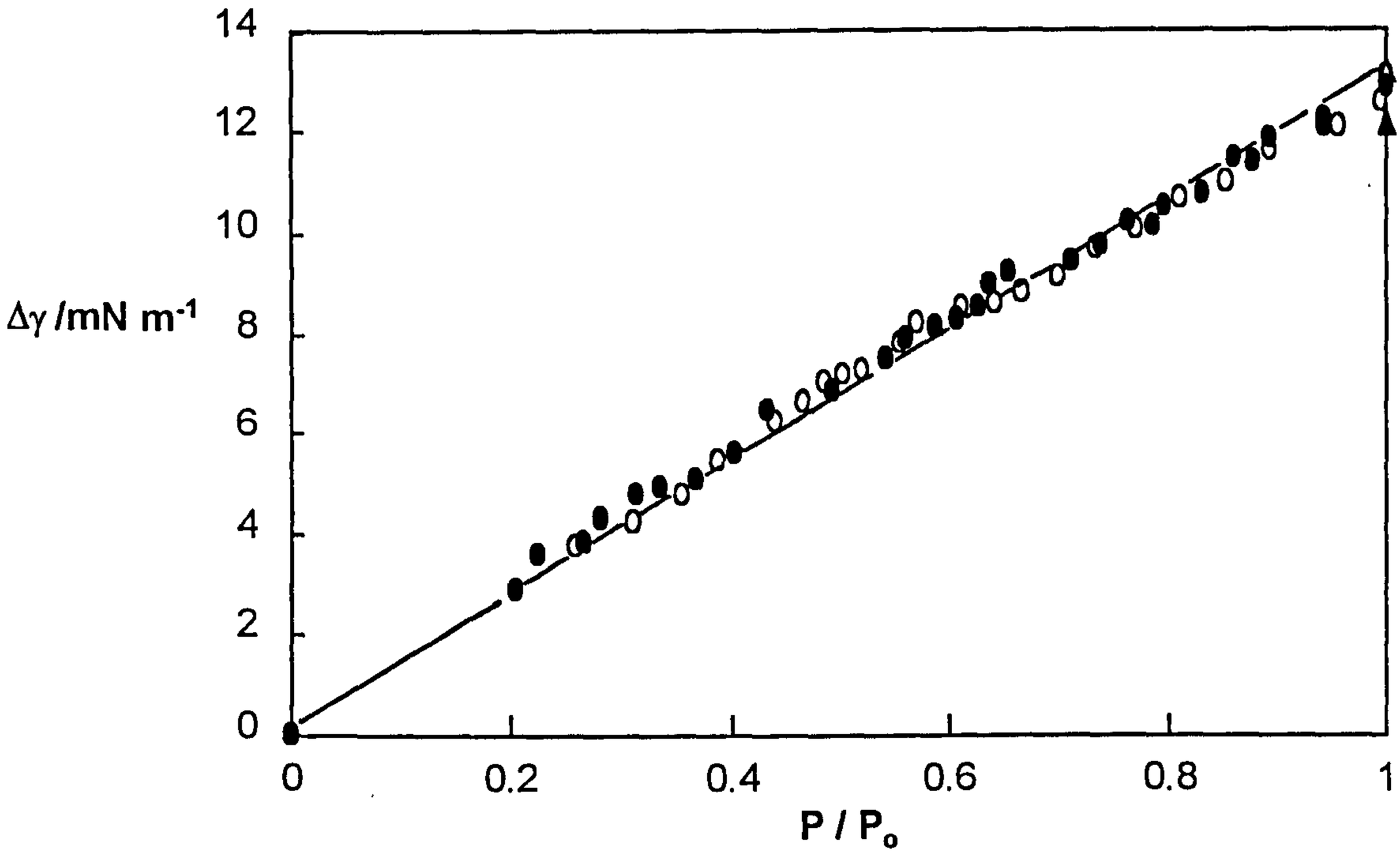

Figure 5.13b

Surface concentration of oil vs oil activity for systems in (a)

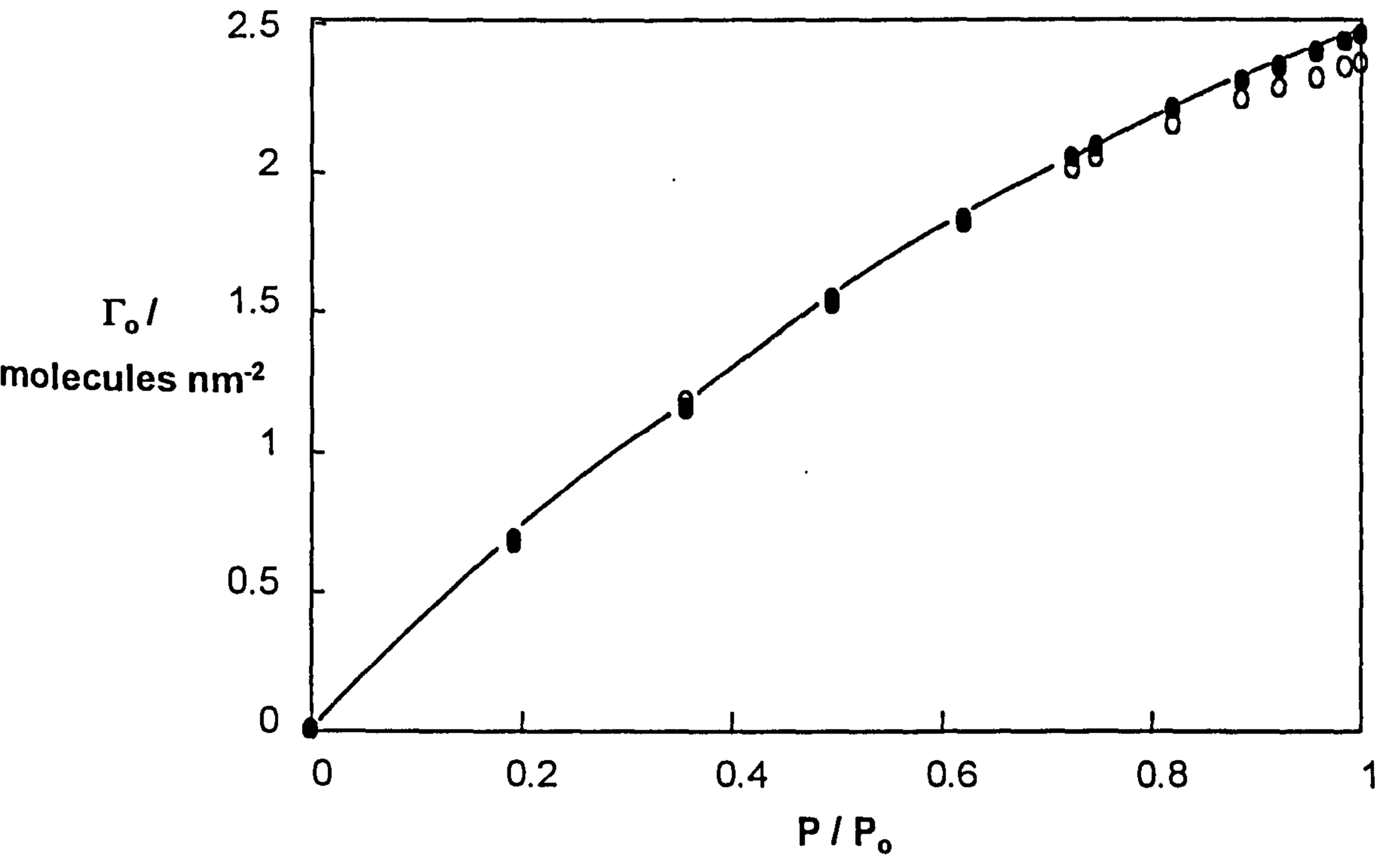

number) and an oil density of 0.76 g cm^{-3}. It is therefore likely that monolayer mixing alone accounts for all the adsorbed oil in this case. If the adsorbed oil has a molecular volume equal to that in the bulk liquid, the effective oil film thickness is 0.8 nm. This is not the total thickness of the surfactant+oil film but only the component contributed by the oil.

It is also sensible to consider the adsorption of oils on a pure water surface. Dodecane does not adsorb on pure water but collects as isolated lenses on the water surface and gives zero surface pressure. 50 cS PDMS oil spreads on water and reduces the surface tension of water by an amount of approximately 10 mN m^{-1}. For the volatile 0.65 cS PDMS oil, we measured the oil adsorption isotherm on pure water, which is shown in Figure 5.14. The $\Delta\gamma$-oil activity data can be fitted linearly and differentiated to yield values of Γ_o. At unit oil activity approximately 3.4 molecules of oil are adsorbed per nm^2 of surface. This amounts to a thickness of 1.2 nm. According to Henry's law,[9] this adsorption isotherm indicates that 0.65 cS PDMS oil forms a monolayer on pure water. Unlike 50 cS PDMS oil, the oil film does not collapse. This behaviour is also different from the wetting behaviour of pentane on water where the van der Waals force across the film is repulsive tending to increase the film thickness and thus favouring the spreading of the liquid on water.[12,44] 0.65 cS PDMS oil molecules contain weak dipole moments which could result in this monolayer adsorption on water.

5.5 Adsorption of PDMS into surfactant monolayers below the cmc

In the previous section, we discussed PDMS oil adsorption into a surfactant monolayer above the cmc and found that the oil adsorption and

Figure 5.14

Lowering of surface tension as a function of oil activity for 0.65 cS PDMS oil on pure water (triangles) and on aqueous solutions of $C_{12}E_5$ at 6.4 mM (circles) and 25°C

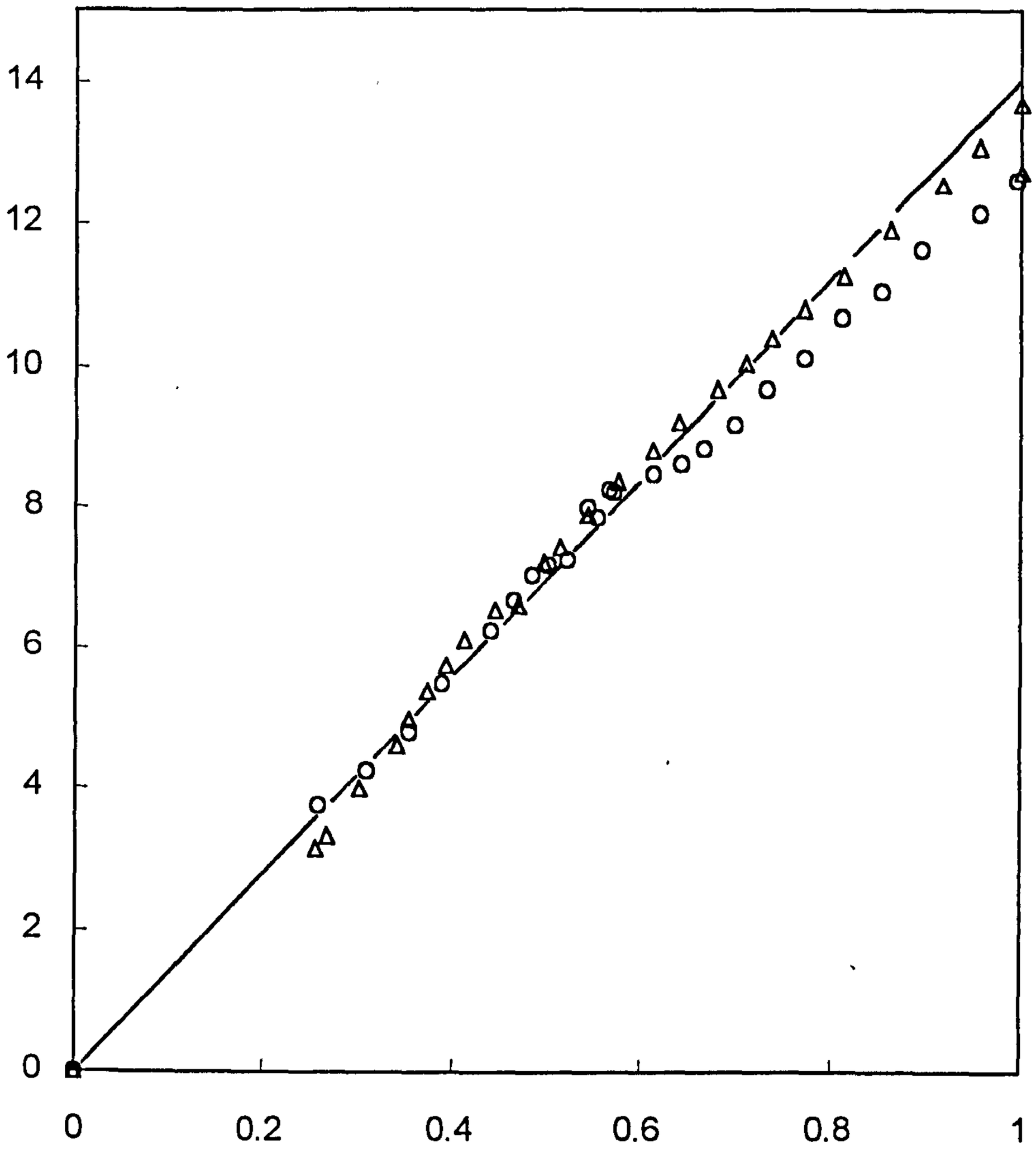

spreading behaviour are dependent on the surfactant structure, especially the headgroup size. Since the PDMS oils are able to spread on pure water, it is of interest to look at whether the presence of the oil at the water surface will affect the surfactant adsorption. In this section, we will discuss the effect of the presence of a liquid drop or oil film of 50 cS PDMS oil on surfactant adsorption. To enhance the understanding of the mixing of oil and surfactant chain region, we have chosen a conventional nonionic surfactant $C_{12}E_5$ and a silicone surfactant Silwet L-77.

5.5.1 $C_{12}E_5$ systems

The way in which drops of 50 cS PDMS oil affect the surfaces of $C_{12}E_5$ solutions has been investigated at concentrations below the cmc of $6x10^{-5}$ M. Figure 5.15 shows the time dependence of the air-water tension following the addition of oil. For all solutions, the oil spreads immediately but the time taken for the tension to become its new value increases as the monolayer is diluted. The tension-surfactant concentration, c, curves with and without oil are shown in Figure 5.16 where it can be seen that the cmc is not affected by the presence of oil. Above the cmc, $\Delta\gamma$ is independent of concentration but depends on concentration below it. $\Delta\gamma$ increases initially as the surface concentration of surfactant, Γ_s, is reduced and then remains about constant with further dilution (Figure 5.17a). We have included the result for spreading on pure water and note that once the surfactant concentration is 1/5 cmc, no further lowering of the tension occurs. Quadratic fits to the curves in Figure 5.16 over the tension range below the cmc yield

Figure 5.15

Surface tension-time plots for aqueous solutions of $C_{12}E_5$ below the cmc at 25°C after addition of 10 μl of 50 cS PDMS oil

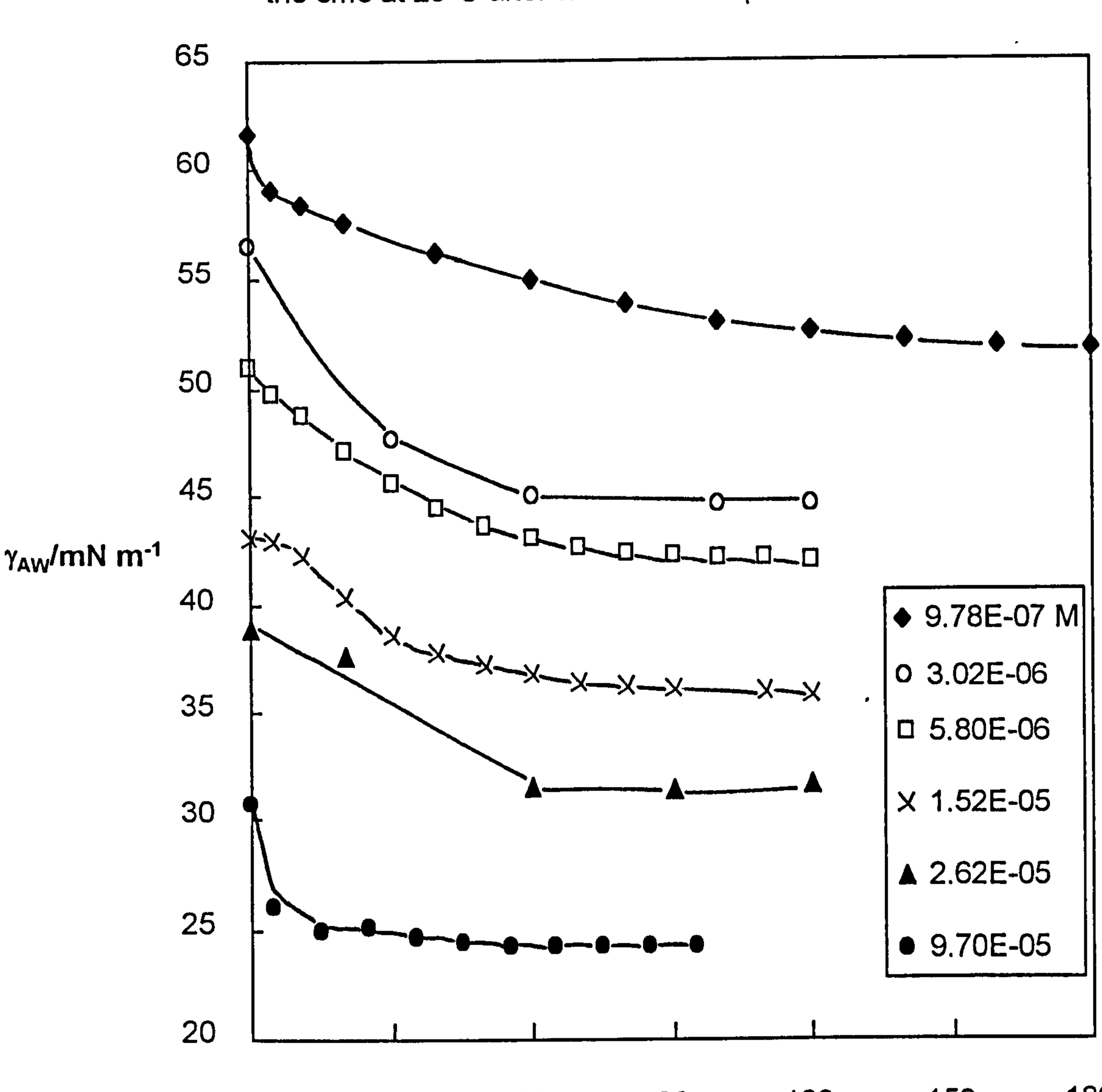

Figure 5.16

Tensions of aqueous $C_{12}E_5$ solutions at 25°C as a function of surfactant concentration in the presence and absence of 50 cS PDMS oil

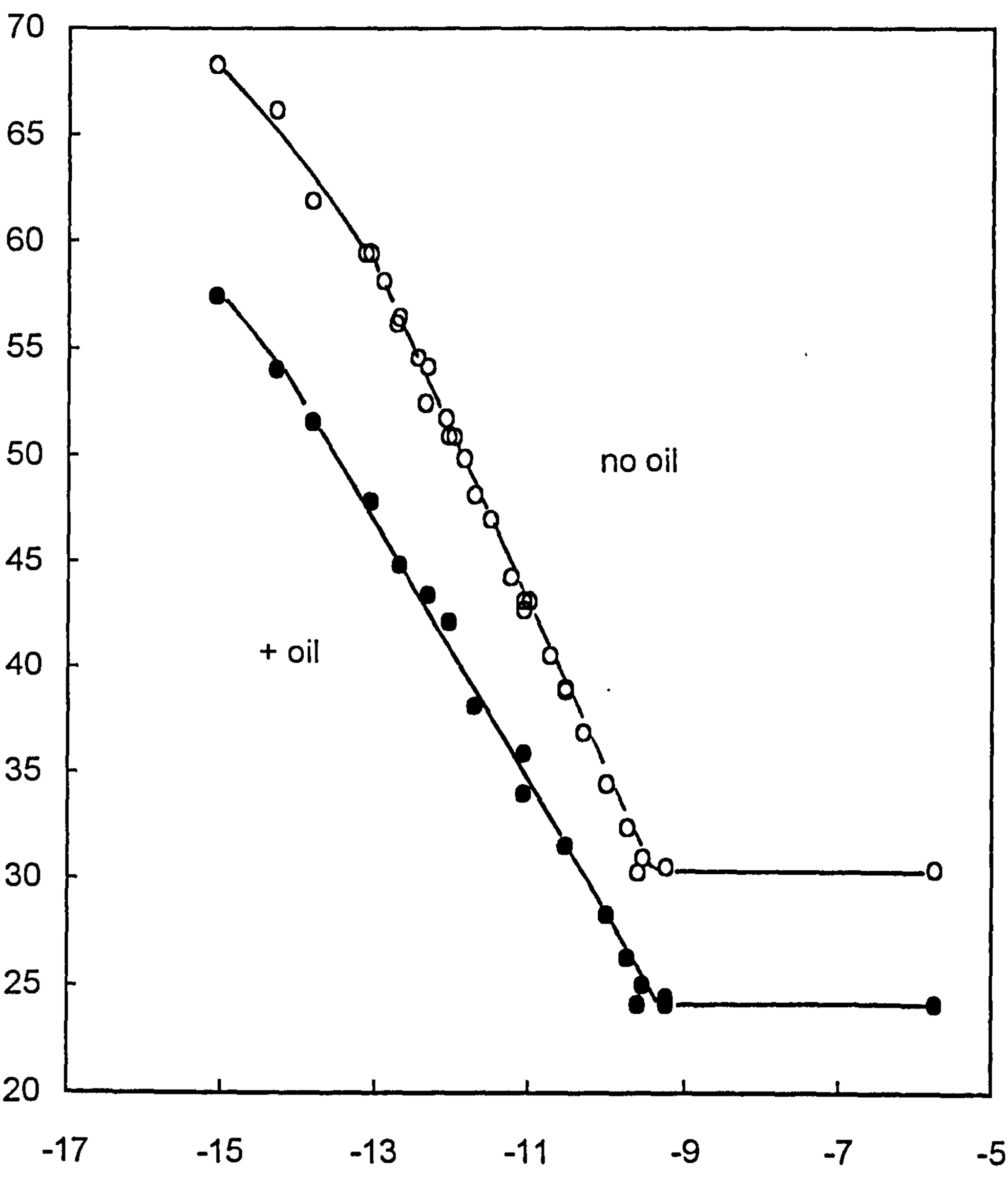

correlation coefficients >0.99 and allow the determination of Γ_s from equation 1.5.

The isotherms for surfactant adsorption given in Figure 5.17b reveal that for very dilute monolayers Γ_s is similar in the two cases. The mixed films at such low concentrations are probably not uniform, maybe consisting of condensed islands in equilibrium with 'gaseous' patches, as observed on pure water.[140] At higher concentrations, PDMS oil competes with surfactant for the surface and actually displaces a fraction of it. This behaviour is very different to that of say dodecane on C_nTAB solutions.[42] Dodecane does not spread on pure water nor is it adsorbed on its surface. The uptake of dodecane is maximum at around half the cmc and rapidly falls to zero for more dilute monolayers. In addition, Γ_s close to the cmc is approximately the same with and without oil since the alkane effectively increases the density of the chain region along with a slight increase in thickness. The enhanced penetration of the silicone oil seen here is thus related to its ability to spread on water, and it seems likely that PDMS oil mixes with both the head group and chain region of the surfactant monolayer. Such hypotheses could be confirmed by direct observation using neutron reflectivity (see later).

5.5.2 L-77 systems

In order to understand what features a surfactant molecule or layer must posses for spreading of oil to occur, we have chosen the silicone surfactant L-77 and conducted a similar investigation. It could be hypothesised that uptake of silicone oils into chains containing silicone groups may be favourable. The shape of the molecules of the surfactant L-

Figure 5.17a

Tension lowering caused by 50 cS PDMS oil as a function of the tension in the presence of oil for the system in Figure 5.16

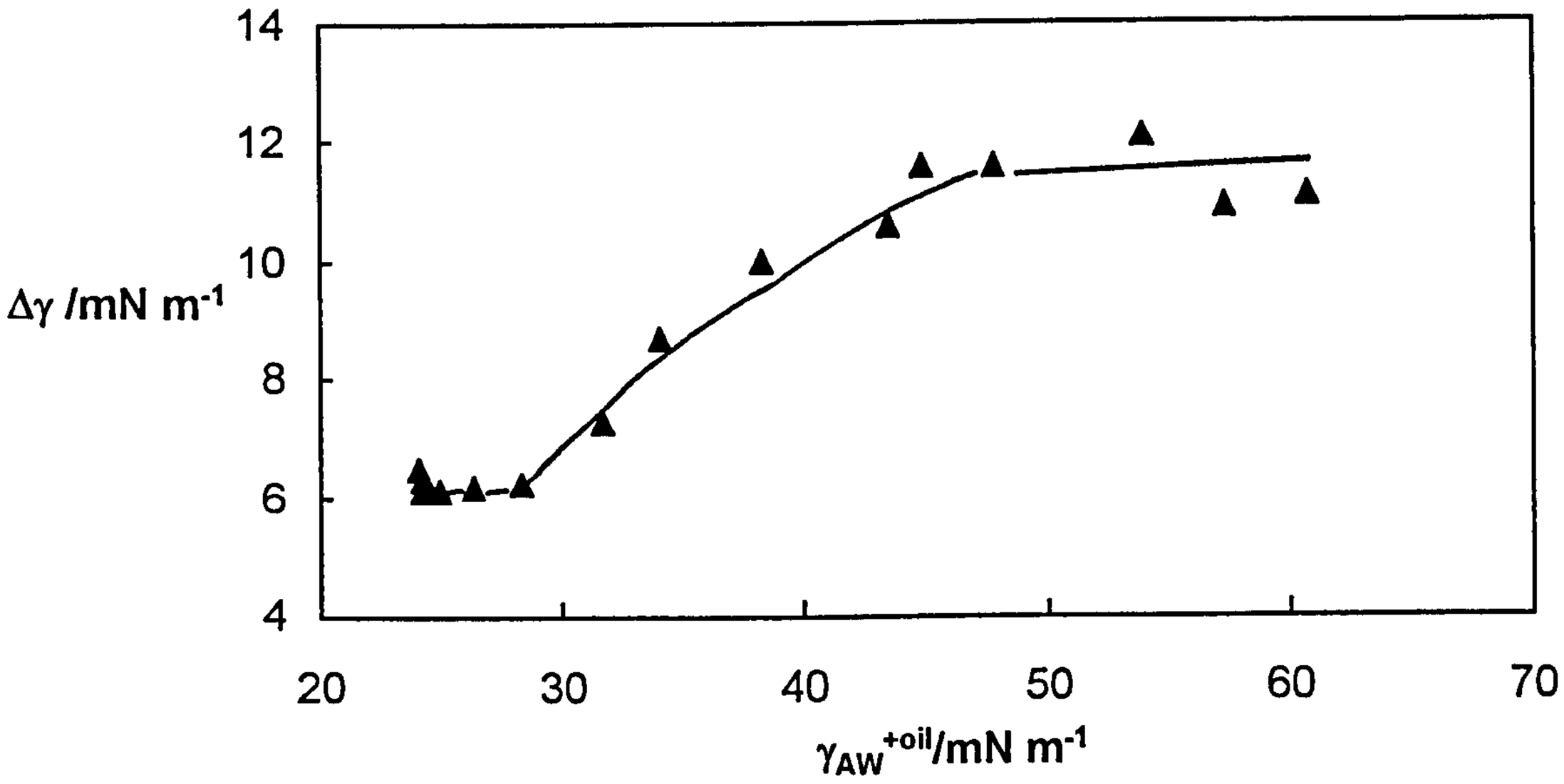

Figure 5.17b

Surface concentration of $C_{12}E_5$ versus its bulk concentration with and without added 50 cS PDMS oil

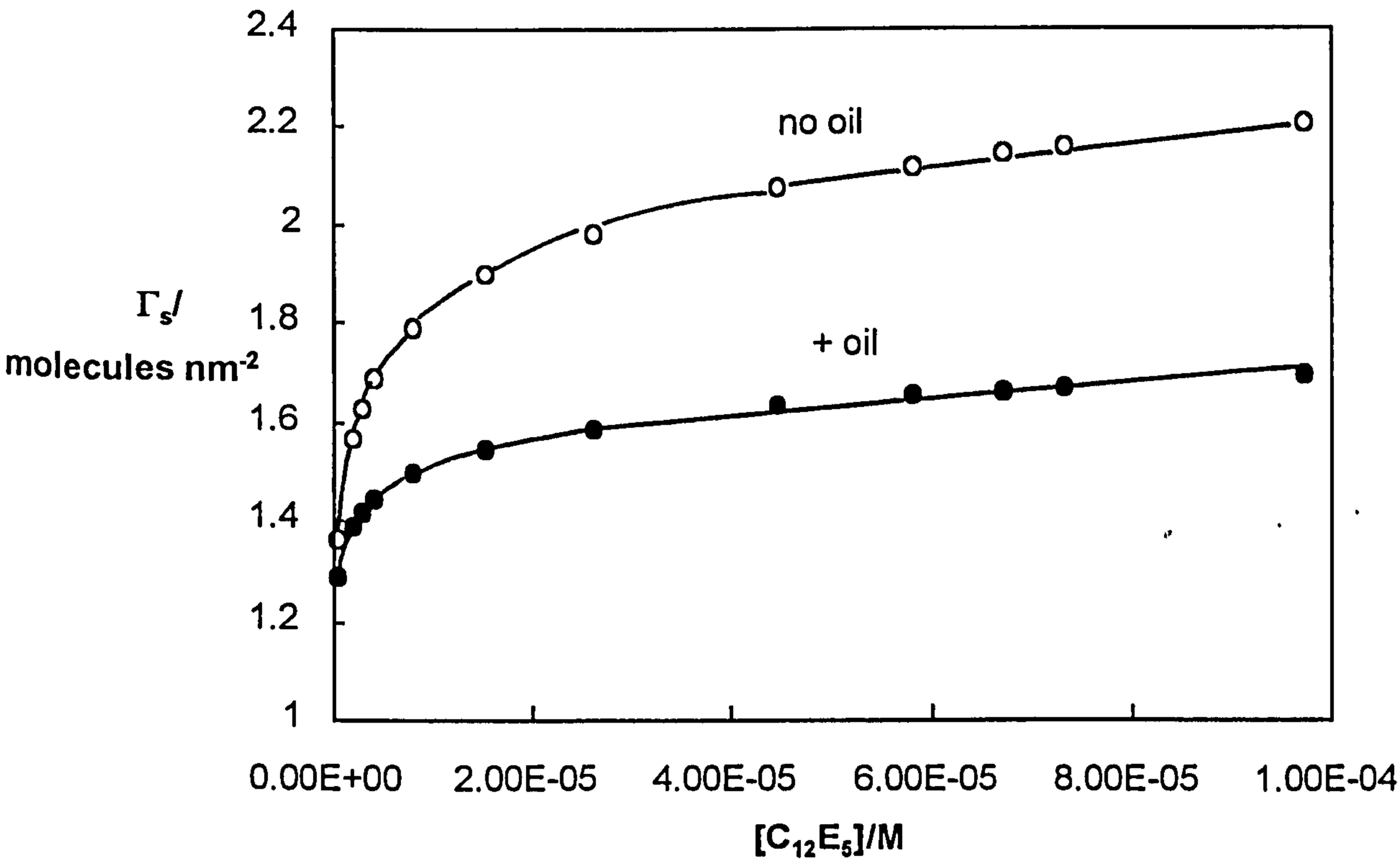

77 has been described as umbrella-like or T-shaped,[121] with the $Si(Me)_3$ groups either side of the central E head group. L-77 adsorbs strongly at the air-water surface like conventional surfactants and has a cmc of 1.2×10^{-4} M at 25°C (open circles in Figure 5.18a). Unlike $C_{12}E_5$, the tension at and above the cmc is quite low, <22 mN m^{-1}. On adding 10 µl of 50 cS PDMS oil to the surfaces of these solutions, the crosses in the figure represent the new surface tensions. Remarkably, the tensions are unchanged in the presence of oil. Above the cmc, no spreading of the oil occurs and a visible lens remains on the surface. The tension is not lowered either, probably because the original tension of 21.2 mN m^{-1} is already close to the surface tension of the oil and this result is consistent. Although by going below the cmc the monolayer is diluted with respect to adsorbed surfactant, the tension is not changed with oil even at values up to 45 mN m^{-1}. Since PDMS oil lowers the tension of water by approximately 10.5 mN m^{-1}, the two curves must eventually diverge at low enough concentrations. Attempts to determine this effect were not reliable due to the long times required for adsorption from these dilute solutions. Consequently, the two sets of data can be fitted together and allow us to calculate the surface concentration of surfactant Γ_s. We see in Figure 5.18b that Γ_s is the same with and without oil present. The lowest concentration corresponds to approximately 1/100 cmc where the area per surfactant molecule has been increased around a factor of 4 from 0.55 nm^2 at the cmc to 2.0 nm^2. Despite this, PDMS oil is not encouraged to mix with this surfactant. The result demonstrates that the *chemical structure* of the surfactant chain is important in determining

Figure 5.18a

Tensions of aqueous L-77 solutions at 25°C as a function of surfactant concentration in the presence (crosses) and absence (circles) of 50 cS PDMS oil

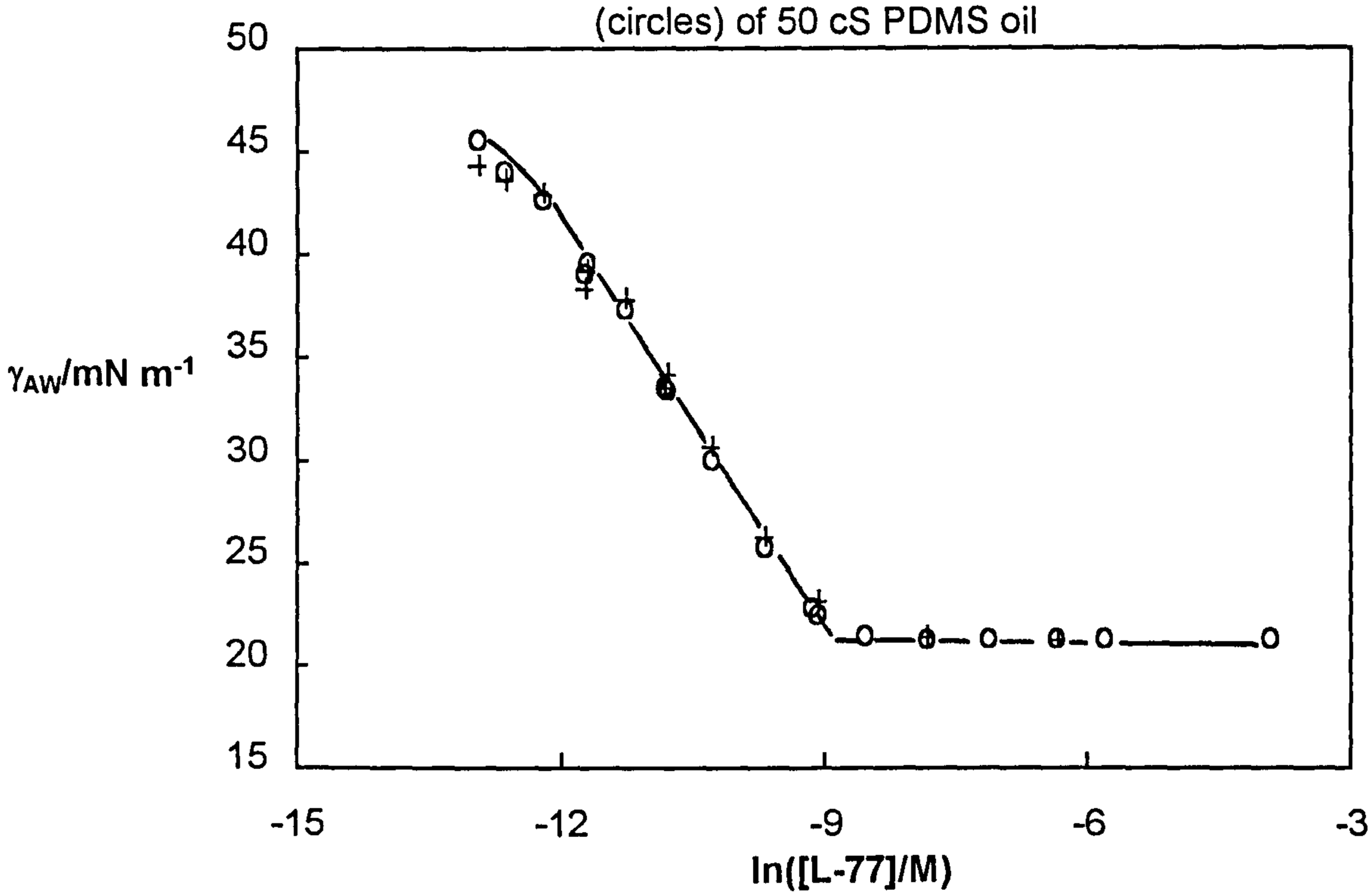

Figure 5.18b

Surface concentration of L-77 versus its bulk concentration with and without added 50 cS PDMS oil

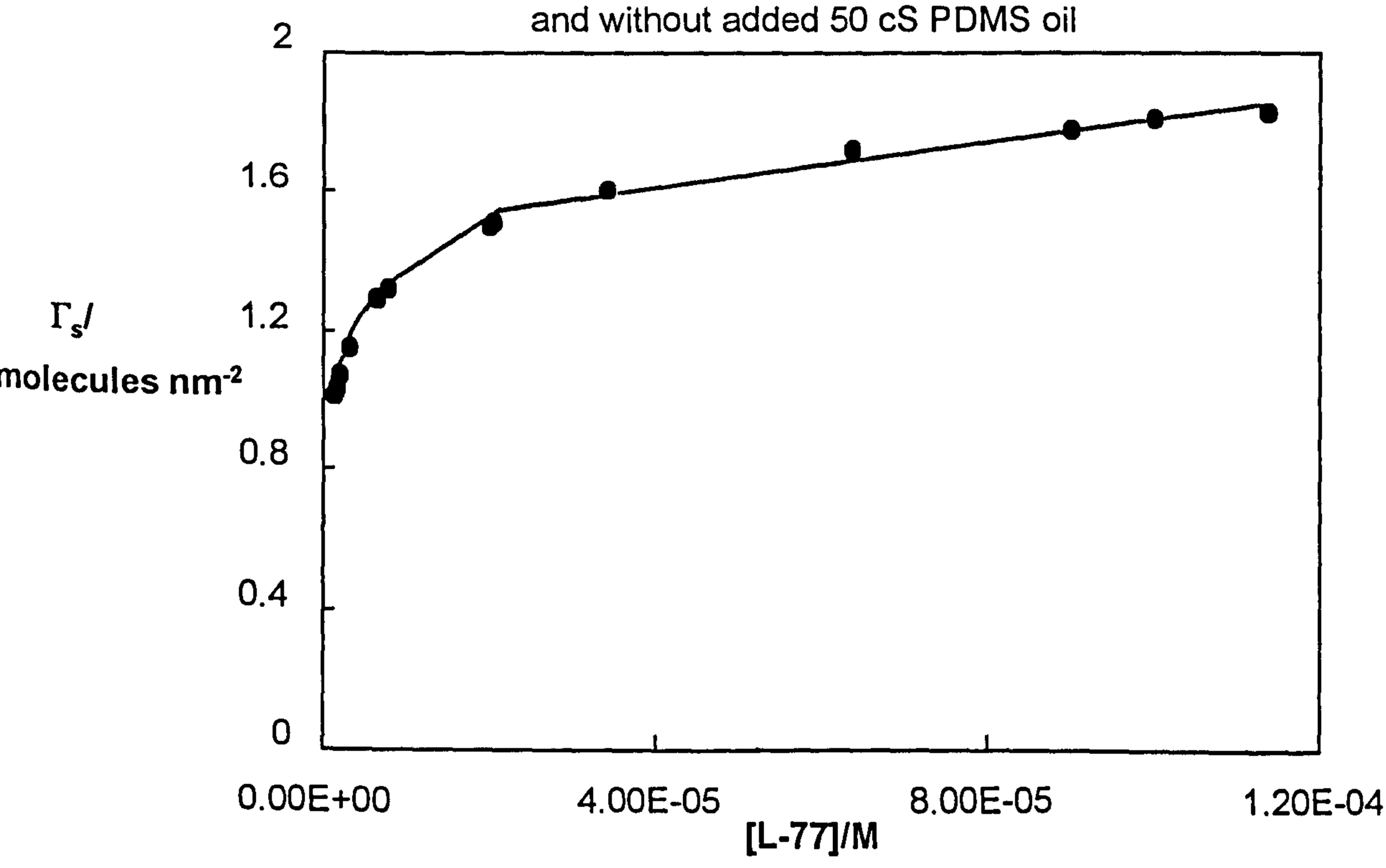

whether oils spread on surfactant solutions or not and shows that matching the oil and surfactant chain *types* is not a sufficient condition.

5.6 Spreading behaviour of PDMS oil studied by neutron reflection

5.6.1 Introduction

Neutron reflection is a powerful technique used to study the composition and structure of interfaces.[141] The neutron refractive index is related to the scattering length density of substances at the interface and hence specular neutron reflection can yield atomic densities normal to the surface from which the composition, average thickness, roughness of a surface film can be obtained. Similar information can be obtained using, for example, x-ray reflection. However, there are many instances where the neutron method provides a distinct advantage. In contrast to x-rays neutron scattering amplitudes vary widely from element to element, and isotopic substitution can be used to produce large contrasts in the scattering density. Of particular importance is the large difference in scattering powers of hydrogen and deuterium; this has been used to great effect in surface chemistry.[142]

The study of mixed films of surfactant and hydrocarbon oil at air-water surfaces by neutron reflectivity has been reported previously by Lu *et al.*[51,138,143] The mixed film of surfactant and oil was formed by the addition of a small amount of liquid oil to the surface of aqueous surfactant solutions. For oils that do not spread macroscopically, the surfactant monolayer solubilises a certain amount of the oil leaving the remainder present as small lenses of the pure oil floating on the surface. By partial isotopic labelling,

detailed neutron reflectivity studies have yielded the relative positions of the solubilised alkane and surfactant head and tail groups within the mixed films. This two-dimensional surface solubilisation is akin to conventional oil solubilisation in micellar solutions and provides detailed information about the interactions between oil and surfactant. For the system of the adsorbed monolayer of C_nTAB and dodecane,[51, 143] neutron reflection measurements for mixed films show that, at saturation adsorption, the adsorbed oil in these systems is almost entirely located within the hydrophobic chain region of the surfactant monolayer. The amount of dodecane solubilised was approximately equal to the free space available assuming the surfactant activity does not change as the oil was solubilised and the surfactant hydrophobic chain is fully extended and perpendicular to the surface. More recently, Binks *et al.*[49] compared the adsorption isotherm of hydrocarbon oils on surfactant solutions by neutron reflectivity and tensiometry methods. It was found that the agreement between the two methods was good.

The adsorption of PDMS oils on surfactant monolayers at the air-water interface has been studied for $C_{10}E_5$ and AOT aqueous solution using neutron reflectivity.[56-59] The studies showed clearly mixed surfactant-PDMS oil layers are a superposition of two layers: a surfactant-rich and an oil-rich layer. The degree of mixing of the components in each layer depends strongly on the nature of the surfactant. Significant penetration of PDMS oil into the $C_{10}E_5$ layer was found. On the contrary, no detectable penetration of PDMS oil into the AOT layer was seen. This difference is thought to be due to either the larger flexibility of the $C_{10}E_5$ molecule and/or to the higher water content in the $C_{10}E_5$ layer. Nonetheless, the space filling mechanism can be

used here since the chain region of $C_{10}E_5$ is larger than that of AOT, hence more free space available to solubilise PDMS oil. The spreading behaviour of 50 cS PDMS oil on C_nE_m surfaces above the cmc by tensiometry determined here indicated that the surfactant headgroup size has a more significant effect than the chain length on the oil spreading coefficients. Here, we report some of the preliminary neutron reflectivity results for PDMS oil added to $C_{12}E_m$ (m = 2, 4, 6) monolayers above the cmc.

5.6.2 Basic terms used in neutron reflection

Before presenting the results we first discuss some basic terms and concepts relevant to the neutron experiment. When a beam of neutrons passes from a less dense (medium 1) to a more dense medium (medium 2), some of the neutrons are bent (or refracted) away from the normal (an imaginary line located perpendicular to the interface) and some are reflected away from the surface at the specular angle, θ. Figure 5.19 depicts a beam of neutrons incident at an interface, refracted and reflected from the surface.

Figure 5.19 A schematic representation of the refraction and reflection of a neutron beam

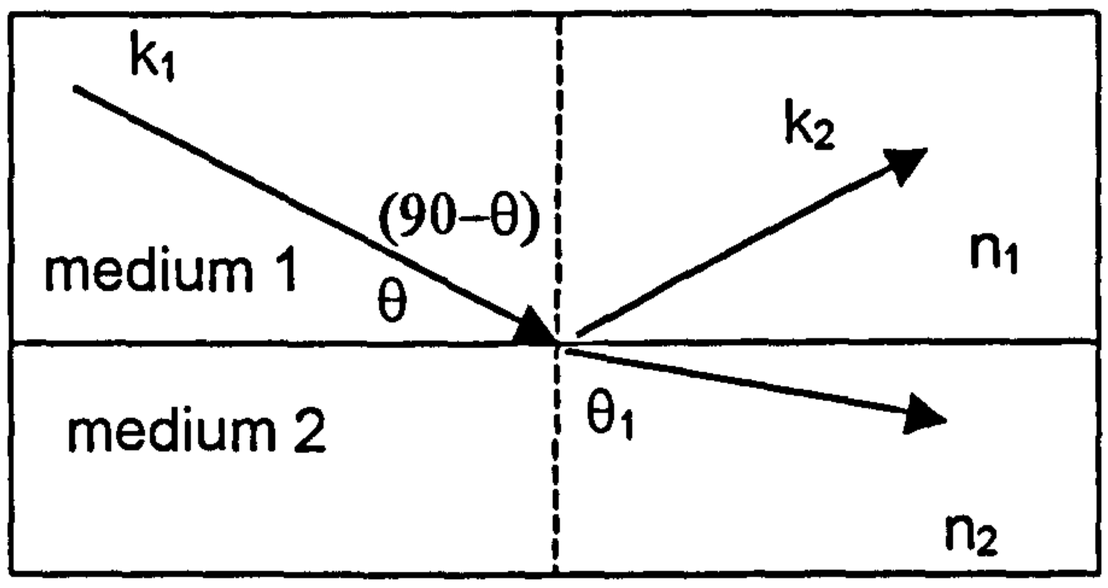

In Figure 5.19, k_1 and k_2 are incident and scattered neutron wave vectors. The neutron wave vector transfer, Q_o is given by,

$$Q_o = k_1 - k_2 = \frac{4\pi \sin\theta}{\lambda} \tag{5.1}$$

where λ is the neutron wavelength. In Figure 5.19 when $\theta_1 = 90^o$, $\theta = \theta_c$, the critical angle. If θ is smaller than θ_c then total external reflection will be achieved, Q_o reaches the critical value Q_c and the reflectivity profile $R(Q) \equiv 1$. R(Q) gives information on the structure normal to an interface, and, as with the reflection of light it is the refractive index normal to the surface that is important. For any material the refractive index (with respect to neutrons) n is wavelength dependent

$$n = 1 - (\lambda^2 / 2\pi)\rho \tag{5.2}$$

where ρ is the scattering length density (SLD) given by,

$$\rho = \frac{\sum_i b_i N_i(z)}{V_i} \tag{5.3}$$

and $N_i(z)$ is the number density profile of species i, b_i is its empirically determined coherent scattering length of the species i[144] and V_i the volume of species i.[144]

5.6.3 Neutron reflection experimental procedure and data analysis models

The neutron reflectivity measurements were carried out on the NG7 reflectometer at the cold source reactor in NIST, Gaithersburg, Maryland, USA. The surfactant solution was contained in a PTFE trough (of surface dimensions 133 x 63 mm). The trough was enclosed in a sealed double-walled temperature controlled compartment, as described elsewhere.[90] 25 µl

of PDMS oil (fully deuterated, molecular weight ~ 3400 and viscosity ~ 50 cS) was syringed on top of the aqueous phase through a small re-sealable inlet. Chloroform was employed as the spreading solvent. The surfactants were dissolved in 100% D_2O and the concentrations were above the cmc to ensure the presence of a saturated monolayer at the surface. A pure D_2O subphase was used to perform the calibration. Deuterated PDMS-protonated surfactant-D_2O contrast was performed. The temperature varies from 10 to 22 °C according to the surfactant used. Table 5.4 shows the calculated SLD for the d-PDMS, D_2O and nonionic surfactants $C_{12}E_2$, $C_{12}E_4$ and $C_{12}E_6$ used in the experiments.

Table 5.4 Calculated scattering length density of each material used in neutron reflection experiment at 25°C

material	dPDMS	D_2O	$C_{12}E_2$	$C_{12}E_4$	$C_{12}E_6$
SLD/10^{-6} Å^{-2}	5.033	6.406	-0.067	0.078	0.177

The optical matrix method[141, 142] was used to analyse the reflectivity data. In this method, the surface region is divided into successive discrete layers with constant refractive indices. For systems where only dPDMS is adsorbed on a pure D_2O, the neutron reflection data was fitted as a single layer model where the adsorbed PDMS film is treated as a single uniform contrast layer. For systems where an adsorbed surfactant monolayer is present on the surface of D_2O, a two layer model was employed in which layer 1 contains mainly PDMS and layer 2 contains mainly the surfactant chains. The changes in the layer thickness and SLD could provide the layer

composition information, i.e. the mixing behaviour of PDMS with surfactant. Figure 5.20 is a schematic illustration of the models.

5.6.4 Results and discussion

Figures 5.21 to 5.24 show the experimental and calculated reflectivity curves and the derived scattering length density profiles for dPDMS on pure D_2O in the absence and presence of surfactant. The fitted profiles are shown by solid lines. It can be seen that, in the absence of surfactant, PDMS forms a single layer on the water surface. In the presence of surfactant, it is necessary to use the two layer model in order to obtain the best fits. The profiles can be fitted with two single layers. The thinning of PDMS layer and a low SLD layer for the surfactant between the D_2O and dPDMS can be seen. As the headgroup size of the surfactant decreased from $C_{12}E_6$ to $C_{12}E_2$, there exists a pronounced minimum in the reflection profile, which shifts to higher wave vector transfer at longer times. The parameters used to fit the profiles are listed in Table 5.5. As seen, the values of the interfacial roughness are large compared to the pure water surface (~ 3 nm) which means that the layer thicknesses are probably not reliable. Furthermore, the assumption that the PDMS layer is uniform may not be correct so the fits assuming uniform layers would give larger errors. In addition, in some cases the data acquisition time may not be sufficient to reach the system equilibrium, therefore, the neutron reflectivity profiles obtained could not represent the equilibrium states. However, in order to obtain correct information from the neutron reflectivity profiles, data of several isotopic contrasts is required.

Figure 5.20

Schematic illustration of the one and two layer models and the corresponding scattering length density profile for each layer

(a) One layer model

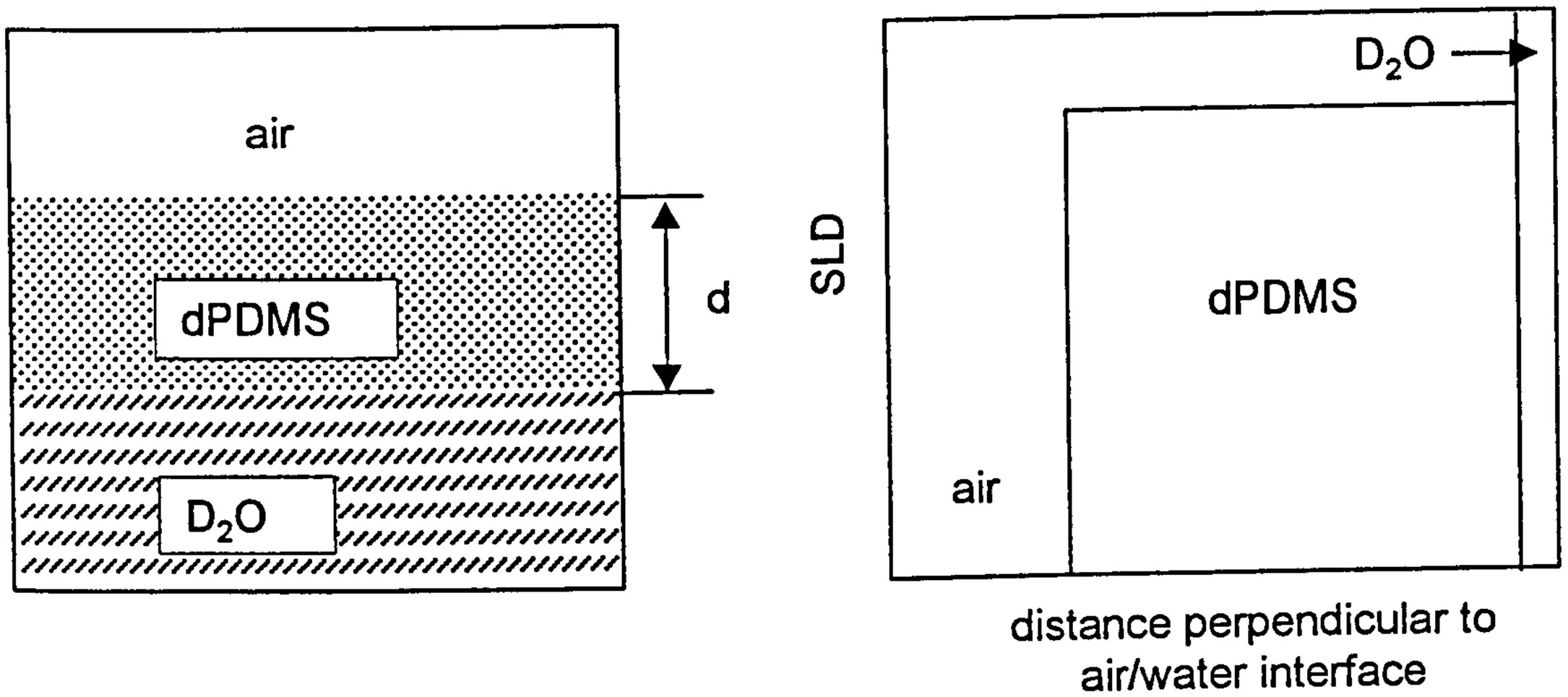

(b) Two layer model

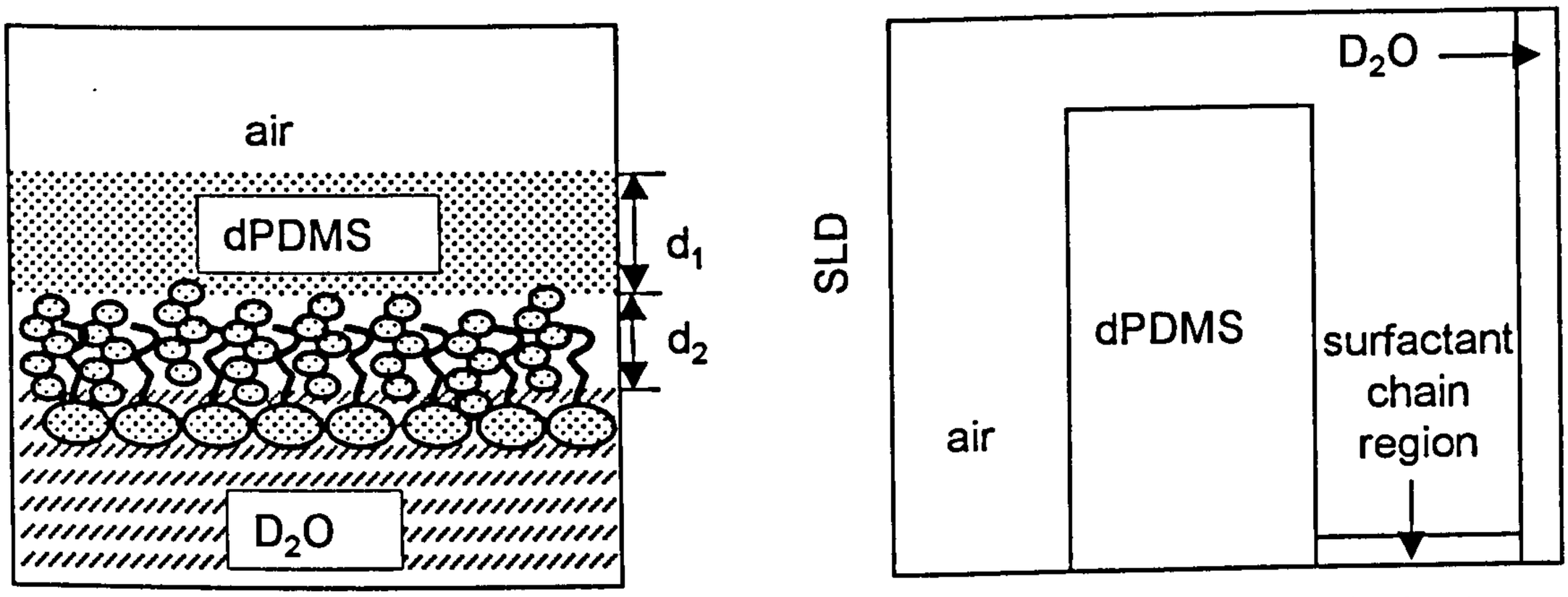

Figure 5.21

(a) Neutron reflection profiles of the system: dPDMS on pure D_2O

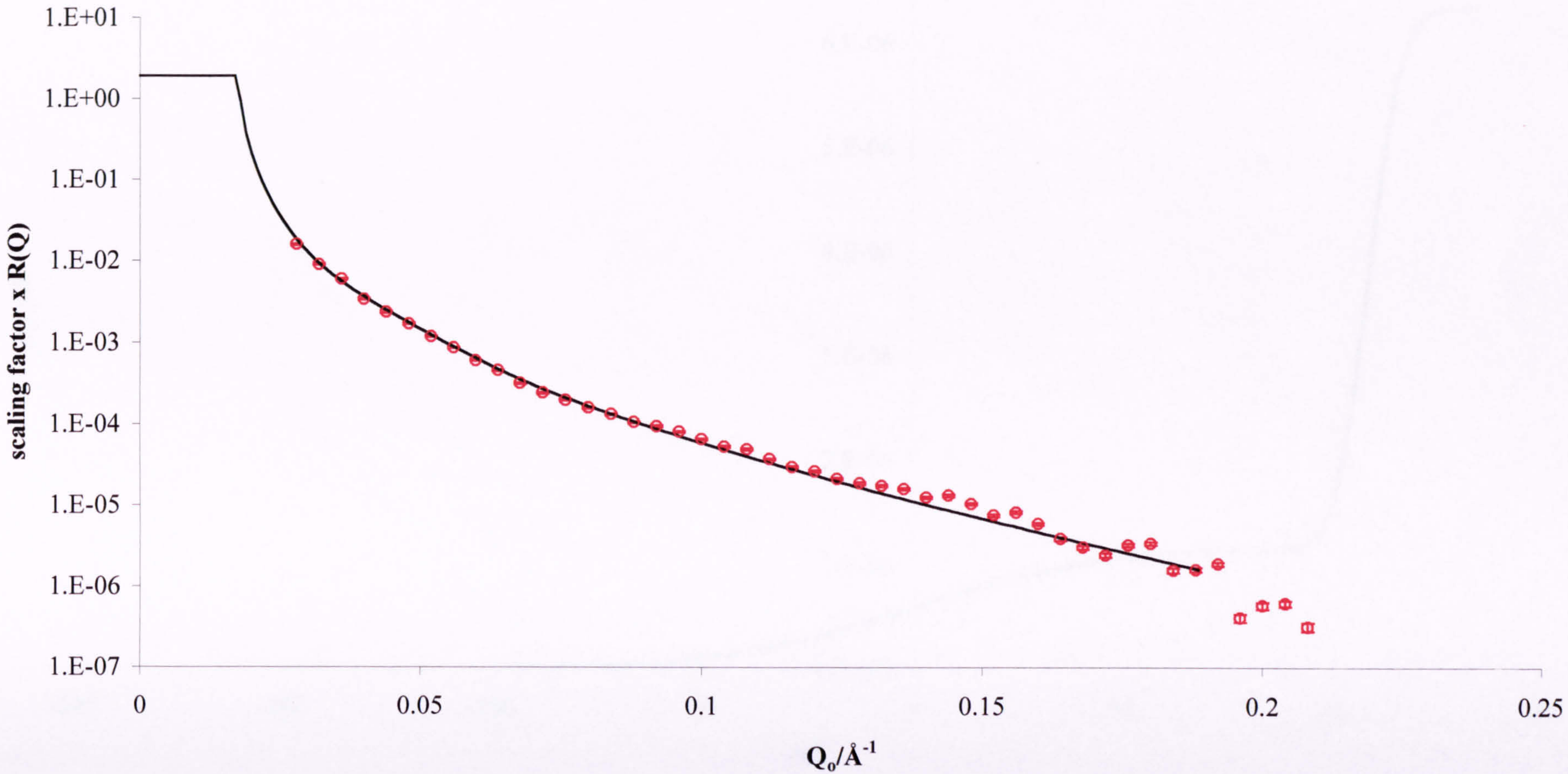

(b) Neutron scattering length density profile of dPDMS on pure D_2O

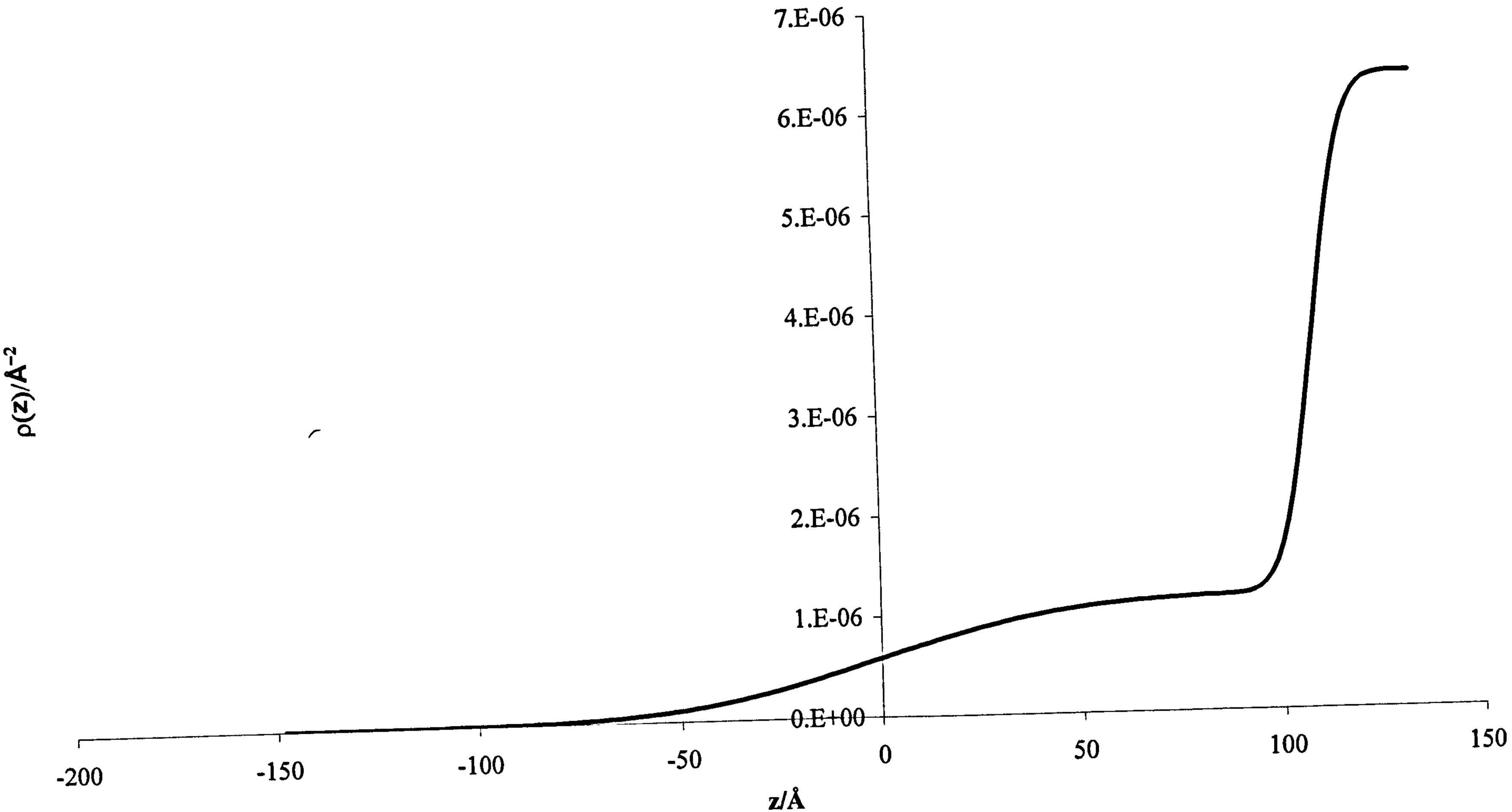

Figure 5.22

(a) Neutron reflectivity profiles of the system: dPDMS/$C_{12}E_2$/D_2O at different times

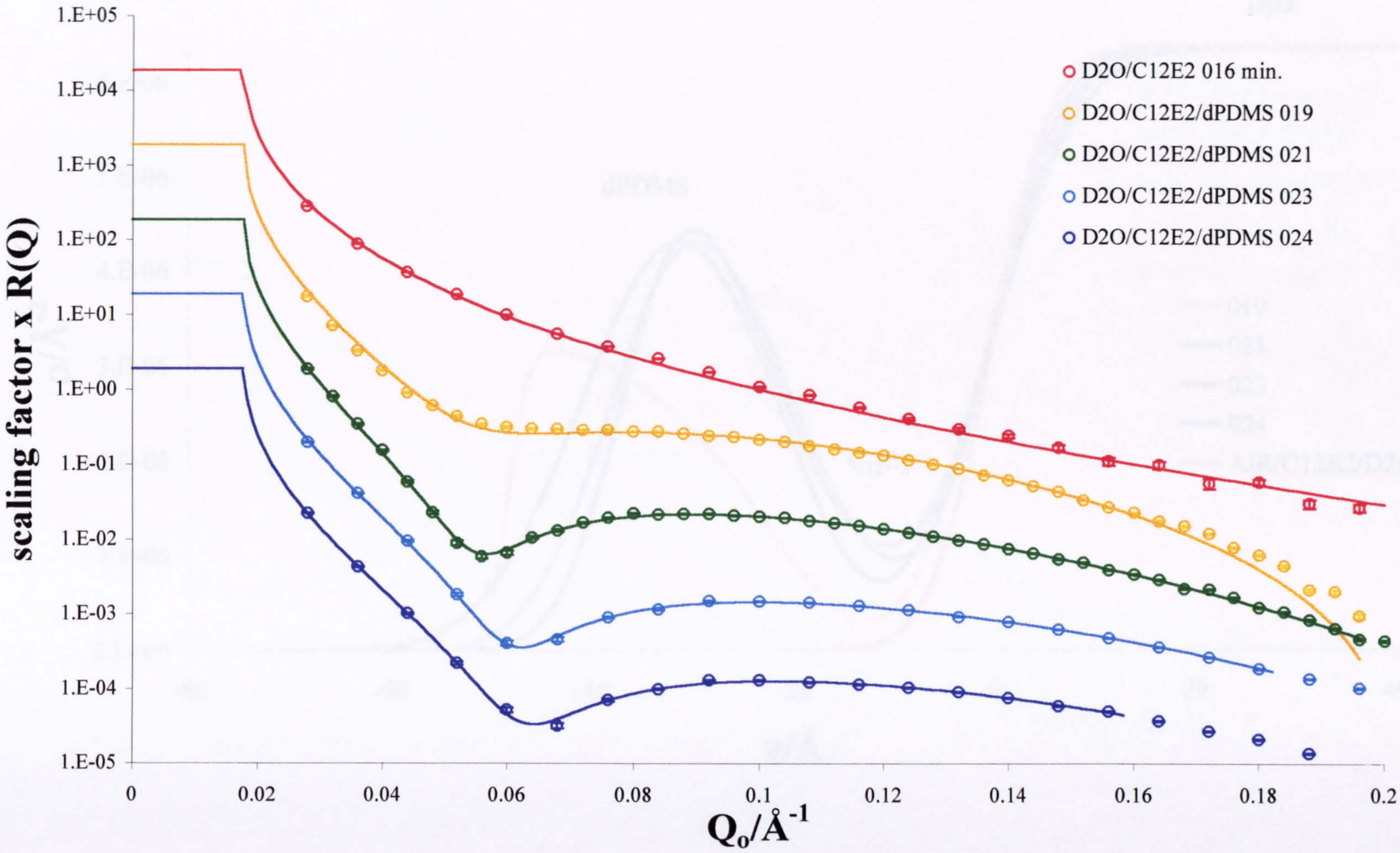

(b) Neutron scattering length density profiles for the system:
dPDMS/$C_{12}E_2$/D_2O at different times

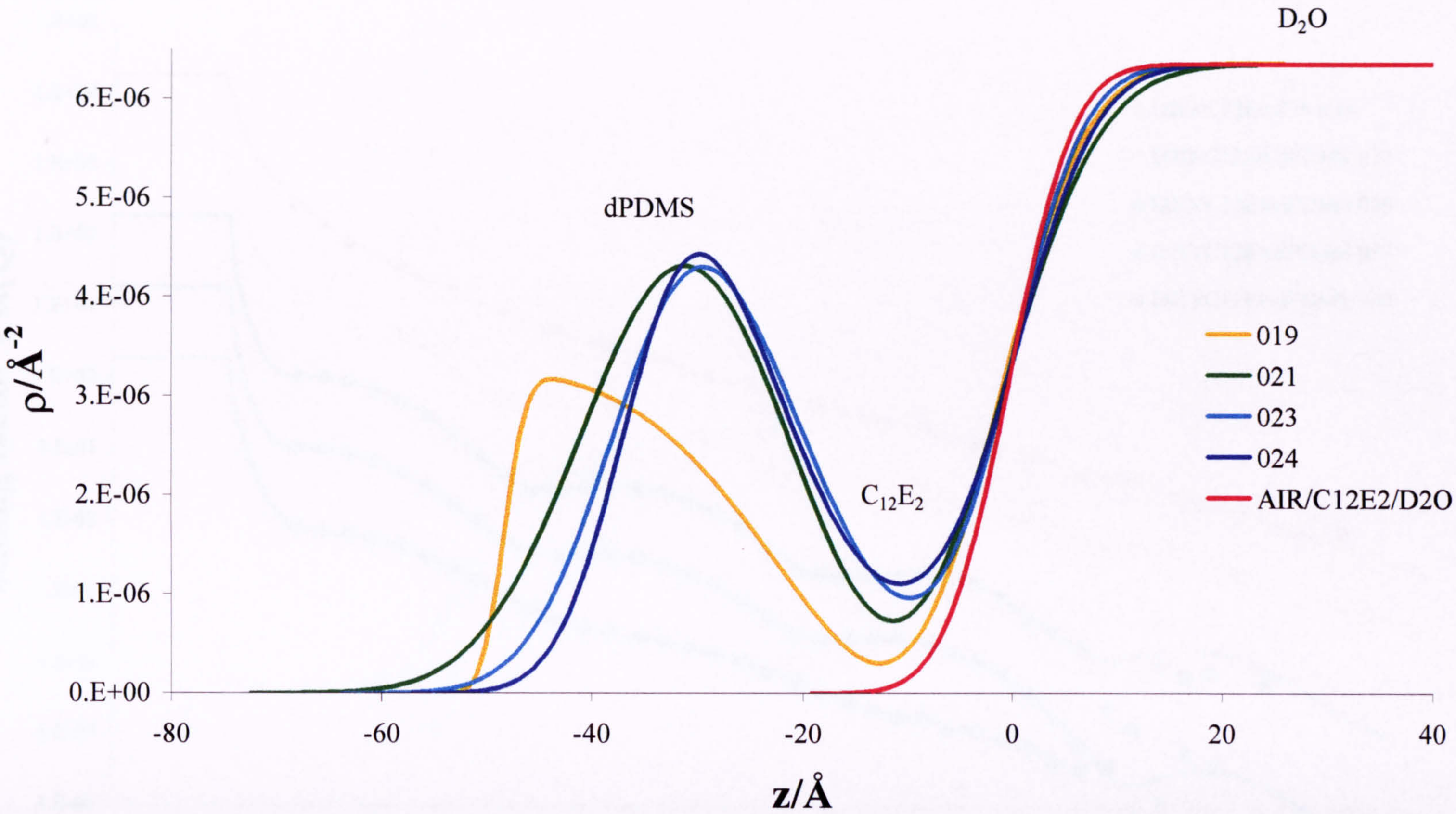

Figure 5.23

(a) Neutron reflectivity profiles of the system: dPDMS/$C_{12}E_4$/D_2O at different times

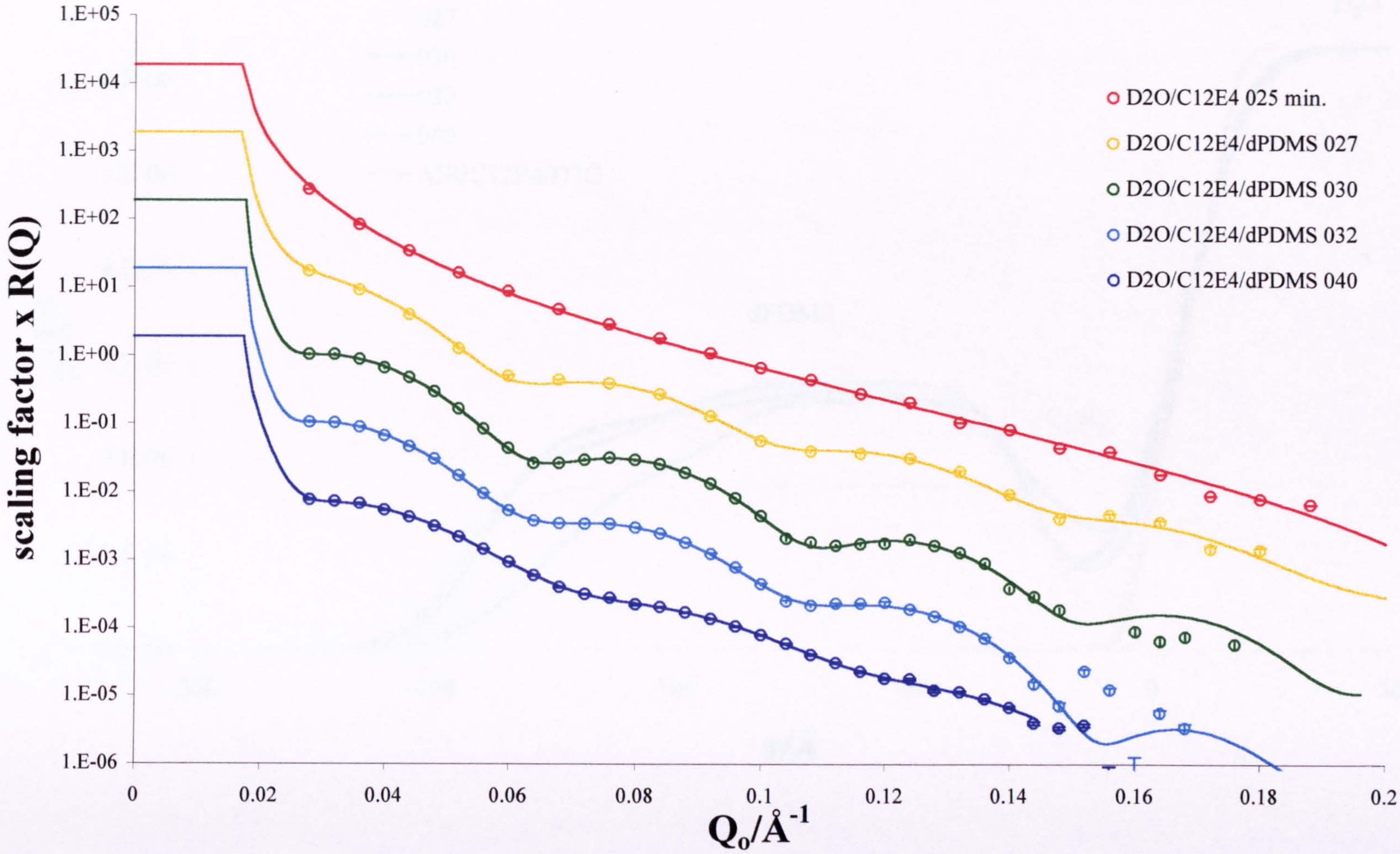

(b) Neutron scattering length profiles of the system:
dPDMS/$C_{12}E_4$/D_2O at different times

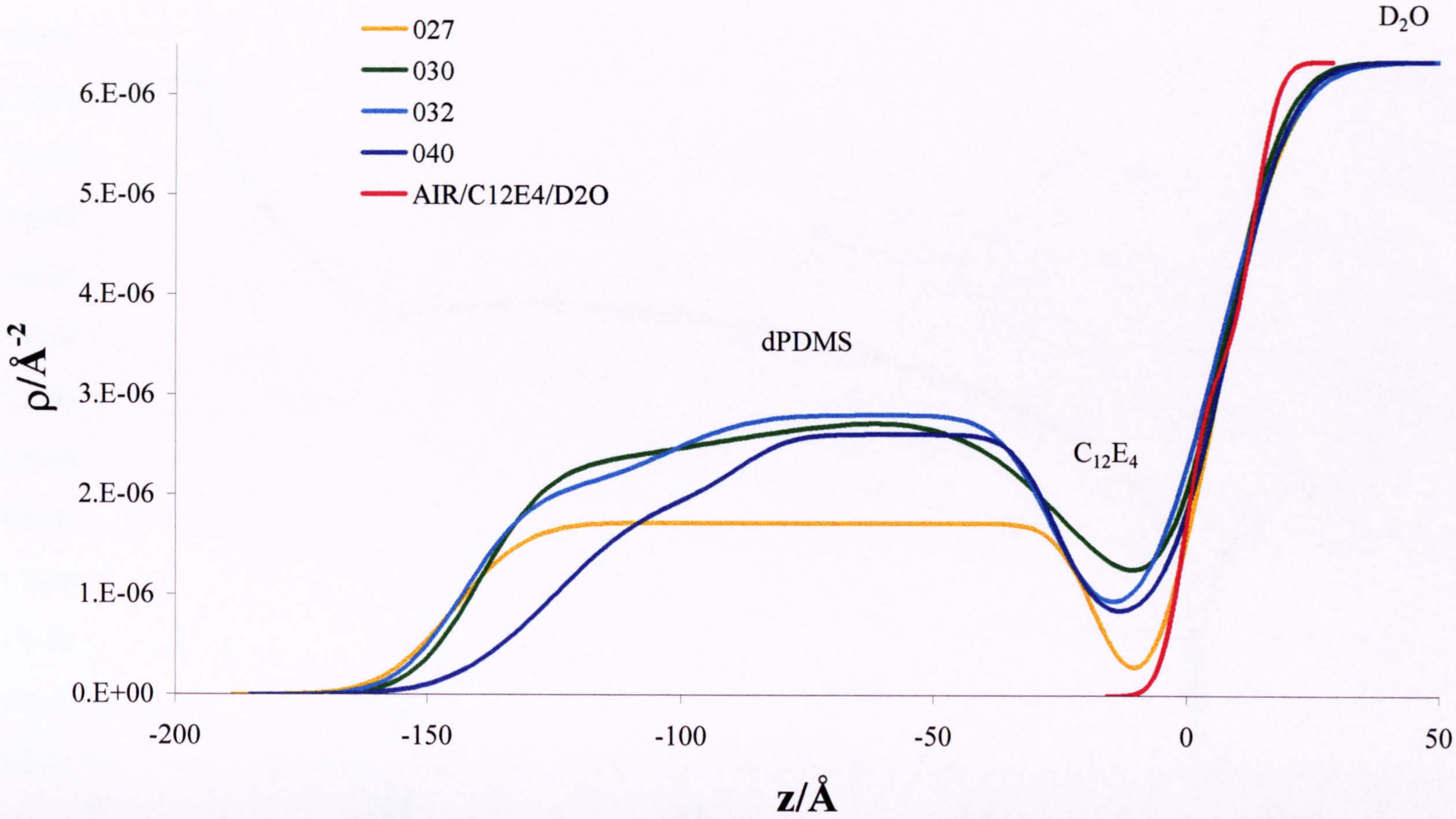

Figure 5.24

(a) Neutron reflectivity profile of the system: $D_2O/C_{12}E_6$/dPDMS

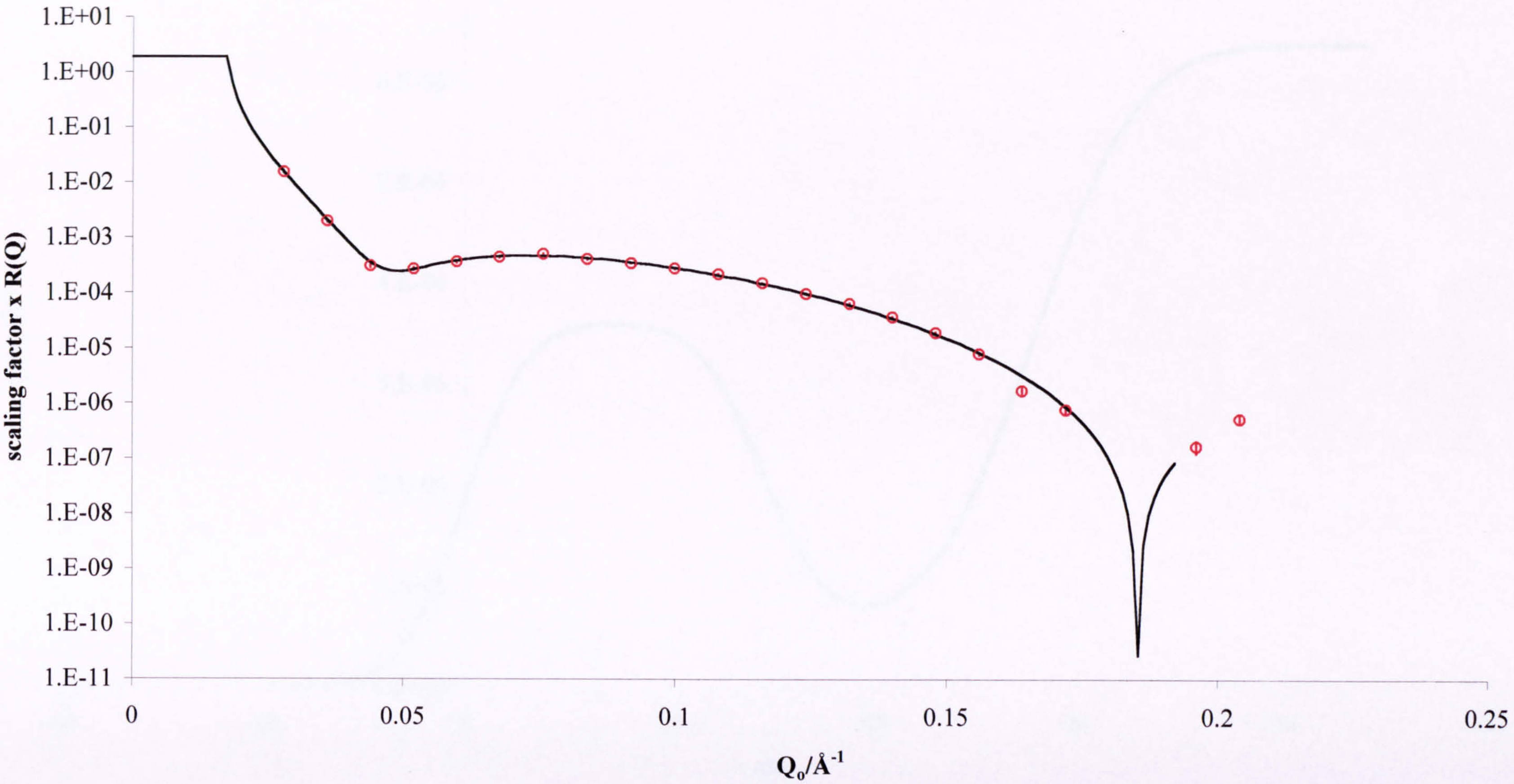

(b) Neutron scattering length density of the system: $D_2O/C_{12}E_6$/dPDMS

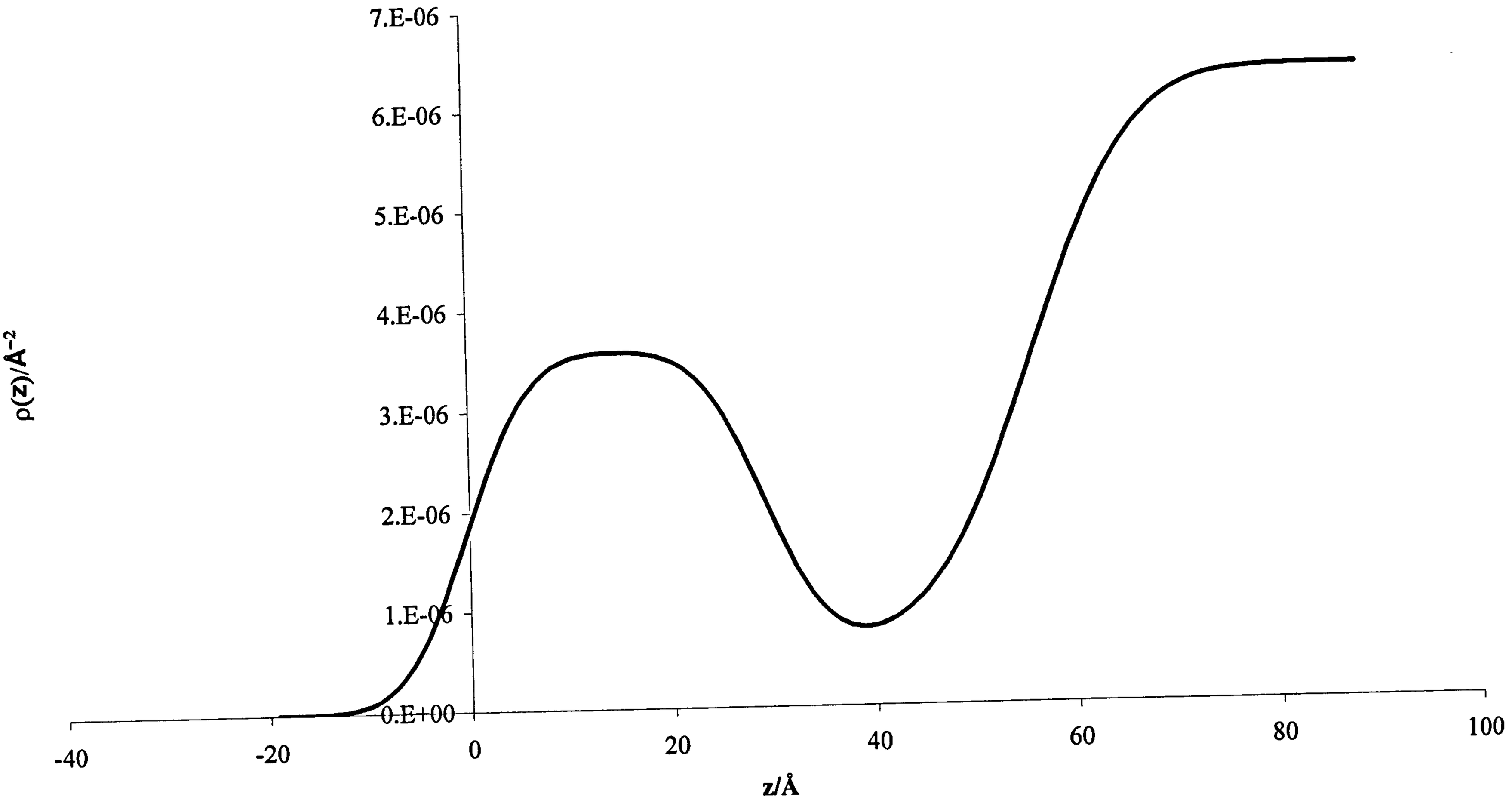

Table 5.5 Parameters used to fit the neutron reflectivity profiles. t denotes the time (min.) since oil addition, d, the thickness of the layer, ρ, the scattering length density and μ, the interfacial roughness*

system	t	layer 1 (PDMS)			layer 2 (surfactant chains)		
		d_1/ nm	$\rho_1/10^{-6}$ Å^{-2}	μ_1/ nm	d_2/ nm	$\rho_2/10^{-6}$ Å^{-2}	μ_2/ nm
D_2O/dPDMS	1	7.895	0.075	6.0514			
D_2O /dPDMS	4	12.75	0.097	7.3268			
D_2O /$C_{12}E_6$/dPDMS	13	8.018	0.54	/	8.3685	0.77	/
D_2O /$C_{12}E_4$	25				0.5354	9.9	/
D_2O /$C_{12}E_4$/dPDMS	27	7.801	0.11	1.0103	13.746	3.3	6.438
D_2O /$C_{12}E_4$/dPDMS	30	0.897	0.094	0.565	0.869	0.066	/
D_2O /$C_{12}E_4$/dPDMS	32	2.765	0.21	1.3114	3.1854	0.29	4.925
D_2O /$C_{12}E_4$/dPDMS	40	7.775	0.17	1.2095	11.264	1.1	4.068
D_2O /$C_{12}E_2$	16				/	/	/
D_2O /$C_{12}E_2$/dPDMS	19	5.543	0.37	1.7694	5.448	0.92	/
D_2O /$C_{12}E_2$/dPDMS	21	140.0	120	19.024	118.86	12	24.83
D_2O /$C_{12}E_2$/dPDMS	23	71.63	45	22.523	64.143	6.2	20.52
D_2O /$C_{12}E_2$/dPDMS	24	406.5	210	59.506	325.99	17	111.2

*The SLD of the subphase D_2O was measured as 6.35 x 10^{-6} Å^{-2}.

5.7 Conclusions

(i) Silicone oils of the PDMS type lower the air-water surface tension of solutions of nonionic surfactants (C_nE_m) above the cmc. For the 50 cS oil, the lowering is weakly dependent on surfactant alkyl chain length (C_n), but increases markedly with head group size (E_m) in line with the increase in the area per surfactant molecule.

(ii) Initial spreading coefficients are positive, reflecting the observation that drops of this oil added to the surface of the surfactant solutions appear to spread. Equilibrium spreading coefficients lie around zero for all systems.

(iii) For $C_{12}E_5$ above the cmc, the lowering of surface tension decreases upon increasing the viscosity of PDMS, and levels off around 50 cS. This is consistent with decreased solubilisation of oil upon increasing the molar volume.

(iv) Using the volatile 0.65 cS oil, the adsorption isotherm has been determined on $C_{12}E_5$. The surface concentration of oil at unit activity corresponds approximately to equal numbers of oil and surfactant molecules in the mixed film.

(v) With $C_{12}E_5$, opening up a close-packed monolayer by dilution below the cmc results in a competition for the surface between the oil and surfactant. Although the cmc is unchanged, the surface concentration of surfactant is reduced substantially in the presence of oil. For the silicone nonionic surfactant L-77 however, no lowering of the tension occurs on addition of oil up to at least 1/50 of the cmc.

(vi) A preliminary neutron reflection study suggested that PDMS forms thin layer on top of the surfactant chain region, further experiments are required to understand the spreading behaviour of PDMS on surfactant solution fully.

CHAPTER SIX

CHAPTER 6

Equilibrium Phase Behaviour in Ionic Surfactant Systems

6.1 Introduction

The previous chapters dealt mainly with the interaction of 50 cS PDMS oil and nonionic surfactants, and showed that PDMS behaves virtually like hydrocarbon oils. Due to its large molecular volume, the solubilisation of the 50 cS PDMS into aqueous micellar solutions is very low for a variety of surfactants (e.g. $C_{12}E_3$, $C_{16}P_8E_1$, L-77). On the contrary, significant solubilisation of the small PDMS oils (e.g. 0.65 cS) into the aqueous micellar solutions such as $C_{12}E_5$ and L-77 is accompanied by a dramatic change in the cloud point. In this and subsequent chapters an ionic surfactant, Aerosol-OT, is employed to investigate the equilibrium phase behaviour, emulsion stability and mixing properties at air-water surfaces of PDMS oils. The majority of the work refers to the small oil hexamethyldisiloxane (0.65 cS), but comparisons are given for certain aspects with higher molecular weight oils.

AOT has been extensively studied[145] in a range of alkane microemulsions especially w/o systems. One of the reasons it is an attractive surfactant for such studies is that its hydrophilic and lipophilic properties are nearly balanced.[146] Furthermore, since microemulsions can be formed without requiring the presence of any cosurfactant such as medium chain

length alcohols, analysis of the phase behaviour is considerably simplified. With alkanes, several aspects of the phase behaviour of the AOT systems such as electrolyte concentration, temperature and variation in hydrocarbon chain length-induced phase transitions have been well established.[45,147] At fixed temperature an increase in salt concentration effects the Winsor phase progression from Winsor I to Winsor II via Winsor III. An increase in temperature, however, has an opposite effect. An ultra-low interfacial tension minimum is usually found to accompany the appearance of Winsor III systems. With PDMS as oil, there are few publications using AOT. Recently, Steytler *et al.*[68] investigated the formation and structure of water-in-silicone oil single phase microemulsions stabilised by AOT. In the case of the low molecular weight PDMS oil hexamethyldisiloxane, the solubilisation of water was measured as a function of temperature with and without 0.1 M NaCl in the dispersed phase. Small angle neutron and dynamic light scattering experiments showed evidence for strong attractive interactions between the water drops, the strength of which was larger than that observed in alkane oils of comparable molecular weight.

In this chapter, we describe the behaviour of PDMS oil-water mixtures containing Aerosol OT. In equilibrium multiphase systems, the effect of salt concentration in the aqueous phase on the distribution of surfactant between coexisting phases has been determined, and linked to the appearance of a low interfacial tension minimum at the PDMS-water interface. The effect of PDMS molecular weight on the surfactant transfer is also discussed. With the small 0.65 cS PDMS oil, such results are compared with the uptake of

both oil into aqueous surfactant solutions and water into oil+surfactant solutions in single phase microemulsions.

6.2 Equilibrium multiphase systems

6.2.1 Effect of electrolyte in 0.65 cS PDMS oil systems

It is known that at fixed temperature, the variation in electrolyte (e.g. NaCl) concentration enables the transfer of AOT aggregates from aqueous to oil phases in hydrocarbon oil systems. At low electrolyte concentrations, the AOT aggregates are oil-in-water (o/w) microemulsion droplets which form in the water phase present in equilibrium with an excess oil phase containing no surfactant. This type of two-phase system is designated as a Winsor I system. At high electrolyte concentrations, the aggregated surfactant forms water-in-oil microemulsion droplets in the oil phase with an excess aqueous phase giving a Winsor II system. The Winsor III phase system occurs at intermediate electrolyte concentrations, where the aggregated surfactant is located entirely in a third phase in equilibrium with both excess oil and water phases. These findings have been rationalised in terms of changes in the spontaneous curvature of the monolayer coating the microemulsion drops, driven by variations in the effective geometry *in situ* of the surfactant adsorbed at the oil-water interface.[31] The inversion of the microemulsion location from water to oil is accompanied by a low interfacial tension minimum. An increase in the chain length of the alkane results in an increase in the salt concentration required for phase inversion and an increase in the magnitude of the minimum tension.[148] In a structural investigation of the types of third phase formed in these systems, small

angle neutron scattering data confirmed the presence of a bicontinuous microemulsion containing roughly equal amounts of oil and water for short alkanes (smaller than decane) and an L_3 phase composed of surfactant bilayers in water swollen slightly by oil for the longer homologues.[114] This change in structure is in line with the decreased penetration of oil into the surfactant chain region upon increasing the oil chain length.

The equilibrium phase behaviour of water-PDMS oil-AOT mixtures has been investigated at 25°C. Equal volumes of aqueous NaCl and PDMS were mixed gently and left to phase separate. For 0.65 cS PDMS, in order to test for distribution equilibrium, two sets of experiments were performed; one in which AOT was initially dissolved in the water phase and one in which it was prepared in the oil phase. The concentration of surfactant (40 mM) chosen is sufficiently greater than the cmc[149] such that solubilisation of oil into aggregates can be distinguished.

(a) AOT initially in water

The appearance of the phases at equilibrium from experiments in which AOT is initially dissolved in water is given in Figure 6.1. Up to 0.06 M NaCl, a clear oil phase coexists with an unbroken emulsion phase. From 0.08-0.12 M, a clear blue phase in water is in equilibrium with a clear oil phase. Three phase systems, in which the third phase forms initially at the bottom of the vessel and is birefringent, exist between 0.13 and 0.18 M NaCl. Between 0.13 and 0.15 M NaCl, the bluish third phase locates at the bottom of the tube, indicating a higher density than the aqueous phase. For 0.16 M to 0.18 M, it becomes the true middle phase with a clear appearance.

Figure 6.1

Phase sequence after 9 weeks for the system: 40 mM AOT initially in aqueous NaCl+0.65cS PDMS oil (1:1 vol) at 25°C. Dashed lines enclose the three phase region and the shaded areas indicate the location of aggregated surfactant

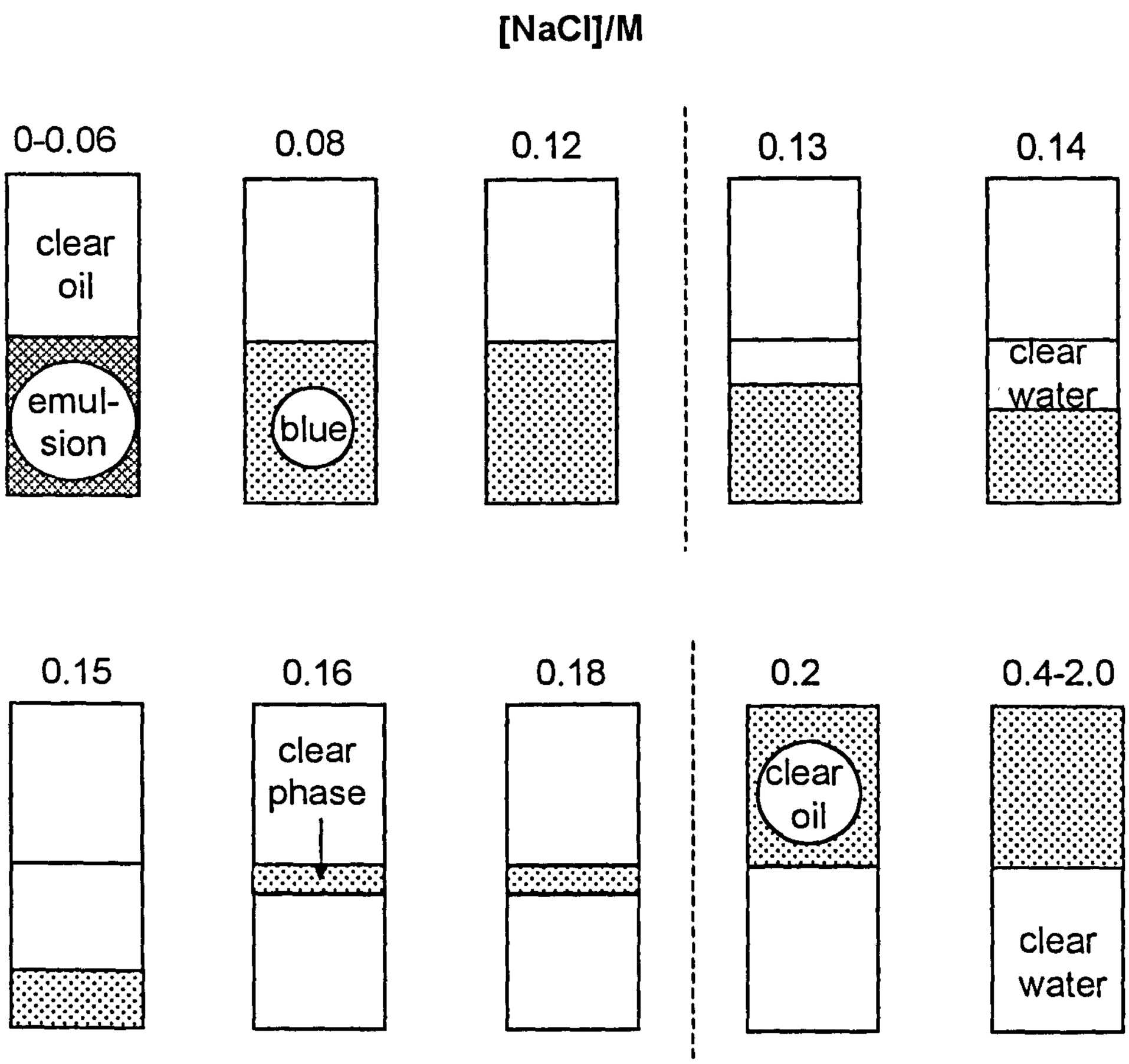

Above 0.18 M NaCl, two clear phases separate. The relative volumes of the coexisting phases are given as a function of [NaCl] in Figure 6.2. Accelerated breaking of emulsions at low salt concentration was achieved by centrifugation for 30 minutes at 5,000 rpm. Although some solubilisation of oil occurs into aqueous phases at low [NaCl] and into third phases at intermediate [NaCl], it amounts to less than 5 vol %. The third phase comprises mainly surfactant+water, its volume fraction decreasing with [NaCl] until close to the Winsor III/II boundary it becomes the true middle phase.

The distribution of AOT between phases has been determined by analysing quantitatively for surfactant using Hyamine titrations. The concentrations of AOT in aqueous and oil phases at equilibrium are shown in Figure 6.3a. Broadly, it can be seen that AOT transfers between water and oil phases, via a third phase (in which the concentration is >0.2 M), upon increasing the salt concentration. However, values in water at low [NaCl] are low (<40 mM and none in oil) and probably a result of the unbroken emulsions which persist in these systems. The percentage of AOT in each phase is given in Figure 6.3b. At low [salt], all the surfactant is located in water in the form of oil-in-water microemulsions in equilibrium with an oil phase containing no surfactant, even as monomers. At high [salt], most of the surfactant resides in the oil phase which coexists with an aqueous phase containing the cmc's worth of surfactant. At intermediate [salt], over 98% of AOT is in the third phase, the rest being in the excess aqueous phase in the form of monomers. Interestingly, for three phase systems close to WIII/WII

Figure 6.2

Relative volume of each phase vs [NaCl] for the system 40 mM AOT initially in aqueous NaCl+0.65 cS PDMS oil at 25°C

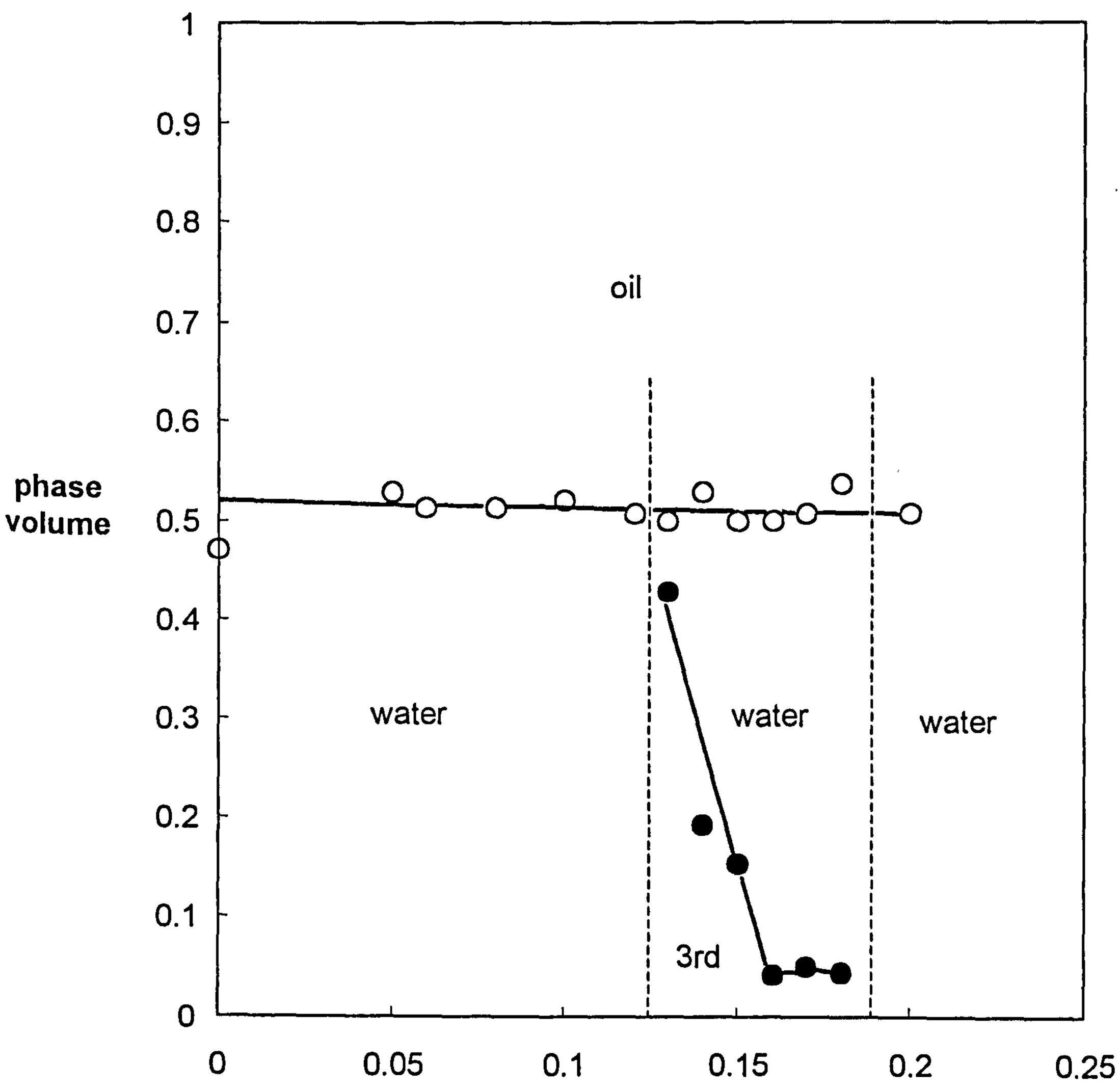

Figure 6.3

(a) Concentration of AOT at equilibrium versus [NaCl] for system in Figure 6.1

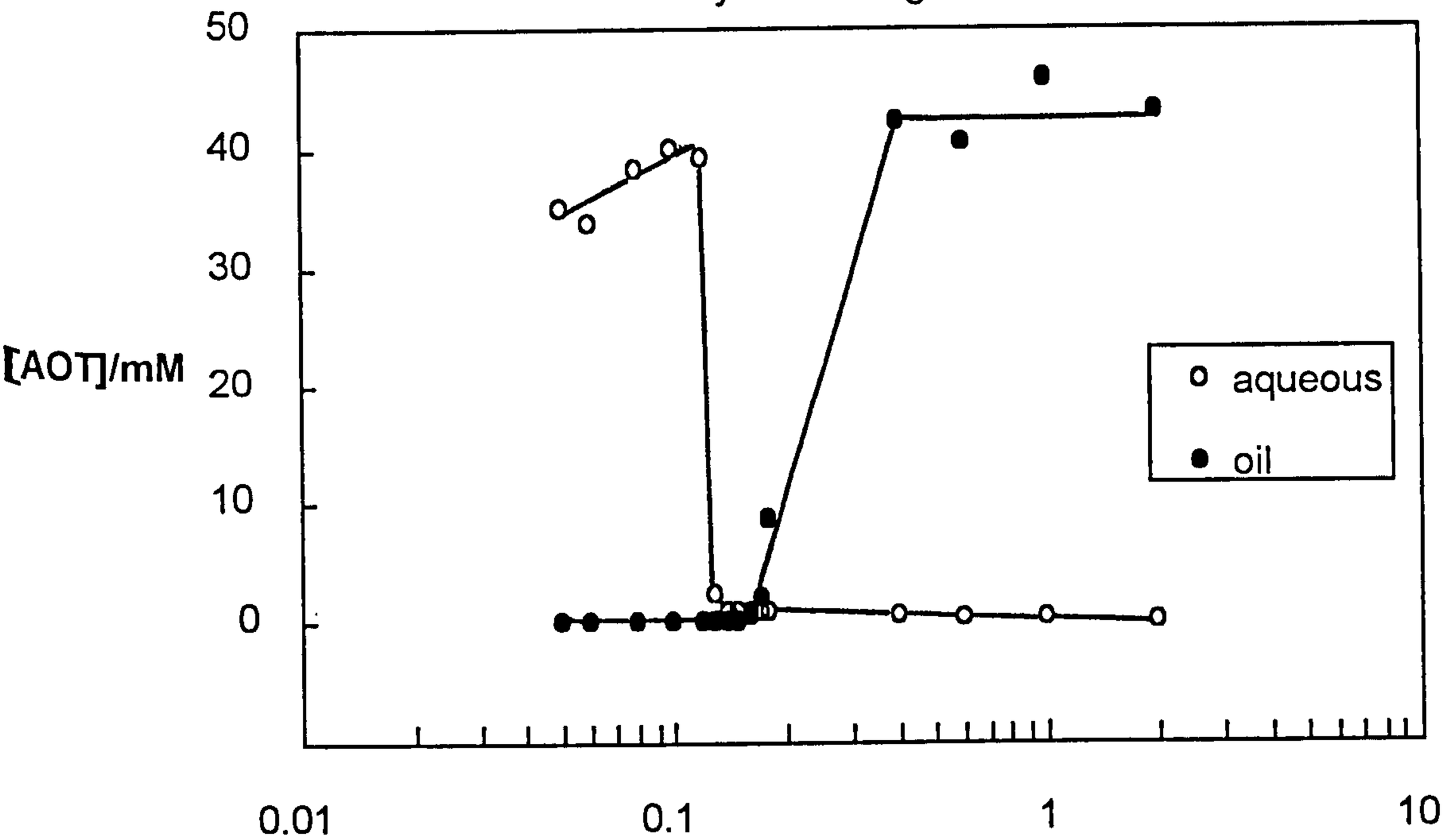

(b) Distribution of AOT between water oil and third phase as a function of [NaCl] for the system in Figure 6.1

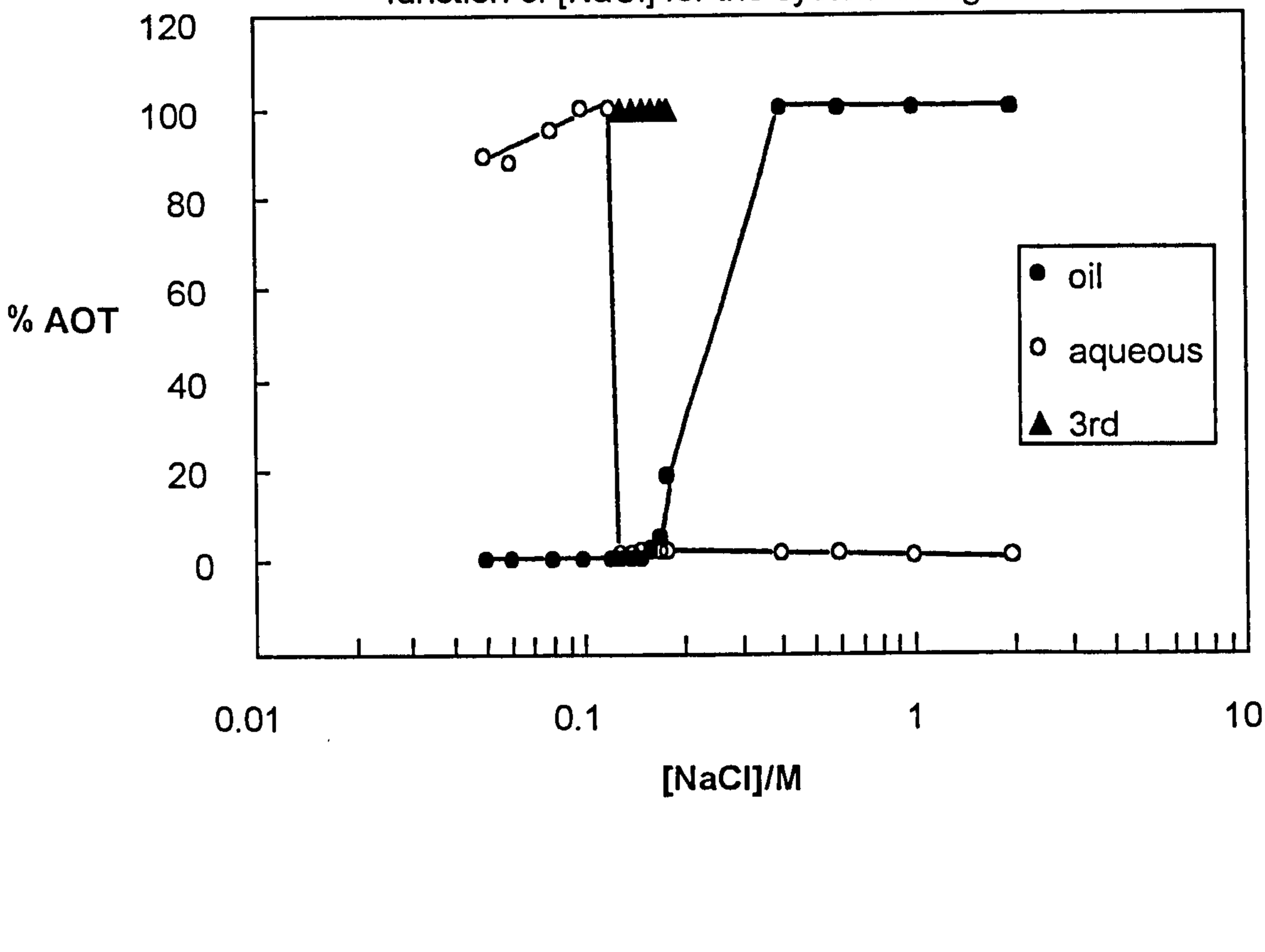

boundary significant transfer of AOT into the excess oil phase occurs prior to virtually complete transfer in Winsor II systems.

(b) AOT initially in oil

For systems with AOT initially in oil phases, very similar separation of the phases occurred at equilibrium with the exception that at low [NaCl] (<0.025 M) emulsion formation was less prone to happen and only turbid phases containing large unsolubilised oil drops appeared. In Figure 6.4 the relative volume of each phase (a) and the concentration of AOT in each phase (b) are plotted as a function of salt concentration. Surfactant transfer is reproducible and more accurate data has been collected.

The excellent agreement between the two sets of data from experiments starting with surfactant in water and in oil is shown in Figure 6.5, and is evidence that equilibrium has been attained. It can be concluded here that the Winsor phase sequence in this system occurs with an increase in salt concentration. There are two interesting features of this equilibrium phase behaviour. Firstly, birefringent liquid crystalline phases appear in equilibrium with excess oil just before the formation of the Winsor III systems, which can be compared with similar phase behaviour found in high alkane chain length systems.[150] Secondly, at the onset of the three-phase region, the microemulsion phase appears as the densest phase instead of appearing between the aqueous and the oil phases as the commonly found "middle-phase" microemulsion. This difference in behaviour is due to the slightly higher density of AOT as compared to other commonly used surfactants which results in the microemulsion being heavier than the excess

Figure 6.4

(a) Relative volume of each phase versus salt concentration for the system: 40 mM AOT initially in 0.65cS PDMS oil + aqueous NaCl (1:1 vol) at 25°C

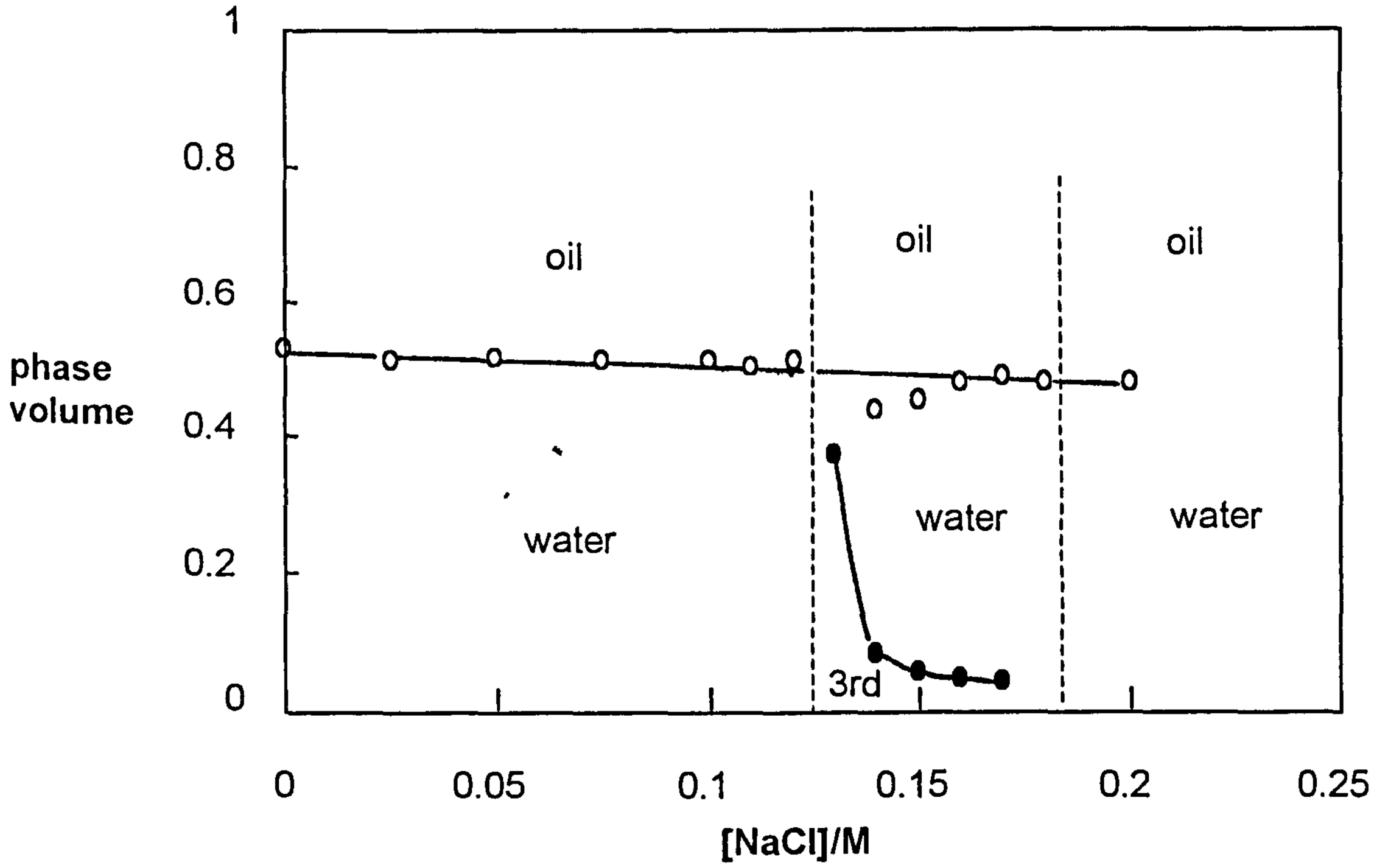

(b) Concentration of AOT in each phase for system above

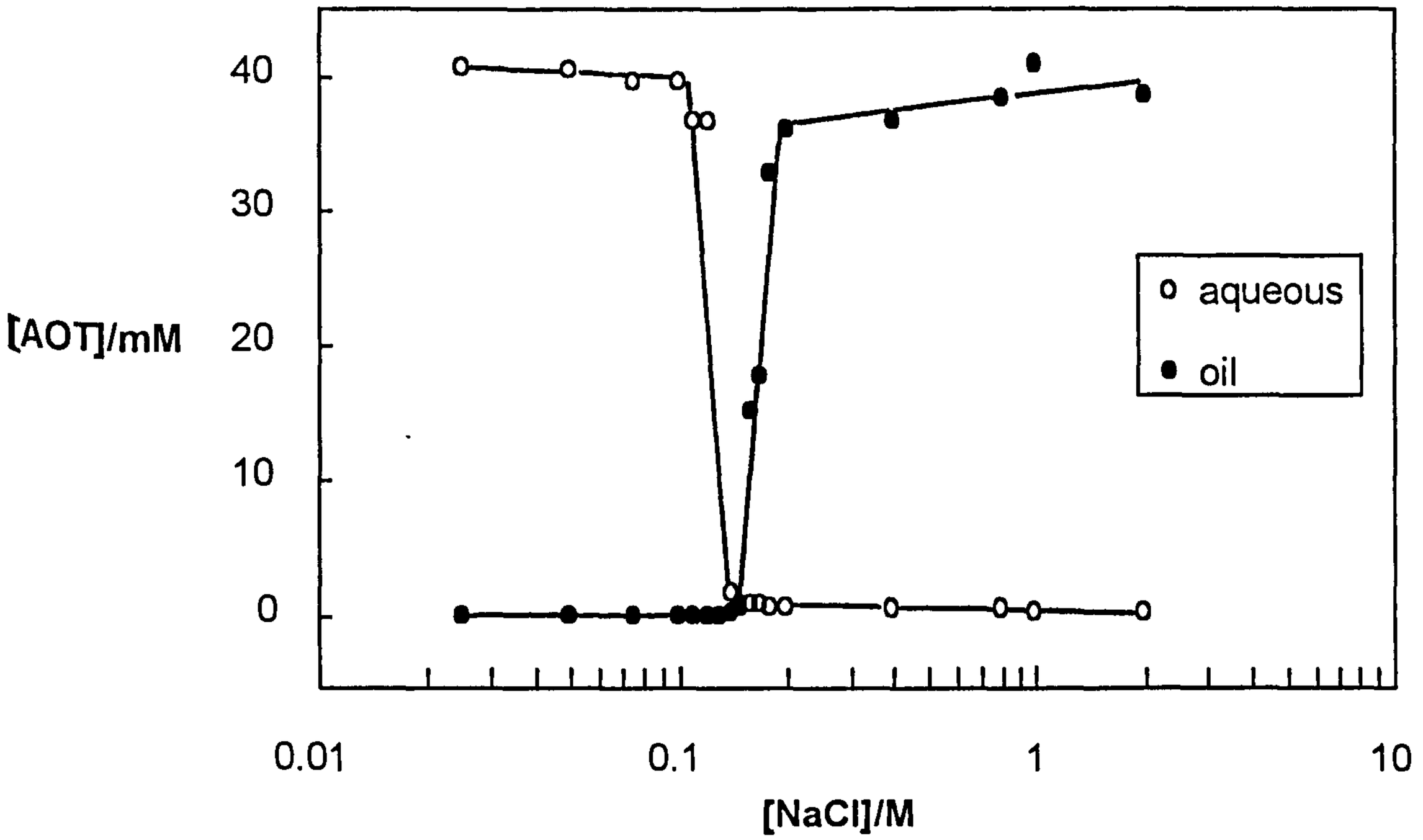

Figure 6.5

Distribution of AOT between water, oil and third phases as a function of salt concentration in the system 40 mM AOT+aqueous NaCl+0.65 cS PDMS at 25°C. Circles refer to water phase, triangles to oil phase and squares to third phase.
Open points: AOT initially in water, filled points: AOT initially in oil

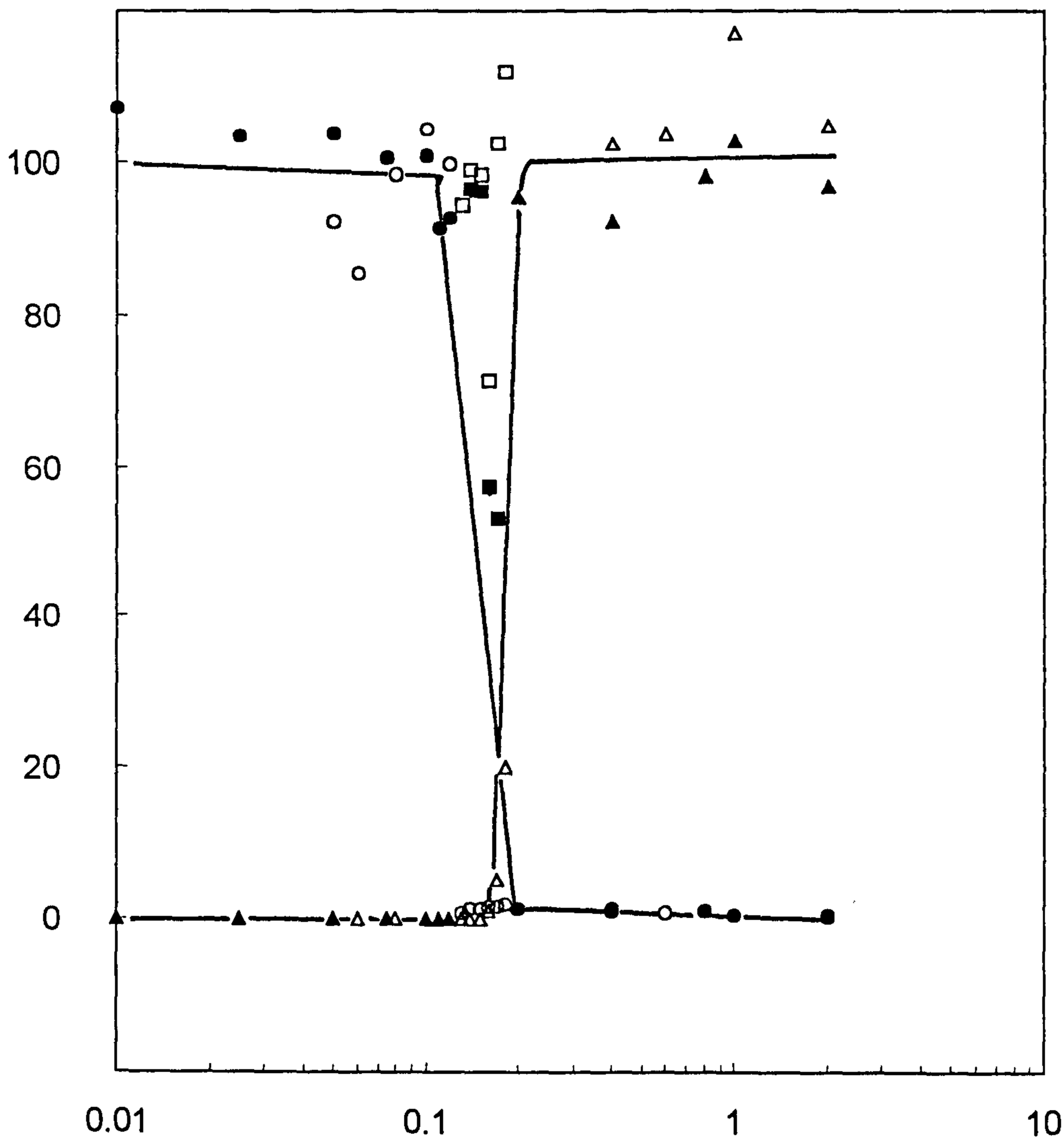

aqueous phase until it solubilises sufficient amount of oil and appears as a "middle-phase".

6.2.2 Nature of Winsor III and Winsor II phases

Kellay *et al.*[45] examined in detail the structure of the Winsor III third phase by neutron scattering. They found that the structure of the third phase in mixtures of AOT+aqueous NaCl+alkane depends on both the salt concentration and the chain length of the alkane. The oil chain length plays an essential role in determining the nature and structure of the phases obtained in the Winsor III systems. Long chain alkanes give third phases which are isotropic and contain very little oil. Shorter chain alkanes on the contrary give lamellar third phases containing more oil. With dodecane as oil, the phase behaviour observed with respect to salt concentration resembles what is observed here for 0.65 cS PDMS. The structure of the third phases appearing as the bottom phase is an L_3 phase constituted of bilayers of surfactant in water, containing virtually no oil. Upon an increase in salt concentration, the structure of the true "middle-phase" is a bicontinuous phase constituted of monolayers of surfactant separating water and oil domains. Given the astonishing similar appearance of the phase behaviour of 0.65 cS PDMS and dodecane in AOT and aqueous NaCl systems, it is reasonable to believe that the explanation of dodecane phase behaviour suits this silicone oil. Actually, there is not a remarkable difference in the molar volume of the two oils (213 cm^3 mol^{-1} for 0.65 cS PDMS, 227 for dodecane).

In Winsor III and Winsor II systems where surfactant aggregation occurs in the third phase and in the oil phase respectively, the concentration of surfactant in excess aqueous phases is close to the cmc in water in the presence of oil. As seen in Figure 6.6a, this concentration falls with increasing salt concentration due to the screening of the charged headgroups by salt leading to a reduction of the cmc. Hall[151] has shown that the variation of the cmc with total sodium ion concentration, $[Na^+]$, (i.e. salt concentration+cmc) is related to the degree of dissociation of surfactant at the micelle surface, α, according to

$$-\frac{d\ln(cmc)}{d\ln[Na^+]} = (1-\alpha) + (2-\alpha)\frac{d\ln f_{\pm}^{NaCl}}{d\ln[Na^+]} \qquad (6.1)$$

where $f_{\pm}^{NaCl}$ is the mean ionic activity coefficient of the electrolyte, assumed to be equal to that of the surfactant. The slope of the plot of ln(cmc) versus $\ln[Na^+]$ shown in Figure 6.6b is –0.53, and using values for $f_{\pm}^{NaCl}$ according to Robinson and Stokes,[152] α calculated using equation (6.1) is around 0.35-0.40 between 0.1 and 1 M NaCl. These are hypothetical values of α if aggregation occurred in the aqueous phase. It is appreciated that the physical meaning of degrees of dissociation of surfactant stabilising water drops in oil will be different to that mentioned above due to the reverse curvature of the interface and the fact that the electrolyte concentration inside the water pools is generally lower than that in the bulk aqueous phase (later). Nonetheless, the apparent α values are similar to those reported for other surfactants like tetradecylpyridinium bromide.[153]

The transfer of aggregated AOT into oil phases in the Winsor II systems is accompanied by the transfer of water because water can be

Figure 6.6

(a) Variation of [AOT] at equilibrium in excess aqueous phase of Winsor III and II systems versus [NaCl].
Open points: AOT initially in water, filled: AOT initially in oil

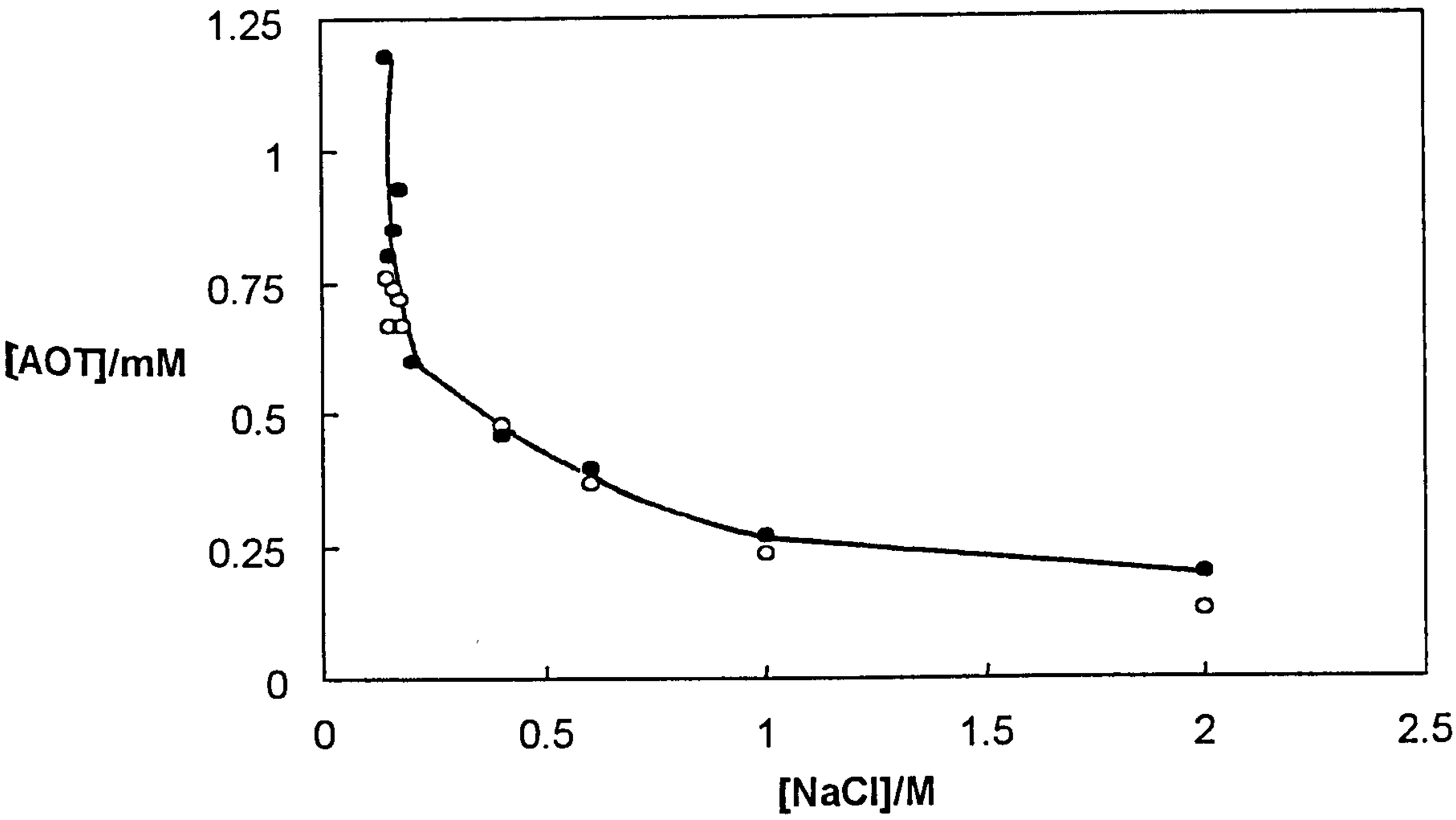

(b) Variation of ln(cmc) with ln[Na^+] in the above system

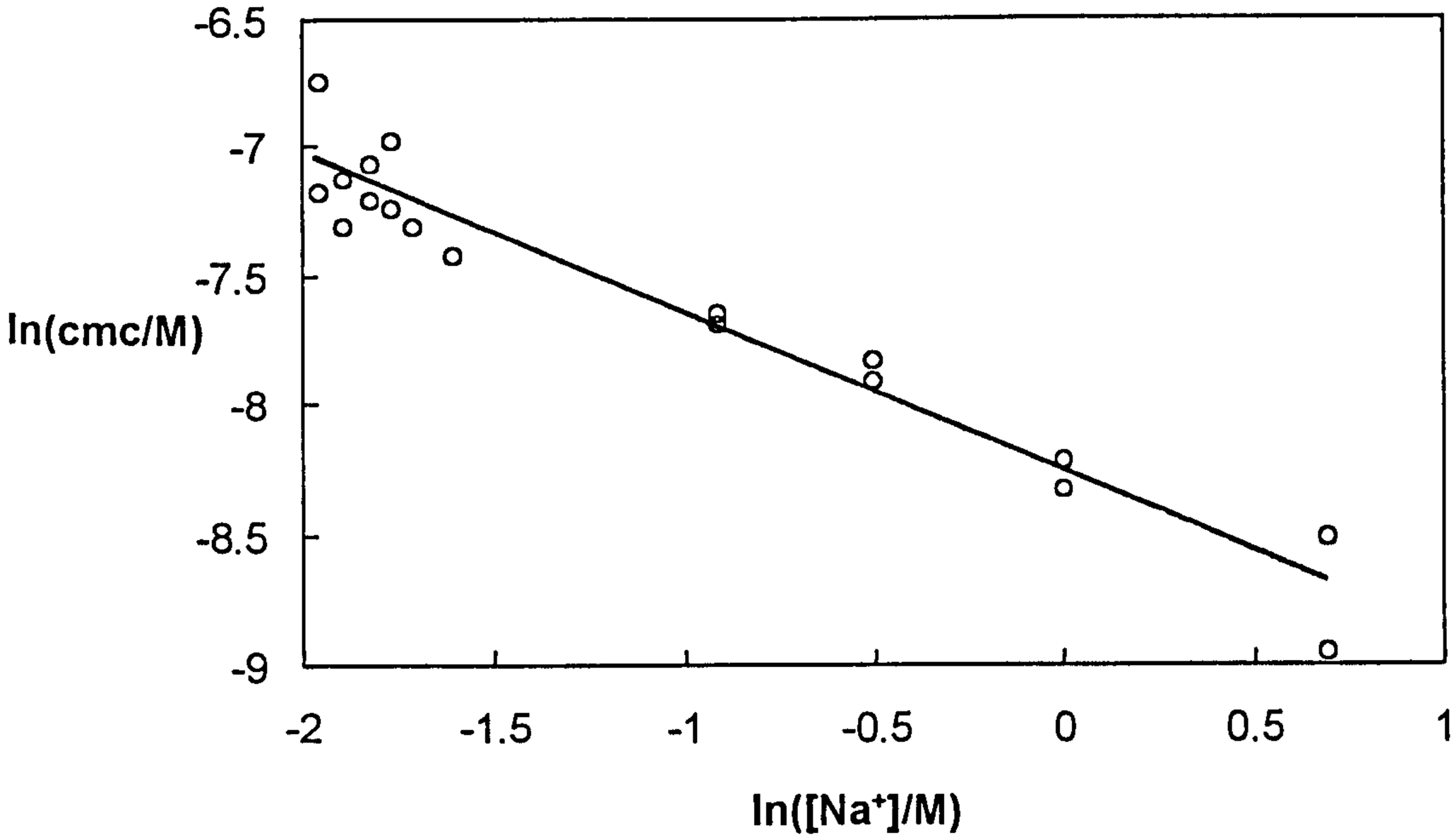

solubilised in the reversed micelles. For constant salt concentration and temperature, we have determined the water concentration in equilibrium oil phases and define the quantity R_W equal to the ratio [water]/[AOT] in silicone oil (R_W). The larger this value, the more water is solubilised as water-in-oil microemulsion droplets per mole of surfactant. Figure 6.7 shows the variation of the maximum solubilisation (R_W) of water in w/o microemulsions when it coexists with the excess aqueous phase for 0.65 cS PDMS oil. Clearly, R_W depends strongly on salt concentration. It falls as [salt] increases and levels off at higher [salt]. This is to be expected because the salt shrinks the electric double layer of the surfactant film at the water-oil interface, which reduces the solubilisation capacity of water. This result agrees well with the equilibrium phase behaviour and interfacial tensions. Near the WIII/WII boundary where the interfacial tension is lowest, the solubilisation capacity of water is the maximum. A similar effect of salt on R_W was reported for alkane systems earlier.[147] If the droplets are assumed to be spherical in shape, simple geometrical considerations yield the following expression relation R_W to the radius of the droplets

$$r_H = \frac{3R_W V_W}{A_s} + t \qquad (6.2)$$

in which r_H is the hydrodynamic radius, V_W is the volume occupied by a water molecule (0.03 nm^3), A_s is the area per surfactant molecule at the droplet surface and t is the thickness of the hydrocarbon chain of the surfactant. Taking the values of A_s as 0.60 nm^2 and t equal to 1.0 nm determined in the same system by neutron scattering,[68] r_H for the water-in-PDMS microemulsions varies from 7 nm at 0.2 NaCl to around 2.5 at 2 M

Figure 6.7

Variation of R_W with salt concentration for oil phases in equilibrated Winsor II systems of aqueous NaCl+0.65 cS PDMS at 25°C

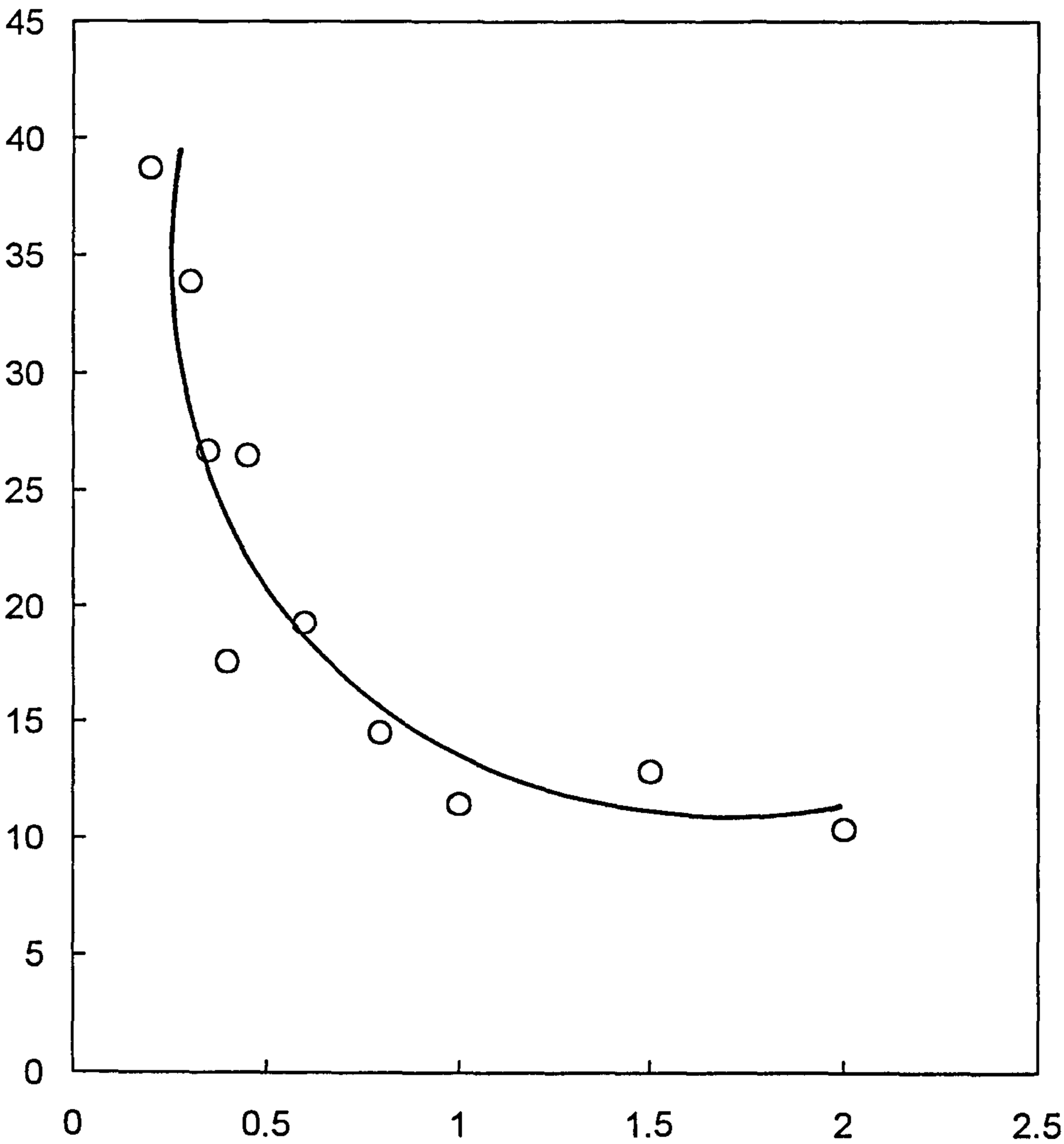

NaCl. It is worth noting that in the w/o microemulsions above which coexist with excess water, the monolayer curvature is the preferred one and the system phase separates at the solubilisation boundary (see later).

6.2.3 Effect of temperature on the Winsor phase behaviour in 0.65 cS oil

It is understood from the phase behaviour of AOT and hydrocarbon systems that temperature has an opposite effect on the equilibrium Winsor phase behaviour in ionic surfactant systems compared with nonionic surfactant systems.[154] For AOT, the progression of Winsor phase system is Winsor II to Winsor I via Winsor III with an increase in temperature. At higher temperature the [NaCl] required to achieve the phase inversion from o/w to w/o moves to a higher value. This is indeed what happens in 0.65 cS PDMS-AOT-water systems. Figure 6.8 shows the appearance and the volume of each phase of mixtures 3 weeks after equilibration at 40°C. Table 6.1 lists the salt concentrations at which the Winsor I/III and Winsor III/II boundaries occur at the two temperatures.

Table 6.1 Comparison of the salt concentration range for the formation of Winsor III systems in 0.65 cS PDMS/AOT/water system

Temperature/°C	Winsor I/III [NaCl] / M	Winsor III/II [NaCl]/ M	[NaCl]/M range
25	0.13	0.18	0.05
40	0.18	0.26-0.28	0.08-0.10

Figure 6.8

(a) Phase sequence at equilibrium for the system: 40 mM AOT initially in 0.65 cS PDMS oil + aqueous NaCl (1:1 vol) at 40°C. Dashed lines enclose the three phase region and the shaded areas indicate the location of aggregated surfactant

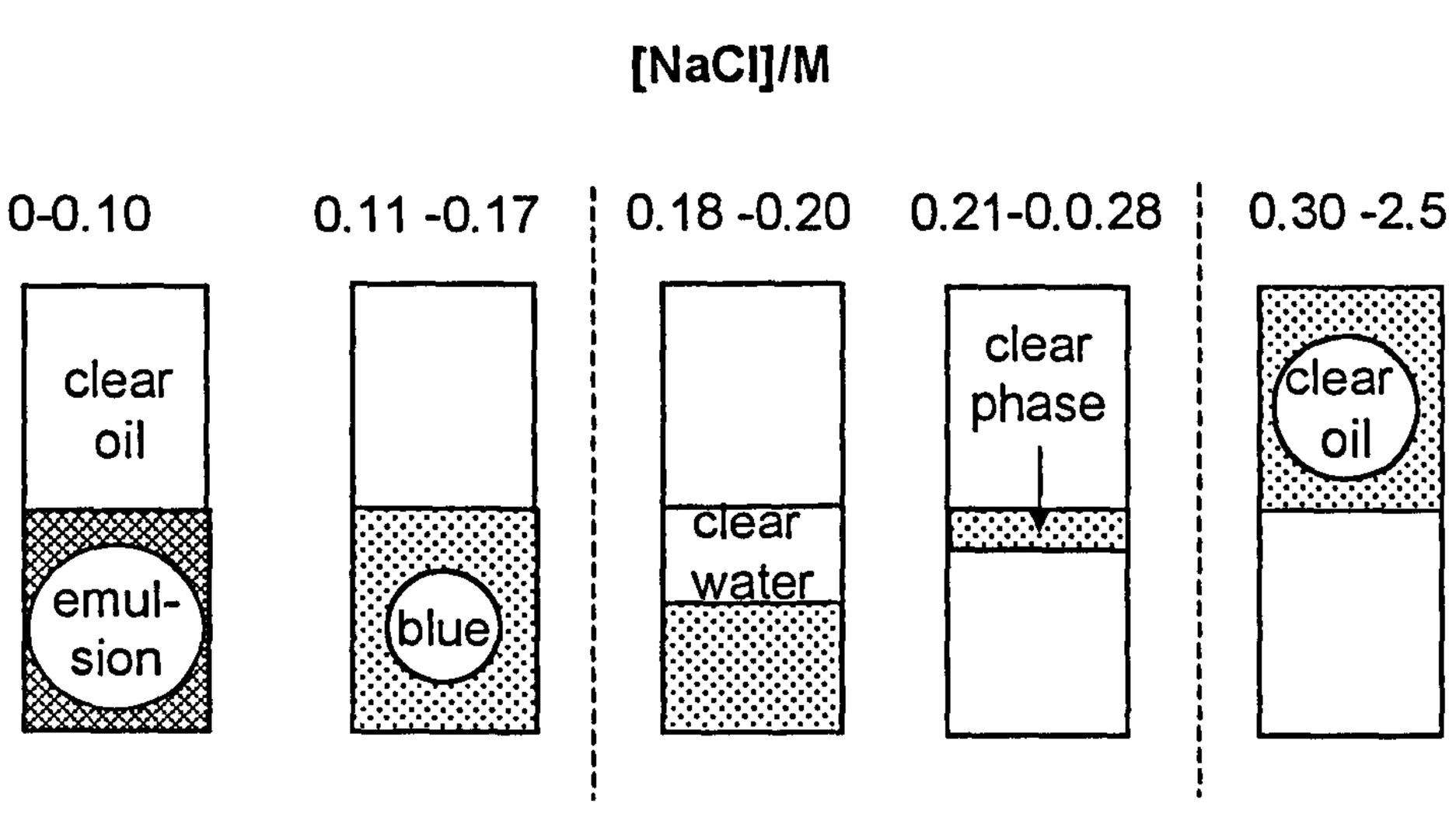

(b) Relative volume of each phase for the above system

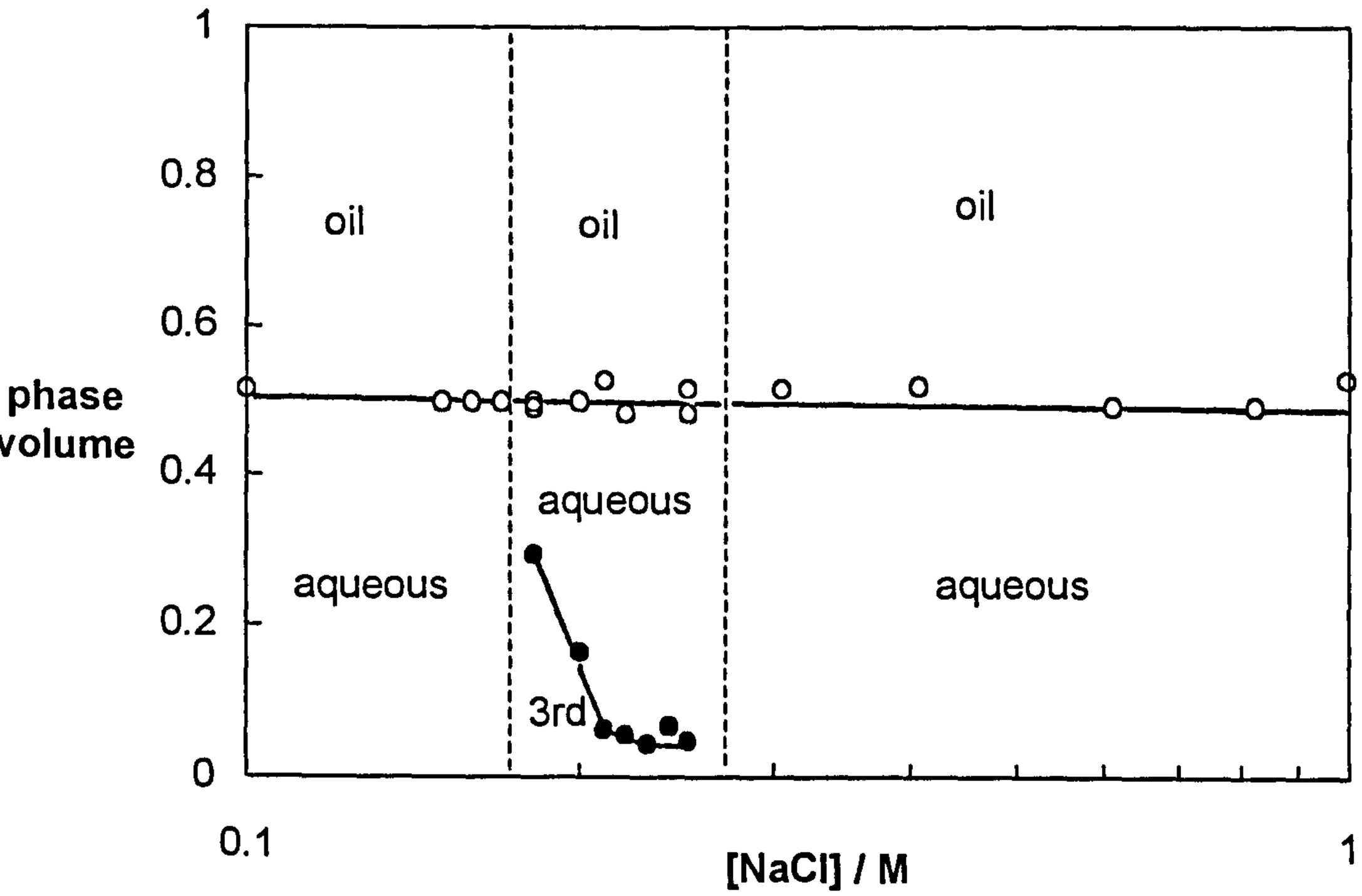

Obviously, at 40°C, the Winsor III range is wider than that at 25°C. From the volume of the excess oil phase, it is obvious that increasing temperature does not improve the solubilisation of oil into the aqueous phase. The solubilisation of oil can be determined experimentally by a turbidity titration method which will be discussed later.

6.2.4 Effect of oil molecular weight on multiphase behaviour

As shown above the addition of NaCl causes the transfer of AOT aggregates from aqueous phases to 0.65 cS PDMS oil phases at 25°C. The microemulsion phase inversion appears to be a typical Winsor phase sequence. In this part the larger molecular weight (or viscosity) PDMS oils are employed to investigate the effect of the size of the PDMS oil on the equilibrium phase behaviour. Similar experimental procedures were adopted to those for the 0.65 cS PDMS oil. The results are shown in Figure 6.9. Although the concentration of salt at the onset of Winsor III systems increases very progressively with oil viscosity from 0.13 to 0.25 M, the concentration of salt at the Winsor III/II boundary increases markedly by about 1.2 M. To the right of the dashed line and above the WIII region, two clear phases coexist with precipitated AOT. Instead of forming a normal phase, which has distinguished boundaries, the solid-like AOT adheres to the walls of the glass vessel.

To confirm the equilibrium phase behaviour observed above, the concentration of AOT in each phase was determined by Hyamine titration. For the systems with 1 cS PDMS, 40 mM AOT was dissolved in the oil initially. The transition of phases is similar to that of 0.65 cS PDMS oil which

Figure 6.9

Electrolyte dependence of three phase systems as a function of oil viscosity for: 40 mM AOT in aqueous NaCl+PDMS oil (1:1 vol) at 25°C

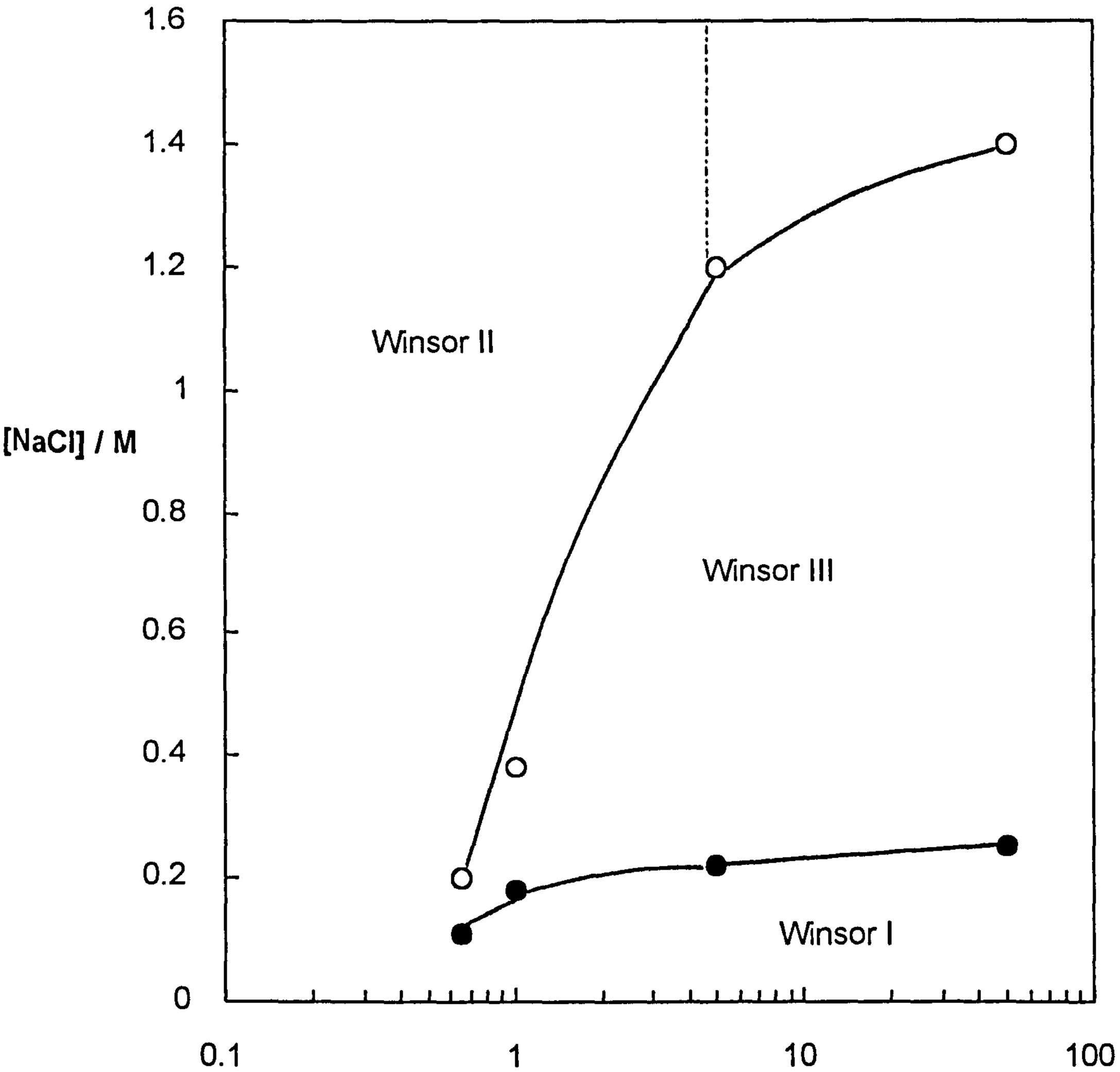

can be appreciated from Figure 6.10a. At low salt concentration (below 0.18 M), all the surfactant resides in the aqueous phase. As the salt concentration is increased (above 0.35 M) transfer of surfactant to the 1 cS PDMS oil occurs and the aqueous phase is left, devoid of micelles, close to its expected cmc. At intermediate salt concentrations, close to conditions corresponding to phase inversion, a third surfactant-rich phase is formed which contains much of the surfactant in the system. For the systems with 5 cS and 50 cS PDMS oils, 40 mM AOT was dispersed in the water because it is not possible to dissolve the surfactant in the oil phase completely. The surfactant distribution for 50 cS oil is shown in Figure 6.10b. A similar decline of surfactant in the aqueous phase can be seen clearly. However the % surfactant in oil phases remains at zero even at very high salt concentration where the third phase is hardly visible. A detectable surfactant-rich third phase is formed between 0.22 and 1.4 M salt. At higher [salt], random solid-like clusters reside at the oil-water interface and on the glass walls. Inversion of microemulsions stabilised by AOT also depends on the chain length of the alkane.[45] For o/w drops, it was shown experimentally that the area of the headgroup region a_h exceeds that of the chain region a_c favouring positive curvature of the monolayer around oil.[155] For w/o drops, the chain area is larger than that of the headgroup and negative curvature around water occurs. Added electrolyte is responsible for reducing a_h by screening the repulsion between headgroups, but a_c may also be enhanced due to oil penetration into the chain region. This latter effect is reduced upon increasing the oil chain length (for entropic reasons), so that in order to invert AOT systems in the presence of longer oils, more salt must be added

Figure 6.10

Distribution of AOT at equilibrium for the system: 40 mM AOT in aqueous NaCl+PDMS oil at 25°C

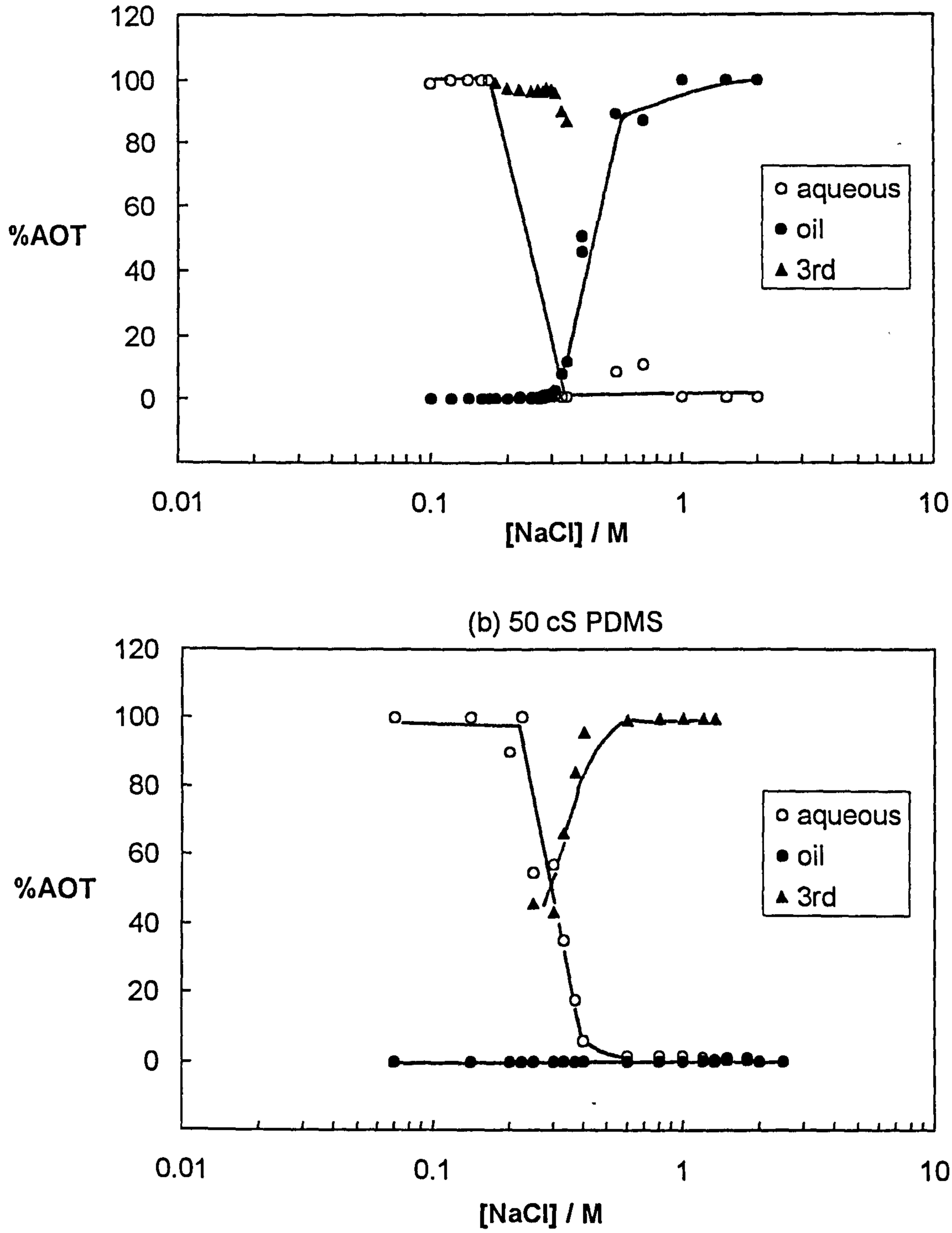

compared with short chain oils. This reasoning appears to apply in the case here with PDMS oils.

For 1 cS PDMS oil the solubilisation of water in the oil phases for the Winsor II systems was also measured and compared with that of 0.65 cS PDMS oil and is shown in Figure 6.11. Surprisingly, there is virtually no difference in water solubilisation for the two oils. The reason is unclear but is probably related to the impurity of the 1 cS oil.

6.2.5 Correlation between phase behaviour and oil-water tensions

In systems where aggregated surfactant distributes between oil and aqueous phases, the macroscopic post-cmc oil-water interfacial tension can pass through a minimum value, and it was shown elsewhere that such low tensions can be obtained through monolayer adsorption.[15] The [salt] required to achieve the minimum is close to that for which Winsor III systems are formed. The longer the alkane chain length, the higher the [NaCl] required to achieve this minimum, and the higher the minimum oil-water interfacial tension.[156] The variation of the PDMS-water interfacial tension with salt concentration is given in Figure 6.12, for an AOT concentration slightly above the cmc in pure water. It can be seen that there is a sharp minimum with a low value (0.021 mN m^{-1}) for 0.65 and 1 cS PDMS oils, while for 5 cS the minimum becomes less pronounced. For 50 cS, tensions fall initially at low salt and then level off with high tensions (1-2 mN m^{-1}). This is in accordance with the results previously for hydrocarbon systems.[157] Interestingly, the oil-water interfacial tension for 1 cS PDMS oil overlaps with that of 0.65 cS PDMS oil, even though the Winsor III phase region is much

Figure 6.11

Comparison of R_W versus [salt] for oil phases in equilibrated WII systems of aqueous NaCl+1 cS PDMS oils at 25°C with that of 0.65 cS PDMS systems

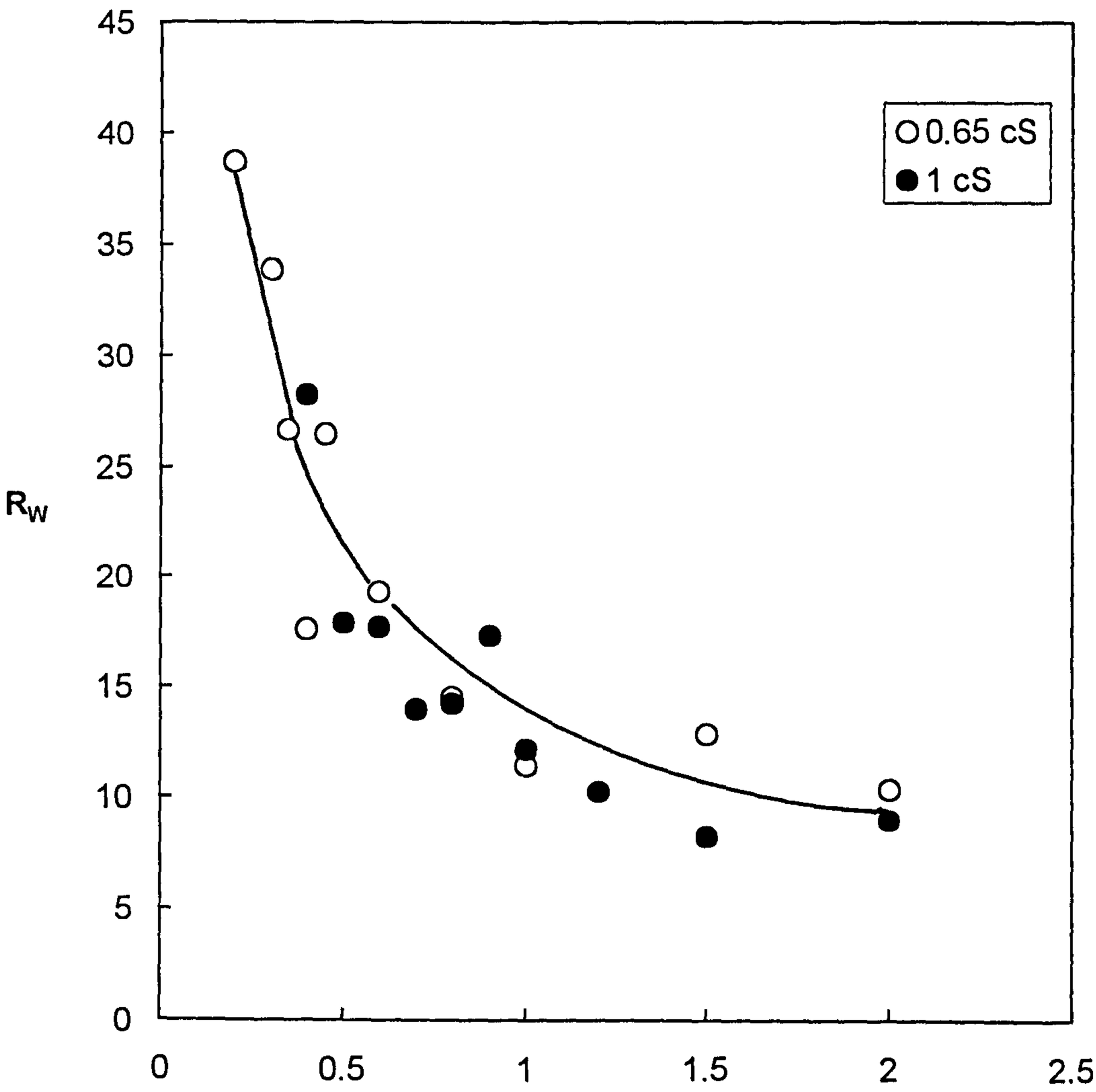

Figure 6.12

Variation of the interfacial tension with total sodium ion concentration for the system: 3 mM AOT in aqueous NaCl solutions plus PDMS oils at 25°C

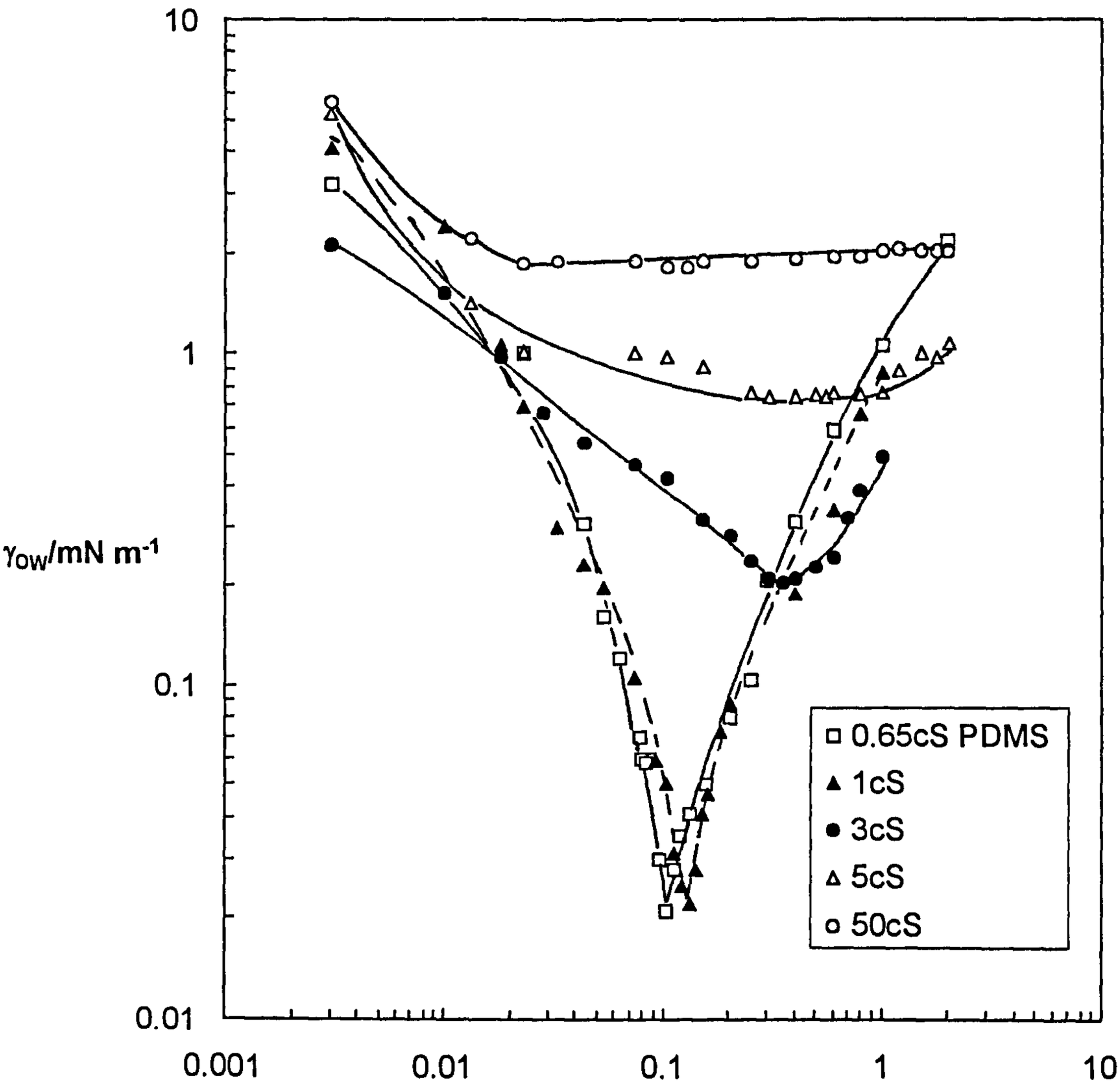

wider with respect to salt. One explanation is that the 1 cS oil is a commercial product which is a mixture of 0.65 cS PDMS oil and higher molecular weight homologues. Only the 0.65 cS oil in the mixture is able to penetrate to some extent into the AOT monolayer hence lower the tension.

It has been shown previously that the low tension is due to the presence of an adsorbed monolayer of surfactant at the oil-water interface.[158] Oil plays a key role in modifying the surfactant monolayer elastic properties. The elastic properties of the surfactant monolayer are characterised by the bending elastic constant (K). By using ellipsometry, Binks *et al.*[148] measured the K value in AOT- aqueous NaCl -alkane systems and found that K is independent of the salt concentration, but depends strongly on the oil chain length. It is of the order of ~1k_BT for short alkanes (N < 11) decreasing to ~0.1 k_BT for longer chain homologues (N > 11). This dependence is related to the differing degrees of oil penetration into the surfactant chain region.[155] As a result of the more favourable entropy of mixing, it is known that, for a given surfactant chain, short alkanes penetrate more strongly than long chain alkanes[159] rendering the film more rigid. Furthermore, it was found that the value of the rigidity K is in accord with the type of third phase formed in Winsor III systems. Large values of K imply the formation of ordered lamellar phases as evidenced for short chain oils (N < 11), while lower rigidities promote disordered phases like the L_3 phase (or a bicontinuous microemulsion) for longer (N > 11) chain oils. In the case of 0.65 cS PDMS oil, from the fact that the type of the third phase in Winsor III systems resembles dodecane behaviour, we can assume that the value of the rigidity K is low (< 0.1 k_BT). In fact, the magnitude of the minimum

tension in the 0.65 cS PDMS and dodecane systems is virtually the same (~0.015 mN m^{-1}) shown in Figure 6.13. For higher molecular weight PDMS oils, the oils are not able to penetrate the surfactant monolayer, which might be the reason that there is no minimum in the interfacial tension. This is consistent with the wide WIII region shown in Figure 6.9.

The effect of temperature on the water-0.65 cS PDMS oil interfacial tension is shown in Figure 6.14. As described before, at higher temperatures, higher salt concentrations are needed to promote the transfer of surfactant to the oil phase. As a result, a higher temperature shifts the tension minimum to higher [salt], which is consistent with the equilibrium phase behaviour in Figure 6.8. The magnitude of the tensions at the two temperatures is similar indicating that the extent of oil solubilisation into the third phase in both cases has not much difference.

6.3 Water-in-oil microemulsion single phase systems

6.3.1 Theory

In comparison with multiphase systems, we need to consider Winsor IV systems, i.e. single phase microemulsion systems. AOT aggregates in oil phases as reverse micelles which swell as water is solubilised. The swollen reversed micelles form the droplets of the w/o microemulsion which is a transparent single phase system. For a given w/o microemulsion there exists an optimal salinity at fixed temperature at which maximum solubilisation results from the counteracting effect of the interfacial bending stress of rigid interfaces and the attractive inter-droplet interactions.[160,161] Hou and Shah[160] used a plausible model to explain the solubilisation

Figure 6.13

Comparison of the oil-water interfacial tensions with salt concentration for the systems of 3 mM AOT in aqueous NaCl solutions plus 0.65 cS PDMS oil (circles) with that of dodecane systems (triangles, after ref.45) at 25°C

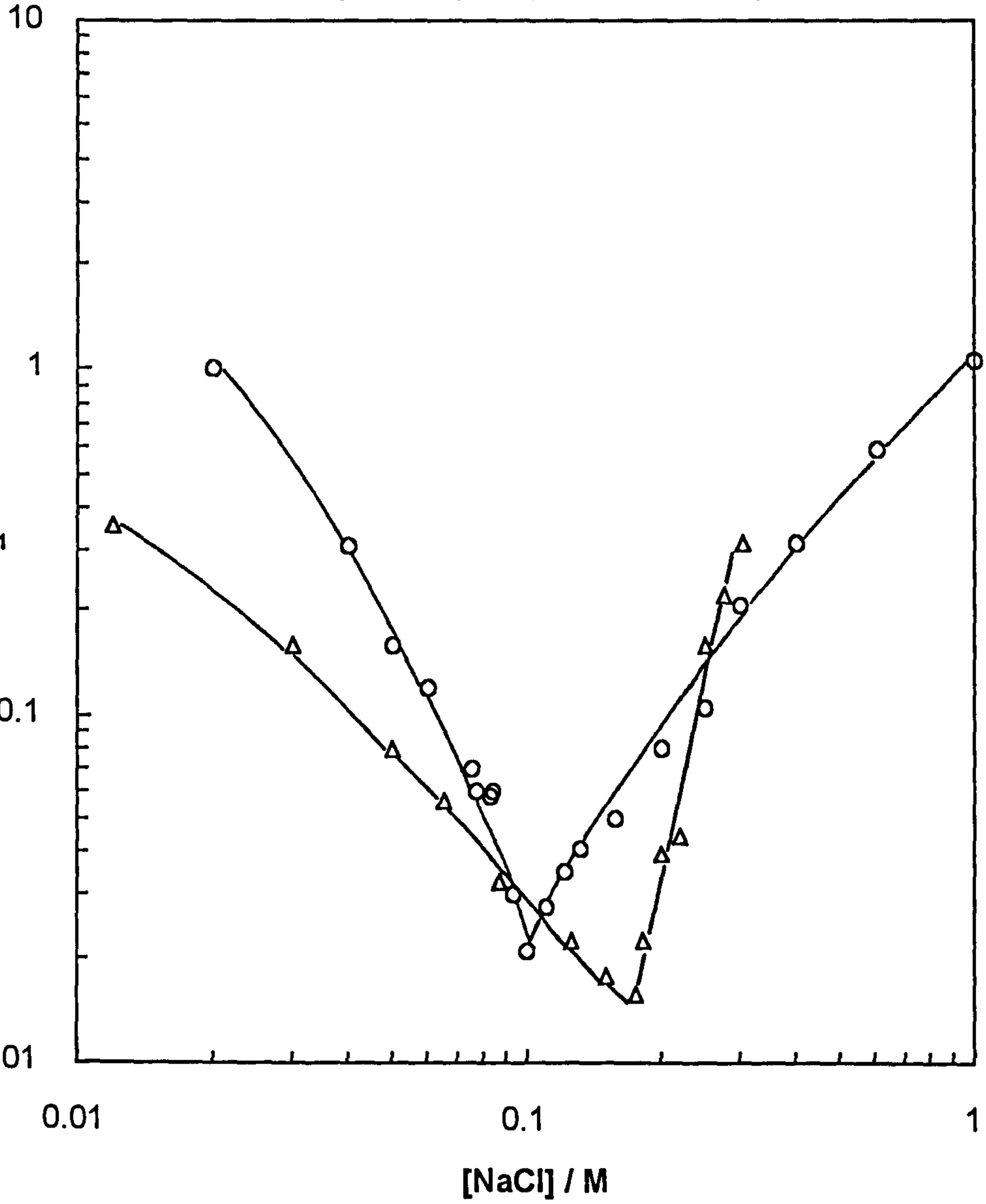

Figure 6.14

Interfacial tensions in the system 3 mM AOT in aqueous NaCl solutions plus 0.65 cS PDMS oil versus total sodium ion concentration at two temperatures

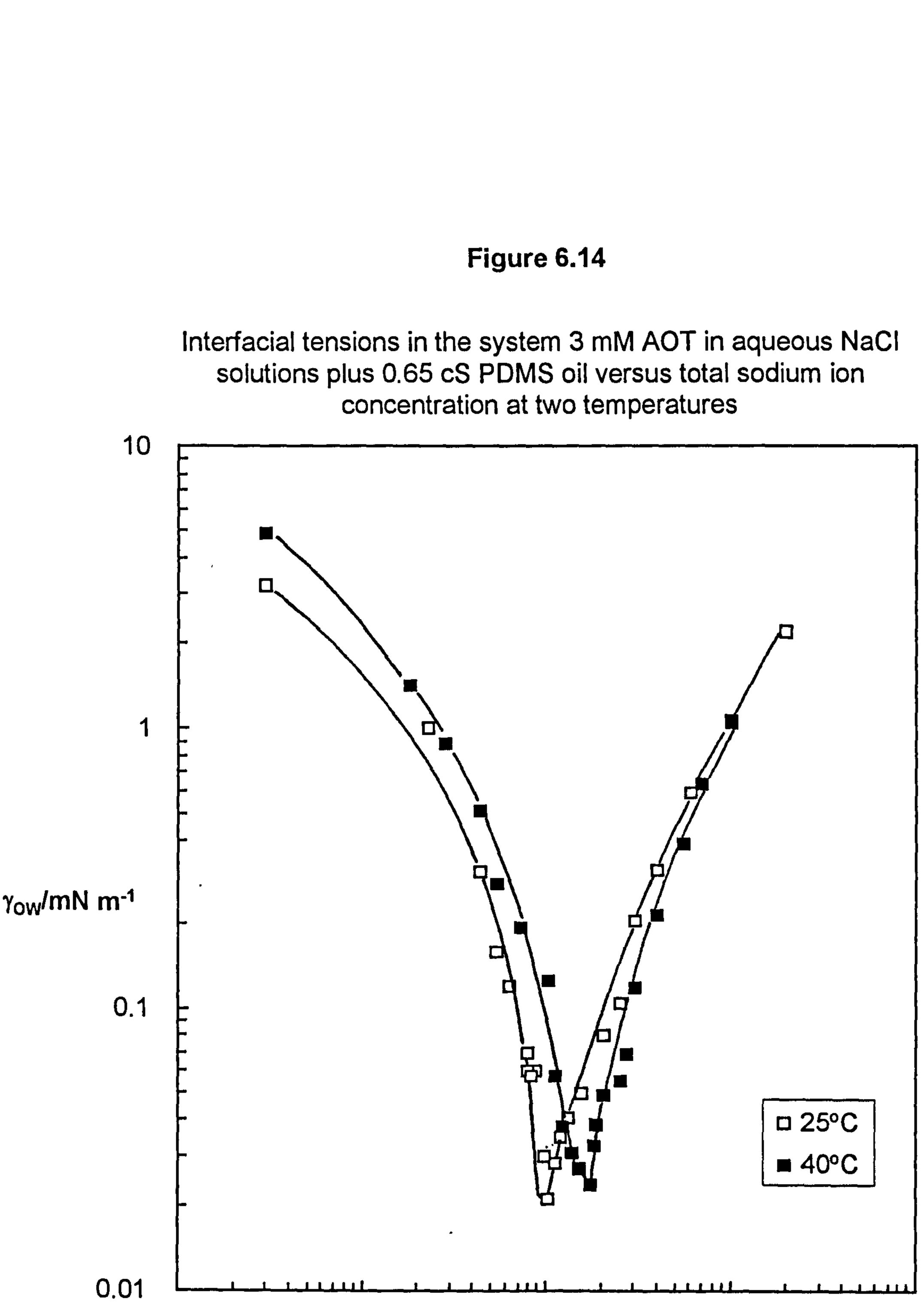

capacity of water in w/o microemulsions. In this model, two types of phase separation are considered, which are shown schematically in Figure 6.15. At the solubilisation boundary (S) where microemulsion droplets behave like hard spheres, the phase separation of the microemulsion into a microemulsion and an excess water phase is driven by the bending stress of a rigid surface. The solubilisation capacity of water is limited by the spontaneous curvature radius (R^o) of the surfactant film, and can be improved by increasing the molecular volume of the oil or decreasing the salinity. At the haze boundary (H), the phase instability (microemulsion separates into a droplet-lean and a droplet-rich phase) is induced by inter-droplet attractions. The uptake capacity of water, which depends on the critical droplet radius (R^c), can be increased by decreasing the molecular volume of oil or increasing the salinity. As a result, any variation has its limitation, and a cusp can be obtained when plotted together.

Similarly, at constant salt concentration, the solubilisation capacity of water in w/o microemulsions can be obtained as a function of temperature. The single-phase microemulsion region exists between an upper and a lower temperature phase boundary (UTPB, LTPB). Instability at the UTPB is driven by short-range attractive interactions[162] between the droplets due to a decline in surfactant/oil compatibility with increasing temperature. The LTPB corresponds to the solubilisation boundary.

6.3.2 Effect of electrolyte concentration in the dispersed aqueous phase

The solubilisation of aqueous NaCl into 0.65 cS PDMS oil solutions containing AOT is shown in Figure 6.16 as a function of dispersed phase salt

Figure 6.15

Schematic illustration of the effect of the variation of the molecular volume of oil and salinity on the radius of spontaneous curvature (R^o) and critical radius (R^c). The arrows point to the direction of the increase in the value of the variable

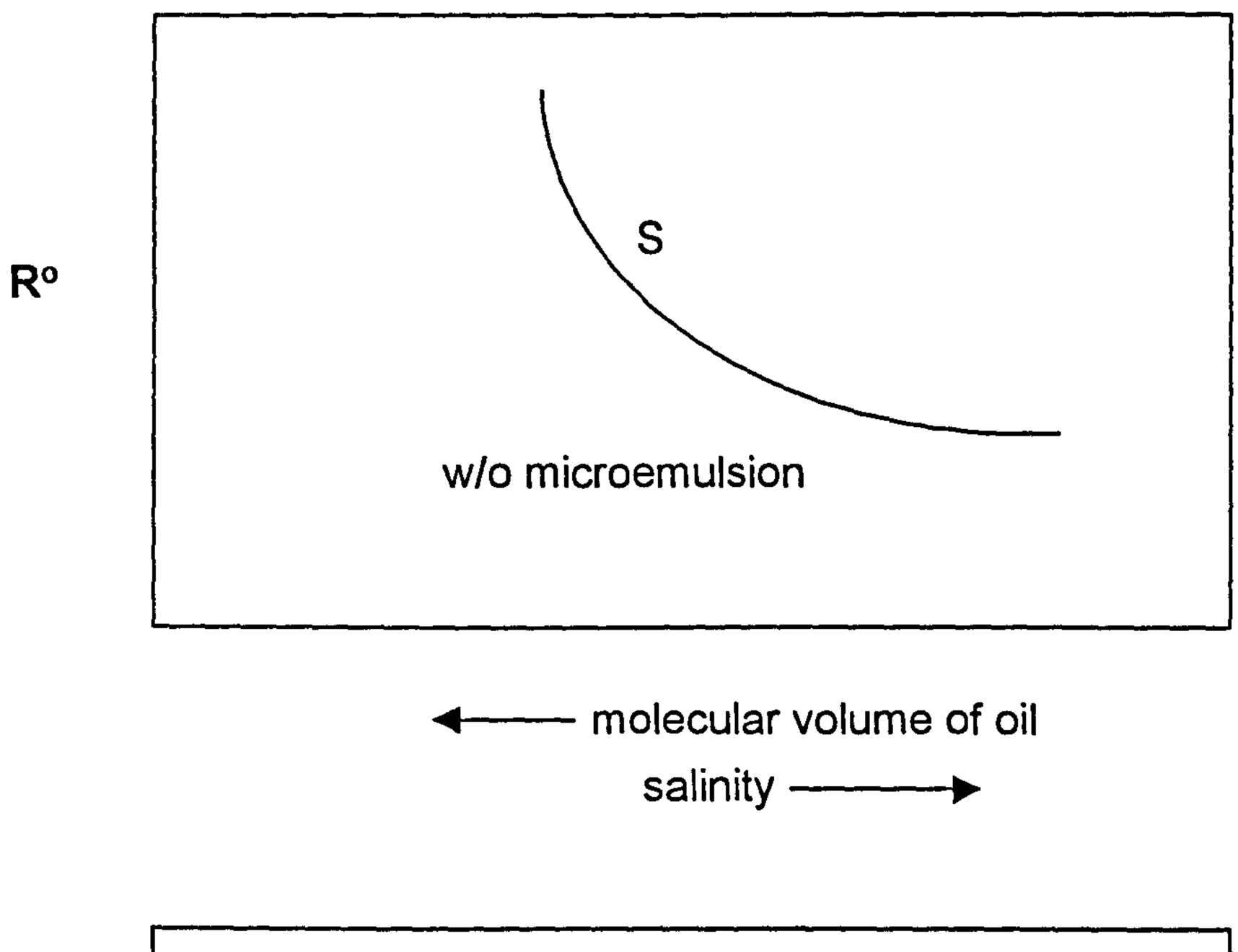

Figure 6.16

Effect of salt concentration on the uptake of water into 0.65 cS PDMS oil phases containing 40 mM AOT at two temperatures

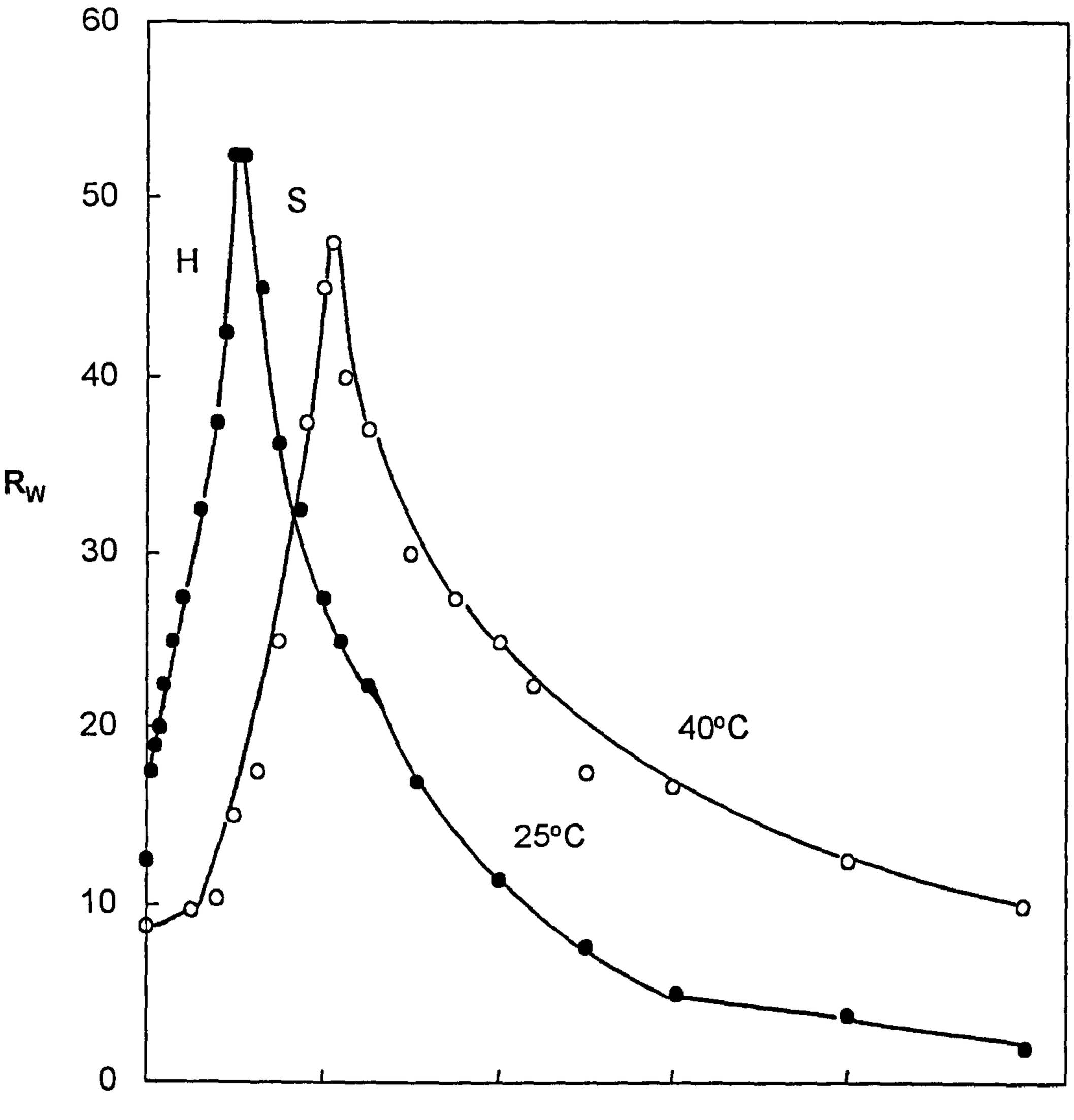

concentration in terms of the R_W value defined as $[H_2O]/[AOT]$. As expected, a maximum in R_W is attained as the electrolyte concentration is varied at fixed temperature. At the haze boundaries, two clear phases were observed while at the solubilisation boundaries, droplets of water were observed. An increase in temperature increases the salt concentration required to reach maximum solubilisation, which is close to that required to form Winsor III systems. This is because an increase in the temperature favours counter-ion dissociation, and so more salt is needed to achieve the preferred droplet curvature. The R_W values at the solubilisation boundary in the single phase microemulsions of Figure 6.16 may be compared with those in equilibrated oil phases in Winsor II systems shown in Figure 6.7 as seen in Figure 6.17a. In the former, the salt concentration refers to that in the dispersed water, $[NaCl]_{dw}$, (expressed as moles of NaCl per unit volume of water in the microemulsion) whereas in the latter the salt concentration is that of the conjugate aqueous phase, $[NaCl]_{aq}$. The two are related via the partition coefficient P of salt between dispersed and bulk water as[163]

$$P = \frac{[NaCl]_{dw}}{[NaCl]_{aq}} \qquad (6.3)$$

Values of P are shown in Figure 6.17b as a function of R_W i.e. droplet size. For small drops, the salt partitions heavily in favour of the excess aqueous phase (P=0.2) but as the drop size increases and discrete water pools appear as distinct from water of hydration around surfactant headgroups, the value of P increases until it approaches unity around R_W=50, where most of the water can be treated as behaving like bulk.

Figure 6.17

(a) Variation of water solubilisation with salt concentration in oil phases of Winsor II systems and Winsor IV systems for aqueous NaCl+0.65 cS PDMS+AOT at 25°C

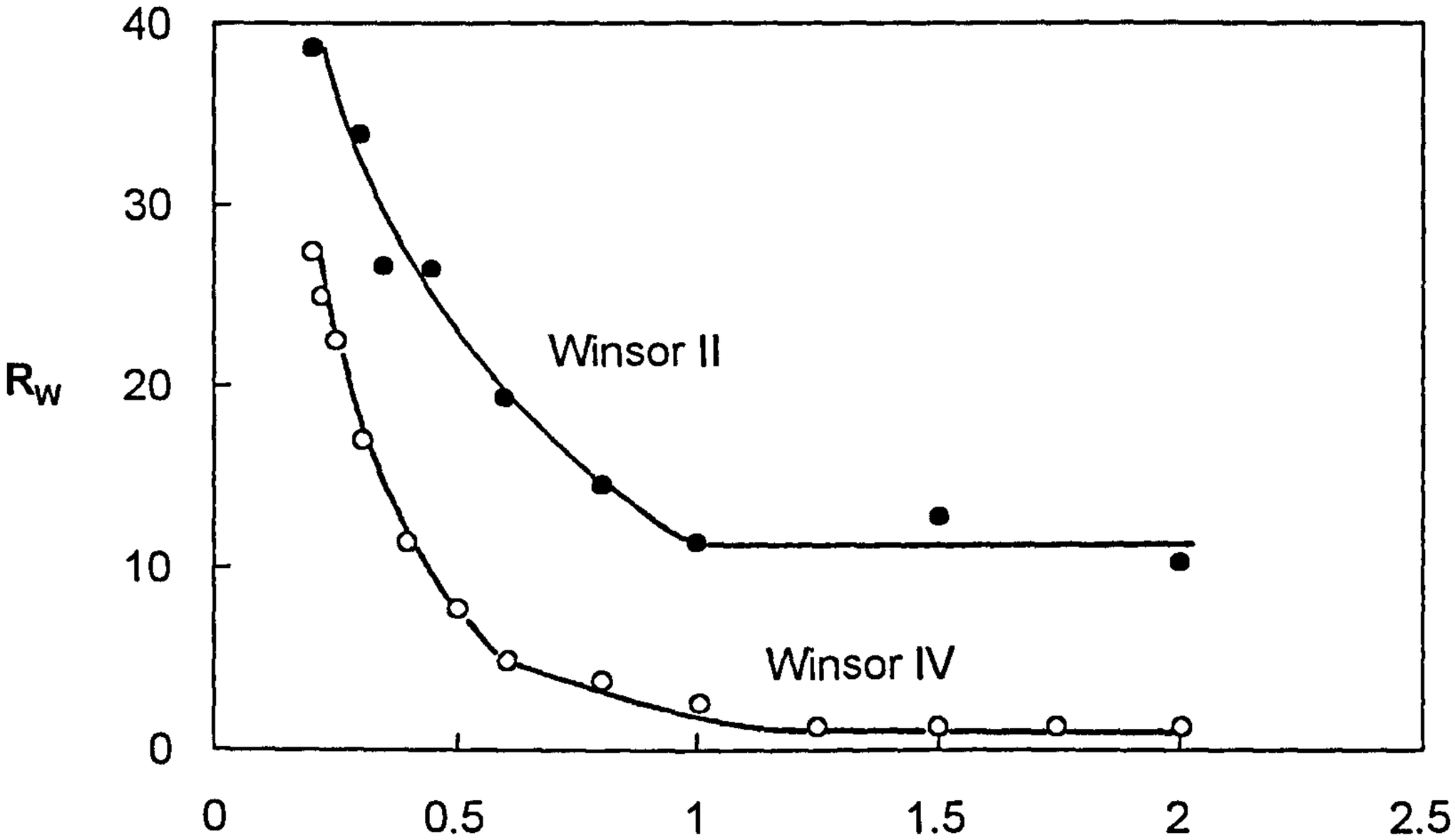

(b) Partition coefficient of salt versus R_W value in Winsor II systems for AOT+aqueous NaCl+0.65 cS PDMS oil at 25°C

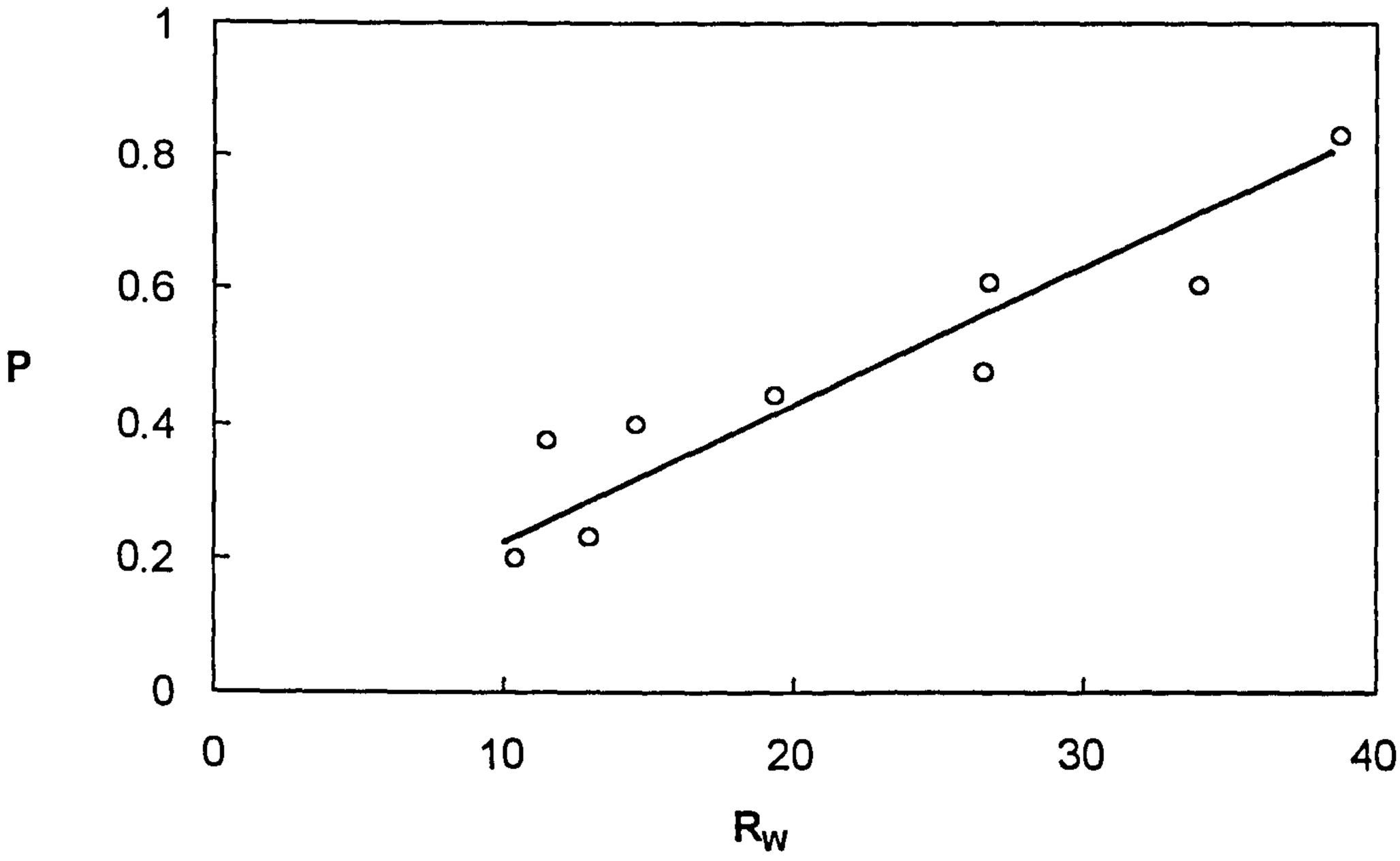

6.3.3 *Effect of temperature*

Figure 6.18 shows the variation of the solubilisation of water with temperature at various salt concentrations. The lower phase boundary, not measurable in the case without salt, is the solubilisation one at which a w/o microemulsion exists with an excess water phase, whilst the upper boundary, driven by attractive interactions between the drops, is the haze one. The temperature around maximum solubilisation is close to the phase inversion temperature (PIT) in multiphase systems, and increases with salt concentration due to increased counter-ion dissociation around headgroups. Reassuringly, phase inversion is around 25°C in 0.1 M NaCl systems as detailed earlier. At the haze boundary, two clear phases separate quickly. In water-in-decane microemulsions of AOT at 44°C, it was demonstrated that the two phases are both w/o microemulsions of the same droplet size differing only in the number density of the droplets.[161] We have studied the separation at various R_W values above the haze boundary at 35°C with PDMS oil using pure water as the dispersed phase (indicated by the dotted line in Figure 6.18). The appearance of the phase separation and the relative volume of each phase are shown in Figure 6.19. The phase separation starts from R_W = 10, which is in agreement with the haze boundary in Figure 6.18. All the upper phases are clear and the AOT and water concentration were found to be negligible. The lower phases are isotropic at low R_W and become bireferengent when R_W exceeds 40, indicating the formation of liquid crystalline phases. Therefore, we can conclude that for 0.65 cS PDMS oil, the two phases above the haze boundary are a pure oil phase and a surfactant-rich phase which solubilises all the water and some oil. The

Figure 6.18

Effect of temperature on the uptake of water into 0.65 cS PDMS oil phases containing 40 mM AOT at three salt concentrations

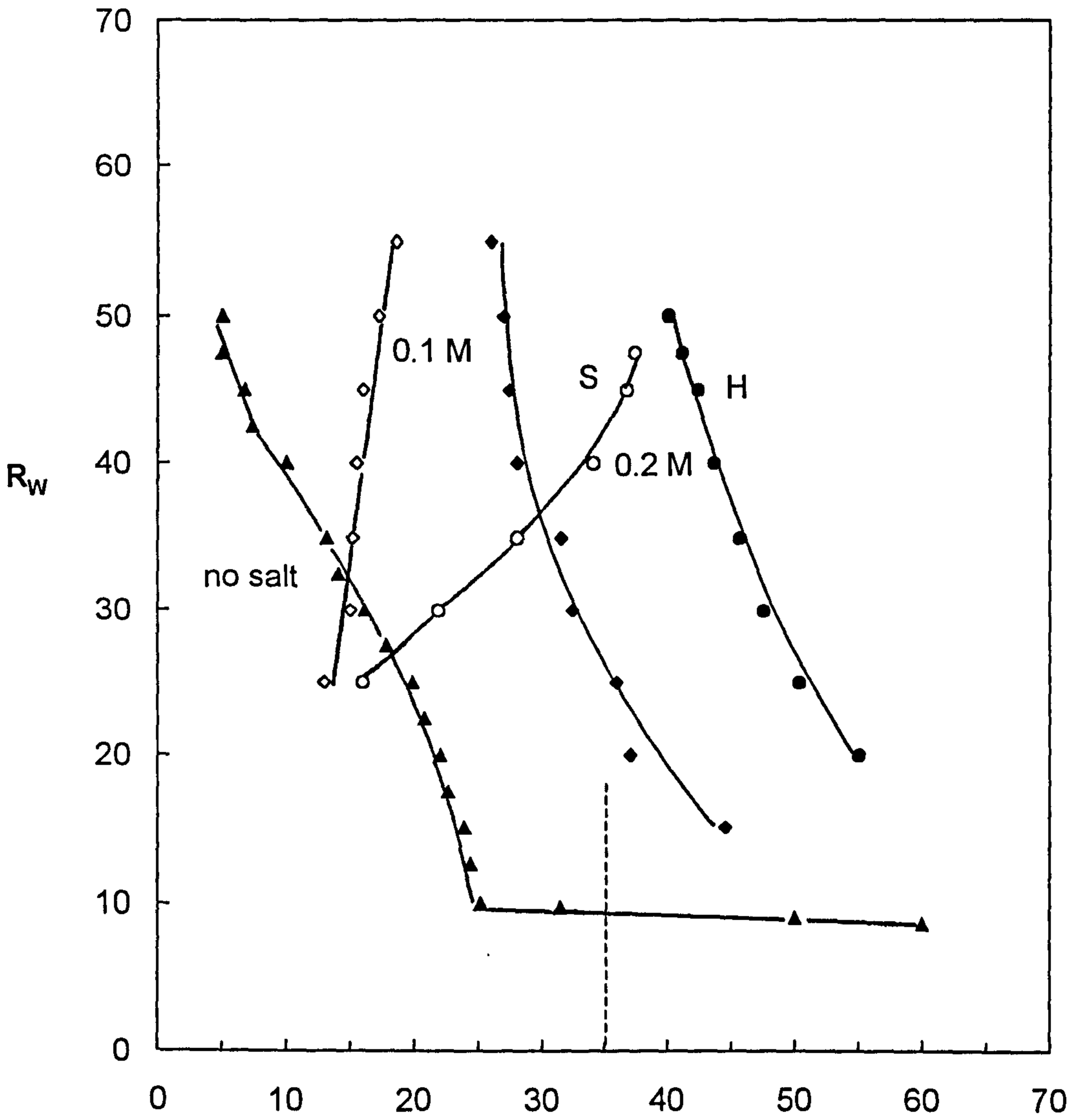

Figure 6.19

Phase separation above the haze boundary for w/o microemulsions without salt at 35°C

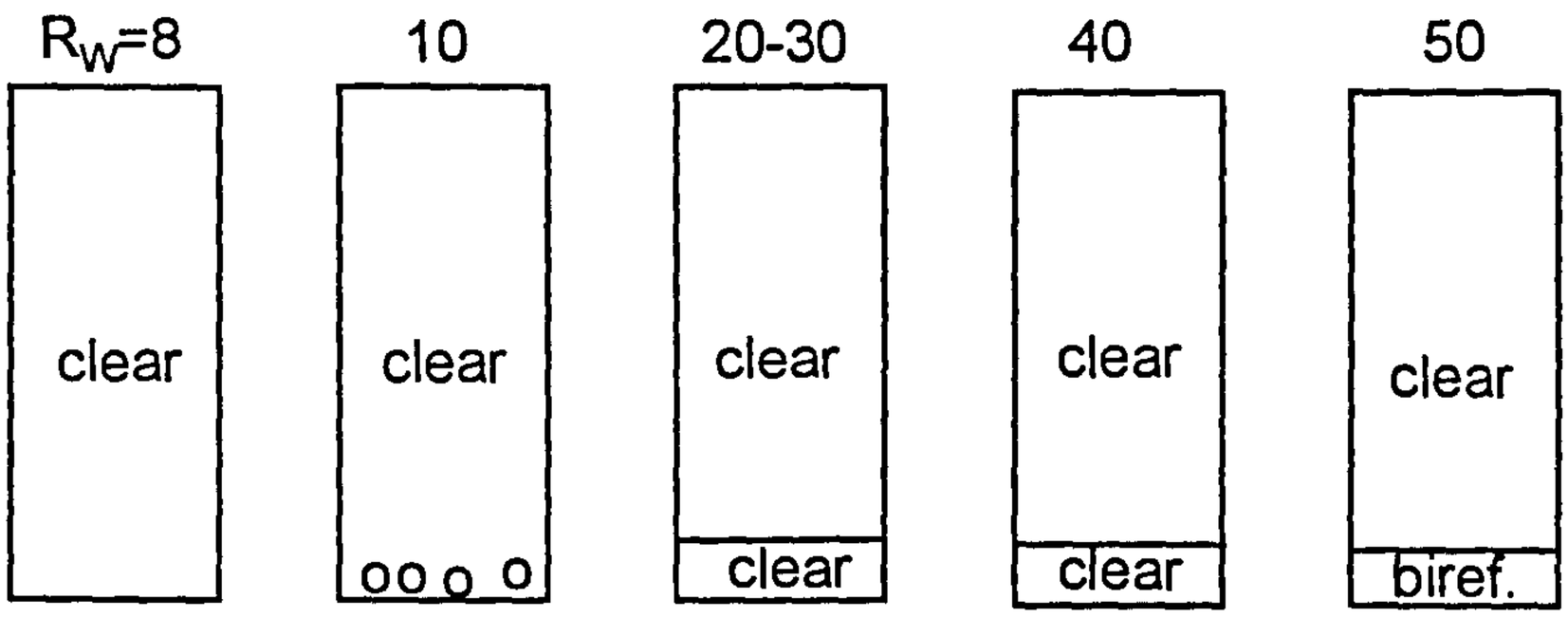

surfactant-rich phase is not necessarily a w/o microemulsion; it may be a lamella or bicontinuous phase. Frank and Zografi[164] discussed similar findings for long chain alkane systems.

6.4 Oil-in-water microemulsion single phase systems

6.4.1 Effect of electrolyte concentration

The precise uptake of oil into aqueous aggregates is best studied via turbidity titrations using single phase microemulsions. At fixed surfactant concentration, we have measured the solubilisation of 0.65 cS PDMS oil as a function of salt concentration and temperature. Figure 6.20 shows the uptake of oil into 3 mM AOT solutions versus salt concentration at 25°C in terms of the R_o value defined as [PDMS]/[AOT]. To the left of the full curve, two phases separate consisting of an aqueous phase containing AOT and oil as an oil-in-water microemulsion and a pure oil phase. This occurs at the solubilisation boundary (S) and is equivalent to the separation in Winsor I systems. The maximum solubilisation of oil occurs around 0.1 M NaCl which corresponds to the salt concentration at the oil-water interfacial tension minimum. Above 0.11 M NaCl, phase separation also occurs at lower R_o values on increasing [NaCl] to give a clear, upper aqueous phase of volume fraction >0.8 and a viscous, bluish lower aqueous phase of low volume fraction. This boundary is denoted the cloud boundary (C) and we have taken it for R_o values above which two phases separate to give a liquid-liquid interface within a few hours following cessation of the stirrer. The phase sequence occurring between the solubilisation and cloud boundaries is more complicated. From 0 to 0.02 M NaCl, aqueous AOT solutions are clear in the

Figure 6.20

Effect of salt concentration on the uptake of 0.65 cS PDMS oil at 25°C into 3 mM AOT aqueous solutions. Open circles are at the solubilisation and cloud boundaries, filled circles are the oil needed to clarify the aqueous phase

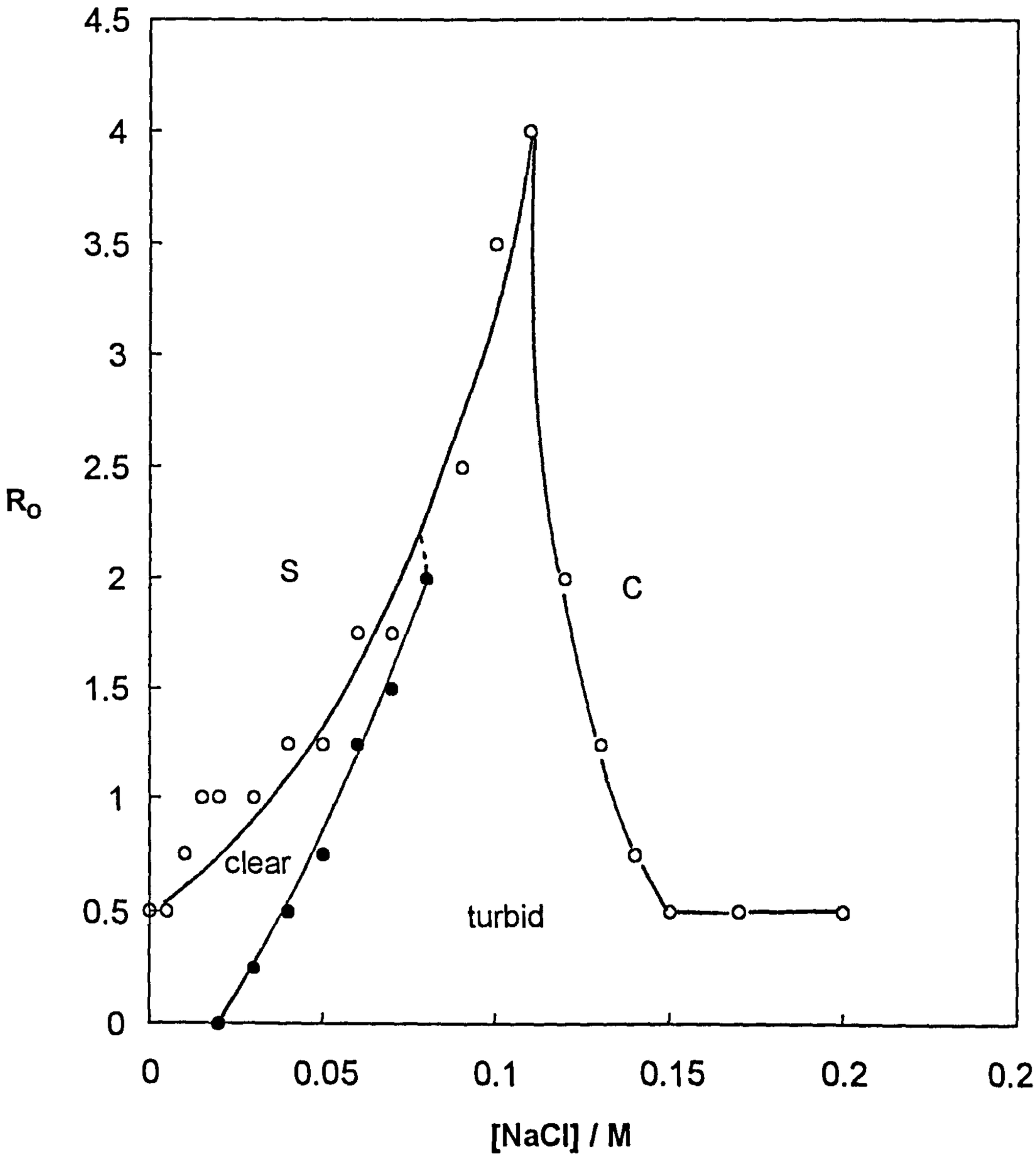

absence of oil. The phase is micellar and denoted L_1. PDMS can be solubilised in the micellar solution until the solubilisation boundary is reached. Between 0.02 and 0.075 M NaCl, the turbid AOT solutions in the absence of oil (due to the coexistence of a vesicle phase L_α with micelles) are cleared following oil solubilisation and microemulsion formation. The filled points indicate the amount of oil needed to clarify the surfactant solutions. Beyond 0.08 M NaCl, the addition of oil does not clear the solutions which remain turbid without any visible phase separation for over one week. The oil is probably solubilised in the lamellar phase as was observed by Gosh and Miller[150] in aqueous AOT solutions containing dodecane.

In order to understand the nature of the phase separation and identify each phase, mixtures were allowed to separate at R_o values equal to 0.25 above the cloud boundary at each salt concentration (0.12-0.20 M) and the coexisting phases were analysed for surfactant. Figure 6.21 (a) and (b) show the appearance of the phase separation and volume of each phase at equilibrium. Upon increasing [NaCl], the volume of the lower phase falls from 0.14 to 0.02 and it contains a high concentration of surfactant which solubilises all of the oil and some water. The concentration of AOT in the upper phases was found to be very close the cmc's given in Figure 6.6. Thus phase separation leads to an aqueous surfactant-rich phase coexisting with an aqueous phase containing monomeric surfactant. This is analogous to the two water-continuous phases, one rich and one lean in micelles, which separate above the cloud point in nonionic surfactant solutions.[126]

Figure 6.21

(a) correlation of R_o and phase separation at the cloud boundary for o/w microemulsions with salt concentration at 25°C

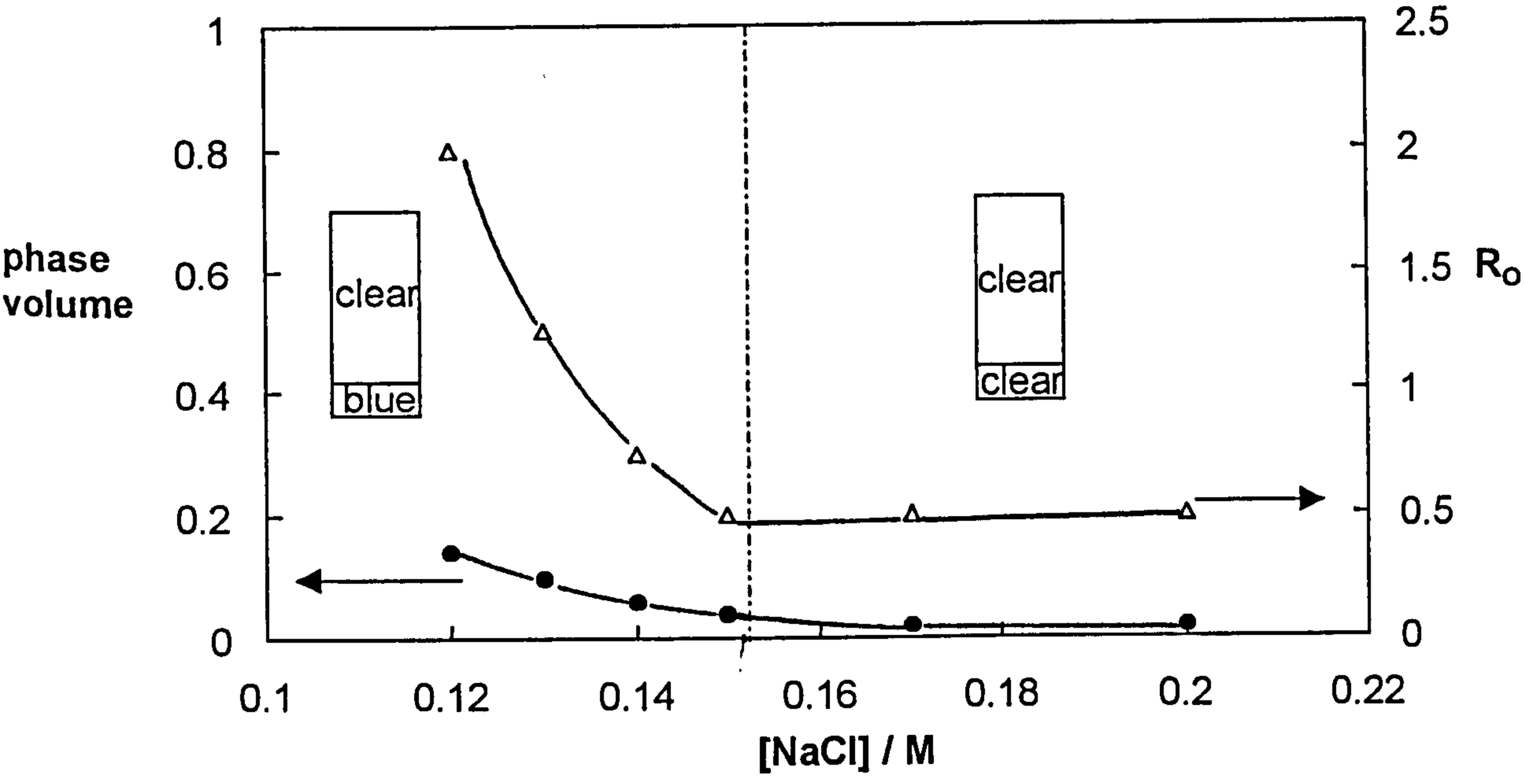

(b) Concentration of AOT in the upper phase versus [NaCl] for above systems (circles). Triangles are cac of AOT in the presence of heptane from ref. 149

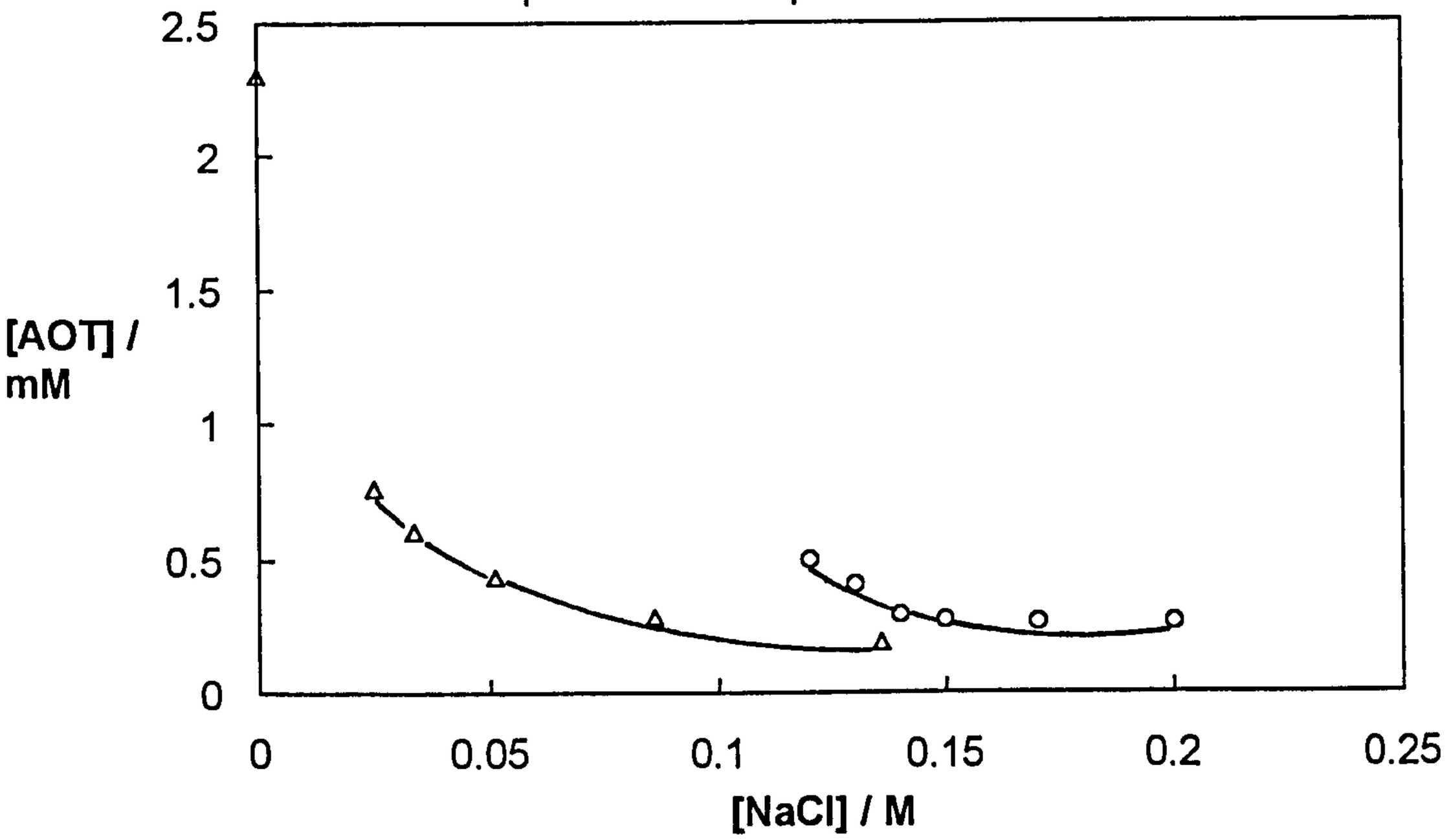

6.4.2 *Effect of temperature*

The maximum solubilisation of oil in o/w microemulsions as a function of temperature at three electrolyte concentrations is shown in Figure 6.22. In which 40 mM AOT was employed as the continuous phase, and 0.65 cS PDMS oil as the dispersed phase. The upper phase boundary is the solubilisation one whilst the lower one is the cloud boundary. This arises since with ionic surfactants like AOT, an increase in temperature drives the system from Winsor II (w/o) to Winsor I (o/w), the opposite sense to salt concentration. The single phase region between the two boundaries is shifted to higher R_o values and higher temperatures as the salt concentration increases. At 37°C and in 0.09 M NaCl, over 6 moles of PDMS oils per mole of AOT can be solubilised. The decreased solubilisation capacity with increasing temperature is most likely linked to the dissociation of the surfactant headgroups which, being an endothermic process, increases with temperature resulting in increased electrostatic repulsion between the headgroups and thus a higher monolayer curvature. Low or near zero degrees of dissociation of AOT in hydrocarbon-in-water microemulsions near the phase inversion condition have been measured recently via conductivity, emf and small angle light scattering measurements.[165] In comparison with Figure 6.20, the variation of R_o at the solubilisation boundary with [NaCl] at higher temperatures is plotted in Figure 6.23. Clearly, the trend is similar to the solubilisation boundary in Figure 6.20. The solubilisation capacity is higher in 40 mM AOT than that in 3 mM AOT aqueous solutions. This apparent dependence of solubilisation capacity on surfactant concentration is because of the counter-ion dissociation of the surfactant. In other words,

Figure 6.22

Effect of temperature on the uptake of 0.65 cS PDMS oil into 40 mM AOT aqueous solutions. Open points mean lower boundaries, filled points mean upper boundaries

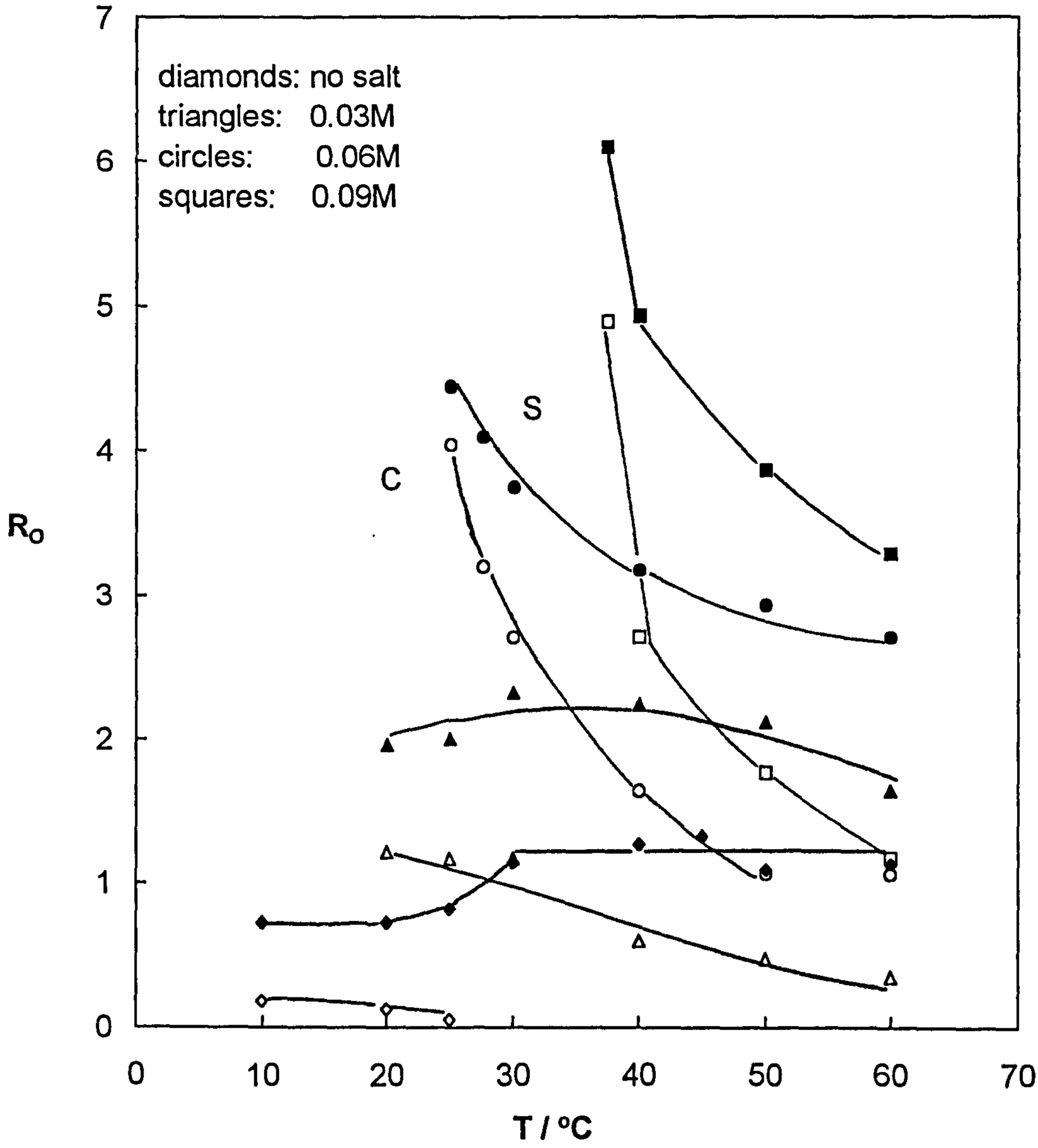

Figure 6.23

Maximum uptake of 0.65 cS PDMS oil into 40 mM AOT aqueous solutions versus [salt] for three temperatures

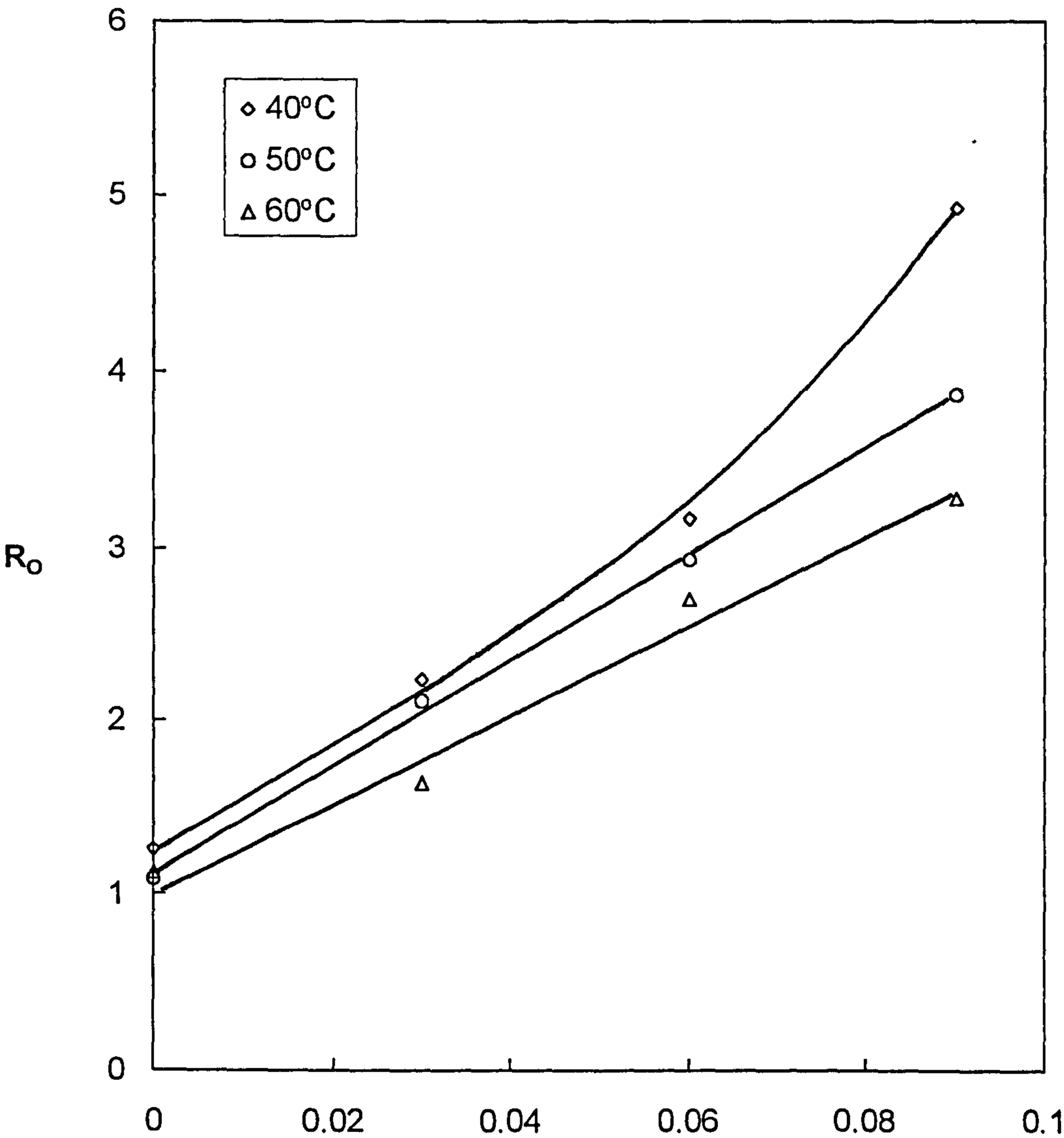

the total sodium ion concentration in the system should be considered rather than just the added salt concentration. Fletcher[166] defined the parameter α to describe this relationship:

$$[NaCl]_{aq} = [NaCl]_{aq}([AOT] \rightarrow 0) + \alpha[AOT]_{aq} \qquad (6.4)$$

where $[NaCl]_{aq}([AOT] \rightarrow 0)$ is the salt concentration in the limit of zero AOT concentration which is the actual system salinity, and α is the proportionality constant (dependent on R_o). The subscript aq indicates that the concentration is expressed per unit volume of water in the microemulsion as opposed to the total volume. The physical meaning of α is that it can be related with the degree of dissociation and is a parameter reflecting the inter-particle interactions which cause the shifts in phase boundary as the AOT concentration is changed.

6.5 Conclusions

The above results allow us to draw the following conclusions for the equilibrium phase behaviour of silicone oils, water and anionic surfactant AOT mixtures.

(a) For the 0.65 cS oil (hexamethyldisiloxane)

(i) At 25°C the progression of Winsor systems I-III-II can be effected by an increase in [NaCl]. Aggregated AOT transfers from water to oil between 0.12 and 0.20 M NaCl, akin to dodecane as oil. Monomeric AOT resides exclusively in aqueous phases in multiphase systems. The third phases contain mainly surfactant and water and are probably of the L_3 type.

Increasing the temperature requires higher [NaCl] to obtain the Winsor phase transition.

(ii) The uptake of oil into aqueous AOT solutions forming single phase o/w microemulsions has been determined as a function of [NaCl] and temperature. The nature of the phases separating at the phase boundaries has been established. Solubilisation of water into AOT solutions in oil forming w/o microemulsions has also been measured for various [NaCl] and at various temperatures. The partitioning of salt between dispersed and excess water phases is in favour of the latter for small drops but becomes more nearly equal with increasing drop size.

(iii) The planar PDMS-water interfacial tension passes through a low minimum (0.02 mN m^{-1}) around salt concentrations where three phases form.

(b) For the higher molecular weight PDMS oils

(i) Three phase systems formed at equilibrium occur at higher [NaCl] with an increase in the molecular weight of the oil. In addition, the extent of the Winsor III region with respect to salt concentration increases markedly from 0.12 M for 0.65 cS to 1.15 M for 50 cS.

(ii) The equilibrium phase behaviour does not vary significantly between 5 and 50 cS PDMS oils. More than 98% of surfactant transfers to the middle phase at intermediate salt concentration, but there is precipitation of AOT in excess of the cmc in the water phase at high salt concentration. Thus transfer of surfactant to the oil phase was not observed.

(iii) The minimum interfacial tension increases by nearly two orders of magnitude in this series, corresponding to the progressive increase of the Winsor III salt concentration range.

CHAPTER SEVEN

CHAPTER 7

Stability of Emulsions Prepared from Equilibrium Winsor Systems

7.1 Introduction

Macroemulsions composed of drops in the micron-size range are not thermodynamically stable and there are various sources of instability leading to ultimate phase separation.[26] Creaming or sedimentation of drops can occur (depending on density differences) and is enhanced by flocculation. For coalescence to occur, the thinning film between two approaching drops must reach a critical rupture thickness. Emulsion type and stability is known to be associated with the equilibrium phase behaviour in surfactant+oil+water systems.[28, 92] The hydrophile-lipophile balance (HLB) of the system (as opposed to the empirical HLB number of the surfactant) is related to the locus of aggregate formation. High HLB systems are those in which o/w microemulsion droplets (or swollen aqueous micelles) form, i.e. Winsor I systems. Low HLB systems are Winsor II systems where a w/o microemulsion (or swollen reverse micelle) coexists with excess water devoid of aggregates. As described earlier, it is frequently observed that the types of emulsions (o/w, w/o or intermediate type) formed by the homogenisation of the equilibrium Winsor systems are the same as those of the equilibrium microemulsions, e.g. emulsification of an o/w microemulsion plus excess oil (Winsor I) generally gives an o/w emulsion, the continuous

phase of which is itself an o/w microemulsion. Both Petsev *et al.*[167] and Kabalnov and Wennerström[37] have advanced arguments, supported experimentally, based on interfacial bending in order to explain the correspondence between emulsion and microemulsion types.

The effects of system HLB on emulsion stability in the region of the Winsor I/III and III/II boundaries appear to be system dependent. Baldauf *et al.*[168] reported that in 2-phase regions the rate of creaming or sedimentation decreased (stability increased) as the Winsor I/III and II/III boundaries were approached whereas the coalescence rates followed the opposite trend. In contrast, Anton and Salager[169] found that stabilities with respect to both creaming/sedimentation and coalescence fell as the 3-phase boundaries were approached from the 2-phase regions. In both studies however, very low stabilities were encountered in the Winsor III region. Hazlett and Schechter[170] studied the emulsion stability through the Winsor phase regions by varying the butanol cosurfactant concentration in the system of toluene, aqueous NaCl and a single chain surfactant (sodium dodecyl sulphate). It was found that the stability to coalescence was low in the triphasic region but rose sharply at both the Winsor III/I and III/II boundaries. Stability in the Winsor II region at higher butanol concentration was then found to fall off. The emulsion stability with the respect to salt concentration (through the Winsor progression) has been investigated in AOT/nonane/aqueous systems by Aveyard *et al.*[171] previously. It was found that in the Winsor I region, a distinct maximum in stability exists with respect to creaming, with instability rising towards the Winsor I/III boundary. In the Winsor II region, the sedimentation is relatively rapid and virtually independent of salt

concentration. In the triphasic Winsor III region, the emulsion is very unstable while the surfactant-rich phase remains highly conducting. There exists an obvious contrast of the emulsion stability near the Winsor I/III and II/III boundaries in systems with and without cosurfactant.

In this chapter, we investigate the long term stability or breakdown of the silicone oil emulsions formed from the Winsor I, III and II equilibrium systems, with the objective of understanding the influence of the curvature properties of the surfactant monolayer, brought about by changes in electrolyte concentration, on these. The system chosen is AOT+0.65 cS PDMS oil+water as a function of electrolyte due to the fact that salt alone can transfer the surfactant from the aqueous phase to the oil phase. In these systems we follow the appearance of separated layers of both the continuous phase and the disperse phase as mentioned earlier. The emulsion phase inversion with higher molecular weight PDMS oils is examined with respect to salt concentration and related to the Winsor phase behaviour and oil-water interfacial tensions.

7.2 Correlation between Winsor phase behaviour, emulsion type and o-w interfacial tensions

Based on the principle that an o/w emulsion conducts and a w/o does not, emulsion conductivity has been used to determine emulsion type.[28, 92] The filled points in Figure 7.1 refer to the conductivity of emulsions in water-0.65 cS PDMS-AOT systems. Below 0.1 M NaCl, the equilibrium phase systems are Winsor I and the conductivity of the emulsions observed here is high indicating the formation of o/w emulsions which are white and highly

Figure 7.1

Variation of the emulsion conductivity (40 mM AOT) and interfacial tension (3 mM AOT) with salt concentration for 0.65 cS PDMS systems

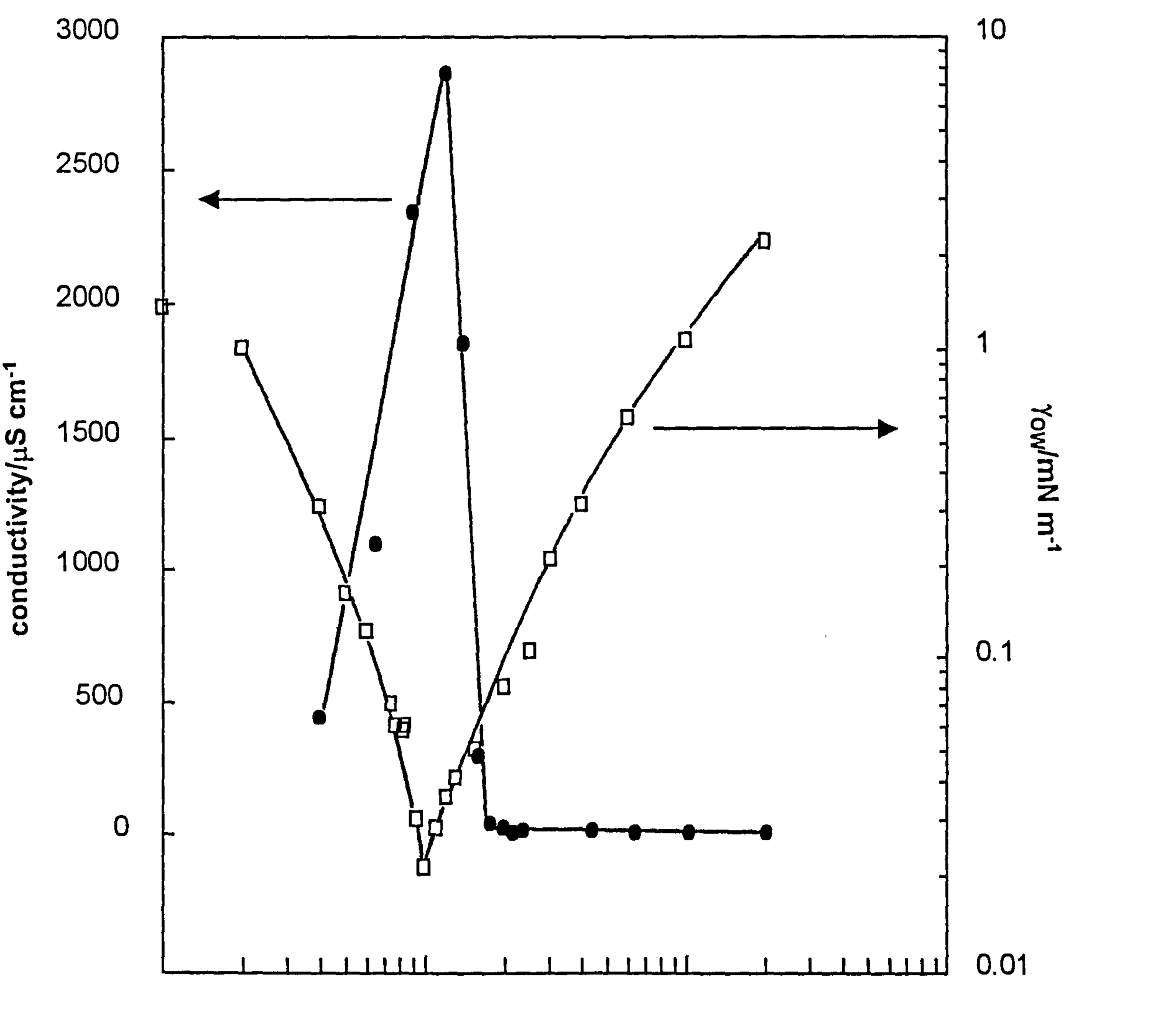

foaming. Above 0.2 M salt, the emulsions become non-conducting corresponding to w/o emulsions. At intermediate salt concentrations, the emulsions are very unstable and we see a clear inversion of the emulsion type around this region. It can be observed in Figure 7.1 that the onset of inversion from high to low conductivity emulsions occurs at the Winsor I/III boundary, indicating the continuous phase becomes less conducting. This is different from the case of alkane emulsions where the onset of inversion happened at the Winsor II/III boundary.[172] Also shown in Figure 7.1 is the oil-water interfacial tension between 0.65 cS PDMS oil and the aqueous phase. Reassuringly, a minimum in tension occurred around the conditions of emulsion phase inversion, demonstrating the correlation between the emulsion and microemulsion in silicone oil systems.

7.3 Effects of salt concentration of the stability of emulsions

In our experiments the time taken for varying amounts of clear phase (either oil or water) to separate was used as a measure of emulsion stability. Figure 7.2 summarises the overall picture regarding the breakdown of the emulsions in 2-phase systems prepared from equal volumes of oil and water. The volumes of both the oil and the aqueous phases separating as a function of time were recorded and plotted separately. Such plots can clearly distinguish between creaming and coalescence. We have also measured the drop-size distribution of selected emulsions in different Winsor regions. We suppose that three different phenomena might be responsible for the stability of the emulsions, depending on the salt concentration- creaming,

Figure 7.2

Sequence of visual changes in Winsor I and II systems for emulsions: 40mM AOT in 0.65 cS PDMS oil plus equal volume of aqueous NaCl at 25°C

Winsor I region

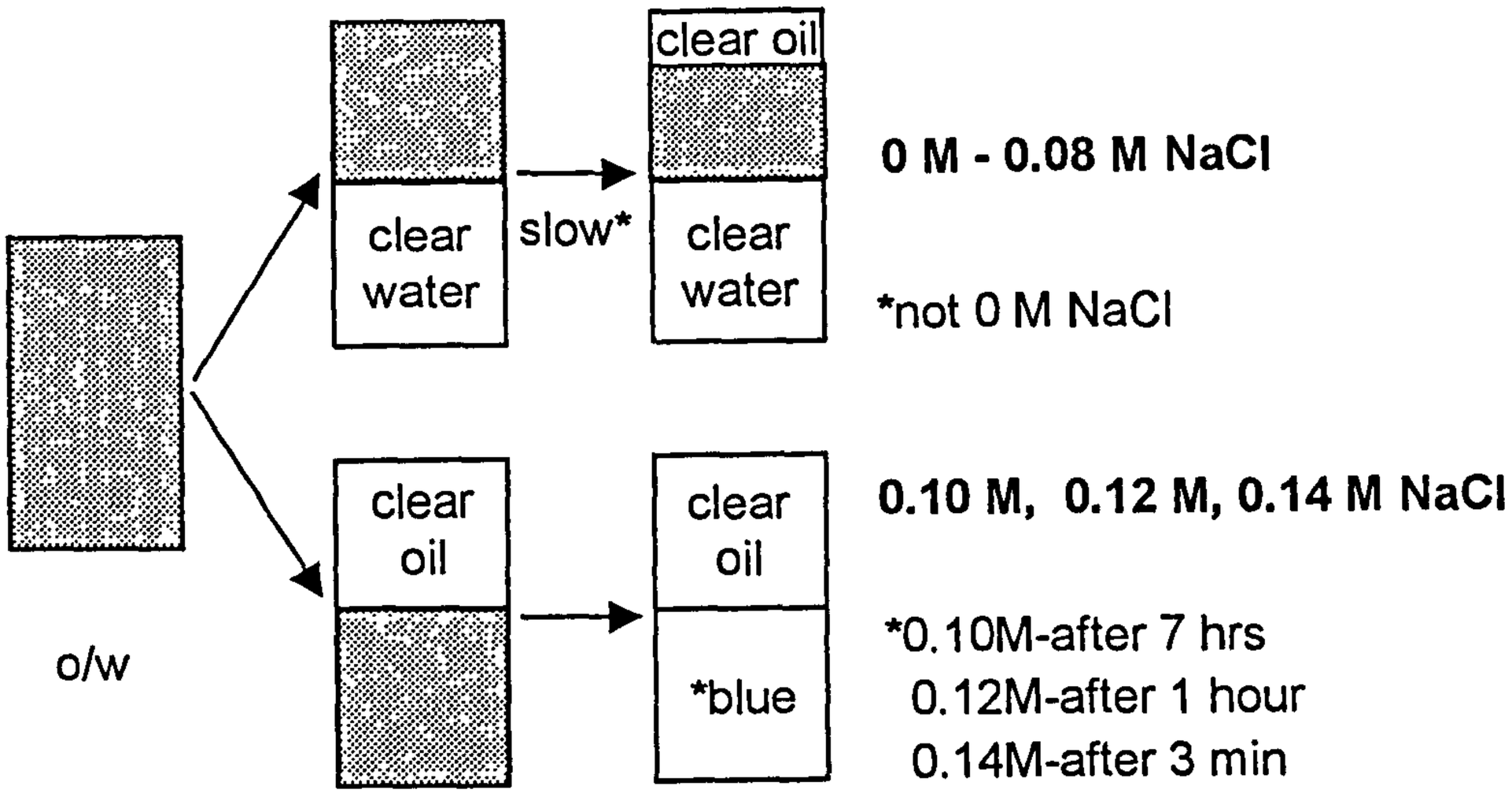

Winsor II region

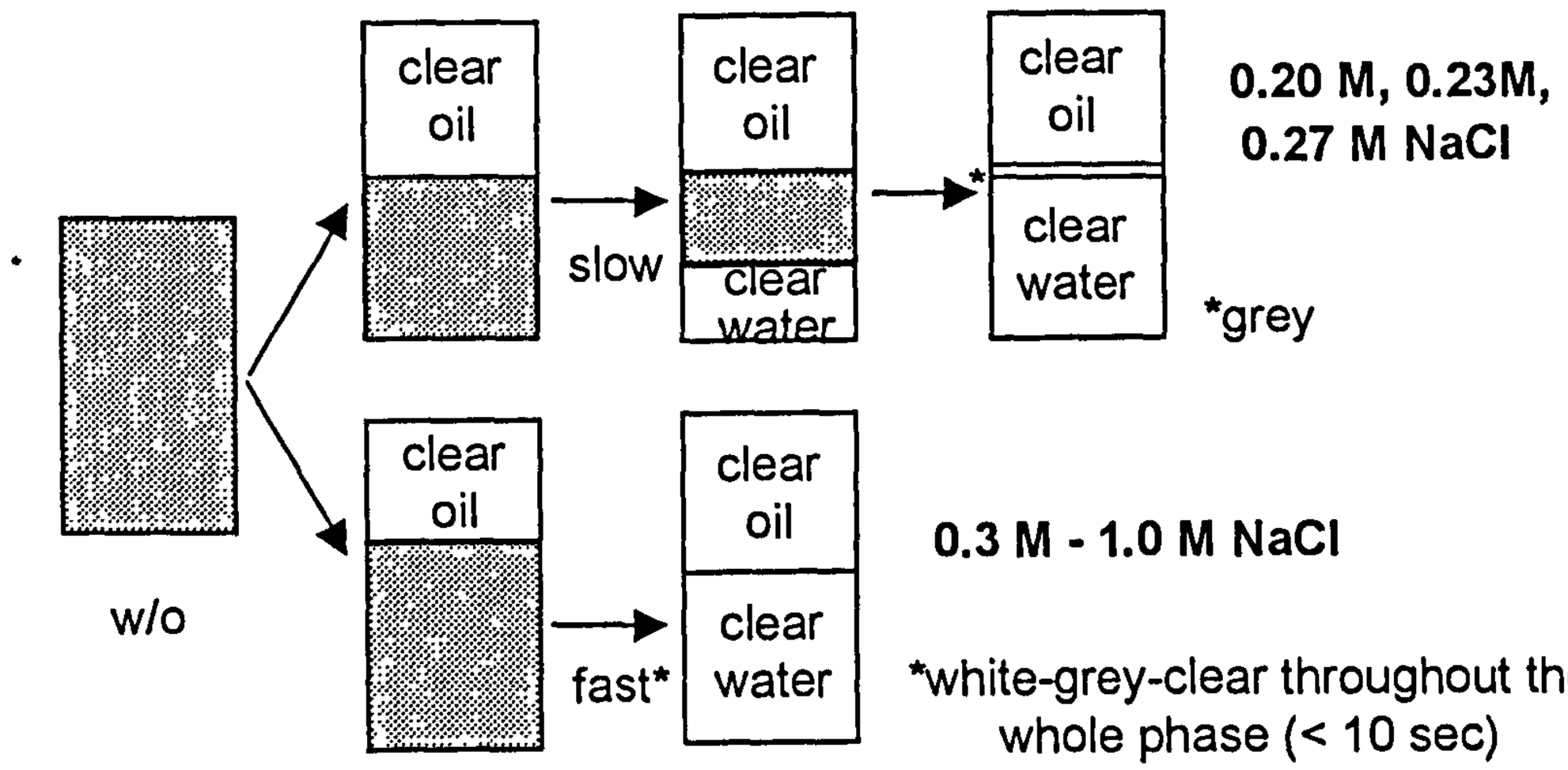

white emulsion

coalescence and Ostwald ripening. It should be noted that droplet flocculation is expected to affect each of the processes.

7.3.1 Stability of o/w emulsions in Winsor I systems

The effect of salt concentration on the stability of the 0.65 cS PDMS oil emulsion systems has been examined at 40 mM AOT. In the Winsor I region, two types of behaviour are seen: creaming and coalescence. Up to 0.08 M NaCl the emulsions were very foamy and no separation of oil was observed within 10 days. However, rapid creaming was apparent which was found to be dependent on salt concentration (Figure 7.3). The creaming rate passes through a minimum in the range 0.04 to 0.06 M NaCl. Coalescence is induced by rupture of the thin film between two droplets that are close to each other. For this to occur, the droplets must be either aggregated or packed in the cream layer. In Figure 7.3 it is shown that the coalescence is initiated once the creamed emulsion becomes concentrated enough when [salt] is below 0.10 M, i.e. after about 85% of continuous water phase separates and increases with increasing salt concentration. The volume fraction of oil in the cream as coalescence commences is around 0.83 which is above that for hexagonal close packing of monodisperse spheres (0.74). This high value is a result of both the polydispersity in drop size and the deformability of the drops allowing enhanced packing. The induction time for the formation of a clear oil layer is at least 200 hours. From Figure 7.4 it can be seen that approaching the Winsor I/III boundary, the non-foamy emulsions for 0.1 M to 0.14 M NaCl coalesce very fast in less than 10 minutes with the lower phase losing its white intensity throughout this time

Figure 7.3

Water (creaming) and oil (coalescence) phase resolution varies with time for different [NaCl] for o/w emulsions formed in Winsor I region at 25°C

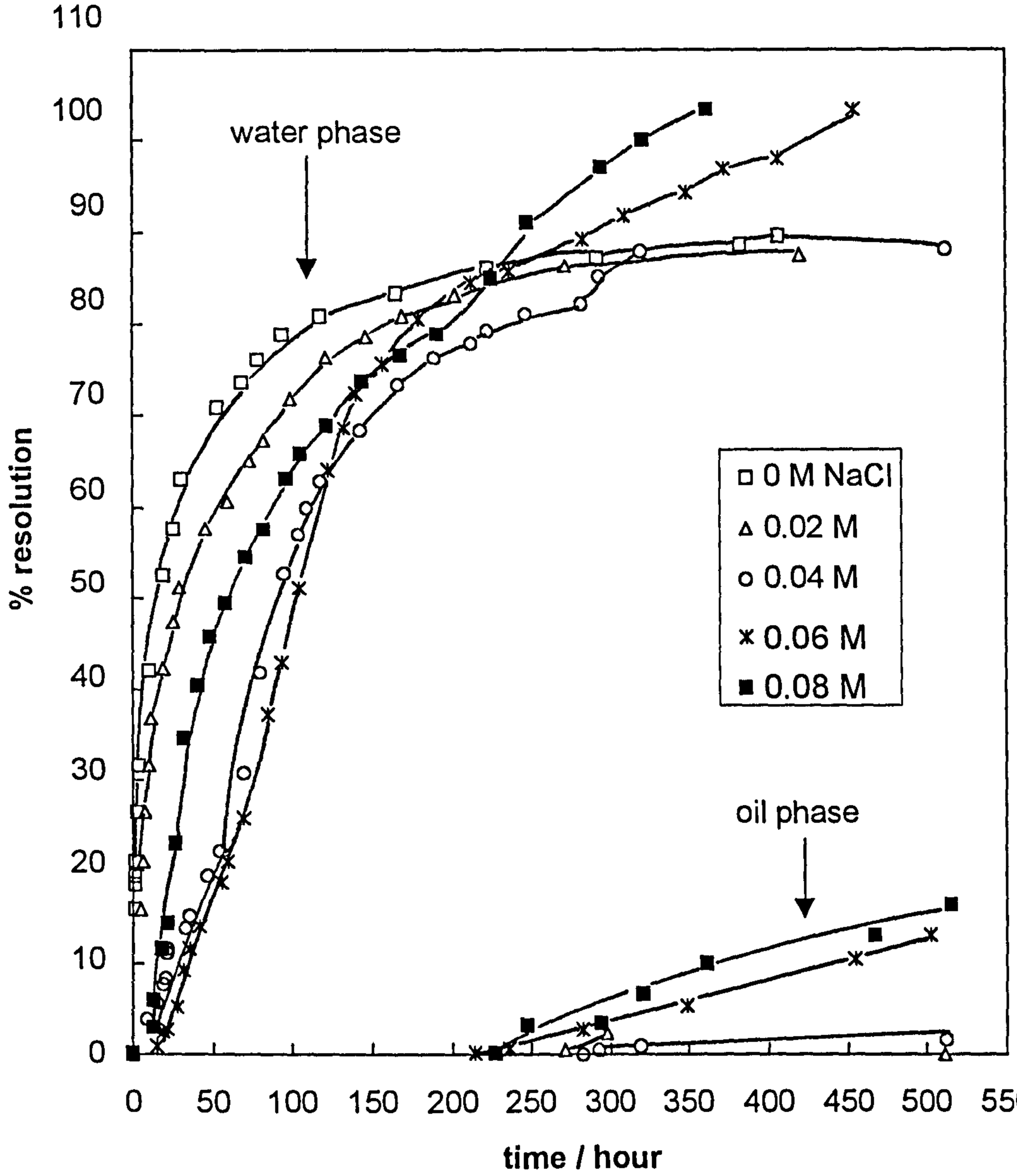

Figure 7.4

Percentage of oil phase resolution (coalescence) versus time for o/w emulsions for 0.10 M, 0.12 M and 0.14 M NaCl formed in Winsor I systems at 25°C

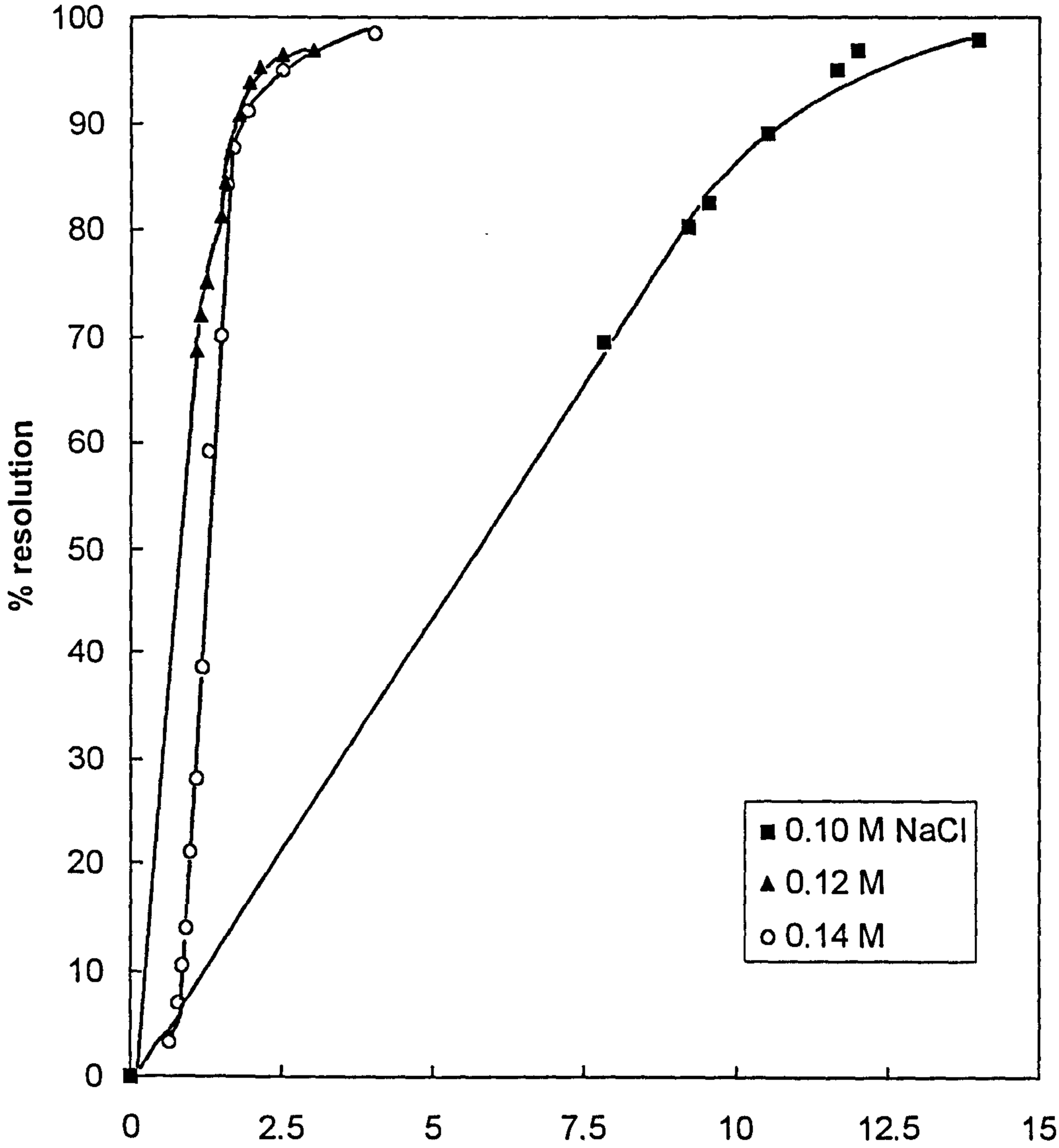

and taking on the clear bluey appearance of the equilibrium o/w microemulsion. No apparent induction period exists for the formation of clear oil phases in this salt range. The stability is extremely low very close to the Winsor I/III boundary (0.12 M NaCl) where complete phase separation is achieved.

As salt concentration increases, there is a gradual decrease followed by a sharp increase in the volume mean diameter of the emulsions (Figure 7.5). We note that the sharp increase occurs close to the Winsor I/III boundary where the oil-water interfacial tension falls sharply also. A minimum in diameter at 0.06 M NaCl was found which corresponds to maximum stability of the emulsions. From Figure 7.6a where the volume size distributions are plotted, it can be seen that the volume size distribution at this [NaCl] is very narrow. In addition, the image analysis in Figure 7.6b shows the emulsion is reasonably monodisperse. Further increase in salt concentration produces a sharp increase in the volume mean diameter, much broader volume size distributions and larger polydispersity, indicating fast coalescence occurs as seen from the stability studies. These findings are very interesting, we therefore chose this system and investigated how the size of the droplets and hence the stability of the emulsion is influenced by the surfactant concentration. The results are presented in Figure 7.7. The filled squares represent the volume mean diameters *d(v, 0.1)*, defined as the diameters such that 10% of the volume distribution of the drops are ≤ this value, while open squares correspond to diameters *d(v, 0.5)* such that 50% of the volume distribution of the drops are ≤ this value. It can be seen that a decrease in the surfactant concentration produces a sharp increase in the

Figure 7.5

Volume mean diameters for emulsions formed in Winsor I systems after dilution vs NaCl concentration at 23°C

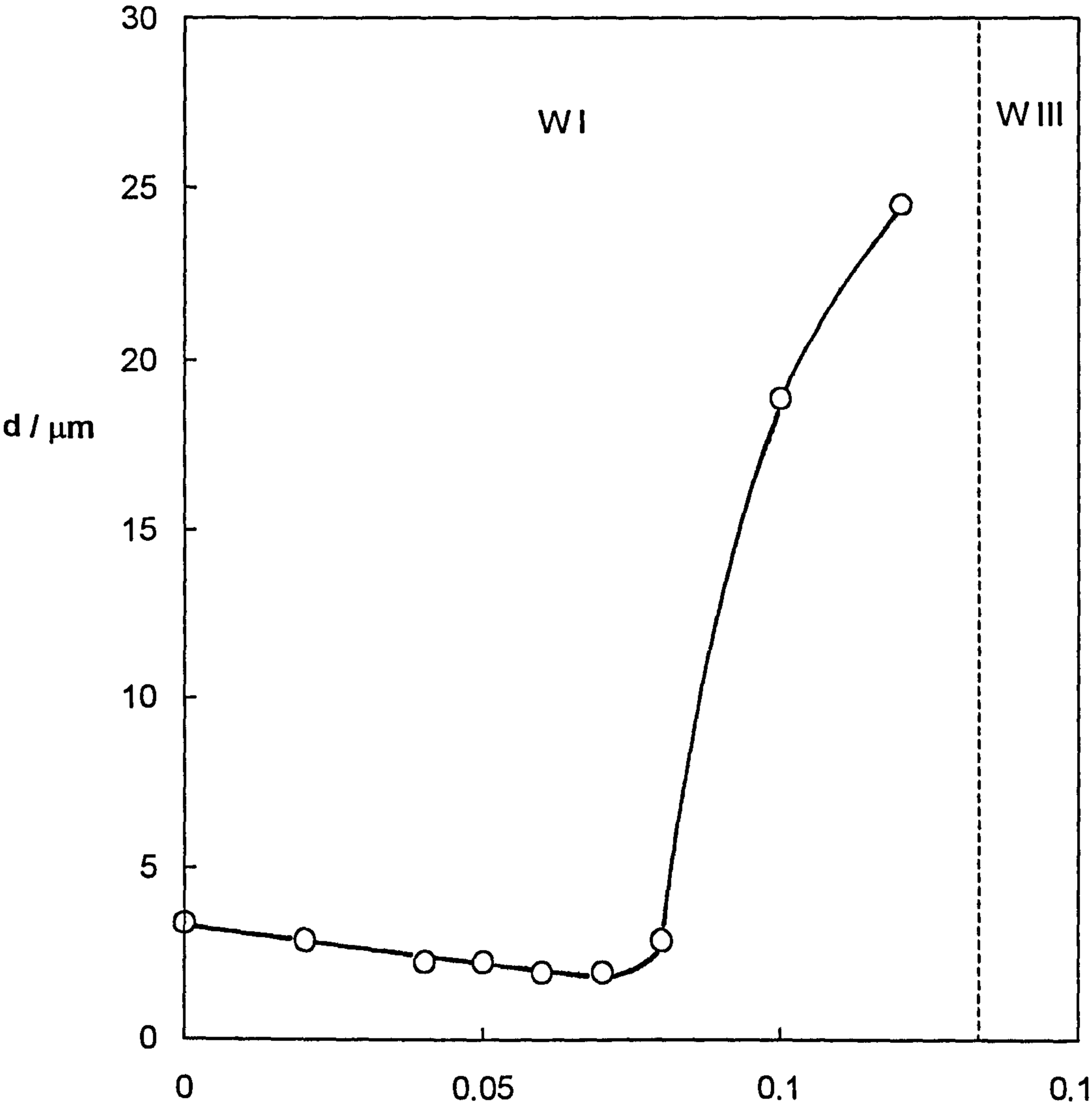

Figure 7.6a

Typical volume diameter distributions for emulsions in the system:
0.65 cS PDMS oil+40 mM AOT+aqueous NaCl after dilution

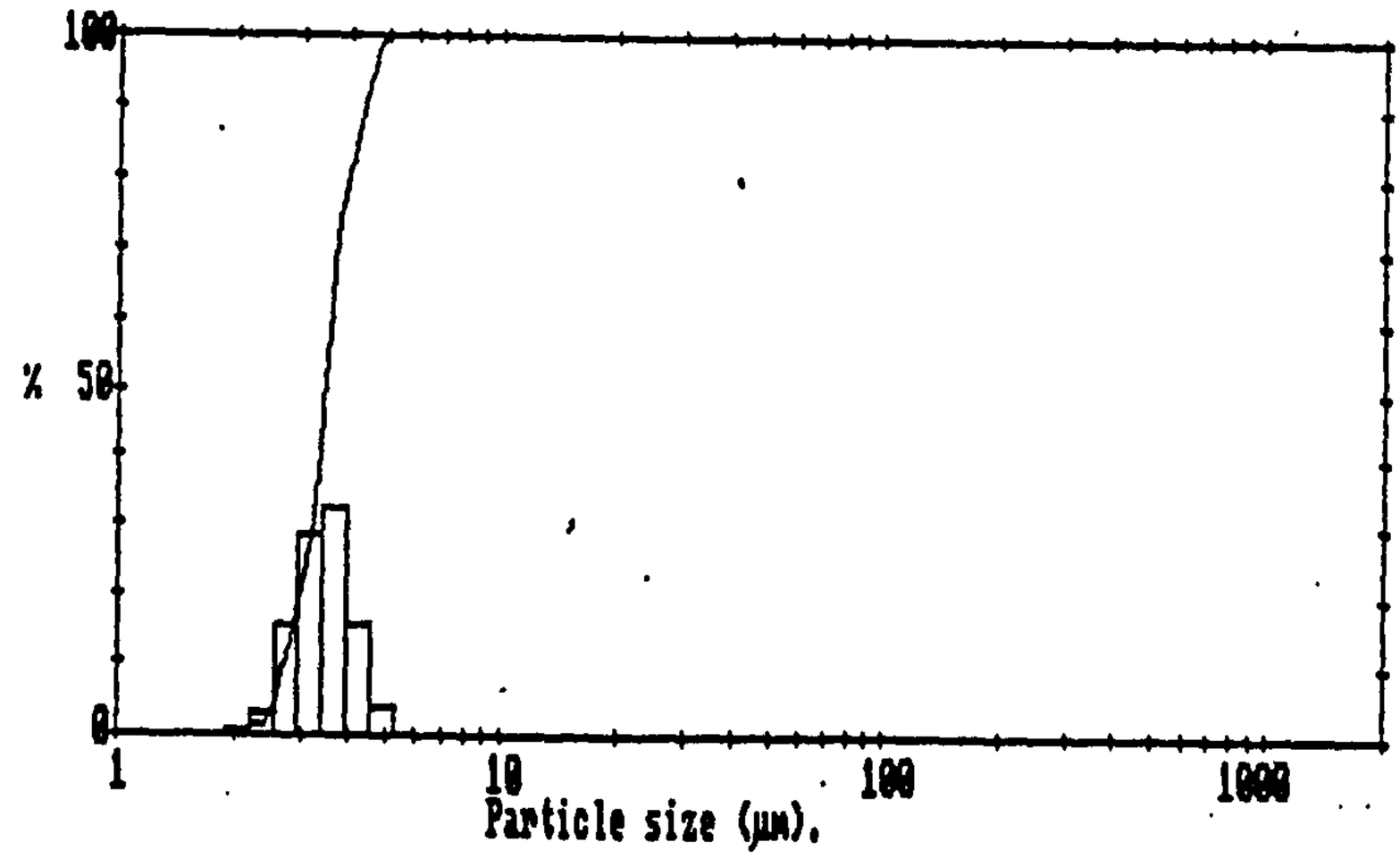

0 M NaCl

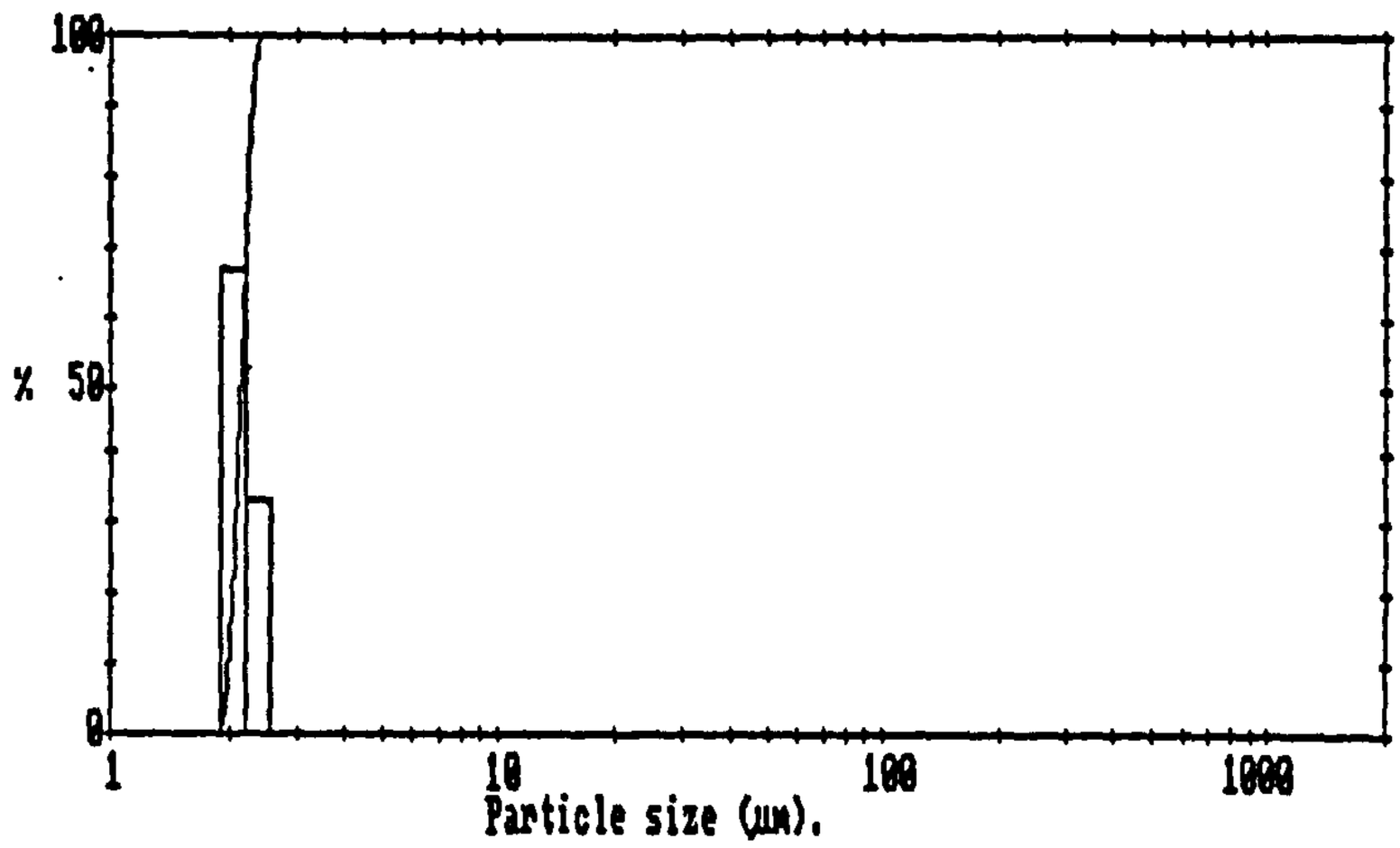

0.06 M

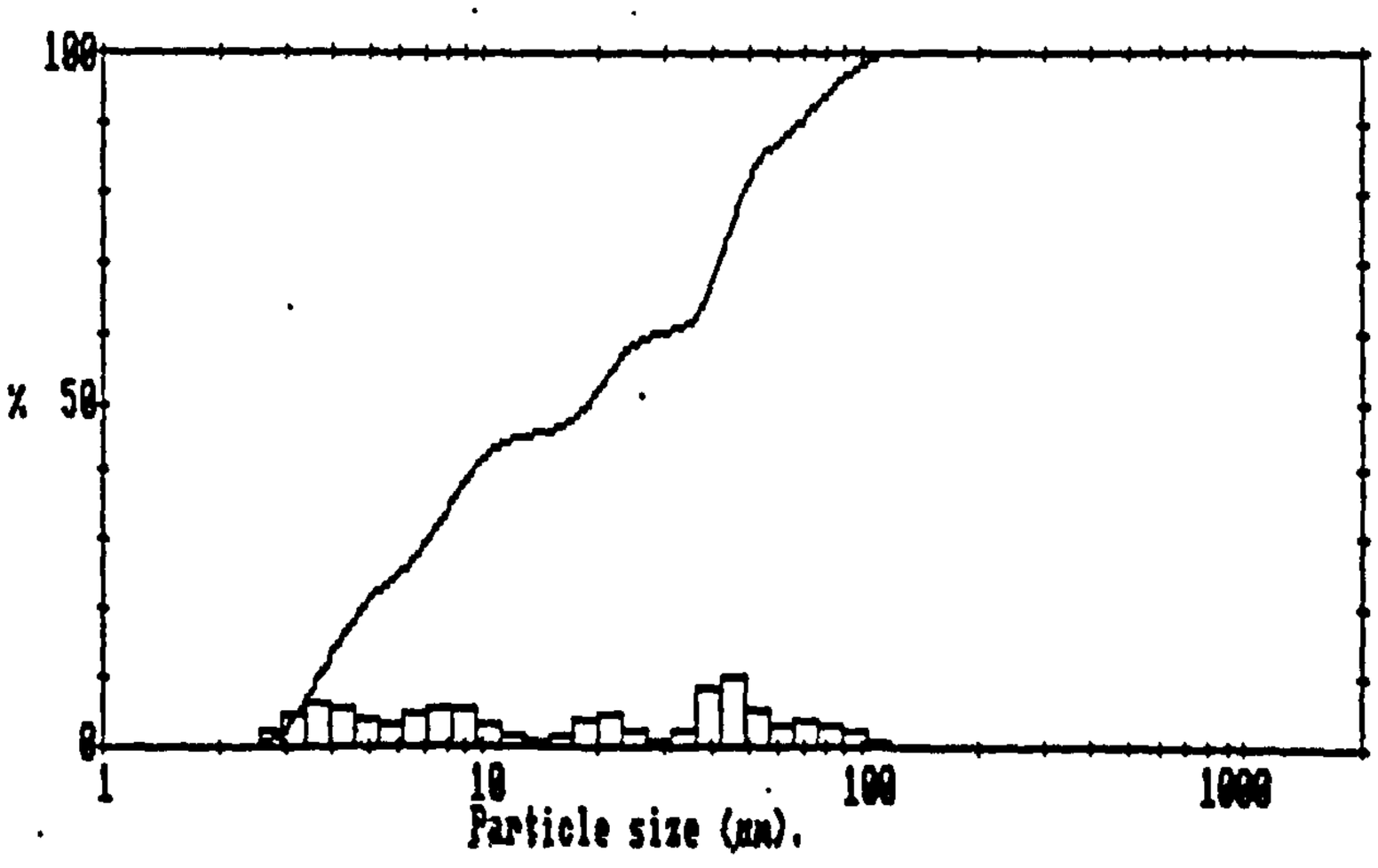

0.10M

Figure 7.6b

Optical microscope images for the emulsions: 5 vol% 0.65 cS PDMS oil in 40 mM AOT plus aqueous NaCl

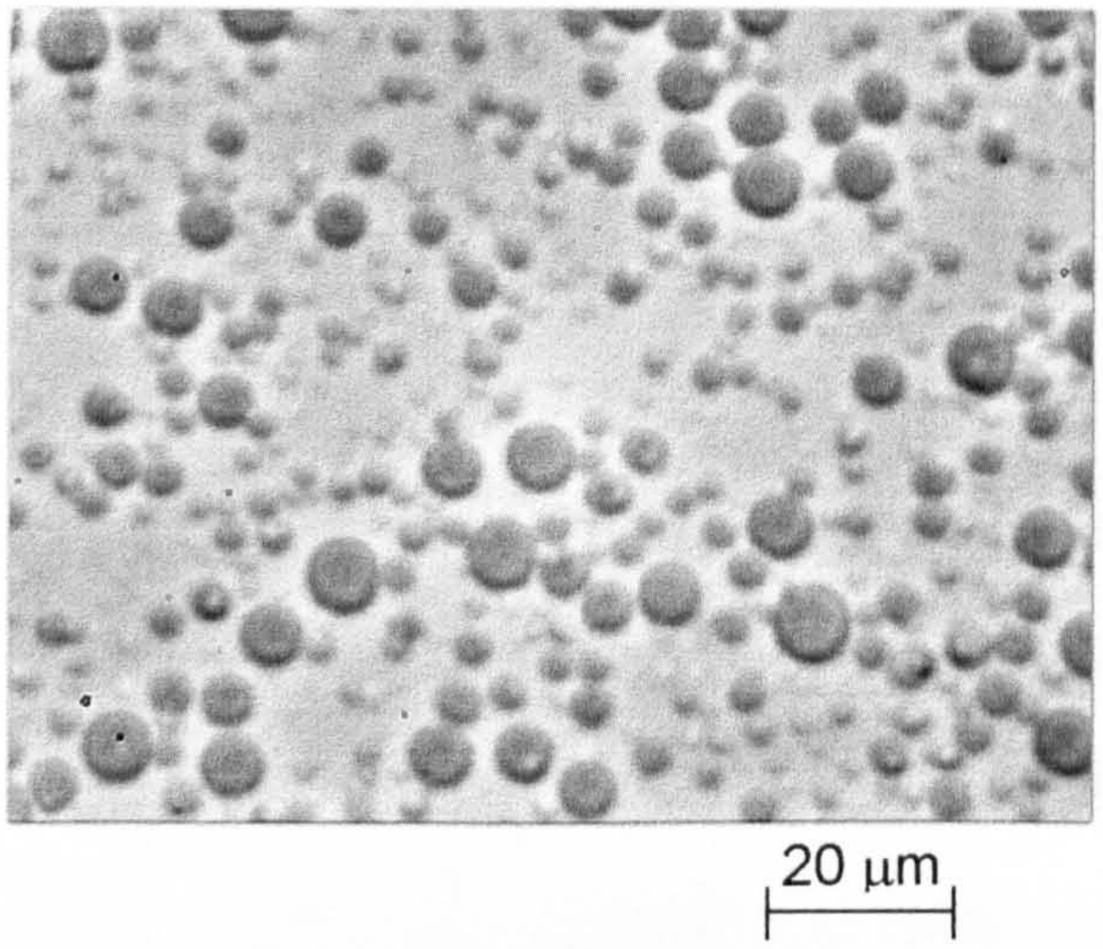

0 M NaCl

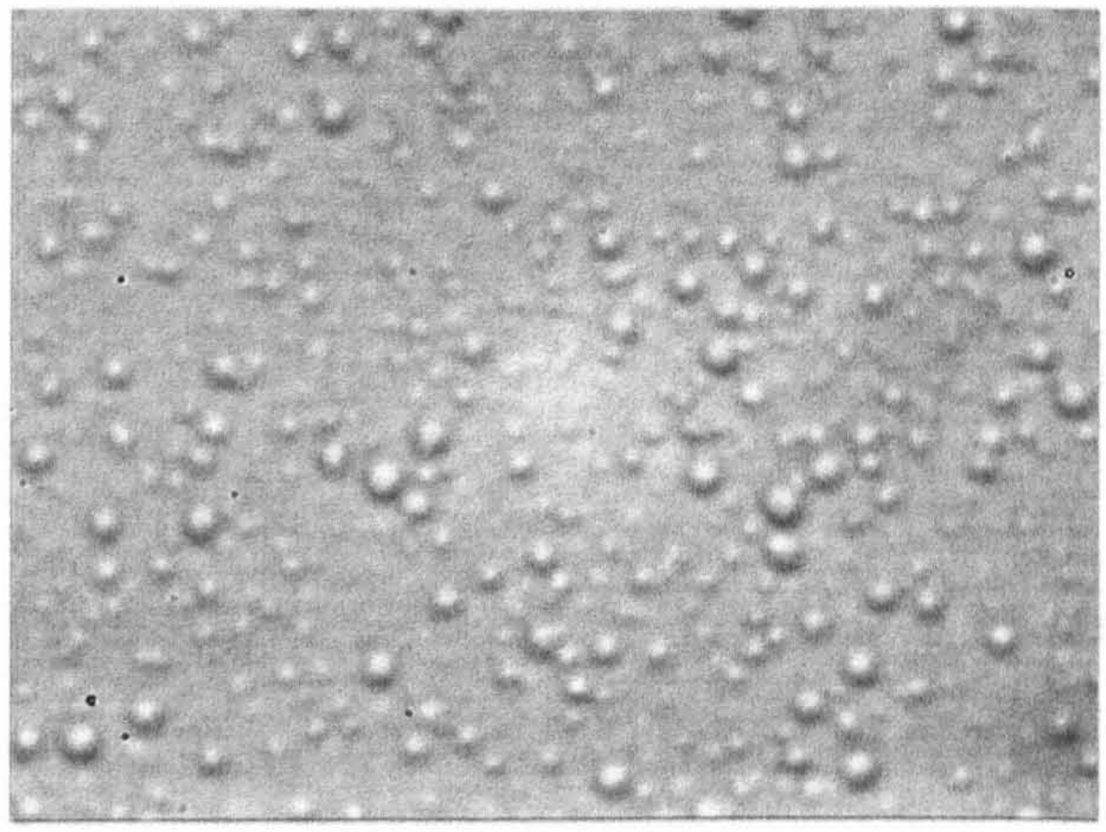

0.06 M

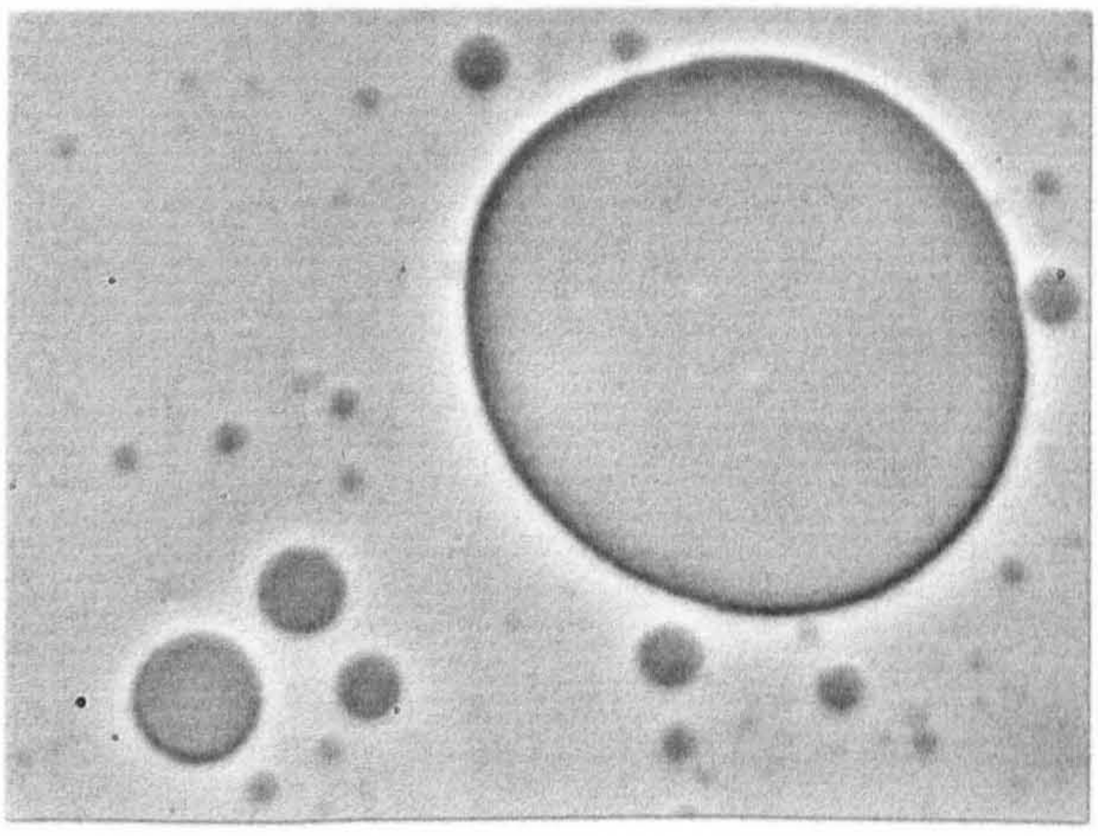

0.10 M

volume mean diameters and broader volume size distributions. One explanation may be that the concentration of surfactant is too low to fully cover the oil droplets, hence the possibility of coalescence is greater and emulsions become unstable.

The maximum in emulsion stability around 0.06 M NaCl for o/w emulsions may be due to several reasons. As shown in Figure 7.1 the oil-water interfacial tension falls to very low values (from 3.2 to 0.1 mN m^{-1}) as the salt concentration increases in this range. As a result the initial volume diameter of the emulsions also decreases, with the smallest drop size and reasonably monodisperse emulsions occurring at 0.06 M NaCl. This is likely to contribute to the initial increase in stability to creaming (up to 0.06 M NaCl), since the creaming rate is proportional to the square of the drop radius.[26] Salt can be expected to progressively reduce the zeta potential for the o/w emulsions by compressing the electrical double layer, which will result in increased flocculation and hence creaming. Further, it has been shown recently that the degree of dissociation of adsorbed AOT, at least around microemulsion drops, decreases to zero close to the Winsor I/III boundary,[164] again favouring flocculation. The maximum stability may arise from competing effects due to drop size (increasing stability) and falling electrical repulsion (decreasing stability). Indeed, the mean drop diameter close to the boundary (>0.08 M) increases to over 15 μm alongwith an increase in polydispersity consistent with rapid coalescence as evidenced in the stability studies. Droplet flocculation will occur if the pair interaction free energy becomes appreciably negative (implying attraction) at a certain

separation. By taking into account the deformability of liquid emulsion drops, Danov *et al.*[173] have shown that such interactions may lead to the formation of a planar film of thickness h and radius r between colliding drops (see Figure 7.8), enhancing the possibility of coalescence. In their model, the total interaction energy W(h,r) between two deformed drops is the sum of several contributions

$$W(h,r) = W^{vdW}(h,r) + W^{e}(h,r) + W^{s}(r) \qquad (7.1)$$

Here W^{vdW} is the van der Waals attractive energy coming from the sum of the interaction energy between the spherical, undeformed parts of two drops and the interaction energy arising across the planar film between the deformed areas. W^{vdW} depends on the Hamaker constant for the interaction oil-water-oil, h, r and the drop radius a. W^{e} is the electrostatic repulsive energy for weakly overlapping double layers, dependent on salt concentration, r, h and the surface potential Ψ_0. The third term W^{s} is a repulsive term due to the increase in surface area following deformation and depends on a, r and the interfacial tension γ. With a knowledge of the various parameters, contour diagrams of W(h,r) may be calculated as a function of h and r for variations in [salt], Ψ_0, a and γ. It turns out that the magnitude of the interfacial tension is very important in determining whether deformation occurs and, if it does, in its extent.[174] Thus, for low [salt] there is virtually no deformation or film formation and the drops interact as non-deformable spheres. With increasing concentrations of salt, the drops become much more attractive (due mainly to a drastic lowering of γ) and deformable such that W(h,r) reaches the values of less than -100 kT and r/a can become as high as 0.4. Not surprisingly coalescence sets in under these conditions.

Figure 7.7

Volume mean diameter for emulsions of AOT in 0.65 cS PDMS oil plus equal volume of 0.06 M aqueous NaCl after dilution vs AOT concentration in oil phase at room temperature

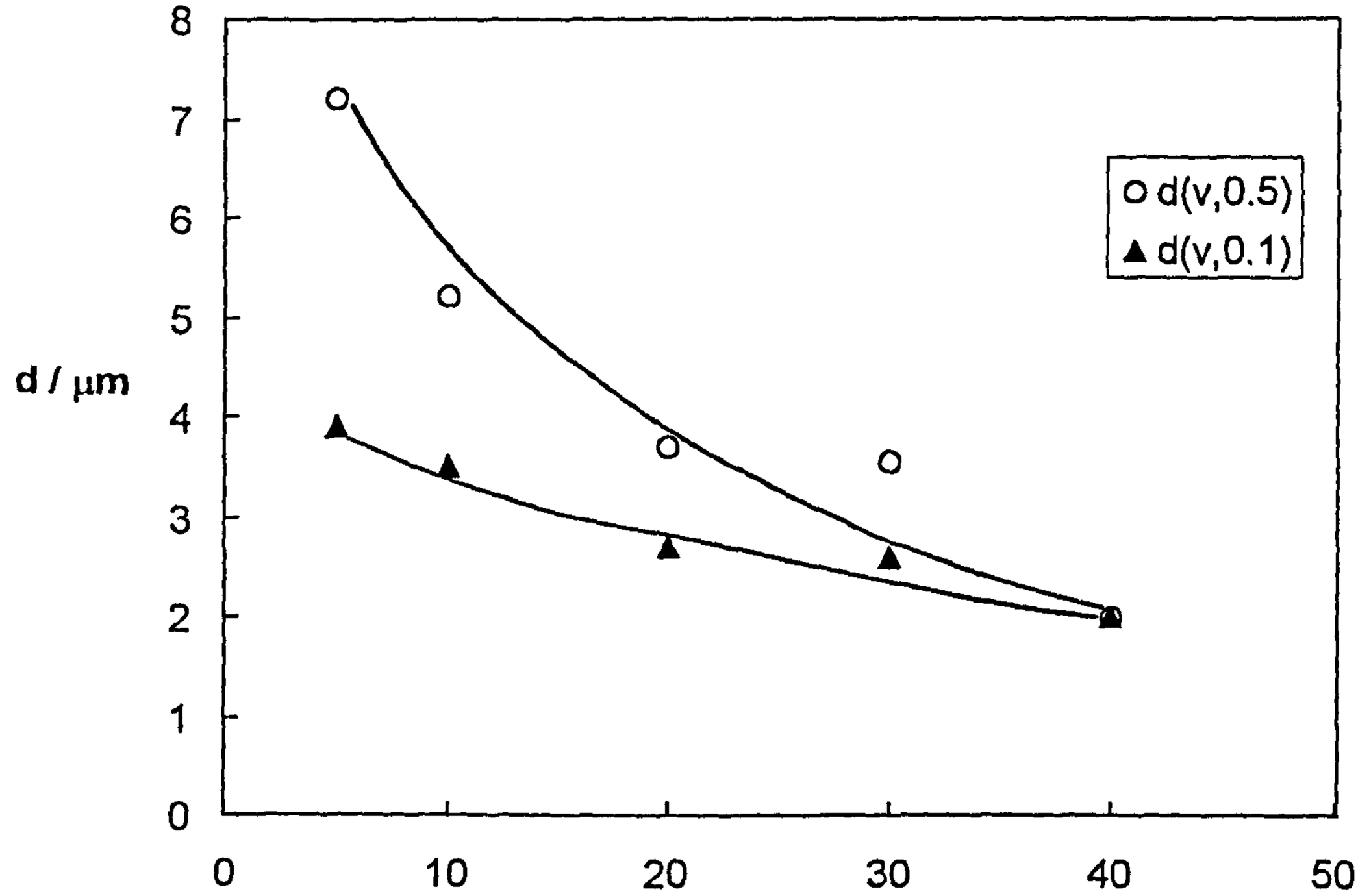

Figure 7.8

Schematic representation of two deformed emulsion droplets

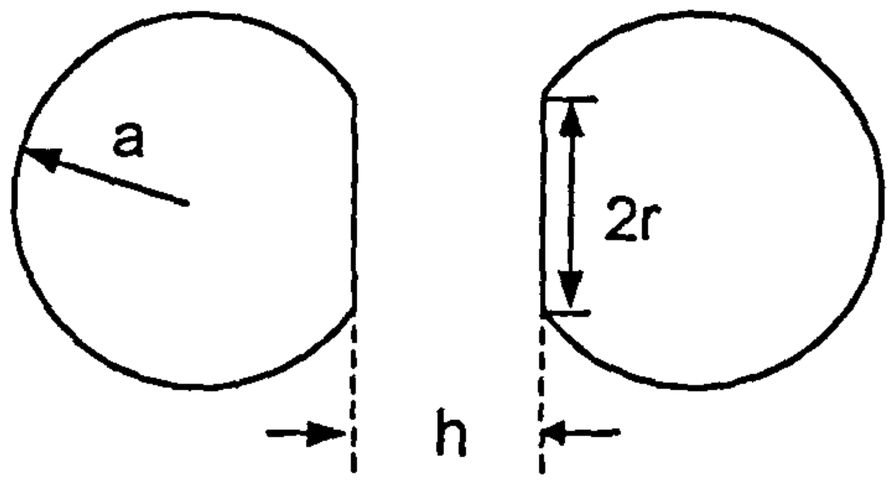

a: drop radius prior to deformation

h: film thickness

r: film radius

Even though these calculations were for heptane as oil, they can be expected to be similar for this small PDMS oil because of the similar lowering of γ as salt concentration increases.

7.3.2 Stability of w/o emulsions in Winsor II systems

In the Winsor II region, a delineation in behaviour is also seen for the w/o emulsions. The emulsions are pretty unstable and they sediment and coalesce fast compared to the creaming and coalescence in Winsor I systems. Figures 7.9 and 7.10 show the percentage of sedimentation and coalescence as a function of time for various salt concentrations. Close to the Winsor III/II boundary (0.20, 0.23 M NaCl) sedimentation occurs rapidly (within 3 minutes) followed by slow coalescence (over days). Above 0.27 M NaCl, rapid sedimentation occurs simultaneously with coalescence. The rates of both processes increase (i.e. stability decreases) on moving away from the Winsor III/II boundary. It has been claimed that a second stability maximum exists in the Winsor II region for alkane systems.[172] In 0.65 cS PDMS oil systems, the stability maximum for sedimentation in Winsor II systems appears at the Winsor III/II boundary. If we compare the onset of emulsion phase inversion in alkane and 0.65 cS PDMS oil systems, inversion from o/w (conducting) to w/o (non-conducting) starts for alkanes at the Winsor III/II boundary and ends in the Winsor II region, whereas for silicone oil systems it starts at the Winsor I/III boundary and ends at the Winsor III/II boundary. It is likely that the secondary maximum in emulsion stability to creaming (sedimentation) in AOT systems is accompanied by the completion of the emulsion phase inversion. The stability of emulsions in

Figure 7.9

Oil phase resolution (sedimentation) versus time for different [NaCl] for w/o emulsions formed in Winsor II systems at 25°C

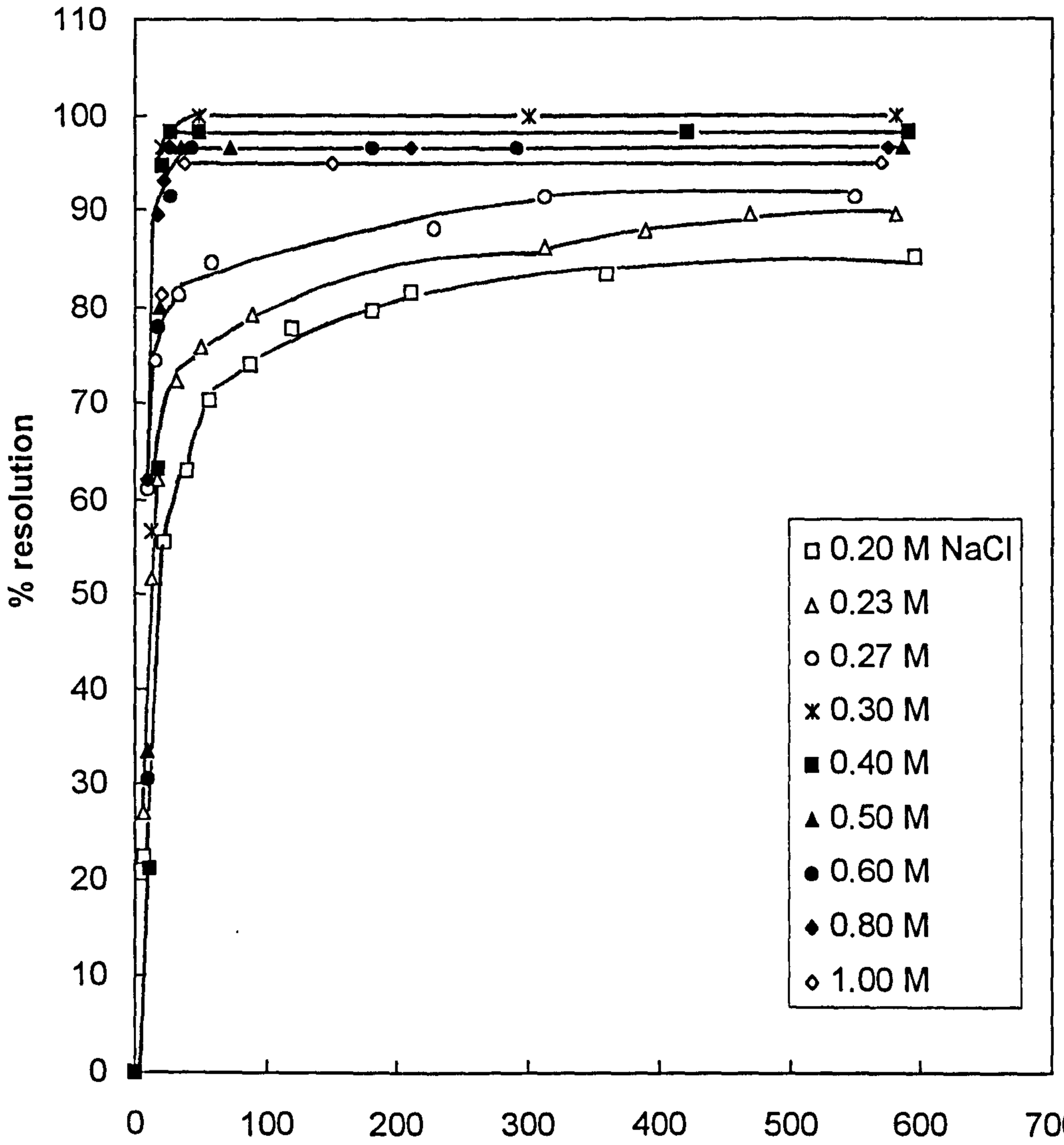

Figure 7.10

Water phase resolution (coalescence) as a function of time for various [salt] for w/o emulsions in Winsor II systems at 25°C

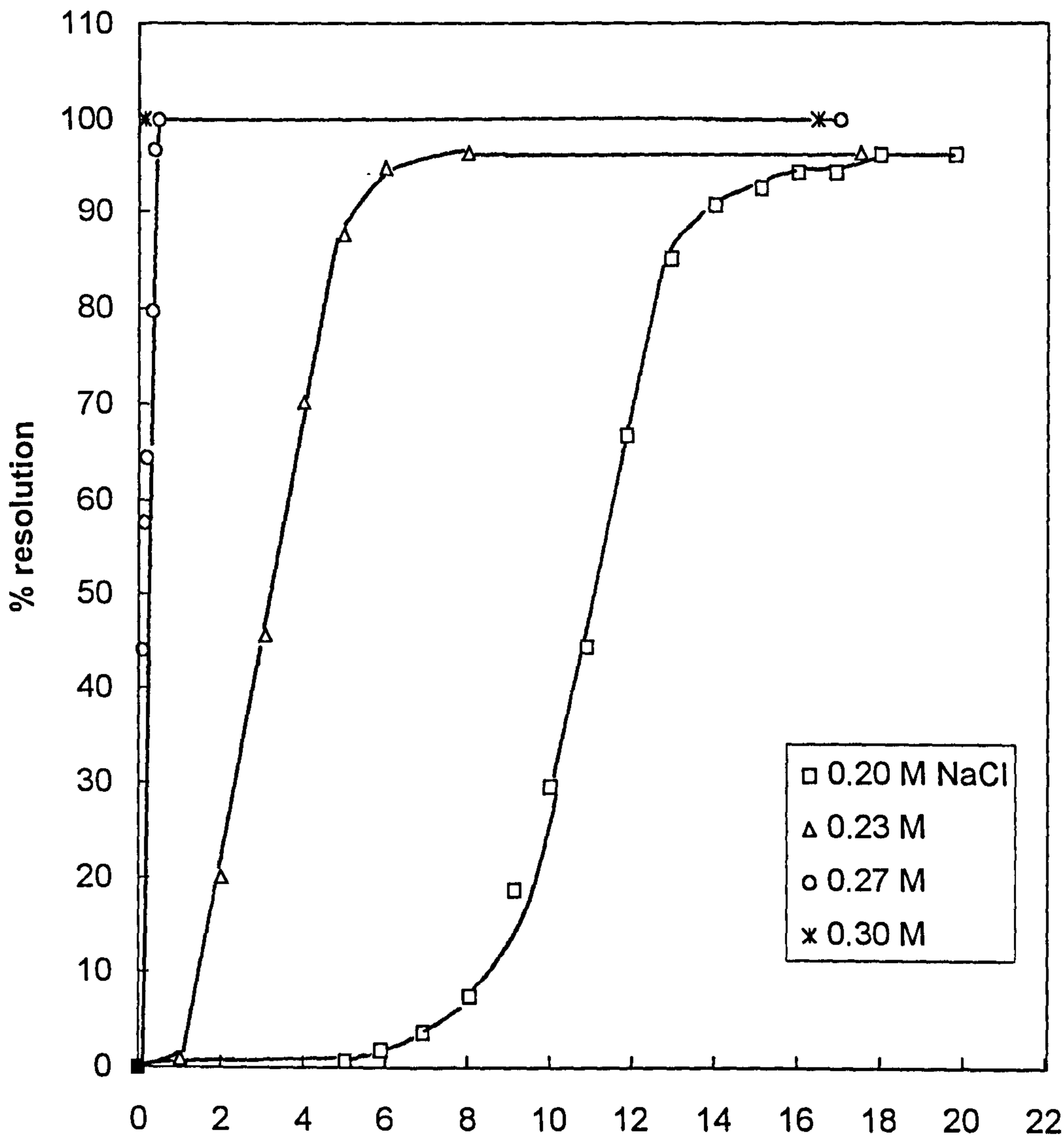

both Winsor I and Winsor II systems as a function of sodium ion concentration is summarised in Figure 7.11.

7.3.3 Stability of emulsions in Winsor III systems

In general, the stability of emulsions in AOT-0.65 cS PDMS-NaCl systems in the Winsor III region is low, in agreement with previous reported work.[172] Homogenisation of the three-phase systems produces white, foaming emulsions which break down immediately after the cessation of the homogenisation. The sequence of visual changes in Winsor III systems is shown in Figure 7.12. Almost immediately an upper oil phase resolves, the lower phase remaining as a foaming white emulsion for a while depending on the salt concentration. As seen from Figure 7.13 the oil resolution does not vary significantly with [NaCl] in this range, about 100% of the oil phase separating within 2 minutes. The emulsion with 0.16 M NaCl ultimately resolves into three phases - upper clear oil phase, clear middle phase and bottom blue phase with probably most of the surfactant. However, the emulsion with 0.18 M NaCl resolves into three colourless phases. For the emulsion with 0.16 M NaCl we were able to record another sequence of visual changes; the appearance of the blue phase, shown in Figure 7.14. At long times, this blue bottom phase resolves into an equilibrium aqueous phase (bottom) and the (clear) surfactant-rich phase. The slow resolution of the two lower phases must be in part due to the similar densities. It has been shown earlier that the oil content in the surfactant-rich phase is small.

In summary, our findings with respect to creaming/sedimentation and coalescence rates are at variance with previous results, which themselves

Figure 7.11

Percentage resolution of continuous and non-continuous phases at different times for emulsions formed in Winsor I and Winsor II systems at 25°C

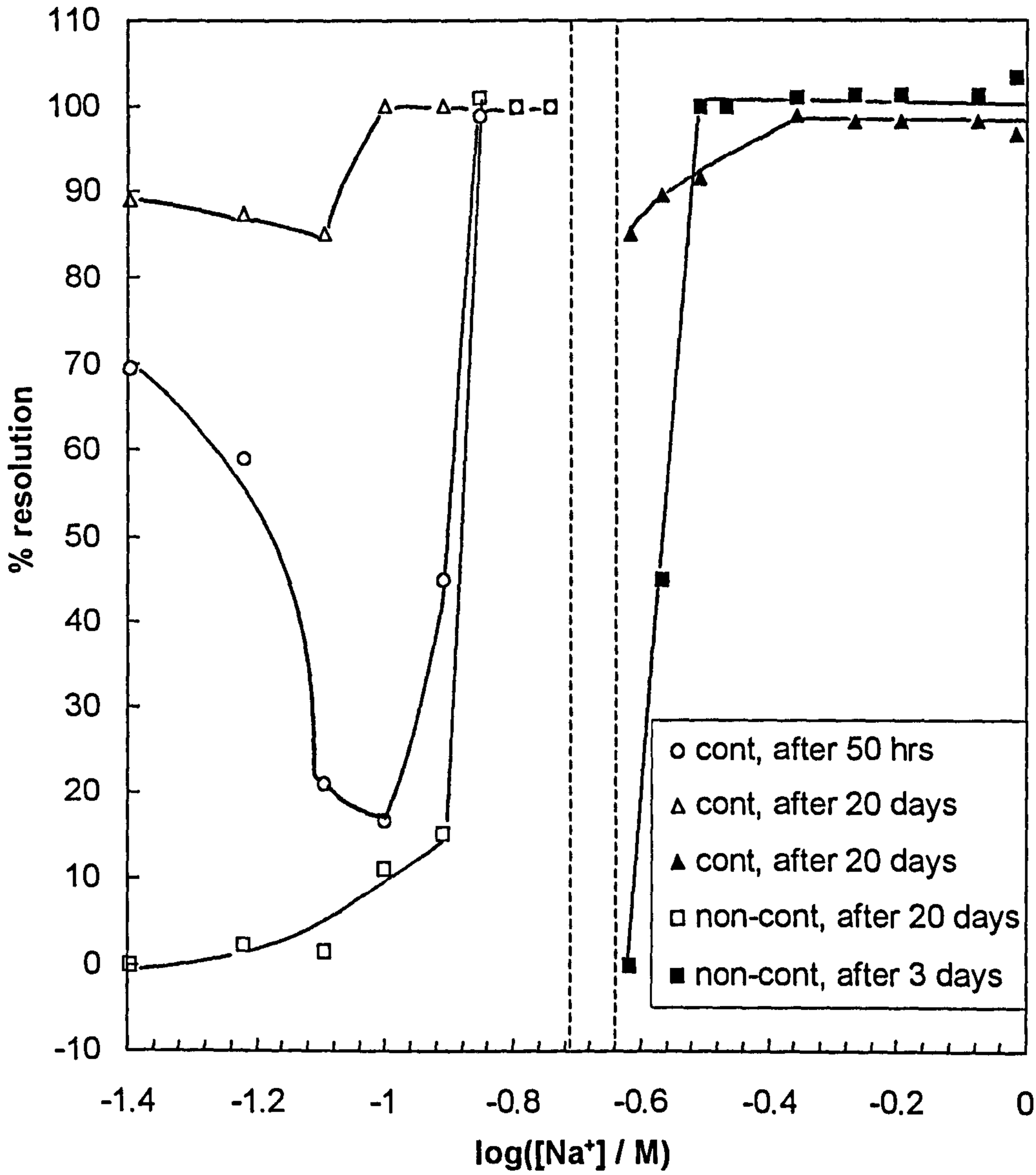

Figure 7.12

Sequence of visual changes in Winsor III systems for emulsions: 40 mM AOT in 0.65 cS PDMS oil plus equal volume of aqueous NaCl at 25°C

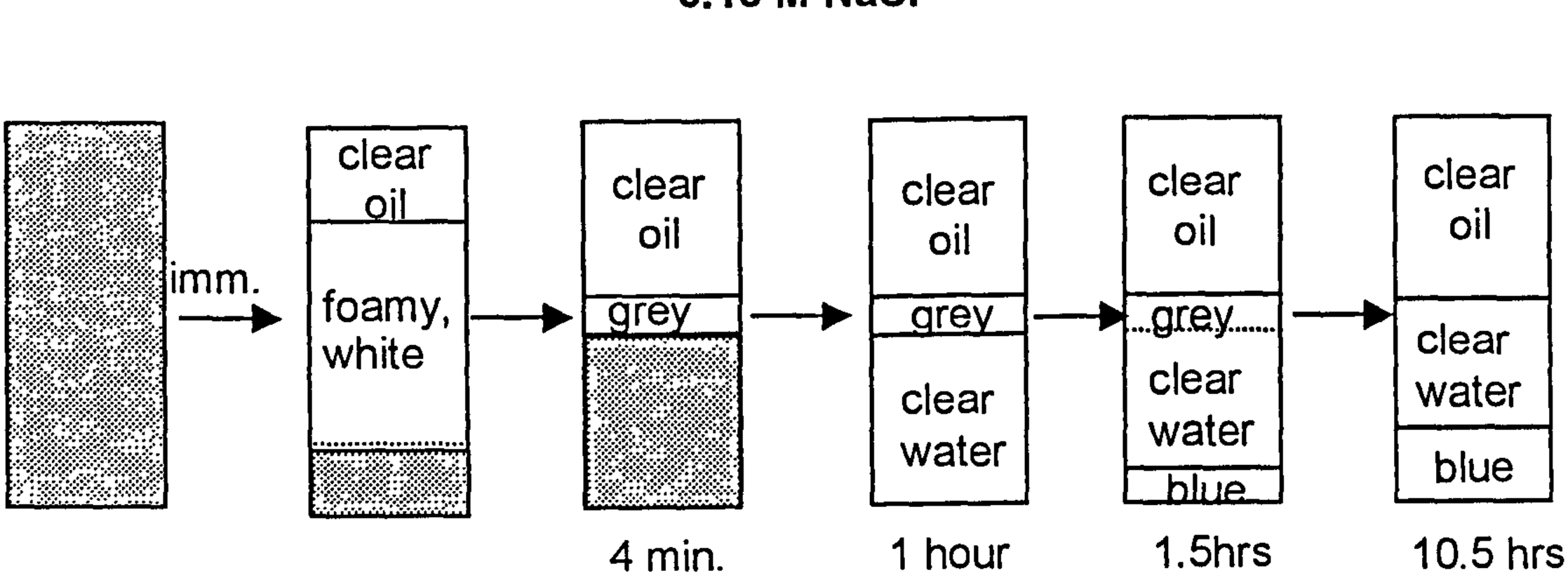

Figure 7.13

Oil phase resolution as a function of time for various [salt] for emulsions in Winsor III region at 25°C

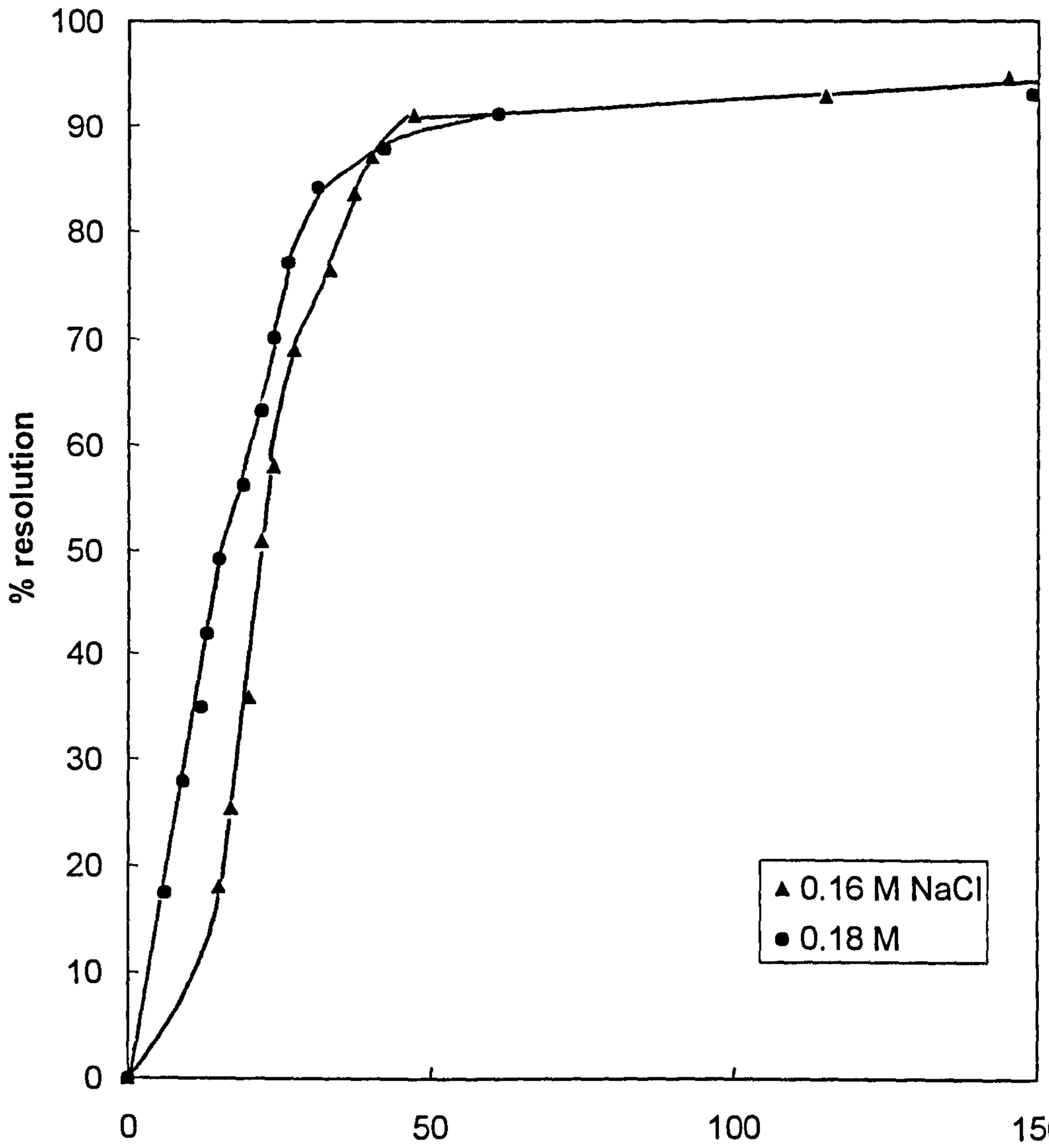

Figure 7.14

Percentage resolution of "blue" phase (relative to the total volume of blue plus water phase, to which the bottom phase ultimately resolves) versus time for 0.16 M NaCl in Winsor III systems at 25°C

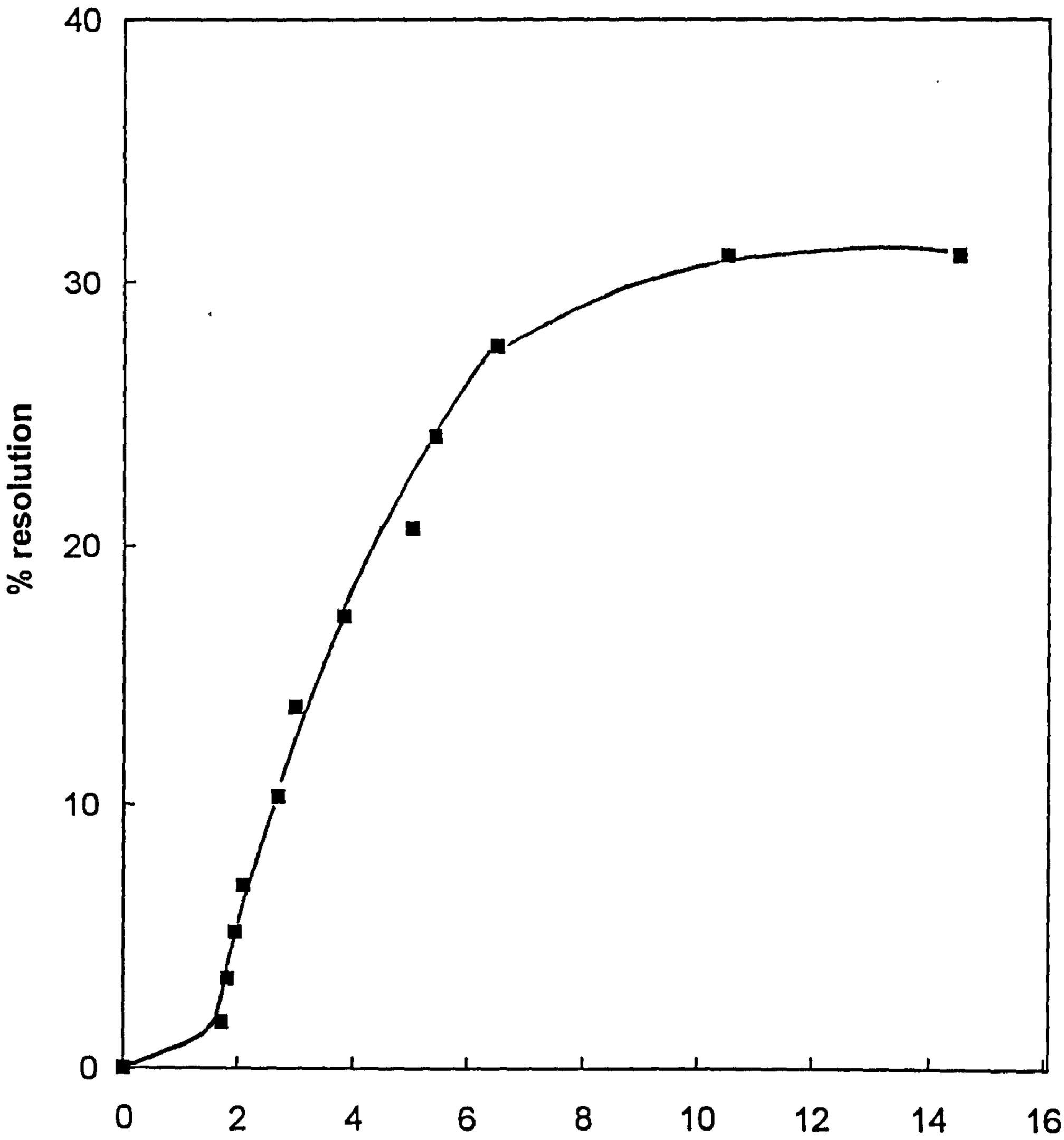

show opposite trends. We observe that stability to both creaming and coalescence falls drastically as Winsor I systems approach the I/III boundary, whereas the stability to both sedimentation and coalescence increases as Winsor II systems approach the II/III boundary. Table 7.1 gives the times for various processes and highlights the extreme variation from seconds to days depending on the Winsor system concerned.

Table 7.1 Summary of emulsion stabilities in 40 mM AOT+0.65 cS PDMS+aqueous NaCl systems at 25°C. The times, t, (in seconds, s, hours, h and days, d) for various percentages of water (w) or oil (o) phase resolution are given as a function of salt concentration.

Winsor system	[NaCl] /M	t (50% w) creaming	t (5% o) coal.	t (50% o)	t (80% o) sedimen.	t (50% w) coal.
I	0	15 h	> 650 h			
I	0.02	28 h	> 650 h			
I	0.04	92 h	> 650 h			
I	0.06	105 h	350 h			
I	0.08	66 h	300 h			
I	0.10	7 h	30 s			
I	0.12	1 h	6 s			
III	0.16			22 s		
III	0.18			15 s		
II	0.20				180 s	11.2 d
II	0.23				100 s	3.2 d
II	0.27				30 s	0.12 d
II	0.30				15 s	0.05 d

7.4 Emulsion inversion and stability for different PDMS oil viscosity

7.4.1 Phase inversion

The correspondence between emulsion and microemulsion type also holds for the higher molecular weight PDMS oils. Figure 7.15 shows the conductivity of emulsions as a function of salt concentration. The surfactant was initially dissolved in the aqueous phase and mixed with an equal volume of oil before emulsification. As seen, emulsions invert from o/w (conducting) at low [NaCl] to w/o (non-conducting) at high [NaCl]. The salt concentration at which the emulsion phase inversion occurred increases with an increase in the molecular weight of the oil from 0.65 cS to 10 cS PDMS. However, little change occurs with a further increase in oil size, similar to the findings on PITs for nonionic surfactant emulsions discussed in chapter 3. For the 0.65 cS oil, inversion takes place between 0.09 and 0.15 M NaCl, increasing to between 0.2 and 2 M for the 100 cS oil. In Figure 7.16, the relationship between emulsion stability for high molecular weight PDMS oils and electrolyte concentration may be seen. For a particular oil viscosity, stable white o/w emulsions are formed below a certain [NaCl]. At intermediate salt concentrations, emulsions were very unstable breaking completely within 5 seconds. Above a higher [NaCl], grey w/o emulsions of reasonable stability were formed having conductivity below 5 $\mu S\ cm^{-1}$. We recall the findings of the equilibrium phase behaviour and water-PDMS oil interfacial tension results. For the 0.65 cS, the salt concentration range where the Winsor III systems occur is narrow and a sharp minimum in γ_{ow} is found. As the molecular weight of PDMS oil increases, it becomes much wider, with a

Figure 7.15

Conductivity of emulsions in the system 40 mM AOT in aqueous NaCl plus PDMS oils (1:1) vs total sodium ion concentration at 25°C

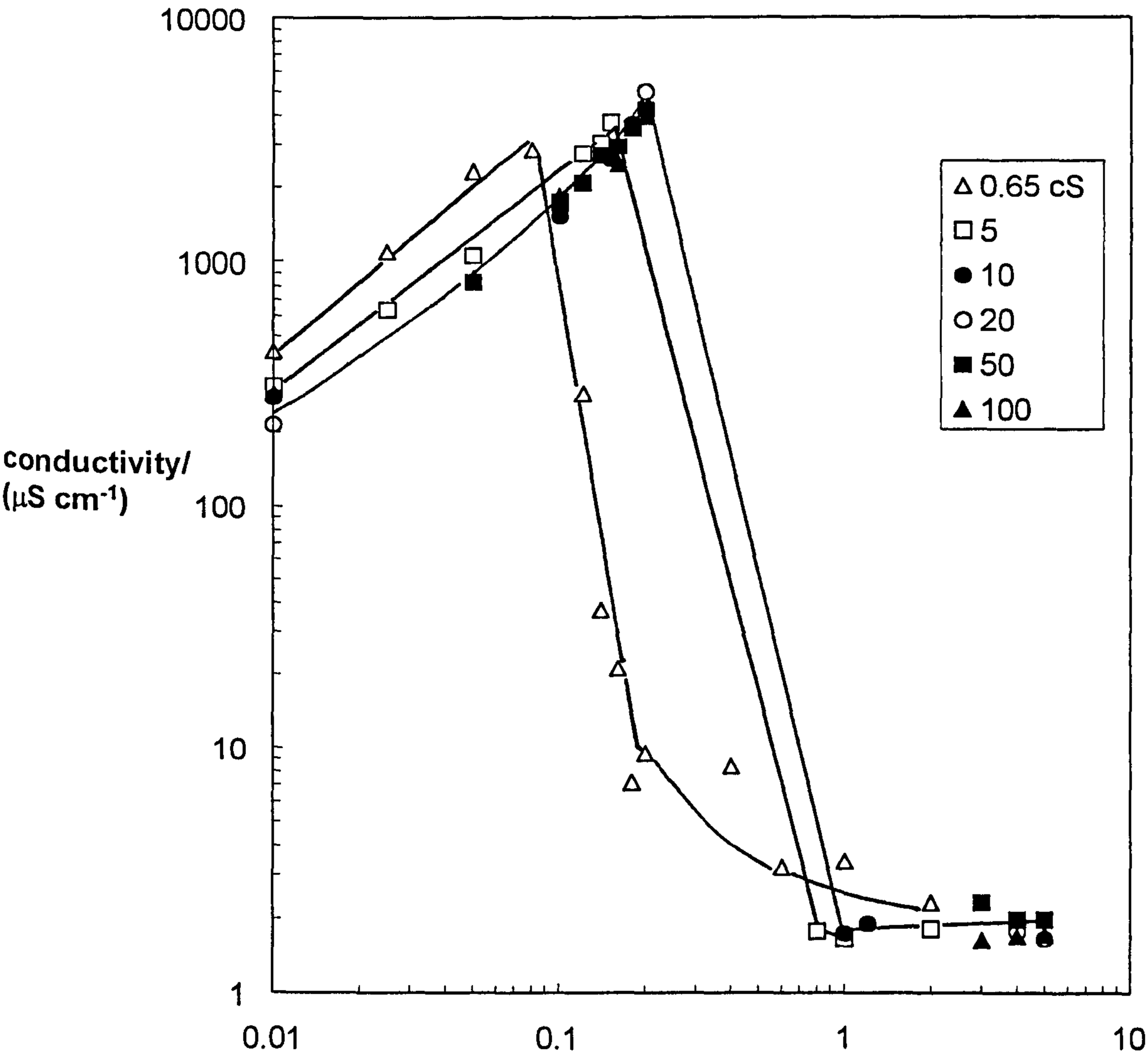

Figure 7.16

Effect of PDMS oils viscosity on the type and stability of the emulsions in Figure 7.15 at different electrolyte concentrations

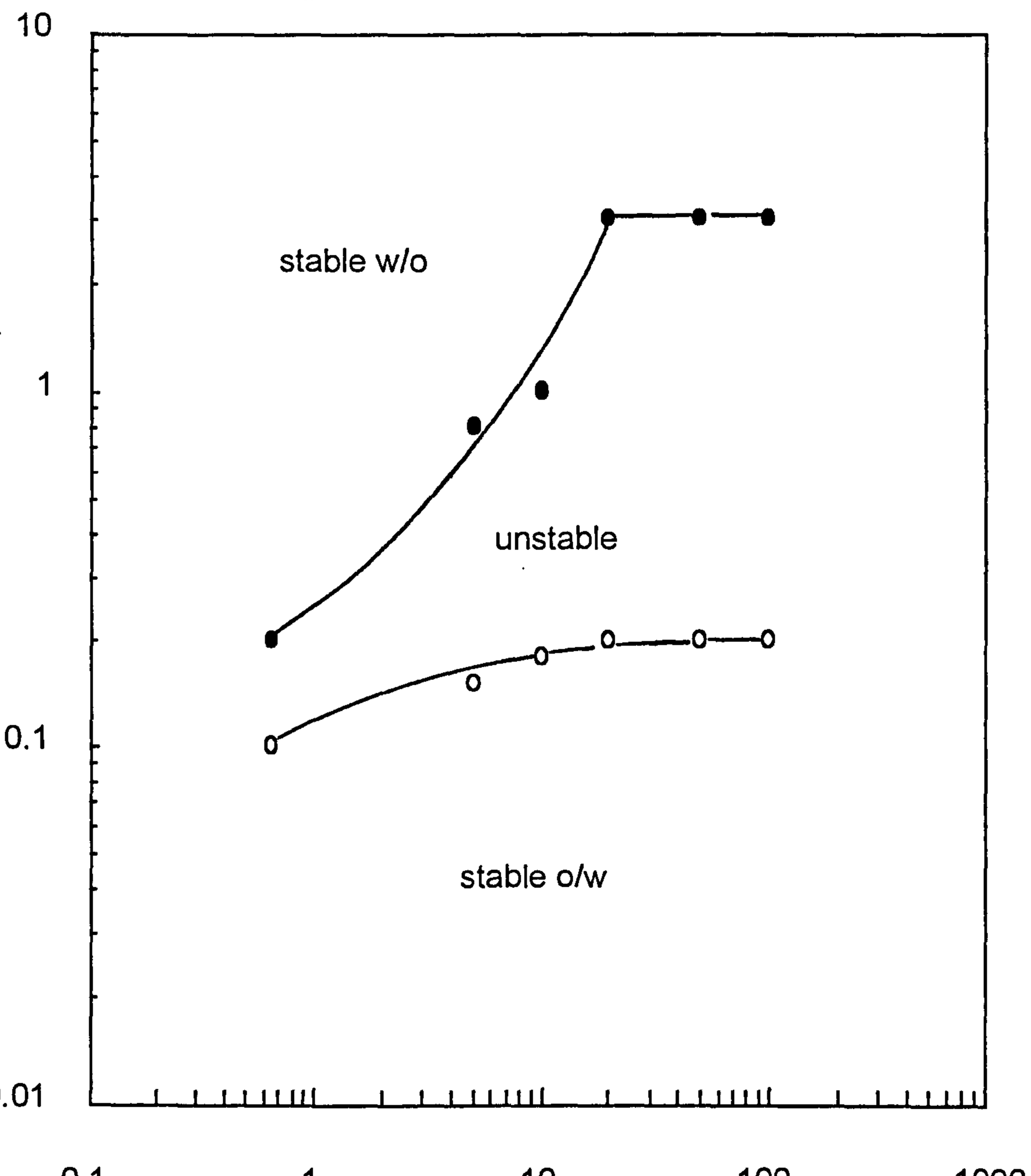

correspondingly higher interfacial tension. It can be seen in Table 7.2 that the salt concentration ranges relating to Winsor III systems coincide well with those in which three phase emulsions are formed and inversion occurs.

Table 7.2 Effect of PDMS oil viscosity on the post-cmc PDMS-water interfacial tension (no salt), γ_{ow}, the minimum post-cmc tension, γ_{min}, the salt concentration range over which Winsor III systems form and the salt concentration range over which very unstable emulsions form in AOT-aqueous NaCl-PDMS mixtures at 25°C

PDMS viscosity/cS	γ_{ow}/mN m^{-1}	γ_{min}/mN m^{-1}	[NaCl]/M for Winsor III	[NaCl]/M for unstable emulsion
0.65	3.18	0.021	0.13-0.19	0.10-0.20
1.0	4.05	0.025	0.18-0.37	0.15-0.40
3.0	4.50	0.21	0.20-0.90	0.17-0.75
5.0	5.18	0.75	0.21-1.1	0.18-0.80
50.0	5.64	1.80	0.25-1.4	0.20-2.0

7.4.2 Drop size and stability

Figure 7.17 shows the variation of the volume mean diameter with salt concentration for various viscosity oils obtained using the laser diffractometer. After homogenisation, the emulsions were diluted with aqueous electrolyte solutions containing AOT at the corresponding cmc. An obvious feature of Figure 7.17 is that the increase in the volume mean diameter with an increase in viscosity from 0.65 cS to 5 cS oil at zero salt concentration is consistent with the increase in the corresponding interfacial

Figure 7.17

Volume mean diameters for emulsions formed in Winsor I systems versus salt concentration at 23°C for three different PDMS oils

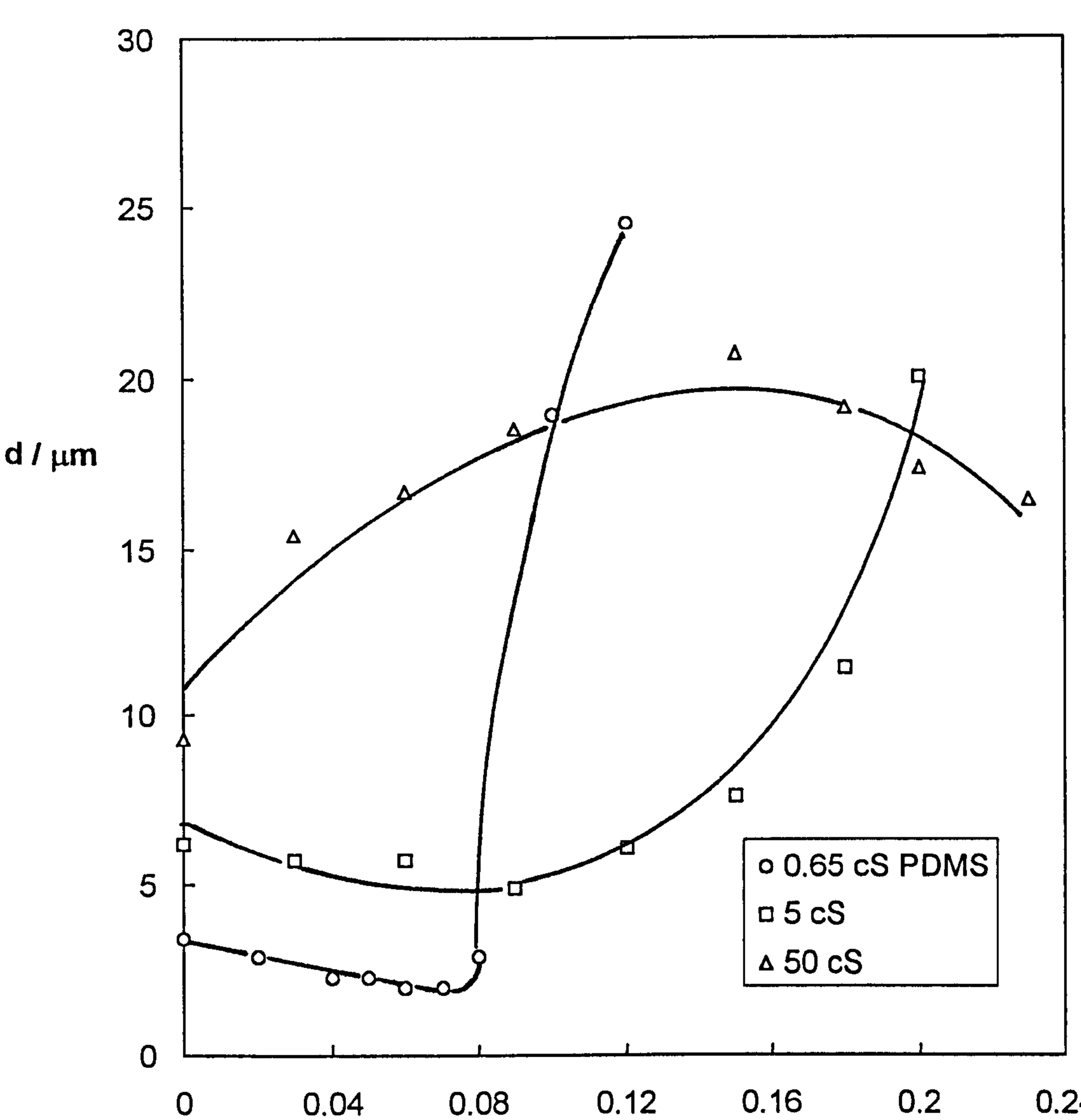

tensions described earlier. It may indicate that in emulsion formation the interfacial tension plays an important role in determining the droplet size. Figure 7.17 also shows that emulsions with 50 cS PDMS oil have a different behaviour compared with emulsions of lower viscosity oil. For this oil, the volume size distributions are very broad indicating large polydispersity. Because of the high viscosity of this oil the energy input might not be high enough to disperse the oil phase.

7.5 Conclusions

The following conclusions can be drawn for emulsions containing water + AOT + NaCl + PDMS oil at 25°C:

(a) For the 0.65 cS oil (hexamethyldisiloxane)

(i) The emulsion inverts from o/w to w/o around the conditions where the minimum in interfacial tension is found.

(ii) For o/w emulsions prepared from Winsor I systems, the stability to creaming and coalescence decreases substantially approaching the Winsor I/III boundary. An argument involving drop deformability is consistent with the findings.

(iii) For w/o emulsions prepared from Winsor II systems, the stability to sedimentation and coalescence both increase approaching the Winsor II/III boundary.

(iv) In Winsor III systems, emulsions are very unstable. Typically fast oil resolution occurs but the surfactant-rich and aqueous phases separate slowly.

(b) For the higher molecular weight PDMS oils

(i) Emulsion phase inversion occurs over the range of salt concentration for which Winsor III systems form. The higher the oil molecular weight, the higher the salt concentration for inversion.

(ii) An increase in the emulsion droplet volume mean diameter with an increase in the oil viscosity from 0.65 cS to 5 cS at zero salt concentration is consistent with the increase in the interfacial tension, showing the important role of interfacial tension in the formation of emulsions.

CHAPTER EIGHT

CHAPTER 8

Mixing of 0.65 cS PDMS Oil with AOT at Air-Water Surfaces

8.1 Introduction

In chapter 5 the mixing behaviour of PDMS oils and nonionic surfactants at the air-water surface was discussed. We learned that the spreading behaviour of PDMS oils on nonionic surfactant solutions is significantly affected by the surfactant structure and the molecular weight of the oil. Nonetheless, it is also related to the molecular weight of the oil. The adsorption isotherm of the 0.65 cS PDMS oil studied by surface tensiometry suggested that an ideal mixed monolayer of oil and $C_{12}E_5$ formed on the aqueous $C_{12}E_5$ solutions. In chapters 6 and 7 the study of the mixing behaviour of silicone oils and AOT at the oil-water interface showed that it is possible to make microemulsions (both o/w and w/o) with 0.65 cS PDMS. The interaction of oils with surfactants is relevant to solubilisation in micellar solutions and to the wetting/spreading behaviour of oils on aqueous surfactant solutions. Hence, it is of interest to investigate the mixing behaviour of 0.65 cS PDMS with AOT at the air-water surface. The possibility to quantify the amount of oil solubilised into the surfactant monolayer at the air-water surface by tension measurements may shed light on the solubilisation of oil into the surfactant monolayer at the oil-water

interface. In this chapter we deal mainly with the adsorption of 0.65 cS PDMS oil at AOT aqueous surfaces with respect to electrolyte concentration. A possible link between the surface pressure due to the adsorption of oil and the surfactant aggregate structure in bulk is made.

8.2 Observation of the spreading behaviour of silicone oils on AOT aqueous surfaces

The method employed to observe the PDMS spreading behaviour on AOT monolayers was similar to that on the nonionic surfactant solutions as described before. The concentration of AOT employed was 3 mM (above the cmc) sufficient to form a surfactant monolayer. Table 8.1 lists the observation of 0.65 cS PDMS oil spreading behaviour on AOT aqueous solutions. In comparison, the spreading behaviour of a larger PDMS oil (50 cS) in the same system is also shown. For 0.65 cS PDMS oil, the oil spreads fast initially and no oil lens was observed after one hour at all salt concentrations investigated. For 50 cS PDMS, the oil spread initially and retracted to oil lenses that then spread slowly. Interference colours were observed in the process. After an hour, oil lenses spread and left a clean surface for higher salt concentrations (above 0.025 M), whereas the oil lenses remained for lower salt concentrations (below 0.02 M). The initial spreading and retraction behaviour is similar to that of benzene on a pure water surface where the mutual solubility between benzene and water is appreciable.[9] The later slower spreading of the oil lenses may be due to low molecular weight PDMS homologues.

Table 8.1 Spreading of silicone oils on 3 mM AOT surfaces

0.65 cS	[NaCl]/M	0 - 0.1		
	initially	oil spread fast, interference colours observed, no oil lens seen		
	1 hour later	clean surface left, no oil lens observed		
50 cS	[NaCl]/M	0 - 0.02	0.025 - 0.04	0.06 – 0.1
	initially	oil spread fast with interference colours, retracting to flat oil lens		
	1 hour later	less flatter oil lens, and small patches of oil with interference colours	no oil lens, interference colours near the edge of the teflon dish	clean surface left, no oil lens, no interference colours

8.3 Effect of electrolyte concentration on the spreading coefficients

The initial and equilibrium spreading coefficients could explain the spreading behaviour of the oil on surfactant solutions. To obtain the spreading coefficients, we need to know the air-oil, air-water and oil-water interfacial tensions. The air-oil and oil-water tensions were discussed earlier (see chapters 5 and 6). The air-water tension with and without oil was measured using the du Noúy ring attachment method. Figure 8.1 shows how the air-water surface tension varies with salt concentration in the presence and in the absence of 0.65 cS PDMS oil. In the absence of oil, the surface tension falls as the salt concentration increases and levels off at 0.02 M NaCl. This is because the repulsion between surfactant head groups is reduced by electrolyte. Therefore, surfactant molecules at the surface

Figure 8.1

Air-water surface tension versus [salt] for 3 mM AOT aqueous solutions in the presence and absence of a liquid drop of 0.65 cS PDMS at 25°C

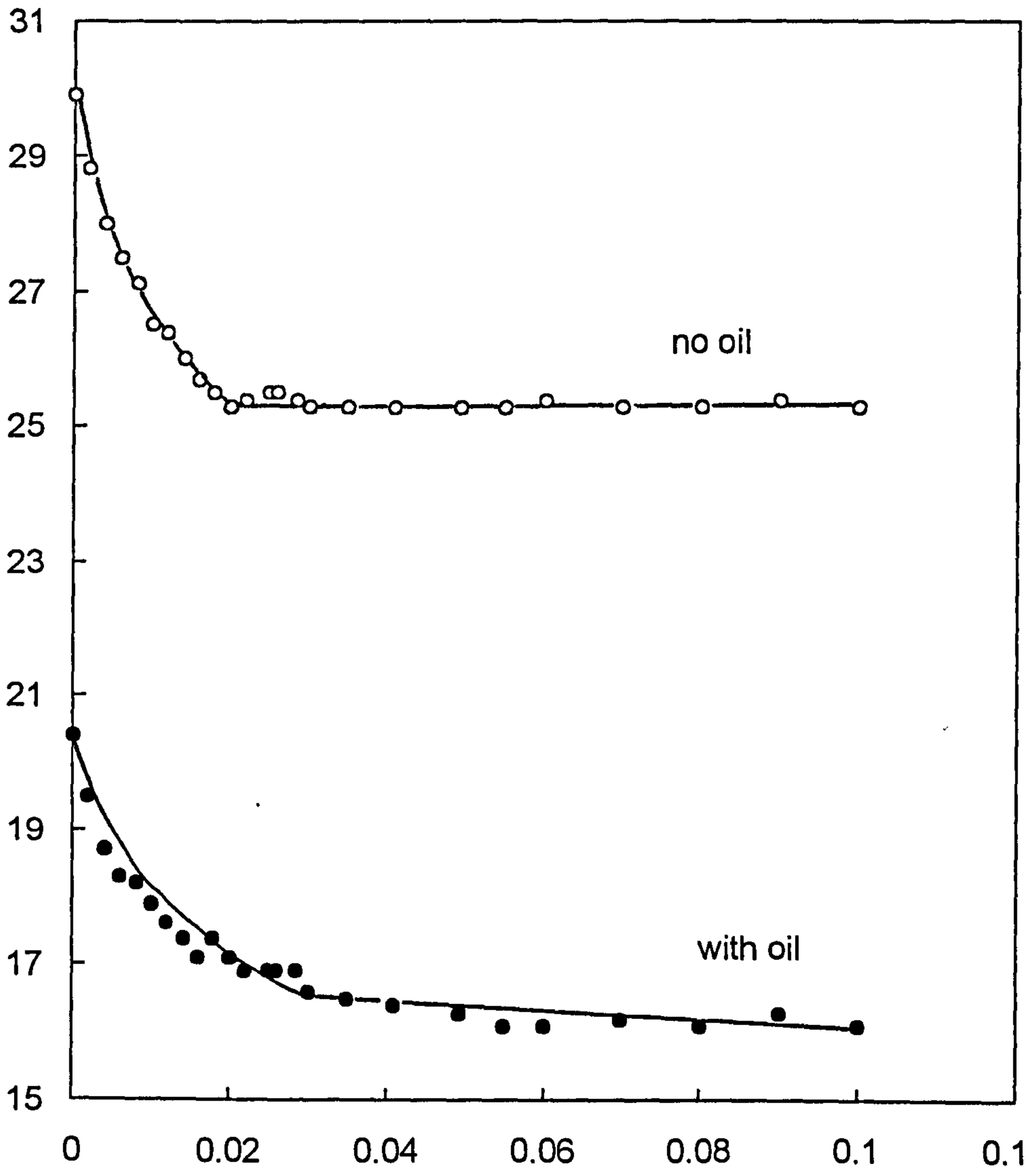

become closer packed which is responsible for the tension reduction. The adsorption of oil causes a lowering of surface tension, such that for [NaCl] ≥ 0.04 M the tension is very close to the surface tension of the oil phase (16 mN m^{-1}). The initial spreading coefficients (S_i), calculated from the three tensions, are all positive with the largest change in magnitude occurring between pure water and 0.01 M NaCl (Figure 8.2). Excluding the case in the absence of salt, the equilibrium spreading coefficients (S_e) lie around zero indicating equilibrium spreading occurs. This finding is analogous to the previous study of cyclohexane spreading on AOT solutions.[42]

8.4 Effect of electrolyte concentration on 0.65 cS oil adsorption

8.4.1 Oil adsorption isotherms

The surface concentration of the adsorbing oil, Γ_o, can be obtained from the measurement of $\Delta\gamma$ (the difference in surface tension with and without the presence of oil) as a function of the oil activity, a_o, as described earlier. Using the vapour adsorption apparatus, we have determined the complete isotherms for the adsorption of 0.65 cS PDMS on AOT monolayers as a function of salt concentration. A selection of these are shown in Figure 8.3, including the adsorption onto a pure water surface (without surfactant). In replacing a pure air-water surface by one coated with an AOT monolayer, the adsorption of PDMS is reduced at all activities. On addition of NaCl to AOT systems, the isotherms move down to lower oil surface pressure initially (0-0.02 M) and then rise again between 0.04-0.1 M NaCl. The $\Delta\gamma/a_o$ data has been fitted and differentiated to yield values of Γ_o (Figure 8.4). As described

Figure 8.2

Spreading coefficients versus salt concentration for 3 mM AOT with 0.65 cS liquid PDMS at 25°C

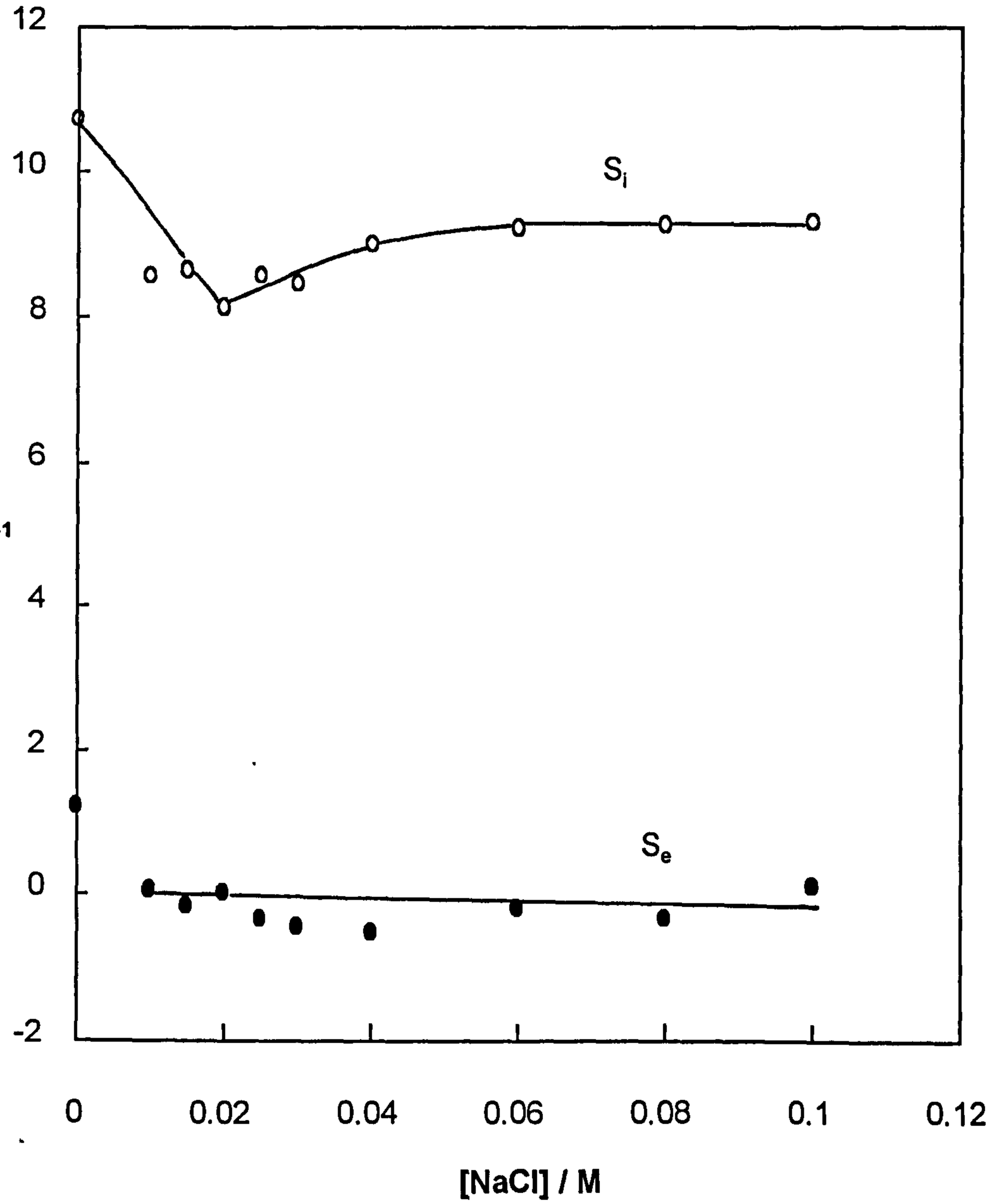

Figure 8.3

Lowering of surface tension with activity of 0.65 cS PDMS oil vapour for pure water and 3 mM AOT monolayers at 25°C

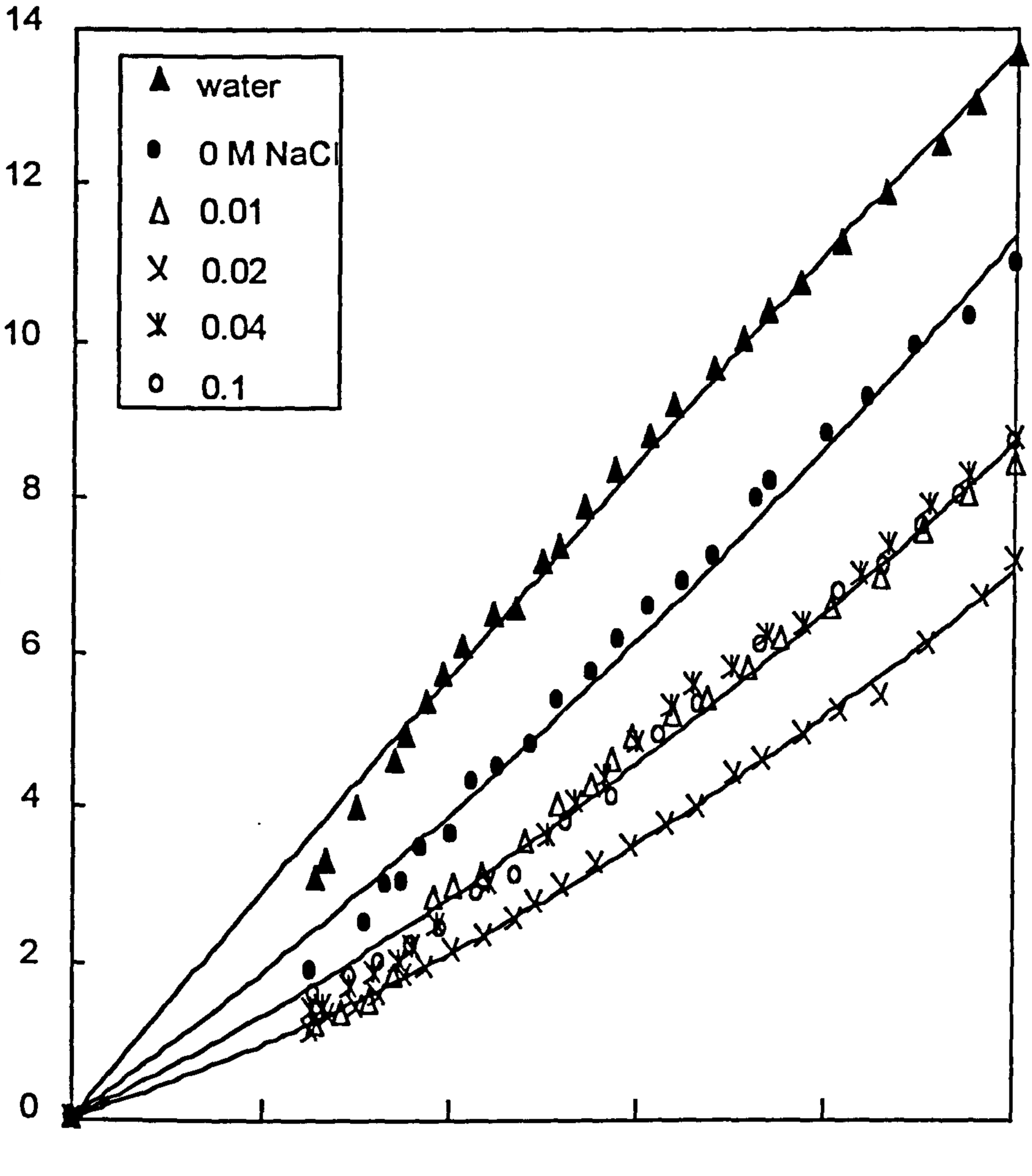

Figure 8.4

Surface concentration of 0.65 cS PDMS oil as a function of oil activity on water and AOT monolayers at 25°C

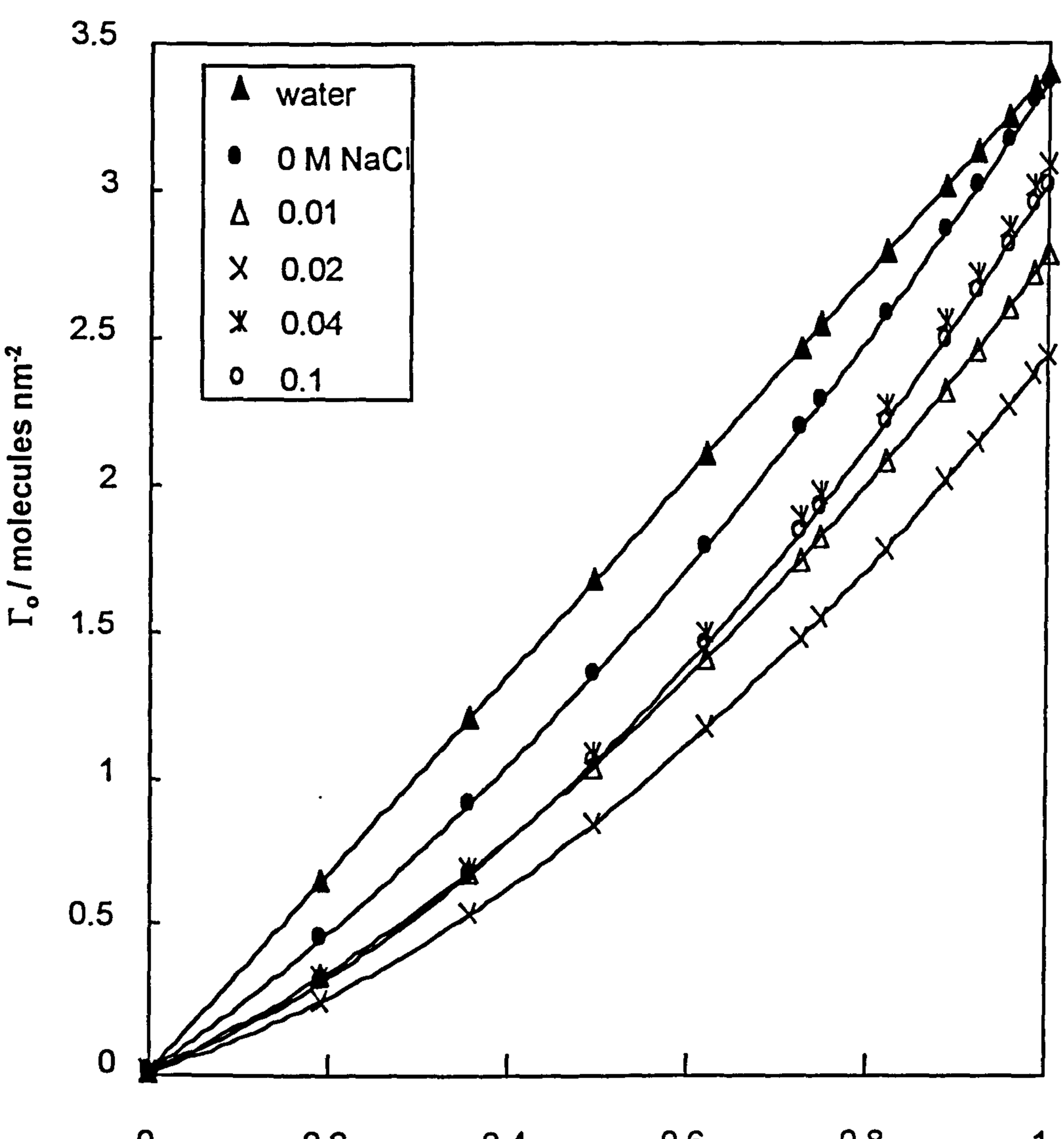

earlier, without surfactant the adsorption isotherm of 0.65 cS PDMS on a pure water surface is ideal, and approximately 3.4 molecules of oil are adsorbed per nm^2 of surface at unit activity, which amounts to a thickness of 1.2 nm. In the presence of surfactant, the situation is more complicated. Unlike on $C_{12}E_5$ surfaces where ideal mixing of surfactant and oil occurred, the isotherms on all salt concentrations of AOT solutions are of the type III of the empirical classification according to Brunauer *et al.*[9] indicating multilayer adsorption.

In the previous study of alkanes with surfactant solutions[42, 49], it has been seen that the chain/air surface in the mixed monolayer is energetically similar to the surface of pure alkane. Binks *et al.*[49] studied the mixing of alkanes and AOT at the air-water surface in detail both by tensiometry and neutron reflectivity. For spreading oils e.g. octane and decane, the adsorption of oils onto surfactant monolayer-coated solution surfaces was depicted as a two stage process. Firstly, oil is adsorbed into the surfactant monolayer to form mixed films in which the oil does not extend significantly beyond the region of hydrophobic surfactant chains. This first stage of adsorption was denoted as the "chain mixing" where the oil adsorption isotherm obeys Henry's law. The second stage was described as film thickening where oil films formed on the top of the mixed monolayer when the oil activity approaches unity (donated here as "oil film adsorption"). Sharp increases in surface pressure were observed at this stage. For dodecane only mixed monolayer formation was observed and the surface pressure caused by the adsorption of dodecane is low. For PDMS adsorbing onto aqueous AOT solutions, Lee *et al.*[59] studied the higher molecular weight

(~84,000) PDMS-AOT films at air-water interfaces by neutron reflectivity and found that the PDMS oil formed a separate layer on top of the AOT monolayer rather than penetrated into it. For a small oil such as 0.65 cS PDMS, firstly oil may penetrate into the surfactant monolayer which will change the area occupied by the surfactant. Secondly, oil may form a duplex layer on top of the mixed monolayer of surfactant and oil. It is not possible to describe the exact structure without the direct measurement for example by neutron reflectivity. However, at unit activity of vapour, the maximum value derived from the isotherms Γ_o is shown in Figure 8.5 as a function of salt concentration. The minimum in Γ_o occurs at 0.02 M NaCl. We will explain this behaviour later.

8.4.2 Correlation between tension lowering and oil-water tension

The lowering of the surface tension of AOT solutions caused either by the presence of a liquid drop of 0.65 cS PDMS oil or by vapour at unit activity is shown in Figure 8.6. Although the error on each point is $\pm$ 0.2 mN m^{-1} and the magnitude in the two sets of data is slightly different, $\Delta\gamma$ appears to decrease initially and then increase to a plateau value at high [salt]. This minimum is distinctive.

It was argued previously that the mixing of surfactant and oil at the air-water interface and at the oil-water interface is related, and the oil-water interfacial tension plays a role in oil adsorption in AOT monolayers. Figure 8.7 shows the variation of the surface concentration of oil with [salt] for selected alkanes and 0.65 cS PDMS oil. In each case, the variation of the oil-water interfacial tension is also shown. For cyclohexane which does not

Figure 8.5

Variation of Γ_o at unit activity (0.65 cS) with [NaCl] at 25°C

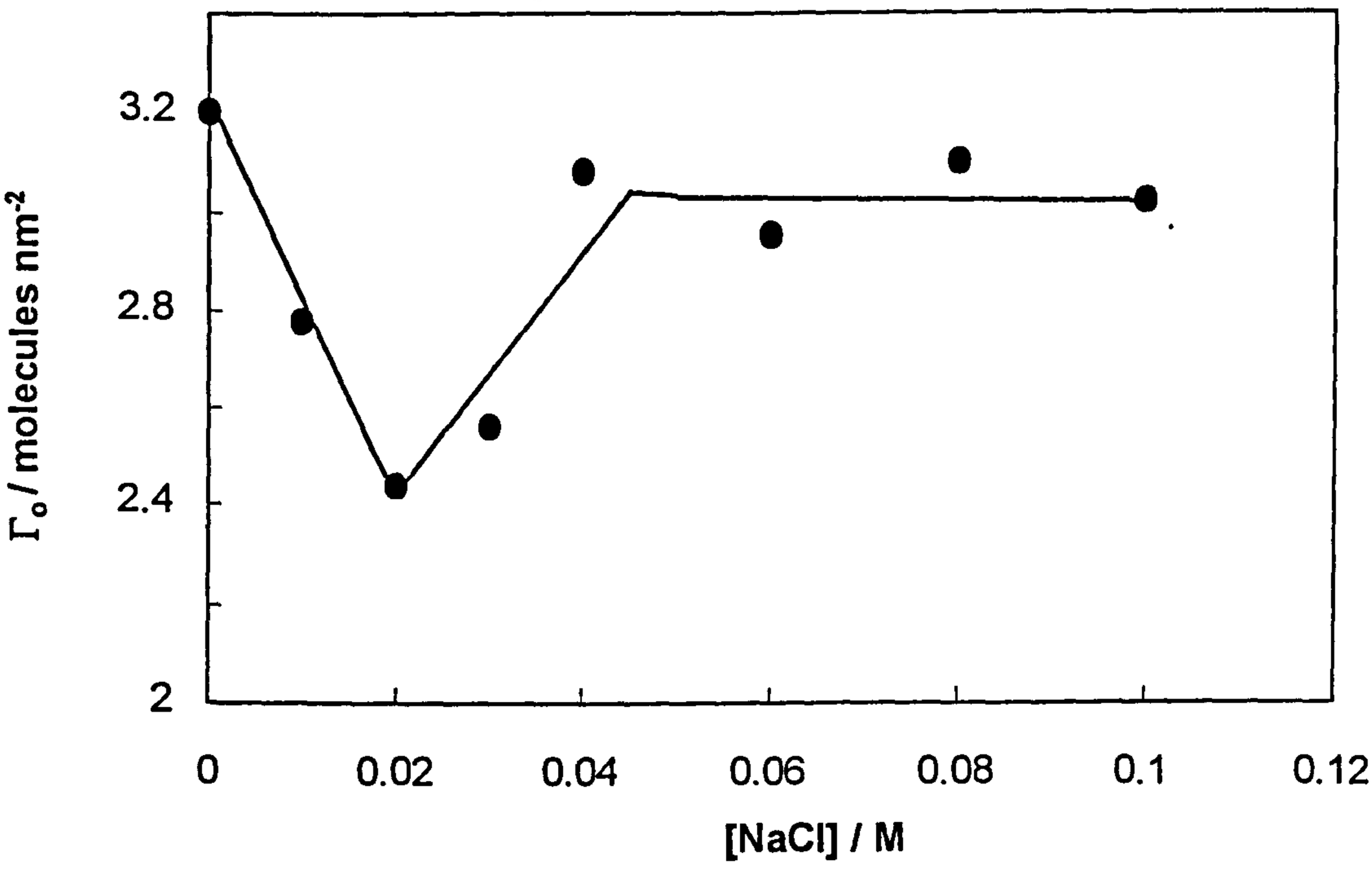

Figure 8.6

Lowering of surface tension caused by the presence of liquid (▲) or 0.65 cS PDMS vapour at unit activity (Δ)

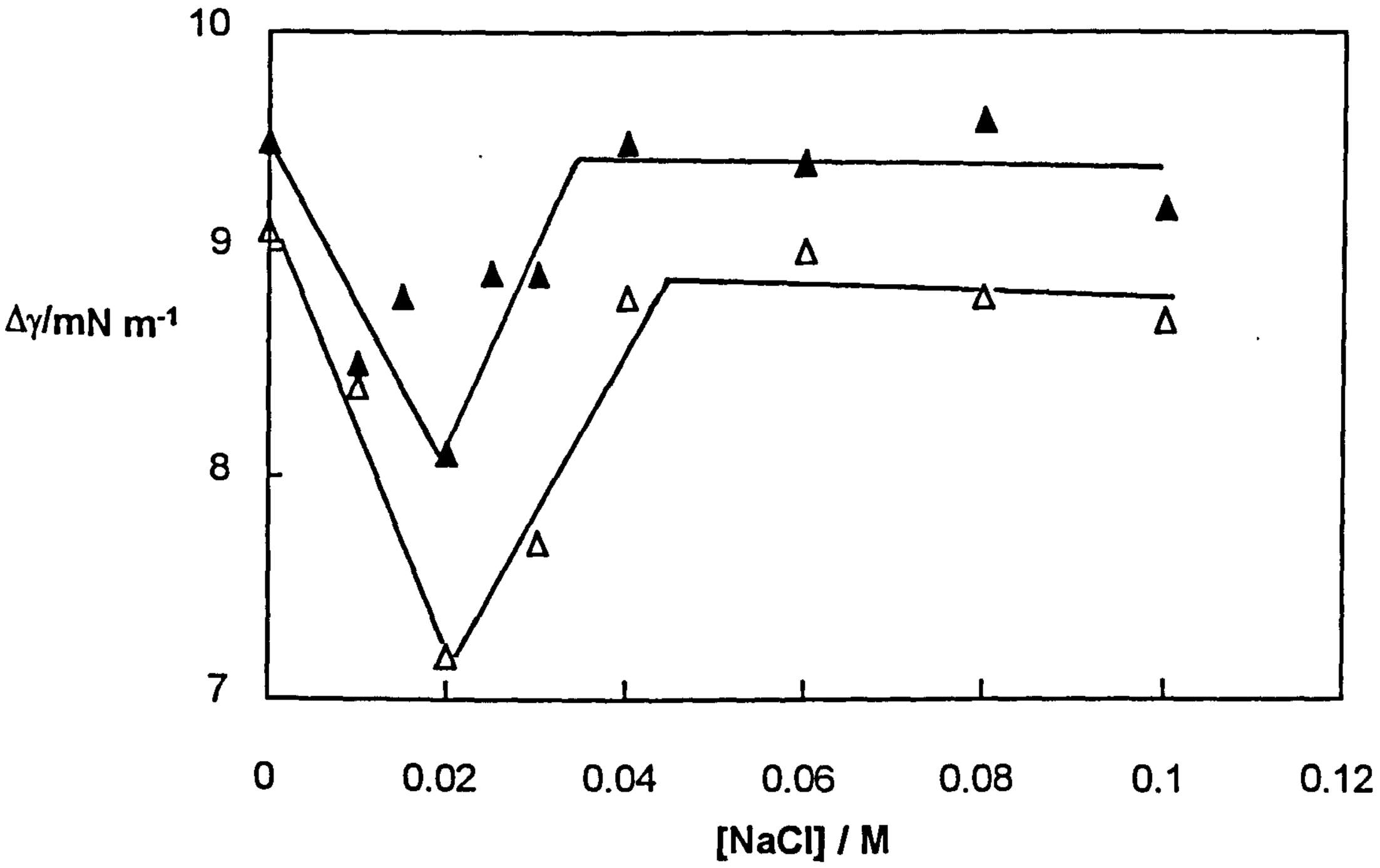

spread on AOT aqueous solutions,[42] the [salt] at which Γ_o become constant corresponds to the formation of the three phase region where the oil-water tension reaches a minimum. This implies that cyclohexane penetration at the air-water surface is similar to that at the oil-water interface. For octane and decane which spread on AOT monolayers, as salt concentration increases, the surface concentration of oil has a maximum when the oil-water tension approaches the minimum.[49] It was shown that an oil film formed on top of the mixed surfactant-oil monolayer. The maximum film thickness is obtained at the [salt] at which the minimum oil-water tension is found. The equilibrium film thickness at unit relative pressure (a_o = 1) has been determined using ellipsometry for similar systems.[45, 175] It was found that the film thickness was maximum when the (ultralow) oil-water tension was minimum. This behaviour was interpreted in terms of contributions to the film disjoining pressure arising from dispersion forces, a steeply decaying short range force of unspecified origin and undulation forces. Undulation forces are due to the suppression of the amplitude of thermal fluctuations of a low tension interface when in close proximity to a hard wall. For oil films on AOT monolayers, the undulation force comes from the interaction of the low tension, undulating AOT monolayer at the oil-water interface pressing against the high tension ("hard wall") oil-air interface. For such a system the contribution, Π_{und}, of the undulation force to the overall disjoining pressure is[45]

$$\Pi_{und} = \frac{k_B T \gamma_{OW}}{2h\pi^2 K\left[\left(\exp\frac{4\pi\mu h^2\gamma_{OW}}{k_B T}\right)-1\right]} \qquad (8.1)$$

Figure 8.7

Correlation between the maximum oil surface concentration (filled points) and oil-water interfacial tension (open points) as a function of [salt] for oils and 3 mM AOT systems at 25°C

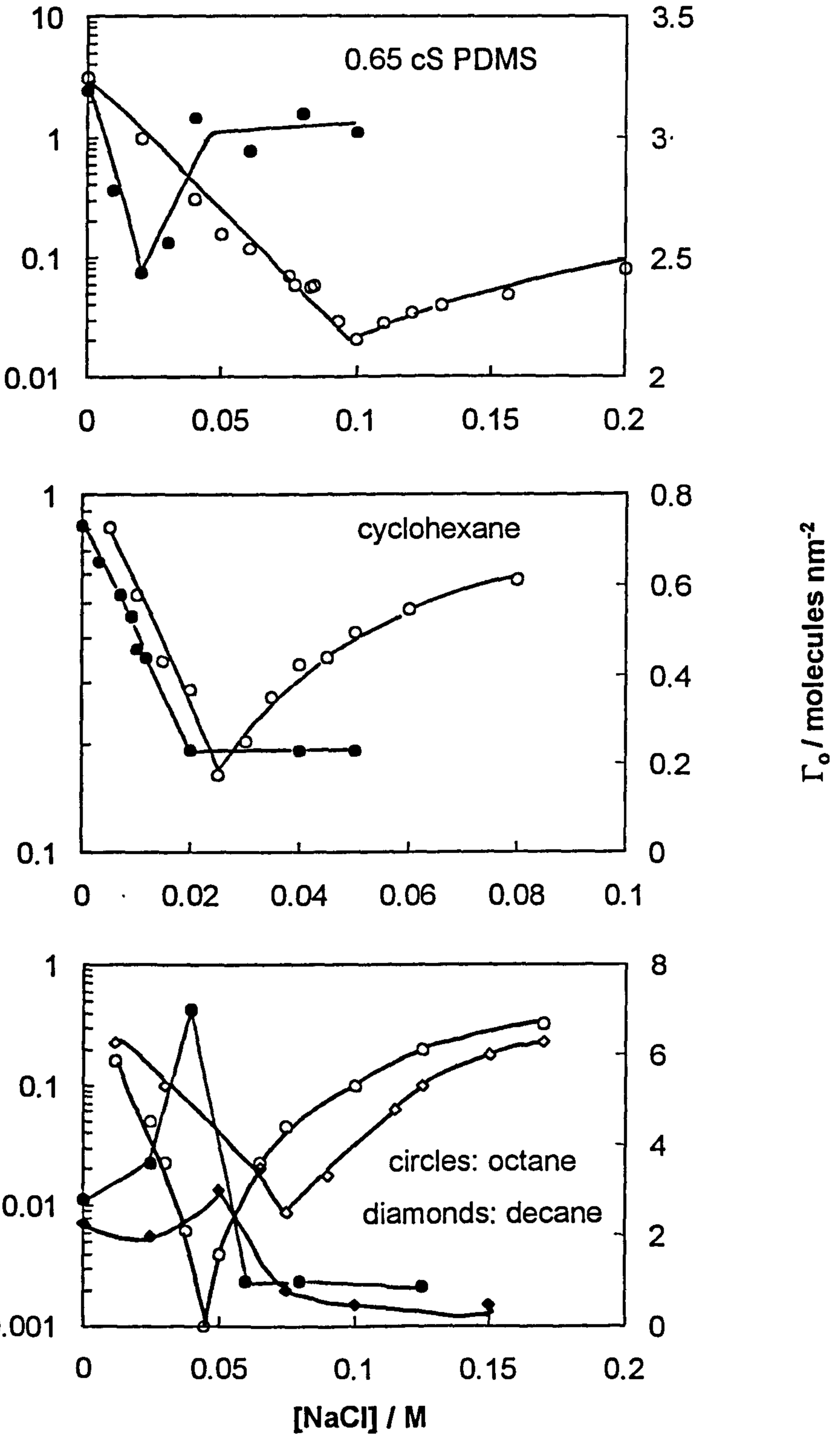

where γ_{ow} is the oil-water tension, h is the equilibrium film thickness, K is the monolayer bending elastic modulus and μ is a numerical constant approximately equal to 1/6. Thus, the repulsive undulation force depends on the bending elastic modulus and the magnitude of the oil-water tension.

For the situation of 0.65 cS PDMS oil, a minimum in oil surface concentration is found at 0.02 M NaCl, which is much lower than the [salt] where the minimum in the oil-water tension occurs (0.1 M). We recall that up to 0.1 M NaCl, Winsor I systems were formed in the multiphase systems. Thus, the changes in the extent of mixing seen arise well before the transition to a three phase region. The initial reduction in $\Delta\gamma$ with [salt] can be understood in the way that the area per surfactant molecule is reduced due to screening with a concomitant reduction in the surface solubilisation of oil. In other words, "chain mixing" plays a major role. The subsequent increase in $\Delta\gamma$ upon further salt addition may be interpreted as the presence of an oil adsorption film which is thickening as undulation force occurs due to the low oil-water tension. As seen from equation 8.1, the magnitude of the undulation force depends on both the oil-water tension and the bending elastic modulus K. For AOT monolayers at the alkane-water interface at 20°C, the value of K has been observed to be independent of salt concentration and to vary with the alkane chain length. The (non re-normalised) values of K/k_BT are 0.83, 0.95 and 0.13 for octane, decane and dodecane respectively.[45, 147] 0.65 cS oil resembles dodecane in mixing with AOT at o/w interface as we discussed earlier, so we could assume that the value of K for 0.65 cS PDMS is low. If this reasoning is correct, we can anticipate that $\Delta\gamma$ will fall again after 0.1 M [NaCl] at which the oil-water

tension minimum occurs. We may say that at low [salt] (0-0.02 M), only "chain mixing" occurs on the adsorption of 0.65 cS PDMS on AOT aqueous solutions, further increase in salt concentration induces "oil film adsorption". However, we should bear in mind that the situation here is extremely complicated due to first of all, the assumption that surfactant activity does not change during the oil adsorption might not be correct. It is true when the solubilisation of oil into surfactant micellar solution is negligible or when the surfactant concentration is below the cmc. Significant solubilisation of 0.65 cS PDMS into 3 mM AOT aqueous solutions was found previously (Chapter 6). Secondly, the van der Waals interaction dominated by the properties of the bulk and the adsorbed film also exists[12] which is even more difficult to quantify since the composition of the film is unknown.

As mentioned earlier PDMS oils spread on both water and organic solvents due to their chain flexibility and low surface tension (16 mN m^{-1}). We can imagine that the conformation of PDMS oils on the different surfaces would not be the same. We may hypothesise in the following way: Below 0.02 M NaCl, PDMS mixes with surfactant molecules and a mixed monolayer is formed. The orientation of the PDMS molecules may be with oxygen atoms towards the water phase and the methyl groups towards air. It may be not only the simple volume filling mechanism but also involve the competition for the water surface between PDMS oil and AOT molecules. Above 0.02 M NaCl, the surfactant monolayer becomes so closely packed that the surface of AOT solutions becomes as hydrophobic as the oil itself. PDMS oil may change its conformation with methyl groups toward the surfactant monolayer and form a thin film. The thickness of this film may

increase as [salt] increases. However, from the adsorption isotherm it can be seen that there is no dramatic increase in Γ_o when unit oil activity is approached, even when the salt concentration is at 0.1 M where the minimum in γ_{ow} occurs. So it is likely there exists a positive undulation force which could thicken the oil film significantly as observed in octane and decane systems. To fully understand the composition of the film and confirm the chain conformational changes in PDMS oils, direct measurements via neutron reflectivity and small angle neutron scattering may be required.

8.5 Correlation between the minimum in the tension lowering and surfactant aggregate structure in bulk

In understanding the mixing behaviour of oil and AOT molecules at air-water surface, one important factor should be taken into account, that is, the structure of AOT aggregates in bulk which is very sensitive to the electrolyte concentration. When oil is present, larger aggregates close to the air-water surface can take up oil and cause turbulence, which may affect the oil adsorption. In this part, we try to understand the minimum in the surface tension lowering of AOT following the adsorption of 0.65 cS PDMS oil from this point of view.

8.5.1 Aggregation of AOT in electrolyte solutions

It is worthwhile summarising the previous studies of the binary phase behaviour of AOT and water. The solubility of AOT in water was found to be about 1.8 wt% (~40 mM) at 30°C, various liquid crystalline phases occur at higher surfactant concentrations beyond this solubility limit. The effect of

electrolyte on the binary phase behaviour of AOT and water is significant. Ghosh and Miller[150] studied the phase behaviour of AOT in aqueous NaCl solutions and found the existence of lamellar phase above 5% AOT at 30°C. With 0.08M NaCl in the system, clusters of monodisperse spherulites were found immersed in an isotropic aqueous phase. The liquid crystalline spherulitic particles increased in number and became more uniformly distributed in the solution as salt concentration increased to 0.2 M NaCl. Bergeron[176] discussed the formation of thick-film regions (microtubes) in thin foam films of 5 mM AOT and 0.1M NaCl. However, no microtubes were found in AOT solutions without salt. Schalchli *et al.*[177] observed vertical soap films of AOT with X-ray reflectivity and found a thick (~9 nm) homogeneous film at the surface of 5 mM AOT solutions with a density about 10% lower than that of the bulk. The thickness of this film was reduced to 8 nm in the presence of 0.017 M NaCl, and increased to 11 nm when the [AOT] was reduced to 0.5 x cmc. The AOT Newton Black Film (thickness 13 nm for 2 x cmc+0.017 M NaCl system) was composed of the bilayers of the thick film rather than surfactant molecular sized bilayers. By contrast, Li *et al.*[178] reported that the structure of AOT at the air-water surface was a surfactant monolayer using neutron reflectivity. The area per surfactant molecule was found to vary between 130-78 $Å^2$ when the concentration of AOT was changed from cmc/300 to the cmc, while the thickness of the monolayer remained virtually constant at 1.8 nm.

Shahidzadeh *et al.*[179] claimed the existence of vesicles which emulsify the oil spontaneously. They brought the vesicular solutions of AOT gently into contact with an oil by means of a micropipette, a flow of the surfactant

aggregates towards the oil phase was observed. The incorporation of the oil into the surfactant bilayers leads to the formation of oil films, with the bilayers that are unstable. The vesicles are consequently destabilised and "explode", thereby dispersing the oil in the aqueous phase. In a system containing 3.2 mM AOT, no vesicles appear below 0.02 M NaCl. Just above 0.02M NaCl the solutions become turbid and vesicles occur. Spherulites and some vesicular structures (cylinder length about 30 μm to 60 μm) were observed by phase contrast microscopy at 0.047 M NaCl. At 0.075 M NaCl, spherical as well as tubular vesicles were observed. After introducing a drop of alkane, due to the incorporation of the alkane in the bilayer, the vesicles swell and burst, spontaneously emulsifying oil in water. The spontaneous emulsification phenomenon was addressed in nonionic surfactant systems as well earlier.[180] In summary, vesicular or liquid crystalline structures exist in AOT water solutions slightly above the cmc; the addition of NaCl promotes and stabilises these structures which emulsify the oil spontaneously.

On preparing 3 mM AOT aqueous solutions, the AOT solutions became cloudy at and above 0.02 M NaCl. Figure 8.8 shows the turbidity of these solutions as a function of [NaCl]. The variation of the cmc[149] of AOT in water with [NaCl] and the appearance of vesicles observed by microscopy is also shown. Observations by phase-contrast microscopy show that just above the cmc large aggregates made up of surfactant bilayers appear in the solution (shown as filled circles in Figure 8.8)[179] There is a good agreement between the cmc measured by tensiometry and the appearance of vesicles seen by microscopy. The sharp increase in turbidity at 0.02 M NaCl is in line with the observation of vesicles by microscopy.[179] It can be

Figure 8.8

Variation of turbidity (triangles) and cmc (open circles) of 3 mM aqueous AOT solution with salt concentration. Filled circles correspond to concentrations for which vesicles start to appear, below which no vesicles were observed by microscopy

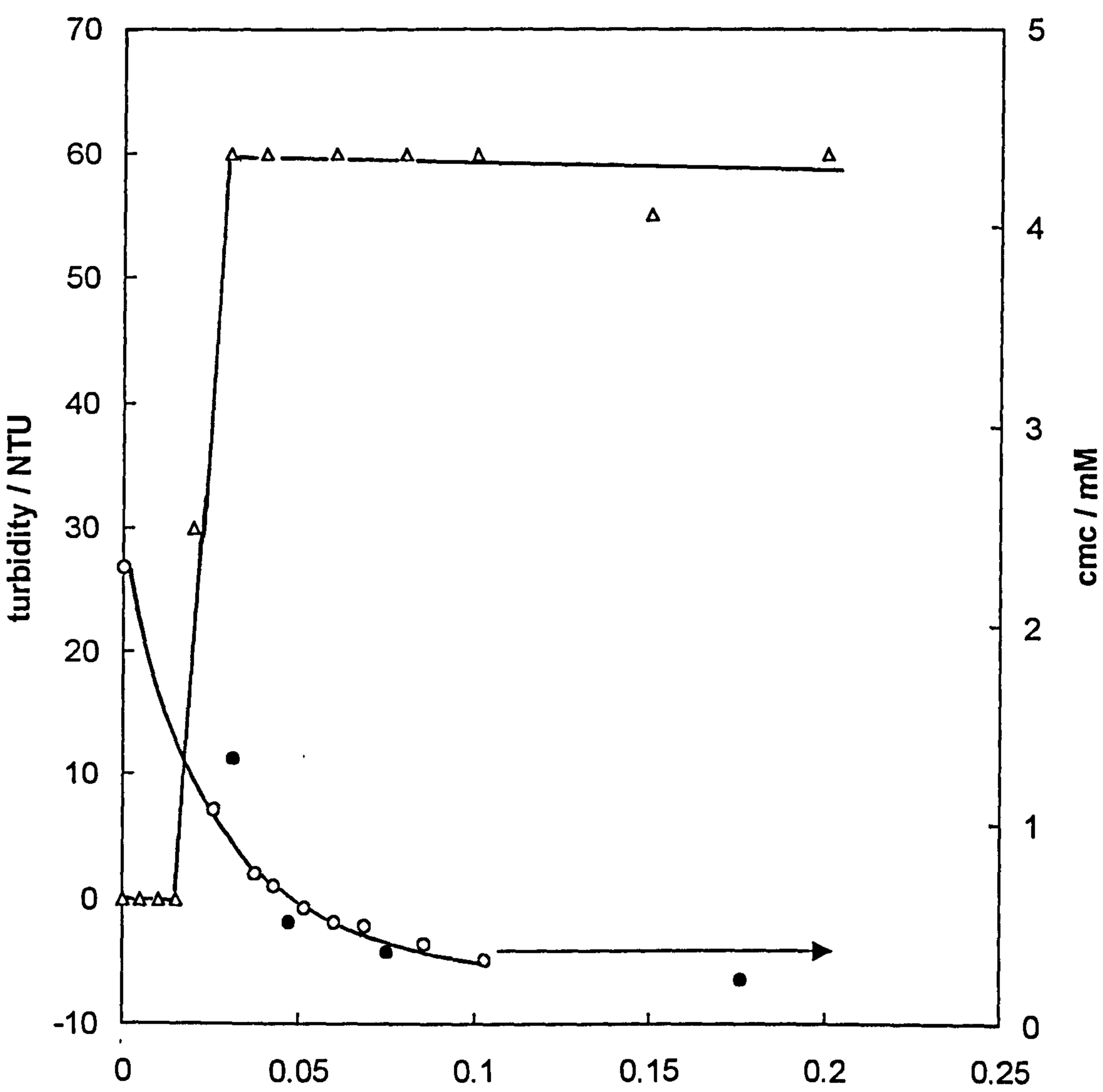

rationalised that below 0.02 M NaCl, the aggregates of AOT are micelles which do not scatter the light and the solutions are clear. Above 0.02 M NaCl, large size vesicles formed and are in equilibrium with the micelles, which cause the turbid appearance of the solutions. Interestingly, the salt concentration here is exactly the [salt] of the minimum in $\Delta\gamma$ observed earlier. For fixed AOT concentration, increasing the electrolyte concentration results in a decrease in the cmc of AOT. Therefore, AOT aggregates (vesicles) increase in size and number. If the vesicles incorporate 0.65 cS PDMS oil and burst in the bulk phase, this process is accompanied by considerable turbulence, which may affect the adsorption of oil into the surfactant monolayer.

8.5.2 Effect of surfactant concentration on $\Delta\gamma$

The question that arises now is: if the vesicles can be removed from the bulk, will the minimum in $\Delta\gamma$ still exist? To address this question, two sets of experiments were carried out. Firstly, the concentration of AOT is reduced to exactly the cmc at each [salt]. The cmc of AOT at each [salt] was taken from reference 149 in which heptane was used. The results are shown in Figure 8.9. Although all the solutions were clear (turbidity < 10 NTU) the minimum in $\Delta\gamma$ still exists but is shifted to higher [NaCl]. Secondly, in Figure 8.10 we see that when the [AOT] is reduced slightly below the cmc (65 % cmc) where a close-packed surfactant monolayer still exists, the minimum disappears. Figure 8.11 shows the comparison of the tension lowering by 0.65 cS PDMS oil in the various surfactant-containing systems. Again, obviously, the apparent minimum in the systems with [AOT] above and at the

Figure 8.9

Air- water surface tension versus [salt] for cmc AOT aqueous solution in the presence and absence of a liquid drop of 0.65 cS PDMS at 25°C

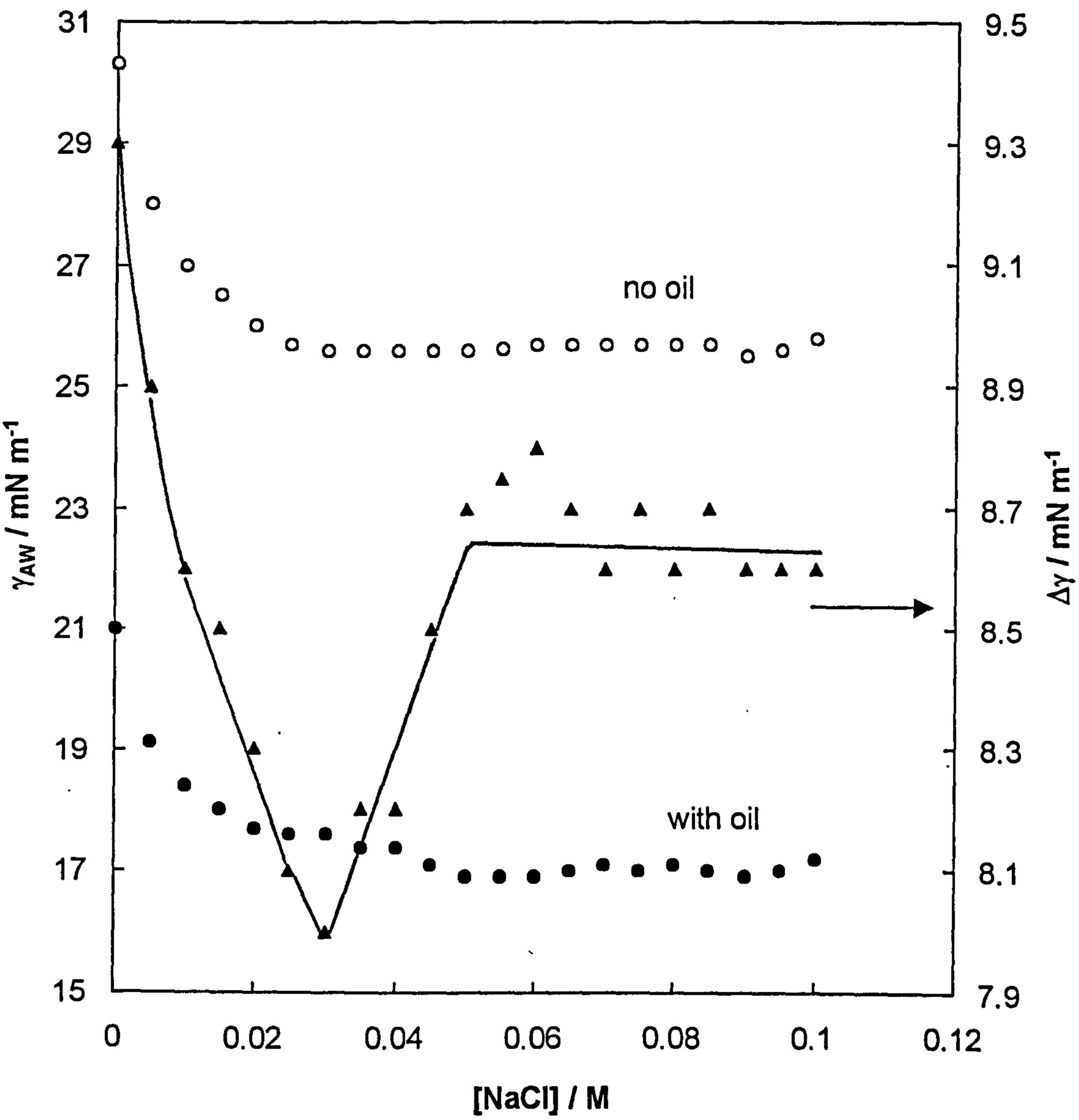

Figure 8.10

Air- water surface tension versus [salt] for 65% cmc AOT aqueous solution in the presence and absence of a liquid drop of 0.65 cS PDMS at 25°C

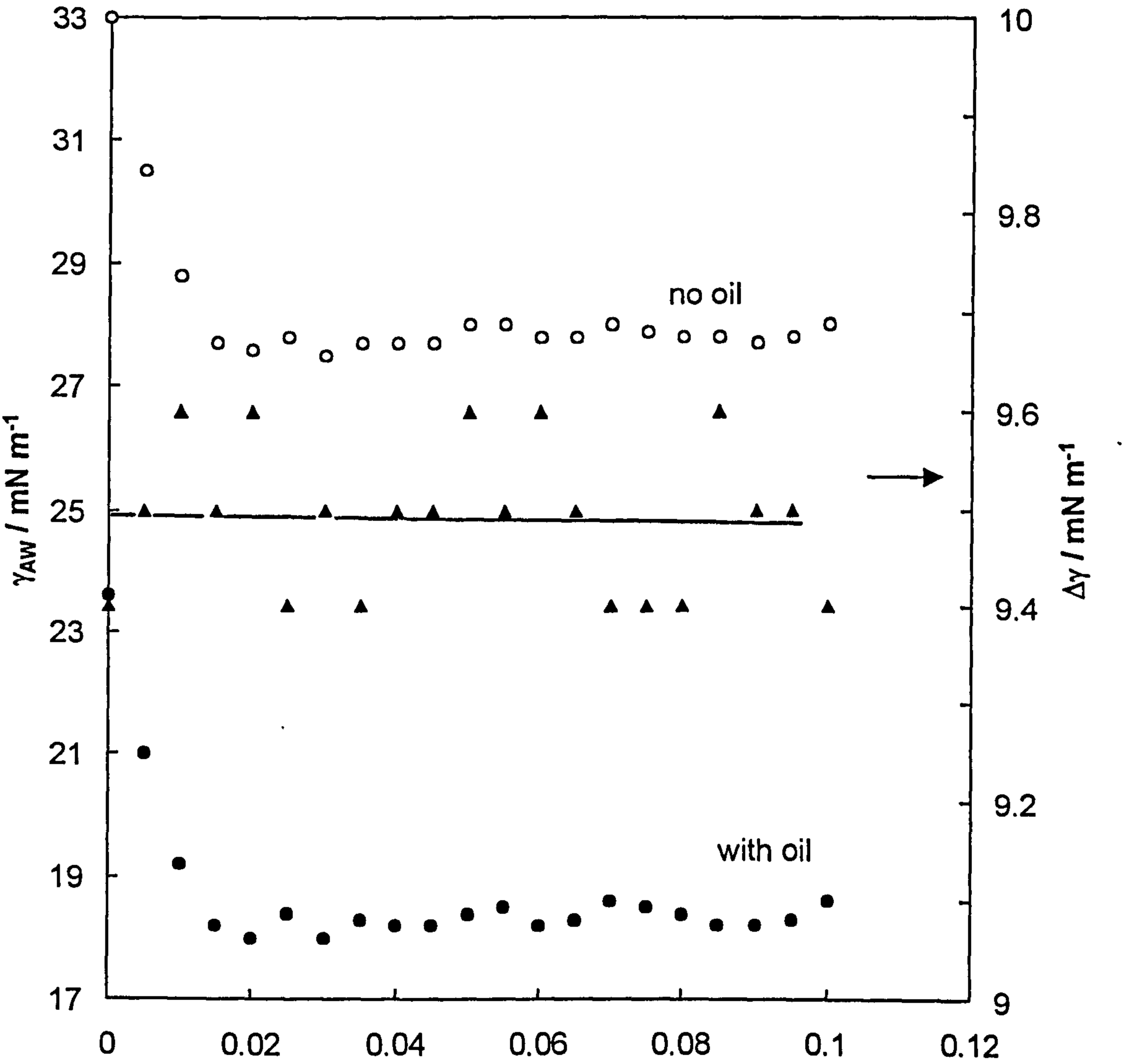

Figure 8.11

Comparison of $\Delta\gamma$ in the various surfactant-containing systems in the presence of a liquid drop of 0.65 cS PDMS at 25°C

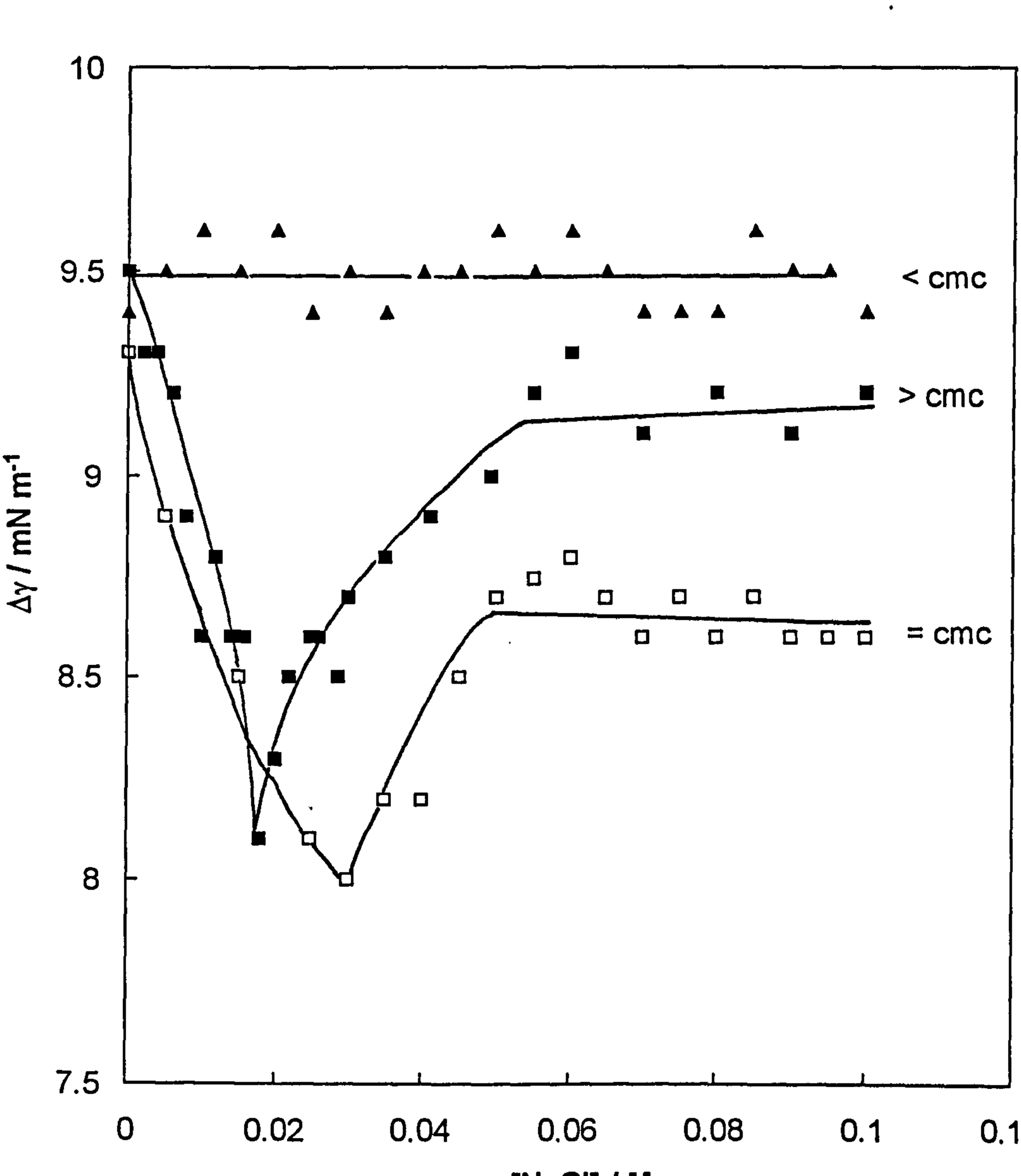

cmc is not apparent in the systems with [AOT] below the cmc. So it is likely that the minimum in $\Delta\gamma$ is related to the vesicles of AOT in the bulk phase.

8.5.3 Effect of equilibrium on the minimum in $\Delta\gamma$

Given the spontaneous emulsification of oil by AOT vesicles is a kinetic process, it is also tempting to know what happens if we allow vesicles to incorporate a sufficient amount of oil before the air-water mixing experiment is carried out. In other words, adding oil to the microemulsion surface instead of the surfactant solution surface. Therefore, the aqueous electrolyte phases with 3 mM AOT and 0.65 cS PDMS oil were first equilibrated (gentle mixing provided occasionally) for 2 days and the surface tension of the pre-equilibrated aqueous phase was then measured. The vapour space above the solution remained saturated with 0.65 cS PDMS oil throughout the measurement. The results are shown in Figure 8.12. As expected, there is no minimum found in the tension lowering as [NaCl] increases. The lower magnitude of $\Delta\gamma$ than that of the non-preequilibrated system may indicate that the monolayer at the air-microemulsion surface is not a pure surfactant, but a mixture of surfactant and oil. This is understandable in the case of PDMS oil since PDMS competes for the surface with surfactant as shown earlier. When the excess oil phase was removed from the equilibrated two phase oil-o/w microemulsion systems, the curved droplets of the microemulsion moved to the air-water surface and create the new flat surface. PDMS molecules could adsorb at the pure water surface and occupy part of it. This means that the surface concentration of surfactant is reduced compared to that of pure surfactant solutions.

Figure 8.12

Comparison of $\Delta\gamma$ in pre-equilibrated (circles) and non-preequilibrated (triangles) oil and 3 mM aqueous AOT phases at 25°C

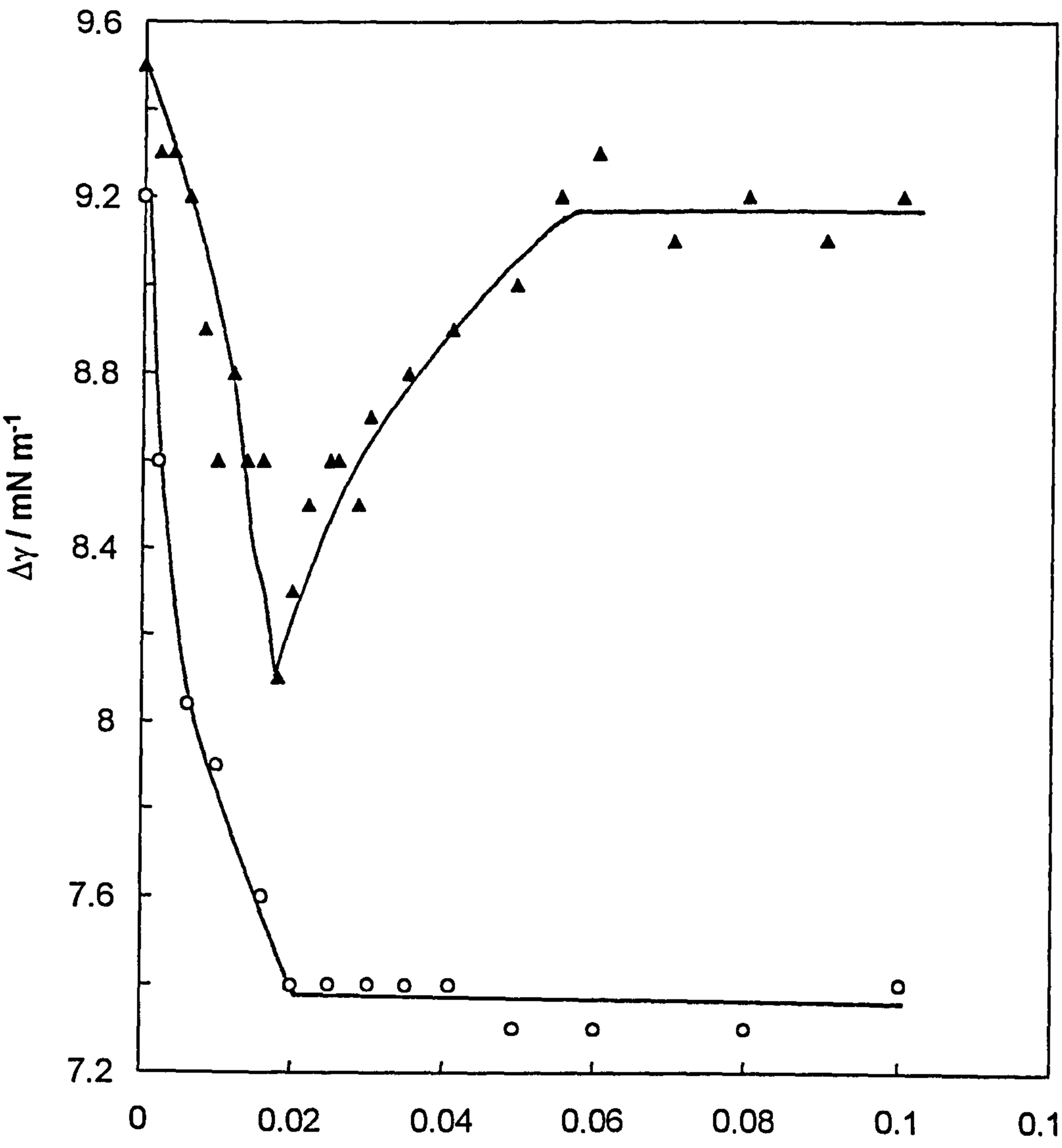

Therefore, the solubilisation of oil into the surfactant monolayer at the air-water surface is expected to be reduced which is responsible for the reduction in $\Delta\gamma$.

It is likely that the surface tension lowering of AOT solutions at and above the cmc is closely related to the formation of vesicles in the bulk aqueous phase. The vesicles can incorporate oil which affects oil adsorption into the surfactant monolayer at the air-water surface.

8.6 Conclusions

(i) 0.65 cS PDMS oil spreads on aqueous AOT solution surfaces over a wide range of bulk electrolyte concentrations. All the initial spreading coefficients are positive and the equilibrium spreading coefficients are close to zero as the bulk salt concentration varies.

(ii) By variation of the oil activity, we quantified the surface concentration of oil and found a minimum in oil surface concentration as the concentration of salt increases. The minimum in $\Delta\gamma$ occurred at much lower salt concentration than that the minimum in oil-water tension occurred

(iii) In understanding the minimum in $\Delta\gamma$, possible reasons such as the existence of a transition from "chain mixing" to two stage oil adsorption, the change in PDMS oil conformation as salt concentration increases, the presence of surfactant aggregates in the bulk are discussed. However, direct neutron reflectivity measurements are required to confirm these findings.

CHAPTER NINE

CHAPTER 9

Overall Conclusions and Summary

The interactions of PDMS oils and surfactant at oil-water and air-water interfaces have been investigated. The results obtained may be conveniently summarised as follows:

(i) In systems containing PDMS oil, water and nonionic surfactants, macroemulsions undergo phase inversion with an increase in temperature. The PIT increases as the surfactant headgroup size increases and decreases as the surfactant chain length increases. Adding a lyotropic electrolyte such as sodium chloride in the system reduces the PIT while a hydrotropic electrolyte such as TBAB raises the PIT. The effect of the increase in the molecular weight of PDMS oil on the PIT is not significant. By using an extended surfactant such as $C_{16}P_8E_1$ very low conductivity (< 5 μS cm^{-1}) emulsions were found, indicating complete phase inversion. However, the silicone surfactant Silwet L-77 does not appear particularly different from $C_{12}E_5$ in the emulsion phase inversion behaviour.

(ii) The equilibrium phase behaviour of the systems containing PDMS oils, water and nonionic surfactants shows clear Winsor phase transitions as the system HLB varies. However, the extent of Winsor III systems is very wide with respect to both the temperature and electrolyte concentration. The third phase is mainly water+surfactant in the case of $C_{12}E_3$. By contrast, it is

mainly oil+surfactant in the case of $C_{16}P_8E_1$. Little solubilisation of 50 cS PDMS oil in the third phase was found in both systems. In the system 50 cS PDMS oil+$C_{12}E_3$+H_2O using TBAB as electrolyte, we found that the electrolyte switches from hydrotropic at low concentrations to lyotropic at higher concentrations. The transition concentration is about 0.5 M at 50 °C. The cloud point of $C_{12}E_5$ and L-77 can be raised by solubilisation of small PDMS oils, indicating the solubilisation of low molecular weight silicone oils into aqueous surfactant micellar solutions. When 50 cS PDMS oil was employed, little change in the cloud point of $C_{12}E_5$ was found. On the other hand, there is significant solubilisation of amino-functionalized PDMS oil (viscosity ~1,500 cS) into L-77 aqueous solutions, which affects the cloud point of L-77, mirrored by the change in the solution viscosity.

(iii) At the air-water surface of nonionic surfactant solutions, PDMS oils spread macroscopically. The initial spreading coefficients are positive. The equilibrium spreading coefficients are all close to zero indicating the spreading status at equilibrium. The surface pressure caused by the adsorption of PDMS oils is related to the surfactant structure. Changing the surfactant headgroup size has a significant effect on the surface pressure, while the effect of surfactant chain length is negligible. The surface pressure of the oil decreases as the viscosity of PDMS oils increases up to 50 cS, then levels off on further increase of the oil viscosity. With volatile PDMS oils, the oil adsorption isotherm can be measured via the vapour adsorption apparatus made in house. On a pure water surface, the spreading of 0.65 cS PDMS oil is ideal, with a thin film of 1.2 nm thickness being formed. In the

presence of surfactant (e.g. $C_{12}E_5$ above cmc), a mixed monolayer composed of approximately 1:1 molar ratio of surfactant and oil is formed. Moreover, we also investigated the effect of the presence of a liquid drop of 50 cS PDMS oil on the adsorption of surfactants. For $C_{12}E_5$, where the oil spreads on all the surfactant concentrations, the surface concentration of surfactant is reduced substantially while leaving the cmc unchanged. There exists a competition for the surface between oil and surfactant. For L-77, no lowering of the tension occurs on addition of oil up to at least 1/50 of the cmc. Oil remains as a flat circular lens on the surface.

(iv) In systems of PDMS oil, water and AOT, at equilibrium the classical Winsor phase sequence was found with respect to [NaCl]. The location of AOT aggregates was determined by the two-phase titration method. The third phase in the Winsor III systems is the lowest phase when the electrolyte concentration is low, and then becomes the middle phase when the [NaCl] is sufficiently high. In Winsor II systems, the solubilisation of water in the w/o microemulsions falls as the salt concentration increases. Very close to the onset of the Winsor III systems, a minimum in the oil-water interfacial tension was found. As the temperature increases, the minimum in the tension moves to higher electrolyte concentration which is associated with the counter-ion dissociation which is endothermic. The increase in the viscosity of PDMS oils results in a higher minimum interfacial tension at higher [salt]. These findings are all consistent with the findings in alkane oil systems.

Studies of the single phase microemulsions (both o/w and w/o) have demonstrated that either o/w or w/o microemulsions with low molecular silicone oil can be formed. For w/o microemulsions, a maximum in the water solubilisation capacity is shown in the R_W~T plot. Adding salt in the dispersed aqueous phase shifts the maximum to higher temperature but lower values. A clear oil phase coexists with a surfactant rich phase which solubilises all the water above the haze boundary. The plot of R_W~[NaCl] also shows a maximum water solubilisation, which can be moved to higher [NaCl] at higher temperatures. The maximum corresponds to the minimum in the oil-water interfacial tension. For o/w microemulsions, the R_O~T phase diagram shows limited solubilisation of the oil in aqueous micelles without electrolyte. Adding NaCl improves the solubilisation of oil but needs higher temperature. A narrow single phase microemulsion region has been found in the R_O~[NaCl] phase diagram. These electrolyte and temperature effects are also observed in alkane systems.

(v) Emulsions made from the equilibrium phases of 0.65 cS PDMS oil-water-AOT systems are of the same type as that of the microemulsions. The study of the stability of the emulsions has been restricted to creaming or sedimentation processes. In Winsor I systems we find a distinct maximum in stability with respect to creaming, accompanied by the virtually monodisperse distribution revealed by the emulsion drop size analysis with instability rising towards the Winsor I/III boundary. In Winsor II systems, sedimentation is relatively rapid and virtually independent of salt

concentration. The triphasic emulsions from the Winsor III region are very unstable.

(vi) The mixing of AOT and 0.65 cS PDMS oil at the air-water surface has been investigated with respect to the bulk salt concentration. The studies from both the oil adsorption isotherms on AOT solutions and the tension lowering of the AOT aqueous solutions at unit oil activity (liquid drop on AOT solution surface) show that there is a minimum in the tension lowering as the salt concentration increases. We linked this finding with the formation of vesicles of AOT in bulk.

(vii) A number of avenues have been opened up for future research. From the spreading behaviour of PDMS oils on surfactant solutions studied by tension, neutron reflection can be employed to reveal the composition of the films. The results will allow us to compare and understand the wetting behaviour of alkane and PDMS oils on aqueous surfactant surfaces fully. From the microemulsion formation in PDMS oil systems, other surfactant systems or mixtures can be used to improve the solubilisation capacity for higher molecular weight oils, which has potential importance in industrial applications. From the effect of AOT vesicles on the PDMS oil adsorption, other oil systems such as alkane and fluorocarbon can be examined to provide evidence to explain the relationship of the solubilisation of oil into surfactant monolayers at oil-water and air-water interfaces.

REFERENCES

REFERENCES

1. MS Silicones Technical Data Sheet G1, Midlands Silicone Co., 7th edn. 1964.
2. J.E. Mark, in 'Silicone-Based Polymer Science', eds. J.M. Ziegler and F.W. G. Feron, Washington DC, ACS, 1990, p. 47.
3. P.J. Flory, Statistical Mechanics of Chain Molecules, Wiley-Interscience, New York, 1969.
4. M.J. Owen, in 'Silicon-Based Polymer Science', eds. J.M. Ziegler and F.W.G. Feron, ACS, Washington DC, 1990, p. 705.
5. H.W. Fox, P.W.Taylor and W.A. Zisman, *Ind. Eng. Chem.*, **39**, 1401 (1947).
6. M.J. Hunter, E.L. Warrick, J.F. Hyde and C.C. Currie, *J. Am. Chem. Soc.*, **68**, 2284 (1946).
7. W.A. Zisman, in 'Contact Angle, Wettability, and Adhesion', Advances in Chemistry 43, ACS, Washington, DC, 1964, p. 1.
8. J.H. Clint, Surfactant Aggregation, Blackie, Glasgow, 1992.
9. R. Aveyard and D.A. Haydon, An Introduction to The Principles of Surface Chemistry, Cambridge University Press, Cambridge, 1973.
10. D.F Evans and H. Wennerström, The Colloidal Domain, Where Physics, Chemistry, Biology, and Technology Meet, VCH, New York, 1994.
11. C. Tanford, The Hydrophobic Effect: Formation of Micelles and Biological Membranes, 2nd edition, Wiley, New York, 1980.
12. J. Israelachvili, Intermolecular & Surface Forces, 2nd edition, Academic Press, London, 1992.
13. P.A. Winsor, *Trans. Faraday Soc.*, **44**, 376 (1948).
14. A.M. Cazabat, D. Langevin, J. Meunier, and A. Pouchelon, *Adv. Colloid Interface. Sci.*, **16**, 175 (1982).
15. R. Aveyard, B.P. Binks, T.A. Lawless and J. Mead, *Can. J. Chem.*, **66**, 3031 (1988).
16. W. Helfrich, *Z. Naturforsch*, **28c**, 693 (1973).
17. P.G. de Gennes and C. Taupin, *J. Phys. Chem.*, **86**, 2294 (1982).

18. D.J. Mitchell and B.W. Ninham, *J. Chem. Soc. Faraday Trans.* 2, **7**, 601 (1981).
19. F. Husson, *Acta Crystallogr.*, **13**, 660 (1960).
20. L. E. Scriven, *Nature*, **263**, 123 (1976).
21. A. de Geyer and J. Tabony, *Chem. Phys. Lett.*, **113**, 83 (1985).
22. G. Porte, J. Apell, P. Bassereau and J. Marignan, *J. Physique (France)*, **50**, 1335 (1989).
23. B.P. Binks, J. Meunier, O. Abillon and D. Langevin, *Langmuir*, **5**, 415 (1989).
24. H. Hoffmann and W. Ulbricht, *J. Colloid Interface Sci.*, **129**, 388 (1989).
25. D. Langevin, *Annu. Rev. Phys. Chem.*, **43**, 341 (1992).
26. B.P. Binks ed, Modern Aspects of Emulsion Science, The Royal Society of Chemistry, Cambridge, 1998.
27. W.D. Bancroft, *J. Phys. Chem.*, **17**, 501 (1913).
28. B.P. Binks, *Langmuir*, **9**, 25 (1993).
29. W.C. Griffin, *J. Soc. Cosmet. Chem.*, **1**, 311 (1949) and **5**, 249 (1954).
30. J.T. Davis, in *Proc. 2nd Int. Cong. Surf. Activity*, London, 417 (1957).
31. R. Aveyard, B.P. Binks and P.D.I. Fletcher, in 'The Structure, Dynamics and Equilibrium Properties of Colloidal Systems', eds. D.M. Bloor and E. Wyn-Jones, Kluwer, Dordrecht, 1990, p. 557.
32. A. Graciaa, J. Lachaise, G. Marion and R.S. Schechter, *Langmuir*, **5**, 1351 (1989).
33. H.T. Davis, *Colloids Surf. A*, **91**, 9 (1994).
34. K. Shinoda and S. Friberg, Emulsions and Solubilisation, Wiley, New York, 1986.
35. H. Kunieda and K. Shinoda, *J. Colloid Interface Sci.*, **106**, 107 (1985).
36. J.L. Salager, G. Lopéz-Castellanos, M. Miñana-Pérez, C. Parra, C. Cucuphat, A. Graciaa and J. Lachaise, *J. Disp. Sci. Technol.*, **12**, 59 (1991).
37. A. Kabalnov and H. Wennerström, *Langmuir*, **12**, 276 (1996).
38. R. Aveyard, B.P. Binks, T.A. Lawless and J. Mead, *J. Chem. Soc. Faraday Trans. 1*, **81**, 2155 (1985).
39. H. Smith, G.C. Covatch and K.-H. Lim, *J. Phys. Chem.*, **95**, 1463 (1991).

40. S. Lehnert, H. Tarabishi and H. Leuenberger, *Colloids Surf. A*, **91**, 227 (1994).
41. R.J. Hunter, Foundation of Colloid Science, Volume II, Clarendon Press, Oxford, 1995.
42. R. Aveyard, P. Cooper and P.D.I. Fletcher, *J. Chem. Soc. Faraday Trans.*, **86**, 3623 (1990).
43. B.P. Binks and J. Dong, *J. Chem. Soc. Faraday Trans.*, **94**, 410 (1998).
44. K. Ragil, J. Menuier, D. Broseta, J.O. Indekeu and D. Bonn, *Phys. Rev. Lett.*, **77**, 1532 (1996).
45. H. Kellay, B.P. Binks, Y. Hendrikx, L.T. Lee and J. Meunier, *Adv. Colloid Interface Sci.*, **49**, 85 (1994).
46. J. S. Rowlinson and B. Widom, Molecular Theory of Capillary, Oxford University Press, Oxford, 1989.
47. R. Aveyard, B.P. Binks, P.D.I. Fletcher and J.R. MacNab, *Langmuir*, **11**, 2515 (1995).
48. D.C. Jones and R.H. Ottewill, *J. Chem. Soc.*, 4076 (1955).
49. B.P. Binks, D. Crichton, P.D.I. Fletcher, J.R. MacNab, Z.X. Li, R.K. Thomas and J. Penfold, *Colloids and Surf. A*, submitted.
50. R. Aveyard, B.P. Binks, P. Cooper, P.D.I. Fletcher and A. Sokolowski, *J. Phys. Chem.*, **96**, 1383, (1992).
51. J.R. Lu, R.K. Thomas, R. Aveyard, B.P. Binks, P. Cooper, P.D.I. Fletcher and A. Sokolowski, *J. Phys. Chem.*, **96**, 10971, (1992).
52. M.K. Bernett and W.A. Zisman, *Macromol.*, **4**, 47 (1971).
53. S. Granick, S.J. Clarkson, T.R. Formoy and J.A. Semlyen, *Polymer*, **26**, 925 (1985).
54. A.H. Ellison and W.A. Zisman, *J. Phys. Chem.*, **60**, 416 (1956).
55. N.L. Jarvis, *J. Colloid Interface Sci.*, **29**, 647 (1969).
56. E.K. Mann and D. Langevin, *Langmuir*, **7**, 1112 (1991).
57. L.T. Lee, E.K. Mann, D. Langevin and B. Farnoux, *Langmuir*, **7**, 3076 (1991).
58. E.K. Mann, L.T. Lee, S. Hénon, D. Langevin and J. Meunier, *Macromol.*, **26**, 7037 (1993).

59. L.T. Lee, E.K. Mann, O. Guiselin, D. Langevin, B. Farnoux and J. Penfold, *Macromol.*, **26**, 7046 (1993).
60. V. Bergeron and D. Langevin, *Macromol.*, **29**, 306 (1996) and *Phys. Rev. Lett.*, **76**, 3152 (1996).
61. A.G. Kanellopoulos and M.J. Owen, *J. Colloid Interface Sci.*, **35**, 120 (1971).
62. J. Rouviere, J.L. Razakarison, J. Marignan and B. Brun, *J. Colloid Interface Sci.*, **133**, 293 (1989).
63. A. Messier, G. Schorsch, J. Rouviere and L. Tenebre, *Progr. Colloid Polym. Sci.*, **79**, 249 (1989).
64. H. Hoffmann and A. Stürmer, *Tenside,* **30**, 335 (1993).
65. H. Katayama, T. Tagawa and K. Kunieda, *J. Colloid Interface Sci.*, **153**, 429 (1992).
66. H. Mayer and M. Roth, *Bautenschuts and Bausanierung*, **13**, 1 (1990).
67. H. Mayer, *Coating*, **27**, 256 (1994) and Wacker-Chemie GmbH, *US Paternt* 4,661,551.
68. D.C. Steytler, P.J. Dowding, B.H. Robinson, J.D. Hague, J.H.S. Rennie, C.A. Leng, J. Eastoe and R.K. Heenan, *Langmuir*, **14**, 3371 (1998).
69. R.P. Gee, *Colloids Surf. A*, **137**, 91 (1998).
70. A.C. John, H. Uchiyama, K. Nakamura and H. Kunieda, *J. Colloid Interface Sci.*, **186**, 294 (1997).
71. J. Dumoulin, Rhone-Poulenc S.A., *US Patent* 3,973,294.
72. A. Harashima, Toray Silicone Co. Ltd., *European Patent* 0 268 982 A3.
73. M. Osaki and I. Ona, Dow Corning Toray Silicone Co. Ltd., *European Patent* 0 404 027 A2.
74. R.P. Gee, Dow Corning Coporation, *US Patent* 4,620,878.
75. T.M. Obey and B. Vincent, *J. Colloid Interface Sci.*, **163**, 454 (1994).
76. K.R. Anderson, T.M. Obey and B. Vincent, *Langmuir*, **10**, 2493 (1994).
77. International Critical Tables, McGraw-Hill, London, **4**, 447 (1928).
78. W.D. Harkins and H.F. Jordan, *J. Am. Chem. Soc.*, **52**, 1751 (1930).
79. B.B. Freud and H.Z. Freud, *J. Am. Chem. Soc.*, **52**, 1772 (1930).
80. H.H. Zuidema and G.W. Waters, *Ind. Eng. Chem.*, **13**, 312 (1941).
81. M.G. Wilkinson, *J. Colloid Interface Sci.*, **40**, 14 (1972).

82. B. Vonnegut, *Rev. Sci. Instr.*, **13**, 6 (1942).
83. A. Couper, R. Newton and C. Nunn, *Colloid Polymer Sci.*, **261**, 371 (1983).
84. H.M. Princen, I.Y.Z. Zia and S.G. Mason, *J. Colloid Interface Sci.*, **23**, 99 (1967).
85. J.C. Slattery and J.D. Chen, *J. Colloid Interface Sci.*, **64**, 373 (1978).
86. P.W. Atkins, Physical Chemistry, 5th edition, Oxford University Press, Oxford, 1994.
87. V.W. Reid, G.F. Longman and E. Heinerth, *Tenside*, **4**, 292 (1967).
88. D.M Smith, W.M.D. Bryant and J. Mitchell, *J. Am. Chem. Soc.*, **61**, 2407 (1939).
89. Malvern 2600 Series: Laser Diffraction Particle Sizer, User Manual, Malvern, 1986.
90. B.J. Clifton, T. Cosgrove, R.M. Richardson, A. Zarbakhsh and J.R.P. Webster, *Physica B*, **248**, 289 (1998).
91. B.W. Brooks, H.N. Richmond and M. Zerfa, in 'Modern Aspects of Emulsion Science', ed. B.P. Binks, The Royal Society of Chemistry, Cambridge, 1998, p. 175.
92. B. P. Binks, *Colloids Surf. A*, **71**, 167 (1993).
93. H. Saito and K. Shinoda, *J. Colloid Interface Sci.*, **32**, 647 (1970).
94. K. Shinoda and S. Friberg, Emulsions and Solubilisation, Wiley, New York, 1986. p. 108.
95. N.M. Van Os, J.R. Haak and L.A. M. Rupert, Physico-chemical Properties of Selected Anionic, Cationic and Nonionic Surfactants, Elsevier, Amsterdam, 1993.
96. M. Kahlweit, *Ber. Bunsenges. Phys. Chem.*, **98**, 490 (1994).
97. P. Becher, *J. Colloid Interface Sci.*, **17**, 325 (1962).
98. K. Shinoda, T. Yamaguchi, and R. Hori, *Bull. Chem. Soc. Jpn.*, **34**, 237 (1961).
99. K. Shinoda and H. Takeda, *J. Colloid Interface Sci.*, **32**, 642 (1970).
100. M. Kahlweit, R. Strey and P. Firman, *J. Phys. Chem.*, **90**, 671 (1986).
101. H. Schott, A.E. Royce, and S.K. Han, *J. Colloid Interface Sci.*, **98**, 196 (1984).

102. K. Shinoda and H. Arai, *J. Phys. Chem.*, **68**, 3485 (1964).
103. K. Shinoda, *J. Colloid Interface Sci.*, **24**, 8 (1967).
104. H. Arai and K. Shinoda, *J. Colloid Interface Sci.*, **25**, 396 (1967).
105. M. Minana-Perez, A. Graciaa, J. Lachaise and J-L. Salager, *Colloids Surf. A*, **100**, 217 (1995).
106. M. Gradzielski, H. Hoffmann, P. Robisch and W. Ulbricht, *Tenside*, **27**, 366 (1990).
107. J.D. Mitchell, G.J.T. Tiddy, L. Waring, T. Bostock and M.P. McDonald, *J. Chem. Soc. Faraday Trans. 1*, **79**, 975 (1983).
108. R.M. Hill, M. He, H.T. Davis and L.E. Scriven, *Langmuir*, **10**, 1724 (1994).
109. J.C. Morgan, R.S. Schechter, and W.H. Wade, in "Solution Chemistry of Surfactants", ed. K.L. Mittal, Plenum Press, New York, (1979), p. 749
110. B. Widom, *J. Phys. Chem.*, **77**, 2196 (1973).
111. R.B. Griffiths, *J. Chem. Phys.*, **60**, 195 (1974).
112. M. Kahlweit and R. Strey, *Angew. Chem., Int. Ed. Engl.* **24,** 654 (1985).
113. R. Aveyard, B.P. Binks and P.D.I. Fletcher, *Langmuir*, **5**, 1210 (1989).
114. H. Kellay, Y. Hendrikx, J. Meunier, B.P. Binks and L.T. Lee, *J. Phys. II France*, **3**, 1747 (1993).
115. R.G. Laughlin, in 'Micelles, Microemulsions and Monolayers', ed. D.O. Shah, Marcel Dekker, New York, 1998, p. 73.
116. R. Aveyard, B.P. Binks, S. Clark and P.D.I. Fletcher, *J. Chem. Soc. Faraday Trans.*, **86**, 3111 (1990).
117. F. Hofmeister, *Arch. Exp. Pathol. Pharmakol.*, **24**, 247 (1888).
118. K.D. Collins and M.W.Q. Washabaugh, *Rev. Biophys.*, **24**, 247 (1985).
119. R. Aveyard, *Can. J. Chem.*, **60**, 1317 (1981).
120. A. Kabalnov, U. Olsson and H. Wennerström, *J. Phys. Chem.*, **99**, 6220 (1995).
121. K.P. Ananthapadmanabhan, E.D. Godard and P. Chandar, *Colloids Surf.* **44**, 281 (1990).
122. M.J. Rosen, A.W. Cohen, M. Dahanayake and X.Y. Hua, *J. Phys. Chem.*, **86**, 541 (1982).

123. M. He, R.M. Hill, Z. Lin, L.E. Scriven and H.T. Davis, *J. Phys. Chem.*, **97**, 8820 (1993).
124. C.J. Drummond, G.G. Warr, F. Grieser, B.W. Ninham and D.F. Evans, *J. Phys. Chem.*, **89**, 2103 (1985).
125. W. Binana-Limbele and R. Zana, *J. Colloid Interface Sci.*, **121**, 81 (1988).
126. R. Aveyard, B.P. Binks, S. Clark and P.D.I. Fletcher, *J. Chem. Tech. Biotechnol.*, **48**, 161 (1990).
127. D.C. Steytler, D.L. Sargeant and B.H. Robinson, *Langmuir*, **10**, 2213 (1994).
128. J.C. Ravey, M. Bouzier and C. Picot, *J. Colloid Interface Sci.*, **97**, 9 (1984).
129. J.C. Ravey and M. Bouzier, *J. Colloid Interface Sci.*, **116**, 30 (1987).
130. R. Aveyard and T.A. Lawless, *J. Chem. Soc. Faraday Trans. 1*, **82**, 2951 (1986).
131. R. Aveyard, B.P. Binks, P.D.I. Fletcher, T-G. Peck and P.R. Garrett, *J. Chem. Soc. Faraday Trans.*, **89**, 4313 (1993).
132. W.D. Harkins, *J. Chem. Phys.*, **9**, 552 (1941).
133. H.W. Fox, E.M. Solomon and W.A. Zisman, *J. Phys. & Colloid Chem.*, **54**, 723 (1950).
134. J. Fang, M. Dennin, C.M. Knobler, Yu.K. Godovsky, N.N. Makarova and H. Yokoyama, *J. Phys. Chem. B*, **101**, 3147 (1997).
135. W.H. Banks, *Nature*, **174**, 365 (1954).
136. N.J. Jarvis, *J. Phys. Chem.*, **70**, 3027 (1966).
137. S. Granick, *Macromol.*, **18**, 1597 (1985).
138. V. Bergeron, *Langmuir*, **13**, 3474 (1997).
139. J.R. Lu, Z.X. Li, R.K. Thomas, B.P. Binks, D. Crichton, P.D.I. Fletcher, J.R. MacNab and J. Penfold, *J. Phys. Chem. B*, **102**, 5785 (1998).
140. E.K. Mann, S. Hénon, D. Langevin and J. Meunier, *J. Phys. II France*, **2**, 1683 (1992).
141. J. Penfold, R.M. Richardson, A. Zarbakhsh, J.R.P. Webster, D.G. Bucknall, A.R. Rennie, R.A.L. Jones, T. Cosgrove, R.K. Thomas, J.S. Higgins, P.D.I. Fletcher, E. Dickinson, S.J. Roser, I.A. McLure, A.R.

Hillman, R.W. Richards, E.J. Staples, A.N. Burgess, E.A. Simister and J.W. White, *J. Chem. Soc. Faraday Trans.*, **93**, 3899 (1997).

142. J. Penfold and R.K. Thomas, *J. Phys., Condens. Matter*, **2**, 1369 (1990).
143. J.R. Lu, R.K. Thomas, B.P. Binks, P.D.I. Fletcher and J. Penfold, *J. Phys. Chem.*, **99**, 4113 (1995).
144. V.F. Sears, *Neutron News*, **3**, 26 (1992).
145. K.D. Tapas, *Adv. Colloid Interface. Sci.*, **59**, 85(1992).
146. K. Shinoda, H. Kunieda, T. Arai and H. Saito, *J. Phys. Chem.*, **88**, 5126 (1984).
147. R. Aveyard, B.P. Binks, S. Clark and J. Mead, *J. Chem. Soc. Faraday Trans. 1,* **82**, 125 (1986).
148. B.P. Binks, H. Kellay and J. Meunier, *Europhys. Lett.,* **16**, 53 (1991).
149. B.P. Binks, PhD thesis, University of Hull, 1986.
150. O. Ghosh and C.A. Miller, *J. Phys. Chem.*, **91**, 4528 (1987).
151. D.G. Hall, in "Aggregation Processes in Solution", eds. E. Wyn-Jones and J. Gormally, Elsevier, Amsterdam, 1983, p.7.
152. R.A. Robinson and R.H. Stokes, Electrolyte Solutions, Butterworths, London, 1959.
153. R. Palepu, D.G. Hall and E. Wyn-Jones, *J. Chem. Soc. Faraday Trans.*, **86**, 1535 (1990).
154. H. Kunieda and K. Shinoda, *J. Colloid Interface Sci.*, **75**, 601(1980).
155. R. Aveyard, B.P. Binks, S. Clark and P.D.I. Fletcher, *J. Chem. Soc. Faraday Trans. 1*, **82**, 1755 (1986).
156. K. Shinoda and Y. Shibata, *Colloids Surf.*, **19**, 185 (1986).
157. G. Granet, R.D. Khadirian and S. Piekarski, *Colloids Surf.*, **49**, 199 (1990).
158. A. Pouchelon, D. Chatenay, J. Meunier and D. Langevin, *J. Colloid Interface Sci.*, **82**, 418 (1981).
159. S. Mukherjee, C.A. Miller and T. Fort, *J. Colloid Interface Sci.*, **91**, 223 (1983).
160. M.J. Hou and D.O. Shah, *Langmuir*, **3**, 1086 (1987).
161. A. Derouiche and C. Tondre, *J. Disp. Sci. Technol.*, **12**, 517 (1991).

162. M. Kotlarchyk, S-H. chen, J. S. Huang and M.W. Kim, *Phys. Rev. A*, **29**, 2054 (1984).
163. P.D.I. Fletcher, *J. Chem. Soc. Faraday Trans. 1*, **82**, 2651 (1986).
164. S.G. Frank and G. Zografi, *J. Colloid Interface Sci.*, **29**, 27 (1969).
165. R. Aveyard, B.P. Binks, P.D.I. Fletcher, C.E. Rutherford, P.J. Dowding and B. Vincent, *Phys. Chem. Chem. Phys.*, in press.
166. P.D.I. Fletcher, *J. Chem. Soc. Faraday Trans. 1*, **83**, 1493 (1987).
167. D.N. Petsev, N.D. Denkov and P.A. Kralchevsky, *J. Colloid Interface Sci.*, **176**, 201 (1995).
168. L.M. Baldauf, R.S. Schechter, W.H. Wade and A. Graciaa, *J. Colloid Interface Sci.*, **85**, 187 (1982).
169. R.E. Anton and J-L. Salager, *J. Colloid Interface Sci.*, **111**, 54 (1986).
170. R.D. Hazlett and R.S. Schechter, *Colloids Surf.*, **29**, 53 (1988).
171. R. Aveyard, B.P. Binks, P.D.I. Fletcher, X. Ye and J.R. Lu, in 'Emulsions – A Fundamental and Practical Approach', ed. J. Sjöblom, Kluwer, Dordrecht, 1992, p. 97.
172. J.R. Lu, PhD thesis, University of Hull, 1990.
173. K.D. Danov, D.N. Petsev, N.D. Denkov and R. Borwankar, *J. Chem. Phys.*, **99**, 7179 (1993).
174. Calculations using experimental values of γ, a, Ψ_o for heptane-in-water emulsions stabilised by AOT. B.P. Binks, W-G. Cho and D.N. Petsev, unpublished results.
175. H. Kellay, J. Meunier and B.P. Binks, *Phys. Rev. Lett.*, **69**, 1220 (1992).
176. V. Bergeron, *Langmuir*, **12**, 5751 (1996).
177. A. Schalchli, D. Sentenac and J.J. Benattar, *J. Chem. Soc. Faraday Trans.*, **92,** 553 (1996).
178. Z.X. Li, J.R. Lu, R.K. Thomas and J. Penfold, *J. Phys. Chem. B*, **101**, 1615 (1997).
179. N. Shahidzadeh, D. Bonn and J. Meunier, *Europhys Lett.*, **40**, 459 (1997).
180. W.J. Benton, K.H. Raney and C.A. Miller, *J. Colloid Interface Sci.*, **110**, 63 (1986).

APPENDICES

Appendix I

FORTRAN program used for calculating the interfacial tension in drop-volume technique

```
a=1.2
b=1.6
      pi=3.1415926536
      print *, 'What is the tip radium / cm?'
      Read *, zadi
      Print *, 'What is the larger density (g/cm3)?'
      Read *, dhi
      Print *, 'What is the smaller density (g/cm3)?'
      Read *, dlo
C     Now calculate density difference, Δd
      Δd=dhi-dlo
      Print *, 'Input mean micrometer increment & standard devn. (mm)?'
      Read *, h, hsd
C     Now calculate max and min values for delta h
      Hmax=h+hsd
      Hmin=h-hsd
      Print *, 'What was the c.s.a of the syringe barrel (cm2)?'
      Read *, csa
      Vmax=0.1*hmax*csa
      Vmin=0.1*hmin*csa
C     Volumes are now in cubic centimetres
C     What was the shape of that drop?
C     calculate x (=r/v^.3333)
      Xmax=zadi/(vmin** (1.0/3.0))
      Xmin=zadi/(vmax**(1.0/3.0))
C     calculate surface tension for upper and lower bounds
     If ((xmin.gt.o). and .(xmin.le.a)) then
```

```
  Fmax=1.0024-1.0587*xmin-.54088*xmin**2+6.0708*xmin**3
  Fmax=fmax-10.495*xmin**4+7.7164*xmin**5-2.0861*xmin**6
Else if (xmin.gt.a).and. (xmin.le.b)) then
  Fmax=4.559+6.2616*xmin+.79498*xmin**2-1.2113*xmin**3
  Fmax=fmax-.93623*xmin**4+.077998*xmin**5-.31847*xmin**6
  Fmax=fmax+.28095*xmin**7+.23758*xmin**8-.13212*xmin**9
Else if ((xmin.gt.b).or.(xmin.le.0)) then
  Print *, 'xmin is out of range – upper limit of gamma is'
  Print *, 'out of range!'
  Print *, 'xmin = ', xmin
End if
If ((xmax.gt.0).and.(xmax.le.a)) then
  Fmin=1.0024-1.0587*xmax-.54088*xmax**2+6.0787*xmax**3
  Fmin=fmin-10.495*xmax**4+7.7164*xmax**5-2.0861*xmax**6
Else if ((xmax.gt.a) and.(xmax.le.b)) then
  Fmin=4.559+6.2616*xmax+.79498*xmax**2-1.2113*xmax**3
  Fmin=fmin-.93623*xmax**4+.077998*xmax**5-.31847*xmax**6
  Fmin=fmin+.28095*xmax**7+.23758*xmax**8-.13212*xmax**9
Else if ((xmax.gt.b).or(xmax.le.0)) then
  Print *, 'xmax is out of range – lower limit of gamma is'
  Print *, 'xmax = ',xmax
End if
Gammin=981*vmin*dd/(2.0*pi*zadi*fmin)
Gammax=981*vmax*dd/(2.0*pi*zadi*fmax)
Print *, 'correction factor, phi ranges from ', fmin' to 'fmax
Ga=(gammin+gammax)/2.0
Gsd=gammax-ga

Print *, 'Tension = ' ,ga, '+/- ', gsd, 'mN/m'
Stop
End
```

Appendix II

Emulsion conductivity (κ) of PDMS+ aqueous surfactant systems

Temperature effect on nonionic surfactant systems:

Table 1 —Surfactant concentration effect: $C_{12}E_5$ as surfactant

5%		10%		15%		20%		30%	
T/°C	κ /μS cm^{-1}	T/°C	κ /μS cm^{-1}	T/°C	κ /μS cm^{-1}	T/°C	κ /μS cm^{-1}	T/°C	κ /μS cm^{-1}
10	433	20	346	24	451	20	194	20	184
12	434	22	344	26	319	22	197	24	185
14	433	24	345	28	318	24	216	26	169
16	432	26	347	30	316	26	216	28	173
18	431	28	349	32	317	28	219	30	173
20	429	30	350	34	319	30	220	32	190
22	428	32	351	36	320	32	221	34	182
24	428	34	356	38	324	34	221	36	174
26	427	36	363	40	341	36	228	38	170
28	424	38	375	42	353	38	229	40	171
30	423	40	376	44	363	40	233	42	171
32	421	42	381	46	373	42	244	44	175
34	421	44	387	48	381	44	254	46	175
36	422	46	389	49	380	46	260	48	187
38	422	48	391	50	388	48	269	50	197
40	433	50	394	52	380	50	275	52	195
42	435	52	395	54	396	52	283	54	213
44	440	54	394	55	397	54	288	57	142
46	444	55	395	56	304	56	213	59	139
48	450	56	392	58	273	58	186	61	114
51	451	57	310	60	245	60	176	62	107
52	452	58	304	62	237	62	162	65	97
54	458	60	286	64	199	63	159	67	91
56	366	62	267	66	195	64	154	69	84
58	328	64	249	68	169	66	135	70	81
60	313	66	236	69	161	67	129	71	80
62	292	69	222	70	172	68	126	72	84
64	276	70	222	71	190	69	121		
66	267	71	240			70	394		
68	319								

Table 2 —Surfactant chain length effect for 10% C_nE_5 systems

n=10		n=12		n=14		n=16	
T/°C	κ/μS cm^{-1}	T/°C	κ/μS cm^{-1}	T/°C	κ/μS cm^{-1}	T/°C	κ/μS cm^{-1}
4.9	612	20	346	20	409	10	244
10.1	584	22	344	22	405	12	242
12.2	580	24	345	24	308	14	242
14.8	569	26	347	26	311	16	241
16.4	572	28	349	28	315	18	247
18.2	570	30	350	30	320	20	219
20	567	32	351	32	322	22	250
22	563	34	356	34	340	24	253
24	560	36	363	36	347	26	252
26	556	38	375	38	350	28	251
28	553	40	376	40	243	30	255
30	556	42	381	42	190	32	154
32.3	548	44	387	44	135	34	145
33.8	563	46	389	46	106	36	116
36.2	557	48	391	48	90	38	116
38.4	560	50	394	50	79	40	113
40.4	572	52	395	52	71	42	112
42.5	570	54	394	54	67	45	108
44.2	572	55	395	56	64	46	106
46.1	577	56	392	58	62	48	100
48	591	57	310	60	60	50	51
50	635	58	304	62	51	52	50
58	638	60	286	64	66	54	51
65	677	62	267			56	53
70	722	64	249			58	54
		66	236			60	55
		69	222				
		70	222				
		71	240				

Table 3 —Surfactant head group effect for 10% $C_{12}E_m$ systems

m=2		m=3		m=4		m=5		m=6	
T/°C	κ /μS cm^{-1}	T/°C	κ /μS cm^{-1}	T/°C	κ /μS cm^{-1}	T/°C	κ /μS cm^{-1}	T/°C	κ /μS cm^{-1}
5	1.6	10	163	10	436	20	346	20	342
10	1.4	12	164	14.6	610	22	344	25	340
12	2.8	14	164	20	643	24	345	30	339
14	2.8	16	162	24	419	26	347	36	338
18	2.5	18	154	26.2	287	28	349	41	373
21	2.3	20	148	28.2	242	30	350	45	397
24	2	22	131	30.8	214	32	351	50	383
31	2	24	116	33	207	34	356	55	370
36	2	26	115	37	189	36	363	60	450
41	1.5	28	106	40.4	139	38	375	66	434
45	1.4	30	76	43	136	40	376	69	500
		32	39	46	113	42	381		
		34	55	49	133	44	387		
		36	129	52	148	46	389		
		38	216			48	391		
		40	253			50	394		
		64	5			52	395		
		66	4			54	394		
		67	5			55	395		
						56	392		
						57	310		
						58	304		
						60	286		
						62	267		
						64	249		
						66	236		
						69	222		
						70	222		
						71	240		

Table 4 —Other surfactants systems: 10% surfactants in aqueous

L-77		$C_{16}P_8E_1$		$C_{16}P_4E_1$	
T/°C	κ /μS cm^{-1}	T/°C	κ /μS cm^{-1}	T/°C	κ /μS cm^{-1}
20	296	5	178	10	322
22	300	7	160	12	327
24	301	10	115	14	226
26	305	13	356	16	156
28	308	15	394	183	128
30	310	16	408	20	110
33	312	18	400	22	69
34	315	20	422	24	30.3
36	316	22	372	26	26
38	318	24	320	28	27
40	322	26	316	30	16
42	322	28.4	318	32	4.6
44	250	30	280	40	2.2
46	196	32	100		
48	182	34			
50	176	36			
52	175	38			
54	188	40			
56	263				

Table 5 —NaCl effect on $C_{12}E_5$ systems: 10% surfactant in aqueous

0.01M		0.1M		0.5M		1M		2M		4M	
T/°C	κ /μS cm^{-1}	T/°C	κ /mS cm^{-1}	T/°C	κ /mS cm^{-1}	T/°C	κ /mS cm^{-1}	T/°C	κ /mS cm^{-1}	T/°C	κ /mS cm^{-1}
20	346	20	6.02	20	11.9	20	17.9	20	41.1	8	55
22	344	22	3.96	22	11.9	22	18.2	22	41.3	9	56
24	345	24	3.95	24	11.8	24	18.4	24	40.4	10	55
26	347	26	3.9	26	11.8	26	18.5	26	39.5	12	54.7
28	349	28	3.89	28	11.7	28	18.7	28	40.8	14	27.5
30	350	30	3.93	30	11.9	30	18.7	30	41.1	16	22.6
32	351	32	3.95	32	12.1	32	19.2	32	31.6	18	20.4
34	356	34	4.3	34	12.2	34	19.6	34	18.9	20	20.1
36	363	36	4.6	36	12.6	36	19.6	36	19	22	19.2
38	375	38	5.07	38	12.6	38	19.8	38	11.1	24	17.8
40	376	41	5,73	40	12.8	40	20	40	9.9	26	15.2
42	381	43	6.5	42	13	42	16.2	42	9.8	28	10.2
44	387	45	5.51	44	13.1	44	14.6	44	9.4	30	12.9
46	389	47	5.45	46	13	46	10.4	46	9.4		
48	391	49	5.42	48	10.1	47	8.1	48	9.7		
50	394	51	5.49	50	8.3	48	7.6	50	11.3		
52	395	53	4.13	52	8.2	49	7				
54	394	55	3.89	54	7.4	50	6.7				
55	395	57	3.23	56	5.6	51	6.6				
56	392	59	2.92	58	5.4	52	6.3				
57	310	61	2.44	60	4.9	54	6.2				
58	304	63	2.36			56	6.3				
60	286	65	2.4			58	6.6				
62	267					60	8				
64	249										
66	236										
69	222										
70	222										
71	240										

Table 6 —TBAB effect on $C_{12}E_3$ systems: 10% surfactant in aqueous

0.01M		0.1M		1M	
T/°C	κ /μS cm^{-1}	T/°C	κ /mS cm^{-1}	T/°C	κ /mS cm^{-1}
5	147	20	0.96	20	10.5
10	142	22	0.92	25	11.3
15	143	24	0.87	30	11.8
20	146	26.5	0.77	35	12.2
25	146	29	0.7	40	12.4
27	81	32	0.61	45	12.7
30	85	34	0.72	50	10.4
35	155	38	1.18	55	15.2
40	354	40	1.88	60	18.4
44	362	42	2.43	65	18.6
		44	2.44	70	19.4
		47	2.71		20.8
		49	2.89		
		52	3.1		
		54	3.57		
		60	3.75		
		65	3.68		
		70	5.4		

Table 7 —Oil viscosity effect on $C_{12}E_2$ systems: 10% surfactant in aqueous

50 cS		100 cS		500 cS		1000 cS	
T/°C	κ /μS cm^{-1}	T/°C	κ /μS cm^{-1}	T/°C	κ /μS cm^{-1}	T/°C	κ /μS cm^{-1}
5	1.4	6	182.3	5	273	5	254
10	1.6	8	175.5	10	153	10	150
12	2.8	10	121.2	13	143	12	130
14	2.8	12	104.9	14	199	14	226
18	2.5	14	135.4	16	246	16	314
21	2.3	16	235	18	276	18	380
24	2	18	290	20	390	36	3.3
31	2	20	414	28	36	40	2
36	2	32	8.9	30	40	50	0
41	1.5	36	4.3	32	11.4	60	0
45	1.4	38	1.4	34	14.6	70	0
		40	1.2	36	1.4		
		42	1	38	1.9		
		44	1	40	0.2		
		46	1	45	0.7		
		48	1	50	0.6		
		50	1				

Table 8 —Oil viscosity effect on $C_{16}P_8E_1$ systems: 10% surfactant in aqueous

50 cS		100cS		500 cS		1000cS	
T/°C	κ /μS cm^{-1}	T/°C	κ /μS cm^{-1}	T/°C	κ /μS cm^{-1}	T/°C	κ /μS cm^{-1}
5	178	6	373	5	16.1	5	140
10	114.5	8	203	7	140	7	120
13	356	10	334	10	210	10	190
15	394	12.5	596	12	520	12	508
16	408	15	594	14	503	14	499
18	400	18.5	591	16	509	16	388
20	422	20	594	18	550	18	
22	436	22	564	20	40	20	
24	428	24	549	22	10	35	1.2
26	415	27	546	25	11.3	40	4
28	412	30	460	27	23.2	45	1.4
30	350	32	320	30	24	50	0.6
32	5	34	14.3	32	2.2	55	0.9
34	3	36	2.2	35	0.8	60	0.8
40	1	40	1	40	1.7	65	0
45	1	45	1	45	4	70	0
50	1	50	136	50	0.3		
55	1	55	170	55	0		
60	1	60	170	60	0.8		
65	1	65	190	65	0		
70	1	70	220	70	0		

Electrolyte concentration effect on AOT systems:

Table 9 —[Salt] effect PDMS-40 mM AOT-NaCl aqueous system at 25°C

0.65 cS		1 cS		5 cS		10 cS	
[NaCl] /M	κ /μS cm^{-1}	[NaCl] /M	κ /μS cm^{-1}	[NaCl] /M	κ /μS cm^{-1}	[NaCl] /M	κ /μS cm^{-1}
0.01	433	0	208	0.01	312	0.01	279
0.025	1090	0.025	830	0.025	634	0.1	1520
0.05	2330	0.05	1510	0.05	1056	0.15	2590
0.08	2860	0.075	1820	0.1	1704	0.18	3640
0.1	1850	0.1	2410	0.12	2770	0.4	
0.12	290	0.12	2520	0.14	3030	0.6	
0.14	37	0.135	2450	0.15	3720	0.7	
0.16	21	0.15	2090	0.8	1.78	0.8	
0.18	7.2	0.175	1850	1	1.66	0.9	
0.2	9.5	0.2	1370	2	1.82	1	1.74
0.4	8.4	0.3	410			1.2	1.91
0.6	3.2	0.4	100				
1	3.4	0.5	55				
2	2.3	0.75	30				

20 cS		50 cS		100 cS	
[NaCl]/M	κ /μS cm^{-1}	[NaCl]/M	κ /μS cm^{-1}	[NaCl]/M	κ /μS cm^{-1}
0.01	216	0.01	303	0.01	288
0.1	1665	0.05	820	0.05	850
0.2	4940	0.1	1762	0.1	1665
4	1.78	0.12	2080	0.16	2480
5	1.67	0.14	2680	0.2	3880
		0.16	2940	3	1.63
		0.18	3510	4	1.68
		0.2	4200	5	1.71
		3	2.32		
		4	1.98		
		5	1.96		

Appendix III

Relative volume (v) of each phase in equilibrium multi-phase behaviour systems

Table 1 —Surfactant concentration effect in $C_{12}E_3$ + 50 cS PDMS oil system at different temperature

$C_{12}E_3$/wt %	30°C			40°C		
	V_{oil}	V_{water}	V_{3rd}	V_{oil}	V_{water}	V_{3rd}
0	0.5	0.5	0	0.5	0.5	0
1	0.493	0.457	0.043	0.5	0.5	0
2	0.493	0.428	0.079	0.499	0.442	0.059
5	0.5	0.4	0.107	0.499	0.371	0.137
10	0.486	0.286	0.214	0.499	0.314	0.187
15	0.479	0.257	0.257	0.571	0.2	0.229
20	0.479	0.1	0.421	0.615	0.1	0.285
$C_{12}E_3$/wt %	50°C			60°C		
	V_{oil}	V_{water}	V_{3rd}	V_{oil}	V_{water}	V_{3rd}
0	0.5	0.5	0	0.5	0.5	0
1	0.5	0.5	0	0.5	0.5	0
2	0.5	0.471	0.029	0.5	0.5	0
5	0.5	0.442	0.058	0.5	0.5	0
10	0.499	0.4	0.101	0.499	0.439	0.062
15	0.497	0.342	0.161	0.499	0.429	0.072
20	0.496	0.3	0.204	0.497	0.407	0.096

Table 2 —NaCl effect in 5% $C_{12}E_3$ + 50 cS PDMS oil system at different temperatures

[NaCl] / M	10°C			18°C			30°C		
	V_{oil}	V_{water}	V_{3rd}	V_{oil}	V_{water}	V_{3rd}	V_{oil}	V_{water}	V_{3rd}
0.01	0.48	0.52	0	0.48	0.52	0.00	0.52	0.09	0.40
0.05	0.43	0.57	0	0.43	0.57	0.00	0.51	0.11	0.37
0.1	0.47	0.53	0	0.47	0.53	0.00	0.53	0.12	0.35
0.2	0.43	0.57	0	0.43	0.57	0.00	0.50	0.11	0.39
0.5	0.55	0.45	0	0.55	0.45	0.00	0.45	0.10	0.45
1	0.45	0.55	0	0.40	0.60	0.00	0.50	0.11	0.39
1.5	0.48	0.52	0	0.45	0.55	0.00	0.49	0.07	0.44
2	0.49	0.51	0	0.49	0.27	0.24	0.49	0.04	0.47
2.4	0.49	0.51	0	0.49	0.41	0.10			
2.7	0.47	0.53	0	0.51	0.42	0.07			
3	0.51	0.22	0.27	0.49	0.42	0.08	0.49	0.04	0.47
3.5	0.51	0.32	0.16	0.49	0.41	0.11	0.49	0.03	0.48
4	0.52	0.37	0.11	0.48	0.42	0.10	0.49	0.03	0.49
4.5	0.51	0.42	0.07	0.49	0.46	0.05	0.49	0.00	0.51
5	0.52	0.44	0.04	0.49	0.48	0.03	0.49	0.00	0.51

[NaCl] / M	41°C			50°C			60°C		
	V_{oil}	V_{water}	V_{3rd}	V_{oil}	V_{water}	V_{3rd}	V_{oil}	V_{water}	V_{3rd}
0.01	0.5	0.371	0.129	0.5	0.45	0.05	0.51	0.49	0
0.05	0.5	0.357	0.143	0.529	0.428	0.04	0.52	0.48	0
0.1	0.508	0.371	0.121	0.5	0.45	0.05	0.5	0.5	0
0.2	0.499	0.388	0.113	0.5	0.457	0.04	0.51	0.49	0
0.5	0.507	0.414	0.079	0.5	0.457	0.04	0.5	0.5	0
1	0.493	0.457	0.05	0.494	0.471	0.04	0.52	0.48	0
2	0.5	0.471	0.029	0.52	0.48	0.00	0.51	0.49	0
2.4	0.5	0.49	0.01	0.5	0.5	0.00	0.5	0.5	0
3	0.507	0.493	0	0.5	0.5	0.00	0.52	0.48	0

Table 3 —TBAB effect in the system: 5% $C_{12}E_3$ + aqueous + 50 cS PDMS oil

[TBAB] / M	41°C			50°C			60°C		
	V_{oil}	V_{water}	V_{3rd}	V_{oil}	V_{water}	V_{3rd}	V_{oil}	V_{water}	V_{3rd}
0.01	0.5	0.36	0.1388	0.506	0.424	0.068	0.512	0.468	0.018
0.05	0.493	0.20	0.3013	0.5	0.418	0.081	0.513	0.459	0.027
0.1	0.5	0.05	0.4459	0.527	0.391	0.081	0.506	0.452	0.041
0.15	0.514	0.48		0.513	0.375	0.111			
0.2	0.459	0.54		0.297	0.513	0.189	0.5	0.445	0.054
0.25	0.516	0.48		0.524	0.262	0.213			
0.35	0.508	0.49		0.516	0.083	0.4			
0.4	0.508	0.49		0.508	0.084	0.406			
0.42	0.506	0.49		0.506	0.054	0.438			
0.45	0.5	0.5		0.506	0.1	0.393			
0.5	0.507	0.49		0.5	0.5		0.5	0.438	0.061
0.52	0.507	0.49							
0.58	0.513	0.43	0.054						
0.6				0.5	0.45	0.05	0.5	0.455	0.044
0.62	0.514	0.41	0.0714						
0.68	0.525	0.4	0.075						
0.7	0.506	0.39	0.0958	0.513	0.418	0.067	0.513	0.418	0.067
0.75	0.507	0.49		0.513	0.486				
0.8	0.514	0.48		0.5	0.5		0.5	0.5	
0.9	0.5	0.5		0.5	0.5		0.5	0.5	
0.96	0.5	0.5		0.513	0.486		0.513	0.486	
1.2	0.5	0.5		0.5	0.5		0.5	0.5	

Table 4 —Electrolyte effect on the relative phase volume of each phase at equilibrium for system: 40 mM AOT initially either in oil or aqueous+0.65 cS PDMS+NaCl aqueous at 25°C

AOT initially in aqueous phase				AOT initially in oil phase			
[NaCl]/M	V_{oil}	V_{3rd}	$V_{aq.}$	[NaCl]/M	V_{oil}	V_{3rd}	$V_{aq.}$
0	0.528	0	0.471	0	0.471	0	0.528
0.05	0.471	0	0.528	0.025	0.489	0	0.510
0.06	0.485	0	0.514	0.05	0.488	0	0.513
0.08	0.486	0	0.513	0.075	0.493	0	0.506
0.1	0.478	0	0.521	0.1	0.493	0	0.506
0.12	0.492	0	0.507	0.11	0.5	0	0.5
0.13	0.5	0.428	0.071	0.12	0.493	0	0.506
0.14	0.47	0.191	0.338	0.13	0.486	0.368	0.145
0.15	0.5	0.152	0.347	0.14	0.486	0.076	0.4375
0.16	0.5	0.042	0.457	0.15	0.5	0.05	0.45
0.17	0.491	0.050	0.457	0.16	0.478	0.042	0.478
0.18	0.462	0.044	0.492	0.17	0.478	0.036	0.485
0.2	0.492	0	0.507	0.2	0.520	0	0.479
0.4	0.478	0	0.521	0.4	0.496	0	0.503
0.6	0.507	0	0.492	0.8	0.507	0	0.492
1	0.508	0	0.491	1	0.5	0	0.5
2	0.485	0	0.514	2	0.5	0	0.5

Table 5 —Electrolyte effect on the AOT concentration and distribution of each phase at equilibrium for system: 40 mM AOT initially in aqueous+0.65 cS PDMS at 25°C

[NaCl]/M	[AOT]/mM			%AOT		
	aqueous	oil	3rd	aqueous	oil	3rd
0.05	35.04	0		92	0	
0.06	33.6	0		85	0	
0.08	38.3	0		98	0	
0.1	39.9	0		104	0	
0.12	39.3	0		99	0	
0.13	2.42	0	43.6	0.8	0	94.2
0.14	0.76	0	102	1.28	0	98.7
0.15	0.67	0	127	1.39	0	98.3
0.16	0.74	0.44	324	1.69	1.1	71.4
0.17	0.72	2	376	1.6	4.99	102.3
0.18	0.67	8.5	393	1.8	20.02	112
0.2						
0.4	0.48	42.2		1.25	102.3	
0.6	0.37	40.5		0.9	103.6	
1	0.24	45.8		0.59	117	
2	0.13	43		0.33	104	

Table 6 —Electrolyte effect on the AOT concentration and distribution of each phase at equilibrium for system: 40 mM AOT initially 0.65 cS PDMS+NaCl aqueous at 25°C

[NaCl]/M	[AOT]/mM			%AOT		
	aqueous	oil	3rd	aqueous	oil	3rd
0.01	40.4	0		107.1		
0.025	40.6	0		103.4		
0.05	40.3	0		103.7		
0.075	39.5	0		100.4		
0.1	39.6	0		100.7		
0.11	36.7	0		91.3		
0.12	36.7	0		92.6		
0.13						94.2
0.14	1.18	0.2	38.62			98.7
0.15	0.8	0.73	38.47			98.3
0.16	0.85	16.2	22.95			71.4
0.17	0.93	17.8	21.27			102.3
0.18						112.0
0.2	0.6	36.1		1.44	95.3	
0.4	0.46	36.7		1.15	92.2	
0.8	0.4	38.28		0.98	98.0	
1	0.27	40.8		0.67	102.7	
2	0.2	38.5		0.5	96.7	

Table 7 —Electrolyte effect on the %AOT distribution of each phase at equilibrium for system: 40 mM AOT+ 1 or 50 cS PDMS+NaCl aqueous at 25°C

1 cS PDMS				50 cS PDMS			
[NaCl]/M	aqueous	oil	3rd	[NaCl]/M	aqueous	oil	3rd
0.1	99	0		0.07	100	0	
0.14	100	0		0.14	100	0	
0.17	100	0		0.2	90	0	
0.18	0	0	98.7	0.225	100	0	
0.2	0	0	97.1	0.25	54.5	0	45.8
0.225	0.64	0	96.53	0.3	57.31	0	43.3
0.25	0.67	0	96	0.33	35.05	0	66.1
0.28	1.1	0.4	96	0.37	17.6	0	84.1
0.29	1	0.6	97	0.4	5.6	0	96
0.31	1	2.6	95.4	0.6	1.07	0	99.3
0.33	0.6	7.9	89.7	0.8	1.08	0	99.5
0.35	0.73	11.7	86.4	1	1.07	0	99.5
0.4	50.6	45.7		1.2	0.57	0	99.8
0.55	8.9	89		1.35	0.52	0	99.8
0.7	11	87.1		1.5	0.57	0.5	
1	0.75	99.6		1.8	0.05	0.76	
1.5	0.56	99.8		2	0	0	
2	0.45	100		2.5	0	0	

Table 8 —Electrolyte concentration effect on the uptake of water (R_W) in w/o microemulsion phase of Winsor II systems at 25°C

0.65 cS PDMS		1 cS PDMS	
[NaCl]/M	R_w	[NaCl]/M	R_w
0.2	38.75	0.4	28.2
0.3	33.9	0.5	17.9
0.35	26.5	0.6	17.7
0.4	17.63	0.7	14
0.45	26.5	0.8	14.3
0.6	19.3	0.9	17.3
0.8	14.58	1	12.25
1	11.47	1.2	10.3
1.5	12.9	1.5	8.2
2	10.38	2	9

Table 9 —Electrolyte concentration effect on the 0.65 PDMS-water interfacial tensions for systems of 3 mM AOT aqueous+PDMS oils by spinning drop technique at two temperatures

25°C		40°C	
$[Na^+]$/M	γ_{ow} mN m^{-1}	$[Na^+]$/M	γ_{ow} mN m^{-1}
0.003	3.18	0.003	4.885
0.023	1	0.018	1.427
0.043	0.31	0.028	0.885
0.053	0.16	0.043	0.5099
0.063	0.12	0.053	0.281
0.079	0.07	0.073	0.196
0.08	0.06	0.103	0.126
0.0832	0.058	0.113	0.0575
0.088	0.06	0.123	0.038
0.097	0.03	0.138	0.0307
0.103	0.021	0.153	0.0269
0.113	0.028	0.173	0.0238
0.121	0.035	0.181	0.0326
0.132	0.041	0.188	0.0385
0.157	0.05	0.203	0.0495
0.203	0.08	0.253	0.055
0.253	0.104	0.273	0.069
0.3012	0.207008	0.303	0.119
0.4012	0.314836	0.403	0.215
0.6032	0.592161	0.553	0.3881
1.006	1.056248	0.703	0.632
1.9975	2.170045	1.003	1.071

Table 10 —Electrolyte concentration effect on the other PDMS oils-water interfacial tensions for systems of 3 mM AOT aqueous+PDMS at 25°C

1 cS		3 cS		5 cS		50 cS	
$[Na^+]$/M	γ_{ow} mN m^{-1}	$[Na^+]$/M	γ_{ow} mN m^{-1}	$[Na^+]$/M	γ_{ow} mN m^{-1}	$[Na^+]$/M	γ_{ow} mN m^{-1}
0.003	4.05	0.003	2.11	0.003	5.177	0.003	5.64
0.01	2.37	0.01	1.52	0.013	1.415	0.013	2.193
0.018	1.056	0.018	0.972	0.023	1.012	0.023	1.87
0.023	0.69	0.028	0.668	0.073	1.0023	0.033	1.889
0.033	0.3	0.043	0.543	0.103	0.9832	0.073	1.875
0.043	0.231	0.073	0.469	0.153	0.91	0.103	1.803
0.053	0.196	0.103	0.424	0.253	0.767	0.128	1.82
0.073	0.105	0.153	0.317	0.303	0.742	0.153	1.889
0.093	0.059	0.203	0.287	0.403	0.741	0.253	1.893
0.103	0.05	0.253	0.238	0.503	0.753	0.403	1.92
0.113	0.031	0.303	0.212	0.553	0.741	0.603	1.93
0.123	0.025	0.353	0.206	0.603	0.768	0.803	1.947
0.133	0.022	0.403	0.212	0.803	0.751	1.003	2.005
0.143	0.028	0.503	0.229	1.003	0.76	1.203	2.05
0.153	0.041	0.603	0.247	1.203	0.893	1.503	2.02
0.163	0.047	0.703	0.321	1.503	0.998	1.803	2.02
0.183	0.073	0.803	0.389	1.803	0.98	2.003	2.02
0.203	0.088	1.003	0.492	2.03	1.07		
0.403	0.19						
0.603	0.34						
0.803	0.66						
1.003	0.877						

Appendix IV

Single phase microemulsion systems

Table 1 —Cloud point (cp) of 0.5 wt% $C_{12}E_5$ affected by the addition of PDMS (µl PDMS oil per 10 ml surfactant solution)

0.65 cS PDMS		1 cS PDMS		5 cS PDMS	
µl / 10ml	cp / °C	µl / 10ml	cp / °C	µl / 10ml	cp / °C
0	31.4	0	31.4	0	31.4
10	31.6	10	37.4	10	46.8
20	34.4	20	43.4	20	50
30	36.7	30	47.8		
40	38.3	40	49.6		
50	39.9	50	51.3		
60	41.5	60	52.7		
70	42.5	70	53.5		
80	44	80	53.8		
90	45.2				
100	45.7				
110	46.2				
130	47.7				
150	48.3				
170	48.5				

Table 2 —Cloud point (cp) of 0.5 wt% L-77 affected by the addition of PDMS

0.65 cS PDMS		1 cS PDMS		5 cS PDMS	
µl / 10ml	cp / °C	µl / 10ml	cp / °C	µl / 10ml	cp / °C
0	11.5	0	11.5	0	11.5
10	9	10	13.5	10	26.5
20	15	20	21.5	20	35
30	20	40	28	30	35.5
40	23	60	28.2	40	36
50	25			60	36
60	26			80	36
70	26.5			100	36
80	27				

Table 3 —Variation of cloud point with added aminofunctionalised PDMS oil for 0.5 wt% aqueous solution of L-77. Also shown is the ratio of the outflow time for solutions containing oil to that of the solution without oil

oil conc./g per 100 ml L-77 aqu.	cloud point /°C	outflow time /s	outflow time ratio
0	10.7	41.72	1
0.0451	18.6	35.95	0.861697
0.0811	19.5	35.32	0.846596
0.1249	21	33.88	0.812081
0.2049	52	33.24	0.79674
0.2911	49.2	33.74	0.808725
0.4092	52.2	33.83	0.810882
0.4434	51	33.44	0.801534
0.4951	37.5	33.42	0.801055

Table 4 —oil uptake at the phase boundaries as a function of [L-77] in 10 cm^{-3} of water for aminofunctionalised PDMS at 10°C

[L-77]/g	[oil]/g at haze boundary	[oil]/g at solubilisation boundary
0	0	0
0.0192	0.029	0.034
0.0379	0.0436	0.0534
0.0646	0.0728	0.1019
0.0835	0.092	0.121
0.094	0.111	0.16
0.13	0.16975	0.218
0.156	0.174	0.243
0.1928	0.208	0.267

Table 5 —Electrolyte effect on the uptake of water (R_W) into w/o microemulsion single phases of the system: 40 mM AOT in 0.65 cS PDMS oil at two temperatures

25°C		40°C	
[NaCl]/M	R_W	[NaCl]/M	R_W
0	12.5	0	8.75
0.005	17.5	0.05	9.75
0.01	19	0.08	10.4
0.015	20	0.1	15
0.02	22.5	0.125	17.5
0.03	25	0.15	25
0.04	27.5	0.18	37.5
0.06	32.5	0.2	45
0.08	37.5	0.21	47.5
0.09	42.5	0.225	40
0.1	52.5	0.25	37
0.105	52.5	0.3	30
0.11	52.5	0.35	27.5
0.13	45	0.4	25
0.15	36.2	0.44	22.5
0.175	32.5	0.5	17.5
0.2	27.5	0.6	16.7
0.22	25	0.8	12.5
0.25	22.5	1	10
0.306	17		
0.4	11.4		
0.5	7.7		
0.604	5		
0.8	3.86		
1.002	2.5		
1.2506	1.25		
1.4995	1.25		
1.7491	1.25		
2.001	1.25		

Table 6—Comparison of the water uptake into w/o microemulsions at solubilisation boundaries in Winsor IV and Winsor II systems at 25°C, P is the partition coefficient of salt between the dispersed phase in w/o microemulsions and the coexisted bulk aqueous phase

Winsor IV systems		Winsor II systems		
[NaCl]/M	R_w	[NaCl]/M	R_w	P
0.2	27.5	0.2	38.75	0.833124
0.22	25	0.8	14.58	0.398664
0.25	22.5	1	11.47	0.374025
0.306	17	2	10.38	0.199836
0.4	11.4	0.3	33.9	0.607001
0.5	7.7	0.35	26.7	0.609693
0.604	5	0.45	26.5	0.476579
0.8	3.86	0.6	19.3	0.441212
1.002	2.5	1.5	12.9	0.230632
1.2506	1.25			
1.4995	1.25			
1.7491	1.25			
2.001	1.25			

Power law fitting of Winsor IV system data: $R_w = 2.6093([NaCl])^{-1.5056}$

Table 7 —Temperature effect on the uptake of water (R_W) into w/o microemulsion single phases of the system: 40 mM AOT in 0.65 cS PDMS oil at 3 electrolyte concentrations, T_h, haze boundary, T_s, solubilisation boundary

0 M NaCl		0.1 M NaCl			0.2 M NaCl		
T_h/°C	R_W	T_s/°C	T_h/°C	R_W	T_s/°C	T_h/°C	R_W
60	8.5		44.5	15		55	20
25.2	10		37	20	16	50.2	25
24.5	12.5	13	35.8	25	22	47.4	30
24	15	15	32.4	30	28	45.6	35
22.7	17.5	15.2	31.5	35	34	43.5	40
22.1	20	15.5	28	40	36.7	42.3	45
20.9	22.5	16	27.4	45	37.2	41	47.5
19.9	25	17.2	27	50	40	40	50
17.8	27.5	18.6	26	55			
16.1	30						
14.1	32.5						
13.1	35						
10	40						
7.3	42.5						
6.7	45						
5	47.5						
5	50						
31.5	9.6						
50	9						

Table 8 —Electrolyte effect on the uptake of 0.65 cS PDMS oil (R_o) into o/w microemulsion single phases of the system: 3 mM AOT in NaCl aqueous at 2 temperatures, R_c is the oil needed to clarify turbid AOT aqueous phase

25°C			40°C*		
[NaCl]/M	R_o	R_c	[NaCl]/M	R_o	R_c
0	0.5		0	0.5	
0.005	0.5		0.005	0.5	
0.01	0.75		0.01	0.5	
0.015	1		0.015	0.5	
0.02	1	0	0.02	0.5	
0.03	1	0.25	0.03	0.5	0
0.04	1.25	0.5	0.04	0.5	0.25
0.05	1.25	0.75	0.05	0.5	0.5
0.06	1.75	1.25	0.06	0.6	
0.07	1.75	1.5	0.07	0.5	
0.08	2	2	0.08	0.75	
0.09	2.5		0.09	1	
0.1	3.5		0.1	1.25	
0.11	4		0.11	1.25	
0.12	2		0.12	1	
0.13	1.25		0.13	0.75	
0.14	0.75		0.14	0.75	
0.15	0.5		0.15	0.75	
0.17	0.5		0.17	0.75	
0.2	0.5		0.18	0.5	

*Data for 40°C are not reliable due to the volatility of the oil.

Table 9 —Temperature effect on the uptake of 0.65 cS PDMS oil (R_o) into o/w microemulsion single phases of the system: 40 mM AOT in NaCl aqueous, R_c is the oil needed to clarify the turbid aqueous phase

0 M NaCl			0.03 M NaCl			0.06 M NaCl			0.09 M NaCl		
T/°C	R_c	R_o	T/°C	R_c	R_o	T/°C	R_c	R_o	T/°C	R_c	R_o
10	0.18	0.72	10			25			10		
20	0.12	0.72	20	1.2	1.96	30	2.7	3.75	20		
25	0.06	0.82	25	1.17	1.99	40	1.64	3.17	25		
30		1.14	30	1.17	2.32	50	1.06	2.93	30		
40		1.26	40	0.59	2.23	60	1.06	2.7	40	2.7	4.93
45		1.32	50	0.47	2.11	27.5	3.2	4.1	50	1.76	3.87
50		1.08	60	0.35	1.64	25	4.05	4.45	60	1.17	3.28
60		1.12							37.5	4.9	6.1

Appendix V

Mixing of surfactants and PDMS at air-water surfaces

Table 1 —Surface tension of C_nE_5 aqueous versus with the presence liquid drops of 50 cS PDMS (10 μl) at 25°C at different bulk concentrations

1.5 x cmc

Time/min	C_8, γ_i=32.3 mN m^{-1}	C_{10}, γ_i=31.1 mN m^{-1}	C_{12}, γ_i=30.7 mN m^{-1}	C_{14}, γ_i=30.4 mN m^{-1}	C_{16}, γ_i=31.5 mN m^{-1}
5	26.1	24.9	26.1	30.6	33.2
11	26.2		25	30.5	32.8
20	26.1	24.9	25.1	25.7	32.4
40	26.1	24.9	24.6	24.2	32
45			24.3	23.9	31.8
55			24.3	23.8	
65			24.3		31.5
75			24.3	23.8	
85			24.2		31.3
95			24.2	23.8	
100					31.2

50 x cmc

Time/min	C_8, γ_i=32.3 mN m^{-1}	C_{10}, γ_i=31.1 mN m^{-1}	C_{12}, γ_i=30.7 mN m^{-1}	C_{14}, γ_i=30.4 mN m^{-1}	C_{16}, γ_i=31.5 mN m^{-1}
5	25.7	24.6	24.2	24.4	35
15	25.7	24.6	24.2	23.8	34.5
30	25.7	24.6	24.2	23.8	33.8
40	25.7	24.6	24.2	23.7	33.3
60	25.7	24.6	24.2	23.7	32.7
55				23.7	32.4
65					32.2
75					32.1
85					31.8
95					31.5
100					31

Adding C_nE_5 in PDMS

%C_nE_5	C_8, γ_i=32.3 mN m^{-1}	C_{10}, γ_i=31.1 mN m^{-1}	C_{12}, γ_i=30.7 mN m^{-1}	C_{14}, γ_i=30.4 mN m^{-1}	C_{16}, γ_i=31.5 mN m^{-1}
0	26.1	24.9	24.2	23.8	31.2
0.2	26.2	24.7	24.1	23.9	25.7
0.5	26.2	24.7	24.2	23.9	25.7
0.8	26	24.7	24.1	23.8	25.6
1	26.1	24.6	24.1	23.8	25.8

Table 2 —Surface tension of $C_{12}E_m$ aqueous versus time with the presence liquid drops of 50 cS PDMS (10 μl) at 25°C at different bulk concentrations

50 x cmc

Time/min.	E_2, γ_i=25.9 mN m^{-1}	E_3, γ_i=27.7 mN m^{-1}	E_4, γ_i=28.8 mN m^{-1}	E_5, γ_i=30.4 mN m^{-1}	E_6, γ_i=32.2 mN m^{-1}
5	23.1	27.7	23.2	24.2	25.4
20	23.1	26.5	23.1	24.2	25.3
30	23.1	23.6	23.1	24.2	25.3
40	23.1	23.8	23	24.2	25.3
60	23.1	23.3	23	24.2	25.3
70		23.3	23	23	

Adding 1% $C_{12}E_m$ in 1.5 x cmc aqueous surfaces

Time /hr.	E_2, γ_i=25.9 mN m^{-1}	E_3, γ_i=27.7 mN m^{-1}	E_4, γ_i=28.8 mN m^{-1}	E_5, γ_i=30.4 mN m^{-1}	E_6, γ_i=32.2 mN m^{-1}
1	22.9	22.9	23.3	24	25.2
2	22.8	23.1	22.9	23.7	24.4
4	22.6	23.1	22.9	23.7	24.8
5	22.6	22.9	22.9	23.6	24.5
6	22.6	23	22.9	23.6	24.6
8	22.6	23	23	23	24.8
10	22.9	23			24.5

Table 3 —Surface tension of 1.5xcmc $C_{12}E_5$ aqueous versus time with the presence of liquid drops of x cS PDMS (10 μl, containing 1 wt% surfactant) at 25°C, γ_l = 30.7 mN m^{-1}

t /min.	5 cS	10	20	50	100	500	1000
5	21.5	22.4	23.1	24.2	24.1	24.2	24.5
30	21.4		23.1	24.2	24	24.1	24.4
40		22.5		24.2		24.2	24.4
60	21.3	22.5	23.1	24.2	24	24.2	24.4
120	21.4						

0.65 cS		1 cS	
Time/min	Tension mN m^{-1}	Time/min	Tension mN m^{-1}
1	16.4	1	18.4
5	17.1	5	17.8
10	18.8	15	17.7
20	17.1	25	17.8
30	16.8	35	17.8
40	16.8	Cover off	
50	16.7	40	28.6
60	16.7	45	30
70	16.6	50	30.1
Cover off			
72	23.5		
75	29.8		

Table 4 —Surface tensions of aqueous $C_{12}E_5$ solutions at 25°C as a function of surfactant concentration in the presence and absence of 50 cS PDMS oil

$[C_{12}E_5]$/M	Ln($[C_{12}E_5]$)	$\gamma_{no\ oil}$ mN m^{-1}	γ^{+oil} mN m^{-1}	$\Delta\gamma$ mN m^{-1}
2.87E-07	-15.0638	68.3	57.4	10.9
6.22E-07	-14.2903	66.1	54	12.1
9.78E-07	-13.8378	61.8	51.6	10.2
2.10E-06	-13.0736	59.4	47.8	11.6
3.02E-06	-12.7103	56.4	44.8	11.6
4.38E-06	-12.3385	54.1	43.5	10.6
5.80E-06	-12.0577	50.9	42.1	8.8
8.20E-06	-11.7114	48.2	38.2	10
1.52E-05	-11.0942	43.1	35.8	7.3
1.55E-05	-11.0747	42.7	34	8.7
2.62E-05	-10.5498	38.9	31.6	7.3
4.48E-05	-10.0133	34.5	28.2	6.3
5.84E-05	-9.74819	32.4	26.2	6.2
6.72E-05	-9.60784	30.3	24.2	6.1
7.34E-05	-9.51959	31.1	24.9	6.2
9.70E-05	-9.2408	30.6	24.1	6.5
9.73E-05	-9.23771	30.6	24.4	6.2
3.25E-03	-5.7291	30.5	24.2	6.3

Polynomial fitting of data:
In the absence of oil: y = -0.2877x2 - 13.985x - 75.855
In the presence of oil: y = -0.1378x2 - 9.3212x - 51.179

Table 5 —Surface tensions of aqueous L-77 solutions at 25°C as a function of surfactant concentration in the presence and absence of 50 cS PDMS oil

[L-77]M	Ln([L-77])	$\gamma_{no\ oil}$ mN m^{-1}	γ^{+oil} mN m^{-1}	$\Delta\gamma$ mN m^{-1}
6.62E-06	-11.9254152	42.4	41	1.4
8.06E-06	-11.728597	39	38.4	0.6
8.24E-06	-11.7071172	39.6	39.7	-0.1
1.30E-05	-11.2482562	37.3	37.8	-0.5
1.35E-05	-11.2128209	40.4	40.4	0
2.03E-05	-10.8048897	33.5	33.6	-0.1
2.06E-05	-10.7902195	33.4	34.3	-0.9
3.42E-05	-10.2832849	29.9	30.6	-0.7
6.37E-05	-9.661326	25.7	26.1	-0.4
1.14E-04	-9.07931211	22.4	23.1	-0.7
2.17E-04	-8.4356132	21.2	21.2	0
4.00E-04	-7.82404601	21.2	21.3	-0.1
1.78E-03	-6.33114191	21.2	21.2	0

Polynomial fitting of data: y = -0.276x2 - 12.557x - 69.07

Table 6 —Surface tensions of aqueous 3 mM AOT solutions at 25°C as a function of electrolyte concentration in the presence and absence of 0.65 cS PDMS oil

[NaCl]/M	$\gamma_{no\ oil}$ mN m^{-1}	γ^{+oil} mN m^{-1}	$\Delta\gamma$ mN m^{-1}
0	29.9	20.4	9.5
0.002	28.8	19.5	9.3
0.004	28	18.7	9.3
0.006	27.5	18.3	9.2
0.008	27.1	18.2	8.9
0.01	25.9	17.4	8.5
0.012	26.4	17.6	8.8
0.014	26	17.4	8.6
0.015	25.8	17	8.8
0.016	25.7	17.1	8.6
0.018	25.5	17.4	8.1
0.02	25.3	16.9	8.4
0.022	25.4	16.9	8.5
0.025	25.5	16.9	8.6
0.026	25.5	16.9	8.6
0.0285	25.4	16.9	8.5
0.03	25.3	16.6	8.7
0.035	25.3	16.5	8.8
0.03	25	16.1	8.9
0.04	25.3	15.8	9.5
0.041	25.3	16.4	8.9
0.0493	25.3	16.3	9
0.06	25.3	15.9	9.4
0.08	25.3	15.7	9.6
0.1	25.3	16.1	9.2

Table 7 —Surface tensions of aqueous cac AOT solutions at 25°C as a function of electrolyte concentration in the presence and absence of 0.65 cS PDMS oil

[NaCl]/M	[AOT]/mM	$\gamma_{no\ oil}$ mN m^{-1}	γ^{+oil} mN m^{-1}	$\Delta\gamma$ mN m^{-1}
0	2.3004	30.3	21	9.3
0.005	1.991556	28	19.1	8.9
0.01	1.720388	27	18.4	8.6
0.015	1.484316	26.5	18	8.5
0.02	1.280766	26	17.7	8.3
0.025	1.107158	25.7	17.6	8.1
0.03	0.960916	25.6	17.6	8
0.035	0.839463	25.6	17.4	8.2
0.04	0.740221	25.6	17.4	8.2
0.045	0.660613	25.6	17.1	8.5
0.05	0.598063	25.6	16.9	8.7
0.055	0.549992	25.65	16.9	8.75
0.06	0.513823	25.7	16.9	8.8
0.065	0.48698	25.7	17	8.7
0.07	0.466885	25.7	17.1	8.6
0.075	0.450961	25.7	17	8.7
0.08	0.43663	25.7	17.1	8.6
0.085	0.421316	25.7	17	8.7
0.09	0.402441	25.5	16.9	8.6
0.095	0.377428	25.6	17	8.6
0.1	0.3437	25.8	17.2	8.6

Table 8 —Surface tensions of aqueous 65% cac AOT solutions at 25°C as a function of electrolyte concentration in the presence and absence of 0.65 cS PDMS oil

[NaCl]/M	[AOT]/mM	$\gamma_{no\ oil}$ mN m^{-1}	γ^{+oil} mN m^{-1}	$\Delta\gamma$ mN m^{-1}
0	1.49526	33	23.6	9.4
0.005	1.294512	30.5	21	9.5
0.01	1.118252	28.8	19.2	9.6
0.015	0.964806	27.7	18.2	9.5
0.02	0.832498	27.6	18	9.6
0.025	0.719653	27.8	18.4	9.4
0.03	0.624595	27.5	18	9.5
0.035	0.545651	27.7	18.3	9.4
0.04	0.481144	27.7	18.2	9.5
0.045	0.429399	27.7	18.2	9.5
0.05	0.388741	28	18.4	9.6
0.055	0.357495	28	18.5	9.5
0.06	0.333985	27.8	18.2	9.6
0.065	0.316537	27.8	18.3	9.5
0.07	0.303475	28	18.6	9.4
0.075	0.293125	27.9	18.5	9.4
0.08	0.28381	27.8	18.4	9.4
0.085	0.273856	27.8	18.2	9.6
0.09	0.261587	27.7	18.2	9.5
0.095	0.245328	27.8	18.3	9.5
0.1	0.223405	28	18.6	9.4

Table 9 —Surface tensions for systems of 3 mM AOT aqueous before and after pre-equilibrated with equal volume of 0.65 cS PDMS oil as a function of electrolyte concentration at 25°C

[NaCl]/M	$\gamma_{no\ oil}$ mN m^{-1}	γ^{+oil} mN m^{-1}	$\Delta\gamma$ mN m^{-1}
0	29.9	20.7	9.2
0.002	28.8	20.2	8.6
0.006	27.5	19.46	8.04
0.01	26.5	18.6	7.9
0.016	25.7	18.1	7.6
0.02	25.3	17.9	7.4
0.025	25.5	18.1	7.4
0.03	25.3	18	7.4
0.035	25.3	17.9	7.4
0.041	25.3	17.9	7.4
0.0493	25.3	18	7.3
0.06	25.3	18	7.3
0.08	25.3	18	7.3
0.1	25.3	17.9	7.4

Appendix VI

Surface tension lowering of surfactant aqueous varies with the activity of volatile PDMS (P/P_o) via vapour adsorption (Hauxwell vapour train) at 25°C

Table 1 —Adsorption of 0.65 cS PDMS on pure water (surfactant free) surface, $\gamma_{no\ oil}$ = 71.4 mN m^{-1}

P/P_o	γ^{+oil} mN m^{-1}	$\Delta\gamma$ mN m^{-1}
0	71.4	0
0.256	68.3	3.12
0.267	68.11	3.31
0.301	67.4	4.02
0.341	66.8	4.62
0.353	66.46	4.96
0.374	66.06	5.36
0.392	65.7	5.72
0.412	65.33	6.09
0.445	64.89	6.53
0.469	64.82	6.6
0.496	64.22	7.2
0.513	64.01	7.41
0.542	63.52	7.9
0.575	63.06	8.36
0.611	62.63	8.79
0.638	62.23	9.19
0.68	61.75	9.67
0.71	61.4	10.02
0.736	61.02	10.4
0.772	60.65	10.77
0.814	60.16	11.26
0.862	59.53	11.89
0.917	58.89	12.53
0.955	58.35	13.07
1	57.76	13.66

Polynomial fitting of tension lowering data: y = 14.001x

Table 2 —Adsorption of 0.65 and 1 cS PDMS on 6.4 mM $C_{12}E_5$ aqueous (100 times cmc of $C_{12}E_5$ in water) surface, $\gamma_{no\ oil}$ = 29.9 mN m^{-1}

0.65 cS PDMS			1 cS PDMS		
P/P_o	γ^{+oil} mN m^{-1}	$\Delta\gamma$ mN m^{-1}	P/P_o	γ^{+oil} mN m^{-1}	$\Delta\gamma$ mN m^{-1}
0	29.9	0	0	29.9	0
0.258	26.15	3.75	0.205	27.01	2.89
0.31	25.65	4.25	0.224	26.3	3.6
0.355	25.12	4.78	0.265	26.04	3.86
0.389	24.41	5.49	0.281	25.64	4.26
0.44	23.66	6.24	0.313	25.16	4.74
0.464	23.24	6.66	0.335	24.98	4.92
0.485	22.86	7.04	0.367	24.83	5.07
0.502	22.71	7.19	0.402	24.28	5.62
0.52	22.66	7.24	0.432	23.41	6.49
0.554	22.05	7.85	0.492	23.02	6.88
0.542	21.88	8.02	0.542	22.41	7.49
0.569	21.68	8.22	0.607	21.62	8.28
0.5645	21.64	8.26	0.637	20.92	8.98
0.611	21.42	8.48	0.559	22.03	7.87
0.641	21.3	8.6	0.588	21.77	8.13
0.666	21.07	8.83	0.628	21.35	8.55
0.698	20.74	9.16	0.654	20.69	9.21
0.733	20.24	9.66	0.712	20.44	9.46
0.772	19.8	10.1	0.74	20.1	9.8
0.81	19.23	10.67	0.763	19.66	10.24
0.853	18.85	11.05	0.786	19.75	10.15
0.894	18.28	11.62	0.796	19.36	10.54
0.955	17.8	12.1	0.83	19.14	10.76
0.995	17.31	12.59	0.861	18.41	11.49
			0.877	18.53	11.37
			0.893	18.05	11.85
			0.942	17.78	12.12
			0.942	17.61	12.29
			1	17.01	12.89

Polynomial fittings of tension lowering data

0.65 cS PDMS: $y = -3.0785x^2 + 15.646x$

1 cS PDMS: $y = -2.4199x^2 + 15.119x + 0.0858$

Table 3 —Adsorption of 0.65 cS PDMS on 3 mM AOT aqueous at different electrolyte concentrations

0 M NaCl, $\gamma_{no\ oil}$ = 28.4 mN m^{-1}

P/P_o	γ^{+oil} mN m^{-1}	$\Delta\gamma$ mN m^{-1}
0	28.4	0
0.253	26.52	1.88
0.312	25.9	2.5
0.333	25.39	3.01
0.349	25.36	3.04
0.37	24.92	3.48
0.401	24.75	3.65
0.424	24.07	4.33
0.451	23.9	4.5
0.485	23.61	4.79
0.515	23.01	5.39
0.551	22.67	5.73
0.579	22.22	6.18
0.611	21.79	6.61
0.647	21.46	6.94
0.68	21.13	7.27
0.725	20.42	7.98
0.741	20.2	8.2
0.801	19.61	8.79
0.844	19.14	9.26
0.894	18.49	9.91
0.95	18.1	10.3
1	17.42	10.98

Polynomial fitting of tension lowering data: $y = 2.5287x^2 + 8.7953x$

0.01M NaCl, $\gamma_{no\ oil}$ = 26.2 mN m^{-1}

P/P_o	γ^{+oil} mN m^{-1}	$\Delta\gamma$ mN m^{-1}
0	26.2	0
0.258	24.97	1.23
0.286	24.82	1.38
0.316	24.67	1.53
0.342	24.36	1.84
0.383	23.34	2.86
0.403	23.22	2.98
0.434	23.07	3.13
0.48	22.64	3.56
0.515	22.16	4.04
0.551	21.89	4.31
0.572	21.59	4.61
0.595	21.29	4.91
0.638	21.01	5.19
0.673	20.79	5.41
0.717	20.39	5.81
0.752	20	6.2
0.805	19.59	6.61
0.857	19.19	7.01
0.903	18.64	7.56
0.95	18.17	8.03
1	17.75	8.45

Polynomial fitting of tension lowering data: $y = 2.7145x^2 + 6.0005x$

0.02M NaCl, $\gamma_{no\ oil}$ = 25.3 mN m^{-1}

P/P_o	γ^{+oil} mN m^{-1}	$\Delta\gamma$ mN m^{-1}
0	25.3	0
0.253	24.18	1.12
0.269	23.95	1.35
0.3	23.87	1.43
0.325	23.71	1.59
0.353	23.47	1.83
0.374	23.34	1.96
0.401	23.15	2.15
0.436	22.94	2.36
0.469	22.73	2.57
0.491	22.52	2.78
0.519	22.3	3
0.554	22.02	3.28
0.591	21.81	3.49
0.631	21.5	3.8
0.662	21.28	4.02
0.702	20.87	4.43
0.733	20.67	4.63
0.776	20.37	4.93
0.814	20.08	5.22
0.857	19.86	5.44
0.907	19.15	6.15
0.964	18.55	6.75
1	18.09	7.21

Polynomial fitting of tension lowering data: $y = 2.9622x^2 + 4.1112x$

0.03M NaCl, $\gamma_{no\ oil}$ = 25.6 mN m^{-1}

P/P_o	γ^{+oil} mN m^{-1}	$\Delta\gamma$ mN m^{-1}
0	25.6	0
0.282	23.75	1.85
0.3	23.59	2.01
0.319	23.51	2.09
0.349	23.39	2.21
0.378	23.12	2.48
0.41	22.92	2.68
0.449	22.57	3.03
0.485	22.22	3.38
0.519	21.92	3.68
0.545	21.72	3.88
0.592	21.37	4.23
0.641	20.83	4.77
0.706	20.17	5.43
0.748	19.86	5.74
0.789	19.48	6.12
0.827	19.11	6.49
0.87	18.72	6.88
0.912	18.3	7.3
0.96	17.92	7.68
1	17.52	8.08

Polynomial fitting of tension lowering data: $y = 2.3553x^2 + 5.8298x$

0.04M NaCl, $\gamma_{no\ oil}$ = 25.3 mN m^{-1}

P/P_o	γ^{+oil} mN m^{-1}	$\Delta\gamma$ mN m^{-1}
0	25.3	0
0.253	23.9	1.4
0.266	23.86	1.44
0.293	23.6	1.7
0.319	23.44	1.86
0.346	23.29	2.01
0.361	23.09	2.21
0.387	22.82	2.48
0.44	22.26	3.04
0.504	21.65	3.65
0.533	21.21	4.09
0.563	20.89	4.41
0.598	20.45	4.85
0.635	20	5.3
0.659	19.72	5.58
0.7	19.48	5.82
0.736	19.06	6.24
0.776	18.9	6.4
0.835	18.25	7.05
0.866	17.92	7.38
0.906	17.39	7.91
0.95	16.99	8.31
1	16.53	8.77

Polynomial fitting of tension lowering data: $y = 3.6053x^2 + 5.4826x$

0.06M NaCl, $\gamma_{no\ oil}$ = 25.3 mN m^{-1}

P/P_o	γ^{+oil} mN m^{-1}	$\Delta\gamma$ mN m^{-1}
0	25.3	0
0.253	23.87	1.43
0.282	23.59	1.71
0.307	23.25	2.05
0.327	23.08	2.22
0.353	22.86	2.44
0.383	22.6	2.7
0.403	22.36	2.94
0.424	22.16	3.14
0.449	21.9	3.4
0.474	21.68	3.62
0.502	21.42	3.88
0.536	21.16	4.14
0.56	20.81	4.49
0.595	20.6	4.7
0.635	20.18	5.12
0.659	19.91	5.39
0.7	19.16	6.14
0.733	19.18	6.12
0.789	18.66	6.64
0.814	18.24	7.06
0.862	17.98	7.32
0.908	17.23	8.07
0.95	16.91	8.39
1	16.31	8.99

Polynomial fitting of tension lowering data: $y = 3.0238x^2 + 6.0847x$

0.1 M NaCl, $\gamma_{no\ oil}$ = 25.2 mN m^{-1}

P/P_o	γ^{+oil} mN m^{-1}	$\Delta\gamma$ mN m^{-1}
0	25.2	0
0.256	24.02	1.58
0.296	23.8	1.8
0.327	23.6	2
0.361	23.4	2.2
0.392	23.2	2.4
0.429	22.7	2.9
0.471	22.5	3.1
0.524	21.8	3.8
0.575	21.5	4.1
0.624	20.7	4.9
0.666	20.3	5.3
0.733	19.5	6.1
0.814	18.8	6.8
0.862	18.5	7.1
0.903	18	7.6
0.941	17.6	8
1	16.9	8.7

Polynomial fitting of tension lowering data: $y = 3.5997x^2 + 5.2338x$

Appendix VII

Emulsion stability in the system of AOT aqueous+0.65 cS PDMS oil at 25°C

Table 1 —Water (creaming) phase resolution ($\%W_{re}$) as a function of time for various salt concentrations for o/w emulsions (40 mM AOT in 0.65 cS PDMS+equal volume of aqueous NaCl solutions) formed in Winsor I region

0 M NaCl		0.02 M		0.04 M		0.06 M		0.08 M	
t/hr.	$\%W_{re}$	t/hr.	$\%W_{re}$	t/hr.	$\%W_{re}$	t/hr.	$\%W_{re}$	t/hr.	$\%W_{re}$
0	0	0	0	0	0	0	0	0	0
1.032	15.8	5.588	15.8	8.254	3.8	15.74	1	12.50	2.8
1.266	18.4	6.338	21	15.25	5.6	19.05	2.4	12.86	5.6
1.471	19.4	8.004	26.4	18.70	7.6	21.12	2.6	18.09	11.1
1.754	21	10.25	31.6	19.70	8.4	27.27	5.2	21.37	13.8
2.471	26.4	11.10	36.8	20.83	11	32.01	9.3	26.34	22.2
3.888	31.6	19.12	42.2	21.77	11.4	35.77	11.6	32.04	33.4
10.69	42	25.54	47.4	32.37	13.8	41.01	13.95	40.0	38.9
18.69	52.6	28.80	51.1	35.44	15	54.90	18.6	47.72	44.2
25.09	57.8	45.37	57.8	46.20	19.4	59.60	21	58.40	47.8
30.32	63.2	58.69	60.7	53.75	22.2	69.17	25.6	71.25	52.8
52.89	71	73.77	65.2	69.70	30.55	84.27	37.2	81.39	55.6
68.72	73.6	82.60	67.4	79.45	41.6	93.44	42.84	95.89	61.1
78.45	76.3	97.94	72	94.54	52.8	108.8	52.4	105.0	63.9
93.22	79	121.4	76.4	103.3	57.14	121.8	61.9	120.4	66.66
117.7	81	145.9	78.7	108.2	60	132.2	66.6	143.9	71.4
165.8	83.4	168.6	80.9	116.7	62.8	140.0	70	168.4	74.2
221.4	86.1	201.6	83.15	142.2	68.6	156.8	73.2	191.1	76.5
291.6	87.3	224.9	85.4	166.7	73.5	179.7	78	224.0	82.35
381.7	88.6	271.8	86.4	189.4	76.5	212.1	81.9	247.4	88.2
511.4	89.55	419.6	87.4	211.7	77.9	235.4	82.93	294.2	93.9
				222.4	79.4	282.3	86.4	320.4	96.87
				245.7	81.2	308.4	88.9	360.4	100
				281.6	82.35	348.4	91.36		
				292.5	85.3	372.4	93.8		
				318.7	87.9	406.2	95		
				512.4	88.24	454.2	100		

Table 2—Oil (coalescence, $\%O_{col}$) phase resolution as a function of time for various salt concentrations for o/w emulsions (40 mM AOT in 0.65 cS PDMS+equal volume of aqueous NaCl solutions) formed in Winsor I region

0.02 M NaCl		0.04 M		0.06 M		0.08 M	
t/hr.	$\%O_{col}$	t/hr.	$\%O_{col}$	t/hr.	$\%O_{col}$	t/hr.	$\%O_{col}$
271	0	282	0	215	0	227	0
297.6	0.5	292.5	0.5	235.4	0.5	247.4	2.94
419.9	2.3	318.7	1	282.3	2.5	294.4	3.17
		512.7	1.5	348.4	5	320.4	6.25
				454.4	10	360.4	9.4
				502.4	12.5	466.2	12.5
						514.4	15.6

0.10 M NaCl		0.12 M		0.14 M	
t/min.	$\%\ O_{col}$	t/min.	$\%\ O_{col}$	t/min.	$\%\ O_{col}$
0	0	0	0	0	0
7.8	69.5	1.0667	68.75	0.63	3.4
9.2	80.3	1.15	71.88	0.76	7
9.55	82.5	1.25	75	0.85	10.6
10.5	89	1.467	81.25	0.9	14
11.65	95	1.567	84.37	0.98	21
12	97	1.8	90.62	1.067	28
14	98	1.967	93.75	1.167	38.6
		2.133	95.31	1.28	59.2
		2.5	96.5	1.47	70.2
		3	97	1.6	84.2
				1.7	87.6
				1.91	91.2
				2.5	95
				4	98.5

Table 3 —Oil (sedimentation, $\%O_{se}$) phase resolution as a function of time for various salt concentrations for w/o emulsions (40 mM AOT in 0.65 cS PDMS+equal volume of aqueous NaCl solutions) formed in Winsor II region

0.20 M NaCl		0.23 M		0.27 M		0.30 m		0.40 M	
t/sec.	$\%O_{se}$	t/sec.	$\%O_{se}$	t/sec.	$\%O_{se}$	t/sec.	$\%O_{se}$	t/sec.	$\%O_{se}$
0	0	0	0	0	0	0	0	0	0
6	22.22	7	27.1	9	61	12	56.67	11	21.05
22	55.55	13	51.7	15	74.6	20	96.67	17	63.16
40	62.96	18	62.1	33	81.4	48	100	21	94.74
57	70.37	32	72.4	58	84.7	98	100	26	98.25
88	74.07	50	76	95	85	300	100	48	98.25
120	77.78	90	79.3	228	88.1	580	100	93	98.25
180	79.63	140	80.85	312	91.5			420	98.25
210	81.48	313	86.2	550	91.5			590	98.25
360	83.33	389	87.9						
595	85.19	470	89.6						

0.50 M NaCl		0.60 M		0.80 M		1.00 M	
t/sec.	$\%O_{se}$	t/sec.	$\%O_{se}$	t/sec.	$\%O_{se}$	t/sec.	$\%O_{se}$
0	0	0	0	0	0	0	0
10	33.33	9	30.51	10	62.07	20	81.36
19	80	17	77.97	18	89.66	27	91.53
34	96.67	27	91.53	22	93.1	37	94.92
45	96.67	42	96.61	26	96.55	44	94.92
72	96.67	49	96.61	43	96.55	95	94.92
90	96.67	87	96.61	85	96.55	570	94.92
585	96.67	180	96.61	210	96.65		
		290	96.61	575	96.65		

Table 4 —Water (coalescence, $\%W_{col}$) phase resolution as a function of time for various salt concentrations for w/o emulsions (40 mM AOT in 0.65 cS PDMS+equal volume of aqueous NaCl solutions) formed in Winsor II region

0.20 M NaCl		0.23 M		0.27 M		0.30 M	
t/days	$\%W_{col}$	t/days	$\%W_{col}$	t/days	$\%W_{col}$	t/days	$\%W_{col}$
0	0	0	0	0	0	0	0
5	0.75	1	1	0.08	44.1	0.125	100
5.89	1.8	2	20	0.166	57.6	16.5	100
6.93	3.7	3.06	45.6	0.19	64.4		
8.07	7.4	4.01	70.2	0.32	79.7		
9.1	18.5	4.98	87.7	0.4	96.6		
10	29.6	6	94.7	0.5	100		
10.9	44.4	8	96.5	17	100		
11.87	66.7	17.5	96.5				
12.93	85.1						
14	90.7						
15.1	92.6						
16	94.4						
16.95	94.4						
18	96.2						
19.8	96.2						

Table 5 —Oil phase resolution ($\%O_{re}$) as a function of time for various salt concentrations for emulsions (40 mM AOT in 0.65 cS PDMS+equal volume of aqueous NaCl solutions) formed in Winsor III region

0.16 M NaCl		0.18 M	
t/sec.	$\%O_{re}$	t/sec.	$\%O_{re}$
0	0	0	0
15	18	6	17.4
17	25.4	9	28
20	36	12	35
22	51	13	42
24	58.1	15	49.2
27	69	19	56.2
33	76.4	22	63.2
37	83.6	24	70.2
40	87.2	26	77.2
47	91	31	84.2
115	92.8	42	87.8
145	94.6	61	91.2
233	94.6	149	93
285	94.6	276	93
		290	93

Table 6 —Percentage resolution of "blue" phase (relative to the total volume of blue plus water phase, to which the bottom phase ultimately resolves) with time for 0.16 M salt concentration in Winsor III region at 25°C

t/hr.	% blue resolution
0	0
1.7044	1.72
1.8303	3.45
1.9544	5.17
2.0878	6.9
2.7044	10.35
2.9877	13.79
3.8544	17.24
5.0211	20.69
5.4378	24.14
6.4878	27.59
10.5211	31.03
14.5211	31.03

Table 7 —Volume mean diameters for emulsions formed in Winsor I region for three PDMS oils after dilution vs NaCl concentration at 23°C

0.65 cS PDMS		5 cS		50 cS	
[NaCl]/M	*d(v,0.5) /μm	[NaCl]/M	d(v,0.5) /μm	[NaCl]/M	d(v,0.5) /μm
0	3.4	0	6.2	0	9.3
0.02	2.9	0.03	5.7	0.03	15.4
0.04	2.3	0.06	5.7	0.06	16.7
0.06	2	0.09	4.9	0.09	18.5
0.08	2.9	0.12	6.1	0.15	20.7
0.1	18.9	0.15	7.6	0.18	19.1
0.12	24.5	0.18	11.4	0.2	17.3
0.05	2.3	0.2	20	0.23	16.4
0.07	2				

Table 8 —Volume mean diameters for emulsions: AOT in 0.65 cS PDMS oil plus equal volume of 0.06 M aqueous NaCl after dilution vs AOT concentration in oil phase at 23°C

[AOT]/mM	d(v,0.5)/μm	[AOT]/mM	*d(v,0.1)/μm
40	2	40	2
30	3.55	30	2.6
20	3.7	20	2.7
10	5.2	10	3.5
5	7.2	5	3.9

* d(v,0.5) is defined as the volume mean diameters such that 50% of the volume distribution of the drops are ≤ this value, similarly, d(v,0.1) means that 10% of the volume distribution of drops are ≤ this value.